Universidad de Huelva

Departamento de Ingeniería Química, Química Física y Ciencias de los Materiales



Biorrefinería hidrolítica y termoquímica para la obtención de productos de valor añadido y energía a partir de cultivos de alta productividad

Memoria para optar al grado de doctora
presentada por:

Susana Lozano Calvo

Fecha de lectura: 29 de octubre de 2025

Bajo la dirección de los doctores:

Francisco López Baldovín

Juan Carlos García Domínguez

Huelva, 2025



UNIVERSIDAD DE HUELVA

Departamento de Ingeniería Química, Química Física y

Ciencias de los Materiales

BIORREFINERÍA HIDROLÍTICA Y TERMOQUÍMICA PARA LA OBTENCIÓN DE PRODUCTOS DE VALOR AÑADIDO Y ENERGÍA A PARTIR DE CULTIVOS DE ALTA PRODUCTIVIDAD.

Tesis Doctoral

Programa de Doctorado en Ciencia y Tecnología

Industrial y Ambiental

SUSANA LOZANO CALVO

2025

Directores:

Dr. Francisco López Baldovín

Dr. Juan Carlos García Domínguez

BIORREFINERÍA HIDROLÍTICA Y TERMOQUÍMICA PARA LA OBTENCIÓN DE PRODUCTOS DE VALOR AÑADIDO Y ENERGÍA A PARTIR DE CULTIVOS DE ALTA PRODUCTIVIDAD.

Memoria presentada por la ingeniera Dña. Susana Lozano Calvo
para optar al Grado de Doctora por la Universidad de Huelva.

Susana Lozano Calvo
Huelva (España), 2025

D. Francisco López Baldovín, Catedrático de Ingeniería Química y D. Juan Carlos García Domínnguez, Catedrático de Ingeniería Química, adscritos al área de Ingeniería Química del Departamento de Ingeniería Química, Química Física y Ciencia de los Materiales de la Escuela Técnica Superior de Ingeniería de la Universidad de Huelva.

CERTIFICAN:

Que la presente memoria titulada **"Biorrefinería hidrolítica y termoquímica para la obtención de productos de valor añadido y energía a partir de cultivos de alta productividad"** presentada por Susana Lozano Calvo para optar al Grado de Doctor por la Universidad de Huelva, ha sido realizada en el Departamento de Ingeniería Química, Química Física y Ciencia de los Materiales bajo nuestra dirección y reúne todos los requisitos exigidos para su defensa como Tesis Doctoral.

V^0 B^0 directores de la Tesis

Dr. Francisco López Baldovín. **Dr. Juan Carlos García Domínguez.**

A mi familia, por todo el amor
incondicional y el apoyo incansable.

A mi pareja, por caminar a mi lado.

Y a quien partió demasiado pronto,
pero sigue iluminando cada sueño.

Este logro también es vuestro ♡

"La naturaleza es el ingeniero más brillante de todos los tiempos"

Frances Arnold

Agradecimientos.

Al mirar hacia atrás en esta etapa tan especial, colmada de horas de investigación, estudio, redacción de publicaciones y, finalmente, la elaboración de esta tesis doctoral, no puedo dejar de recordar los muchos momentos vividos en el laboratorio y en la Universidad de Huelva, donde no solo he crecido como investigadora, sino también como persona (y, por qué no decirlo, también en edad). Sobre todo, he tenido la fortuna de conocer y compartir el camino con personas que han dejado una huella imborrable en este proceso. A ellas, y a mi familia, que ha sido un apoyo constante e incondicional a lo largo de todo este recorrido, quiero dedicarles estas líneas de profundo agradecimiento por toda la ayuda que me han brindado.

En primer lugar, quiero expresar mi agradecimiento a mis directores de tesis, los catedráticos **Francisco López Baldovín** y **Juan Carlos García Domínguez**, por brindarme la oportunidad de trabajar junto a ellos y por su supervisión y orientación a lo largo de este recorrido académico. Agradezco también la libertad que me han brindado para tomar mis propias decisiones, lo que me ha permitido desarrollarme de forma autónoma y adquirir valiosas habilidades en la gestión de la investigación. Esta independencia ha sido, sin duda, clave en mi crecimiento como investigadora.

Quiero dedicar una mención especial al catedrático **Manuel Jesús Díaz Blanco**, por la confianza depositada en mí desde el primer momento, por su cercanía y por haberme ofrecido las herramientas necesarias para crecer con autonomía. Su visión de la investigación, basada en el compromiso, el rigor y la honestidad, ha sido una fuente constante de inspiración. Haber trabajado codo a codo con él durante estos años ha sido, sin duda, una de las experiencias más enriquecedoras de esta etapa. Le agradezco profundamente no solo su guía académica, sino también su calidad humana. Gracias, Jesús, por estar siempre dispuesto a escuchar, por priorizar mi desarrollo personal y profesional, y por ser, más que un superior, un verdadero amigo.

Quisiera expresar también mi agradecimiento a los profesores del Departamento de Ingeniería Química, Química Física y Ciencia de los Materiales, y muy especialmente a los integrantes del grupo de investigación "**Pro^{2}tecs**", por haberme hecho sentir parte de una familia desde el primer día. Agradezco sinceramente a **Mercedes Ruiz Montoya**, **Inmaculada Giráldez Díaz**, **Francisco Javier Navarro Domínguez** y a tantos otros por su cercanía, por su interés constante en el desarrollo de mi tesis y por estar siempre pendientes de mi evolución como investigadora. En particular, quiero reconocer a **Pedro Partal**, quien fue el investigador principal en mi primer contrato dentro del grupo, por darme la primera oportunidad profesional en este entorno académico que ha sido tan importante en mi trayectoria.

No quiero dejar de agradecer a mis compañeros de laboratorio, con quienes he compartido tanto dentro como fuera del ámbito académico. Al **Dr. Javier Mauricio Loaiza Rodríguez**, por todos los aprendizajes que me brindó en los inicios de esta trayectoria, y por las incontables horas de conversación sobre investigación, ambiciones y sobre la vida misma. A la **Dra. María Trinidad García Domínguez**, por ser mi primera tutora cuando comencé a dar mis primeros pasos en el laboratorio durante el trabajo fin de grado, por tu luz, tu apoyo constante y esas sonrisas que siempre consiguen animar el día. Al **Dr. Alberto Palma López**, por tus enseñanzas, tus sabios consejos, y por ser un ejemplo inspirador de que, con esfuerzo y dedicación, es posible abrirse camino en el mundo universitario. Mi más sincera enhorabuena también por tus logros.

Tampoco puedo dejar de mencionar al Dr. Sergio Clemente, por haber compartido conmigo parte de esta intensa y, a veces, impredecible aventura que supone una tesis doctoral. Agradezco también profundamente a **Natalia Almagro** y **Rocío Rengel**, por ser mucho más que compañeras: por su amistad, por el apoyo constante que me han dado, y continúan dando, a lo largo de este camino, y por permitirme formar parte de sus vidas. Su presencia ha sido esencial para mantener el equilibrio entre el trabajo y lo personal en esta etapa.

A lo largo de esta etapa, también he tenido la suerte y oportunidad de colaborar con investigadores de otras instituciones, experiencias que me han aportado un valioso aprendizaje adicional. En este sentido, deseo agradecer especialmente a la **Dra. María Eugenia Eugenio**, del centro ICIFOR (Madrid), y a todo su equipo, por el tiempo compartido, por el ambiente tan enriquecedor que encontré durante mi estancia y por la cercanía y profesionalidad con la que me acogieron. Asimismo, quiero expresar mi agradecimiento al **Dr. Duarte Neiva** y a su equipo de ForTec (Lisboa), por facilitarme enormemente mi estancia internacional, por acercarme con calidez a la cultura y al idioma portugués, y por compartir sus conocimientos con tanta generosidad. Gracias a ellos, me sentí como en casa, incluso estando lejos.

Llegado a este punto, tras haber recorrido las personas que han formado parte de mi trayectoria académica, no puedo olvidar a dos grandes amigos que me llevo de estos años: **Rodri** y **Manolo**, compañeros de Green Asphalt. Gracias por vuestra amistad sincera, por las innumerables risas compartidas (también alguna que otra lágrima), por el apoyo constante, y por aparecer y permanecer en mi vida. Aprecio profundamente la calidad humana que tenéis, las conversaciones profundas que hemos tenido y, sobre todo, que me hayáis permitido ser siempre quien realmente soy. Gracias de todo corazón, gracias, amigos.

También quiero dedicar unas palabras a esa familia que se elige: los amigos. Gracias a quienes, con su compañía y cariño, han sido refugio en los días difíciles y celebración en los momentos felices.

En especial, a ti, **Paco**, mi gran amigo y compañero de vida. Gracias por estar siempre ahí, por tu apoyo constante sin pedir nada a cambio, por compartir mis inquietudes y mis logros. Tu lealtad y tu manera de cuidarme son esenciales. Gracias, de corazón.

El cierre de estos agradecimientos, como no podría ser de otra manera, está reservado para mi familia, el pilar fundamental de mi desarrollo personal y crecimiento profesional. Sin su apoyo incondicional, nada de esto habría sido posible.

A mis padres, **Balbino** y **Ángeles**, por ser la base sólida sobre la que se ha construido toda mi formación académica y personal, y por ser fuentes constantes de inspiración, consuelo e impulso en todo momento. A mi madre, por ser mi más mejor amiga y por escucharme siempre con paciencia y cariño. A mi padre, por ser mi mayor ejemplo de constancia, esfuerzo y fortaleza, un pilar que nunca se tambalea. Gracias por darme todo vuestro amor, no pude tener más suerte que la de nacer de vosotros.

A mi hermana **Mónica**, por ser mi defensora incondicional, por estar siempre a mi lado, por ayudarme a seguir adelante y por ser la fuerza y la alegría de papá y mamá. Gracias por tanto, por quererme como lo haces, y por darme el mayor regalo: mi sobrino **Izan**, quien me recuerda cada día la alegría de lo simple. Juntos somos más fuertes que cualquier adversidad.

A mi tío **Silverio**, por ser como un segundo padre, por darme tanto amor y por ser el apoyo incondicional de mi padre. Gracias, tito, por todo lo que me das.

Gracias a ti, **Balbi**, por seguir siendo luz en cada uno de mis sueños y por cuidarnos desde ahí arriba. Algún día nos volveremos a ver. Te quiero.

Y no por ser el último es menos importante: quiero expresar mi más profundo agradecimiento a mi pareja, **Jorge**, por acompañarme en este camino, por animarme a seguir en todo momento, por aparecer en mi vida justo cuando más necesitaba luz, por hacerme soñar despierta y por enseñarme lo que significa un amor de verdad. Gracias por caminar a mi lado con paciencia, por entender mis silencios y celebrar mis logros como si fueran tuyos. Siempre 19.

Finalmente, deseo expresar mi agradecimiento al Ministerio de Ciencia e Innovación por la financiación recibida a través de la ayuda para contratos predoctorales para la formación de doctores (PRE2021-097925), que hizo posible la realización de esta tesis.

Al concluir esta etapa tan significativa de mi vida, soy consciente de que todo final implica también un nuevo comienzo. Los caminos que se separan de algunas personas, las experiencias vividas y los aprendizajes obtenidos, conforman la esencia de nuestro crecimiento personal y profesional. Esta tesis no solo representa un logro académico, sino también un viaje de transformación, en el que he

descubierto fortalezas, enfrentado desafíos y construido mi propio camino. Aunque algunas rutas se bifurquen, el legado de quienes me han acompañado permanece intacto y guía cada paso que doy hacia el futuro. Con gratitud y esperanza, abrazo esta nueva etapa con la convicción de seguir creciendo y aprendiendo.

Índice.

Resumen. 1

Abstract. 5

Capítulo 1: Introducción.

1.1. Contextualizando los procesos de Biorrefinería. La transición Energética: de fósiles a renovables. 11

1.2. El futuro de las refinerías convencionales ante la transición energética. 13

1.3. El papel de la biomasa como fuente de energía renovable. 13

1.4. Las biorrefinerías como evolución del uso de la biomasa: tipología y panorama actual. 15

1.5. Biomasa lignocelulósica: características, clasificación y relevancia en las biorrefinerías. 17

1.6. El clon AF2 de *Populus x euramericana*: características, cultivo y relevancia en las Biorrefinerías. 23

1.7. Pretratamientos de la biomasa lignocelulósica en Biorrefinería. 27

1.8. Procesos termoquímicos de conversión de biomasa. 32

1.9. Extracción alcalina en frío como pretratamiento de la biomasa lignocelulósica. 35

Bibliografía. 38

Capítulo 2: Objetivos y Plan de trabajo.

2. Objetivos. 53

2.1. Objetivo General. 53

2.2. Objetivos Específicos. 54

2.3. Plan de trabajo. 55

Capítulo 3: Resultados y Discusión.

3.1. Extracción Alcalina en frío. 59

3.1.1. Extracción Alcalina en Frío de Hierba Elefante. 60

PUBLICACIÓN 1.

3.1.2. Extracción Alcalina en Frío del Clon AF2 de *Populus x euramericana*. 91

PUBLICACIÓN 2.

3.1.3. Extracción Alcalina en Frío de la *Robinia Pseudoacacia*. 119

3.2. Análisis Cinético y Producción de Hidrógeno en la Valorización Secuencial del Clon AF2 de *Populus* mediante Extracción Alcalina en Frío y Pirólisis. 129

PUBLICACIÓN 3.

3.3. Valorización Secuencial del Clon AF2 de *Populus* mediante Extracción Alcalina en Frío y Deslignificación Organosolv. 157

3.4. Valorización del Clon AF2 de *Populus* mediante Explosión de vapor, extracción de compuestos bioactivos con disolventes verdes e hidrólisis enzimática..... 187

3.5. Análisis de la influencia del origen de la biomasa y los métodos de fraccionamiento en la pirólisis de las principales fracciones lignocelulósicas. 205

PUBLICACIÓN 4.

Capítulo 4: Conclusiones.

4.1. Conclusiones..... 243

4.2. Conclusions. 245

Anexos.

1. Publicaciones. 249

2. Comunicaciones en congresos. 311

Resumen.

La transición energética y el desarrollo de productos químicos sostenibles son ejes fundamentales en la actual estrategia para reducir la dependencia de los recursos fósiles. En este contexto, la valorización de biomasa lignocelulósica a través del concepto de biorrefinería representa un enfoque sostenible, ambiental y energético para la obtención de productos de valor añadido, como combustibles, energía y compuestos químicos. Sin embargo, aún persisten desafíos que dificultan la implementación a gran escala de estas biorrefinerías, es por ello por lo que es necesaria la continua investigación técnica y económica especialmente en las fases de pretratamiento, procesamiento y gestión de materias primas y productos intermedios.

Actualmente, existe una amplia variedad de métodos de fraccionamiento y conversión destinados a optimizar la valorización de la biomasa. El objetivo final es establecer biorrefinerías compuestas por etapas integradas y optimizadas. En este marco, la extracción alcalina en frío (EAF) ha surgido como una tecnología de pretratamiento prometedora por su capacidad para fraccionar selectivamente sin necesidad de altas temperaturas ni elevado consumo energético. Asimismo, las tecnologías termoquímicas, como la pirolisis y la gasificación, se perfilan como herramientas clave, ya sea aplicadas directamente sobre la biomasa o en combinación con pretratamientos previos, permitiendo obtener fracciones sólidas, líquidas y gaseosas con alto valor.

Otro reto fundamental para el desarrollo de biorrefinerías es garantizar un suministro estable y continuo de biomasa lignocelulósica. En este sentido, los cultivos energéticos de alta productividad y rotación corta representan una alternativa estratégica. Entre ellos, el género *Populus* destaca por su rápido crecimiento, adaptabilidad y diversidad de híbridos y clones. En la presente Tesis Doctoral se seleccionó el clon AF2 de *Populus x euramericana,* debido a su elevada producción de biomasa, alta tolerancia a condiciones hídricas variables y capacidad de acumulación de carbono.

El objetivo de esta Tesis Doctoral fue evaluar el potencial del clon AF2 de *Populus x euramericana* en el marco de una biorrefinería lignocelulósica, mediante la integración de etapas suaves e intensivas orientadas a optimizar el proceso global en términos de rendimiento y eficiencia energética.

Para alcanzar este objetivo, se modelizaron y optimizaron los distintos tratamientos y etapas mediante la aplicación de diseños experimentales de composición central, considerando variables independientes como la temperatura, el tiempo y la concentración de reactivos. Las respuestas analizadas incluyeron propiedades de las fases sólidas y líquidas obtenidas, características de las pastas celulósicas, propiedades de las hojas de papel y parámetros de la lignina recuperada.

La presente Tesis Doctoral se estructuró en cinco bloques principales de trabajo, que se resumen a continuación:

1. Extracción alcalina en frío (EAF).

Se aplicó este pretratamiento a tres biomasas: hierba elefante (*Pennisetum Purpureum Schum*), el clon AF2 de *Populus x euroamericana* y *Robinia pseudoacacia*, con el objetivo de optimizar las condiciones de operación para maximizar la extracción selectiva de hemicelulosas, preservando la celulosa y la lignina. Los mejores resultados se obtuvieron en el clon AF2, donde el uso simultáneo de ultrasonidos mejoró significativamente la solubilización de hemicelulosas (hasta un 42,3% del contenido inicial presente en la biomasa). La eficiencia fue menor en la *Robinia pseudoacacia*, incluso con la asistencia de ultrasonidos. En general, la EAF demostró ser eficaz para solubilizar selectivamente hemicelulosas y preservar las otras fracciones lignocelulósicas, especialmente la de celulosa.

2. Análisis cinético y producción de hidrógeno en la valorización secuencial del clon AF2 de *Populus* mediante extracción alcalina en frío y pirólisis.

Se evaluó la fracción sólida obtenida tras el pretratamiento de EAF con ultrasonidos aplicado al clon AF2 en un proceso termoquímico de pirólisis. Se analizó el modelo cinético en términos de energía de activación y producción de hidrógeno, demostrando que dicho pretratamiento redujo la energía requerida e incrementó la generación de hidrógeno. Entre las variables de operación, la concentración de álcali en la etapa de EAF resultó ser la más influyente sobre la energía de activación del proceso.

3. Valorización secuencial del clon AF2 de *Populus* mediante extracción alcalina en frío y deslignificación organosolv.

En este bloque de trabajo se propuso un enfoque de biorrefinería en cascada, basado en una estrategia de doble etapa para el fraccionamiento del clon AF2, combinando la EAF con ultrasonidos y un posterior tratamiento organosolv. La etapa alcalina previa permitió suavizar las condiciones del proceso organosolv, reduciendo tanto la temperatura como la proporción de etanol necesarias sin comprometer la calidad de la pasta celulósica ni la recuperación de lignina.

Como resultado de esta integración, se obtuvo una pasta con mayor contenido de glucano (62,5%) y menor contenido de lignina (20,5%) al operar a 150 ºC durante 90 minutos y con un 65% de etanol. En comparación, el proceso organosolv convencional (sin etapa alcalina previa) requirió operar a 180 ºC bajo las mismas condiciones de tiempo y etanol, produciendo una pasta con un contenido de glucano del 50,1% y un 32,5% de lignina.

4. Valorización del clon AF2 de *Populus* mediante explosión de vapor, extracción de compuestos bioactivos con disolventes verdes e hidrólisis enzimática.

Este bloque estudió la combinación del pretratamiento de explosión de vapor con la extracción de compuestos bioactivos y la producción de azúcares fermentables a partir del clon AF2. Se observó que la aplicación de una etapa de extracción con disolventes verdes (acetato y lactato de etilo) tras la explosión de vapor mejoró significativamente la eficiencia de la hidrólisis enzimática.

Como resultado, se obtuvieron concentraciones cercanas a 36 g L^{-1} de azúcares fermentables, así como la recuperación de compuesto fenólicos con alta capacidad antioxidante, alcanzando valores de hasta 62,58 mg GAE/g biomasa seca.

5. Análisis de la influencia del origen de la biomasa y los métodos de fraccionamiento en la pirólisis de las principales fracciones lignocelulósicas.

Se evaluó el comportamiento cinético de las fracciones de celulosa, hemicelulosa y lignina durante el proceso termoquímico de pirólisis, considerando tres tipos de biomasa: paja de trigo (herbácea), tagasaste (arbustiva) y el clon AF2 de *Populus x euramericana (arbórea)*. Asimismo, se analizaron distintos métodos de fraccionamiento, incluyendo EAF, proceso Kraft y sosa-antraquinona.

Los resultados mostraron que la energía de activación está influenciada por múltiples factores, entre ellos el tipo de fracción lignocelulósica, el origen de la biomasa y el método de fraccionamiento empleado. La lignina fue la fracción que presentó la mayor variabilidad cinética y se mostró especialmente sensible a la técnica de fraccionamiento.

Los resultados obtenidos en esta Tesis Doctoral demuestran el potencial del clon AF2 de *Populus x euramericana* como materia prima para biorrefinerías sostenibles. La integración de pretratamientos suaves, procesos en cascada y conversión termoquímica permiten avanzar hacia esquemas eficientes para la valorización integral de la biomasa lignocelulósica, contribuyendo al desarrollo de modelos alternativos basados en recursos renovables y procesos ambientalmente responsables.

Abstract.

The energy transition and the development of sustainable chemicals are central to current strategies aimed at reducing dependence on fossil resources. In this context, the valorisation of lignocellulosic biomass through the biorefinery concept represents a sustainable, environmentally friendly, and energy-efficient approach for the production of value-added products such as fuels, energy and chemical compounds. Nevertheless, significant challenges remain that hinder the large-scale implementation of these biorefineries. Therefore, continued technical and economic research is essential, particularly in the areas of pretreatment, processing and the management of feedstock and intermediate products.

A wide range of fractionation and conversion methods is currently available to optimise biomass valorisation. The ultimate aim is to establish biorefineries composed of integrated and highly optimised stages. Within this framework, cold alkaline extraction (CAE) has emerged as a promising pretreatment technology, owing to its ability to selectively fractionate biomass without the need for high temperatures or high energy input. In parallel, thermochemical technologies, such as pyrolysis and gasification, are gaining attention key approaches. These methods can be applied directly to raw biomass or used in combination with pretreatment, enabling the production of high-value solid, liquid and gaseous fractions.

Another key challenge for the development of biorefineries is ensuring a stable and continuous supply of lignocellulosic biomass. In this regard, highly productive, short-rotation energy crops represents a strategic alternative. Among these, the *Populus* genus is particularly notable for its fast growth, broad adaptability, and wide diversity of hybrids and clones. In this Doctoral Thesis, the clone AF2 of *Populus x euramericana* was selected due its high biomass yield, strong tolerance to variable water conditions, and significant carbon sequestration capacity.

The objective of this Doctoral Thesis was to evaluate the potential of the clone AF2 of *Populus x euramericana* within the framework of a lignocellulosic biorefinery, by integrating both mild and intensive processing stages aimed at optimising overall process perfomance in terms of product yields and energy efficiency.

To achieve this objective, the different treatments and processing stages were modeled and optimised using central composition experimental designs. The independent variables included temperature, reaction time, and reagent concentration. The responses analysed encompassed the properties of both the solid and liquid fractions obtained, the characteristics of the resulting cellulosic pulps, the properties of produced paper sheets, and specific parameters related to the recovered lignin.

This Doctoral Thesis was structured into five main research blocks, which are summarised below:

1. **Cold alkaline extraction (CAE).**

This pretreatment was applied to three type of biomass: elephant grass (*Pennisetum Purpureum Schum*), clone AF2 of *Populus x euramericana* and *Robinia pseudoacacia*, with the aim of optimising the selective extraction of hemicelluloses while preserving cellulose and lignin. The best results were obtained with clone AF2, where the simultaneous use of ultrasound significantly enhanced the solubilisation of hemicelluloses (reaching up to 42.3% of the initial content present in the biomass). In contrast, *Robinia pseudoacacia* showed lower efficiency, even with ultrasound assistance. Overall, CAE proved effective in selectively solubilising hemicelluloses while preserving the other lignocellulosic fractions, particularly celllulose.

2. **Kinetic and hydrogen production anlaysis in the sequential valorisation of *Populus* clone AF2 via cold alkaline extraction and pyrolysis.**

The solid fraction obtained after CAE pretreatment assisted by ultrasound was evaluated though a thermochemical process of pyrolysis. The kinetic model was analysed in terms of activation energy and hydrogen production, revealing that the pretreatment reduced the energy requirement and increased hydrogen generation. Among the operating variables, the alklali concentration during the CAE stage was identified as the most influential factor affecting the activation energy of the process.

3. **Sequential valorisation of *Populus* clone AF2 via cold alkaline extraction and organosolv delignification.**

In this section of the study, a cascade biorefinery approach was proposed, based on a dual-stage fractionation strategy for the AF2 clone, combining CAE with ultrasound with a subsequent organosolv treatment. The alklaline pretreatment allowed to milder organosolv processing conditions, enabling reductions in both temperature and etanol concentration without compromising the quality of the cellulosic pulp or the recovery of lignin.

As a result of this integrated process, a pulp with a higher glucan content (62.5%) and lower lignin content (20.5%) was obtained under conditions of 150 ºC, 90 minutes, and 65% etanol. In contrast, the conventional organosolv process (without the prior alkaline step) required a higher temperature of 180 ºC under the same time and ethanol concentration, producing a pulp with 50.1% glucan and 32.5% lignin.

4. **Valorisation of *Populus* clone AF2 via steam explosion, green solvent extraction of bioactive compounds, and enzymatic hydrolysis.**

This section studied the combination of steam explosion pretreatment with the extraction of bioactive compounds and the production of fermentable sugars from clone AF2. The application of green solvent extraction step (using ethyl acetate and ethyl lactate) after steam explosion significantly enhanced the efficiency of enzymatic hydrolysis.

As a result, fermentable sugar concentrations close to 36 g L^{-1} were achieved, along with recovery of phenolic compounds exhibiting high antioxidant capacity, reaching values of up to 62.58 mg GAE/g dry biomass.

5. **Analysis of the influence of biomass origin and fractionation methods on the pyrolysis of the main lignocellulosic fractions.**

The kinetic behaviour of cellulose, hemicellulose, and lignin fractions during pyrolysis was evaluated using three type of biomass: wheat straw (herbaceous), tagasaste (bushy) and clone AF2 of *Populus x euramericana* (arboreal). Different fractionation methods were also analysed, including CAE, Kraft process and soda-antraquinone.

The results showed that the activation energy is influenced by multiple factors, including the type of lignocellulosic fraction, the biomass origin, and the fractionation method used. Among the three fractions, lignin exhibited the highest kinetic variability and was particularly sensitive to the chosen fractionation technique.

The results obtained in this Doctoral Thesis demonstrates the potential of clone AF2 of *Populus x euramericana* as a feedstock for sustainable biorefineries. The integration of mind pretreatments, cascade processing, and thermochemical conversion contributes to the development of efficient strategies for the integral valorisation of lignocellulosic biomass. This work supports the advancement of alternative models based on renewable resources and enviromentally friendly processes.

CAPÍTULO 1

Introducción



1.1. Contextualizando los procesos de Biorrefinería. La transición Energética: de fósiles a renovables.

El presente trabajo de Tesis Doctoral se enmarca en la necesaria evolución industrial hacia procesos más respetuosos con el medio ambiente y en la transición hacia recursos renovables y sostenibles que permitan reducir progresivamente la dependencia actual de los recursos fósiles. Esta transformación industrial abarca dos aspectos fundamentales: la transición energética, centrada en los biocombustibles y las energías renovables, y la transición hacia la producción de nuevos productos químicos sostenibles de toda índole.

Entre estos aspectos, la transición energética ha captado una mayor atención de la ciudadanía, y de la opinión pública, especialmente en lo relacionado con el desarrollo de biocombustibles, la energía eléctrica para la movilidad y los biocombustibles sólidos destinados a la generación de electricidad. Por este motivo, este apartado introductorio de la Tesis Doctoral comienza revisando estos temas, para contextualizar los avances recientes y su relevancia en el marco de las biorrefinerías.

Actualmente, los avances en la lucha contra el cambio climático presentan un panorama preocupante, como lo reflejan los datos del Emissions Gap Report 2023 del programa de las Naciones Unidas para el Medio Ambiente (UNEP). Según este informe [1]:

1. En septiembre de 2023, la temperatura media mundial se situó 1,8 °C por encima de los niveles preindustriales. Las proyecciones convierten a 2023 como el año más cálido registrado hasta ahora.
2. Las emisiones globales de gases de efecto invernadero alcanzaron un récord de 57,4 gigatoneladas de dióxido de carbono (CO_2) equivalentes en 2022, un aumento del 1,2% respecto a 2021.
3. Las concentraciones atmosféricas de CO_2 aumentaron hasta 417,9 ± 0,2 partes por millón en 2022.
4. El sector energético fue el que generó mayores emisiones, representando un 36% del total; seguido por la industria (25% del total), agricultura (18% del total), transporte (14% del total) y edificios (6,7% del total).

A pesar de algunos avances desde la firma del Acuerdo de París en 2015, las políticas actuales no son suficientes para evitar que el calentamiento global supere los 2 °C. Inicialmente, se proyectaba un aumento del 16% en las emisiones de gases de efecto invernadero para 2030, pero gracias a las medidas implementadas, el incremento previsto ha bajado al 3%. Sin embargo, se necesitan reducciones del 28% para limitar el calentamiento a 2 °C y del 42% para lograr la meta más ambiciosa

de 1,5 °C. Ningún país del G20 está reduciendo sus emisiones al ritmo necesario para cumplir con las metas de emisiones netas cero [1].

En el caso de la Unión Europea (UE) se han implementado medidas significativas contra el cambio climático, logrando reducir sus emisiones en más del 31% en 2022 respecto a los niveles de 1990 [2]. A pesar de este avance, la UE sigue siendo el cuarto mayor emisor a nivel global, contribuyendo con un 6% de las emisiones mundiales [3].

Esta reducción en las emisiones de gases de efecto invernadero por parte de la UE fue especialmente promovida por la mejora de la eficiencia energética. Entre 2005 y 2022, las emisiones por unidad de energía utilizada disminuyeron un 10%, debido al cambio hacia combustibles fósiles que emiten menos CO_2 y el aumento del empleo de las energías renovables [2]. La cuota total de energías renovables en el consumo final bruto de energía pasó del 10,3% en 2005 al 21,8% en 2021 [2].

A pesar de estos logros, según el informe publicado por la Agencia Europea Medioambiental en julio de 2023 [2], las proyecciones de la UE aún no son suficientes para lograr el "objetivo 55", que persigue disminuir las emisiones en al menos un 55% para 2030 y alcanzar la neutralidad climática en 2050. Es necesario acelerar los esfuerzos tanto a nivel europeo como global para evitar los impactos más severos del cambio climático.

Hoy en día, el cambio climático, impulsado en gran medida por las emisiones de gases de efecto invernadero, sigue siendo un desafío crítico. En este contexto, aumentar el uso de las energías renovables se presenta como una pieza clave en la transición hacia una economía más limpia y sostenible. Esto se refleja en las medidas adoptadas por el Parlamento Europeo dentro del marco del "objetivo 55", que establece alcanzar una cuota de 42,5% de energías renovables en el consumo final de energía de la UE para 2030.

A esto se suma la incertidumbre respecto al agotamiento de los combustibles fósiles, cuya demanda sigue creciendo a un ritmo alarmante debido al desarrollo industrial y el crecimiento poblacional [4]. En este escenario de creciente dependencia de combustibles no renovables y el agravamiento del calentamiento global, la transición hacia fuentes renovables ya no es solo una opción, sino una necesidad urgente para asegurar un futuro energético seguro y sostenible.

En este marco, se hace imprescindible avanzar en la investigación científica y en la aplicabilidad de los procesos de biorrefinería, especialmente aquellos que utilizan biomasa lignocelulósica como materia prima renovable y sostenible.

1.2. El futuro de las refinerías convencionales ante la transición energética.

De acuerdo con lo expresado en el apartado anterior, las políticas climáticas orientadas hacia la neutralidad climática para 2050 repercuten directamente a las refinerías convencionales, ya que se persigue una reducción significativa en la demanda de combustibles fósiles. Como resultado, se plantea a las refinerías tradicionales la obligación de adaptarse para suministrar energías más limpias. En este contexto, surge la necesidad de transformar estas instalaciones para integrarse en un sistema energético descarbonizado.

Según un estudio de la firma consultora Ricardo para Transport & Environment [5], la transformación de las refinerías implica una transición de los combustibles con alto contenido de carbono hacia alternativas de bajo o nulo contenido de carbono, como los biocombustibles, combustibles sintéticos y electrocombustibles derivados del hidrógeno verde. El informe destaca el potencial de las refinerías convencionales para desempeñar un papel crucial en la producción de hidrógeno y e-combustibles, aprovechando su infraestructura y sus conocimientos técnicos, a la vez que se integran nuevas tecnologías para la producción de combustibles más limpios.

Asimismo, el informe prevé que el futuro de las refinerías convencionales se orienta hacia un modelo híbrido, donde los procesos de refinado tradicionales coexistan con tecnologías emergentes para la generación de combustibles bajos en carbono. Aquellas refinerías que loguen adaptarse a estas nuevas exigencias del mercado energético podrán mantener su relevancia y contribuir a la transición energética. Por el contrario, aquellas que no implementen estos cambios corren el riesgo de quedar obsoletas.

El informe subraya que el futuro de las refinerías convencionales depende de su capacidad para adaptarse a la transición hacia la descarbonización, adoptando nuevas tecnologías y ajustándose a la evolución de los marcos políticos para lograr la neutralidad climática.

1.3. El papel de la biomasa como fuente de energía renovable.

En contraposición a lo anterior, los avances en tecnología, desarrollo e implementación de las energías renovables están en auge y, como resultado, en 2023 estas energías más limpias representaron el 23% del consumo energético de la Unión Europea. Existe una gran multitud de fuentes renovables, entre las que destacan la solar, la eólica, la geotérmica y la hidroeléctrica. Sin embargo, estas fuentes se enfrentan a retos como la intermitencia debido a variaciones estacionales o medioambientales, así como la incapacidad de producir combustibles sintéticos. En este contexto, la biomasa lignocelulósica destaca como una alternativa decisiva por su disponibilidad, renovabilidad

y capacidad para generar biocombustibles, productos químicos y materiales respetuosos con el medioambiente, sin la intermitencia indicada, lo que la convierte en un recurso valioso para la transición energética [6].

La biomasa lignocelulósica, una fuente de energía renovable y neutra en emisiones de CO_2, está ampliamente disponible en todo el mundo y actualmente es la cuarta fuente de energía más importante del mundo, después del petróleo, el gas natural y el carbón [7]. Además, la biomasa lignocelulósica es el único recurso natural y renovable de carbono con una abundante disponibilidad, lo que la convierte en un sustituto adecuado de los combustibles fósiles. Entendemos más apropiada la utilización de la "biomasa lignocelulósica", frente a la biomasa en general, que abarca una gran variedad de organismos acuáticos y terrestres, vegetación, árboles, biomasa virgen y biomasa residual, como los residuos sólidos urbanos (RSU), biosólidos de aguas residuales, estiércol de desechos animales, residuos forestales, agrícolas y algunos residuos industriales. A diferencia de los combustibles fósiles, que tardan millones de años en formarse, la biomasa en general y la lignocelulósica en particular, se considera renovable, ya que puede reemplazarse o sustituirse en un plazo relativamente corto [8].

La contribución clave de la biomasa lignocelulósica a la transición energética es su uso directo para la generación de electricidad y calor, la generación de biocombustibles a través de procesos de fermentación y conversión química, su ciclo cerrado de carbono, ya que el CO_2 liberado durante la combustión es reabsorbido por las plantas durante su crecimiento, y adicionalmente, la utilización de la biomasa procedente de residuos agrícolas, forestales y municipales, que incorpora el concepto de gestión eficiente y sostenible de los residuos.

Es importante señalar que el uso de la biomasa como fuente de energía renovable también enfrenta ciertos desafíos actualmente, que requieren continuos esfuerzos de investigación y desarrollo para su optimización. Quizá muchos de ellos son falsas polémicas generadas en lo relacionado con la industria energética tradicional y que al menos son muy discutibles. Entre estos retos figuran la competencia con la producción de alimentos, los posibles efectos negativos sobre los ecosistemas acuáticos y la salud de los suelos, la incertidumbre del suministro, la falta de conocimiento profundo sobre la variabilidad y composición de esta materia prima y análisis del ciclo de vida más completos que determinen la eficiencia en la producción de biocombustibles [9]. En general, para hacer frente a estos retos se necesita más investigación técnica y económica que abarque las fases de pretratamiento, procesamiento y gestión de productos y materias primas.

1.4. Las biorrefinerías como evolución del uso de la biomasa: tipología y panorama actual.

Una biorrefinería es una instalación industrial integrada, inspirada en el modelo de una refinería de petróleo convencional, diseñada para transformar materia prima de origen biológico en una amplia gama de productos de valor añadido y bioenergía. Estos productos incluyen biocombustibles, electricidad, calor y una diversidad de bioproductos, como materiales, productos químicos, alimentos y piensos [10-13]. Para alcanzar esta variedad de productos, es esencial la integración de múltiples procesos y tecnologías de conversión dentro de una misma planta [13].

El funcionamiento de una biorrefinería se basa en la valorización de biomasa a través de diversas tecnologías, cuya selección depende del tipo de biomasa empleada y de los productos finales deseados. Esta flexibilidad permite a las biorrefinerías adaptarse a diferentes fuentes de biomasa y responder a demandas específicas del mercado [13]. Por ello, representan un pilar clave en la transición hacia una economía más sostenible, basada en recursos renovables.

La gran diversidad de materias primas de origen biológico disponibles ha dado lugar a la existencia de múltiples tipos de biorrefinerías, clasificadas según criterios como [11,13]:

Materias primas: se refiere a la biomasa inicial empleada en la biorrefinería, que puede variar según el origen y características.

Procesos de conversión: engloba los métodos y tecnologías utilizadas para convertir la biomasa en productos, los cuales se seleccionan en función de las características de la materia prima y de los productos finales deseados.

Plataformas: incluye los productos intermedios generados durante los procesos de conversión, que sirven como base para obtener una amplia gama de productos finales.

Productos: comprende los bioproductos finales generados por la biorrefinería.

Entre las clasificaciones más extendidas destaca la basada en el tipo de materia prima utilizada y el grado de desarrollo tecnológico, dando lugar a las siguientes categorías [14]:

Biorrefinerías de primera generación: utilizan biomasa agrícola y forestal convencional, como cultivos de almidón (maíz, trigo), de azúcar (caña de azúcar, remolacha azucarera) y oleaginosos, para producir principalmente bioetanol y biodiésel. Su principal inconveniente es la competencia entre la materia prima y la demanda de alimentos, además del impacto ambiental en el suelo.

Biorrefinerías de segunda generación: emplean biomasa lignocelulósica (residuos agrícolas, forestales, urbanos y cultivos energéticos e industriales). Estas ofrecen ventajas significativas, como

la abundancia y no competencia con los cultivos alimentarios, además de su capacidad para producir biocombustibles, bioquímicos y biomateriales.

Biorrefinerías de tercera generación: utilizan biomasa acuática, como algas y microalgas, para obtener biocombustibles más limpios (biodiésel y bioetanol), productos de valor añadido (cosméticos, terapéuticos, piensos y alimentos) y soluciones innovadoras para la gestión de residuos. Su principal ventaja es la rápida producción de biomasa en períodos cortos.

Biorrefinerías de cuarta generación: basadas en cultivos o microorganismos modificados genéticamente, estas biorrefinerías están diseñadas para capturar y almacenar carbono, contribuyendo así a alcanzar emisiones negativas de carbono.

El desarrollo conceptual y tecnológico de las biorrefinerías ha permitido su implementación en diversas regiones del mundo, siendo Europa uno de los tres principales líderes en este campo. Según datos de la Comisión Europea, actualmente existen 298 biorrefinerías a escala comercial [15]. De estas, el 75% procesan biomasa agrícola, el 28% biomasa forestal, el 10% de residuos y un 4% de biomasa marina.

La distribución geográfica de estas instalaciones muestra una alta concentración en países como Francia (89), Alemania (59), los Países Bajos (31), Bélgica y Finlandia (21 cada uno). En España se contabilizan 13 biorrefinerías, de las cuales el 85% procesan biomasa agrícola. En las Figuras 1 y 2 se detalla la distribución de las biorrefinerías existentes en la actualidad, según el tipo de materia prima procesada, tanto en Europa como en España.

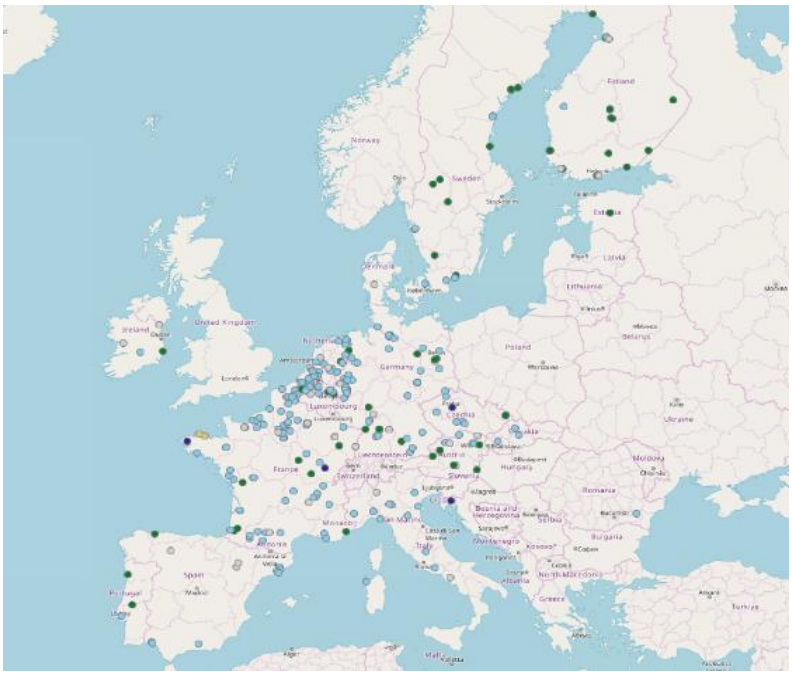


Figura 1. Localización de las biorrefinerías dentro de la Unión Europea según las materias primas (Agrícola en azul, Forestal en verde, Marina en amarillo, Residuos en morado y en gris biorrefinerías con más de una materia prima). Fuente: plataforma Biorrefinerías químicas y de materiales en la UE [15].

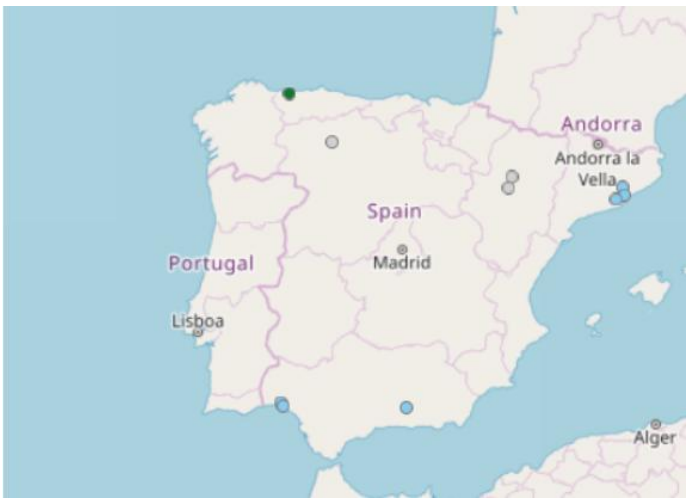


Figura 2. Localización de las biorrefinerías en España en la actualidad según la materia prima empleada (Agrícola en azul, Forestal en verde, y más de una materia prima en gris). Fuente: plataforma Biorrefinerías químicas y de materiales en la UE [15].

1.5. Biomasa lignocelulósica: características, clasificación y relevancia en las biorrefinerías.

A continuación, se resume de manera breve las principales características químicas y morfológicas de la biomasa lignocelulósica, estableciendo las bases para abordar, más adelante, los aspectos específicos de los materiales utilizados en el presente trabajo de Tesis Doctoral.

La biomasa lignocelulósica se ha consolidado como una de las materias primas más prometedoras para el desarrollo de las biorrefinerías de segunda generación. Su abundancia, bajo costo y el hecho de que no compite directamente con los cultivos alimentarios la convierten en una opción sostenible para la producción de bioproductos y biocombustibles.

En términos general, la biomasa lignocelulósica presenta una estructura compleja formada por tres componentes principales: celulosa, hemicelulosa y lignina. Estos polímeros desempeñan un papel estructural esencial en las plantas, proporcionando rigidez y resistencia a las paredes celulares [16]. La proporción de estos componentes varía significativamente en función de diversos factores, como la especie vegetal, las condiciones ambientales y la edad de la planta, lo que a su vez determina las propiedades fisicoquímicas específicas de cada biomasa.

Los componentes de los materiales lignocelulósicos (MLC) se pueden desglosar en dos grandes grupos: **componentes estructurales de la pared celular**, que suponen entre un 80-90% del peso total, y **componentes no estructurales**, grupo más heterogéneo que incluye compuestos secundarios y extractivos.

Componentes estructurales de la pared celular.

El complejo lignocelulósico es una estructura robusta y organizada donde la celulosa, como núcleo principal, mantiene su configuración fibrosa y cristalina. Rodeando a la celulosa, la hemicelulosa se sitúa entre microfibrillas y macrofibrillas, mientras que la lignina forma una matriz que integra ambos componentes. Esta red polimérica está sostenida por cuatro tipos principales de enlaces, garantizando la cohesión tanto dentro de cada componente polimérico (enlaces intrapoliméricos), como entre ellos (enlaces interpoliméricos), definiendo la estabilidad y funcionalidad del complejo. La Tabla 1 detalla los principales enlaces, y la Figura 3 ilustra las interacciones entre celulosa, hemicelulosa y lignina.

Tabla 1. Resumen de enlaces intrapoliméricos y enlaces interpoliméricos.

Tipo de enlace	Enlaces intrapoliméricos	Enlaces interpoliméricos
Enlace éter	Celulosa, hemicelulosa y lignina	Celulosa-Lignina Hemicelulosa-Lignina
Puente de hidrógeno	Celulosa	Celulosa-Hemicelulosa Hemicelulosa-Lignina Celulosa-Lignina
Enlace éster	Hemicelulosa	Hemicelulosa-Lignina
Enlace Carbono-Carbono	Lignina	

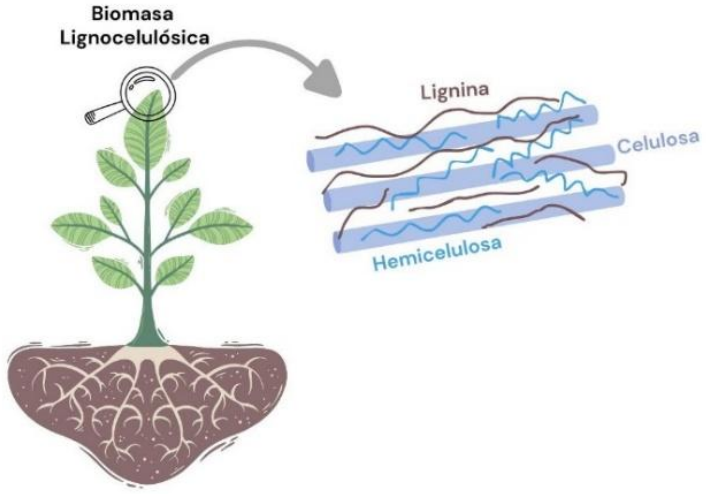


Figura 3. Estructura de los materiales lignocelulósicos (celulosa, hemicelulosa y lignina). Figura adaptada Tomme et al. [17].

Celulosa.

La celulosa es el principal componente estructural de los MLC, representando entre el 25-40% del peso en materiales agrícolas y el 40-50% en maderas. Este polímero lineal de fórmula $(C_6H_{10}O_5)_n$, tiene un grado de polimerización que varía entre 500 y 15000 unidades, dependiendo de su origen.

Este polímero lineal de β-D-glucosa, con enlaces β-(1→4), tiene una estructura cristalina que le confiere una baja solubilidad en agua y una alta resistencia química y enzimática [18]. Las moléculas

de celulosa se organizan en cadenas lineales que, mediante enlaces de hidrógeno, se agrupan en fibrillas elementales compuestas aproximadamente por 36 cadenas individuales. Estas fibrillas forman microfibrillas de estructuras cristalinas, que se ensamblan para constituir fibras de celulosa, las cuales interactúan con la hemicelulosa y la lignina para reforzar la rigidez estructural de las paredes celulares vegetales [19].

Existen varios polimorfos de celulosa cristalina [20], siendo los más relevantes la celulosa I y la celulosa II. La celulosa I, también conocida como celulosa nativa, es como se encuentra naturalmente en las plantas, algas y bacterias. Esta forma es termodinámicamente metaestable y puede transformarse en celulosa II o III [20-22]. La celulosa II se genera a partir de procesos de regeneración o mercerización [20]. La celulosa II es más estable desde un punto de vista termodinámico y posee una estructura monoclínica, se utiliza ampliamente en la producción de celofán y fibras textiles [23].

Dado que el 50% del carbono orgánico de la biosfera se encuentra en forma de celulosa, su conversión en productos químicos y combustibles es de gran relevancia para el desarrollo de una bioeconomía circular [24].

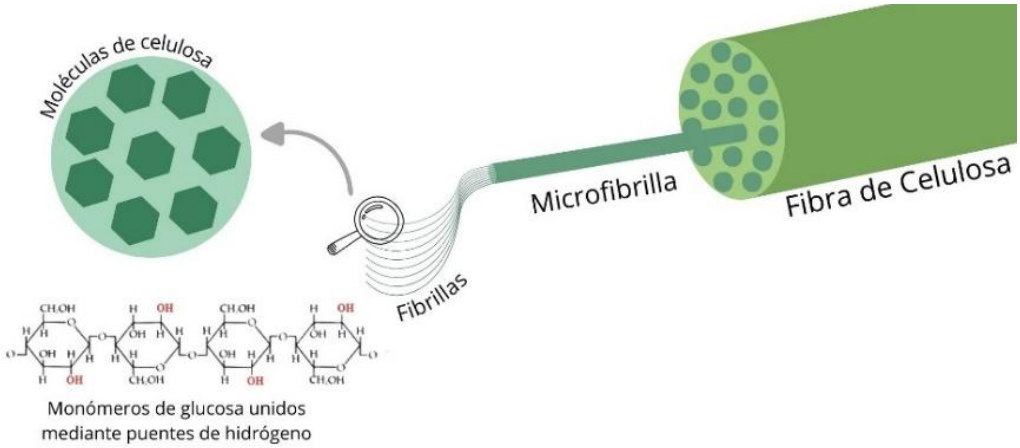


Figura 4. Estructura de la celulosa en la pared celular. Figura adaptada Spanevello et al. [25].

Hemicelulosa.

La hemicelulosa es el segundo biopolímero más abundante en los MLC y destaca por su naturaleza heterogénea. Está compuesta principalmente por mezclas de polisacáridos como pentosas (D-xilosa y L-arabinosa), hexosas (D-glucosa, D-manosa y D-galactosa), ácidos urónicos (ácido glucurónico y galacturónico), y desoxihexosas (ramnosa y fucosa). Dependiendo de la fuente de biomasa, puede representar entre un 10-45% en peso del material, con un grado de polimerización que varía entre 50 y 300 unidades [26]. Su estructura amorfa, altamente ramificada y el menor grado de polimerización facilita su hidrolización en medios ácidos o acuosos calientes [27].

En maderas blandas, representa entre el 18-23% en peso, predominando el xiloglucano, galactoglucomanano y arabinoglucuronoxilano [26,28]. En las maderas duras, su contenido varía entre un 10-15% en peso, estando compuesta principalmente por glucuronoxilano, glucomanano y xiloglucano [26,28]. Por su parte, las plantas herbáceas contienen entre un 20-25%, predominando el xiloglucano y el glucuronoarabinoxilano [29].

Además de ser una interfase estructural entre la celulosa y la lignina, la hemicelulosa regula la expansión celular y puede actuar como almacén de sustancias de reserva. Su relativa facilidad de conversión enzimática y química la convierte en un recurso valioso para aplicaciones industriales.

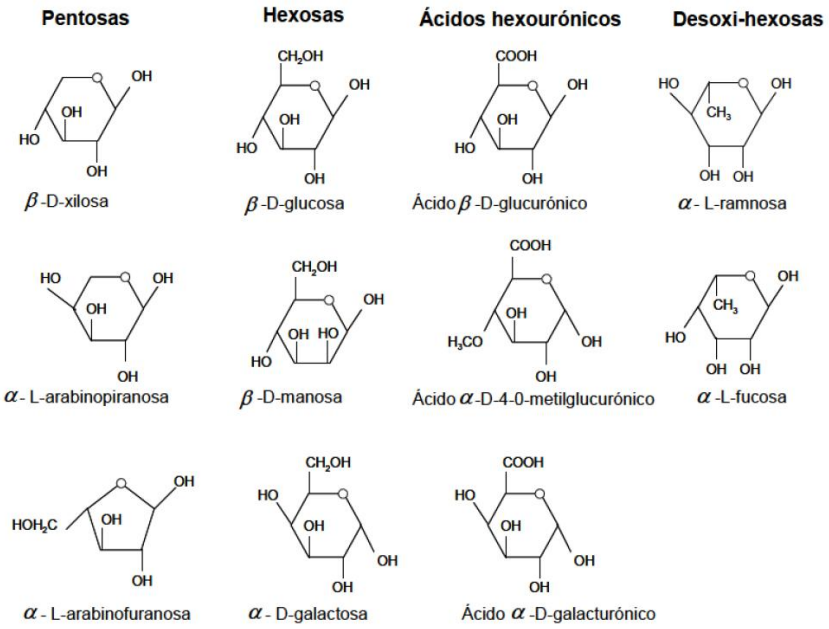


Figura 5. Principales monosacáridos de las hemicelulosas [30].

Lignina.

La lignina es uno de los polímeros orgánicos más complejos y heterogéneo en la naturaleza. Representa típicamente entre el 10-25% del peso seco de la biomasa vegetal, variando según la fuente: es más abundante en maderas (hasta el 34%) y menos prevalente en materiales agrícolas (10-20%) [31,32]. Se trata de un polímero tridimensional amorfo, formado principalmente por unidades monoméricas de fenil-propano [33], desempeña funciones estructurales clave, como proporcionar cohesión celular, resistencia mecánica, elasticidad, y protección contra pérdidas de agua y ataques biológicos [34-36].

Está formada por tres tipos de unidades monoméricas, derivadas de los monolignoles: alcohol p-cumarílico, el alcohol coniferílico y el alcohol sinapílico. Estas unidades se combinan para formar tres tipos de lignina: p-hidroxifenilo (H), guayacilo (G) y siringilo (S) [27,37]. Estos varían según la biomasa, en el caso de las maderas blandas predominan las unidades G, mientras que las maderas

duras poseen una mezcla más equilibrada de unidades S y G. En las gramíneas, como el trigo, predominan las unidades H [38,39].

La lignina ocupa los espacios intercelulares y rodea la matriz de celulosa y hemicelulosa, estabilizando y rigidizando la pared celular mediante entrecruzamientos entre los diferentes polímeros [40,41]. Gracias a su estructura altamente ramificada, reticulada y polimérica, tiene un elevado peso molecular y un poder calorífico de 23,3-25,6 MJ kg^{-1}, superando en aproximadamente un 30% el de la celulosa y la hemicelulosa combinadas. Esto se debe a que la lignina contiene compuestos menos oxidados, lo que le otorga una mayor densidad energética [42,43].

Tradicionalmente utilizada como combustible de bajo valor [44], la lignina es cada vez más valorizada en la bioeconomía circular por su estructura aromática, que la hace adecuada para producir productos químicos, combustibles y materiales avanzados [45,46]. Sin embargo, su separación eficiente de la celulosa y hemicelulosa sigue siendo un desafío, requiriendo métodos robustos pero delicados para preservar la calidad de los componentes extraídos [47].

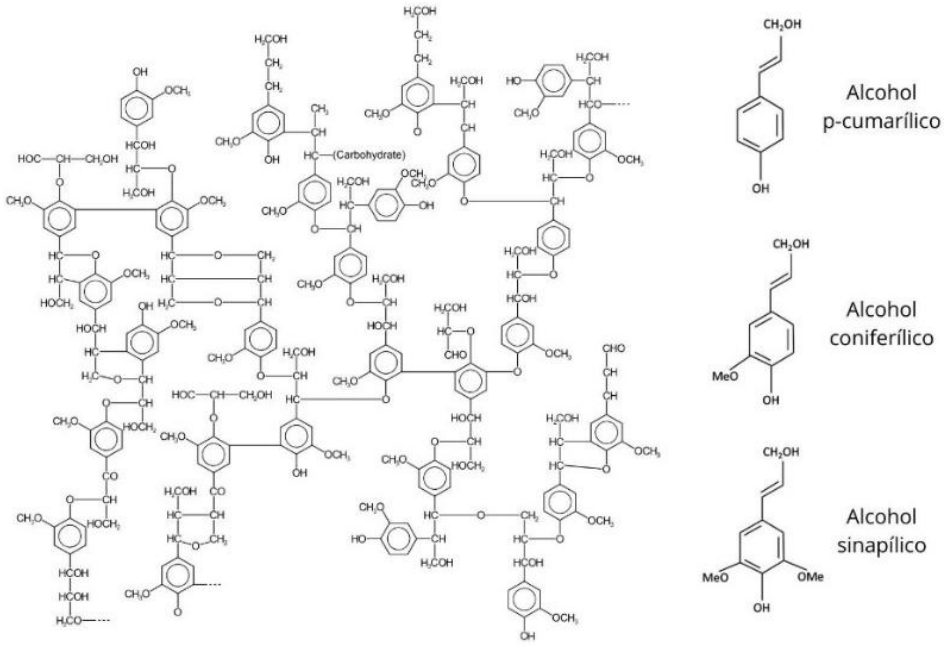


Figura 6. Estructura de la lignina y sus precursores principales (monolignoles) [48].

Componentes no estructurales de la pared celular.

Aunque no forman parte de la estructura primaria de la pared celular, los componentes no estructurales representan una fracción importante de la biomasa, con proporciones que pueden variar entre un 5-10%, y en algunos casos, alcanzar hasta el 40% en peso. Su principal característica es la relativa facilidad con la que pueden ser separados de la materia prima, lo que los hace interesantes desde el punto de vista de su valorización [49]. Entre estos componentes destacan:

Agua: presente en forma de fluidos biológicos y debido al carácter higroscópico de los MLC. Su contenido varía según las condiciones ambientales, oscilando entre el 8-10% en peso respecto al material seco.

Cenizas: residuo inorgánico que queda tras la combustión completa de la biomasa. Están compuestas por una mezcla de elementos y minerales como silicatos, carbonatos, fosfatos, calcio, magnesio, sodio y potasio, entre otros [50]. La proporción de cenizas varía significativamente según la fuente de biomasa: los materiales leñosos, en general, contienen un bajo porcentaje, alrededor del 1%, mientras que los residuos agrícolas y otros materiales herbáceos pueden alcanzar proporciones mucho mayores, de hasta un 14% [27].

Extractos: compuestos solubles en agua o disolventes orgánicos como etanol o hexano, se tratan de diversos biopolímeros como terpenos, terpenoides, esteroides, ceras, grasas, lípidos, proteínas y compuestos fenólicos como lignanos, taninos y estilbenos [51]. Tienen un gran interés comercial gracias a sus propiedades aromáticas, medicinales y antioxidantes.

Proteínas: presentes en pequeñas cantidades, participan en procesos celulares clave como el reconocimiento célula-célula y la reparación tisular, además de integrarse en las estructuras de soporte de la pared celular.

Pectinas: polímeros ricos en ácido D-galacturónico que se localizan entre los microfilamentos de celulosa [27]. Contribuyen a la cohesión de la matriz celular y al mantenimiento estructural.

Clasificación de la biomasa lignocelulósica.

Dada la diversidad composicional y funcional de los MLC, su clasificación puede basarse en diversos criterios [52]. Uno de los más comunes es según su origen, agrupándose en las siguientes categorías:

Origen Forestal. Representan más del 70% del total de los MLC, proviniendo de bosques y cultivando especies leñosas como coníferas (maderas blandas) y frondosas (maderas duras), así como de residuos de actividades forestales como podas o cortezas.

Origen Agrícola. Incluye cultivos y residuos de la producción agrícola, caracterizándose por su abundancia, bajo coste y ciclos de crecimientos cortos. Se subdivide en tres grupos: cultivos destinados a la industria textil y papelera (lino, cáñamo), cultivos alimentarios (cereales que generan residuos como la paja), y, por último, el tercer grupo que engloba hierbas silvestres (bambú, hierba elefante), cultivos energéticos especializados (alfalfa, pasto varilla), y cultivos de rápido crecimiento (tagasaste, leucaena).

Origen Urbano. Incluye residuos sólidos urbanos, compuestos por MLC como papel, cartón, desechos de comidas, además de restos de poda y acondicionamiento urbano. Este flujo de residuos está aumentando anualmente entre un 2-6%, lo que resalta la necesidad de soluciones sostenibles para su valorización.

Origen Industrial. Incluye subproductos y residuos de procesos industriales, como el bagazo de caña de azúcar, cáscaras de arroz, orujo de aceituna, aguas residuales de industrias alimentarias y desechos de la transformación de madera.

1.6. El clon AF2 de *Populus x euramericana*: características, cultivo y relevancia en las Biorrefinerías.

En las últimas décadas, los cultivos energéticos han adquirido un interés creciente como una solución estratégica para diversificar las fuentes de energía renovable, posicionándose como una pieza clave en las políticas energéticas. La Unión Europea y sus estados miembros los han identificado como un elemento fundamental para alcanzar sus metas de sostenibilidad a corto y medio plazo.

Dentro de este contexto, el género *Populus* (conocido comúnmente como álamos o chopos) destaca por su rápido crecimiento y adaptabilidad. Su nombre, derivado del latín que significa "popular", hace referencia su abundancia en ecosistemas templados y fríos del hemisferio norte, especialmente en zonas ribereñas. Este género, perteneciente a la familia Salicáceas junto con el género *Salix* (sauces), comprende aproximadamente 40 especies.

Los álamos son árboles caducifolios de rápido crecimiento, capaces de producir hasta 12 m^3 ha^{-1} $año^{-1}$, lo que permite obtener cosechas productivas en ciclos cortos. Prosperan óptimamente en suelos con alta disponibilidad de agua y luz y presentan una gran facilidad para la hibridación, lo que ha permitido el desarrollo de variedades adaptadas a necesidades específicas. Además, su capacidad de propagación vegetativa facilita la reproducción masiva de individuos con características favorables, consolidando al género *Populus* como un recurso idóneo para plantaciones energéticas.

La diversidad dentro del género *Populus* se debe, en gran medida, a su naturaleza dioica, es decir, sus individuos son masculinos o femeninos, lo que facilita el cruzamiento entre ellos. Se conoce por hibridación al proceso de cruzamiento entre individuos de diferentes especies, pudiendo ocurrir de forma natural, cuando coexisten en la misma zona, o de manera artificial, entre especies diferentes y geográficamente alejadas entre sí. En la Figura 7 y en la Tabla 2 se recogen los diferentes subgéneros, secciones, especies, híbridos y clones del género *Populus*.

Además, este género sobresale por su capacidad para reproducirse vegetativamente mediante estaquillado, permitiendo la multiplicación masiva de individuos seleccionados, un proceso conocido como clonación, siendo un proceso clave para establecer plantaciones homogéneas y productivas.

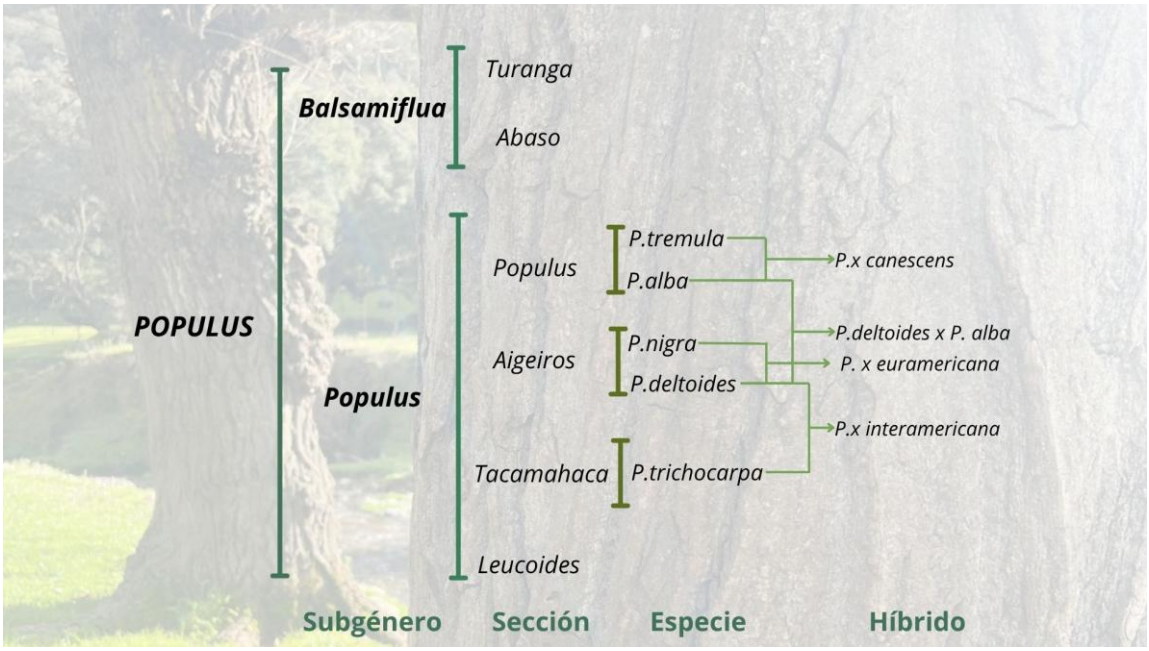


Figura 7. Del género *Populus* a sus híbridos. Información adaptada del Catálogo Nacional de Materiales de Base 2016 [53].

El género *Populus* se divide en seis secciones principales: *Turanga, Abaso, Populus* (o Leuce), *Aigeiros, Tacamahaca* y *Leucoides*. En Europa, los clones más empleados pertenecen a las siguientes especies e híbridos:

- ***Populus nigra*** (chopo negro europeo): tolera mejor la escasez de agua, pero su crecimiento es más lento.
- ***Populus deltoides*** (chopo negro americano): crece rápidamente y se emplea en híbridos, aunque requiere suelos aluviales fértiles.
- ***Populus trichocarpa*** (chopos balsamíferos): tolera suelos poco profundos, arcillosos, con pH bajos y con encharcamiento temporal.
- ***Populus x interamericana*** (híbrido de *P. deltoides* y *P. trichocarpa)*: posee un desarrollo radical rápido, aunque no se adapta bien a suelos demasiado arcillosos o con pH elevado.
- ***Populus x euramericana*** (híbrido de *P. deltoides* y *P. nigra)*: presenta características intermedias entre ambas especies, adaptándose bien a suelos aluviales y con pH próximo a la neutralidad, aunque no tolera altos contenidos de arcilla (>20-25%).

Tabla 2. Lista de clones del género *Populus*. Información adaptada del Catálogo Nacional de Materiales de Base 2016 [53].

Especie/híbrido	Clones
Populus nigra	Anadolu, Ankum, Bordils, Brandaris, Jean Pourtet, Loenen, Lombardo Leonés, San Giorgio, Vereecken.
Populus deltoides	Alcinde, Baldo, Carolin, Delgas, Dellinois, Delrive, Delvignac, Dvina, Harvard, Lena, Lincoln, Lux, Marquette, Oglio, Onda, Peoria, Viriato.
Populus x euramericana	A4A, Adda, AF2, AF4, Agathe F, Albelo, Aleramo, Arno, Ballottino, Bellini, Blanc du Poitou, Branagesi, Brenta, B-1M, Canadá Blanco, Carpaccio, Cima, Culant, Degrosso, Dorskamp, Degrosso, Ellert, Enza, Flevo, Florence Biondi, Gaver, Ghoy, Gibecq, Guardi, Guariento, Hees, I-45/51, I-214, I-262, I454/40, I-488, Imola, Koster, Lambro, Lima, Luisa Avanzo, MC, Mella, Muur, Neva, Ogy, Orba, Oudenberg, Pannonia, Pinseque, Polargo, Robusta, San Martino, Sanosol, Soligo, Ticino, Trebbia, Triplo, 2000 Verde.
Populus trichocarpa	Blom, Columbia River, Fritzi Pauley, Muhle Larsen, Scott Pauley, Trichobel
Populus x interamericana	Barn, Beaupré, Boelare, Donk, Hazendans, Hoogvorst, Hunnegem, Rap, Raspalje, Unal, USA 49-177
Populus deltoides x Populus alba	I-144/69

En esta tesis doctoral se ha empleado el clon AF2, perteneciente al híbrido *Populus x euramericana*. Este clon es una variedad de nueva generación desarrollada en 1994 por la empresa italiana Alasia. Su progenitora materna es *P. deltoides* 145-86 (Illinois, USA) y su progenitor paterno es *P. nigra* 40 (Piemonte, Italia), lo que dio lugar a un clon masculino.

El clon AF2 presenta una alta producción de biomasa. Pannacci. et al. [54] analizaron cuatro clones en plantaciones de alta densidad en Italia central y concluyeron que el clon AF2 mostró una de las mayores productividades, alcanzando una producción promedia de 6,04 toneladas de materia seca por hectárea al año. En la misma región, Matteo et al. [55] evaluaron tres clones modernos de *Populus* en condiciones no irrigadas y subóptimas como plantación de corta rotación. Los resultados indicaron que el clon AF2 mostró tolerancia a la sequía estival, manteniendo altos valores de conductancia estomática, tasas de asimilación fotosintética y eficiencia intrínseca del uso del agua. Además, su cierre estomático gradual estuvo asociado a un mayor rendimiento en biomasa, lo que lo hace especialmente adecuado para ambientes mediterráneos afectados por la sequía, especialmente en la fase de establecimiento, cuando las plantas son más sensibles.

En España, Sixto et al. [56] estudiaron el crecimiento de nueve clones de *Populus* en distintas localizaciones, determinando que el clon AF2 destacaba por su mayor crecimiento en altura, productividad de biomasa total y capacidad de adaptación. Esta última característica lo hace idóneo

para su cultivo en zonas con escasa información sobre las condiciones del terreno, ya que ofrece una mayor garantía de éxito en el establecimiento y crecimiento inicial.

Sin embargo, un estudio realizado en la Universidad Politécnica de Madrid señaló que el clon AF2 presenta un menor número de brotes tras las cortas, en comparación con otros clones estudiados. Este resultado sugiere que su elevado crecimiento se debe principalmente a un mayor diámetro y altura, en lugar de a la capacidad de rebrote [57].

Respecto al uso de agua, Fontenla-Razzetto et al. [58] analizaron el comportamiento del clon AF2 en suelos arenosos de Eslovaquia occidental con distintos niveles de acceso al agua subterránea. Sus resultados mostraron que, si bien el consumo hídrico era mayor en sitios con un nivel freático más alto y la transpiración se veía limitada en condiciones más secas, el clon AF2 logró tasas de crecimiento similares en diámetro a lo largo de la temporada de crecimiento. Esto evidencia su capacidad de adaptación a diferentes condiciones hídricas, lo que refuerza su potencial como recurso para plantaciones energéticas en entornos variables.

Por otro lado, Schroeder [59] estudió la resistencia de diferentes clones de *Populus* a insectos fitófagos a través de la defoliación. Durante los cuatro años de análisis, la pérdida de hojas se mantuvo en general en rangos del 5,8-13,4%, y el clon AF2 presentó una defoliación del 11,5%. En el ranking de resistencia, el clon AF2 ocupó la posición 18/20 entre 2012 y 2015, y la posición 4/8 en 2016. Estos resultados indican que el clon AF2 presenta una resistencia moderada a especies comunes como *Chrysomela populi* y *Phratora sp*.

Los cultivos de corta rotación, como es el caso del clon AF2, además de su uso en la producción de biomasa, también tienen interés en el secuestro de carbono a corto y medio plazo. Olivera et al. [60] analizaron la acumulación de carbono sobre y bajo el suelo en tres clones de *Populus* y determinaron que el clon AF2 fue el que acumuló la mayor cantidad de carbono, con 6,44 Mg ha^{-1} $año^{-1}$ en biomasa aérea y 0,91 Mg ha^{-1} $año^{-1}$ en biomasa subterránea.

En cuanto a su composición química, estudios han reportado valores de celulosa entre 39-49%, hemicelulosa entre 21-29% y lignina entre 16-24%, con un contenido total de extractivos que varían entre 1,4-12,8%. Estos valores dependen de la parte del árbol analizada, la edad de la planta y las condiciones ambientales de cultivo [61,62].

1.7. Pretratamientos de la biomasa lignocelulósica en Biorrefinería.

El concepto de biorrefinería es análogo al de las refinerías de petróleo, con la diferencia fundamental en la materia prima utilizada. Su objetivo es la transformación integral de la biomasa en energía y productos de alto valor añadido. Para maximizar el aprovechamiento de los componentes de la biomasa lignocelulósica es fundamental desarrollar procesos de conversión eficientes [63].

Uno de los principales desafíos que presenta la biomasa lignocelulósica es su carácter recalcitrante, el cual dificulta su conversión en productos de interés. Su estructura robusta limita la acción de enzimas y catalizadores, reduciendo así el rendimiento en la producción de biocombustibles y otros compuestos derivados. Por ello, el pretratamiento es un paso esencial dentro de un esquema de biorrefinería, ya que mejora la accesibilidad de biomasa y optimiza su conversión. Este proceso modifica la estructura física y química de la biomasa mediante diferentes mecanismos, como la eliminación parcial de la lignina y la hemicelulosa, la reducción de la cristalinidad de la celulosa y el incremento del área superficial accesible para la acción enzimática [64]. Sin embargo, debe evitarse la degradación de los azúcares liberados y la formación de compuestos inhibidores, como furfural, hidroximetilfurfural (HMF) y ciertos ácidos orgánicos, que pueden afectar negativamente las etapas posteriores del proceso [65].

Dado que la eficiencia del pretratamiento está directamente relacionada con las características estructurales de la biomasa, la conversión de MLC depende no solo de su composición química, sino también de la organización de sus constituyentes y la interacción entre ellos. Factores como la cristalinidad de la celulosa, la estructura de las hemicelulosas, el área superficial estructural y el volumen de poros, así como la composición, el contenido y la reticulación de la lignina, varían según la especie vegetal, los tejidos específicos, la parte de la planta utilizada y su grado de madurez, lo que influye en la elección y eficacia del método de pretratamiento más adecuado [66-68].

Los pretratamientos tradicionalmente se clasifican en físicos, químicos, fisicoquímicos y biológicos. Cada uno presenta ventajas y limitaciones, y su elección depende de la materia prima utilizada, el proceso de conversión posterior y la composición del producto deseado. La combinación de diferentes estrategias de pretratamiento es una práctica común para optimizar la eficiencia del proceso y maximizar la recuperación de compuestos valiosos [69-71].

Una de las variables más relevantes en la efectividad y selectividad de los pretratamientos es el pH, ya que determina qué fracciones de la biomasa se solubilizan o permanecen en estado sólido. Un pH bajo favorece la hidrólisis de la hemicelulosa a azúcares monoméricos sin afectar significativamente la celulosa ni la lignina. En cambio, un pH neutro genera una hidrólisis parcial, dejando la hemicelulosa mayormente en forma oligomérica o polimérica. Por otro lado, un pH alto

facilita la disolución de la lignina, mientras que la celulosa y hemicelulosa permanecen en estado sólido. En el caso de ciertos disolventes, su efecto puede ser similar al de un pH alto [65].

Además del pH, la efectividad de los pretratamientos también depende del mecanismo utilizado para modificar la estructura de la biomasa. Entre estos métodos, los **pretratamientos físicos** se emplean principalmente para reducir el tamaño de partícula, aumentando así el área superficial y facilitando la acción de enzimas y reactivos químicos. A continuación, se presentan las principales estrategias utilizadas en esta categoría.

- **La molienda** y otros **procesos mecánicos** disminuyen la cristalinidad de la celulosa y mejoran la accesibilidad de los reactivos [72].
- **La extrusión**, por su parte, combina alta presión y temperatura para aumentar la porosidad y facilitar la hidrólisis enzimática [73].
- **La irradiación con microondas** permite un calentamiento rápido, volumétrico y selectivo, favoreciendo la alteración de la matriz lignocelulósica y mejorando la disponibilidad de celulosa y hemicelulosa; su combinación con tratamientos químicos aumenta la eficacia [74-77].
- **Los ultrasonidos** generan cavitación acústica, lo que provoca la formación de microburbujas que, al colapsar generan ondas de choque y radicales oxidantes. Estos efectos contribuyen a la desintegración de la biomasa. Este método es prometedor, aumentando su eficacia al ser combinado con agentes químicos [72,78-80].

A pesar de sus ventajas en la mejora de la accesibilidad y la modificación estructural, los pretratamientos físicos suelen requerir una inversión energética significativa, lo que puede limitar su escalabilidad industrial.

A diferencia de los métodos físicos, los **pretratamientos químicos** se basan en el uso de reactivos que modifican la estructura de la lignina, la celulosa y la hemicelulosa, facilitando la posterior conversión de la biomasa lignocelulósica. Se presentan a continuación los métodos más estudiados y empleados:

- **La hidrólisis ácida**, es de los más tradicionales, es altamente efectivo en la solubilización de la hemicelulosa, dejando expuesta la celulosa para su posterior conversión [72]. Se emplean tanto ácidos concentrados, como el sulfúrico y el clorhídrico, como ácidos diluidos a temperaturas más elevadas [81]. La principal ventaja del uso de ácidos concentrados es que el proceso puede realizarse a temperaturas relativamente bajas, reduciendo el consumo energético [72]. Sin embargo, presenta una alta corrosividad y genera compuestos inhibidores [40,82]. En contraste, el uso de ácidos diluidos requiere temperaturas más altas y tiempos de

reacción más prolongados, pero minimiza la formación de inhibidores y facilita la recuperación de los reactivos, lo que mejora su sostenibilidad [40].

- **La hidrólisis alcalina**, favorece la eliminación de la lignina y la disrupción estructural [40,73]. Se emplean bases como hidróxido de sodio, potasio o amonio para la degradación de la biomasa. A diferencia de la hidrólisis ácida, este método requiere de reactores sencillos, ya que opera a temperaturas y presiones más bajas [83]. No obstante, presentan algunas limitaciones, como la necesidad de largos tiempos de operación y el alto consumo de agua para la eliminación de residuos alcalinos, lo que incrementa los costos operativos y el impacto ambiental [84].
- **El método organosolv** utiliza disolventes orgánicos, como etanol, metanol, acetona o tetrahidrofurfurílico, pudiendo ser combinado con ácidos o bases [85], para solubilizar principalmente la lignina. Además, es particularmente efectivo en el fraccionamiento de la biomasa en sus tres componentes principales [86], así como una recuperación de la lignina con una estructura relativamente intacta, lo que la hace valiosa para aplicaciones industriales [87]. Sin embargo, este método tiene ciertas desventajas, como el alto costo de los disolventes, las altas presiones de operación, la necesidad de sistemas de recuperación eficientes y el riesgo de una alta inflamabilidad por parte de alguno de los solventes [88].
- **Los líquidos iónicos (IL) y los solventes eutécticos profundos (DES)** han surgido como alternativas adecuadas. Estos solventes pueden disolver la lignina y alterar la estructura cristalina de la celulosa [72]. Los IL presentan propiedades únicas, como baja volatilidad y estabilidad química y térmica, pero su elevado costo y la dificultad en su recuperación limitan su aplicación a gran escala [65,89,90]. Por otro lado, los DES han ganado interés debido a su bajo impacto ambiental, biodegradabilidad y facilidad de síntesis a partir de compuestos económicos como sales de amonio, ácidos orgánicos y carbohidratos. Además, los DES permiten la eliminación selectiva de la lignina sin degradar la celulosa ni la hemicelulosa, lo que los convierte en una opción prometedora para procesos más ecológicos [91].

A pesar de sus múltiples ventajas, como la alta eficiencia en la degradación de la biomasa, la solubilización de componentes específicos y la mejora en la accesibilidad enzimática para procesos posteriores, los pretratamientos químicos también poseen desventajas, como el alto costo de los reactivos, la necesidad de manejo seguro de productos corrosivos o tóxicos, la generación de residuos y la posible formación de compuestos inhibidores. La elección del pretratamiento químico más adecuado dependerá del tipo de biomasa utilizada, los costos asociados y la viabilidad de recuperación de los reactivos empleados.

Los **pretratamientos biológicos** emplean microorganismos para degradar y modificar la estructura de la biomasa lignocelulósica, ofreciendo ventajas como un bajo impacto ambiental y un menor consumo energético en comparación con los pretratamientos anteriores [40].

Este tipo de pretratamiento puede realizarse mediante hongos con distintos mecanismos: los hongos de podredumbre blanca atacan la lignina, los de podredumbre blanda degradan la celulosa y los de podredumbre parda afectan tanto a la hemicelulosa como la celulosa. Además, también se emplean bacterias con capacidad de degradar varios componentes lignocelulósicos [65].

A pesar de sus ventajas, este método está limitado por su baja tasa de degradación, ya que los microorganismos requieren de largos periodos de tratamiento [65]. No obstante, se han propuesto estrategias para su optimización, como la aplicación de hongos altamente selectivos, la ingeniería genética de bacterias y la combinación del pretratamiento biológico con otros métodos [40,65,92].

Como se ha observado, cada tipo de pretratamiento presenta limitaciones inherentes que afectan su eficiencia y viabilidad. En general, los pretratamientos aplicados de manera aislada suelen estar asociados con una baja eficiencia, una alta formación de subproductos y elevados costos [93]. Para superar estas limitaciones, se propone la implantación de pretratamientos combinados, que consisten en la integración de métodos físicos, químicos y biológicos, con el objetivo de mejorar la degradabilidad y eficiencia [94].

El pretratamiento combinado tiene la ventaja obvia del efecto sinérgico y una aplicabilidad más extensa. Las combinaciones de pretratamientos posibles serían fisicoquímicos, físico-biológicos, químicos-biológicos y químico-químico [84].

En cuanto a los **pretratamientos fisicoquímicos**, como su nombre indica, combinan métodos físicos y químicos para mejorar la degradación y conversión de la biomasa. Algunos de estos pretratamientos son:

- **La explosión de vapor.** Usa el vapor a alta temperatura y presión descomponiendo parcialmente la hemicelulosa y lignina, mejorando así la accesibilidad de la celulosa [84]. Se trata de un pretratamiento fisicoquímico ya que su mecanismo de operación se basa en la descompresión explosiva a alta temperatura y presión, y a los efectos químicos al generar ácido acético a partir de la hidrólisis de los grupos acetilo asociados a las hemicelulosas [95]. Además, se puede combinar con el pretratamiento ácido para optimizar aún más la hidrólisis y conversión de los azúcares. Sin embargo, se trata de una tecnología con un alto consumo energético y operativamente compleja por lo que requiere su optimización [84].
- **Explosión de fibra de amoniaco.** Consiste en tratar la biomasa con amoniaco anhidro líquido a temperaturas moderadas y alta presión, seguido de una despresurización rápida, lo que

provoca la expansión de las fibras de la biomasa. En este proceso, los efectos físicos y químicos combinados mejoran la conversión enzimática de celulosa y hemicelulosa en azúcares fermentables al solubilizar la lignina, hidrolizar la hemicelulosa y aumentar el área superficial [84,95].

- **Trituración mecánica con pretratamientos químicos** (ácidos, álcalis u oxidantes), con el fin de aumentar la superficie y la porosidad de la biomasa, al mismo tiempo que mejora la hidrólisis enzimática y la eliminación de la lignina. Este tratamiento disminuye el consumo de reactivos químicos, pero tiene un alto consumo energético [84].
- **Calor húmedo y álcali.** El vapor a alta temperatura y presión debilita la estructura de la biomasa, facilitando la posterior acción de soluciones alcalinas, que penetran mejor en la celulosa y hemicelulosa. Esta combinación reduce el tiempo de tratamiento, disminuye el consumo de álcali y mejora la eficiencia del pretratamiento [84].

Si seguimos con las posibilidades de combinación de los pretratamientos, el siguiente grupo sería los **físico-biológico**. En este caso, consiste más en realizar el pretratamiento físico seguido del biológico. Algún ejemplo de estos son la pulverización mecánica con pretratamiento biológico, explosión de vapor con pretratamiento biológico o el pretratamiento hidrotermal-biológico. Estas combinaciones consiguen reducir el tiempo de tratamiento [84].

En cuanto a los **pretratamientos químicos-biológicos**, la primera etapa consistiría en un proceso químico (ácido o alcalino) alterando la estructura de la biomasa y facilitando el acceso de los microorganismos o enzimas de la etapa biológica posterior. Este enfoque optimiza la degradación de la celulosa y la hemicelulosa, aumentando la producción de azúcares fermentables y reduciendo la formación de inhibidores, lo que mejora la eficiencia de la fermentación. Además, la combinación de ambos métodos puede disminuir los costos de procesamiento y el tiempo de pretratamiento [84].

Y por último los **pretratamientos químicos-químicos**, los cuales combinan diferentes métodos para optimizar por lo general la hidrólisis posterior a través de la degradación de la lignina y hemicelulosa. Pudiendo combinarse ácido-álcali, ácido-oxidante, alcalino-oxidante o disolventes eutécticos profundos y ácidos/álcalis [84].

Por lo tanto, tras revisar la literatura actual sobre los diferentes métodos de pretratamiento, se concluye que el desarrollo de tecnologías de pretratamiento eficientes y sostenibles es crucial para la conversión comercial de la biomasa lignocelulósica. Aunque los métodos actuales han mejorado significativamente la descomposición de la biomasa, aún enfrentan desafíos importantes, como la reducción de costos, la minimización del impacto ambiental y la mejora en la eficiencia de conversión.

Uno de los principales retos es lograr un fraccionamiento selectivo y controlado de la celulosa, hemicelulosa y lignina sin generar compuestos inhibidores que afecten las etapas posteriores del proceso. Además, la variabilidad en la calidad de la biomasa, las dificultades logísticas y la falta de integración entre las distintas estrategias de pretratamiento siguen limitando la escalabilidad industrial.

En este contexto, las investigaciones futuras deben enfocarse en el desarrollo de procesos más selectivos y adaptativos, que puedan ajustarse a diferentes tipos de biomasa y condiciones operativas. La optimización de pretratamientos combinados, la implementación de catalizadores más eficientes y el diseño de sistemas para la recuperación de reactivos serán fundamentales para mejorar la viabilidad de estos procesos a gran escala.

1.8. Procesos termoquímicos de conversión de biomasa.

La conversión de biomasa se ha consolidado como una estrategia clave para mitigar la dependencia de los combustibles fósiles y reducir los efectos del cambio climático. En el marco de las biorrefinerías, diversos enfoques de valorización se han desarrollado en los últimos años, entre los cuales destacan los procesos termoquímicos por su gran potencial e interés por parte de la comunidad científica, política e industrial [96].

Los procesos termoquímicos transforman la biomasa mediante la aplicación de calor, a menudo en presencia de catalizadores, y sin necesidad estricta de pretratamientos complejos, además de ser procesos con velocidades de reacción más rápidas [97-99]. Esta conversión permite la obtención de biocombustibles líquidos (bioaceite), sólidos (biocarbón) y gaseosos (gas de síntesis), a través de reacciones que implican la ruptura de enlaces moleculares y la recomposición de la materia orgánica [99,100].

Las principales tecnologías termoquímicas incluyen la pirólisis, la gasificación, la licuefacción, la combustión y la torrefacción, entre otros. La selección del proceso más adecuado depende en gran medida de la naturaleza de la biomasa (composición lignocelulósica, humedad, cenizas, densidad energética), así como de los objetivos del proceso (tipo de producto, eficiencia energética, escalabilidad), ya que todo ello afecta a los parámetros del proceso (velocidad de reacción, rendimientos y calidad de los productos) [99,100].

En la Tabla 3 se recogen las características principales de alguno de los procesos de conversión termoquímicos, con el fin de destacar sus condiciones operativas, productos predominantes y posibles aplicaciones dentro de un esquema de valorización de biomasa.

Entre las tecnologías termoquímicas de conversión de biomasa, la pirólisis y la gasificación destacan por su tecnología y potencial de aplicación [96]. En particular, la pirólisis de biomasa ha ganado relevancia en los últimos años [101,102].

La principal diferencia entre ambos procesos reside en los productos generados. Mientras que la gasificación produce fundamentalmente gas de síntesis, la pirólisis convierte la biomasa en una fracción líquida conocida como bio-oil, además de biocarbón y gases no condensables. Al tratarse de un combustible líquido, el bio-oil presenta ventajas logísticas frente al gas, ya que puede almacenarse y transportarse con mayor facilidad [100,103].

Tabla 3. Comparativa de procesos termoquímicos.

Proceso	Reacción	Atmosfera	Productos	Temperaturas
Combustión	Oxidación completa	Aire	Calor, CO_2 Agua	800-1000 ºC
Pirólisis	Descomposición térmica	Inerte	Biocarbón Bio-oil Gases	300-700 ºC
Gasificación	Oxidación parcial	Oxigeno limitado, vapor o aire	Gas de síntesis Cenizas	800-1200 ºC
Licuefacción	Craking	En agua, ausencia de aire. Presiones de 5-20MPa.	Crudo de bio-oil	240-380 ºC
Torrefacción	Deshidratación	Inerte	Biomasa carbonizada Agua CO_2 Gases	200-300 ºC

La pirólisis se lleva a cabo en un ambiente inerte, sin presencia de oxígeno, a temperaturas que varían entre los 300 ºC y los 700 ºC. Durante este proceso, la materia orgánica de la biomasa experimenta una reacción de descomposición termoquímica irreversible que da lugar a los productos mencionados [100,101].

En función de la velocidad de calentamiento y el tiempo de residencia, la tecnología de pirólisis se clasifica en tres tipos principales [104,105]:

- **Pirólisis lenta:** considerada el método termoquímico más antiguo. Se caracteriza por tiempos de residencia prolongados (de 5 minutos a varios días) y bajas velocidades de calentamiento (0,1-1 ºC s^{-1}) [96,106]. Generalmente opera a temperaturas entre 300 ºC y 500 ºC y permite el procesamiento de una amplia variedad de tamaños de partícula [101,107]. Este tipo, también es conocido como carbonización, se emplea principalmente para la producción de carbón

vegetal, ya que las condiciones de operación favorecen las reacciones de repolimerización que maximizan el rendimiento de sólidos [101,106].

- **Pirólisis rápida:** se distingue por tasas de calentamiento elevadas (10-200 ºC s^{-1}) y tiempos de residencia muy cortos (entre 0,2 y 10 segundos) [96,106]. Este proceso opera, en la mayoría de los casos, a temperaturas comprendidas entre 400 ºC y 700 ºC, siendo 500 ºC el valor más común para diversas biomasas [100,107,108]. Esta modalidad de pirólisis se emplea principalmente cuando el objetivo es maximizar la fracción líquida. El rápido enfriamiento de los vapores generados es esencial para maximizar la producción de bio-oil, que puede alcanzar rendimientos del 50-75% [101,109]. Para lograr estos valores, se requiere el uso de partículas por lo general inferiores a 3 mm, para así garantizar una alta transferencia de calor [108].
- **Pirólisis flash:** se caracteriza por tasas de calentamiento extremadamente altas (>1000 ºC s^{-1}) y tiempos de residencia de solo décimas de segundo o menos [106,107]. Este proceso opera a temperaturas entre 800 ºC y 1000 ºC, y se destaca por la alta eficiencia en la producción de bio-oil, con rendimientos que pueden alcanzar hasta un 75-80% [101,106,107]. Los tiempos de residencia tan cortos son fundamentales para evitar la repolimerización de los productos descompuestos [110].

Además de los tipos de pirólisis ya mencionados, existen otros procesos que operan bajo condiciones similares. Un ejemplo es la **pirólisis intermedia**, que busca obtener una mezcla de productos de la pirólisis lenta y rápida. Este proceso se realiza a temperaturas de hasta 500 ºC, con velocidades de calentamiento de 0,1-10 ºC min^{-1} y tiempos de residencia de 0,5 a 25 minutos [111,112]. Otro tipo emergente es la **hidropirólisis**, que es similar a la pirólisis rápida, pero se lleva a cabo en un ambiente inerte con hidrógeno y a presiones superiores a la atmosférica. Este proceso se utiliza para obtener un bio-oil de mayor calidad, debido a la reducción de hidrocarburos insaturados [111].

El uso de catalizadores en la pirólisis de biomasa ha ganado relevancia en los últimos años, con el objetivo de mejorar la calidad y distribución de los productos obtenidos. Los catalizadores más utilizados son los óxidos metálicos y las zeolitas [113].

Los rendimientos y la composición de los productos dependen no solo de las condiciones de operación (como la velocidad de calentamiento, el tiempo de residencia, el tamaño de partícula, la temperatura, el diseño del reactor y la presencia de catalizador), sino también de la composición específicos de la biomasa lignocelulósica utilizada.

Cada uno de los constituyentes principales de la biomasa sigue vías de reacción específicas, lo que influye en la distribución de los productos. Por ejemplo, la celulosa produce un bio-oil rico en

levoglucosano y otros azúcares anhidros; las hemicelulosas generan principalmente gases y un bio-oil acuoso con compuestos fenólicos y cetonas; mientras que la lignina favorece la formación de un biocarbón y un bio-oil con alto contenido de fenoles [101,114].

Además, la combinación estructural de estos componentes varía entre tipos de biomasa, lo que altera las interacciones entre ellos y, en consecuencia, el rendimiento global de la pirólisis. Por ejemplo, la presencia de material mineral puede influir en la distribución y proporción de los productos, debido a su efecto catalítico durante la pirólisis [115,116].

Para optimizar los rendimientos de los productos específicos, es fundamental centrar la atención en las reacciones de pirólisis. En este sentido, el pretratamiento de la biomasa lignocelulósica puede emplearse para favorecer reacciones selectivas que maximicen la formación de los productos deseados.

1.9. Extracción alcalina en frío como pretratamiento de la biomasa lignocelulósica.

Entre los distintos pretratamientos aplicados a la biomasa lignocelulósica en biorrefinería, la elección del método más adecuado depende de varios factores, siendo actualmente uno de los más determinantes la viabilidad económica y ambiental del proceso. En este contexto, la extracción alcalina en frío (EAF) ha surgido como una alternativa prometedora dentro de los tratamientos químicos con álcali, gracias a su capacidad para modificar selectivamente la matriz lignocelulósica sin requerir altas temperaturas ni grandes consumos energéticos.

La EAF, también conocida como extracción cáustica en frío, permite la modificación selectiva de la biomasa lignocelulósica sin recurrir a altas temperaturas, generalmente entre 20 ºC y 40 ºC [117,118]. A diferencia de los tratamientos alcalinos convencionales a altas temperaturas, que promueven una deslignificación significativa, la EAF se caracteriza por su alta selectividad, favoreciendo principalmente la eliminación de hemicelulosas y preservando casi intacta la celulosa [119,120]. Este comportamiento se debe a que las hemicelulosas, debido a su menor grado de polimerización y estructura amorfa, son más susceptibles a la hidrólisis alcalina que la celulosa [118]. Además, este proceso se basa en la mayor solubilidad de las hemicelulosas en soluciones alcalinas en comparación con las ácidas, lo que permite su eliminación con un menor grado de degradación a compuesto furfural [121,122]. Este enfoque ha demostrado ser una estrategia prometedora para la extracción de hemicelulosas en aplicaciones industriales, incluyendo el procesamiento de pulpa y papel, la obtención de bioproductos y la optimización de la hidrólisis enzimática de la celulosa. Gracias a su aplicación a temperaturas moderadas y su bajo consumo de reactivos, este método presenta un menor impacto ambiental en comparación con otros pretratamientos más agresivos [122].

Existen actualmente dos aplicaciones principales de este método, aunque una de ellas es más extendida. La EAF se emplea, principalmente, para la obtención de pastas solubles con una alta pureza de celulosa. Además, también puede aplicarse como pretratamiento en procesos de biorrefinería, ya sea para la producción de pasta celulósica o para la obtención de otros productos de alto valor añadido a partir de biomasa lignocelulósica.

La EAF ha sido ampliamente utilizada en la producción de pulpas solubles de alta pureza, ya que permite eliminar selectivamente las hemicelulosas sin afectar significativamente la celulosa [123,124]. Este proceso es clave para obtener pulpas con un contenido de celulosa superior al 90%, reduciendo al mínimo las impurezas orgánicas e inorgánicas [125]. Durante el tratamiento, la solución alcalina penetra en la estructura de la fibra, provocando su hinchamiento y la disolución progresiva de las hemicelulosas, que posteriormente se difunden hacia la solución [124]. En comparación con otras estrategias de purificación, como la prehidrólisis o la extracción alcalina en caliente, la EAF ha demostrado ser una alternativa eficaz y ambientalmente sostenible, ya que facilita la recuperación de los productos químicos utilizados y no requiere etapas adicionales de digestión [126]. No obstante, el proceso debe ser cuidadosamente controlado para evitar la conversión parcial de celulosa I a celulosa II, lo que podría afectar la reactividad de la pulpa en aplicaciones posteriores, como la producción de fibras artificiales o productos químicos derivados de la celulosa [127].

Mientras que el empleo de la EAF con otras perspectivas industriales actualmente ha sido menos estudiado, (como puede ser la producción de etanol o favorecer un tratamiento escalonado para fraccionar la biomasa lignocelulósica en sus tres principales componentes), existen indicios de su potencial en estos ámbitos. La EAF facilita la separación selectiva de los componentes químicos de la biomasa, permitiendo la obtención de lignina soluble en álcali, hemicelulosas y otros residuos con mínimas alteraciones estructurales y químicas [119,128]. Este proceso, que puede llevarse a cabo sin presión y a temperatura ambiente, es particularmente prometedor para el pretratamiento de biomasas con el fin de valorizar sus fracciones [119,129]. En particular, las hemicelulosas extraídas pueden ser utilizadas para la producción de nuevos materiales como biopelículas o aditivos alimentarios, mientras que la lignina residual puede transformarse en productos de alto valor añadido como fibra de carbono y adhesivos [119,122,130]. Además, la eliminación selectiva de xilano de materiales lignocelulósicos mediante pre-extracción alcalina ha demostrado mejorar la extracción de lignina sin afectar negativamente la producción de papel [122,130]. Finalmente, la pre-extracción alcalina ha sido identificada como un método que podría mitigar el problema del silicio en biomasa no maderera, el cual puede afectar la eficiencia de los procesos de pulpeo alcalino [122]. Estos hallazgos resaltan el potencial de la EAF no solo en la producción de pulpa de alta pureza, sino también en estrategias de biorrefinería para la conversión integral de biomasa lignocelulósica en bioproductos sostenibles.

Sin embargo, la eficacia de la EAF depende en gran medida del material lignocelulósico procesado, lo que requiere una optimización específica de las variables de operación (temperatura, tiempo de reacción, carga alcalina y relación licor/biomasa) para cada tipo de biomasa [119]. En general, este tratamiento presenta un mayor rendimiento de extracción en biomasas herbáceas que en biomasas madereras [130,131], lo que ha impulsado el desarrollo de estrategias complementarias para mejorar su eficiencia. Por ejemplo, algunos estudios han demostrado que la aplicación de un pretratamiento mecánico como el refinado de la pasta, puede aumentar la extracción de hemicelulosas durante la EAF [132]. Otra estrategia en auge es la combinación de nuevas tecnologías, como la aplicación simultanea de ultrasonidos. Sun et al. [133] investigaron el efecto de la combinación de ultrasonidos con la EAF en una pasta quimitermo-mecánica de *Populus* (tratamiento químico y vapor, seguido de una trituración), encontrando que esta técnica mejoró significativamente la eliminación de hemicelulosas. Además, se observó que la aplicación de ultrasonidos permitió reducir la concentración de álcali de 5% a 2%, logrando una eficiencia de extracción similar a la del tratamiento tradicional sin ultrasonidos. También se evidenció que el rendimiento del proceso con 2% de NaOH asistido por ultrasonidos fue mayor que el de la extracción alcalina convencional con 5% de NaOH [133]. Estos hallazgos destacan el potencial de la EAF asistida por ultrasonidos como una alternativa eficiente y sostenible para la valorización de biomasa lignocelulósica.

Bibliografía.

[1] United Nations Environment Programme, Emissions gap report 2023: broken record—temperatures hit new highs, yet world fails to cut emissions (again), (2023).

[2] European Environment Agency, Trends and projections in Europe 2023, Publications Office of the European Union, (2023).

[3] European Environment Agency, Climate change mitigation: reducing emissions | European Environment Agency's home page. https://www.eea.europa.eu/en/topics/in-depth/climate-change-mitigation-reducing-emissions#eu-greenhouse-gases-in-numbers (accessed June 27, 2025).

[4] T. Mathimani, T.S. Kumar, M. Chandrasekar, L. Uma, D. Prabaharan, Assessment of fuel properties, engine performance and emission characteristics of outdoor grown marine Chlorella vulgaris BDUG 91771 biodiesel, Renew Energy 105 (2017) 637–646. https://doi.org/10.1016/j.renene.2016.12.090.

[5] T. Scarbrough, What Future Role For Convetional Refineries In The Decarbonisation Transittion?, (2022).

[6] P. Zhu, O.Y. Abdelaziz, C.P. Hulteberg, A. Riisager, New synthetic approaches to biofuels from lignocellulosic biomass, Curr Opin Green Sustain Chem 21 (2020) 16–21. https://doi.org/10.1016/j.cogsc.2019.08.005.

[7] S.M. Mousavi, E. Thorin, F.M. Schmidt, A. Sepman, X.-S. Bai, H. Fatehi, Numerical Study and Experimental Verification of Biomass Conversion and Potassium Release in a 140 kW Entrained Flow Gasifier, Energy & Fuels 37 (2023) 1116–1130. https://doi.org/10.1021/acs.energyfuels.2c03107.

[8] D.L. Klass, Biomass for renewable energy and fuels, Encyclopedia of Energy 1 (2004) 193–212.

[9] S. V Vassilev, C.G. Vassileva, V.S. Vassilev, Advantages and disadvantages of composition and properties of biomass in comparison with coal: An overview, Fuel 158 (2015) 330–350. https://doi.org/10.1016/j.fuel.2015.05.050.

[10] E. de Jong, A. Higson, P. Walsh, M. Wellisch, Bio-based chemicals value added products from biorefineries, IEA Bioenergy, Task42 Biorefinery 34 (2012) 1–33.

[11] R. Platt, A. Bauen, P. Reumerman, C. Geier, R. van Ree, I.V. Gürsel, L.Y.G. Chavez, M. Behrens, P. von Bothmer, J. Howes, EU Biorefinery Outlook to 2030 (Lot 3): Studies on support to research and innovation policy in the area of bio-based products and services, (2021). https://doi.org/10.2777/103465.

[12] B. US Department of Energy–Office of Energy Efficiency and Renewable Energy, Energy, Environmental, and Economics (E3) Handbook, (1997).

[13] S. España, Manual sobre biorrefinerías en España, (2017).

[14] J.K. Saini, R. Gupta, hemansi, A. Verma, P. Gaur, R. Saini, R. Sukla, R.C. Kuhad, Integrated Lignocellulosic Biorefinery for Sustainable Bio-Based Economy, in: M. and M.P.K. and U.S.N. and R.P.W. and G.V.K. Srivastava Neha and Srivastava (Ed.), Sustainable Approaches for Biofuels Production Technologies: From Current Status to Practical Implementation, Springer International Publishing, Cham, (2019) 25–46. https://doi.org/10.1007/978-3-319-94797-6_2.

[15] E. Baldoni, P. Reumerman, C. Parisi, R. Platt, H. González Hermoso, K. Vikla, J. Vos, R. M'barek, Chemical and material biorefineries in the EU, (2021). http://data.europa.eu/89h/24e98d11-ef06-4233-8f69-1e123938e891 (accessed June 27, 2025).

[16] B. Kamm, P.R. Gruber, M. Kamm, Biorefineries-industrial processes and products, Wiley-VCH Weinheim, (2006).

[17] P. Tomme, R.A.J. Warren, N.R. Gilkes, Cellulose hydrolysis by bacteria and fungi, Adv Microb Physiol 37 (1995) 1–81. https://doi.org/10.1016/S0065-2911(08)60143-5.

[18] B.C. Saha, Hemicellulose bioconversion, J Ind Microbiol Biotechnol 30 (2003) 279–291. https://doi.org/10.1007/s10295-003-0049-x.

[19] Y. Habibi, L.A. Lucia, O.J. Rojas, Cellulose nanocrystals: chemistry, self-assembly, and applications, Chem Rev 110 (2010) 3479–3500. https://doi.org/10.1021/cr900339w.

[20] A.C. O'sullivan, Cellulose: the structure slowly unravels, Cellulose 4 (1997) 173–207. https://doi.org/10.1023/A:1018431705579.

[21] R.J. Moon, A. Martini, J. Nairn, J. Simonsen, J. Youngblood, Cellulose nanomaterials review: structure, properties and nanocomposites, Chem Soc Rev 40 (2011) 3941–3994. https://doi.org/10.1039/C0CS00108B.

[22] M. Martínez-Sanz, M.J. Gidley, E.P. Gilbert, Application of X-ray and neutron small angle scattering techniques to study the hierarchical structure of plant cell walls: a review, Carbohydr Polym 125 (2015) 120–134. https://doi.org/10.1016/j.carbpol.2015.02.010.

[23] D. Klemm, B. Heublein, H. Fink, A. Bohn, Cellulose: fascinating biopolymer and sustainable raw material, Angewandte Chemie International Edition 44 (2005) 3358–3393. https://doi.org/10.1002/anie.200460587.

[24] F.H. Isikgor, C.R. Becer, Lignocellulosic biomass: a sustainable platform for the production of bio-based chemicals and polymers, Polym Chem 6 (2015) 4497–4559. https://doi.org/10.1039/C5PY00263J.

[25] R.A. Spanevello, A.G. Suárez, A.M. Sarotti, Fuentes alternativas de materia prima, Educación Química 24 (2013) 124–131. https://doi.org/10.1016/S0187-893X(13)72505-9.

[26] F.M. Gírio, C. Fonseca, F. Carvalheiro, L.C. Duarte, S. Marques, R. Bogel-Łukasik, Hemicelluloses for fuel ethanol: a review, Bioresour Technol 101 (2010) 4775–4800. https://doi.org/10.1016/j.biortech.2010.01.088.

[27] H. Chen, H. Chen, Chemical composition and structure of natural lignocellulose, Biotechnology of Lignocellulose: Theory and Practice (2014) 25–71. https://doi.org/10.1007/978-94-007-6898-7_2.

[28] S. Wang, G. Dai, H. Yang, Z. Luo, Lignocellulosic biomass pyrolysis mechanism: A state-of-the-art review, Prog Energy Combust Sci 62 (2017) 33–86. https://doi.org/10.1016/j.pecs.2017.05.004.

[29] A.J. Ragauskas, M. Nagy, D.H. Kim, C.A. Eckert, J.P. Hallett, C.L. Liotta, From wood to fuels: integrating biofuels and pulp production, Industrial Biotechnology 2 (2006) 55–65. https://doi.org/10.1089/ind.2006.2.55.

[30] D. Fengel, G. Wegener, Wood: chemistry, ultrastructure, Reactions 613 (1984) 1960–1982.

[31] D. Tarasov, M. Leitch, P. Fatehi, Lignin–carbohydrate complexes: properties, applications, analyses, and methods of extraction: a review, Biotechnol Biofuels 11 (2018) 1–28. https://doi.org/10.1186/s13068-018-1262-1.

[32] A.J. Ragauskas, G.T. Beckham, M.J. Biddy, R. Chandra, F. Chen, M.F. Davis, B.H. Davison, R.A. Dixon, P. Gilna, M. Keller, Lignin valorization: improving lignin processing in the biorefinery, Science 344 (2014) 1246843. https://doi.org/10.1126/science.1246843.

[33] N.G. Lewis, E. Yamamoto, Lignin: occurrence, biogenesis and biodegradation., (1990).

[34] E. Ten, W. Vermerris, Functionalized polymers from lignocellulosic biomass: State of the art, Polymers (Basel) 5 (2013) 600–642. https://doi.org/10.3390/polym5020600.

[35] R. Hückelhoven, Cell wall–associated mechanisms of disease resistance and susceptibility, Annu. Rev. Phytopathol. 45 (2007) 101–127. https://doi.org/10.1146/annurev.phyto.45.062806.094325.

[36] M. Schuetz, A. Benske, R.A. Smith, Y. Watanabe, Y. Tobimatsu, J. Ralph, T. Demura, B. Ellis, A.L. Samuels, Laccases direct lignification in the discrete secondary cell wall domains of protoxylem, Plant Physiol 166 (2014) 798–807. https://doi.org/10.1104/pp.114.245597.

[37] R. Vanholme, B. Demedts, K. Morreel, J. Ralph, W. Boerjan, Lignin biosynthesis and structure, Plant Physiol 153 (2010) 895–905. https://doi.org/10.1104/pp.110.155119.

[38] A. Lourenço, H. Pereira, Compositional variability of lignin in biomass, Lignin-Trends and Applications (2018) 65–98.

[39] C. Xu, R.A.D. Arancon, J. Labidi, R. Luque, Lignin depolymerisation strategies: towards valuable chemicals and fuels, Chem Soc Rev 43 (2014) 7485–7500. https://doi.org/10.1039/C4CS00235K.

[40] Z. Anwar, M. Gulfraz, M. Irshad, Agro-industrial lignocellulosic biomass a key to unlock the future bio-energy: a brief review, J Radiat Res Appl Sci 7 (2014) 163–173. https://doi.org/10.1016/j.jrras.2014.02.003.

[41] D. Fougere, S. Nanda, K. Clarke, J.A. Kozinski, K. Li, Effect of acidic pretreatment on the chemistry and distribution of lignin in aspen wood and wheat straw substrates, Biomass Bioenergy 91 (2016) 56–68. https://doi.org/10.1016/j.biombioe.2016.03.027.

[42] F. Shafizadeh, P.P.S. Chin, Thermal deterioration of wood, ACS Publications (1977). https://doi.org/10.1021/bk-1977-0043.ch005.

[43] R.H. White, Effect of lignin content and extractives on the higher heating value of wood, Wood and Fiber Science (1987) 446–452.

[44] A. Agarwal, M. Rana, J.-H. Park, Advancement in technologies for the depolymerization of lignin, Fuel Processing Technology 181 (2018) 115–132. https://doi.org/10.1016/j.fuproc.2018.09.017.

[45] V.V. Andhalkar, D. Montané, F. Medina, M. Constantí, Biorefinery design with combined deacetylation and microwave pretreatment for enhanced production of polyhydroxyalkanoates and efficient carbon utilization from lignocellulose, Chemical Engineering Journal 486 (2024) 149754. https://doi.org/10.1016/j.cej.2024.149754.

[46] Y. Tong, T. Yang, J. Wang, B. Li, Y. Zhai, R. Li, A review on the overall process of lignin to phenolic compounds for chemicals and fuels: from separation and extraction of lignin to transformation, J Anal Appl Pyrolysis (2024) 106663. https://doi.org/10.1016/j.jaap.2024.106663.

[47] H. Kaur, D. Goyal, Lignin extraction from lignocellulosic biomass and its valorization to therapeutic phenolic compounds, J Environ Manage 372 (2024) 123334. https://doi.org/10.1016/j.jenvman.2024.123334.

[48] I. Burgert, E. Zürich, Werkstoffe I Teil 2-Holz und Holzwerkstoffe Bauingenieurwissenschaften-Bachelor, Skript zur Vorlesung, (n.d).

[49] L.T. Fan, Y.-H. Lee, M.M. Gharpuray, The nature of lignocellulosics and their pretreatments for enzymatic hydrolysis, in: Microbial Reactions, Springer, (2005) 157–187. https://doi.org/10.1007/3540116982_4.

[50] S. V Vassilev, D. Baxter, L.K. Andersen, C.G. Vassileva, T.J. Morgan, An overview of the organic and inorganic phase composition of biomass, Fuel 94 (2012) 1–33. https://doi.org/10.1016/j.fuel.2011.09.030.

[51] S. Nanda, P. Mohanty, K.K. Pant, S. Naik, J.A. Kozinski, A.K. Dalai, Characterization of North American lignocellulosic biomass and biochars in terms of their candidacy for alternate renewable fuels, Bioenergy Res 6 (2013) 663–677. https://doi.org/10.1007/s12155-012-9281-4.

[52] N. Afanasjeva, L.C. Castillo, J.C. Sinisterra, Biomasa Lignocelulósica. Parte I: Transformación de biomasa, J. Sci. Technol. Appl 3 (2017) 27–43.

[53] Rueda, A. Padró, J.M. Grau, H. Sixto, C. Villar, J.L. García Caballero, F. Martínez Sierra, M. Aránzazu Prada, V. Garavilla, A. de Lucas, Clones de chopos del Catálogo Nacional de Materiales de Base, Consejería de Fomento y Medio Ambiente, Junta de Castilla y León. Valladolid. Versión Febrero De (2016).

[54] E. Pannacci, S. Bartolini, G. Covarelli, Evaluation of four poplar clones in a short rotation forestry in Central Italy, Italian Journal of Agronomy 4 (2009) 191–198. https://doi.org/10.4081/ija.2009.4.191.

[55] G. Di Matteo, P. Nardi, S. Verani, G. Sperandio, Physiological adaptability of Poplar clones selected for bioenergy purposes under non-irrigated and suboptimal site conditions: A case study in Central Italy, Biomass Bioenergy 81 (2015) 183–189.

[56] H. Sixto, J. Salvia, M. Barrio, M.P. Ciria, I. Cañellas, Genetic variation and genotype-environment interactions in short rotation Populus plantations in southern Europe, New For (Dordr) 42 (2011) 163–177. https://doi.org/10.1007/s11056-010-9244-6.

[57] J. Plaza del Pino, Evaluación de la capacidad de rebrote en clones híbridos de Populus destinados a la producción de biomasa para energía., 2011. https://oa.upm.es/10909/2/PFC_JAVIER_PLAZA_DEL_PINO_a.pdf (accessed February 1, 2025).

[58] G. Fontenla-Razzetto, F.T. Wahren, D. Heilig, B. Heil, G. Kovacs, K.-H. Feger, S. Julich, Water Use of Hybrid Poplar (Populus deltoides Bart. ex Marsh x P. nigra L. “AF2”) Growing Across Contrasting Site and Groundwater Conditions in Western Slovakia, Bioenergy Res 16 (2023) 379–397. https://doi.org/10.1007/s12155-022-10445-x.

[59] H. Schroeder, Poplar clones differ in their resistance against insects feeding, (2016). https://doi.org/10.3220/LBF1534394196000.

[60] N. Oliveira, R. Rodríguez-Soalleiro, C. Pérez-Cruzado, I. Cañellas, H. Sixto, R. Ceulemans, Above-and below-ground carbon accumulation and biomass allocation in poplar short rotation plantations under Mediterranean conditions, For Ecol Manage 428 (2018) 57–65. https://doi.org/10.1016/j.foreco.2018.06.031.

[61] A. Fuertes, N. Oliveira, I. Cañellas, H. Sixto, R. Rodríguez-Soalleiro, M. Hanewinkel, D. Sperlich, Assessing the potential of poplar short rotation plantations to contribute to a low-carbon bioeconomy under water-limited conditions, J Environ Manage 347 (2023) 119062. https://doi.org/10.1016/j.jenvman.2023.119062.

[62] M.B. Folgueras, J.M. Gómez-Martín, M.A. Diez, How height-related variations in hybrid poplars affect composition and pyrolytic behaviour: The key role of lignin maturity during woody-biomass pyrolysis, J Anal Appl Pyrolysis 169 (2023) 105861. https://doi.org/10.1016/j.jaap.2023.105861.

[63] D. Cantero, R. Jara, A. Navarrete, L. Pelaz, J. Queiroz, S. Rodríguez-Rojo, M.J. Cocero, Pretreatment processes of biomass for biorefineries: current status and prospects, Annu Rev Chem Biomol Eng 10 (2019) 289–310. https://doi.org/10.1146/annurev-chembioeng-060718-030354.

[64] S.I. Mussatto, Biomass fractionation technologies for a lignocellulosic feedstock based biorefinery, Elsevier, (2016).

[65] M. Galbe, O. Wallberg, Pretreatment for biorefineries: a review of common methods for efficient utilisation of lignocellulosic materials, Biotechnol Biofuels 12 (2019) 294. https://doi.org/10.1186/s13068-019-1634-1.

[66] F. Monlau, A. Barakat, E. Trably, C. Dumas, J.-P. Steyer, H. Carrère, Lignocellulosic materials into biohydrogen and biomethane: impact of structural features and pretreatment, Crit Rev Environ Sci Technol 43 (2013) 260–322. .

[67] L. Zhu, J.P. O'Dwyer, V.S. Chang, C.B. Granda, M.T. Holtzapple, Structural features affecting biomass enzymatic digestibility, Bioresour Technol 99 (2008) 3817–3828. https://doi.org/10.1016/j.biortech.2007.07.033.

[68] A. Barakat, H. de Vries, X. Rouau, Dry fractionation process as an important step in current and future lignocellulose biorefineries: A review, Bioresour Technol 134 (2013) 362–373. https://doi.org/10.1016/J.BIORTECH.2013.01.169.

[69] S.H. Mood, A.H. Golfeshan, M. Tabatabaei, G.S. Jouzani, G.H. Najafi, M. Gholami, M. Ardjmand, Lignocellulosic biomass to bioethanol, a comprehensive review with a focus on pretreatment, Renewable and Sustainable Energy Reviews 27 (2013) 77–93. https://doi.org/10.1016/j.rser.2013.06.033.

[70] H.P. Vu, L.N. Nguyen, M.T. Vu, M.A.H. Johir, R. McLaughlan, L.D. Nghiem, A comprehensive review on the framework to valorise lignocellulosic biomass as biorefinery feedstocks, Science of the Total Environment 743 (2020) 140630. https://doi.org/10.1016/j.scitotenv.2020.140630.

[71] U. Brémond, R. de Buyer, J.-P. Steyer, N. Bernet, H. Carrere, Biological pretreatments of biomass for improving biogas production: an overview from lab scale to full-scale, Renewable and Sustainable Energy Reviews 90 (2018) 583–604. https://doi.org/10.1016/j.rser.2018.03.103.

[72] A.R. Mankar, A. Pandey, A. Modak, K.K. Pant, Pretreatment of lignocellulosic biomass: A review on recent advances, Bioresour Technol 334 (2021) 125235. https://doi.org/10.1016/J.BIORTECH.2021.125235.

[73] B. Kumar, N. Bhardwaj, K. Agrawal, V. Chaturvedi, P. Verma, Current perspective on pretreatment technologies using lignocellulosic biomass: An emerging biorefinery concept, Fuel Processing Technology 199 (2020) 106244. https://doi.org/10.1016/j.fuproc.2019.106244.

[74] C. Yin, Microwave-assisted pyrolysis of biomass for liquid biofuels production, Bioresour Technol 120 (2012) 273–284. https://doi.org/10.1016/j.biortech.2012.06.016.

[75] G.D. Stefanidis, A.N. Muñoz, G.S.J. Sturm, A. Stankiewicz, A helicopter view of microwave application to chemical processes: reactions, separations, and equipment concepts, Reviews in Chemical Engineering 30 (2014) 233–259. https://doi.org/10.1515/revce-2013-0033.

[76] M. Regier, H. Schubert, Microwave processing, Thermal Technologies in Food Processing (2001) 178–207.

[77] Y. Niu, A. Rogiewicz, C. Wan, M. Guo, F. Huang, B.A. Slominski, Effect of microwave treatment on the efficacy of expeller pressing of Brassica napus rapeseed and Brassica juncea mustard seeds, J Agric Food Chem 63 (2015) 3078–3084. https://doi.org/10.1021/jf504872x.

[78] M.W. Easson, B. Condon, B.S. Dien, L. Iten, R. Slopek, M. Yoshioka-Tarver, A. Lambert, J. Smith, The application of ultrasound in the enzymatic hydrolysis of switchgrass, Appl Biochem Biotechnol 165 (2011) 1322–1331. https://doi.org/10.1007/s12010-011-9349-1.

[79] J. Luo, Z. Fang, R.L. Smith Jr, Ultrasound-enhanced conversion of biomass to biofuels, Prog Energy Combust Sci 41 (2014) 56–93. https://doi.org/10.1016/j.pecs.2013.11.001.

[80] M. Ashokkumar, The characterization of acoustic cavitation bubbles–an overview, Ultrason Sonochem 18 (2011) 864–872. https://doi.org/10.1016/j.ultsonch.2010.11.016.

[81] W. Den, V.K. Sharma, M. Lee, G. Nadadur, R.S. Varma, Lignocellulosic biomass transformations via greener oxidative pretreatment processes: access to energy and value-added chemicals, Front Chem 6 (2018) 141. https://doi.org/10.3389/fchem.2018.00141.

[82] A.L. Woiciechowski, C.J.D. Neto, L.P. de Souza Vandenberghe, D.P. de Carvalho Neto, A.C.N. Sydney, L.A.J. Letti, S.G. Karp, L.A.Z. Torres, C.R. Soccol, Lignocellulosic biomass: Acid and alkaline pretreatments and their effects on biomass recalcitrance–Conventional processing and recent advances, Bioresour Technol 304 (2020) 122848. https://doi.org/10.1016/j.biortech.2020.122848.

[83] F. Hu, A. Ragauskas, Pretreatment and lignocellulosic chemistry, Bioenergy Res 5 (2012) 1043–1066. https://doi.org/10.1007/s12155-012-9208-0.

[84] J. Chen, X. Ma, M. Liang, Z. Guo, Y. Cai, C. Zhu, Z. Wang, S. Wang, J. Xu, H. Ying, Physical–Chemical–Biological Pretreatment for Biomass Degradation and Industrial Applications: A Review, in: Waste, MDPI, (2024) 451–473. https://doi.org/10.3390/waste2040024.

[85] W.Y. Cheah, R. Sankaran, P.L. Show, T. Ibrahim, T.N. Baizura, K.W. Chew, A. Culaba, J.-S. Chang, Pretreatment methods for lignocellulosic biofuels production: current advances, challenges and future prospects, Biofuel Research Journal 7 (2020) 1115–1127.

[86] N. Brosse, M.H. Hussin, A.A. Rahim, Organosolv processes, Biorefineries (2019) 153–176. https://doi.org/10.1007/10_2016_61.

[87] N. Brosse, M.N. Mohamad Ibrahim, A. Abdul Rahim, Biomass to bioethanol: initiatives of the future for lignin, Int Sch Res Notices 2011 (2011) 461482. https://doi.org/10.5402/2011/461482.

[88] A.K. Kumar, S. Sharma, Recent updates on different methods of pretreatment of lignocellulosic feedstocks: a review, Bioresour Bioprocess 4 (2017) 7. https://doi.org/10.1186/s40643-017-0137-9.

[89] Q. Zhang, J. Hu, D.-J. Lee, Pretreatment of biomass using ionic liquids: research updates, Renew Energy 111 (2017) 77–84. https://doi.org/10.1016/j.renene.2017.03.093.

[90] Y. Feng, Q. Li, G. Kang, G. Ji, Y. Tang, J. Tu, Aqueous two-phase/reverse micelle continuous process for recycling and simultaneous purification of polar ionic liquid from enzymatic hydrolysate, Journal of Chemical Technology & Biotechnology 91 (2016) 394–399. https://doi.org/10.1002/jctb.4587.

[91] E. Pereira, D.T.V. Pereira, S.C. Rabelo, R. Ceriani, A.C. da Costa, Green solvent pretreatments for lignocellulosic biorefineries: A review, J Environ Chem Eng (2025) 115303. https://doi.org/10.1016/j.jece.2024.115303.

[92] H. Chen, J. Liu, X. Chang, D. Chen, Y. Xue, P. Liu, H. Lin, S. Han, A review on the pretreatment of lignocellulose for high-value chemicals, Fuel Processing Technology 160 (2017) 196–206. https://doi.org/10.1016/j.fuproc.2016.12.007.

[93] B. Basak, R. Kumar, A.S. Bharadwaj, T.H. Kim, J.R. Kim, M. Jang, S.-E. Oh, H.-S. Roh, B.-H. Jeon, Advances in physicochemical pretreatment strategies for lignocellulose biomass and their effectiveness in bioconversion for biofuel production, Bioresour Technol 369 (2023) 128413. https://doi.org/10.1016/j.biortech.2022.128413.

[94] S. Meenakshisundaram, A. Fayeulle, E. Leonard, C. Ceballos, A. Pauss, Fiber degradation and carbohydrate production by combined biological and chemical/physicochemical pretreatment methods of lignocellulosic biomass–a review, Bioresour Technol 331 (2021) 125053. https://doi.org/10.1016/j.biortech.2021.125053.

[95] N. Mosier, C. Wyman, B. Dale, R. Elander, Y.Y. Lee, M. Holtzapple, M. Ladisch, Features of promising technologies for pretreatment of lignocellulosic biomass, Bioresour Technol 96 (2005) 673–686. https://doi.org/10.1016/j.biortech.2004.06.025.

[96] M.-K. Bahng, C. Mukarakate, D.J. Robichaud, M.R. Nimlos, Current technologies for analysis of biomass thermochemical processing: A review, Anal Chim Acta 651 (2009) 117–138. https://doi.org/10.1016/j.aca.2009.08.016.

[97] R. Singh, B.B. Krishna, G. Mishra, J. Kumar, T. Bhaskar, Strategies for selection of thermo-chemical processes for the valorisation of biomass, Renew Energy 98 (2016) 226–237. https://doi.org/10.1016/j.renene.2016.03.023.

[98] J. Santos, H. Jahangiri, M.A. Bashir, A. Hornung, M. Ouadi, The upgrading of bio-oil from the intermediate pyrolysis of waste biomass using steel slag as a catalyst, ACS Sustain Chem Eng 8 (2020) 18420–18432. https://doi.org/10.1021/acssuschemeng.0c05536.

[99] S. Jha, S. Nanda, B. Acharya, A.K. Dalai, A review of thermochemical conversion of waste biomass to biofuels, Energies (Basel) 15 (2022) 6352. https://doi.org/10.3390/en15176352.

[100] S.Y. Lee, R. Sankaran, K.W. Chew, C.H. Tan, R. Krishnamoorthy, D.-T. Chu, P.-L. Show, Waste to bioenergy: a review on the recent conversion technologies, BMC Energy 1 (2019) 4. https://doi.org/10.1186/s42500-019-0004-7.

[101] T. Kan, V. Strezov, T.J. Evans, Lignocellulosic biomass pyrolysis: A review of product properties and effects of pyrolysis parameters, Renewable and Sustainable Energy Reviews 57 (2016) 1126–1140. https://doi.org/10.1016/J.RSER.2015.12.185.

[102] G. Wang, Y. Dai, H. Yang, Q. Xiong, K. Wang, J. Zhou, Y. Li, S. Wang, A review of recent advances in biomass pyrolysis, Energy & Fuels 34 (2020) 15557–15578. https://doi.org/10.1021/acs.energyfuels.0c03107.

[103] V. Dhyani, T. Bhaskar, A comprehensive review on the pyrolysis of lignocellulosic biomass, Renew Energy 129 (2018) 695–716. https://doi.org/10.1016/J.RENENE.2017.04.035.

[104] M.F. Demirbas, M. Balat, Biomass pyrolysis for liquid fuels and chemicals: A review, (2007).

[105] M. Balat, M. Balat, E. Kirtay, H. Balat, Main routes for the thermo-conversion of biomass into fuels and chemicals. Part 1: Pyrolysis systems, Energy Convers Manag 50 (2009) 3147–3157. https://doi.org/10.1016/J.ENCONMAN.2009.08.014.

[106] A. Demirbas, G. Arin, An overview of biomass pyrolysis, Energy Sources 24 (2002) 471–482. https://doi.org/10.1080/00908310252889979.

[107] S. Jha, J.A. Okolie, S. Nanda, A.K. Dalai, A review of biomass resources and thermochemical conversion technologies, Chem Eng Technol 45 (2022) 791–799. https://doi.org/10.1002/ceat.202100503.

[108] A. V. Bridgwater, Review of fast pyrolysis of biomass and product upgrading, Biomass Bioenergy 38 (2012) 68–94. https://doi.org/10.1016/J.BIOMBIOE.2011.01.048.

[109] M.I. Jahirul, M.G. Rasul, A.A. Chowdhury, N. Ashwath, Biofuels production through biomass pyrolysis—a technological review, Energies (Basel) 5 (2012) 4952–5001. https://doi.org/10.3390/en5124952.

[110] J. Akhtar, N. Saidina Amin, A review on operating parameters for optimum liquid oil yield in biomass pyrolysis, Renewable and Sustainable Energy Reviews 16 (2012) 5101–5109. https://doi.org/10.1016/J.RSER.2012.05.033.

[111] M. Tripathi, J.N. Sahu, P. Ganesan, Effect of process parameters on production of biochar from biomass waste through pyrolysis: A review, Renewable and Sustainable Energy Reviews 55 (2016) 467–481. https://doi.org/10.1016/J.RSER.2015.10.122.

[112] K. Kebelmann, A. Hornung, U. Karsten, G. Griffiths, Intermediate pyrolysis and product identification by TGA and Py-GC/MS of green microalgae and their extracted protein and lipid components, Biomass Bioenergy 49 (2013) 38–48. https://doi.org/10.1016/J.BIOMBIOE.2012.12.006.

[113] G. Chen, J. Andries, H. Spliethoff, Catalytic pyrolysis of biomass for hydrogen rich fuel gas production, Energy Convers Manag 44 (2003) 2289–2296. https://doi.org/10.1016/S0196-8904(02)00254-6.

[114] S.D. Stefanidis, K.G. Kalogiannis, E.F. Iliopoulou, C.M. Michailof, P.A. Pilavachi, A.A. Lappas, A study of lignocellulosic biomass pyrolysis via the pyrolysis of cellulose, hemicellulose and lignin, J Anal Appl Pyrolysis 105 (2014) 143–150. https://doi.org/10.1016/J.JAAP.2013.10.013.

[115] R. Fahmi, A. V Bridgwater, I. Donnison, N. Yates, J.M. Jones, The effect of lignin and inorganic species in biomass on pyrolysis oil yields, quality and stability, Fuel 87 (2008) 1230–1240. https://doi.org/10.1016/j.fuel.2007.07.026.

[116] R. Fahmi, A. V Bridgwater, L.I. Darvell, J.M. Jones, N. Yates, S. Thain, I.S. Donnison, The effect of alkali metals on combustion and pyrolysis of Lolium and Festuca grasses, switchgrass and willow, Fuel 86 (2007) 1560–1569. https://doi.org/10.1016/j.fuel.2006.11.030.

[117] G. Jayme, E. Roffael, Einfluss von Natriumhyroxidlösungen verschiedener Konzentration auf die Feinstruktur und die Reaktivität der Cellulose, Das Papier 23 (1969) 405–412.

[118] C. Hutterer, G. Schild, A. Potthast, A precise study on effects that trigger alkaline hemicellulose extraction efficiency, Bioresour Technol 214 (2016) 460–467. https://doi.org/10.1016/j.biortech.2016.04.114.

[119] D.M. de Carvalho, O. Sevastyanova, J.H. de Queiroz, J.L. Colodette, Cold alkaline extraction as a pretreatment for bioethanol production from eucalyptus, sugarcane bagasse and sugarcane straw, Energy Convers Manag 124 (2016) 315–324. https://doi.org/10.1016/J.ENCONMAN.2016.07.029.

[120] S. Ghahramani, S. Hedjazi, S. Izadyar, S. Fischer, A. Abdulkhani, Influence of different pulping processes, cold caustic extraction, and bleaching as common post-treatments on properties of produced lignocellulose nanocrystals (LCNCs) from bagasse, Int J Biol Macromol (2025) 141448. https://doi.org/10.1016/J.IJBIOMAC.2025.141448.

[121] H. Cheng, H. Zhan, S. Fu, L.A. Lucia, Alkali extraction of hemicellulose from depithed corn stover and effects on soda-AQ pulping, Bioresources 6 (2011) 196–206.

[122] M.T. García, A. Alfaro, J.C. Garcia, M.A.M. Zamudio, A.B. Morales, F. López, Obtainment of hemicellulose derivatives and cellulose pulp from wheat straw following cold alkaline extraction, Cellul Chem Technol 51 (2017) 465–475.

[123] J. Li, S. Zhang, H. Li, X. Ouyang, L. Huang, Y. Ni, L. Chen, Cellulase pretreatment for enhancing cold caustic extraction-based separation of hemicelluloses and cellulose from cellulosic fibers, Bioresour Technol 251 (2018) 1–6. https://doi.org/10.1016/J.BIORTECH.2017.12.026.

[124] J. Li, H. Hu, H. Li, L. Huang, L. Chen, Y. Ni, Kinetics and mechanism of hemicelluloses removal from cellulosic fibers during the cold caustic extraction process, Bioresour Technol 234 (2017) 61–66. https://doi.org/10.1016/J.BIORTECH.2017.03.026.

[125] H. Sixta, Handbook of pulp, 2 volume set, John Wiley & Sons, 2006.

[126] X. Dou, Y. Tang, The Influence of Cold Caustic Extraction on the Purity, Accessibility and Reactivity of Dissolving-Grade Pulp, ChemistrySelect 2 (2017) 11462–11468. https://doi.org/10.1002/slct.201701551.

[127] H.A. Krässig, H.A. Krässig, H.A. Krässig, Cellulose: structure, accessibility and reactivity. 1993, Yverdon, Switzerland: Gordon and Beach Science Publishers (n.d.) 167–169.

[128] S. McIntosh, T. Vancov, Optimisation of dilute alkaline pretreatment for enzymatic saccharification of wheat straw, Biomass Bioenergy 35 (2011) 3094–3103. https://doi.org/10.1016/j.biombioe.2011.04.018.

[129] F. Peng, J.-L. Ren, F. Xu, J. Bian, P. Peng, R.-C. Sun, Comparative study of hemicelluloses obtained by graded ethanol precipitation from sugarcane bagasse, J Agric Food Chem 57 (2009) 6305–6317. https://doi.org/10.1021/jf900986b.

[130] J.C. García, M.J. Díaz, M.T. Garcia, M.J. Feria, D.M. Gómez, F. López, Search for optimum conditions of wheat straw hemicelluloses cold alkaline extraction process, Biochem Eng J 71 (2013) 127–133. https://doi.org/10.1016/j.bej.2012.12.008.

[131] Y.C. Park, J.S. Kim, Comparison of various alkaline pretreatment methods of lignocellulosic biomass, Energy 47 (2012) 31–35. https://doi.org/10.1016/j.energy.2012.08.010.

[132] J. Li, Y. Liu, C. Duan, H. Zhang, Y. Ni, Mechanical pretreatment improving hemicelluloses removal from cellulosic fibers during cold caustic extraction, Bioresour Technol 192 (2015) 501–506. https://doi.org/10.1016/J.BIORTECH.2015.06.011.

[133] Q. Sun, G. Yang, J. Chen, M. He, S. Niu, Effect of ultrasonic-assisted cold caustic extraction on the properties of ctmp poplar fibers, 펄프· 종이기술 49 (2017) 5–15. http://dx.doi.org/10.7584/JKTAPPI.2017.08.49.4.5.

CAPÍTULO 2

Objetivos y Plan de Trabajo



2. Objetivos.

El concepto de biorrefinería ha ganado un gran interés como una de las estrategias más prometedoras para hacer frente al agotamiento de los recursos fósiles y mitigar los efectos del cambio climático. Las biorrefinerías permiten avanzar hacia la descarbonización mediante la producción de bioproductos y biocombustibles que pueden sustituir parcial o totalmente a los derivados del petróleo. Sin embargo, a escala industrial, su éxito comercial sigue siendo limitado, en gran parte debido a la irregularidad en el suministro de la biomasa.

En este contexto, los cultivos energéticos de alta productividad y corta rotación representan una alternativa viable para garantizar un suministro estable y sostenible de biomasa. En esta línea, la presente Tesis Doctoral se centra en la valorización del clon AF2 de *Populus x euramericana* como recurso lignocelulósico para aplicaciones en biorrefinería.

2.1. Objetivo General.

Así, el objetivo principal de esta Tesis Doctoral es evaluar el potencial del clon AF2 de *Populus x euramericana*, un taxón de alta producción de biomasa, en el marco de un esquema de biorrefinería lignocelulósica.

Esta investigación se enmarca en las líneas de trabajo del grupo de investigación en **Tecnologías de Recursos Renovables y Contaminación Ambiental** (PAIDI RNM-371), adscrito al **Centro de investigación en Tecnología de Productos y Procesos (Pro^{2}TecS)**, del Departamento de Ingeniería Química, Química Física y Ciencia de los Materiales de la Universidad de Huelva.

La presente tesis se ha desarrollado en el contexto del **Programa de Doctorado en Ciencia y Tecnología Industrial y Ambiental**, perteneciente a la Escuela de Doctorado de la Universidad de Huelva, concretamente dentro de la línea de investigación de **Biorrefinería Industrial y Tecnología forestal**.

El trabajo ha sido financiado y conceptualizado en el marco del proyecto del Ministerio de Ciencia e Innovación: ***Residuos Forestales Y Especies De Maderas Duras De Alta Productividad. Biorrefinería Hidrolítica Y Termoquímica Para La Obtención De Productos Químicos De Valor Añadido*** **(PID2020-112875RB-C21)**. Inicialmente, estos estudios de doctorado fueron impulsados por el proyecto FEDER/Agencia IDEA-Consejería de Economía, Conocimiento, Empresa y Universidad de la Junta de Andalucía: ***Unidad de Innovación Conjunta sobre Valorización de residuos agroforestales en materiales y tecnologías de construcción avanzados*** **(UIC-GREEN ASPHALT, 802C1800001).**

Cabe destacar la colaboración del grupo de investigación en **Análisis y Planificación del Medio Natural** del departamento de Ciencias Agroforestales de la Universidad de Huelva, especialmente en lo referente al suministro y disposición de las materias primas empleadas durante todo el proceso experimental.

2.2. Objetivos Específicos.

Dentro del marco del objetivo general de la presente Tesis Doctoral, se han planteado los siguientes objetivos específicos, que estructuran y dan contenido a los distintos apartados del capítulo de resultados:

- Optimizar la etapa de extracción de derivados hemicelulósicos a partir de distintas especies lignocelulósicas: una especie herbácea (hierba elefante) y dos taxones leñosos (clon AF2 de *Populus x euramericana* y *Robinia pseudoacacia*), mediante extracción alcalina en frío asistida por ultrasonidos.
- Evaluar y optimizar una segunda etapa de tratamiento termoquímico centrada en el clon AF2 de *Populus x euramericana*, posterior a la extracción alcalina en frío. Cuantificar el grado de conversión de las fases sólidas, realizar un análisis cinético para la evolución de la energía de activación y optimizar la producción de hidrógeno.
- Estudiar y optimizar las condiciones del proceso de deslignificación organosolv aplicado a la madera del clon AF2 de *Populus x euramericana* tras la etapa alcalina, evaluando el efecto catalítico del medio básico residual. Comparar los resultados con un proceso organosolv convencional (sin alcalinidad previa) y analizar las propiedades fisicoquímicas de las pulpas obtenidas.
- Analizar y caracterizar las ligninas obtenidas mediante ambos enfoques del proceso organosolv (alcalino y convencional), con el fin de evaluar su composición, estructura y estabilidad térmica.
- Evaluar el efecto del pretratamiento de explosión de vapor (steam explosion) sobre el clon AF2 de *Populus x euramericana* orientado a la obtención de compuestos bioactivos mediante el empleo de disolventes verdes. Además, estudiar la posterior hidrólisis enzimática de los pretratados, tras su desintoxicación para mejorar la eficiencia del proceso.
- Comparar el comportamiento termoquímico de las principales fracciones de biomasa lignocelulósica, obtenidas a partir de diferentes especies y métodos de fraccionamiento. Realizar un análisis cinético, estimar la energía de activación y estudiar la composición de los gases generados durante el proceso de pirólisis.

2.3. Plan de trabajo.

Con el propósito de alcanzar los objetivos específicos planteados y desarrollar el objetivo general de la presente Tesis Doctoral, se ha diseñado un plan de trabajo compuesto por seis actividades principales, cada una de las cuales está respaldada por un conjunto de tareas. Estas actividades se presentan a continuación, estructuradas de manera secuencial y complementaria, garantizando así el desarrollo de la investigación.

Actividades principales:

1. Selección y caracterización de materias primas lignocelulósicas.
2. Optimización del proceso de extracción alcalina en frío (EAF).
3. Estudio termoquímico de los sólidos procedentes de la EAF.
4. Aplicación de una segunda etapa de fraccionamiento mediante un proceso organosolv, tras la etapa previa de EAF.
5. Evaluación del pretratamiento por explosión de vapor y extracción con disolventes verdes.
6. Estudio termoquímico de las principales fracciones lignocelulósicas.

Tareas:

A continuación, se detallan las tareas asociadas a cada una de las actividades principales del plan de trabajo:

1. Selección y caracterización de materias primas.

1.1. Caracterización de las materias primas conforme a normas y estándares internacionalmente aceptadas.

1.2. Evaluación y selección de especies vegetales lignocelulósicas, con especial atención en especies de rápido crecimiento y alta disponibilidad, en colaboración con el departamento de Ciencias Agroforestales de la Universidad de Huelva.

2. Optimización del proceso de extracción alcalina en frío (EAF).

2.1. Optimización del proceso de extracción alcalina en frío sobre la hierba elefante (*Pennisetum Purpureum Schum*).

2.2. Optimización y estudio comparativo de la aplicación combinada de EAF y ultrasonidos sobre el clon AF2 de *Populus x euramericana* y *Robinia pseudoacacia.*

3. Estudio termoquímico de los sólidos post-EAF.

3.1. Estudio cinético del proceso de pirólisis mediante termogravimetría (TGA) de los sólidos obtenidos tras la EAF aplicada al clon AF2.

3.2. Evaluación del hidrógeno generado durante el proceso de pirólisis.

4. Aplicación de una segunda etapa organosolv.

4.1. Optimización del proceso organosolv del clon AF2 previamente tratado con EAF.

4.2. Estudio comparativo entre el proceso organosolv y la versión combinada con pretratamiento alcalino.

4.3. Análisis estructural y evaluación de la estabilidad térmica de las ligninas obtenidas mediante el proceso organosolv como del proceso combinado con pretratamiento alcalino.

5. Pretratamiento por explosión de vapor y disolventes verdes.

5.1. Influencia de las variables del proceso de explosión de vapor en el tratamiento del clon AF2 *Populus x euramericana*.

5.2. Evaluación del efecto de distintos disolventes verdes sobre la reducción de compuestos inhibidores.

5.3. Estudio de la eficacia de la hidrólisis enzimática en función del disolvente empleado y protocolo de lavado.

5.4. Análisis y cuantificación de compuestos bioactivos extraídos.

6. Estudio termoquímico de fracciones lignocelulósicas.

6.1. Aplicación de distintos tratamientos de fraccionamiento a tres especies lignocelulósicas para la obtención de celulosa, hemicelulosa y lignina.

6.2. Estudio cinético y efectos de cada método de fraccionamiento sobre la evolución de la energía de activación del proceso de pirólisis.

6.3. Análisis de gases generados en la descomposición térmica.

CAPÍTULO 3

Resultados y Discusión



3.1. Extracción Alcalina en frío.

El fraccionamiento de la biomasa lignocelulósica ha despertado un creciente interés debido a su potencial para producir productos de alto valor añadido, así como para generar energía a partir de una fuente renovable.

La fracción con menor resistencia a la hidrólisis es la hemicelulosa, cuya fragmentación permite iniciar un esquema de biorrefinería operando en condiciones suaves. Como se mencionó en la introducción de esta tesis doctoral, las hemicelulosas representan entre el 15% y el 30% del contenido de la biomasa, dependiendo del tipo específico. Además, esta fracción presenta una amplia gama de aplicaciones en industrias como la papelera, alimentaria, farmacéutica, química, etc., como en su aplicación en la producción de aditivos alimenticios.

Debido al creciente interés en aislar hemicelulosas mediante métodos selectivos que eviten su degradación, actualmente está en permanente estudio diversos tratamientos. Uno de los más prometedores es la extracción alcalina en frío (EAF), que permite operar a temperaturas inferiores a 40 ºC, lo que simplifica el diseño de los reactores al requerir bajas presiones, además de ofrecer ahorros energéticos y económicos, y minimizar la degradación de las hemicelulosas. Sin embargo, su efectividad depende en gran medida del tipo de biomasa seleccionada, por lo general suele ser más efectiva en biomasas herbáceas que en madereras.

En el marco de esta tesis doctoral, se ha aplicado este tratamiento a tres tipos de biomasa: una especie herbácea, la hierba elefante, y dos taxones de alta productividad, el clon AF2 de *Populus x euramericana* y *Robinia pseudoacacia*. A continuación, se presentan los resultados obtenidos para cada una de estas especies.

3.1.1. Extracción Alcalina en Frío de Hierba Elefante.

Los resultados obtenidos en este estudio se detallan en el artículo: **Cold Alkaline Extraction Of Elephant Grass For Optimal Subsequent Extraction Of Hemicelluloses And Energy Production.** J.C. García, A. Alfaro, J.M. Loaiza, S. Lozano-Calvo & F. López. Biomass Conversion and Biorefinery, 14(7), 8307-8320. (**Publicación 1**).

A continuación, se proporciona un resumen conciso y una contextualización de la presente aportación.

En el contexto de la búsqueda de recursos alternativos para mitigar los efectos negativos del uso de recursos fósiles y no renovables, están ganando un gran interés las especies bioenergéticas. Destacando las fuentes de biomasa de segunda generación, como los cultivos energéticos y las gramíneas perennes.

Pennisetum Purpureum Schum., comúnmente conocida como hierba elefante, es una gramínea perenne de la familia *Poaceae* que se caracteriza por su rápido crecimiento, sus bajas demandas de recursos y su capacidad de adaptación a diversos climas, resistiendo a sequías y generando altos rendimientos de biomasa en suelos marginales. Los rendimientos promedios de esta gramínea oscilan entre 30 y 40 toneladas métricas por hectárea al año, con ciclos de crecimiento rápidos que permiten entre tres y cuatro cultivos anuales. Además, presenta importantes beneficios ambientales, como su capacidad para secuestrar hasta 40 toneladas de dióxido de carbono por hectárea.

El objetivo principal de este apartado es someter la hierba elefante al tratamiento de extracción alcalina en frío, con el fin de obtener un licor rico en hemicelulosas y un residuo sólido apto para la producción de energía con una mayor eficiencia. Este enfoque sigue los principios de la economía circular y busca optimizar la eficiencia de la hierba elefante como cultivo energético.

La hierba elefante empleada en este estudio fue cultivada experimentalmente en las instalaciones del Departamento de Celulosa y Papel de la Universidad Federal de Viçosa (Minas Gerais, Brasil). Esta biomasa fue caracterizada químicamente, presentando un contenido de celulosa del 41,7% (medido como glucano), un contenido de lignina de 20,9% (suma de lignina soluble y lignina Klason) y un 27,4% de hemicelulosas (compuestas por xilano, arabano, galactano y manano). La determinación de estos azúcares se realizó mediante cromatografía líquida de alta resolución (HPLC), utilizando una columna BioRad Aminex HPX-87H, a 50 ºC, con H_2SO_4 a 0,005 M como fase móvil y un caudal de 0,6 mL min^{-1}, con un detector de índice de refracción. Además, se caracterizó en términos energéticos mediante la determinación de su poder calorífico superior a volumen constante, siguiendo las normas CEN/TS 14.918 (2005) y UNE 16.001 EX (2005), utilizando un calorímetro automático de bomba isoperibol Parr 6300. El poder calorífico superior fue de 18,44 MJ Kg^{-1}.

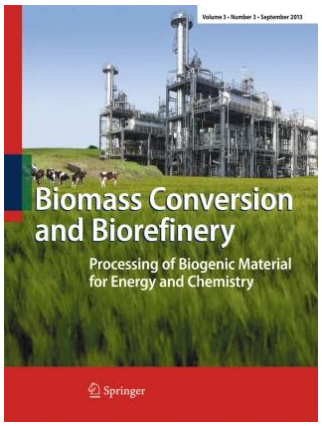
Para el estudio de optimización de las condiciones de extracción alcalina en frio sobre la hierba elefante, se seleccionaron como variables independientes la concentración de hidróxido de sodio, la temperatura y el tiempo de operación, dentro de un diseño experimental de composición central. Las concentraciones de hidróxido de sodio variaron entre 80 g L^{-1} y 120 g L^{-1}, las temperaturas entre 20ºC y 40ºC, y los tiempos de operación entre 30 y 90 minutos. En todos los ensayos se utilizó un hidromódulo (relación líquido/sólido) fijo de 15.

A modo de resumen, las condiciones más favorables y que se consideraron óptimas dentro del diseño experimental en la extracción alcalina en frío sobre la hierba elefante fueron una concentración de hidróxido de sodio de 100 g L^{-1}, una temperatura de 30 ºC y un tiempo de operación de 30 minutos. Estas condiciones incrementaron en un 4% el poder calorífico del sólido residual respecto a la materia prima de partida sin tratar, además de obtener una separación relativamente selectiva de las hemicelulosas frente a la celulosa y lignina, obteniendo en el licor un 30,1% de las hemicelulosas y permaneciendo el 93% y el 82,1% de celulosa y lignina en el sólido, respectivamente.

PUBLICACIÓN 1.

Cold alkaline extraction of Elephant Grass for optimal subsequent extraction of Hemicelluloses and energy production.

J.C. García, A. Alfaro, J.M. Loaiza, S. Lozano-Calvo & F. López.



Biomass Conversion and Biorefinery
Springer
Volumen 14, página 8307-8320, (2024).
DOI:10.1007/s13399-022-03054-3

Categoría	Clasificación revista/Número total de revistas	Cuartil (Porcentaje)
Ingeniería Química	63/170	Q2 (63,2%)
Energía y combustibles	94/171	Q3 (45,3%)
Factor de impacto	3,5	

Cold alkaline extraction of Elephant grass for optimal subsequent extraction of hemicelluloses and energy production.

J. C. García[1] · A. Alfaro[2]✉ · J. M. Loaiza[1] · S. Lozano-Calvo[1] · F. López[1]

✉ A. Alfaro · ascension.alfaro@uhu.es

[1] Research Center in Technology of Products and Chemical Processes, PRO2TECS- Chemical Engineering Department, University of Huelva, Av. 3 de marzo s/n, 21071 Huelva, Spain
[2] Department of Forest Engineering, University of Huelva, Huelva, Spain

Abstract

There is growing scientific and industrial interest in obtaining useful substances by fractionating lignocellulosic biomass from non-food plant crops for use by the bioenergy industry. The primary goals are to ensure process sustainability and to comply with the principles of circular economy. In this work, we optimized energy production from Elephant grass by previously using cold alkaline extraction to remove its hemicellulose fraction. Elephant grass contains a high proportion of lignin (20%) and hemicelluloses (27.4%), and therefore is an excellent alternative to wood materials for energy production by direct burning. Energy production was optimized to identify the best operating conditions among those tested, namely: alkali concentrations of 80–120 g NaOH L^{-1}, temperatures of 20–40 °C, and treatment times of 30–90 min. Using the optimum conditions thus established (viz., 100 g NaOH L^{-1}, 30°C, and 30 min) raised the high heating value (HHV) to 19.151 MJ kg^{-1} (i.e., by 4% relative to the starting material). Also, it allowed the content in elemental C to be preserved, that in H increased by 4.86% and, more environmentally significant, most sulphur (46.9%) to be removed from the solid phase upon treatment. Cold alkaline extraction of the raw material additionally enabled relatively selective separation of the hemicellulose fraction from the cellulose and lignin fractions. Thus, 30.1% of all hemicellulose was dissolved in the treatment liquor and made valorizable while 93.0% of cellulose and 82.1% of lignin present in the raw material remained in the solid phase.

Keywords Biorefinery · Cold alkaline extraction · Elephant grass · Hemicelluloses · Bioenergy

1 Introduction.

Biorefining is becoming increasingly essential to ensure sustainable development, especially when using raw materials based on non-food plants such as perennial grasses, which escape the food versus fuel dilemma [1–3]. In fact, using biomass as a renewable energy source can be useful to fulfil the goals of the current European energy policy, which is increasingly favouring the establishment of sustainable energy crops not compromising food production [4, 5]. A fraction of 17.9% of all energy used in the word in 2018 was obtained from renewable sources—and 67% of it from biomass—2.2% from nuclear power and 79.9% from fossil fuels [6]. The European Union has set the goal that, by 2030, 37% of all energy should be produced from renewable sources [7, 8]. In the process, fossil fuels

https://doi.org/10.1007/s13399-022-03054-3

should be gradually replaced with renewable energy sources to reduce greenhouse gas emissions, diversify energy supply, and alleviate the currently strong dependence on oil markets while creating new jobs, fostering industrial entrepreneurship, and boosting economic growth [9, 10].

Energy from biomass can be used in the traditional manner (i.e., by burning, which uses 57.7% of lignocellulosic biomass) or as "modern bioenergy," which uses the remainder portion of biomass (specifically, 20.8% for industrial heating, 10% for home heating, 8.3% for transportation, and 3.3% for electricity production) [6].

A number of plant species are currently being used for energy production worldwide. Especially prominent among the non-wood species are perennial grasses such as giant reed (*Arundo donax, L.*), miscanthus (*Miscanthus x giganteus*), energy cane (*Saccharum spontaneum hybrids*), switchgrass (*Panicum virgatum L.),* bulbous canary grass (*Phalaris aquatica L.*), elephant grass (*Pennisetum purpureum Schum.*) [11–13], and bagasse from eating sugarcane [14, 15]. These plants are especially suitable for energy production by virtue of their low cropping costs, and also of their ability to grow in a variety of environments or even on marginal land [16]. Also, they produce large amounts of biomass [17], use water and nutrients highly efficiently [18, 19], contain more cellulose and lignin than deciduous species, and have a relatively low moisture content at the end of their growth cycle [2, 20, 21]. Even more important, they have the potential for use on marginal land and hence for improving the social and economic status of some rural areas [22].

Pennisetum purpureum Schum is a perennial grass of the family Poaceae from tropical Africa. Popularly known by the names "Elephant grass," "giant zacate," "fake sugarcane," "Napier grass," "merkeron," "Uganda grass" and "king grass," this plant has traditionally been used as fodder in tropical and subtropical countries. Each plant of Elephant grass has a number of branching stems radiating from the same stand. Its stems can be up to 8 m tall and 2.5 cm thick, and resemble those of sugarcane in appearance [1, 23]. Elephant grass grows well in temperate, subtropical, and tropical regions with a dry season. Also, it can grow in many types of land, but especially on thick, light-textured, well-drained soils [24], as well as on acid soils previously amended with biochar [25]. This species is highly resistant to disease and tolerant of drought [26]. Its ability to grow on contaminated soils has allowed its cropping in engineered wetlands to exploit its phytoremediating effects and use the resulting biomass for ethanol and butanol production [27]. Among others, elephant grass has additionally been used to reclaim water bodies contaminated with high concentrations of arsenic [21].

Like miscanthus and switchgrass, Elephant grass is a C4-type plant whose high photosynthetic efficiency leads to also high lignocellulose production [17, 28–30]. In fact, Elephant grass produces in the region of 45 t dry matter ha^{-1} $year^{-1}$ [1, 23, 31, 32] depending on the particular genotype, soil

https://doi.org/10.1007/s13399-022-03054-3

fertility, and crop management practices. Thus, Basso et al. [33] and Rengsirikul et al. [34] reported yields of 12–150 and 45–67 t ha^{-1} $year^{-1}$, respectively, so high biomass production yields, and the fact that Elephant grass can be harvested up to four times each year, make it especially attractive for energy production [1, 33].

Industrially, Elephant grass has been used to obtain chemicals such as cellulose and xylanase [35], monosaccharides and ethanol [36], xylitol and ethanol [37], hemicelluloses [38, 39], lignin nanoparticles [40], cellulose pulp [32, 41], and corrosion inhibitor extracts [42]. Also, it has been used to obtain fuels such as ethanol [33, 34, 43–45] or methane [24, 46–48], pyrolysis products [34, 49–52], thermal and electrical energy [17, 24, 53–58], and densified solid biofuels [19]. These uses testify to the high potential of Elephant grass for energy production and have fostered research into genetic breeding methods for improving its properties as a raw material and optimizing its use [24, 53, 59–61].

In this scenario, our group envisaged the development of a process for obtaining energy from Elephant grass and using its lignocellulose fraction as a source of chemicals. This is the way biorefining schemes are typically used to fractionate lignocellulosic materials stepwise for optimal use of the ensuing fractions. In this work, we used cold alkaline extraction (CAE) prior to fractionation of Elephant grass on the grounds of its operational and environmental advantages over other alkaline and hydrolysis treatments [26, 62]. The most salient advantage of CAE over alternative biomass fractionation methods is its ability to separate hemicelluloses in a selective manner for their subsequent alcoholic precipitation with minimal degradation to furfural [63–67]. In addition, CAE requires no high temperatures or pressures, and hence uses energy sparingly. In fact, most CAE-based processes are conducted at mild temperatures (20–40 °C) [68]. However, the efficiency of the CAE treatment is strongly dependent on the particular raw material and greater with grassy lignocellulosic materials than with woody plants (i.e., it allows lignocellulose to be more efficiently extracted from grasses) [63, 69–71].

With the aims of ensuring sustainability in the process and complying with the principles of circular economy, in this work, we optimized the efficiency of Elephant grass as an energy crop by subjecting the raw material to cold alkaline extraction in order to remove its hemicellulose fraction in the treatment liquor and use the resulting solid phase for energy production with increased economic and environmental efficiency in the overall process.

https://doi.org/10.1007/s13399-022-03054-3

2 Materials and methods.

Figure 1 shows the sequential scheme of the experimental work carried out with the Elephant grass.

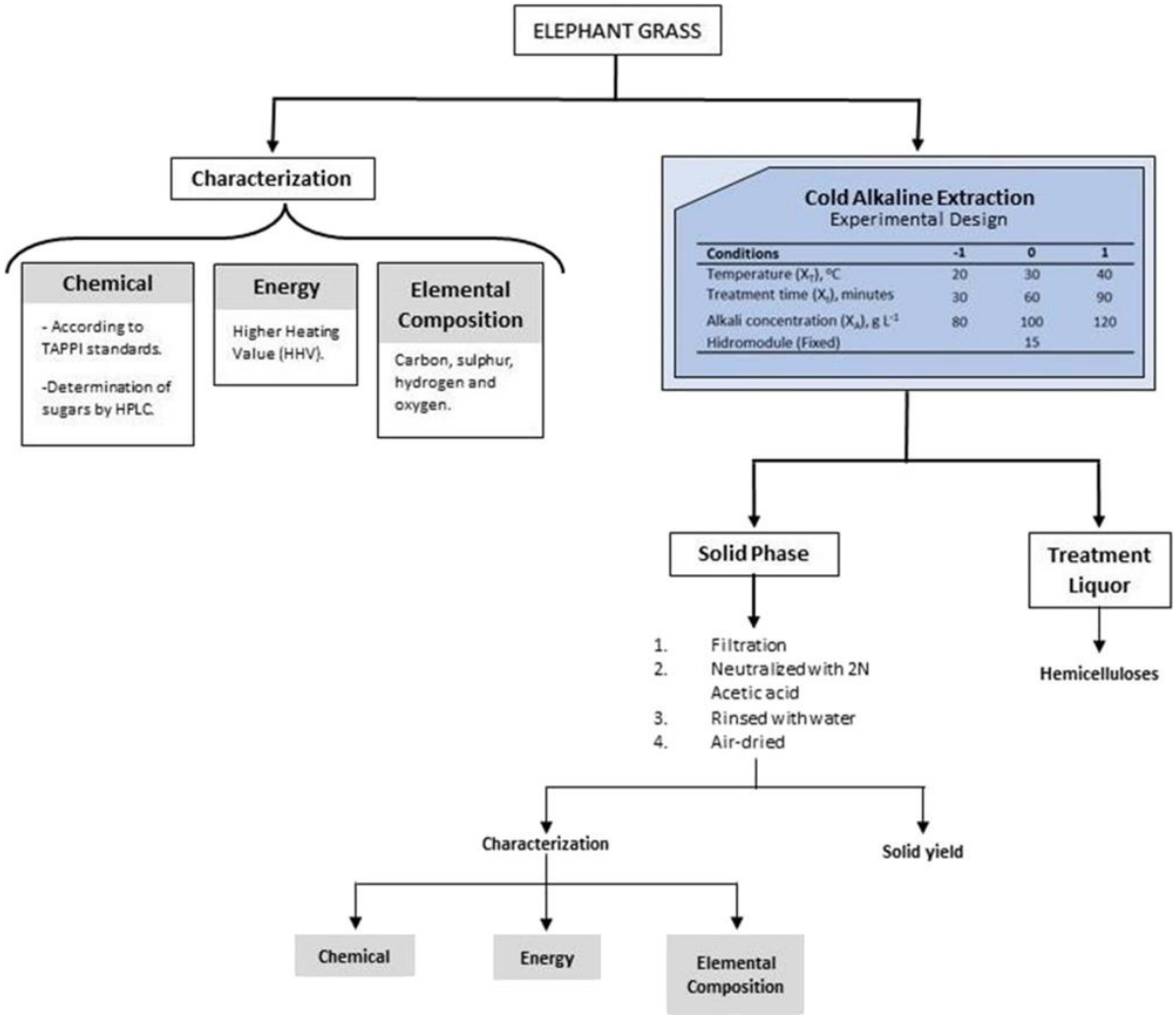


Figure 1. Scheme of the work carried out.

2.1 Chemical and energy characterization.

The material studied was elephant grass grown at an experimental station of the Pulp and Paper Laboratory of the Federal University of Viçosa (Minas Gerais, Brazil) that was ground by hand to obtain fragments of variable length and 1–4 cm in width. The material was characterized in chemical and energy terms by using the same methods as with the CAE liquor and solid phase.

For chemical analysis, samples were ground to variably sized particles in Wiley mill. The particles were sieved according to TAPPI T257-cm85 and those ranging from 40 to 60 mm in size retained. Moisture was determined by drying to a constant weight at 105°C (TAPPI T-264-cm-07). The samples, raw material, and CAE solid phase were all hydrolysed with 5 mL of 72% H_2SO_4 acid at 30°C for 1 h and the hydrolysed by adding water to reduce the acid concentration down to 4% while heating at 121°C for 60 min according to TAPPI T 249 cm-09. The resulting solid residue was

https://doi.org/10.1007/s13399-022-03054-3

recovered by filtration and labelled Klason lignin (TAPPI T 222 om-06). Soluble lignin was determined according to TAPPI T UM 25, and the hydrolysate used to determine, glucan, and hemicelluloses (xylan, araban, galactan, and mannan) in the material on an Agilent 1100 HPLC instrument equipped with a BioRaden ion-exchange column and a refractive index detector. The working temperature was 50°C, and the mobile phase consisted of 0.005 M H_2SO_4 and was circulated at 0–0.6 mL/min. All measurements were made in triplicate and the resulting coefficient of variation was less than 4%.

The raw materials and the solid phases were analysed for carbon, sulphur, hydrogen, and oxygen on an Eltra Helios CHS analyser. Also, they were used to determine their higher heating value (HHV) at a constant volume in accordance with CEN/TS 14,918 (2005) and UNE 16,001 EX (2005) on a Parr 6300 automatic isoperibol bomb calorimeter.

2.2 Cold alkaline extraction and determination of hemicelluloses.

Alkaline extraction was done by immersing the raw material in a bath containing an NaOH solution, using a constant solid/liquid ratio on a dry basis of 15 in all tests. The independent variables of the process were the soda concentration, temperature, and treatment time.

The solid fraction was recovered by filtration, neutralized with 2 N acetic acid, rinsed with water, and air-dried for weighing in order to estimate yield. The proportions of glucan and hemicelluloses from the raw material present in the extraction liquor were determined as described in the previous Sect. (2.1). The solid fraction was also subjected to the determinations described in it.

2.3 Multiple regression models and experimental design of cold alkaline extraction.

The CAE process was modelled in order to maximize extraction of hemicellulose derivatives while ensuring that the resulting solid would have a high heating value for energy production. A $2n$ factorial design with a central point was used to reduce the number of tests needed and also to avoid significant covariances between the dependent variables. The number of tests needed, N, was calculated as 2^n+2n+n_C, where 2^n is the number of points constituting the design, $2n$ that of axial points and n_C that of central points.

The independent variables were normalized by using the following Eq. (1):

$$X_n = \frac{X-\bar{X}}{(X_{max}-X_{min})/2} \qquad (1)$$

where X is the absolute value of the variable concerned, and $\bar{X}$, X_{max}, and X_{min} are its mean, maximum, and minimum value, respectively.

As can be seen in Table 1, each independent variable was examined at three different values. The results were used to establish second-order polynomials for each dependent variable, the polynomials

https://doi.org/10.1007/s13399-022-03054-3

including linear and quadratic terms of the independent variables, and their mutual interactions, and being fitted by multiple regression:

$$Y = a_0 + \sum_{i=1}^{n} b_i X_{ni} + \sum_{i=1}^{n} c_i X_{ni}^2 + \sum_{i=1,j=1}^{n} d_{ij} X_{ni} X_{nj} \quad (i<j) \quad (2)$$

where X denotes independent variables, Y dependent variables, and coefficients a_o, b_i, c_i, and d_{ij} are constants for each model obtained from the experimental results. The dependent variables were yield, glucan, xylan, araban, galactan, mannan, Klason lignin, and soluble lignin, and the independent variables were soda concentration, temperature, and time.

The independent variables present in the polynomials are those which exhibited statistically significant coefficients. In fact, no term with $p< 0.05$ as per Student's t-test or spanning a confidence interval narrower than 95% was included.

The results were processed with the software Statistica v. 10.0 (StatSoft, Inc., Tulsa, OK, USA) and additionally used to calculate R^2 and Snedecor's F-value, those with $R^2 > 0.85$ or $F > 5$ being deemed acceptable.

Table 1. Conditions of CAE experimental design.

Conditions	-1	0	1
Temperature (X_T), ºC	20	30	40
Treatment time (X_t), minutes	30	60	90
Alkali concentration (X_A), g L^{-1}	80	100	120
Hidromodule (fixed)		15	

3 Results and discusión.

As noted earlier, the primary aims of this work were to optimize the use of Elephant grass by subjecting the raw material to cold alkaline extraction (CAE) in order to remove its hemicellulose fraction in the treatment liquor and facilitate energy production from the resulting solid phase under the assumption that CAE would increase the heat capacity and decrease the sulphur content of the solid phase while enabling selective extraction of hemicellulose derivatives for their valorization. For this purpose, the starting material was characterized in chemical and energy terms, and the CAE process was modelled for optimal energy production. Finally, the efficiency with which hemicellulose derivatives were extracted, and its dependence on the operating conditions, were assessed.

3.1 Chemical and energy characterization.

Based on recent studies [24], Elephant grass can store dry matter more efficiently than other plant species. This results in favourable quality-related biomass properties including high heating value (HHV), and cellulose, hemicellulose, lignin, and ash contents. These properties make elephant grass an effective alternative to lignocellulosic raw materials for energy production by burning. Table 2 shows the chemical composition of Elephant grass as determined by our group and other authors. As

can be seen, coefficients of variation were relatively high (viz. 136% for cellulose, 105% hemicellulose, 69% for lignin, and 25% for ash), which can be ascribed to differences in plant growth environment. In any case, our results fall within the chemical composition ranges previously reported by other authors. Also, the differences in composition can have arisen from differences among the 85 genotypes studied [33], which spanned cellulose and lignin contents over the range 38.5–48.9% and 6.4–12.4%, respectively.

Table 2. Chemical characterization of Elephant grass.

Component (%)	**This work**	**Oluwasina** [38]	**Gomes** [32]	**Pandey** [21]	**Cardona** [72]	**De Conto** [49]
Glucan	41.7	55.33	38.2	36.34	22.6	30.37
Xylan	23.1	–	9.6	–	–	–
Arabinan	2.9	–	0.2	–	–	–
Galactan	0.95	–	0.8	–	–	–
Manan	0.45	–	0.6	–	–	–
Hemicelluloses	27.4	16.6	–	34.12	20.9	31.31
Klason lignin	19.3	2.79	–	–	–	–
Soluble lignin	1.56	24.0	2.2	–	–	–
Lignin	20.9	–	18	30.40	19.4	26.02
Holocelluloses	69.1	69.60	–	–	–	–
Ash	–	8.87	–	–	11.1	–

The chemical composition of Elephant grass is compared with those of other grass species and a reference material (*Eucalyptus globulus*) used for bioenergy production and other industrial purposes in Table 3. The cellulose content of the plant material used here (41.7%) was higher than that of other grasses such as switchgrass (31.0%) and sugarcane bagasse (39.0%), but somewhat lower than that of *Miscanthus giganteus* (48.6%) and eucalyptus wood (48.1%). The material had a high content in hemicellulose (27.4%), which is especially useful for biorefining by selective extraction of the hemicellulose fraction. This content exceeds the combined xylan and araban content reported by Oluwasina [38] for the same species (17.6%) and is comparable to the upper ends of the ranges for other materials such as rice straw (23–28%), wheat straw (26–32%), sugarcane bagasse (27–32%), and bamboo (15–26%) [80]. Xylan was the major component of the hemicellulose fraction and present in considerably higher proportions (23.1%) than in other materials (e.g., 8.4% in eucalyptus wood or 17.3% in sugarcane bagasse) [81]. The proportion of lignin in Elephant grass (20.9%) was higher than those in other residual grass materials such as wheat straw, tricolor sorghum, or corn stover (18.6%) [73], but slightly lower than those of grass species such as *M. Giganteus* and sugarcane bagasse, and wood species such as eucalyptus (26.9%), poplar (25.2%), and leucaena (24%) [75, 77, 82, 83]. Finally, the lignin contents of elephant straw were similar to those of other raw materials such as rice straw (15–25%) [84, 85] and fell in the overall ranges for grass species (10–30%) [73].

https://doi.org/10.1007/s13399-022-03054-3

Table 3. Chemical composition of selected lignocellulosic crops of industrial and bioenergetic interest.

Component (%)	**Switchgrass** [73, 74]	***Miscanthus* x *giganteus*** [75, 76]	**Sugarcane bagasse** [32]	**Eucalyptus** [73, 77, 78]	**Wheat straw** [73, 79]	**Bicolor sorghum** [73]
Glucan	30.97, 38	48.64, 39.5	39.01	48.07, 49.4, 46.8	32.64, 41.8	34.01
Xylan	20.42, 22.8	nd, 19.0	22.05	10.42, 12, 16.6	19.22, 25.4	14.14
Arabinan	2.75, 3.7	nd, 1.8	2.06	0.3, 0.3, 0.5	2.35, 2.5	1.65
Galactan	0.92, 1.3	–	0.46	0.74, 1.2	0.75, 0.7	0.52
Mannan	0.29	–	0.35	1.23, 0.9	0.31	0.2
Hemicelluloses	24.55	18.67	–	–	–	–
Lignin	17.56, 22.1	27.2	23.09	26.91, 27.2, 22.9	16.85	16.09
Holocellulose	–	67.31	–	nd, nd, 66.9	–	–
Ash	5.76, 3.7	5.49	3.66	1.22	10.22	5.04
Extractives	16.99	–	3.76	4.15	12.95	22.03

In terms of energy potential, the high heating value (HHV) of Elephant grass, calculated as described under Materials and Methods, was 18.44 MJ kg^{-1}, which is very similar to that reported by Reza et al. [50] (18.55 MJ kg^{-1}) but higher than that obtained by Tsai [86] (16.3 MJ kg^{-1}). These differences are quite normal because HHV changes with plant age (e.g., from 16.96 MJ kg^{-1} at 4 months to 22.04 MJ kg^{-1} at 6) [87]. HHV for Elephant grass was similar to the values for a number of wood species (in the region of 20 MJ kg^{-1}) according to Raveendran et al. [88], and also similar to or slightly greater than those of short-lifecycle plant species used for energy production such as *Leucaena leucocephala* (19.3–20.6 MJ kg^{-1}) [83], switchgrass (18.8 MJ kg^{-1}), or wheat straw (18.55 MJ kg^{-1}) [74].

Table 4. Elemental composition of Elephant grass and other lignocellulosic materials.

Species	**C** (%)	**H** (%)	**S** (%)	**O** (%)
Elephant grass [(1)]	48.999	6.790	0.12125	44.09
Elephant grass [(2)]	43.23	5.8	0.11	50,86
Clone AF2 *Populus* [(1)]	52.101	6.023	0.016	41.86
Leucaena [(1)]	50.623	6.117	0.024	43.236
Robinia [(1)]	51.38	6.301	0.023	42.296
Eucalyptus globulus [(1)]	51.924	6.326	0.01	41.74
Elm [(1)]	52.916	6.406	0.017	40.661
Pine [(1)]	57.746	6.942	0.12	35.192
Ethiopian rapeseed [(3)]	46.3	6.1	0.49	47.11
Populus [(3)]	48.19	5.9	0.05	45.86

[(1)] This work, [(2)] [50], [(3)] [89]

An elemental composition analysis conducted as described under Materials and Methods provided the C, O, H, and S contents that are compared with those reported by Reza et al. [50] and those for various other raw materials in Table 4. The chemical composition of a raw material can be expected to influence that of the gases it releases and the amount of heat it produces upon burning. The fact that the C and H contents of Elephant grass were somewhat higher than those of other materials suggested that it might be more efficient for energy production. On the other hand, the S content of

Elephant grass was similar to those of other lignocellulosic raw materials and substantially lower than those of fossil fuels.

3.2 Modelling and optimization of the higher heating value and elemental composition of the post-CAE liquor and solid phase.

Table 5 shows the HHV and elemental composition (C, H, S, and O) of the solid fraction from the CAE treatment as determined under variable operating conditions selected in accordance with the experimental design used. The polynomial equations of the design are shown in Table 6, which includes one for CAE solid yield. As can be seen, the differences between observed and calculated values never exceeded 10% and correlation coefficients were all higher than 0.95. Table 5 also includes CAE yield.

Table 5. HHV and elemental composition of the post-CAE solid phase obtained under different operating conditions.

T (ºC), ***t*** (min), **NaOH concentration** (g L^{-1})	**C** (%)	**H** (%)	**S** (%)	**O** (%)	**HHV** (MJ/kg)	**Yield** (%)
0 0 0	47.581	7.089	0.0865	52.333	18.745	74.6
0 0 0	47.656	7.061	0.0827	52.261	18.863	75.3
1 1 1	47.185	6.747	0.0019	52.813	18.200	66.9
1 1 -1	46.170	6.724	0.0018	53.828	17.777	71.8
1 -1 1	47.027	6.862	0.0040	52.969	18.449	79.4
1 -1 -1	46.866	6.931	0.0035	53.131	18.045	82.8
-1 1 1	47.052	6.755	0.0084	52.940	18.122	75.3
-1 1 -1	46.956	6.703	0.0118	53.032	18.278	72.1
-1 -1 1	46.956	6.810	0.0384	53.006	18.429	84.7
-1 -1 -1	47.585	6.850	0.0384	52.377	18.374	86.8
1 0 0	46.172	6.975	0.0232	53.805	18.435	70.5
-1 0 0	46.263	6.869	0.0520	53.685	18.402	76.1
0 1 0	48.388	7.056	0.0613	51.551	18.866	70.6
0 -1 0	48.871	7.067	0.0891	51.040	19.244	82.5
0 0 1	46.891	6.982	0.0831	53.026	18.590	77.4
0 0 -1	47.077	6.975	0.0844	52.839	18.470	80.6
Raw material	48.999	6.790	0.12125	57.912	18.440	–

Y_{HHV} high heating value (HHV). Y_C, Y_H and Y_S content in carbon, hydrogen and Sulphur (%). Y_{yield} CAE yield (%). X_A, X_T, X_t normalized alkali concentration, temperature and treatment time, respectively.

As can be seen from Eq. 1 in Table 6, HHV for the post-CAE solid phase from Elephant grass was strongly dependent on the quadratic terms of the process variables. Clearly, the values and signs of the coefficients for the treatment time suggest that times in the lower end of the operating range should result in increased HHV levels. Also clearly, using alkali concentrations and temperatures at the ends of the operating ranges would detract from HHV as the very likely result of poor extraction of hemicelluloses into the CAE liquor at low temperatures and excessive extraction of polyphenols

https://doi.org/10.1007/s13399-022-03054-3

(lignin) at high temperatures. As confirmed by Figure 2A, it was therefore advisable to use medium alkali concentrations and temperatures. Thus, Eq. 1 in Table 6 predicts HHV = 19.151 MJ kg^{-1}, which was nearly 4% higher than the value for the starting material.

Equations 2 and 4 in Table 6 show the modelled results for the C and H contents of the post-CAE solid phase. The conditions needed to maximize HHV and both contents were identical. Again, the quadratic terms were especially influential and interaction terms virtually uninfluential. As with HHV, maximizing the C and H contents of the post-CAE solid phase would require using medium alkali concentrations and temperatures in combination with short treatment times. Under these conditions, Eqs. 2 and 4 in Table 6 predict a content in C of 48.961% and one in H of 7.120%. While the C content was similar to that of the raw material, the H content was 4.86% higher. The response surface for the C content, not shown, was similar to that of Figure 2A.

Based on the predictions of Eq. 3 in Table 6, the operating conditions maximizing energy production, and the C and H contents, should lead to increased S contents in the post-CAE solid phase. Although this might be an unwanted outcome of the treatment, the S content of the starting biomass was so low that it was unlikely to raise environmental concerns. Also, the CAE treatment considerably reduced the S content by 26.6–98.5% depending on the particular conditions (46.9% with the optimum settings). In this way, CAE facilitated use of the material for energy production with little emission of sulphur dioxide. This is an added advantage to the above-mentioned increased energy yield and valorization of the hemicellulose fraction relative to burning of the raw material. Also, the increased energy yield need not be accompanied by an excessive decrease in solid yield. In fact, hemicellulose extraction should be selective providing most cellulose and lignin remain in the post-CAE solid phase.

Table 6. Polynomial models for HHV, C, H, S, and yield.

Eq.	Polynomial	R^2	F
1	$Y_{HHV} = 18.850 + 0.0938X_A - 0.121X_t - 0.070X_T - 0.346X_A^2 + 0.179X_t^2 - 0.458X_T^2 + 0.116X_AX_T$	0.94	34.5
2	$Y_C = 47.513 - 0.279X_t - 0.302X_T - 0.476X_A^2 + 1.170X_t^2 - 1.242X_T^2$	0.95	52.6
3	$Y_S = 0.0887 - 0.0097X_t - 0.0112X_T - 0.0070X_A^2 - 0.0156X_t^2 - 0.0532X_T^2 + 0.0070X_TX_t$	0.98	140.4
4	$Y_H = 7.073 - 0.047X_t + 0.035 \cdot X_T - 0.104X_A^2 - 0.160X_T^2 + 0.0316X_AX_t$	0.96	66.9
5	$Y_{yield} = 75.56 - 2.35X_T - 5.96X_t - 1.04X_A - 1.94X_T^2 + 3.78X_A^2 - 1.19X_tX_A$	0.99	57.61

Y_{HHV} high heating value (HHV), Y_C, Y_H, and Y_S content in carbon, hydrogen, and sulphur (%). Y_{yield} CAE yield (%). X_A, X_T, X_t normalized alkali concentration, temperatura, and treatment time, respectively.

As can be seen from Table 5, the CAE treatment resulted in little biomass loss. Thus, solid yields ranged from 66.9 to 86.8% and exceeded those obtained by García et al. [63] treating wheat straw (viz., 61.1% by using a NaOH concentration of 100 g L^{-1}, a temperature of 40 °C, and a treatment time of 90 min). The yield from Elephant grass under similar temperature and time conditions amounted to 71.8 and 66.9% with a NaOH concentration of 80 and 120 g L^{-1}, respectively. There

https://doi.org/10.1007/s13399-022-03054-3

were no substantial changes in yield with temperature or the alkali concentration, however. By contrast, time considerably influenced the results. Thus, the highest yields were obtained at short times (30 min, normalized value –1) and, with little difference, low temperatures (20°C, –1) and high alkali concentrations (120 g NaOH L^{-1}, + 1). As can be seen from Figure 2B, using short treatment times and medium temperatures (normalized value 0) provided the highest solid yields. Based on Eq. 5 in Table 6, using medium temperatures and alkali concentrations in combination with short times (–1) would lead to a yield of 81.5% in the post-CAE solid phase. This is quite acceptable if one considers that the highest possible yield was 85.6% (Eq. 5, Table 6).

3.3 Modelling and optimization of monosaccharide contents in the post-CAE liquor and solid phase.

Table 7 shows the contents in Klason and soluble lignin, individual monomers from the polysaccharide fraction, their combination, and monomers from the hemicellulose fraction (xylan, arabinan, galactan, and mannan) of the post-CAE solid fraction as a function of the operating conditions used. The results were used to calculate the proportion of each fraction that was extracted into the CAE liquor. Table 8 shows the proportions such fractions but relative to the percent content of each polymer in the starting material.

Table 7. Composition of the solid resulting from the CAE in percentage with respect to the raw material.

T (°C), **t** (min),	**Lignin**, %		**Carbohydrates**, %						**Total**
Conc.NaOH (g/L)	Klason	Soluble	Glucan	Xylan	Arabinan	Galactan	Mannan	Total CHO	**hemicelluloses**
0 0 0	13.6	0.8	36.3	13.3	2.2	0.7	0.2	52.8	16.4
0 0 0	13.4	0.8	36.7	13.5	2.2	0.7	0.2	53.2	16.6
1 1 1	10.4	0.6	36.0	9.3	1.8	0.6	0.3	48.1	12.1
1 1 -1	11.3	0.6	36.8	10.7	1.9	0.7	0.3	50.4	13.5
1 -1 1	14.0	0.9	37.0	12.8	2.5	0.9	0.4	53.7	16.6
1 -1 -1	14.3	1.0	37.2	13.3	2.6	0.9	0.4	54.4	17.2
-1 1 1	13.5	0.8	36.3	13.4	2.4	0.8	0.3	53.1	16.8
-1 1 -1	12.4	1.0	36.9	13.0	2.5	0.8	0.3	53.5	16.6
-1 -1 1	16.1	1.4	38.9	16.4	2.8	0.9	0.3	59.3	20.4
-1 -1 -1	15.9	1.5	35.8	16.0	2.7	0.9	0.4	55.8	20.0
1 0 0	11.2	0.9	33.3	9.7	2.0	0.7	0.3	46.0	12.7
-1 0 0	13.3	1.2	33.9	13.6	2.3	0.8	0.3	50.9	17.0
0 1 0	12.2	0.5	37.9	12.3	2.1	0.7	0.1	53.1	15.2
0 -1 0	16.2	0.8	38.8	15.7	2.5	0.9	0.2	58.0	19.2
0 0 1	13.8	0.8	37.7	13.7	2.5	0.7	0.3	54.8	17.1
0 0 -1	14.2	0.8	38.5	14.6	2.3	0.8	0.3	56.5	18.0

Not all chemical characterization results shown in Tables 7 and 8 were modelled. In fact, some components were present in too small amounts in both the raw material and the post-CAE solid phase for any useful conclusions to be drawn. Rather, we used multiple regression on the major dependent variables suggested by the experimental design in addition to total hemicellulose in order to consider two minor saccharides (mannan and galactan). On the other hand, the liquid fraction was modelled for extracted lignin, extracted glucan, and total extracted hemicellulose (viz., the combination of all monomers listed in Table 8 except glucan). The models used, and their statistical figures of merit, are

shown in Table 9. As can be seen, the differences between experimental and calculated values never exceeded 10% and correlation coefficients (R^2) were all higher than 0.95.

Table 8. Percentages of extraction in liquid phase relative to the percent content of each polymer in the starting material.

T (°C), **t** (min), **Conc.NaOH** (g/L)	**Extraction in percentage in liquid phase with respect to the initial polymer** (%)							**% Total Hemicelluloses extracted in liquid**
	Klason lignin	Soluble lignin	Glucan	Xylan	Arabinan	Galactan	Mannan	
0 0 0	29.5	49.5	12.8	42.3	25.4	24.4	53.9	40.0
0 0 0	30.8	50.4	11.9	41.8	24.8	24.9	51.1	39.5
1 1 1	46.4	64.1	13.5	59.6	36.6	33.1	40.6	55.9
1 1 -1	41.2	62.2	11.6	53.8	34.4	28.9	36.2	50.6
1 -1 1	27.7	44.9	11.1	44.7	12.4	3.9	11.8	39.3
1 -1 -1	26.0	33.9	10.8	42.3	10.0	4.1	17.2	37.1
-1 1 1	30.3	50.7	12.9	42.0	18.2	20.7	33.1	38.6
-1 1 -1	35.5	35.6	11.5	43.9	132.0	12.8	36.0	39.4
-1 -1 1	16.8	10.4	6.6	29.2	3.1	1.9	24.7	25.4
-1 -1 -1	17.7	0.8	14.1	30.7	5.7	4.0	22.8	27.0
1 0 0	42.1	40.2	20.1	58.0	30.7	25.8	36.4	53.7
-1 0 0	31.2	21.5	18.7	41.1	20.0	19.9	32.4	38.0
0 1 0	36.7	71.2	9.1	46.7	29.2	22.0	76.5	44.4
0 -1 0	16.3	49.1	7.0	32.0	14.7	4.6	63.4	29.8
0 0 1	28.4	50.0	9.6	40.9	14.6	26.8	31.2	37.4
0 0 -1	26.3	51.5	7.7	36.8	19.4	19.4	28.4	34.3

The values of the dependent variables of Table 9 were used to construct response surfaces in order to facilitate comparisons and identification of the optimum CAE conditions. The *z*-axis represents each of the most influential variables at two different response levels (+ 1 and –1).

CAE allowed hemicelluloses to be relatively selectively extracted in the form of highly pure polymers [90]. In fact, only 6.6–20.1% of all glucan present in the raw material—which accounted for an average 11.3% in it—was removed (i.e., 2.8–84% of all starting material). By contrast, 25.4–56.0% of the whole hemicellulose fraction (viz., 7.0–15.3% of raw material) was extracted. CAE additionally resulted in substantial delignification. Thus, 16.3–46.4% of the initial amount of Klason lignin (3.2–9.0% of all raw material) was extracted into the CAE liquor.

The post-CAE liquor contained various monomers, xylo-oligomers, minerals, proteins, degradation products (furfural and 5-hydroxymethylfurfural), gluco-oligomers, arabanoligomers, extractables, dissolved lignin, and non-volatile solids [83]. Overall, hemicelluloses were the most efficiently extracted lignocellulosic fraction (especially xylan). Galactan and mannan monomers supplied only small amounts of monosaccharides to the post-CAE liquor owing to their low proportion in the raw material (less than 1% and 0.5%, respectively). Also, araban was less markedly extracted into the CAE liquor than was xylan. As expected, extraction peaked under the most drastic operating conditions.

https://doi.org/10.1007/s13399-022-03054-3

Table 9. Models for the dependent variables after the CAE process.

No. Eq	Solid residue equations	R^2	*F*-Snedecor
1	$YligK = 13.48 - 1.00X_T - 1.65X_t - 1.25X_T^2 + 0.70X_t^2 + 0.54X_A^2 - 0.32X_TX_A$	0.98	92.7
2	$Yglu = 36.52 - 0.38X_t - 2.96X_T^2 + 1.78X_t^2 + 1.52X_A^2 - 0.44X_TX_A - 0.55X_tX_A$	0.94	24.4
3	$Yxyl = 13.36 - 1.65X_T - 1.55X_t - 0.21X_A - 1.69X_T^2 + 0.69X_t^2 + 0.77X_A^2 - 0.33X_TX_A$	0.98	72.4
4	$Yara = 2.19 - 0.20X_T - 0.26X_t + 0.23X_A^2 - 0.07X_TX_t$	0.94	47.3
5	$Yhmt = 16.49 - 1.87X_T - 1.93X_t - 0.23X_A - 1.65X_T^2 + 0.74X_t^2 + 1.08X_A^2 - 0.34X_TX_A$	0.99	138.9
No. Eq	**Extraction liquor equations**	R^2	*F*-Snedecor
6	$Yligex = 30.16 + 5.18X_T + 8.55X_t + 6.50X_T^2 - 3.64X_t^2 - 2.81X_A^2 + 1.63X_TX_A$	0.94	92.7
7	$Ygluex = 12.33 + 0.90X_t + 7.11X_T^2 - 4.28X_t^2 - 3.66X_A^2 + 1.05X_TX_A + 1.32X_tX_A$	0.94	24.4
8	$Yhmtex = 39.80 + 6.83X_T + 7.04X_t + 0.83X_A + 6.01X_T^2 - 2.69X_t^2 - 3.95X_A^2 + 1.22X_TX_A$	0.99	138.9

YligK, klason lignin content in the solid; Yglu, glucan content in the solid; Yxil, xylan content in the solid; Yara, araban content in the solid; Yhmt, hemicelluloses conten in the solid; Yligex, lignin extracted; Ygluex, glucan extracted; Yhmtex, hemicelluloses extracted; X_A, X_T, X_t, normalized value of the alkali concentration, temperature, and time, respectively.

Figure 2C illustrates the dependence of hemicellulose extraction into the CAE liquor on the operating conditions. As can be seen, the highest proportion of hemicellulose in the liquor (57.1%) was obtained by using a medium alkali concentration (100 g NaOH L^{-1}, normalized value = 0), a high temperature (40°C, + 1), and a long treatment time (90 min, + 1). In any case, the first variable was scarcely influential. Other authors previously reported similar hemicellulose extraction values. Thus, Sun et al. [91] dissolved 89.3% of all hemicelluloses in poplar wood by using a similar alkali concentration (8.5% vs 10% here) but a much longer treatment time (16 h). Cheng et al. [65] obtained high xylan extraction yields (> 90%) from corn stover by using an NaOH concentration of 10%, a temperature of 75 °C and a time of 2 h. Under optimum conditions (viz., an alkaline mass fraction of 9.5%, 78°C, and 252 min), Shao [92] obtained a hemicellulose extraction yield of 52.8% from poplar wood.

In this work, we chose to restrict hemicellulose extraction in order to avoid cellulose depolymerization and extensive delignification—which would have diminished the high heating value (HHV) of the post-CAE solid phase. In fact, biomass for thermal energy production by burning should contain high proportions of lignin and cellulose, and possess a high C/N ratio, and high heating value but low moisture, ash, and nitrogen contents [57]. Thus, although the glucan fraction supplied monosaccharides to the CAE liquor, cellulose should ideally remain in the solid phase as a polymer in order to preserve its heating value—and so should lignin, which possesses a high thermal potential. Specifically, cellulose, hemicellulose, and lignin have an HHV of 17.36, 17.54, and 25.8 MJ kg^{-1}, respectively (i.e., cellulose and hemicellulose have a similar HHV which, however, is 48% lower than that of lignin) [93]. Using the operating conditions needed to maximize HHV in the post-CAE solid phase resulted in a hemicellulose extraction yield of 30.1%, which was lower than that obtained under the most drastic conditions (55.1%) but allowed relatively selective extraction of hemicelluloses over glucan and lignin.

https://doi.org/10.1007/s13399-022-03054-3

As can be seen from Figure. 2D, minimizing the proportion of cellulose dissolved in the post-CAE liquor would require using high alkali concentrations, medium temperatures, and short treatment times.

It is necessary to take into account the synergy of the operating variables on the extraction of glucan. In our case, time and temperature are much more influential than the alkali concentration (see Eq. 2 in Table 9 or Figure 2D). As the NaOH concentration is scarcely influential, so it allowed medium values to be used instead of high levels (i.e., the most suitable conditions for maximizing energy production). The percentages of glucan in solid can also rise if the extraction process is more selective towards the other fractions. As predicted by Eq. 2 in Table 9, such conditions would lead to a proportion of 38.7% of cellulose (glucan) in the post-CAE solid phase (i.e., 93% of all cellulose present in the starting material would remain in that phase). Also, as predicted by Eq. 7 in Table 9, only 7.15% of the initial amount of glucan would be dissolved in the CAE liquor (compared to 30.1% of all hemicellulose). These numbers testify to the ability of CAE to selectively extract hemicelluloses over cellulose.

Restricting delignification in order to allow as much lignin as possible to remain in the solid phase (Figure 2E) would require using low temperatures and short treatment times with any alkali concentration. As can be seen, however, normalized temperatures over the range –1 to 0 scarcely influenced the lignin content of the post-CAE solid phase. As predicted by Eq. 6 in Table 9, the conditions needed to maximize HHV would result in 18.0% of all lignin being extracted into the CAE liquor.

Based on the foregoing, increasing the heating value of the post-CAE solid phase while ensuring adequate, selective extraction of hemicelluloses would require using the following, optimum conditions: a medium alkali concentration (100 g NaOH L^{-1}, normalized value = 0), a medium temperature (30°C, 0), and a short treatment time (30 min, –1). These conditions are milder than those used by García et al. [63] to obtain a hemicellulose-rich valorizable liquor and a solid fraction suitable for producing cellulose pulp (viz., 100 g NaOH L^{-1}, 40°C, and 90 min, which allowed them to extract all hemicellulose present in the raw material and 10.3% of lignin). As predicted by Eq. 8 in Table 9, these conditions would allow 55.1% of all hemicellulose and 46.8% of all lignin present in elephant grass to be extracted. Therefore, as suggested by the results of García et al. [63], the alkaline treatment was more efficient with elephant grass than it was with wheat straw. Also, based on the results of De Carvalho et al. [94], it was comparably efficient for extraction from sugarcane straw. Thus, using 110 g NaOH L^{-1}, 30°C, and 60 min in combination allowed them to extract 52.5% of all hemicellulose in their raw material compared to 25.7–55.1% from elephant grass here.

https://doi.org/10.1007/s13399-022-03054-3

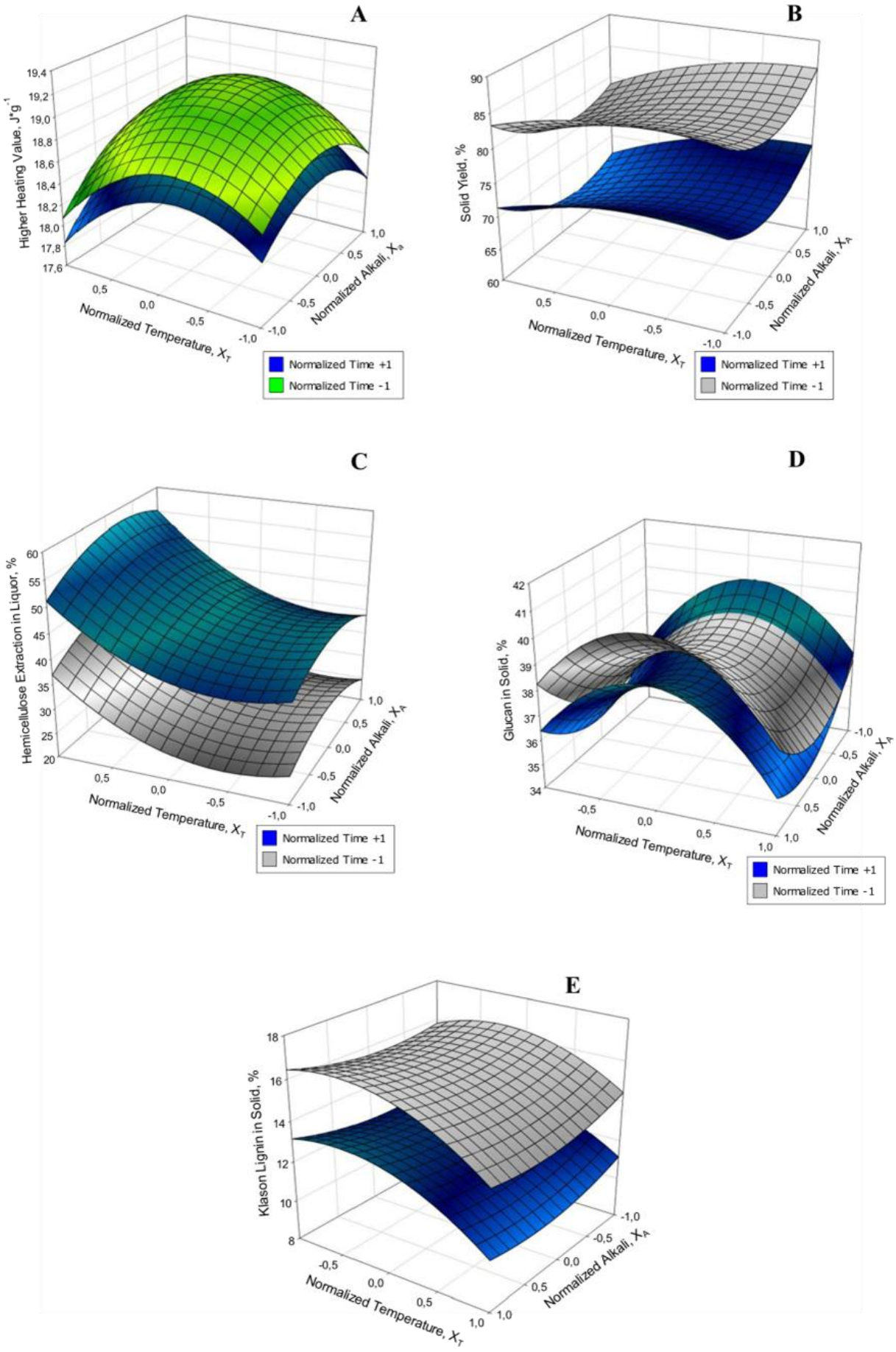


Figure 2 A. HHV response surface. **B** CAE yield response surface. **C** Hemicellulose extraction in the CAE liquor. **D** Percent cellulose content, as glucan, in the post-CAE solid phase. **E** Percent Klason lignin in the post-CAE solid phase.

https://doi.org/10.1007/s13399-022-03054-3

4 Conclusions.

Elephant grass has been deemed an excellent alternative to woody materials for energy production by direct burning, basically by virtue of its substantial contents in lignin (20.86%) and hemicelluloses (27.4%).

Using the optimal operating conditions for pre-burning cold alkaline extraction (CAE) of Elephant grass (viz., an alkali concentration of 100 g NaOH L^{-1}, a temperature of 30°C, and a treatment time of 30 min) allowed its high heating value to be raised by 4% (to 19.151 MJ kg^{-1}) while preserving the proportion of elemental C and increasing that of H with respect to the raw material, and deriving the environmental advantage of reducing the sulphur content by 46.9% from the starting material to the post-CAE solid phase.

Cold alkaline extraction of the raw material additionally enabled relatively selective separation of the hemicellulose fraction from the cellulose and lignin fractions. Thus, 30.1% of all hemicellulose was dissolved in the treatment liquor and made valorizable while 93.0% of cellulose and 82.1% of lignin present in the raw material remained in the solid phase.

Author contribution

All authors contributed to the study conception and design and have collaborated in the different phases of the work. The aspects on which the authors have worked most intensively are highlighted as follows: **Juan Carlos García**: contribution in the methodology, statistical analysis, and making graphics. **Ascensión Alfaro**: writing in the first draft, review, and editing; data analysis; and results and graphs. **Javier Mauricio Loaiza**: contribution in experimental work and methology and writing in the first draft. **Susana Lozano-Calvo**: contribution in experimental work and methodology and writing in the first draft. **Francisco López**: conceptualización, funding acquision, project manager, and general supervision.

Funding

Open Access funding provided thanks to the CRUE-CSIC agreement with Springer Nature. Funding for open acces charge: Universidad de Huelva/CBUA. This study was funded by the Spanish Ministry of Economy and Competitiveness through the National Programme for Research Aimed at the Challenges of Society (CTQ201785251-C2-1and 2-R and PID2020-112875RB-C21), additional cofunding, in an 80:20 proportion, by FEDER (Project Green Asphalt, ref. 802C1800001) and the Andalusian Regional Government (Economy, Knowledge, Enterprises and University Council/IDEA Agency) and by micro-projects of research “Cátedra de la provincia” of the University of Huelva.

Acknowledgement

The authors would like to thank the Laboratorio de Celulosa e Paper of the Federal University of Viçosa, Minas Gerais, Brazil, where part of the work of this paper was developed.

Declarations

Conflict of interest

The authors declare no competing interests.

Open Access

This article is licensed under a Creative Commons Attribution 4.0 International License, which permits use, sharing, adaptation, distribution and reproduction in any medium or format, as long as you give appropriate credit to the original author(s) and the source, provide a link to the Creative Commons licence, and indicate if changes were made. The images or other third party material in this article are included in the article's Creative Commons licence, unless indicated otherwise in a credit line to the material. If material is not included in the article's Creative Commons licence and your intended use is not permitted by statutory regulation or exceeds the permitted use, you will need to obtain permission directly from the copyright holder. To view a copy of this licence, visit http://creativecommons.org/licenses/by/4.0/.

References

[1] Singh BP, Singh HP, Obeng E (2013) Elephantgrass. In: Singh BP (ed) Biofuel crops: production, physiology and genetics. CABI, Wallingford, pp 271–291.

[2] Chen HG, Zhang Y-HHP (2015) New biorefineries and sustainable agriculture: increased food, biofuels, and ecosystem security. Renew Sustain Energy Rev 47:117–132.

[3] Yadav P, Priyanka P, Kumar D et al (2019) Bioenergy crops: recent advances and future outlook. pp 315–335.

[4] Hulthom T, Robertsen L, Lönnberg B et al (1998) The IDE process. A new concept suitable for softwood, hardwood and non-wood, p 577–588.

[5] European Parliament (2006) Report on a strategy for biomass and biofuels (2006/2082 (INI)). https://www.europarl.europa.eu/doceo/document/A-6-2006-0347_EN.html Accessed 8 Nov 2021. Accessed 8 Nov 2021.

[6] REN21 (2020) Renewables 2020. https://www.ren21.net/gsr-2020/. Accessed 9 Nov 2021.

[7] European Parliament (2021) Fact sheets on the European Union. Renewable energy. https://www.europarl.europa.eu/factsheets/en/section/192/industrial-energy-and-research-policies. Accessed 8 Nov 2021.

[8] Eurostat (2021) Database. In: Share Renew. energy gross Final energy Consum. https://ec.europa.eu/eurostat/databrowser/view/t2020_31/default/bar?lang=en. Accessed 9 Nov 2021.

[9] European Commission (2020) In focus: Renewable energy in Europe. https://ec.europa.eu/info/news/focus-renewable-energy-europe-2020-mar-18_en. Accessed on 9 Nov 2021.

[10] Haribabu K, Sivasubramanian V, Deepanraj B, Ong HC (2021) Thematic issue: bioenergy and biorefinery approaches for environmental sustainability. Biomass Convers Biorefin. https://doi.org/10.1007/s13399-021-01989-7.

[11] Korndörfer (2011) Biomass and energy yields of bioenergy germplasm grown on sandy soils in Florida. University of Florida.

[12] Nazli RI, Tansi V, Öztürk HH, Kusvuran A (2018) Miscanthus, switchgrass, giant reed, and bulbous canary grass as potential bioenergy crops in a semi-arid Mediterranean environment. Ind Crops Prod 125:9–23. https://doi.org/10.1016/j.indcrop.2018.08.090.

[13] Cosentino SL, Scordia D, Testa G et al (2018) The importance of perennial grasses as a feedstock for bioenergy and bioproducts. In: Perennial Grasses for Bioenergy and Bioproducts. pp 1–33

[14] Nie S, Zhang C, Zhang Q et al (2018) Enzymatic and cold alkaline pretreatments of sugarcane bagasse pulp to produce cellulose nanofibrils using a mechanical method. Ind Crops Prod 124:435441. https://doi.org/10.1016/j.indcrop.2018.08.033.

[15] Lu Y, Tao P, Zhang N, Nie S (2020) Preparation and thermal stability evaluation of cellulose nanofibrils from bagasse pulp with differing hemicelluloses contents. Carbohydr Polym 245:116463. https://doi.org/10.1016/j.carbpol.2020.116463.

[16] Sosa LL, Jozami E, Oakley LJ et al (2019) Using C4 perennial rangeland grasses for bioenergy. Biomass Bioenergy 128:105299. https://doi.org/10.1016/j.biombioe.2019.105299.

[17] McKendry P (2002) Energy production from biomass (part 1): Overview of biomass. Bioresour Technol 83:37–46. https://doi.org/10.1016/S0960-8524(01)00118-3

[18] Lewandowski I, Scurlock JMO, Lindvall E, Christou M (2003) The development and current status of perennial rhizomatous grasses as energy crops in the US and Europe. Biomass Bioenergy 25:335–361. https://doi.org/10.1016/S0961-9534(03)00030-8

[19] Samson R, Mani S, Boddey R et al (2005) The potential of C4 perennial grasses for developing a global BIOHEAT Industry. CRC Crit Rev Plant Sci 24:461–495.

[20] Dien BS, Jung HJG, Vogel KP et al (2006) Chemical composition and response to dilute-acid pretreatment and enzymatic saccharification of alfalfa, reed canarygrass, and switchgrass. Biomass Bioenergy 30:880–891. https://doi.org/10.1016/j.biombioe.2006.02.004.

[21] Pandey VC, Patel D, Jasrotia S, Singh DP (2020) Potential of Napier grass (Pennisetum purpureum Schumach.) for phytoremediation and biofuel production. In: Phytoremediation Potential of Perennial Grasses. Elsevier, pp 283–302.

[22] Scordia D, Cosentino S (2019) Perennial energy grasses: resilient crops in a changing European agriculture. Agriculture 9:169. https://doi.org/10.3390/agriculture9080169.

[23] Martín Torrealba B, Diaz Dominguez A, Chinea Correa E, Delgado Hdez B (1989) Posibilidad de cultivo y aprovechamiento del "pasto elefante" (“pennisetum purpureum” schum) en Tenerife (Islas Canarias). Pastos 79–86.

[24] Marafon AC, Machado JC, Cavalcante de Amorim EL et al (2021) Elephant grass as a feedstoc for bioenergy production. BSS Mag.

[25] Nguyen BT, Le LB, Pham LP et al (2021) The effects of biochar on the biomass yield of elephant grass (Pennisetum Purpureum Schumach) and properties of acidic soils. Ind Crops Prod 161:113224. https://doi.org/10.1016/j.indcrop.2020.113224.

[26] Negawo AT, Teshome A, Kumar A et al (2017) Opportunities for napier grass (Pennisetum purpureum) improvement using molecular genetics. Agronomy 7:28.

[27] Osman NA, Roslan AM, Ibrahim MF, Hassan MA (2020) Potential use of pennisetum purpureum for phytoremediation and bioenergy production: a mini review. Asia-Pac J Mol Biol Biotechnol 28:14–26. https://doi.org/10.35118/apjmbb.2020.028.1.02.

[28] Byrt CS, Grof CPL, Furbank RT (2011) C4 Plants as biofuel feed-stocks: optimising biomass production and feedstock quality from a lignocellulosic perspective. J Integr Plant Biol 53:120–135.

[29] Varnero CS, Urrutia MV, Ibaceta SV (2018) Bioenergy from perennial grasses. In: Advances in Biofuels and Bioenergy. InTech, p.

[30] van der Weijde T, Alvim Kamei CL, Torres AF et al (2013) The potential of C4 grasses for cellulosic biofuel production. Front Plant Sci 4:107.

[31] Cerdas R, Vallejos E (2010) Productividad del pasto Camerún (Pennisetum purpureum) con varias dosis de nitrógeno y frecuencias de corte en la zona seca de Costa Rica. InterSedes Rev las Sedes Reg XI:180–195.

[32] Gomes FJB, Colodette JL, Burnet A et al (2013) Potential of elephant grass for pulp production. BioResources 8:4359–4379. https://doi.org/10.15376/biores.8.3.4359-4379.

[33] Basso V, Machado JC, da Silva Lédo FJ et al (2014) Different elephant grass (Pennisetum purpureum) accessions as substrates for enzyme production for the hydrolysis of lignocellulosic materials. Biomass Bioenergy 71:155–161. https://doi.org/10.1016/j.biombioe.2014.10.011.

[34] Rengsirikul K, Ishii Y, Kangvansaichol K et al (2013) Biomass yield, chemical composition and potential ethanol yields of 8 cultivars of napiergrass (Pennisetum purpureum Schumach.) harvested 3-monthly in Central Thailand. J Sustain Bioenergy Syst 03:107–112. https://doi.org/10.4236/jsbs.2013.32015.

[35] Menegol D, Scholl AL, Dillon AJP, Camassola M (2016) Influence of different chemical pretreatments of elephant grass (Pennisetum purpureum, Schum.) used as a substrate for cellulase and xylanase production in submerged cultivation. Bioprocess Biosyst Eng 39:1455–1464. https://doi.org/10.1007/s00449-016-1623-8.

[36] Dien BS, Anderson WF, Cheng MH et al (2020) Field productivities of napier grass for production of sugars and ethanol. ACS Sustain Chem Eng 8:2052–2060. https://doi.org/10.1021/acssuschemeng.9b06637.

[37] Antunes FAF, Machado PEM, Rocha TM et al (2021) Column reactors in fluidized bed configuration as intensification system for xylitol and ethanol production from napier grass (Pennisetum Purpureum). Chem Eng Process Process Intensif 164. https://doi.org/10.1016/j.cep.2021.108399.

[38] Oluwasina OO, Lajide L (2016) Evaluation of compositional properties of some plant wastes for industrial applications. FUTA J Res Sci 12:180–187.

[39] Haldar D, Purkait MK (2020) Thermochemical pretreatment enhanced bioconversion of elephant grass (Pennisetum purpureum): insight on the production of sugars and lignin. Biomass Convers Biorefin. https://doi.org/10.1007/s13399-020-00689-y.

[40] Trevisan H, Rezende CA (2020) Pure, stable and highly antioxidant lignin nanoparticles from elephant grass. Ind Crops Prod 145. https://doi.org/10.1016/j.indcrop.2020.112105.

[41] Nandal P, Arora A, Virmani S (2021) An appraisal on valorization of lignin: a byproduct from biorefineries and paper industries. Biomass Bioenergy 155:106295. https://doi.org/10.1016/j.biombioe.2021.106295.

[42] Alaneme KK, Olusegun SJ, Alo AW (2016) Co rrosion inhibitory properties of elephant grass (Pennisetum purpureum) extract: effect on mild steel corrosion in 1 M HCl solution. Alex Eng J 55:1069–1076. https://doi.org/10.1016/j.aej.2016.03.012.

[43] Campos BB, Diniz RHS, da Silveira FA et al (2019) ELEPHANT GRASS (Pennisetum purpureum Schumach) IS A PROMISING FEEDSTOCK FOR ETHANOL PRODUCTION BY THE THERMOTOLERANT YEAST Kluyveromyces marxianus CCT 7735. Brazilian J Chem Eng 36:43–49. https://doi.org/10.1590/0104-6632.20190361s20170263.

[44] Rueda JA, de Guerrero-Rodríguez JD, Ramírez-Ordoñes S et al (2020) Morphological composition and fiber partitioning along regrowth in elephant grass CT115 intended for ethanol production. Sci Rep 10. https://doi.org/10.1038/s41598-020-72169-2.

[45] Yasuda M, Ishii Y, Ohta K (2014) Napier grass (Pennisetum purpureum Schumach) as raw material for bioethanol production: pretreatment, saccharification, and fermentation. Biotechnol Bioprocess Eng 19:943–950.

[46] Rocha-Meneses L, Otor OF, Bonturi N et al (2020) Bioenergy yields from sequential bioethanol and biomethane production: an optimized process flow. Sustain 12:1–19. https://doi.org/10.3390/su12010272.

[47] Pardang P, Sonwai A, Pholchan P et al (2020) Potential of lignin-rich grass, pennisetum purpureum × pennisetum typhoideum, as a feedstock for biogas production. J Environ Eng 146:04020074. https://doi.org/10.1061/(ASCE)EE.1943-7870.0001741.

[48] Phuttaro C, Reungsang A, Boonsawang P, Chaiprapat S (2019) Integrative effects of sonication and particle size on biomethanation of tropical grass Pennisetum purpureum using superior diverse inocula cultures. Energies 12:4226. https://doi.org/10.3390/en12224226.

[49] De Conto D, Silvestre WP, Baldasso C, Godinho M (2016) Performance of rotary kiln reactor for the elephant grass pyrolysis. Bioresour Technol 218:153–160. https://doi.org/10.1016/j.biortech.2016.06.082.

[50] Reza MS, Islam SN, Afroze S et al (2020) Evaluation of the bioenergy potential of invasive Pennisetum purpureum through pyrolysis and thermogravimetric analysis. Energy Ecol Environ 5:118–133. https://doi.org/10.1007/s40974-019-00139-0.

[51] Cai C, Wang L, Wang G et al (2020) Effects of dry explosion pretreatment on physicochemical and fuel properties of hybrid pennisetum (Pennisetum americanum × P. purpureum). Bioresour Technol 297:122–508. https://doi.org/10.1016/j.biortech.2019.122508.

[52] Strezov V, Evans TJ, Hayman C (2008) Thermal conversion of elephant grass (Pennisetum Purpureum Schum) to bio-gas, bio-oil and charcoal. Bioresour Technol 99:8394–8399. https://doi.org/10.1016/j.biortech.2008.02.039.

[53] de Morais RF, de Souza BJ, Leite JM et al (2009) Elephant grass genotypes for bioenergy production by direct biomass combustion. Pesqui Agropecuária Bras 44:133–140. https://doi.org/10.1590/s0100-204x2009000200004.

[54] Brandon AG, Scheller HV (2020) Engineering of bioenergy crops: dominant genetic approaches to improve polysaccharide properties and composition in biomass. Front Plant Sci 11.

[55] Danquah JA, Roberts CO, Appiah M (2018) Elephant grass (Pennisetum purpureum): a potential source of biomass for power generation in Ghana. Curr J Appl Sci Technol 30:1–12. https://doi.org/10.9734/cjast/2018/45224.

[56] do Amaral Santos de Carvalho Rocha JR, Machado JC, Carneiro PCS et al (2017) Bioenergetic potential and genetic diversity of elephantgrass via morpho-agronomic and biomass quality traits. Ind Crops Prod 95:485–492. https://doi.org/10.1016/j.indcrop.2016.10.060.

[57] do Amaral Santos de Carvalho Rocha JR, Machado JC, Carneiro PCS et al (2017) Elephant grass ecotypes for bioenergy production via direct combustion of biomass. Ind Crops Prod 95:27–32. https://doi.org/10.1016/j.indcrop.2016.10.014.

[58] Marafon AC, Amaral AFC, Machado JC et al (2021) Chemical composition and calorific value of elephant grass varieties and other feedstocks intended for direct combustion. Grassl Sci 67:241–249. https://doi.org/10.1111/grs.12311.

[59] Brito da Silva V, Daher RF, de Souza YP et al (2020) Assessment of energy production in full-sibling families of elephant grass by mixed models. Renew Energy 146:744–749. https://doi.org/10.1016/j.renene.2019.06.152.

[60] Flores RA, Urquiaga S, Alves BJR et al (2012) Yield and quality of elephant grass biomass produced in the cerrados region for bioenergy. Eng Agric 32:831–839. https://doi.org/10.1590/S0100-69162012000500003.

[61] Ferreira FM, do Amaral JR, Lopes L et al (2021) Optimal harvest number and genotypic evaluation of total dry biomass, stability, and adaptability of elephant grass clones for bioenergy purposes. Biomass Bioenergy 149.

[62] Kumar AK, Sharma S (2017) Recent updates on different methods of pretreatment of lignocellulosic feedstocks: a review. Bioresour Bioprocess 4:7. https://doi.org/10.1186/s40643-017-0137-9.

[63] García JC, Díaz MJ, Garcia MT et al (2013) Search for optimum conditions of wheat straw hemicelluloses cold alkaline extraction process. Biochem Eng J 71:127–133. https://doi.org/10.1016/j.bej.2012.12.008.

[64] García MT, Alfaro A, Garcia JC et al (2017) Obtainment of hemicellulose derivatives and cellulose pulp from wheat straw following cold alkaline extraction. Cellul Chem Technol 51:465–475.

[65] Cheng H, Zhan H, Fu S, Lucia LA (2011) Alkali extraction of hemicellulose from depithed corn stover and effects on soda-AQ pulping. Bioresources 6:196–206. https://doi.org/10.15376/biores.6.1.196-206.

[66] Arnoul-Jarriault B, Lachenal D, Chirat C, Heux L (2015) Upgrading softwood bleached kraft pulp to dissolving pulp by cold caustic treatment and acid-hot caustic treatment. Ind Crops Prod 65:565–571. https://doi.org/10.1016/j.indcrop.2014.09.051.

[67] Steinbach D, Kruse A, Sauer J (2017) Pretreatment technologies of lignocellulosic biomass in water in view of furfural and 5-hydroxymethylfurfural production- a review. Biomass Convers Biorefinery 7:247–274. https://doi.org/10.1007/s13399-017-0243-0.

[68] Peng F, Peng P, Xu F, Sun RC (2012) Fractional purification and bioconversion of hemicelluloses. Biotechnol Adv 30:879–903.

[69] Longue Júnior D, Colodette JL, Gomes VJ (2010) Remoção de hemiceluloses da madeira por tratamento de lixiviação alcalina com NaOH. Cerne 16:423–429. https://doi.org/10.1590/S0104-77602010000400001.

[70] Hutterer C, Schild G, Potthast A (2016) A precise study on effects that trigger alkaline hemicellulose extraction efficiency. Bioresour Technol 214:460–467. https://doi.org/10.1016/j.biortech.2016.04.114.

[71] Park YC, Kim JS (2012) Comparison of various alkaline pretreatment methods of lignocellulosic biomass. Energy 47:31–35. https://doi.org/10.1016/j.energy.2012.08.010.

[72] Cardona EM, Rios JA, Peña JD, Rios LA (2013) Pretratamiento Alcalino de Pasto Elefante (Pennisetum sp) y King Grass (Pennisetum hybridum) Cultivados en Colombia para la Producción de Bioetanol. Inf Tecnol 24:69–80. https://doi.org/10.4067/S0718-07642013000500009.

[73] Prinsen P (2010) Composición química de diversos materiales lignocelulósicos de interés industrial y análisis estructural de sus ligninas.

[74] Hu Z, Sykes R, Davis MF et al (2010) Chemical profiles of switchgrass. Bioresour Technol 101:3253–3257. https://doi.org/10.1016/j.biortech.2009.12.033.

[75] Tsalagkas D, Börcsök Z, Pásztory Z et al (2021) Assessment of the papermaking potential of processed Miscanthus × giganteus stalks using alkaline pre-treatment and hydrodynamic cavitation for delignification. Ultrason Sonochem 72:105462. https://doi.org/10.1016/j.ultsonch.2021.105462.

[76] Devrije T (2002) Pretreatment of Miscanthus for hydrogen production by Thermotoga elfii. Int J Hydrog Energy 27:1381–1390. https://doi.org/10.1016/S0360-3199(02)00124-6.

[77] Matei JC, Soares M, Bonato ACH et al (2020) Enzymatic delignification of sugar cane bagasse and rice husks and its effect in saccharification. Renew Energy 157:987–997. https://doi.org/10.1016/j.renene.2020.05.028.

[78] Garrote G (2003) Hydrothermal and pulp processing of Eucalyptus. Bioresour Technol 88:61–68. https://doi.org/10.1016/S0960-8524(02)00256-0.

[79] Persson T, Ren JL, Joelsson E, Jönsson A-S (2009) Fractionation of wheat and barley straw to access high-molecular-mass hemicelluloses prior to ethanol production. Bioresour Technol 100:3906–3913. https://doi.org/10.1016/j.biortech.2009.02.063.

[80] Finell M (2003) The use of reed canary-grass (Phalaris arundinacea) as a short fibre raw material for the pulp and paper industry. Swedish University of Agricultural Sciences. Umea, Sweden.

[81] de Carvalho DM, de Queiroz JH, Colodette JL (2016) Assessment of alkaline pretreatment for the production of bioethanol from eucalyptus, sugarcane bagasse and sugarcane straw. Ind Crops Prod 94:932–941. https://doi.org/10.1016/j.indcrop.2016.09.069.

[82] Ai J, Tschirner U (2010) Fiber length and pulping characteristics of switchgrass, alfalfa stems, hybrid poplar and willow biomasses. Bioresour Technol 101:215–221. https://doi.org/10.1016/j.biortech.2009.07.090.

[83] Feria MJ, López F, García JC et al (2011) Valorization of Leucaena leucocephala for energy and chemicals from autohydrolysis. Biomass Bioenergy 35:2224–2233. https://doi.org/10.1016/j.biombioe.2011.02.038.

[84] Jeetah P, Golaup N, Buddynauth K (2015) Production of cardboard from waste rice husk. J Environ Chem Eng 3:52–59. https://doi.org/10.1016/j.jece.2014.11.013.

[85] Gao Y, Guo X, Liu Y et al (2018) A full utilization of rice husk to evaluate phytochemical bioactivities and prepare cellulose nanocrystals. Sci Rep 8. https://doi.org/10.1038/s41598-018-27635-3.

[86] Tsai WT, Tsai YL (2016) Thermochemical characterization of napier grass as an energy source and its environmental and economic benefit analysis. Energy Sources B Econ Plan Policy 11:130–136. https://doi.org/10.1080/15567249.2011.590847.

[87] Rodriguez B, Romero J (2017) EVALUACIÓN DEL POTENCIAL ENERGÉTICO DEL ZACATE “KING GRASS” (Pennisetum purpureum). Universidad del Salvador, EN EL SALVADOR.

[88] Raveendran K, Ganesh A (1996) Heating value of biomass and biomass pyrolysis products. Fuel 75:1715–1720. https://doi.org/10.1016/S0016-2361(96)00158-5.

[89] Martínez S (2009) Evaluación de la biomasa como recurso energético renovable en Cataluña.

[90] Glasser WG, Kaar WE, Jain RK, Sealey JE (2000) Isolation options for non-cellulosic heteropolysaccharides (HetPS). Cellulose 7:299–317. https://doi.org/10.1023/A:1009277009836.

[91] Sun RC, Fang JM, Tomkinson J et al (2001) Fractional isolation, physico-chemical characterization and homogeneous esterification of hemicelluloses from fast-growing poplar wood. Carbohydr Polym 44:29–39. https://doi.org/10.1016/S0144-8617(00)00196-X.

[92] Shao H, Hu Y, Sun H et al (2019) Response surface optimization of alkali extraction and characterization of poplar hemicellulose. Bioresources 14:3844–3859. https://doi.org/10.15376/biores.14.2.3844-3859.

[93] Maksimuk Y, Antonava Z, Krouk V et al (2021) Prediction of higher heating value (HHV) based on the structural composition for biomass. Fuel 299:120860. https://doi.org/10.1016/j.fuel.2021.120860.

[94] de Carvalho DM, Sevastyanova O, de Queiroz JH, Colodette JL (2016) Cold alkaline extraction as a pretreatment for bioethanol production from eucalyptus, sugarcane bagasse and sugarcane straw. Energy Convers Manag 124:315–324. https://doi.org/10.1016/j.enconman.2016.07.029.

Publisher's Note

Springer Nature remains neutral with regard to jurisdictional claims in published maps and institutional affiliations.

According to the journal policy, we confirm that neither the manuscript nor any parts of its content are currently under consideration or published in another journal and its publication is approved by all the authors.

3.1.2. Extracción Alcalina en Frío del Clon AF2 de *Populus x euramericana*.

Los resultados de este estudio han sido publicados en el artículo: **Ultrasound-Assisted Cold Alkaline Extraction: Increasing Hemicellulose Extraction And Energy Production From *Populus* Wood.** S. Lozano-Calvo, J.M. Loaiza, J.C. García, M.T. García and F. López. Forests 2024, 15, 109. (**Publicación 2**).

A continuación, se ofrece un resumen sintético y una contextualización detallada de esta contribución.

En el contexto del creciente uso de la biomasa para transformar el mercado de las energías renovables, destacan las biomasas leñosas por no competir con las aplicaciones alimentarias y por su mayor densidad en comparación con las biomasas herbáceas.

Varias especies de los géneros *Populus, Salix, Eucalyptus, Miscanthus, Cynara, Paulownia, Robinia, Casuarina* y *Leucaena,* entre otros, se están utilizando como cultivos energéticos de rotación corta a escala global. En particular, el género *Populus* tiene la ventaja de adaptarse a una amplia variedad de condiciones ambientales, además de una alta capacidad de hibridación y facilidad de propagación vegetal, lo que ha impulsado un importante desarrollo en la clonación de esta especie. En este estudio, se empleó el clon AF2 de *Populus x euramericana,* cosechado a intervalos de tres años en la provincia de Huelva (España).

Diversas investigaciones han demostrado que la extracción alcalina en frío es menos eficiente en materiales leñosos en comparación con los herbáceos. Para mejorar esta eficacia, en este estudio se incorporó la tecnología de ultrasonidos. Esta tecnología mejora la extracción al inducir la cavitación acústica, que provoca la creación y colapso de microburbujas. Este proceso genera choques y puntos calientes, liberando altas temperaturas y presiones, lo que descompone la cristalinidad de las partículas sólidas.

Por lo tanto, el objetivo principal de este apartado es aplicar el tratamiento de extracción alcalina en frío al clon AF2 de *Populus x euramericana*, incorporando la tecnología de ultrasonidos. Se comparó la efectividad del tratamiento con y sin ultrasonidos, evaluando la obtención de un licor rico en hemicelulosas y un residuo sólido apto para la producción de energía con una mayor eficiencia.

Al igual que con la biomasa de hierba elefante, se seleccionaron como variables independientes la concentración de hidróxido de sodio, la temperatura y el tiempo de operación, dentro de un diseño experimental de composición central. La concentración de hidróxido de sodio varío entre 80 g L^{-1} y 120 g L^{-1}, las temperaturas entre 20 ºC y 40 ºC, y los tiempos de operación entre 30 y 90 minutos. En

todos los ensayos se utilizó un hidromódulo (relación líquido/sólido) fijo de 15. Se llevó a cabo un diseño con y sin la aplicación de ultrasonidos.

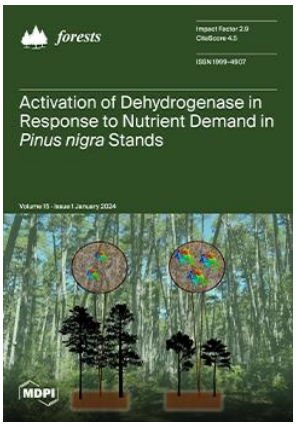
En este caso, la materia prima también fue caracterizada química y energéticamente siguiendo normas estándar. El clon AF2 de *Populus x euramericana* contenía un 40,3% de celulosa (medido como glucano), un 20% de hemicelulosa (medido como xilano y grupos acetilo) y un 25,1% de lignina Klason. Presentando un poder calorífico superior de 19,98 MJ kg^{-1}.

En resumen, los resultados demostraron que el uso de ultrasonidos incrementó la selectividad del tratamiento de extracción alcalina en frío hacia las fracciones de hemicelulosa y lignina. Se obtuvo un sólido con mayor poder calorífico y un licor rico en hemicelulosas. Al operar con tiempos prolongados, temperaturas moderadas y concentraciones medias-altas de álcali en el clon AF2 de *Populus x euramericana,* junto con la aplicación de ultrasonidos, se maximizó el contenido de glucano en el sólido residual, así como su contenido energético.

PUBLICACIÓN 2.

Ultrasound-Assisted Cold Alkaline Extraction: Increasing Hemicellulose Extraction and Energy Production from Populus Wood.

S. Lozano-Calvo, J.M. Loaiza, J.C. García, M.T. García and F. López.



Forests
MDPI
Volumen 15(1), número: 109 (2024).
DOI: 10.3390/f15010109

Categoría	**Clasificación revista/Número total de revistas**	**Cuartil (Porcentaje)**
Forestal	21/89	Q1 (77%)
Factor de impacto	2,4	

Ultrasound-Assisted Cold Alkaline Extraction: Increasing Hemicellulose Extraction and Energy Production from Populus Wood.

S. Lozano-Calvo *, J. M. Loaiza, J. C. García, M. T. García and F. López

*Correspondence: susana.lozano@diq.uhu.es

Research Centre for Technology of Products and Chemical Processes (PRO2TECS), Department of Chemical Engineering, University of Huelva, Av. 3 de marzo s/n, 21071 Huelva, Spain; javiermauricio.loiza@diq.uhu.es (J.M.L.); juan.garcia@diq.uhu.es (J.C.G.); mtrinidad.garcia@diq.uhu.es (M.T.G.); baldovin@diq.uhu.es (F.L.)

Abstract

Alkaline pretreatments are considered highly effective for the separation of the different components of lignocellulosic biomass. However, cold alkaline extraction (CAE) exhibits minimal modification/degradation of hemicellulosic fraction and successfully accomplishes efficient delignification. In this research, the fast-growing clone AF2 of *Populus x euramericana* wood was utilized as the raw material and subjected to ultrasound-assisted CAE. The objective of incorporating ultrasound into cold alkaline extraction is to increase the yield of a hemicellulosic-rich liquid phase that can be used to produce high-value products such as furfural or xylitol. Simultaneously, it aims to obtain a solid phase with a higher calorific value compared to the raw material. The results, obtained from a central composite factorial design, demonstrated that the CAE process for 90 min at a sodium hydroxide concentration of 100 g L^{-1}, a temperature of 30 ºC, and with ultrasound assistance maximized hemicellulose extraction in the liquid phase (60.8% was extracted) and improved the heating value of solid phase.

Keywords: biomass; delignification; hemicelluloses; pre-treatment; ultrasound.

1 Introduction.

International commitments of the European Union to mitigate climate change have promoted a search for clean, renewable energy sources including biomass [1]. More than 60% of the amount of energy produced from biomass in the world is obtained from renewable sources, which account for up to 19.3% of the whole energy output [2]. The use of lignocellulosic biomass has expanded steadily in recent times and is expected to continue to grow in the coming years by virtue of the value-added products that can be obtained from chips, pellets, biogas, and other biorefinery materials [3,4]. However, conventional agroforestry systems cannot by themselves meet the growing demand, so fast-growing woody species are being increasingly planted for this purpose [5]. In this scenario, converting biomass through biorefinery processes has a high potential judging by their sustainability, and also by the fact that they use waste materials to provide alternative energies and high value-added products according to the principles of sustainable development [6,7]. In addition, commitments to a

https://doi.org/10.3390/f15010109

circular economy, the need to reduce the dependence on raw materials from non-renewable fossil resources, and the consequences of climate change all necessitate the adoption of novel technologies within conventional production sectors. This transition aims to supplant the prevailing industrialization model with efficient use of natural resources as far as possible [8,9].

A number of plant species of the genera *Populus, Salix, Eucalyptus, Miscanthus, Cynara, Paulownia, Robinia, Casuarina,* and *Leucaena*, among others, are being used as short-rotation energy crops on a global scale [6,10,11]. Some are multi-purpose species that provide a variety of goods such as forage or paper pulp, and services such as soil restoration or carbon sequestration. These industrial lignocellulosic crops are expected to cover 5–10% of the global forest area by 2050 [12]. In Europe alone, farmland has undergone degradation to such an extent that 45% of its soils have low organic matter contents (<2%); also, 15% have problems due to over-fertilization with inorganic nitrogen, and more than 147 million hectares are seriously eroded [13]. Fortunately, at least 70% of all degraded land is under a climate allowing plants such as *Robinia pseudoacacia, Ulmus pumila, Eucalyptus* sp., and/or *Populus* sp. to grow. It can thus be useful to assess biomass production, industrial use, and the environmental impact of their intensive production on already poor, degraded soils with a view to their potential exploitation [14]. The limited research carried out in this area has indicated that the results are influenced by specific plant species, cultivation conditions, and environmental factors [15,16].

Recent studies have shown the genus *Populus* can easily adapt to varying environmental conditions; also, it possesses a high hybridization capacity and ease of vegetative propagation. These advantages, together with its fast growth, have boosted the development of a very broad clonal offer that allows clones to be selected for optimal growth at specific sites and for specific purposes [11].

The principal components of lignocellulosic biomass are cellulose, hemicellulose, and lignin. All of these components have the potential to yield high-value products. However, achieving this goal necessitates the utilization of a biorefinery scheme for the selective separation and recovery of these fractions [17]. Often, it is particularly useful to carry out the fractionation in two steps. The first step involves hydrolysis under relatively mild conditions to extract the hemicelluloses (which have low resistance). Additionally, this helps prevent excessive degradation of cellulose fibers. The second step involves oxidative delignification or organosolv treatment to remove the lignin fraction [18]. Among the various pretreatment methods available, alkaline pretreatment offers significant advantages, including the use of environmentally friendly and non-corrosive chemicals, as well as milder operating conditions [19]. Cold Alkaline Extraction (CAE) is one such pretreatment that offers the added benefit of yielding hemicelluloses for use as food additives or in the production of furfural and polymers [12]. The CAE, conducted at 20-40 ºC, does not necessitate high pressures, resulting in

reduced energy consumption [20]. Nevertheless, the primary advantage of CAE compared to other biomass fractionation techniques lies in its capacity to selectively extract hemicelluloses with minimal degradation and enable straightforward separation through alcoholic precipitation [21].

However, CAE has its disadvantages, and the most significant one is likely its efficiency, which strongly depends on the specific raw material. This pretreatment has been extensively studied for various applications, and it has been observed that the extraction of hemicelluloses is more efficient in herbaceous lignocellulosic materials than in wood [21–24].

The pretreatment's effectiveness can be enhanced through supplementary procedures, including prehydrolysis, impregnation, or novel techniques such as ultrasound-assisted extraction, sub-critical and supercritical fluid extraction, microwave-assisted extraction, or solvent-accelerated extraction [25,26]. The application of ultrasound can be employed as either a pretreatment step or during the treatment process, providing a clean and eco-friendly extraction method with several benefits [25,27]. Extraction is improved by the transmission of ultrasound, which induces acoustic cavitation. This, in turn, triggers the spontaneous creation of microbubbles. When these microbubbles collapse, they produce localized shock waves and hot spots, releasing high temperatures and pressure. This disintegrates the crystalline structure of solid particles [28]. Ultrasound-assisted fractionation improves the efficiency of conventional processes, and results in a high product yield and selectivity [29]. A. García et al. [29] investigated various lignocellulosic biomass fractionation processes with ultrasound assistance. The results showed that this technology produced a liquid richer in hemicelluloses and lignin compared to when it was not used.

On the other hand, direct combustion is a method for generating chemical energy. This process leads to the emission of CO_2, particulate matter, sulfur dioxide, and other compounds. However, the quantities released are relatively lower than those produced by the combustion of fossil fuels [30,31].

There are numerous scientific investigations on the extraction of hemicellulosic derivatives using various alkaline processes, both with and without ultrasound assistance [32,33]. In this work, we combined a cold alkaline treatment with ultrasound technology. This approach lacks references in the literature, representing a significant aspect of academic originality and scientific novelty. Furthermore, the efficiency of CAE is highly dependent on the raw material used, adding another point of scientific and academic novelty when testing these processes on a raw material such as the AF2 clone of *Populus x euramericana*. To the best of the authors' knowledge, there are no bibliographic references exploring its utilization for the simultaneous valorization of the hemicellulosic liquid and energy application of the solid residue, despite numerous studies on the value-added product of hemicellulosic, as demonstrated by A. Tareen et al. [34]. The AF2 clone of

Populus x euramericana is a high-yield energy crop, and optimizing the conditions for the industrial biorefinery process holds great potential, especially for potential scaling to a semi-industrial or industrial level of exploitation.

For these purposes, the AF2 clone of *Populus x euramericana* was evaluated as a raw material for hemicellulose extraction using CAE, both with and without ultrasound assistance. The process included modeling and optimization through multiple regression, a widely employed approach for optimizing biomass and waste stream valorization [35,36]. The aim was to obtain a high-value liquid fraction and energy from the resulting solid residue, within the context of comprehensive utilization (biorefining).

2 Materials and Methods.

2.1 Characterization and Storage of Raw Materials.

The raw material utilized was wood from the AF2 clone of *Populus x euramericana*, from the province of Huelva, located in southwestern Spain. The material was subject to cold grinding in a Resch mill for 4 min and then sieved to obtain chips approximately 1–3 cm long and 0.5 cm wide. These chips were allowed to equilibrate with ambient moisture and temperature before being stored in tightly closed containers during the period between obtaining the wood chips and their use in the CAE process.

For characterization, the chips were further ground to a size of less than 0.5 mm using an Ika Werke mill. Tests were conducted following international standards, including TAPPI T264 cm-07 for moisture [37], TAPPI 211 om-02 for ash [38], and TAPPI T204 cm-07 in combination with Soxhlet extraction (95% ethanol, 5 h) for extractives [39].

Following gravimetric testing, the material was subjected to quantitative acid hydrolysis with 72% H_2SO_4, and the hydrolysate was analyzed for monomeric sugars (glucose, xylose, and arabinose) according to TAPPI T249 cm-09 [40]. This analysis was conducted using high-performance liquid chromatography (HPLC) with an AMinex HPX-87H ionexchange column (Bio-Rad Laboratories, Alcobendas, Madrid, Spain) at 30 ºC as the stationary phase and 0.005 M H_2SO_4 at a flow rate of 0.6 mL min^{-1} as the mobile phase [41]. Klason lignin was determined following the guidelines of TAPPI T222 om-11 [42].

2.2 Cold Alkaline Extraction (CAE) with and without Ultrasound.

Hemicelluloses were subjected to CAE in a Power Sonic Series 500 ultrasonic bath, using a constant liquid/solid ratio of 15 Kg of water per Kg of raw material on a dry basis (odb). The independent operational variables of the process were temperature (20, 30, or 40 °C), time (30, 60, or 90 min), and sodium hydroxide concentration (80, 100, or 120 g L^{-1}).

https://doi.org/10.3390/f15010109

The resulting CAE liquor was filtered, and the solid residue was washed with water. Then, the solid fraction was air-dried to determine moisture content and weighed to calculate the process yield. The solid fraction underwent chemical characterization using the same test as the raw material. Additionally, it was analyzed for calorific value following CEN/TS 14918:2005 E [43] and UNE 16001 EX [44]. This analysis used a Parr 6300 automatic Isoperibol calorimeter (Parr Instrument Company. Moline, Illinois. USA), a CGA 540 connector, 99.5% pure oxygen, and a maximum pressure of 2500 psig. Furthermore, the solid was subjected to elemental analysis (C, N, O, and H) using a C/H/S-Analyser autosampler Eltra Helos.

The statistical dispersion of the results from chemical and energetic characterization will not be analyzed using the typical parameters of univariate statistics (standard deviation). As this is a multivariate modeling approach aimed at replicating experimental results, it is important to take into account the dispersion between the experimental values and those calculated using the models detailed in Section 2.3, expressed in terms of the coefficient of variation. The analysis and discussion of this coefficient will be conducted in the results section.

2.3 Modeling and Optimization by Multiple Regression-Experimental Design.

The CAE process was modeled by multiple regression with provision for linear, quadratic, and interaction terms among the independent variables:

$$Y = a_0 + \sum_{i=1}^{n} b_i X_{ni} + \sum_{i=1}^{n} c_i X_{ni}^2 + \sum_{i=1,j=1}^{n} d_{ij} X_{ni} X_{nj} \ \text{(i<j)} \quad (1)$$

The number of tests needed was decreased and covariance between variables was reduced by using a central composition design with N tests such that $N=2^n + 2\cdot n + n_c$, 2^n being the number of points constituting the design, $2\cdot n$ that of axial points and n_c that of central points. The effect of the different ranges spanned by the variables was suppressed by normalizing their values to 0, 1, and –1 with the following equation:

$$X_n = \frac{X - \bar{X}}{(X_{max} - X_{min})/2} \quad (2)$$

where X, $\bar{X}$, X_{max}, and X_{min} represent the value of a particular independent variable, and its mean, maximum, and minimum values, respectively. The dependent variables under examination included yield, glucan, xylan, Klason lignin, and lower heating value (LHV).

The statistical models developed in this study to represent the various dependent variables should exhibit globally significant model values, such as the R-squared (R^2) and Snedecor F statistics, that are sufficiently high for the models to have statistical relevance. The "appropriate" threshold for these statistics will vary depending on the type of results and models used, whether working with variables of a more "social" nature or more deterministic ones, as in laboratory experiments. However, in the context of our study, values of R^2 greater than 0.85 and Snedecor F values above 5 are considered

very appropriate. In the results section, the statistical significance of each model will be addressed according to these criteria. Furthermore, the statistical importance of each coefficient associated with the independent variables will be evaluated. In this context, a conventional criterion is used, which considers an independent variable to be statistically significant in the model when its significance level "p" is less than 0.05 or the value of the Student-*t* test is greater than 2. The variables included in the models presented in the results section adhere to this conventional criterion.

Furthermore, in order to simplify interpretation, polynomial equations were employed to generate response surfaces. These surfaces were created by plotting two of the three independent process variables on two horizontal axes while displaying the maximum and minimum levels of the third independent variable. This enables a comprehensive representation of the entire range of variation for each dependent variable in relation to all independent process variables (in our case, alkali concentration, treatment time, and temperature).

3 Results and Discussion.

The initial hypothesis was that the cold alkaline extraction (CAE) of clone AF2 of *Populus x euramericana* would be more efficient than that of other woody species such as eucalyptus (the reference species here). Furthermore, it was hypothesized that the use of ultrasound during the process would result in increased extraction of hemicelluloses in the liquor. If the process were highly selective for hemicelluloses, there would be the additional benefit of an increased calorific value in the solid residue from CAE. This hypothesis was tested by analyzing the raw material and modeling the results obtained with and without ultrasound for comparison.

3.1 Chemical Characterization of the Raw Material.

As previously mentioned, *Populus x euramericana* is a tree species with a wide range of clones [45,46]. In this work, we selected clone AF2 due to its fast growth and adaptability. Under the conditions described above, this clone yielded over 25 tons of dry biomass per hectare per year when harvested at 3-year intervals. The biomass used in this study primarily consisted of stems and branches with a thickness of 2.5–10.0 cm, accounting for 67.5% of the total biomass. The bark content of the biomass, which should ideally be minimized to maintain quality, ranged from 31% in the thickest stems to 12% in those 5.0–10.0 cm thick. The primary criterion for selecting this poplar clone was its sustainability as a crop. Indeed, after 9 years, the target plantation had significantly improved soil quality by increasing the organic matter content by 0.23 percentage points (from 0.80% -typical values in poor soils- to 1.03%) and the nitrogen content by 0.03 percentage points (from 0.12% to 0.15%).

Table 1 displays the results of chip characterization and compares them with the results from Constantí et al. [47] for the *Populus* genus and those from studies on other lignocellulosic raw materials conducted elsewhere. These results represent various raw materials obtained prior to the extraction process and were acquired by different authors following international standards (TAPPI standards). The table also shows the higher heating value (HHV) for the clone and the other materials. Additional determinations for AF2 included the contents of extractives soluble in 1% NaOH (22.3%, -1.95-), hot water (4.22%, -0.12-), and ethanol–acetone mixtures (2.8%, -0.15-). The similarity between the content of xylan and that in NaOH-soluble extractives suggests that the hemicellulose fraction of the studied clone is primarily composed of that polysaccharide. The elemental composition of the biomass was 6.11% hydrogen (H), 0.00019% sulfur (S), 48.67% carbon (C), and 44.13% oxygen (O).

As shown in Table 1, the lignin and xylan contents of the clone exceeded those of most of the species compared, especially the reference material (*E. globulus*) and the Populus species examined by Constantí et al. and Ebringerová et al. [47,48]. These differences are quite normal as the materials had different natures despite their common origin. In line with the results of Constantí et al. and Ebringerová et al. [47,48], clone AF2 contained no arabinan. Additionally, its α-cellulose and glucan contents were slightly lower, yet still similar to those of E. globulus and those reported by Constantí et al. and Ebringerová et al. [47,48] for a different *Populus* species. In contrast, the higher heating value (HHV) significantly exceeded that of most of the other materials, including *E. globulus*.

Table 1. Chemical Composition and Higher Calorific Value (HCV) of Clone AF2 of *Populus euramericana*, and Comparison with Other Materials.

Composition	(1)	(2)	(3)	(4)	(5)	(6)	(7)	(8)
α Cellulose (glucan) (%)	40.3±0.85	41.1±2.1	38.9±3.4	38.0±2.4	44.0±3.3	42.8±2.0	33.8±1.6	55.4±2.6
Klason Lignin (%)	25.1±0.16	24.1±1.8	19.8±1.9	19.0±2.5	27.8±1.1	21.2±0.9	19.9±0.5	16±0.3
Xylan (%)	19.3±0.09	17.0±0.5	19.9±1.3	15.7±0.1	15.7±0.2	17.1±0.3	23.9±0.1	34.6±0.4
Araban (%)	0	–	0.6±0.3	1.5±0.3	1.1±0.1	0.7±0.1	0.37±0.2	5.6±0.3
Acetyl groups (%)	0.7±0.02	–	4.4±0.6	3.3±0.5	4.4±0.2	3.5±0.1	4.32±0.1	–
HHV, KJul/kg od.b.	19982 ±30	–	19592±28	18981±95	20300±53	19326±84	17259±25	–

Raw material percentages (100 kg dry matter); 1—Genus *Populus* (Poplar clone AF2). Present study; 2—Genus *Populus* [47]; 3—Tagasaste (*Chamaecytisus proliferus*) [49,50]; 4—Leucaena (*Leucaena di-versifolia*) [51,52]; 5—Paulownia trihybrid (*fortunei x tormentose x elongata*) [53,54]; 6—*Eucalyptus globulus* [55,56]; 7—Sunflower stalks [52]; 8—Wheat straw [57].

3.2 Cold Alkaline Extraction of Hemicelluloses with and without Ultrasound Assistance.

Table 2 presents the yields, glucan, xylan, and lignin results obtained at each point in the experimental design for the CAE process with and without ultrasound. The values in the table are expressed as a percentage of each polymer in the initial raw material. They could be converted into percentages relative to the raw material by multiplying the value by the corresponding amount in the

initial raw material and dividing by 100. However, if this value is divided by the yield and then multiplied by 100, it would represent the percentage of the polymer relative to the solid phase.

Table 2. Normalized values of the process variables and composition of the solid fractions obtained in the two processes of cold alkaline extraction with and without ultrasound assistance of the *Populus x euramericana* (Clone AF2). Additionally, the glucan, xylan, and lignin contents are expressed as percentages relative to the raw material.

Variables			**With ultrasound**				**Without ultrasound**			
X_A	X_t	X_T	Yield (%)	Glucan (%)	Xylan (%)	Klason Lignin (%)	Yield (%)	Glucan (%)	Xylan (%)	Klason Lignin (%)
0	0	0	68.8	86.4	40.4	67.0	73.2	89.8	45.4	88.5
0	0	0	68.8	86.4	40.4	67.0	73.2	89.8	45.4	88.5
1	1	1	63.3	80.4	45.0	58.4	68.5	93.2	56.8	80.1
1	1	-1	67.9	84.3	43.5	62.4	77.8	95.7	49.3	83.4
1	-1	1	69.0	84.8	49.5	73.9	73.3	96.5	54.7	97.5
1	-1	-1	75.0	95.8	50.2	67.4	80.8	98.2	47.4	90.6
-1	1	1	64.7	96.2	47.2	51.5	69.3	98.1	43.3	71.6
-1	1	-1	70.9	96.2	51.6	66.7	77.6	98.2	51.3	90.9
-1	-1	1	69.5	85.7	49.9	69.2	71.6	89.8	53.0	89.5
-1	-1	-1	74.6	87.6	55.7	77.7	78.5	92.1	60.2	98.9
1	0	0	67.3	91.0	44.4	60.9	72.7	98.7	47.4	79.7
-1	0	0	69.4	95.6	50.3	61.3	73.1	97.4	47.6	79.6
0	1	0	66.5	81.7	39.2	68.7	73.7	88.1	46.4	93.3
0	-1	0	71.0	84.6	44.2	74.4	75.4	85.1	52.0	98.1
0	0	1	68.6	82.1	40.9	68.4	71.1	86.3	49.5	90.6
0	0	-1	73.5	84.1	42.6	72.9	78.7	87.8	50.1	96.0

X_A alkali concentration, X_t time, X_T temperature.

The results were modeled using Equations (3)–(10) from Table 3, as described in Sections 2.2 and 2.3. By analyzing the residuals between the experimental (observed) values and those predicted by the polynomial multiple regression models, it was observed that the prediction errors were all less than 10% and, in some cases, even less than 5%. This percentage is understood as the percentage change within the range of each dependent variable, rather than as the percentage change in the maximum or minimum value. Therefore, the obtained values demonstrate the robustness of the models.

Also, the quadratic regression coefficients, R^2, all exceeded 0.95, which was considered acceptable given the simultaneous calculations involving several independent variables. The Snedecor's *F*-values significantly exceeded 5, which is the minimum value required to assume a good fit. All independent variables included in the models had individual Student's *t*-values greater than 2 or *p*-values less than 0.05, including their statistical significance at the 95% confidence level. For easier

interpretation, the polynomial equations were employed to create the response surfaces in Figures 1 and 2 (refer to Section 2.3).

Table 3. Equations of the polynomial models for the dependent variables of the cold alkaline extraction (CAE) with and without ultrasound assistance of the *Populus x euramericana* wood (Clone AF2).

Equation with ultrasounds	**Equation number**	**Adjusted R^2 / Snedecor's *F-value***
$YI=68.5 - 0.67X_A - 2.57X_t - 2.66X_T - 1.83X_t^2 + 2.58X_T^2$	(3)	0.95 / 56
$GL=87.0 - 2.50X_A - 1.87X_T + 5.98X_A^2 - 4.03X_T^2 - 4.39X_AX_t - 1.6X_AX_T + 1.19X_tX_T$	(4)	0.98 / 59
$X=40.2 - 2.28X_A - 2.24X_t - 1.12X_T + 7.23X_A^2 + 1.62X_T^2 - 0.56X_AX_t + 1.37X_AX_T + 0.44X_tX_T$	(5)	0.98 / 138
$KL=66.6 - 5.96X_t - 2.57X_T - 5.33X_A^2 + 4.58X_T^2 + 1.04X_AX_t + 3.28X_AX_T - 2.34X_tX_T$	(6)	0.98 / 114
Equation without ultrasounds	**Equation number**	**Adjusted R^2 / Snedecor's *F-value***
$YI=73.0 + 0.3\ X_A - 1.38X_t - 3.97X_T + 1.68X_T^2 - 0.57X_AX_t - 0.42X_tX_T$	(7)	0.98 / 202
$GL=89.7 + 0.67X_A + 1.16X_t - 0.80X_T + 8.37X_A^2 - 2.86X_TX_T - 2.53X_AX_t$	(8)	0.99 / 189
$X=45.2 - 2.02X_t + 2.39X_A^2 + 4.39X_T^2 + 2.84X_AX_t + 3.76X_AX_T$	(9)	0.99 / 211
$KL=88.04 - 6.08X_t - 3.05X_T - 8.14X_A^2 + 2.61X_t^2 + 5.24X_T^2 + 4.05X_AX_T - 2.75X_tX_T$	(10)	0.99 / 251

Dependent variables: YI yield (%), GL glucan (%), X xylan (%), KL Klason lignin (%). Independent variables: X_A: alkali concentration, X_t and X_T: treatment time and temperature. The differences between the experimental values and those estimated using the equations never exceeded 10% of the former.

The values predicted by the quadratic Equations (3)–(15) can be easily calculated using these equations and, as mentioned, replicate the experimental results with coefficients of variation below 10% of the range of variation of each dependent variable.

Before delving into the data in Tables 2 and 3, it is important to note that our initial hypothesis was confirmed (i.e., clone AF2 of *Populus x euramericana* proved a suitable raw material for the intended purpose). The CAE yields obtained in the absence of ultrasound were significantly higher than those obtained by Carvalho et al. and Fernández et al. [20,58] with eucalyptus (ranging 3.2% to 5.0%), but lower than those observed for grassy materials such as wheat (ranging from 25.5% 38.8%; [21,16]). A lower yield implies a higher extraction yield in the liquid phase. These results are consistent with our earlier discussion on the introduction that CAE efficiency depends on the specific raw material. For instance, eucalyptus wood, which is resistant to CAE fractionation [20], can be efficiently extracted at temperatures, such as those used by Alfaro et al. and Carvalho et al. [49,20], which reached temperatures of up to 175 °C, resulting in yields of 5.0% to 32.9%. This confirmation aligns with the proportions of different polymers extracted in our study.

Based on Equations (3) and (7) in Table 3, it is evident that temperature had the most significant impact on yield as an individual operational variable, both in the presence and absence of ultrasound. Figures 1A and 2A depict a similar response to the other two independent variables, although over considerably different ranges, ranging from 63.3% to 75.0% with sonication and from 68.5% to 80.8% without it. These findings underscore the pronounced influence of ultrasound on CAE yield. Indeed, experimental yields were notably lower with ultrasound, which was reflected in their mean values and the predictions made by the multiple regression models presented in Equations (3) and (7), particularly at the central points of the experimental design (68.5% with ultrasound and 73.0% without it). It is important to note that a lower yield was preferable as CAE efficiently removed structural components (cellulose, hemicellulose, and lignin) from the raw material. In fact, ultrasound-assisted CAE removed 25.0% to 36.7% of these initial structural components present in the material.

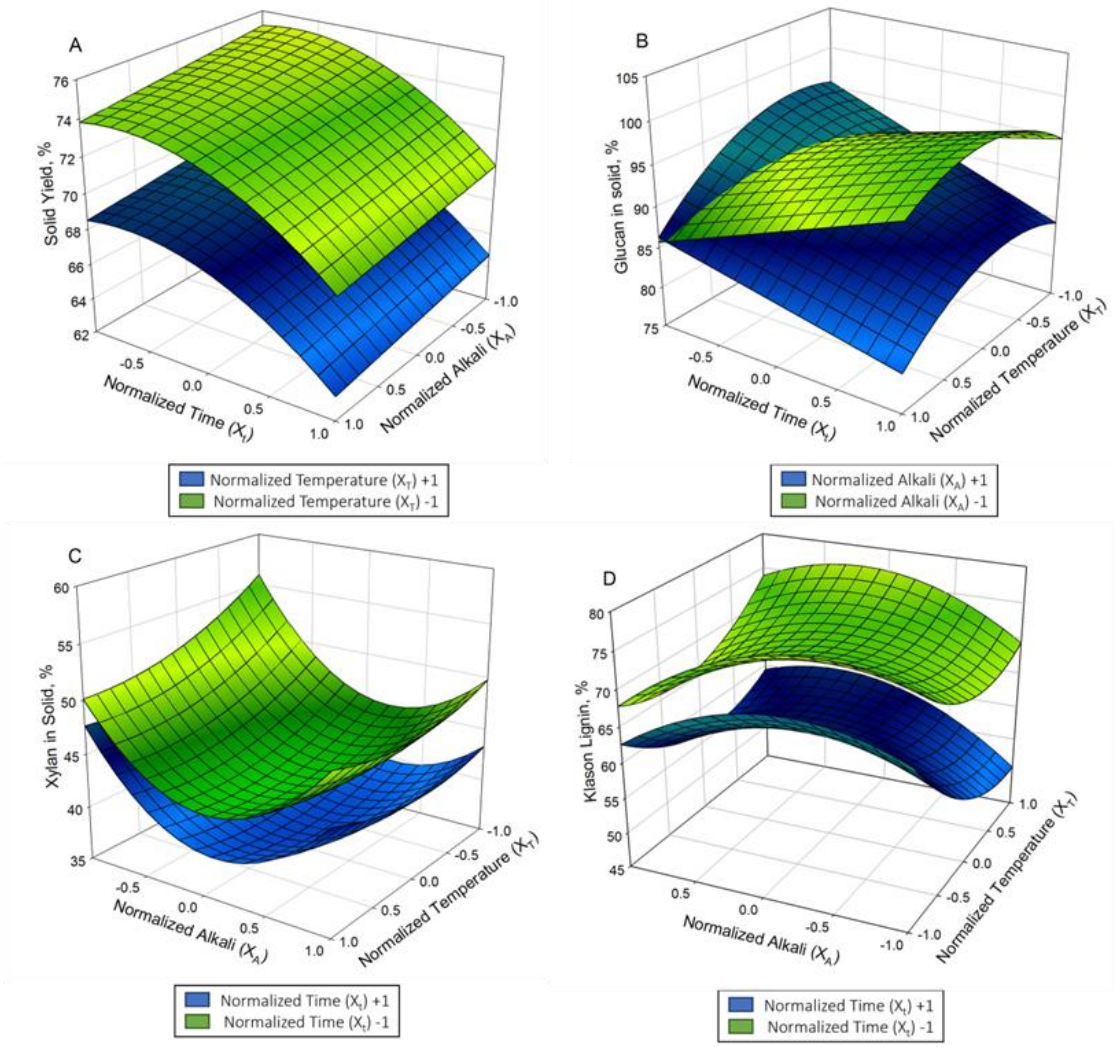


Figure 1. Surface responses for yield (**A**), as well as the glucan (**B**), xylan (**C**), and lignin contents (**D**) (percentage relative to the polymer content in raw material) in the solid residue obtained from the process of Cold Alkaline Extraction using ultrasound on the Popular Wood (clone AF2).

As observed in the glucan surface responses shown in Figures 1 and 2, the glucan content of the CAE solid residue decreased with increasing alkali concentration, treatment time, and solid yield. However, according to Equations (4) and (8), the alkali concentration was the most influential variable on the glucan content. Furthermore, the difference between the predicted values for glucan content at the central point of the experimental design (87.0% with ultrasound and 89.7% without it) was much smaller than that of the corresponding mean yields. Therefore, the yield ranges, both with (81.7%–95.6%) and without ultrasound (85.1%–98.7%), were more similar. Therefore, as previously found by García et al. and Carvalho et al. [20,21], ultrasound had a notably selective effect on the hemicellulose and lignin fractions. This was particularly true for xylan, the primary component of the hemicellulose fraction, characterized by its low polymerization and non-crystallinity structure that makes it more susceptible to decomposition into monosaccharides. These findings support the initial hypothesis that ultrasound enhances hemicellulose extraction in the CAE liquor while preserving or even increasing the calorific potential of the solid residue.

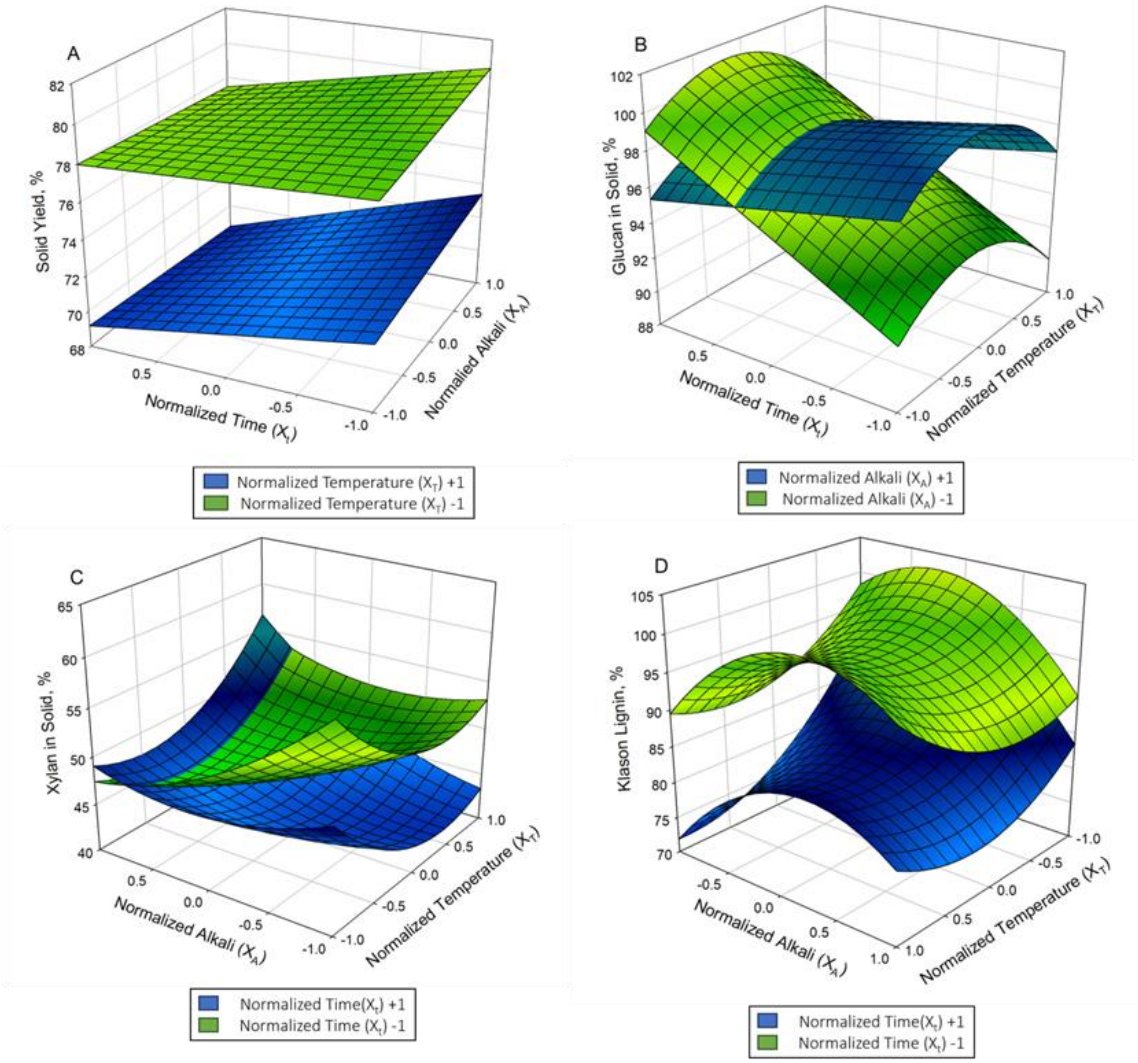


Figure 2. Surface responses for yield (**A**), as well as the glucan (**B**), xylan (**C**), and lignin contents (**D**) (percentage relative to the polymer content in raw material) in the solid residue obtained from the process of Cold Alkaline Extraction without ultrasound on the Popular Wood (clone AF2).

https://doi.org/10.3390/f15010109

In fact, when comparing the experimental ranges for hemicelluloses (xylan) extraction in the presence and absence of ultrasound (44.3%–60.8% vs. 39.8%–56.7%) with the predicted values at the central points based on Equations (5) and (9) (59.8% and 54.8%, respectively), it becomes evident that CAE had a much more selective effect on the hemicellulose fraction (xylan) than on the cellulose fraction (glucan). This difference was even more pronounced in the presence of ultrasound. This suggests that, notably, the CAE process exhibits a high selectivity for hemicelluloses while preserving the integrity of glucan. Alkaline treatments typically alter the structure of lignocellulosic materials by reducing the crystallinity and degree of polymerization of cellulose, thereby increasing the inner surface area, and facilitating release into the extraction medium [59].

Equations (6) and (10) do not provide a clear indication of the independent variable with the strongest influence on hemicellulose extraction into the CAE liquor. Figures 1C and 2C represent extreme values of treatment time, as it was clearly the independent variable that most strongly influenced CAE yield in a linear manner, without ultrasound. In the presence of ultrasound, the highest xylan contents of the solid residue (i.e., the lowest extraction of xylan into the CAE liquor) were achieved with extended treatment times, moderate alkali concentrations, and temperatures. The alkali concentration had little influence. Xylan extraction without ultrasound yielded similar results, although with lower hemicellulose extraction levels. These results were considerably higher than those reported by Carvalho et al. and Fernández et al. [20,60] for eucalyptus (46%) but comparable to those of García et al. and Madejón et al. [21,16] for wheat straw.

In theory, preserving glucan integrity while maximizing hemicellulose extraction into the CAE liquor would be easiest by using a long treatment time, a medium temperature, and a medium-to-high alkali concentration. Below are described the results of the elemental analysis of the CAE solid residue in the presence of ultrasound to confirm the practicality of these operating conditions.

Obviously, preserving most of the glucan in the raw material in the CAE solid residue is of interest when considering the thermal stability of this component. In fact, the cellulose fraction has the highest energy content among the constituents of lignocellulosic biomass [60].

The amount of lignin remaining in the solid was also interest. Cold alkaline extraction partially delignifies the raw material, potentially facilitating subsequent delignification of the solid residue, making it useful for applications such as cellulose pulping, or increasing energy production through thermochemical treatment. Lignin acts as a seal protecting the lignocellulosic fraction, which needs to be broken down to fully exploit the raw material. Due to its abundance of benzene rings, lignin has the highest activation energy and thermal stability [61]. The use of ultrasound significantly facilitated its extraction. Delignification at the central point of the experimental design was estimated to be

33.4% in the presence of ultrasound and 12.0% in its absence (Table 3). Lignin was extracted by 22.3%–48.5% with ultrasound and 1.9%–28.4% without it (Table 2). However, lignin was consistently extracted to a lesser extent than hemicelluloses, indicating that CAE was less selective toward the lignin fraction. Therefore, longer treatment times at the upper end of the range (Equations (4) and (8)), along with medium temperatures (Figure 1D) and alkali concentrations (Figure 2D), may be suitable for effective delignification and hemicellulose extraction while preserving glucan integrity. Since lignin is the most structurally complex component and resistant to extraction from lignocellulosic materials, the treatment time will be especially influential on the efficiency of the chemical treatment and the cavitational effects of ultrasound, leading to cleavage of lignin–cellulose bonds [62].

In summary, these comparisons regarding the yield, glucan, hemicelluloses, and lignin content in the CAE processes with and without ultrasound assistance confirm the initial hypothesis and demonstrate a significant synergistic effect when ultrasound and CAE are applied simultaneously, enhancing both the selectivity and efficiency of hemicellulose extraction and the potential for increased energy yield from the post-treatment solid phase.

Table 4. Values of the process variables and elemental composition (hydrogen, H; Sulphur, S; Carbon, C; and Oxygen, O) of the solid fractions obtained in the Cold alkaline extraction (CAE) with and without the use of ultrasound on *Populus x euramericana* wood (Clone AF2).

Normalized values			**Cold alkaline extraction (CAE) with ultrasound**					
X_A	X_t	X_T	H (%)	S (%)	C (%)	O (%)	Moisture (%)	LHV at constant volume (J/g o.d.b.)
0	0	0	6.105	0.00018	45.60	47.19	9.9	18843
1	1	1	5.867	0.00000	41.01	52.03	8.2	19233
1	1	-1	5.872	0.00000	42.36	50.68	7.8	19033
1	-1	1	5.918	0.00024	44.70	48.23	10.0	18115
1	-1	-1	5.922	0.00011	45.18	47.81	8.1	18570
-1	1	1	5.841	0.00000	42.00	51.07	11.2	18504
-1	1	-1	5.858	0.00016	43.88	49.17	8.2	18530
-1	-1	1	5.861	0.00020	43.85	49.20	10.0	18516
-1	-1	-1	5.908	0.00032	44.15	48.86	8.9	18675
1	0	0	6.023	0.00014	44.00	49.01	11.2	18965
-1	0	0	5.981	0.00030	44.25	48.71	8.8	18872
0	1	0	5.972	0.00004	44.69	48.25	8.2	18734
0	-1	0	5.962	0.000140	45.547	47.4	8.1	18477
0	0	1	5.870	0.000165	44.359	48.78	9.8	18482
0	0	-1	5.890	0.000205	45.076	47.78	9.7	18686

Another interesting point is the dependence of the elemental composition of the CAE solid residue on the operating conditions in the presence of ultrasound. This information can be useful for

identifying the optimal operating conditions for extracting hemicelluloses from the target clone. The results are presented in Table 4, along with the lower heating value (LHV) (it is considered that the water vapor generated during combustion does not condense into liquid water, unlike in the case of higher heating value, where vapor condensation is taken into account) and moisture content. Table 5 displays the equations of the polynomial models derived from these results. Figure 3 illustrates the response surfaces for the contents in C, H, S and O, while Figure 4 shows the response surface for LHV.

As shown in Figure 3A, the lowest hydrogen contents in the solid residues from ultrasound-assisted CAE were obtained at extreme temperatures and were scarcely dependent on the other independent variables. The sulfur content exhibited a similar behavior to the extraction yield and glucan content; thus, it decreased with increasing values of the three independent variables. In contrast, the carbon and oxygen contents increased with rising temperature, alkali concentration, and treatment time. This is consistent with the fact that the latter was a derivative quantity, and the former was the major element. The amount of carbon present in the CAE solid residue peaked at treatment times in the lower end of the range, where the temperature and alkali concentration had little influence, even though the highest carbon contents in the residue were obtained in the central ranges of the two variables. Since the carbon and hydrogen contents have contradictory effects on LHV, it is uncertain whether it is better to use treatment times in the lower or upper end of the range. Nevertheless, medium temperatures and alkali concentrations are the best choices to maximize LHV.

Table 5. Equations of the polynomial models for the dependent variables of the cold alkaline extraction (CAE) with ultrasound assistance of the clone AF2 of *Populus x euramericana.*

Equation with ultrasounds	Equation number	Adjusted R^2 / Snedecor's *F-value*
$H=6.100 + 0.015X_A - 0.016X_t - 0.093X_A^2 + 0.092X_t^2 - 0.220X_T^2$	(11)	0.96 / 70
$S=0.000180 - 0.000049X_A - 0.000086X_t - 0.000019X_T + 0.000036X_A^2 - 0.000089X_t^2 + 0.000050X_AX_T - 0.000023X_tX_T$	(12)	0.95 / 40
$C=45.62 - 1.02X_t - 0.470X_T - 1.514X_A^2 - 0.711X_T^2 - 0.549X_AX_t - 0.363X_tX_T$	(13)	0.97 / 77
$O=47.22 + 1.04X_t + 0.50X_T + 1.60X_A^2 + 0.81X_T^2 + 0.56X_AX_t$	(14)	0.97 / 79
$LHV=18881 + 82X_A + 186X_t - 64X_T - 251X_T^2 + 217X_AX_t + 90X_tX_T$	(15)	0.95 / 27

Dependent variables: Hydrogen (%), Sulphur (%), Carbon (%), Oxygen (%), and LHV Low heating value. Independent variables: XA: alkali concentration, Xt and XT: treatment time and temperature of the cold alkaline extraction (CAE) with ultrasound of the target clone. The differences between the experimental values and those estimated using the equations never exceeded 10% of the former.

The H and C contents influence the calorific value of the material. LHV should increase with a decrease in H content and an increase in C content—although the former element is present in much smaller amounts than C. As demonstrated by Equation (11) in Table 5, the quadratic term of

temperature had the most significant impact on the H content of the CAE solid residue obtained with ultrasound. Additionally, the lowest H contents were observed at low temperatures, regardless of the alkali concentration and treatment time employed. Nonetheless, the highest lower heating values, and consequently the greatest energy output, were achieved with longer treatment times, along with medium temperatures and alkali concentrations.

Overall, utilizing extended durations, medium-to-high alkali concentrations, and moderate temperatures in conjunction with ultrasound yielded CAE solid residues with the highest glucan contents and lowest lignin contents. It also maximized hemicellulose extraction into the CAE liquor and the energy content (LHV) of the solid residue.

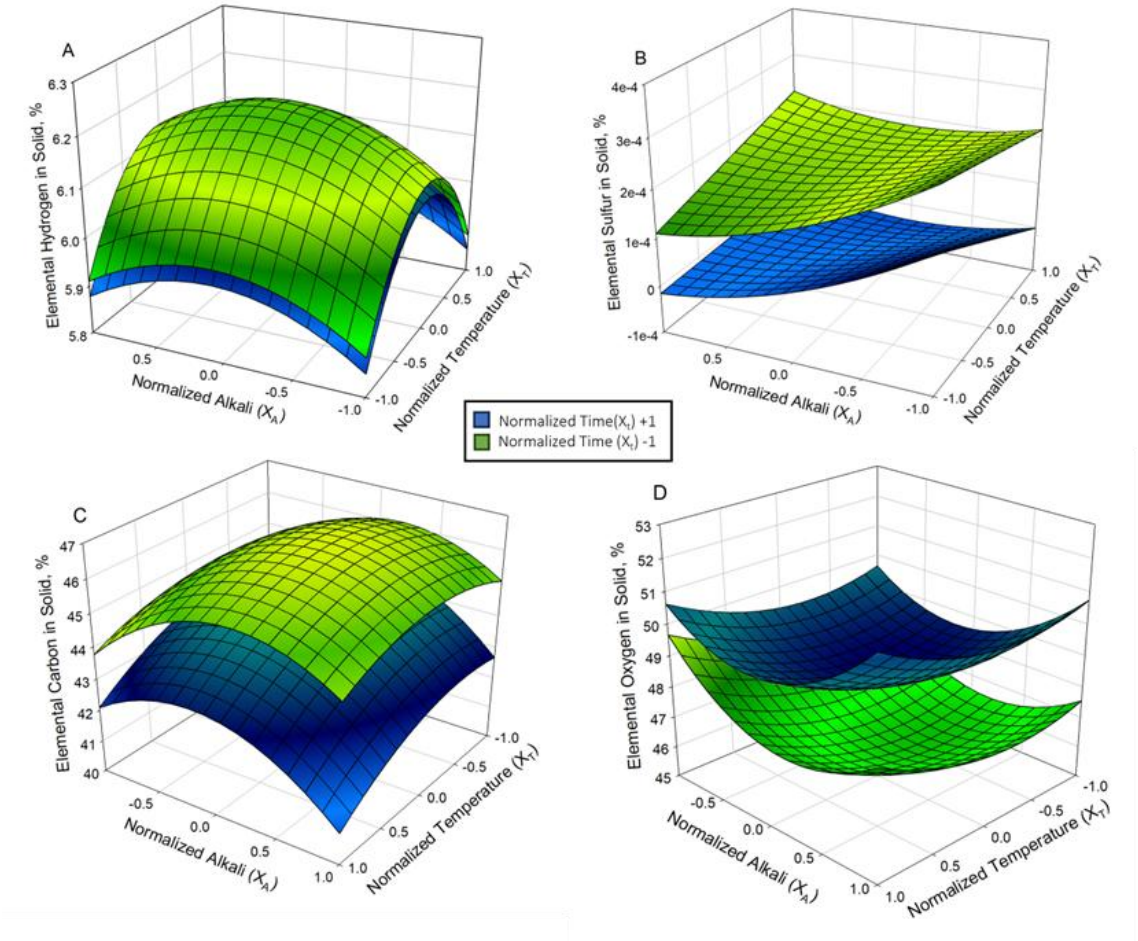


Figure 3. Response surfaces for elemental hydrogen (**A**), sulfur (**B**), carbon (**C**), and oxygen (**D**), all presented as percentages in the solid residue obtained from the Cold Alkaline Extraction process using ultrasound on the Popular Wood (clone AF2).

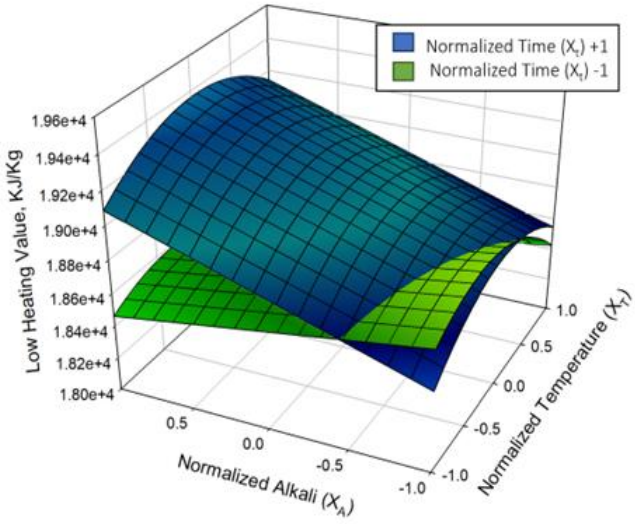


Figure 4. Response surface for lower heating values in the solid residue from the Cold Alkaline Extraction process using ultrasound on the Popular Wood (clone AF2).

One other noteworthy point is the influence of ultrasound on LHV and the hemicellulose content of the CAE solid residue. As depicted in Figure 5, illustrating their variations at a constant treatment time (90 min, +1), it becomes evident that LHV was significantly influenced by the presence of ultrasound. Therefore, LHV=20.880−44.85×hemicellulose content of solid (Equation (16)) (R^2 = 0.79). When ultrasound was employed, longer treatment times increased LHV and reduced the proportion of hemicelluloses in the CAE solid residue, subsequently increasing their concentration in the liquor. The effect was more pronounced at medium temperatures and, to a somewhat lesser extent, at medium alkali concentrations.

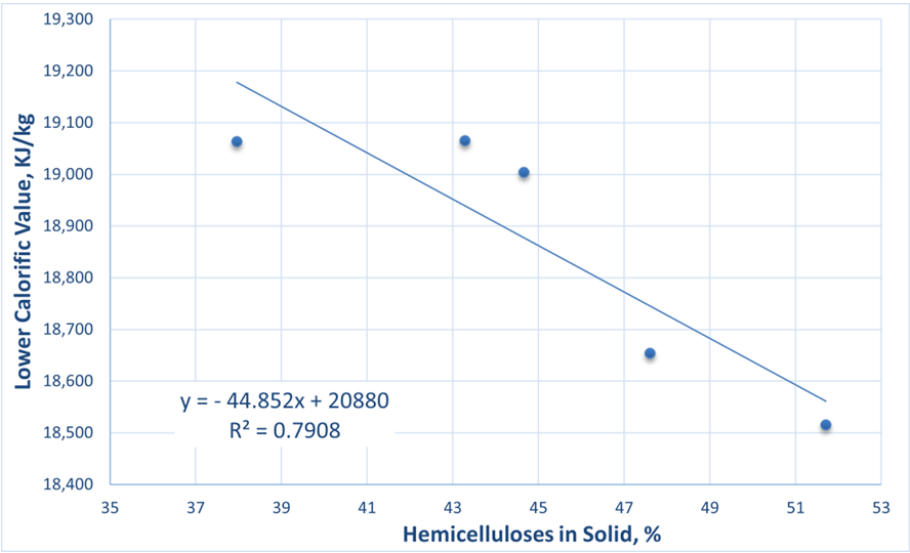


Figure 5. Predicted LHV (Equation (15)) against predicted xylan content (Equation (5)) of the solid residue obtained from the process of Cold Alkaline Extraction using ultrasound of the Popular Wood (clone AF2) at a constant treatment time of 90 min (experimental point, normalized time value = +1).

4 Conclusions.

Clone AF2 of *Populus x euramericana* was found to have lignin and xylan contents slightly higher than those of *Eucalyptus globulus* and other species containing large amounts of biomass. Also, in common with other *Populus* species, the hemicellulose fraction of the clone contained no arabinan derivatives. However, its lower heating value (LHV) was considerably higher than that of *E. globulus* and other energy crops, and, unlike that of *Eucalyptus*, which was used as a reference here, it is suitable for the cold alkaline extraction (CAE) of hemicelluloses.

Using ultrasound increased the selectivity of CAE toward the hemicellulose and lignin fractions in the raw material. Thus, it increased hemicellulose extraction into the liquor while preserving or increasing the calorific value of the solid residue due to the cellulose fraction remaining in it.

The optimal conditions vary depending on the performance and property indices. However, overall, utilizing extended treatment times, medium-to-high alkali concentrations, and moderate temperatures with ultrasound-assisted CAE maximized the glucan content and minimized the lignin content of the resulting solid residue. It also maximized the extraction of hemicelluloses into the liquor and the energy content (LHV) of the solid residue.

Author Contributions

S.L.-C.: Conceptualization, Methodology, Investigation, Formal analysis, Data curation, Visualization, Review. **J.M.L.**: Conceptualization, Methodology, Investigation, Formal analysis, Data curation, Visualization. **J.C.G.**: Conceptualization, Methodology, Funding acquisition, Supervision, Writing—review and editing. **M.T.G.**: Conceptualization, Methodology, Investigation, Formal analysis, Data curation, Visualization. **López. F**: Conceptualization, Methodology, Data curation, Funding acquisition, Supervision, Writing—original draft, Project administration. All authors have read and agreed to the published version of the manuscript.

Funding

This work was funded by Spain's Ministry of Science and Innovation, and also by the National Research Program Oriented to the Challenges of Society (Project PID2020-112875RB-C21, MCIN/AEI /10.13039/501100011033), also this publication is part of the PRE2021-097925 support (funded by MCIN/AEI/10.13039/501100011033 and by the FSE+), and the University of Huelva/CBUA.

Acknowledgments

Not applicable.

Data Availability Statement

All data generated or analyzed during this work are included in this published article.

Conflicts of Interest

The authors declare that they have no competing interests.

References

[1] European Parliament. Directive (EU) 2018/2001 of the European Parliament and of the Council on the promotion of the use of energy from renewable sources. Off. J. Eur. Union 2018, 2018, 82–209.

[2] REN21. Renewables 2020 Global Status Report; Renewable and Sustainable Energy Reviews; REN21 Secretariat: Paris, France, 2020; ISBN 978-3-948393-00-7. Available online: https://www.ren21.net/gsr-2020/ (accessed on 11 December 2023).

[3] Domínguez, E.; Nóvoa, T.; del Río, P.G.; Garrote, G.; Romaní, A. Sequential two-stage autohydrolysis biorefinery for the production of bioethanol from fast-growing Paulownia biomass. Energy Convers. Manag. 2020, 226, 113517. https://doi.org/10.1016/j.enconman.2020.113517.

[4] Ginni, G.; Kavitha, S.; Kannah, Y.; Bhatia, S.K.; Kumar, A.; Rajkumar, M.; Kumar, G.; Pugazhendhi, A.; Chi, N.T.L.; J,R.B. Valorization of agricultural residues: Different biorefinery routes. J. Environ. Chem. Eng. 2021, 9, 105435. https://doi.org/10.1016/j.jece.2021.105435.

[5] World Energy Outlook 2017 [Internet]. OECD; 2017. Available online: https://www.oecd-ilibrary.org/energy/world-energy-outlook-2017_weo-2017-en (accessed on 11 May 2021).

[6] Seserman, D.-M.; Pohle, I.; Veste, M.; Freese, D. Simulating climate change impacts on hybrid-poplar and black locust short rotation coppices. Forests 2018, 9, 419. https://doi.org/10.3390/f9070419.

[7] Montero, G.; Serrada, R. La Situación de los Bosques y el Sector Forestal en España; ISFE: Pontevedra, Spain, 2013.

[8] Contreras M del, M.; Romero, I.; Moya, M.; Castro, E. Olive-derived biomass as a renewable source of value-added products. Process Biochem. 2020, 97, 43–56. https://doi.org/10.1016/j.procbio.2020.06.013.

[9] Ning, P.; Yang, G.; Hu, L.; Sun, J.; Shi, L.; Zhou, Y.; Wang, Z.; Yang, J. Recent advances in the valorization of plant biomass. Biotechnol. Biofuels 2021 14, 102. https://doi.org/10.1186/s13068-021-01949-3.

[10] Cristóbal, J.; Matos, C.T.; Aurambout, J.P.; Manfredi, S.; Kavalov, B. Environmental sustainability assessment of bioeconomy value chains. Biomass Bioenergy 2016, 89, 159–171. https://doi.org/10.1016/j.biombioe.2016.02.002.

[11] Ruiz, H.A.; Conrad, M.; Sun, S.N.; Sanchez, A.; Rocha, G.J.M.; Romaní, A.; Castro, E.; Torres, A.; Rodríguez-Jasso, R.M.; Andrade, L.P.; et al. Engineering aspects of hydrothermal pretreatment: From batch to continuous operation, scale-up and pilot reactor under biorefinery concept. Bioresour. Technol. 2020, 299, 122685. https://doi.org/10.1016/j.biortech.2019.122685.

[12] Sixto, H.; Cañellas, I.; van Arendonk, J.; Ciria, P.; Camps, F.; Sánchez, M.; Sánchez-González, M. Growth potential of different species and genotypes for biomass production in short rotation in Mediterranean environments. For. Ecol. Manag. 2015, 354, 291–299. https://doi.org/10.1016/j.foreco.2015.05.038.

[13] FAO. 2017. The future of food and agriculture – Trends and challenges. Rome. ISBN 978-92-5-109551-5. Available online: https://www.fao.org/3/i6583e/i6583e.pdf (accessed on 11 December 2023).

[14] Lauri, P.; Havlík, P.; Kindermann, G.; Forsell, N.; Böttcher, H.; Obersteiner, M. Woody biomass energy potential in 2050. Energy Policy 2014, 66, 19–31. https://doi.org/10.1016/j.enpol.2013.11.033.

[15] Vanguelova, E.; Pitman, R. Impacts of short rotation forestry on soil sustainability. Short rotation forestry: Review of growth and environmental impacts. For. Res. Monogr. 2011, 2, 37–77.

[16] Madejón, P.; Alaejos, J.; García-Álbala, J.; Fernández, M.; Madejón, E. Three-year study of fast-growing trees in degraded soils amended with composts: Effects on soil fertility and productivity. J. Environ. Manag. 2016, 169, 18–26. https://doi.org/10.1016/j.jenvman.2015.11.050.

[17] Madadi, M.; Song, G.; Karimi, K.; Zhu, D.; Elsayed, M.; Sun, F.; Abomohra, A. One-step lignocellulose fractionation using acid/pentanol pretreatment for enhanced fermentable sugar and reactive lignin production with efficient pentanol retrieva-bility. Bioresour. Technol. 2022, 359, 127503. https://doi.org/10.1016/j.biortech.2022.127503.

[18] Penín, L.; Peleteiro, S.; Rivas, S.; Santos, V.; Parajó, J.C. Production of 5-hydroxymethylfurfural from pine wood via biorefinery technologies based on fractionation and reaction in ionic liquids. Bioresources 2019, 14, 4733–4747. https://doi.org/10.15376/biores.14.2.4733-4747.

[19] Kim, J.S.; Lee, Y.Y.; Kim, T.H. A review on alkaline pretreatment technology for bioconversion of lignocellulosic biomass. Bioresour. Technol. 2016, 199, 42–48. https://doi.org/10.1016/j.biortech.2015.08.085.

[20] de Carvalho, D.M.; Sevastyanova, O.; de Queiroz, J.H.; Colodette, J.L. Cold alkaline extraction as a pretreatment for bioethanol production from eucalyptus, sugarcane bagasse and sugarcane straw. Energy Convers. Manag. 2016, 124, 315–324. https://doi.org/10.1016/j.enconman.2016.07.029.

[21] García, J.C.; Díaz, M.J.; Garcia, M.T.; Feria, M.J.; Gómez, D.M.; López, F. Search for optimum conditions of wheat straw hemicelluloses cold alkaline extraction process. Biochem. Eng. J. 2013, 71, 127–133. https://doi.org/10.1016/j.bej.2012.12.008.

[22] Hutterer, C.; Schild, G.; Potthast, A. A precise study on effects that trigger alkaline hemicellulose extraction efficiency. Bioresour. Technol. 2016, 214, 460–467. https://doi.org/10.1016/j.biortech.2016.04.114.

[23] Park, Y.C.; Kim, J.S. Comparison of various alkaline pretreatment methods of lignocellulosic biomass. Energy 2012, 47, 31–35. https://doi.org/10.1016/j.energy.2012.08.010.

[24] Longue Júnior, D.; Colodette, J.L.; Gomes, V.J. Extraction of wood hemicelluloses through NaOH leaching | Remoção de hemiceluloses da madeira por tratamento de lixiviação alcalina com NaOH. Cerne 2010, 16, 423–429. https://doi.org/10.1590/S0104-77602010000400001.

[25] Tiwari, B.K. Ultrasound: A clean, green extraction technology. TrAC-Trends Anal. Chem. 2015, 71, 100–109. https://doi.org/10.1016/j.trac.2015.04.013.

[26] Yuan, Z.; Long, J.; Wang, T.; Shu, R.; Zhang, Q.; Ma, L. Process intensification effect of ball milling on the hydrothermal pretreatment for corn straw enzymolysis. Energy Convers. Manag. 2015, 101, 481–488. https://doi.org/10.1016/j.enconman.2015.05.057.

[27] Saikia, M.; Das, T.; Hower, J.C.; Silva, L.F.O.; Fan, X.; Saikia, B.K. Oxidative chemical beneficiation of low-quality coals under low-energy ultrasonic and microwave irradiation: An environmental-friendly approach. J. Environ. Chem. Eng. 2021, 9, 104830. https://doi.org/10.1016/j.jece.2020.104830.

[28] Ashokkumar, M. The characterization of acoustic cavitation bubbles—An overview. Ultrason. Sonochem. 2011, 18, 864–872. https://doi.org/10.1016/j.ultsonch.2010.11.016.

[29] García, A.; Alriols, M.G.; Llano-Ponte, R.; Labidi, J. Ultrasound-assisted fractionation of the lignocellulosic material. Bioresour. Technol. 2011, 102, 6326–6330. https://doi.org/10.1016/j.biortech.2011.02.045.

[30] Raihan, A.; Ibrahim, S.; Muhtasim, D.A. Dynamic impacts of economic growth, energy use, tourism, and agricultural productivity on carbon dioxide emissions in Egypt. World Dev. Sustain. 2023, 2, 100059. https://doi.org/10.1016/j.wds.2023.100059.

[31] Li, F.; Li, Y.; Novoselov, K.S.; Liang, F.; Meng, J.; Ho, S.-H.; Zhao, T.; Zhou, H.; Ahmad, A.; Zhu, Y.; et al. Bioresource Upgrade for Sustainable Energy, Environment, and Biomedicine. Nano-Micro Lett. 2023, 15, 35. https://doi.org/10.1007/s40820-022-00993-4.

[32] Puițel, A.C.; Suditu, G.D.; Drăgoi, E.N.; Danu, M.; Ailiesei, G.-L.; Balan, C.D.; Chicet, D.-L.; Nechita, M.T. Optimization of Alkaline Extraction of Xylan-Based Hemicelluloses from Wheat Straws: Effects of Microwave, Ultrasound, and Freeze–Thaw Cycles. Polymers 2023, 15, 1038. https://doi.org/10.3390/polym15041038.

[33] Gufe, C.; Thantsha, M.S.; Malgas, S. Recovery of xylan from Acacia mearnsii using ultrasound-assisted alkaline extraction. Biofuels Bioprod. Biorefining 2023, 17, 976–987. https://doi.org/10.1002/bbb.2491.

[34] Tareen, A.K.; Punsuvon, V.; Parakulsuksatid, P. Conversion of steam exploded hydrolyzate of oil palm trunk to furfural by using sulfuric acid, solid acid, and base catalysts in one pot. Energy Sources Part A Recovery Util. Environ. Eff. 2020, 1–12. https://doi.org/10.1080/15567036.2020.1741733.

[35] Gil, M.V.; Jablonka, K.M.; García, S.; Pevida, C.; Smit, B. Biomass to energy: A machine learning model for optimum gasification pathways. Digit. Discov. 2023, 2. https://doi.org/10.26434/chemrxiv-2023-xl3vr.

[36] Tofani, G.; Cornet, I.; Tavernier, S. Multiple linear regression to predict the brightness of waste fibres mixtures before bleaching. Chem. Pap. 2022, 76, 4351–4365. https://doi.org/10.1007/s11696-022-02181-5.

[37] TAPPI T264 cm-07; Preparation of Wood for Chemical Analysis. TAPPI Press: Atlanta, GA, USA, 2007.

[38] TAPPI 211 om-02; Ash in Wood, Pulp, Paper and Paperboard: Combustion at 525 °C. TAPPI Press: Atlanta, GA, USA, 2002.

[39] TAPPI T204 cm-07; Solvent Extractives of Wood and Pulp. TAPPI Press: Atlanta, GA, USA, 2007.

[40] TAPPI T249 cm-09; Carbohydrate Composition of Extractive-Free Wood and Wood Pulp by Gas-liquid Chromatography. TAPPI Press: Atlanta, GA, USA, 2009.

[41] Romaní, A.; Garrote, G.; Ballesteros, I.; Ballesteros, M. Second generation bioethanol from steam exploded Eucalyptus globulus wood. Fuel 2013, 111, 66–74. https://doi.org/10.1016/j.fuel.2013.04.076.

[42] TAPPI T222 om-11; Acid-Insoluble Lignin in Wood and Pulp. TAPPI Press: Atlanta, GA, USA, 2011.

[43] CEN/TS Solid Biofuels-Method for the Determination of Calorific Value CEN/TS 14918:2005. 2005. Available from: https://standards.iteh.ai/catalog/standards/cen/21f53010-bfdf-41aa-8f73-3ad9e2ab444f/cen-ts-14918-2005 (accessed on 11 December 2023).

[44] UNE 16001, E.X. Solid Biofuels, Method for the determination of calorific value. Spanish Association for Standardization, Madrid, Spain. 2005. Available online: https://infostore.saiglobal.com/preview/is/en/2005/i.s.cents14918-2005.pdf?sku=675235 (accessed on 11 December 2023).

[45] Civitarese, V.; Faugno, S.; Picchio, R.; Assirelli, A.; Sperandio, G.; Saulino, L.; Crimaldi, M.; Sannino, M. Production of selected short-rotation wood crop species and quality of obtained biomass. Eur. J. For. Res. 2018, 137, 541–552. https://doi.org/10.1007/s10342-018-1122-3.

[46] Magagnotti, N.; Spinelli, R.; Kärhä, K.; Mederski, P.S. Multi-tree cut-to-length harvesting of short-rotation poplar plantations. Eur. J. For. Res. 2020, 140, 345–354. https://doi.org/10.1007/s10342-020-01335-y.

[47] Constantí, M.; Reguant, C.; Poblet, M.; Zamora, F.; Mas, A.; Guillamón, J.M. Molecular analysis of yeast population dynamics: Effect of sulphur dioxide and inoculum on must fermentation. Int. J. Food Microbiol. 1998, 41, 169–175. https://doi.org/10.1016/S0168-1605(98)00041-5.

[48] Ebringerová, A.; Hromádková, Z. An overview on the application of ultrasound in extraction, separation and purification of plant polysaccharides. Cent. Eur. J. Chem. 2010, 8, 243–257. https://doi.org/10.2478/s11532-010-0006-2.

[49] Alfaro, A.; López, F.; Pérez, A.; García, J.C.; Rodríguez, A. Integral valorization of tagasaste (Chamaecytisus proliferus) under hydrothermal and pulp processing. Bioresour. Technol. 2010, 101, 7635–7640. https://doi.org/10.1016/j.biortech.2010.04.059.

[50] López, F.; Alfaro, A.; García, M.; Díaz, M.J.; Calero, A.M.; Ariza, J. Pulp and paper from tagasaste (Chamaecytisus proliferus L.F. ssp. palmensis). Chem. Eng. Res. Des. 2004, 82, 1029–1036. https://doi.org/10.1205/0263876041580730.

[51] Feria, M.J.; García, J.C.; Pérez, A.; Gomide, J.L.; Colodette, J.L.; López, F. Process optimization in kraft pulping, bleaching, and beating of Leucaena diversifolia. Bioresources 2012, 7, 283–297. https://doi.org/10.15376/biores.7.1.283-297.

[52] Caparrós, S.; Ariza, J.; López, F.; Nacimiento, J.A.; Garrote, G.; Jiménez, L. Hydrothermal treatment and ethanol pulping of sunflower stalks. Bioresour. Technol. 2008, 99, 1368–1372. https://doi.org/10.1016/j.biortech.2007.01.045.

[53] García, J.C.; Zamudio, M.A.M.; Pérez, A.; De Alva, H.E.; López, F. Paulownia as a raw material for the production of pulp by soda-anthraquinone cooking with or without previous autohydrolysis. J. Chem. Technol. Biotechnol. 2011, 86, 608–615. https://doi.org/10.1002/jctb.2563.

[54] López, F.; Pérez, A.; Zamudio, M.A.M.; De Alva, H.E.; García, J.C. Paulownia as raw material for solid biofuel and cellulose pulp. Biomass Bioenergy 2012, 45, 77–86. https://doi.org/10.1016/j.biombioe.2012.05.010.

[55] Loaiza, J.M.; López, F.; García, M.T.; Fernández, O.; Díaz, M.J.; García, J.C. Selecting the pre-hydrolysis conditions for eucalyptus wood in a fractional exploitation biorefining scheme. J. Wood Chem. Technol. 2016, 36, 211–223. https://doi.org/10.1080/02773813.2015.1112402.

[56] López, F.; García, M.; Feria, M.; García, J.; de Diego, C.; Zamudio, M.; Díaz, M. Optimization of furfural production by acid hydrolysis of eucalyptus globulus in two stages. Chem. Eng. J. 2014, 240, 195–201. https://doi.org/10.1016/j.cej.2013.11.073.

[57] Pan, X.; Sano, Y. Fractionation of wheat straw by atmospheric acetic acid process. Bioresour. Technol. 2005, 96, 1256–1263. https://doi.org/10.1016/j.biortech.2004.10.018.

[58] Fernández, M.; Alaejos, J.; Andivia, E.; Madejón, P.; Díaz, M.J.; Tapias, R. Short rotation coppice of leguminous tree Leucaena spp. improves soil fertility while producing high biomass yields in Mediterranean environment. Ind. Crops Prod. 2020, 157, 112911. https://doi.org/10.1016/j.indcrop.2020.112911.

[59] Hu, M.; Chen, Z.; Wang, S.; Guo, D.; Ma, C.; Zhou, Y.; Chen, J.; Laghari, M.; Fazal, S.; Xiao, B.; et al. Thermogravimetric kinetics of lignocellulosic biomass slow pyrolysis using distributed activation energy model, Fraser-Suzuki deconvolution, and iso-conversional method. Energy Convers. Manag. 2016, 118, 1–11. https://doi.org/10.1016/j.enconman.2016.03.058.

[60] Fernández, M.; Alaejos, J.; Andivia, E.; Vázquez-Piqué, J.; Ruiz, F.; López, F.; Tapias, R. Eucalyptus x urograndis biomass production for energy purposes exposed to a Mediterranean climate under different irrigation and fertilisation regimes. Biomass Bioenergy 2018, 111, 22–30. https://doi.org/10.1016/j.biombioe.2018.01.020.

[61] Chen, Z.; Zhu, Q.; Wang, X.; Xiao, B.; Liu, S. Pyrolysis behaviors and kinetic studies on Eucalyptus residues using thermo-gravimetric analysis. Energy Convers. Manag. 2015, 105, 251–259. https://doi.org/10.1016/j.enconman.2015.07.077.

[62] Methrath Liyakathali, N.A.; Muley, P.D.; Aita, G.; Boldor, D. Effect of frequency and reaction time in focused ultrasonic pretreatment of energy cane bagasse for bioethanol production. Bioresour. Technol. 2016, 200, 262–271. https://doi.org/10.1016/j.biortech.2015.10.028.

Forests.

Disclaimer/Publisher's Note:

The statements, opinions and data contained in all publications are solely those of the individual author(s) and contributor(s) and not of MDPI and/or the editor(s). MDPI and/or the editor(s) disclaim responsibility for any injury to people or property resulting from any ideas, methods, instructions or products referred to in the content.

https://doi.org/10.3390/f15010109

3.1.3. Extracción Alcalina en Frío de la *Robinia Pseudoacacia*.

1 Introducción.

Otro de los géneros que están destacando para ser empleados como cultivos energéticos es la *Robinia Pseudoacacia*, siendo un cultivo de corta rotación. Además, esta especie es fijadora de nitrógeno contribuyendo así a la reducción del uso de fertilizantes inorgánicos nitrogenados [1,2]. La *Robinia Pseudoacacia* crece en una amplia gama de condiciones, incluyendo paisajes post-minería [1]. El rendimiento de producción de biomasa de esta especie va desde 3 toneladas por hectárea al año [3] hasta 19 toneladas por hectárea al año [4].

A lo largo de los resultados expuestos en esta tesis doctoral, así como en la literatura publicada, se ha observado que la eficacia de la extracción alcalina en frío depende significativamente del tipo de biomasa sometida al pretratamiento, siendo mucho más eficaz en materiales herbáceos comparados con materiales madereros [5-8]. En este contexto, se evalúa el rendimiento de la extracción alcalina en frío con la aplicación simultanea de ultrasonidos sobre la *Robinia Pseudoacacia,* como en el caso del clon AF2 de *Populus x euramericana*, con el objetivo de mejorar la eficiencia del proceso en esta biomasa leñosa.

El objetivo principal de este apartado es estudiar la efectividad de la extracción alcalina en frío, con y sin ultrasonidos, sobre la *Robinia Pseudoacacia.* Se busca optimizar la valorización de esta materia prima, generando una fase líquida rica en hemicelulosa y un residuo sólido valorizable energéticamente.

2 Material y Metodología.

La biomasa en estudio, *Robinia Pseudoacacia*, procede de las plantaciones experimentales del departamento de Ciencias Agroforestales de la Universidad de Huelva. Esta biomasa se sometió a un proceso de acondicionamiento, para obtener unas condiciones de tamaño y secado óptimas para ser sometida a la extracción alcalina en frío. Además, se caracterizó acorde con las normas Tappi para conocer su composición de partida [9,10].

Las variables independientes de la extracción alcalina en frío fueron la temperatura (20-40 ºC), el tiempo de operación (30-90 minutos), la concentración de álcali (80-12 g L^{-1}) y un hidromódulo fijo de 15. El tratamiento se realizó con y sin ultrasonidos (potencia de 120 W), utilizando un baño Power Sonic Series 510, que permitía la aplicación simultánea de ultrasonidos para optimizar el rendimiento. Tras el proceso, el material sólido fue filtrado, lavado, neutralizado y lavado antes de su caracterización química y evaluación de rendimiento energético.

Para optimizar el proceso de EAF, se aplicó un diseño experimental de composición central, evaluando la influencia de las variables de temperatura, tiempo y concentración de NaOH sobre el rendimiento del proceso y el contenido de las distintas fracciones lignocelulósicas. Este diseño permitió reducir el número de experimentos a 15, normalizando los valores para facilitar la interpretación de los efectos de cada variable independiente. La modelización estadística se realizó mediante regresión múltiple, empleando el software Statistica, y considerando términos lineales, cuadráticos y de interacción entre variables para identificar los parámetros óptimos con significancia estadística $p < 0,05$.

La caracterización energética de la *Robinia Pseudoacacia* y de los sólidos residuales obtenidos en la extracción alcalina en frío con ultrasonidos, en cuanto a poder calorífico superior a volumen constante y a una temperatura de referencia de 25 ºC, se realizó conforme a las normas CEN/TS 14918 y UNE 164001 [11,12]. El análisis se llevó a cabo en un calorímetro automático Isoperibol Parr 6300, calibrado con ácido benzoico, empleando oxígeno puro al 99,5%, hilo de ignición de níquel-cromo y una presión máxima de 2500 psig.

3 Resultados y Discusión.

La caracterización de la *Robinia Pseudoacacia* se muestra en la Tabla 1 en términos de porcentaje de materia prima seca, comparándola con los resultados de Martín-Sampedro et al. [13] y otros materiales lignocelulósicos caracterizados por otros autores. La composición química presenta valores superiores de glucano y arabano, lo cual es consistente y aceptable dado que la composición de la biomasa puede variar según el sitio de cultivo, el momento de la cosecha y las condiciones ambientales.

Tabla 1. Composición química y poder calorífico superior (PCS) de la *Robinia Pseudoacacia* y otras materias primas.

Composición Química	***Robinia Pseudoacacia***	***Robinia Pseudoacacia*** [13]	**Tagasaste** [14,15]	***Eucalyptus globulus*** [16,17]	**Paja de Trigo** [18]
α Celulosa (glucano) (%)	47,1	39,1	38,9 ± 3,4	42,8 ± 2,0	55,4 ± 2,6
Lignina Klason (%)	19,6	18,1	19,8 ± 1,9	21,2 ± 0,9	16 ± 0,3
Xilano (%)	18,8	18,6	19,9 ± 1,3	17,1 ± 0,3	34,6 ± 0,4
Arabano (%)	2,2	0,8	0,6 ± 0,3	0,7 ± 0,1	5,6 ± 0,3
Grupos acetilo (%)	1,4	-	4,4 ± 0,6	3,5 ± 0,1	-
PCS, kJ kg^{-1} od.b.	18362±222	-	19592 ± 28	19326 ± 84	-

Las fases sólidas obtenidas en cada una de las condiciones de operación del diseño experimental, con y sin ultrasonidos, se emplearon para calcular el rendimiento del tratamiento y analizar su composición química (lignina Klason, glucano y hemicelulosas totales, que incluyen xilano, arabano y grupos acetilos). Estos datos permiten desarrollar distintos modelos polinómicos que identifican las

variables de operación con mayor influencia y aproximan los intervalos óptimos de operación que maximizan la tasa de extracción de xilosa en la fase líquida. En la Tabla 2 se muestran los distintos modelos polinómicos obtenidos en este estudio.

Los rendimientos respecto al sólido en ambos procesos, con y sin ultrasonidos, fueron altos, lo cual indica una baja extracción en la fase líquida. En la EAF sin ultrasonidos, los rendimientos oscilaron entre 89,7% y 91%, mientras que la incorporación de ultrasonidos resultó en un rango de 88,2% a 90,8%. Estos resultados confirman lo discutido en esta tesis sobre la dependencia del tratamiento de extracción alcalina en frío con el tipo de biomasa utilizada. En estudios previos, materiales herbáceos como la paja de trigo muestran mejores rendimientos en la fase sólida de entre 25,5% y 38,8% [5], mientras que para especies leñosas como el *Eucalyptus urophylla x Eucalylptus grandis,* se han reportado rendimientos de 95,5% [19] o en el caso del apartado anterior donde se analizó la EAF con y sin ultrasonidos sobre el clon AF2 de *Populus x euramericana* se conseguían rendimientos de hasta el 68,5% [20].

Tabla 2. Ecuaciones de los modelos polinómicos para las variables dependientes de la extracción alcalina en frío con y sin ultrasonidos.

Variable Dependientes	Ecuaciones de la Extracción Alcalina en Frío sin ultrasonidos
Rendimiento	$89,74+0,07X_a-0,28X_t-0,08X_T+0,3X_t^2+0,54X_T^2+0,1X_aX_t+0,13X_aX_T-0,13X_tX_T$
Lignina Klason	$18,5+0,11X_a+0,15X_t+0,27X_t^2-0,36X_T^2+0,09X_aX_t+0,07X_aX_T+0,09X_tX_T$
Glucano	$45,85+0,14X_a-0,12X_t+0,68X_T+0,28X_a^2-0,81X_t^2-0,24X_T^2+0,45X_aX_t+ 0,45X_aX_T$
Hemicelulosas totales	$19,03+0,34X_a+0,59X_T-0,35X_a^2+0,37X_t^2+0,22X_T^2-0,11X_aX_t+0,24X_aX_T-0,18X_tX_T$
	Ecuaciones de la Extracción Alcalina en Frío con ultrasonidos
Rendimiento	$89,19-0,25X_a-0,44X_t-0,6X_T+0,57X_a^2-0,47X_T^2+0,16X_aX_t$
Lignina Klason	$17,84-0,2X_a-0,13X_t+0,39X_t^2-0,65X_T^2-0,86X_aX_t-0,39X_tX_T$
Glucano	$44,62-0,6X_a-0,28X_T+1,13X_a^2-1,19X_T^2$
Hemicelulosas totales	$19,09-0,19X_a-0,26X_t+0,29X_a^2+0,54X_t^2-0,84X_T^2+0,22X_aX_t+0,28X_aX_T-0,07X_tX_T$

Donde X_a es la concentración de NaOH, X_t el tiempo de operación y X_T la temperatura del proceso.

Para comprobar las ventajas que aporta la aplicación simultanea de ultrasonidos en la extracción alcalina en frío, así como facilitar el análisis de influencia de las distintas variables independientes sobre las variables dependientes, se representan los modelos polinómicos recogidos en la Tabla 2.

En la Figura 1 se representa la superficie de respuesta de los rendimientos en el sólido residual de la EAF con y sin ultrasonidos, en función de la variable de temperatura en su valor máximo (40 ºC), donde se observan los menores rendimientos en el sólido, lo que implica la máxima extracción hacia la fase líquida. Este análisis permite concluir que la extracción alcalina en frío asistida con ultrasonidos genera un menor rendimiento en la fase sólida en comparación con el proceso sin

ultrasonidos, lo que indica que el ultrasonidos mejora la solubilización de polisacáridos hacia la fase líquida, aumentando la efectividad del proceso. Sin embargo, cabe reiterar que, en ambos tratamientos aplicados a la *Robinia Pseudoacacia*, los rendimientos del sólido residual siguen siendo elevados.

En el proceso sin ultrasonidos, la variable de mayor influencia sobre el rendimiento es el tiempo de operación, como se observa por su peso en el modelo polinómico, especialmente en el término lineal. En cambio, en el caso de la EAF con ultrasonidos, la temperatura destaca como la variable con mayor impacto en el rendimiento del sólido, debido a sus contribuciones en los términos lineal y cuadrático del modelo.

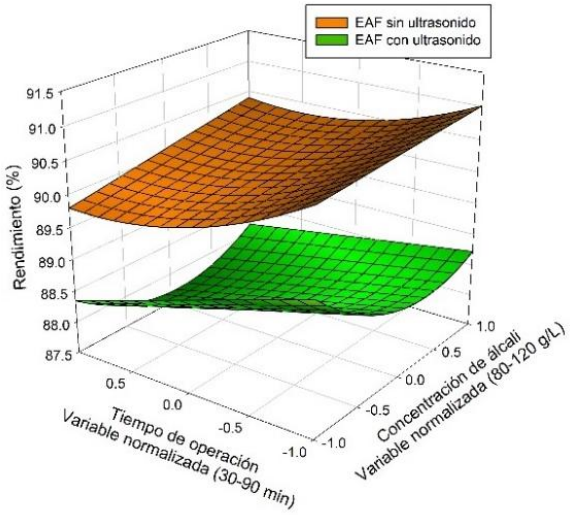


Figura 1. Variación del rendimiento en el sólido en función de la concentración de álcali y el tiempo, en los procesos de EAF con y sin ultrasonidos, a una temperatura de operación máxima de 40 ºC.

En la Figura 2 se representa la superficie de respuesta de los modelos polinómicos del contenido de lignina Klason en las fases sólidas obtenidas en al EAF con y sin ultrasonidos. En este caso, se ha fijado el tiempo de operación en su valor mínimo (30 minutos), esto implica una mayor extracción de lignina hacia la fase líquida. Como se puede observar en esta figura, el uso de ultrasonidos, combinado con bajas concentraciones de álcali y bajas temperaturas, permite extraer una mayor cantidad de la fracción polifenólica, lo que sugiere que el ultrasonidos tiene un ligero efecto selectivo sobre la lignina. Esta mayor extracción de lignina es ventajosa para el aprovechamiento energético del sólido, ya que la lignina, al estar compuesta por una cantidad abundante de anillos bencénicos, presenta una mayor energía de activación y estabilidad térmica [21].

El tiempo de operación se presenta como la variable con mayor influencia sobre el contenido en lignina Klason en el sólido residual procedente del tratamiento alcalino en frío con y sin ultrasonidos, esto se observa en los pesos de los términos lineales y cuadráticos de ambos modelos polinómicos.

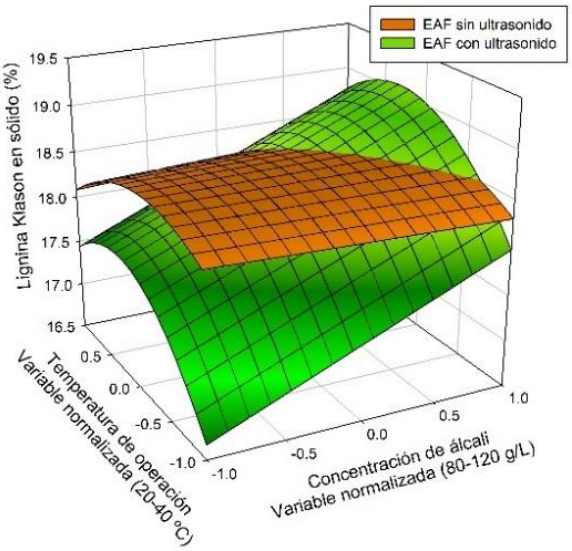


Figura 3. Variación del contenido de lignina Klason en el sólido en función de la concentración de álcali y la temperatura, en los procesos de EAF con y sin ultrasonidos, en un tiempo de operación mínimo de 30 minutos.

La superficie de respuesta de los modelos polinómicos que representan el contenido de glucano en los sólidos tras la EAF, tanto con cómo sin ultrasonidos, se muestra en la Figura 4. En este caso, el tiempo de operación se ha fijado en su valor intermedio (60 minutos), permitiendo así representar el mayor contenido de glucano retenido en el sólido. En general, se observa que la ausencia de ultrasonidos implica una extracción ligeramente menor de la fracción de celulosa hacia la fase líquida en comparación con el tratamiento en el que se aplica ultrasonidos.

Como se observa en los modelos polinómicos del contenido de glucano en los sólidos residuales, la variable con mayor influencia es la temperatura, tanto en el tratamiento con ultrasonidos como sin él. Además, en el proceso de EAF con ultrasonidos, el contenido de glucano en el sólido no depende del tiempo de operación.

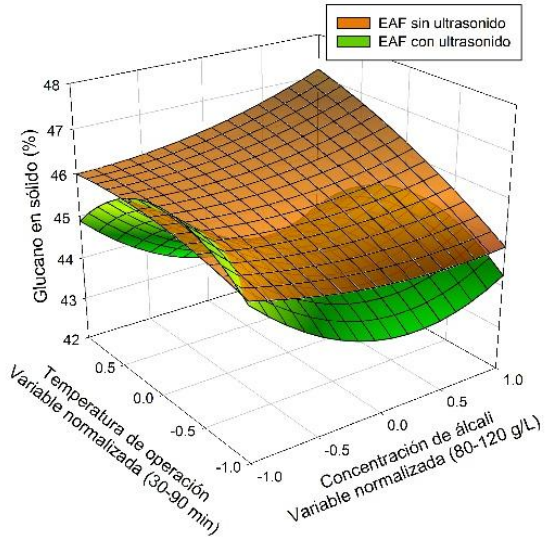


Figura 4. Variación del contenido de glucano en el sólido en función de la concentración de álcali y la temperatura, en los procesos de EAF con y sin ultrasonidos, en un tiempo de operación máximo de 60 minutos.

Finalmente, se analiza el modelo polinómico del contenido de hemicelulosas totales en el sólido residual tras la EAF, con y sin ultrasonidos, en función del tiempo de operación y la concentración de álcali. Los resultados muestran comportamientos opuestos entre ambos tratamientos: sin ultrasonidos, la mayor extracción de hemicelulosas a la fase líquida ocurre operando con una temperatura mínima (20 ºC), mientras que, con ultrasonidos, la extracción es óptima a la temperatura máxima (40 ºC), lo cual se refleja en las superficies de respuestas que se muestran en la Figura 5. Aunque la diferencia en el contenido de hemicelulosas en los sólidos residuales de ambos tratamientos es leve, se registraron rangos de 81,4-92,5 % para la EAF sin ultrasonidos y de 81,3-89,1 % con ultrasonidos, respecto a la materia prima inicial. De forma más específica, el ultrasonidos favorece una extracción más selectiva de xilosa, mientras que sin su aplicación se extraen con una mayor cantidad de arabinosa y grupos acetilos. En conclusión, la ventaja de ultrasonidos radica en una mayor uniformidad del contenido de hemicelulosas en todo el diseño experimental y una ligera mejora en la extracción, aunque en general la eficacia de la EAF sobre la *Robinia Pseudoacacia* fue limitada.

La temperatura, a través sus términos lineal y cuadrático del modelo polinómico, fue la variable con mayor influencia sobre la extracción de hemicelulosas hacia la fase líquida en el tratamiento sin ultrasonidos. En cambio, en el proceso con ultrasonidos, el contenido de hemicelulosas en la fase líquida depende más del tiempo de operación.

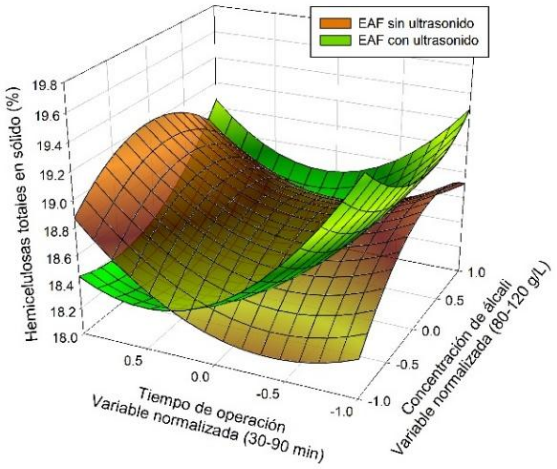


Figura 5. Variación del contenido de hemicelulosas totales en el sólido residual en función de la concentración de álcali y el tiempo, en los procesos de EAF con y sin ultrasonidos, a temperaturas óptimas para su extracción.

Se evaluó el potencial energético de los sólidos obtenidos en la extracción alcalina en frío con y sin ultrasonidos, analizando su poder calorífico superior a volumen constante tras el tratamiento. Este análisis parte de la hipótesis de que la extracción a la fase líquida de componentes hemicelulósicos y

polifenólicos durante la EAF puede preservar e incluso aumentar el poder calorífico de estos sólidos respecto a la materia prima de partida.

Para identificar la influencia de las variables independientes del proceso (concentración de álcali, tiempo y temperatura) en el poder calorífico de los sólido post-EAF, se obtuvieron modelos matemáticos polinómicos, resumidos en la Tabla 3. Los valores utilizados para obtener estas ecuaciones se derivan del promedio de tres mediciones calorimétricas realizadas para asegurar la precisión de estos modelos.

Tabla 3. Ecuaciones para el poder calorífico superior del sólido residual de la EAF con y sin ultrasonidos.

	Poder calorífico superior del sólido residual
EAF sin ultrasonidos	$19023{,}4+104{,}7X_a-89{,}1X_t+102{,}5X_T-67{,}2X_aX_t-67{,}2X_aX_T+60{,}7X_tX_T$
EAF con ultrasonidos	$19098{,}9+74{,}3X_t+74{,}9X_T-381{,}2X_a^2+142{,}2X_t^2+80{,}2X_T^2+111{,}2X_tX_T$

La Figura 6 muestra los valores máximos del poder calorífico superior (PCS) de los sólidos residuales obtenidos en la EAF con y sin ultrasonidos en función de la temperatura y la concentración de álcali. En el caso del tratamiento con ultrasonidos, los máximos valores de PCS se alcanzaron al operar durante el mayor tiempo (90 minutos), mientras que, en el proceso sin ultrasonidos, los mayores valores se observaron en los tiempos de operación más cortos (30 minutos). En la gráfica también se incluye el poder calorífico de la *Robinia Pseudoacacia* como refencia de partida.

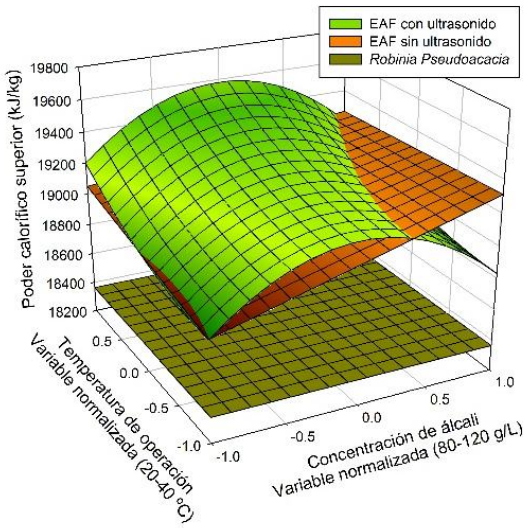


Figura 6. Variación de los máximos valores del poder calorífico superior del sólido residual, en función de la concentración de álcali y la temperatura, para los procesos de EAF con y sin ultrasonidos, y la materia prima.

La grafica demuestra que la extracción de hemicelulosas y lignina durante la EAF contribuye al aumento del PCS de los sólidos residuales post-EAF en comparación con la biomasa sin tratar. Además, los sólidos residuales del tratamiento con ultrasonidos muestran un mayor poder calorífico que aquellos obtenidos de la EAF sin ultrasonidos. El poder calorífico del sólido residual incrementa

de 18362,7 kJ kg^{-1} en la materia prima inicial hasta alcanzar unos valores máximos de aproximadamente 19600 kJ kg^{-1} en los sólidos obtenidos mediante EAF con ultrasonidos. Como se observa en la figura, estos niveles de PCS se logran al trabajar con concentraciones medias de álcali y temperaturas altas, condiciones que también corresponden a máximos de extracción de hemicelulosas y niveles medio-altos de extracción de lignina Klason en la fase líquida.

4 Conclusiones.

La extracción alcalina en frío aplicada a la *Robinia Pseudoacacia* con y sin ultrasonidos resultó menos eficiente que el clon AF2 del *Populus x euramericana*, aunque superior que en el caso del *Eucalyptus urophylla x Eucalylptus grandis*.

Sin el uso de ultrasonidos, las mayores cantidades de hemicelulosas extraídas a la fase líquida ocurrieron en condiciones bajas de concentración de álcali, tiempo y temperatura. En cambio, al aplicar ultrasonidos, los mayores rendimientos de hemicelulosas en el licor se lograron con concentraciones de álcali intermedias, tiempos intermedios y temperaturas bajas.

La aplicación de ultrasonidos no solo mejoró la extracción de polisacáridos en la fase líquida, sino que también aumentó la selectividad hacia las fracciones de hemicelulosas (principalmente xilano) y la fracción polifenólica. Además, el tratamiento permitió obtener un residuo sólido con mayor potencial energético que la materia prima original, incrementando aún más el poder calorífico cuando se empleó ultrasonidos, lo que sugiere una valorización energética viable para la fase sólida.

Referencias

[1] H. Grünewald, C. Böhm, A. Quinkenstein, P. Grundmann, J. Eberts, G. von Wühlisch, Robinia pseudoacacia L.: A lesser known tree species for biomass production, Bioenergy Res 2 (2009) 123–133. https://doi.org/10.1007/s12155-009-9038-x.

[2] N. Oliveira, M. del Río, D.I. Forrester, R. Rodríguez-Soalleiro, C. Pérez-Cruzado, I. Cañellas, H. Sixto, Mixed short rotation plantations of Populus alba and Robinia pseudoacacia for biomass yield, For Ecol Manage 410 (2018) 48–55. https://doi.org/https://doi.org/10.1016/j.foreco.2017.12.034.

[3] K. Rédei, Black locust (Robinia pseudoacacia L.) growing in Hungary, (1998).

[4] A. Werner, A. Vetter, G. Reinhold, Leitlinie zur effizienten und umweltverträglichen Erzeugung von Energieholz, (2006).

[5] J.C. García, M.J. Díaz, M.T. Garcia, M.J. Feria, D.M. Gómez, F. López, Search for optimum conditions of wheat straw hemicelluloses cold alkaline extraction process, Biochem Eng J 71 (2013) 127–133. https://doi.org/10.1016/j.bej.2012.12.008.

[6] C. Hutterer, G. Schild, A. Potthast, A precise study on effects that trigger alkaline hemicellulose extraction efficiency, Bioresour Technol 214 (2016) 460–467. https://doi.org/10.1016/j.biortech.2016.04.114.

[7] D. Longue Júnior, J.L. Colodette, V.J. Gomes, Extraction of wood hemicelluloses through NaOH leaching | Remoção de hemiceluloses da madeira por tratamento de lixiviação alcalina com NaOH, Cerne 16 (2010) 423–429. https://doi.org/10.1590/s0104-77602010000400001.

[8] Y.C. Park, J.S. Kim, Comparison of various alkaline pretreatment methods of lignocellulosic biomass, Energy 47 (2012) 31–35. https://doi.org/10.1016/j.energy.2012.08.010.

[9] TAPPI T249 cm-09, Carbohydrate composition of extractive-free wood and wood pulp by gas-liquid chromatography. TAPPI Press, Atlanta, GA., (2009).

[10] TAPPI T222 om-11, Acid-insoluble lignin in wood and pulp. TAPPI Press, Atlanta, GA., (2011).

[11] CEN/TS, Solid Biofuels-Method for the Determination of Calorific Value CEN/TS 14918:2005, (2005). https://standards.iteh.ai/catalog/standards/cen/21f53010-bfdf-41aa-8f73-3ad9e2ab444f/cen-ts-14918-2005.

[12] UNE 16001 EX, Solid Biofuels, Method for the determination of calorific value, (2005).

[13] R. Martín-Sampedro, J.I. Santos, M.E. Eugenio, B. Wicklein, L. Jiménez-López, D. Ibarra, Chemical and thermal analysis of lignin streams from Robinia pseudoacacia L. generated during organosolv and acid hydrolysis pre-treatments and subsequent enzymatic hydrolysis, Int J Biol Macromol 140 (2019) 311–322. https://doi.org/10.1016/j.ijbiomac.2019.08.029.

[14] M. Constantí, C. Reguant, M. Poblet, F. Zamora, A. Mas, J.M. Guillamón, Molecular analysis of yeast population dynamics: Effect of sulphur dioxide and inoculum on must fermentation, Int J Food Microbiol 41 (1998) 169–175. https://doi.org/10.1016/S0168-1605(98)00041-5.

[15] F. López, A. Alfaro, M. García, M.J. Díaz, A.M. Calero, J. Ariza, Pulp and paper from tagasaste (Chamaecytisus proliferus L.F. ssp. palmensis), Chemical Engineering Research and Design 82 (2004) 1029–1036. https://doi.org/10.1205/0263876041580730.

[16] J.M. Loaiza, F. López, M.T. García, O. Fernández, M.J. Díaz, J.C. García, Selecting the pre-hydrolysis conditions for eucalyptus wood in a fractional exploitation biorefining scheme, Journal of Wood Chemistry and Technology 36 (2016) 211–223. https://doi.org/10.1080/02773813.2015.1112402.

[17] F. López, M.T. García, M.J. Feria, J.C. García, C.M. de Diego, M.A.M. Zamudio, M.J. Díaz, Optimization of furfural production by acid hydrolysis of eucalyptus globulus in two stages, Chemical Engineering Journal 240 (2014) 195–201. https://doi.org/10.1016/j.cej.2013.11.073.

[18] X. Pan, Y. Sano, Fractionation of wheat straw by atmospheric acetic acid process, Bioresour Technol 96 (2005) 1256–1263. https://doi.org/10.1016/j.biortech.2004.10.018.

[19] D.M. de Carvalho, O. Sevastyanova, J.H. de Queiroz, J.L. Colodette, Cold alkaline extraction as a pretreatment for bioethanol production from eucalyptus, sugarcane bagasse and sugarcane straw, Energy Convers Manag 124 (2016) 315–324. https://doi.org/10.1016/J.ENCONMAN.2016.07.029.

[20] S. Lozano-Calvo, J.M. Loaiza, J.C. García, M.T. García, F. López, Ultrasound-Assisted Cold Alkaline Extraction: Increasing Hemicellulose Extraction and Energy Production from Populus Wood, Forests 15 (2024) 109. https://doi.org/10.3390/f15010109.

[21] Z. Chen, Q. Zhu, X. Wang, B. Xiao, S. Liu, Pyrolysis behaviors and kinetic studies on Eucalyptus residues using thermogravimetric analysis, Energy Convers Manag 105 (2015) 251–259. https://doi.org/10.1016/j.enconman.2015.07.077.

3.2. Análisis Cinético y Producción de Hidrógeno en la Valorización Secuencial del Clon AF2 de *Populus* mediante Extracción Alcalina en Frío y Pirólisis.

Los resultados obtenidos en este estudio se detallan en la publicación: **Kinetic and hydrogen production analysis in the sequential valorization of a Populus clone by cold alkaline extraction and pyrolysis.** S. Lozano-Calvo, J.M. Loaiza, J.C. García, R. Tapias and F. López. Scientific Reports 2024, 14, 1509. (**Publicación 3**).

A continuación, se expone brevemente un resumen de los resultados obtenidos, así como su contextualización.

El desarrollo económico global, ligado al consumo excesivo de combustibles fósiles, ha intensificado el cambio climático y el deterioro ambiental. En respuesta, los esquemas de biorrefinería han surgido como una solución sostenible para aprovechar la biomasa lignocelulósica y a partir de ella producir biocombustibles y productos de alto valor añadido. En este contexto, el clon AF2 de *Populus x euramericana* es una opción prometedora, debido a su rápido crecimiento, alta productividad y adaptabilidad a climas mediterráneos.

En línea con los resultados obtenidos en el apartado anterior, donde se destacó la eficacia de la extracción alcalina en frío (EAF) con ultrasonidos sobre el clon AF2 para mejorar el fraccionamiento selectivo de hemicelulosa y lignina, este nuevo análisis aborda la valorización secuencial de la fase sólida a través de tratamientos termoquímicos. La integración de etapas secuenciales en los esquemas de biorrefinería permite maximizar el aprovechamiento de la biomasa lignocelulósica.

En particular, la pirólisis es empleada como una tecnología clave para la obtención de biocombustibles y bioproductos, destacando la posibilidad de producir hidrógeno (H_2), un vector energético esencial para la descarbonización global.

Siendo el objetivo de este estudio el aprovechamiento del clon AF2 del género *Populus* mediante un esquema de biorrefinería en dos etapas: una extracción alcalina en frío asistida por ultrasonidos, seguida de un tratamiento termoquímica mediante pirólisis de las fases sólidas resultantes. Se busca cuantificar el grado de conversión de las fases sólidas a través de análisis termogravimétrico (TGA) y calcular los parámetros cinéticos no isotérmicos mediante el método isoconversional diferencial de Friedman. Además, se modela la cinética del proceso pirolítico en términos de energía de activación (E_a) con el fin de optimizar la producción de hidrógeno. Finalmente, se optimiza la generación de hidrógeno evaluando la influencia de las condiciones de operación de la etapa inicial de extracción alcalina. La hipótesis planteada fue que la reducción en el contenido de lignina de los sólidos tras

EAF, en comparación con la biomasa original, disminuiría la energía de activación requerida en el proceso de pirólisis, además de una mayor producción de hidrógeno.

Resumiendo, el análisis de los resultados obtenidos hace concluir que los sólidos obtenidos tras la extracción alcalina en frío con ultrasonidos presentan una mayor reactividad y, en general, una menor energía de activación durante el proceso de pirólisis en comparación con la biomasa inicial del clon AF2 de *Populus*. Entre las variables operativas de la etapa de extracción alcalina, la concentración de álcali se identificó como el factor más determinante sobre la E_a, observándose una disminución de esta a medida que aumenta la proporción de glucano en los sólidos. Asimismo, se demostró que la EAF con ultrasonidos mejora significativamente la producción de hidrógeno. Por lo tanto, el esquema integrado de extracción alcalina en frío asistida por ultrasonidos y pirólisis representa una estrategia prometedora para la valorización eficiente de esta materia prima lignocelulósica.

PUBLICACIÓN 3.

Kinetic and hydrogen production analysis in the sequential valorization of a *Populus* clone by cold alkaline extraction and pyrolysis.

S. Lozano-Calvo, J.M. Loaiza, J.C. García, R. Tapias & F. López.



Scientific reports

Nature

Volumen: 14(1), número: 1509 (2024)

DOI: 10.1038/s41598-024-52052-0

Categoría	Clasificación revista/Número total de revistas	Cuartil (Porcentaje)
Ciencias multidisciplinarias	25/134	Q1 (81,7%)
Factor de impacto	3,8	

Sequential valorization of a Populus clone by cold alkaline extraction and pyrolysis. Kinetic and hydrogen production analysis.

Lozano-Calvo, S.,[a]✉ Loaiza, J.M.,[a] García, J.C.,[a] Tapias, R.,[b] López, F.[a]

✉Corresponding author: susana.lozano@diq.uhu.es

[a]Research Centre for Technology of Products and Chemical Processes (PRO²TECS), Department of Chemical Engineering, University of Huelva, Av. 3 de Marzo s/n, 21071 Huelva, Spain.
[b]Department of Forest Engineering, University of Huelva.

Abstract

This work employed a two-step biorefining process, consisting of a hemicellulose-rich liquor production through ultrasound-assisted cold alkaline extraction (CAE), followed by thermochemical treatment of the resultant solid phase. The post-CAE solid phase's pyrolytic potential was assessed by application of thermogravimetric analysis (TGA) and Friedman's isoconversional method, and also from hydrogen production. The solid phases remaining after the CAE treatment were more reactive than the untreated raw material. Notably, the alkali concentration employed in the first step was the individual variable most pronounced influence on their activation energy (E_a). Thus, at a degree of conversion $\alpha = 0.50$, E_a ranged from 109.7 to 254.3 kJ/mol for the solid phases, compared to 177 kJ/mol for the raw material; this value decreased with rising glucan content. At maximal degradation, the post-CAE solid phases produced up to 15.57% v/v more hydrogen than did the untreated raw material.

1 Introduction.

Economic growth and expansive economies have led to an increasingly poorer environmental quality in many countries, especially as regards ecological systems, biodiversity and human health. Economic development is closely related to energy consumption [1] and, at present, 81% of all primary energy is obtained from fossil fuels, 5% from nuclear fission and only 14% from renewable sources [2]. As a result, atmospheric CO2 levels continue to rise steadily. In fact, they have risen by 42% since 1950 and worsened the global problem posed by climate change [3]. In response to this pressing challenge, international institutions have adopted initiatives such as the Paris Agreement, by which countries such as United Kingdom, Spain, France and New Zealand have committed to be carbon-neutral by 2050, and others such as Sweden and Norway expect to meet this goal by 2045 and 2030, respectively [4]. Because societies can hardly be sustainable unless they use low-carbon fuels [5], growing concern with dramatic climate events and the exhaustion of fossil fuels has emerged over the last few decades that has boosted a search for renewable sources of energy on a global scale [6].

https://doi.org/10.1038/s41598-024-52052-0

Biomass is a clean, sustainable choice for a smooth transition from oil-based to biorenewable energy [7,8]. Lignocellulosic biomass is especially effective as a renewable resource because it is widely available in vast amounts, and also because its chemical components are highly suitable and its production does not compete with that of food [8,9]. As a result, second-generation biofuels are being increasingly obtained from lignocellulosic biomass for the production of renewable energy [10].

Biorefining lignocellulosic materials allows biomass to be fractioned into its three main precursors (cellulose, hemicellulose and lignin) and the precursors to be processed in order to obtain products with a high added value [11]. One of the treatments used for this purpose is cold alkaline extraction, which is especially advantageous in operational and environmental terms. Also, however, it is subject to one major disadvantage: the optimum operating conditions depend on the particular type of biomass to be treated. Thus, CAE is usually much more efficient with grass than it is with wood [12] and the latter usually requires additional measures for efficient processing [13]. Also, CAE removes both hemicelluloses and polyphenols [14]. The potential applications of the hemicellulosic franction are extensive and have been explored by numerous researchers. For instance, sugar extracted from hemicellulose can subjected to biological conversion for biofuel production, such as ethanol; utilized in chemical processes for the production of substances like xylitol or lactic acid; or chemical conversion produces furfural, 5-hydroxyfurfural, and levulinic acid, crucial precursors for synthesizing various organic derivatives [15]. In addition, the CAE decreases the lignin content of the material and leading to a reduced activation energy upon thermochemical treatment as a result of the polyphenol fraction consisting largely of benzene rings —which possess increased Ea values and thermal stability [16].

Thermochemical treatments of lignocellulosic biomass provide a promising technology for producing fuels with a high added value [17]. Highlighting pyrolysis as the most popular and versatile process [18] for the efficient production of bio-coal, bio-oil and pyrolytic gas (a mixture of carbon monoxide and dioxide, hydrogen, light hydrocarbons and small amounts of other compounds) [19]. Pyrolysing lignocellulosic biomass affects its three main components (cellulose, hemicellulose and lignin) [20] and involves a number of chemical reactions the span three steps, namely: (1) evaporation of moisture; (2) primary degradation of biomass (200−400 °C); and (3) side reactions [21]. A number of studies have examined the pyrolysis of various types of lignocellulosic biomass and their individual fractions with a view to better understanding their rate and extent of thermal degradation, the products formed and their proportions [22].

Pyrolysing biomass is also one way of obtaining hydrogen (H_2) from renewable resources [23]. Hydrogen is one of the major energy vectors for decarbonization strategies in Europe [24] and

pyrolysis produces not only gaseous hydrogen, but also additional hydrogen formed in water−gas exchange reactions with carbon monoxide [25]. Hydrogen production is influenced by several variable, and it has been observed that as the pyrolysis temperature rises, the output of gaseous products increases while the formation of biochar and bio-oil decreases [26]. Thus, a temperature of 750 °C produces about 50% of hydrogen, whereas one of 500 °C gives only about 35% [25]. This is a result of the gas forming in very small amounts in primary reactions relative to tar cracking, reforming and coal decomposition at increased temperatures [27,28].

Hydrogen production also increases with increasing proportion of cellulose and hemicelluloses, but not lignin [29,30]. In fact, hydrogen forms largely from the cellulose fraction [31]. Ligneous biomass has been found to provide more hydrogen than agricultural residues [32]. Thus, Loaiza et al. [33] found extracting hemicelluloses from *Eucalytpus urograndis* by pyrolysis to provide solids whose pyrolysis led to a decreased activation energy and increased hydrogen production (6−8%) relative to the untreated, raw material.

The lignocellulosic biomass used in this work was obtained from clone AF2 of the genus *Populus* (viz., *Populus nigra x Populus deltoides*). *Populus* is a fast-growing plant that affords short, highly productive rotation [34]. Also, it is especially well adapted to Mediterranean areas with cold winters [35] and adequate soil moisture [36], so its productivity can be affected by climate change [34]. This has promoted the use of hybrid clones capable of growing under suboptimal conditions [37]. Some studies have shown clone AF2 of *Populus* to outperform others under conditions of limited water availability and long droughts [38].

The main aim of this work was to optimize exploitation of clone AF2 by using a two-step biorefining scheme involving ultrasound-assisted CAE and the subsequent pyrolysis of the resulting solid phase. The degree of conversion was assessed by thermogravimetric analysis (TGA) and non-isothermal kinetic parameters were determined by using Friedman's differential isoconversional method. Also, the kinetics of the pyrolytic process was modelled in terms of E_a in order to maximize hydrogen production, which was quantified as a function of the operating conditions of the ultrasound-assisted CAE treatment.

2 Materials and methods.

2.1 Characterization of the raw material.

The lignocellulosic biomass used was from clone AF2 of *Populus* and collected from plantations on La Rabida Campus (University of Huelva, Spain). The collected material was cold ground to obtain chips approximately 1−3 cm long and 0.5 cm wide.

The raw material was previously characterized by some members of our group in terms of moisture [39], solubility in 1% soda [40], solubility in hot water [41], ethanol−acetone extractives [42] and ash [43]. In addition, the material was subjected to acid hydrolysis in two steps involving treatment with 72% sulphuric acid at 30 °C for 1h to cleave polysaccharides into oligomers and 4% sulphuric acid at 121°C for 1 h to convert the oligomers into monomers. Monomeric sugars and Klason lignin were determined by HPLC according to TAPPI T-249 [44] and TAPPI T-222 [45], respectively. The results of the previous determinations are summarized in Table 1.

Table 1. Percent composition of the raw material.

1% NaOH extractives	22.3 ± 1.95
Hot water extractives	4.22 ± 0.12
Ethanol−acetone extractives	2.8 ± 0.15
α-Cellulose (glucan)	40.3 ± 0.85
Klason lignin	25.1 ± 0.16
Xylan	19.3 ± 0.09
Arabinan	0
Acetyl groups	0.7 ± 0.02
Ash	1.14 ± 0.04

2.2 Ultrasound-assisted cold alkaline extraction.

A CAE treatment was used to maximize extraction of hemicelluloses into the liquor and ensure that they would remain stable for potential subsequent processing. The treatment was conducted in a Power Sonic Series 500 bath, using a water modulus (i.e., a liquid/solid ratio) of 15 kg water/ kg raw material on a dry basis, an ultrasound power of 120 W, an alkali concentration of 80–120 g/L, a temperature of 20–40 °C (temperature was kept constant by cooling the bath) and a treatment time of 30–90 min. The process was followed by filtration to separate the liquor from the remaining solid phase.

The CAE liquor was neutralized with 37% v/v hydrochloric acid, and the hemicellulose fraction precipitated with ethanol. The solid phase was neutralized with acetic acid, rinsed in water, centrifuged and dried at room temperature to determine moisture as described in Section "Characterization of the raw material" and calculate CAE yield by weighing. The solid was additionally hydrolysed in two steps as described in Section "Characterization of the raw material" in order to determine its composition.

The previous conditions were used in combination with a central composite factor design and response surface análisis [46] to optimize the CAE treatment by examining the influence of the independent variables of the process (viz., alkali concentration, temperature and treatment time) on the composition of the post-CAE solid phase (viz., glucan, xylan and Klason lignin), the activation energy of the solid and its pyrolytic hydrogen production capacity.

https://doi.org/10.1038/s41598-024-52052-0

The factor design used allowed second-order polynomials to be established whose coefficients were a measure of the statistical significance of the influence of each independent variable on the dependent variables. For easier comparison, the independent variables were normalized by using the following equation:

$$X_n = 2 * \frac{X - \bar{X}}{(X_{max} - X_{min})/2} \qquad (1)$$

where X, $\bar{X}$, X_{max} and X_{min} are the absolute, mean, maximum and minimum value, respectively, of the variable concerned. The design was applied at three different alkali concentrations (80, 100 and 120 g/L), temperatures (20, 30 and 40 °C) and treatment times (30, 60 and 90 min). It encompassed three groups of experimental points, namely: 2^n points for the factor design proper, $2n$ axial points and n_c central points. Therefore, the total number of experiments required, given by $2^n + 2n + n_c$, was 16.

Experimental data were modelled by fitting the results for the dependent variables to the following polynomial equation:

$$Y = a_0 + \sum_{i=1}^{n} b_i X_{ni} + \sum_{i=1}^{n} c_i X_{ni}^2 + \sum_{i=1,j=1}^{n} d_{ij} X_{ni} X_{nj} \ \text{(i<j)} \qquad (2)$$

where X denotes independent variables and Y dependent variables, and the coefficients a_0, b_i, c_i and d_{ij} were estimated individually for each independent variable.

The independent terms selected were those having a statistically significant coefficient ($p < 0.05$). The conditions imposed on the overall statistics were $R^2 > 0.9$ and $F_{Snedecor} > 5$. All statistical processing was done with the software Statistica v. 10.0 from Statsoft, Inc. (Tulsa, OK, USA).

2.3 Thermogravimetric analyses.

The raw material and the different post-CAE solid phases were subjected to non-isothermal thermogravimetric analysis (TGA) on a TGA/DSC1 STARe System from Mettler Toledo. In each test, an amount of ca. 13 g of sample was heated from 25 to 800 °C at four different rates (5, 10, 15 and 20 °C/min), using nitrogen at a flow-rate of 10 mL/min as inert gas. The experiments were performed in triplicate recorded the average values.

2.4 Friedman's analytical method.

Friedman's method was used here to examine the kinetics of the pyrolysis reactions and determine their activation energy. The overall kinetics of the biomass pyrolysis process can be represented as follows:

$$\frac{d\alpha}{dt} = k(T) \cdot f(\alpha) \qquad (3)$$

where α is the conversion fraction $[(W_0 - W_t)/(W_0 - W_\infty)]$, W denoting the mass of sample, and W_0, W_t and W_∞ its initial value, that at time t and that at the end of the process, respectively; $f(\alpha)$ the

differential conversion function; T (K) temperature; and k(T) the rate constant in the Arrhenius equation [k(T) = $A \cdot \exp(-E_a/RT)$, with A the pre-exponential factor, E_a the apparent activation energy and R the universal gas constant (8.314 J/mol·K)]. The reaction rate can be expressed as follows:

$$\frac{d\alpha}{dT} = \left(\frac{A}{\delta}\right) \cdot \exp\left(-\frac{Ea}{R \cdot T}\right) \cdot f(\alpha) \qquad (4)$$

where δ is the linear heating rate (δ = dT/dt), which is constant.

For convenience, eq. (4) can be expressed in integral form:

$$\int_0^{\alpha} \frac{d\alpha}{f(\alpha)} = G(\alpha) = \left(\frac{A}{\beta}\right) \cdot \int_{T_0}^{T} \exp\left(-\frac{E_a}{R \cdot T}\right) dT = \left(\frac{A}{\beta}\right) \cdot p(x) \qquad (5)$$

where G(α) and p(x) are the integrals of the conversion function and temperature, respectively. The latter function cannot be solved exactly, so it has to be estimated or integrated numerically [47].

Some empirical methods allow the kinetic parameters to be calculated from the data for the thermal analysis. Such methods are of either the isoconversional or the fitting type. In this work, we used an isoconversional method to calculate the kinetic parameters for no specific form of the reaction model to enable the accurate determination of the activation energy [48,49]. The most widely used isoconversional method is Friedman's differential method [50]. In natural logarithmic form, eq. (4) becomes:

$$\ln\left(\beta \cdot \frac{d\alpha}{dT}\right) = \ln[A \cdot f(\alpha)] - \frac{E_a}{R \cdot T} \qquad (6)$$

Friedman's method assumes the extent of biomass decomposition to depend solely on the mass loss rate. Therefore, a plot of ln (dα/dt) against 1/T allows he activation energy to be calculated from the slope ($-E_a$/R) and conversion from the intercept [ln [A·f(α)].

2.5 Modeling and optimization of activation energy.

The modeling and optimization of the E_a results, as a function of the independent operating variables of the CAE process with ultrasounds, has been conducted following the methodology outlined in section "Thermogravimetric analysis (TGA) of the pyrolytic process".

The experimental design points for the central composite design are consistent with those utilized for modeling and optimizing the composition of the solid phase.

The same procedures, including response surface analysis, normalization of independent variables, analysis of coefficients, statistical assessment of model validity and/or uncertainty, and the selection of statistically significant coefficients, have been applied. It is noteworthy that the results of the dependent variable (E_a) were obtained in accordance with the description provided in sections "Thermogravimetric analyses" and "Friedman's analytical method".

2.6 Quantifying hydrogen production in a pyrolytic reactor.

The amount of hydrogen resulting from pyrolysis of the lignocellulosic biomass and the CAE solid phases was evaluated using a laboratory-scale reactor. The reactor consisted of a 140 cm length and 10 mm wide quartz tube, within which approximately 2 g of the sample was uniformly introduced and placed in a furnace at a constant temperature for 4 min, using nitrogen at a flow-rate of 150 mL/min as carrier gas. The operating variables of this laboratory-scale reactor are the furnace temperature, the residence time of the sample in the furnace, and the flow-rate of carrier gas. While it is at a laboratory scale, we believe the results would be scalable. The reactor design is an original design from the research group, and efforts have been made to operate it in a manner resembling that of a semi-pilot reactor.

Hydrogen production was measured by collecting samples in Tedlar bags at the reactor outlet. Samples were collected at the highest degradation temperature in each test for 1 minute. Four different samples were taken in each experiment to determine the maximum H_2, which was produced between minutes 2 and 3. These samples were analyzed using a precalibrated MultiRAE IR PGM-54 gas analyser from RAE Systems (San José, CA, USA). All measurements were made in triplicate and averaged to calculate the volume of pyrolytic gas of the analyzed sample and disregarding the carrier gas.

3 Results.

3.1 Ultrasound-assisted cold alkaline extraction of hemicellulose.

Previous studies by our group [51] revealed that using ultrasound in the CAE of clone AF2 of *Populus* resulted in increased extraction of all lignocellulosic fractions but especially those of hemicelluloses and polyphenols. Specifically, extraction of hemicelluloses, measured as xylan, from the raw material into the CAE liquor ranged from 39.8 to 56.7% in the absence of ultrasound and from 44.3 to 60.8% in its presence. Also, the hemicellulose content of the post-CAE solid phase decreased from 60.2–43.3% to 55.7 – 39.2% of the content in the starting material. On the other hand, the lignin content of the solid increased from 51.5–77.7% with sonication to 71.6–98.9% without it. Finally, cellulose was scarcely extracted into the CAE liquor and remained in the solid phase by 80.4–96.2% with ultrasound and by 85.1–98.7% without it.

These results allowed polynomial models relating the dependent variables (glucan, xylan and Klason lignin in the post-CAE solid phase) to the independent variables (alkali concentration, temperature and treatment time) to be developed. Table 2 shows the equations for the models, which were used to predict the effect of each independent variable of the ultrasound-assisted CAE process on the cellulose, hemicellulose and polyphenol contents of the resulting solid phase. Such contents

(specifically, those of glucan, xylan and Klason lignin) are referred to their initial levels in the starting, raw material.

As can be seen from eq. (8) in Table 2, the alkali concentration was the most influential variable on the glucan content of the post-CAE solid phase. Cellulose extraction into the liquor was maximal at the greatest alkali concentration, temperature and time values studied. As noted earlier, however, glucan was scarcely extracted into the liquor (20.22% at most).

Table 2. Equations of the polynomial models for the dependent variables in the ultrasound-assisted CAE treatment.

Equation	Adjusted R^2	Adjusted Snedecor's F
$GL=87.0-2.50X_A-1.87X_T+5.98X_A^2-4.03X_T^2-4.39X_AX_t-1.60X_AX_T+1.19X_tX_T$ (8)	0.98	59
$X=40.2-2.28X_A-2.24X_t-1.12X_T+7.23X_A^2+1.62X_T^2-0.56X_AX_t+1.37X_A X_T+0.44X_tX_T$ (9)	0.89	138
$KL=66.6-5.96X_t-2.57X_T-5.33X_A^2+4.58X_T^2+1.04X_AX_t+3.28X_AX_T-2.34X_tX_T$ (10)	0.98	114

Dependent variables: GL glucan (%), X xylan (%), KL Klason lignin (%). Independent variables: X_A alkali concentration, X_T temperature, X_t treatment time. The differences between the experimental values and those estimated with the equations never exceeded 10% of the former.

Based on eq. (9) in Table 2, medium alkali concentrations and temperatures in combination with long treatment times should result in maximal hemicellulose extraction into the CAE liquor. Finally, eq. (10) suggests that long CAE treatment times should result in increased delignification (i.e., in increased proportions of lignin in the CAE liquor). This prediction is consistent with the results of Methrath Liyakathali et al. [52], who found the treatment time and sonication to influence the cleavage of lignin−cellulose bonds to an extent increasing with the former variable. Accordingly, lignin extraction into the CAE liquor was especially high in the upper range of treatment times (90 min).

The post-CAE solid phase was rich in cellulose, but poor in lignin by effect of the polyphenol fraction being largely extracted into the liquor. In theory, this must decrease the pyrolysis activation energy since the polyphenol fraction is that with the highest E_a value [16]. Also, it should result in increased hydrogen production relative to the starting material [53]. These two expectations warranted the present work, where we examined the pyrolytic process as described below.

3.2 Thermogravimetric analysis (TGA) of the pyrolytic process.

The CAE treatment provided a highly valorizable liquor by effect of the extraction process being especially selective for hemicelluloses. Also, the treatment provided a solid phase enriched with a cellulose fraction potentially useful for purposes such as producing energy, hydrogen, biofuels, pulp, paper or polyphenol derivatives. In this work, we examined the potential of the process for obtaining

energy and a high added value product: hydrogen. Removing most of the hemicellulose fraction and part of the polyphenol fraction decreased the activation energy of the pyrolysis process [16,33], thereby presumably facilitating it. It should be noted that, as shown for treatments other than CAE, the operating conditions —or rather, their combination—influence the activation energy and kinetics of the thermal treatment [54].

Because using all 16 points of the experimental design would have been impractical, we selected those corresponding to the lowest and highest extraction of hemicelluloses (viz., 80 g/L, 90 min, 20°C and 100 g/L, 60 min, 30 °C, respectively) and the lowest and highest extraction of Klason lignin (viz., 80 g/L, 30 min, 20 °C and 80 g/L, 90 min, 40 °C, respectively) in addition to the raw material.

Figure 1 is a weight loss versus temperature plot. As can be seen, the initial temperature of the second step of process, known as "active pyrolysis", was higher for the raw material (224 °C) than it was with the lowest and highest extraction of hemicelluloses (172 and 180 °C, respectively) and lignin (177 and 172 °C, respectively). The decreased temperatures for the post-CAE solid phases relative to the raw material can be ascribed to selective extraction of hemicelluloses and polyphenols into the CAE liquor. Also, residual lignin in the resulting solid contained fewer bonds and was thus less thermally stable. The affinity of alkaline treatments for soluble lignin and the cleavage of C–C bonds in polyphenols remaining in the solid fraction was previously observed by other authors [54]. The cleavage of bonds in the lignin fraction decreases its strength and degree of polymerization, thus facilitating hydrolysis of polysaccharides [55].

Heating the post-CAE solid phase with the highest content in hemicelluloses at 5 °C/min led to an extended loss of fixed carbon that was not considered in calculating the activation energy. Nor was the result for the residue heated at 15 °C/min leading to the lowest extraction of lignin.

3.3 Derivative thermogravimetry (DTG).

Figure 2 shows the rate of weight loss (%/min) as a function of temperature (i.e., the DTG curves) for the raw material and the four post-CAE solid phases examined in the previous section. As can be seen, there were three distinct regions typical of biomass pyrolysis corresponding to water evaporation, active pyrolysis ad side reactions [21]. The main pyrolysis step spanned the range 200–400 °C and two sub-steps involving degradation of the cellulose and hemicellulose fractions. Whereas the raw material exhibited two well-defined peaks, the post-CAE solid phases showed a poorly defined peak for hemicellulose degradation. This was a result of structural and compositional differences between the samples directly influencing hemicellulose and cellulose degradation [56].

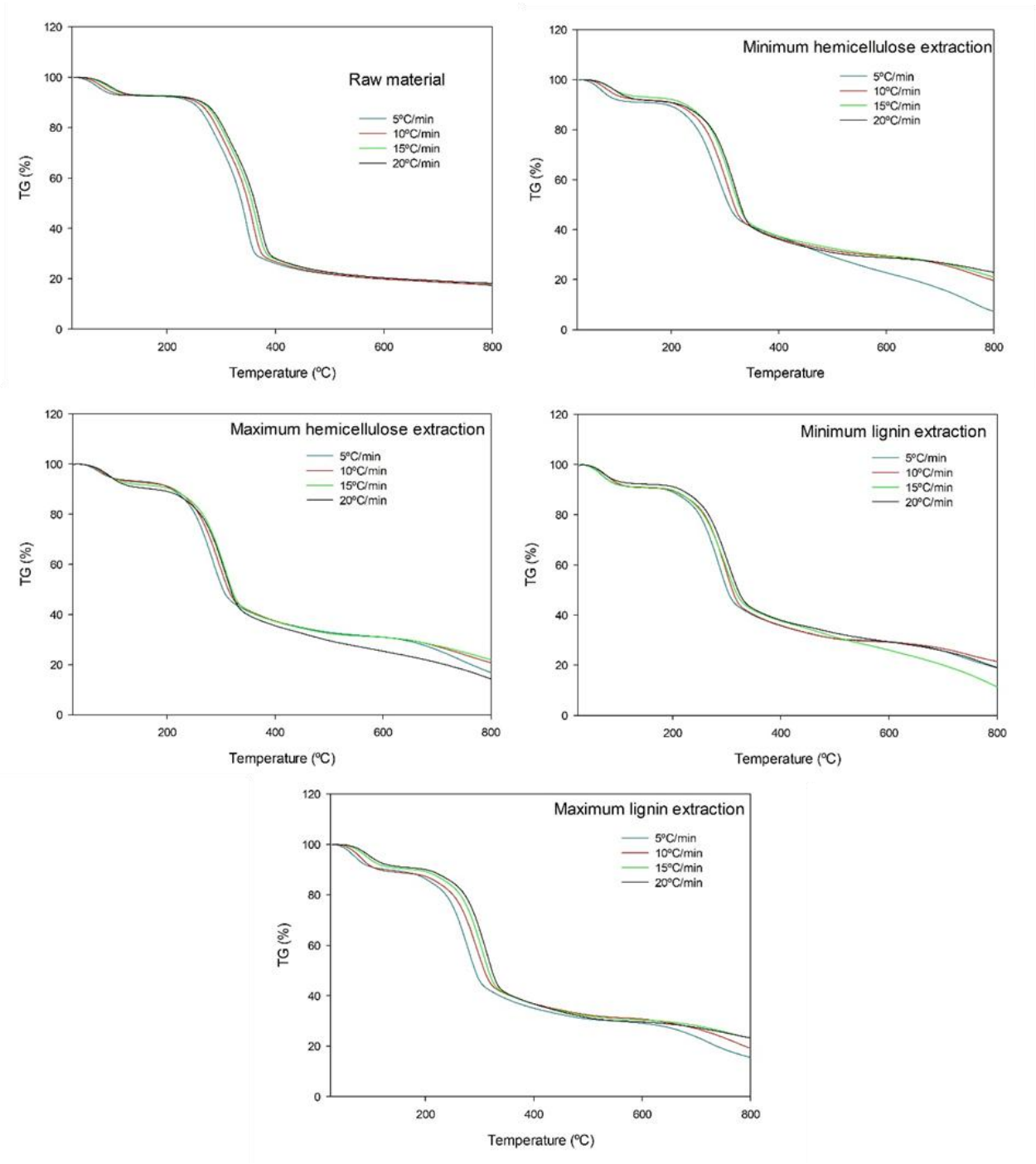


Figure 1. TGA at different heating rates of the raw material and the four post-CAE solid phases.

Thermal degradation in the active pyrolysis step started at 230 °C in the raw material and at around 190 °C in the post-CAE solid phases, possibly as a result of increased extraction of hemicelluloses and lignin from the latter. Thus, the CAE treatment caused a portion of the polyphenolic fraction to be extracted into the liquor and the rest, which remained in the solid, to break more easily as a consequence of its having a decreased number of C–C bonds —and being less thermally stable as a result [57].

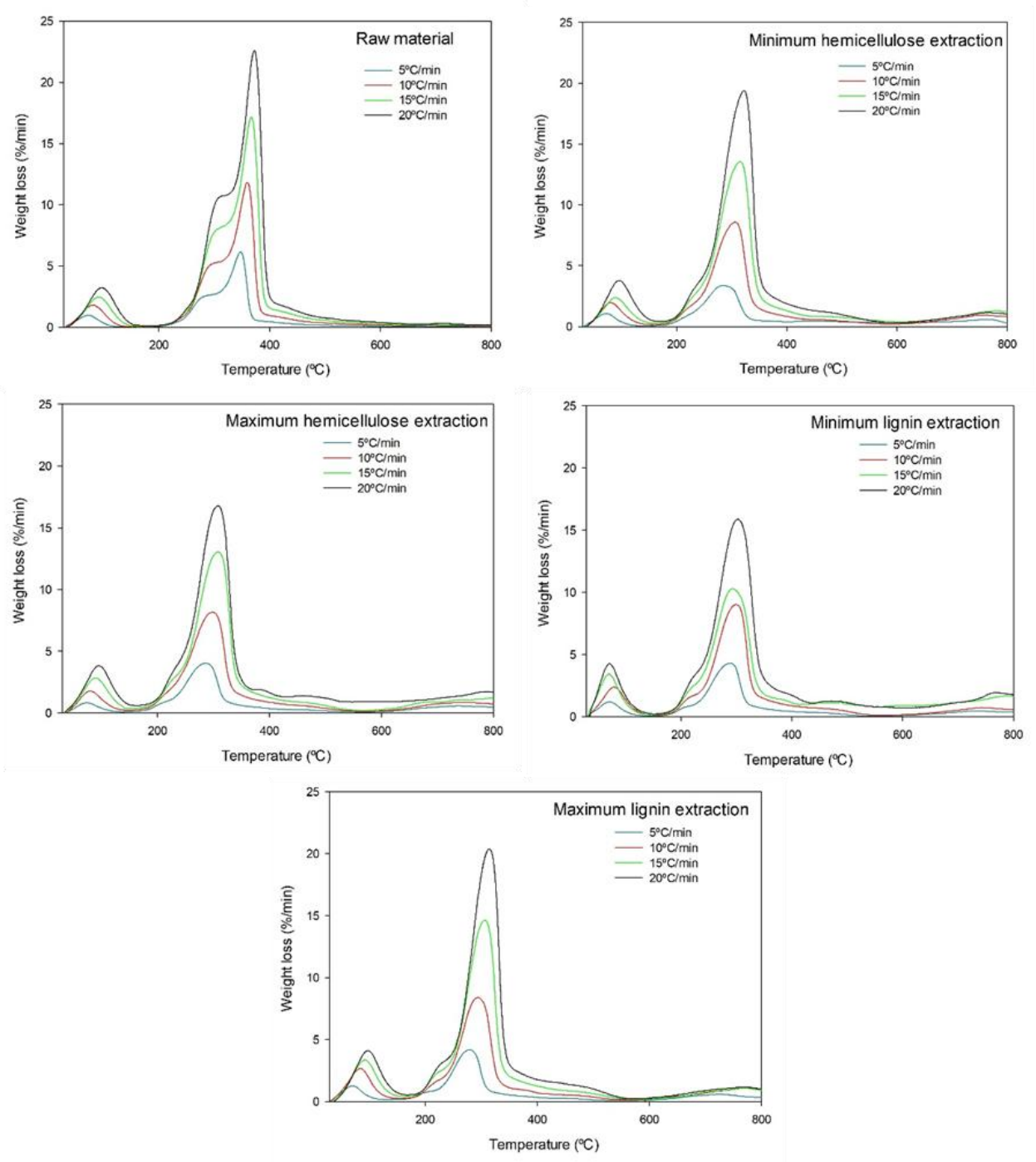


Figure 2. DTG of the raw material and the four post-CAE solid phases.

As can also be seen from Figure 2, the maximum loss temperature (T_{max}) was 372 °C for the raw material and lower (302–320 °C) for the post-CAE solid phases. T_{max} is known to be inversely related to reactivity [58]. Again, the post-CAE solid phases were less thermally stable than the raw material. Also, T_{max} coincided with the main peak in the DTG curves, which was primarily associated with cellulose degradation [55].

The maximum reaction rate at a heating rate of 20 °C/min was 22.59%/min for the raw material (40.3 wt% glucan), about 19.50%/min for the post-CAE solid phases resulting from the lowest extraction of hemicelluloses and highest extraction of lignin (38.3 and 39.0 wt% glucan, respectively),

and in the region of 16.3%/min for those with the highest extraction of hemicelluloses and lowest extraction of lignin (35.0 and 35.7 wt% glucan, respectively). Therefore, it can be observed that the maximum reaction rate increases alongside the glucan content. It can be asserted that the primary degradation, which occurs in this peak of the DTG curves, largely corresponds to the degradation of the cellulose fraction.

3.4 Kinetic analysis of the pyrolytic process.

The pyrolysis kinetics of the raw material and the post-CAE solid phases allowed the influence of the independent variables of the treatment on the thermochemistry of the process to be established. The activation energy E_a at a given degree of conversion α was calculated by applying Friedman's isoconversional method to the results obtained at the heating rates 5, 10, 15 and 20 °C/min. Table 3 shows the E_a values thus obtained as the average of at least three determinations each. The relative standard deviation was less than 5% in all instances.

E_a for the raw material was 168, 177 and 179 kJ/mol at a degree of conversion of 0.25, 0.50 and 0.75, respectively. As can be seen, the activation energy changed with α, both in the raw material and in the post-CAE solid phases. This was a result of the pyrolysis of such highly complex materials as lignocellulosic biomass being an intricate process involving a number of steps. Some authors have reported an average E_a value for the whole conversion range whereas others believe that the effective activation energy of lignocellulosic biomass depends on those of decomposition of each fraction [59–61].

Table 3. Activation energy as calculated with Friedman's isoconversional method at different degrees of conversion for the post-CAE solid phases.

Operating conditions (X_A, X_t, X_T)			**E_a (kJ/mol)**		
			α = 0.25	α = 0.50	α= 0.75
0	0	0	145.7	179.5	285.9
1	1	1	215.4	227.1	139.1
1	1	-1	152.9	195.3	135.1
1	-1	1	127.6	158.8	195.4
1	-1	-1	131.9	164.4	265.4
-1	1	1	177.6	153.6	253.3
-1	1	-1	165.8	211.9	262.7
-1	-1	1	154.8	190.5	167.3
-1	-1	-1	186.8	262.2	255.4
1	0	0	141.1	170.9	282.9
-1	0	0	174.5	209.6	312.8
0	1	0	133.8	166.1	198.3
0	-1	0	108.2	145.1	222.9
0	0	1	156.5	183.2	212.3
0	0	-1	152.9	185.8	290.3

Independent variables: X_A alkali concentration, X_T temperature, X_t treatment time.

https://doi.org/10.1038/s41598-024-52052-0

The data in Table3 were subjected to multiple regression analysis on E_a as a function of the three independent variables (alkali concentration, temperature, and treatment time) at the different degrees of conversion considered. The equations for the models thus established are shown in Table 4. The coefficients of variation between the predicted and experimental results were all less than 10% and the quadratic regression coefficients, R^2, greater than 0.95. Student's-*t* values for the individual variables were all greater than 2, so the results were statistically significant at $p < 0.05$.

Table 4. Equations of the polynomial models for the activation energy.

Equation	α
$E_a = 137.91 - 9.18X_A + 13.73X_t + 21.81X_A^2 - 14.95X_t^2 + 18.74X_T^2 + 13.50X_AX_t + 12.04X_AX_T + 11.57X_tX_T$ (11)	0.25
$E_a = 173.91 - 16.18X_A + 8.3X_t + 18.68X_A^2 - 16.01X_t^2 + 12.92X_T^2 + 29.62X_AX_t + 25.57X_AX_T$ (12)	0.50
$E_a = 276.27 - 18.69X_A - 16.48X_t - 28.84X_T + 23.98X_A^2 - 63.23X_t^2 - 22.54X_T^2 - 40.84X_AX_t + 23.22X_tX_T$ (13)	0.75

Independent variables: X_A alkali concentration, X_T temperature, X_t treatment time.

Figures 3, 4, 5 show the response surfaces for the models, which were used to identify the ranges of the independent variables leading to the lowest activation energy for the post-CAE solid phases relative to the raw material. Surfaces were plotted at two different levels of alkali concentration, which was the individual independent variable most strongly influencing E_a. For easier viewing and understanding, the activation energy for the initial, untreated biomass was plotted on a fixed plane so it would not change along the axes representing the CAE operating conditions.

Figure 3, which corresponds to Eq. (11), shows the variation of E_a for the post-CAE solid phases as a function of temperature and time at the highest and lowest alkali concentration studied. As can be seen, E_a was independent of both variables throughout their operation ranges. Also, at $\alpha = 0.25$ it was lower for the post-CAE solid phases than it was for the raw material. Thus, E_a spanned the range 108.4–205.1 kJ/mol, which is similar to those for hemicelluloses reported by other authors. Some overall kinetic methods for hemicellulose pyrolysis have provided E_a values from 100 to 220 kJ/mol [62].

It should be noted that E_a was lowest for the post-CAE solid phases resulting from treatments at high alkali concentrations and short times, the temperature having little effect on the results.

Figure 4 shows the variation of E_a with the treatment temperature and time at the highest and lowest alkali concentration —the most influential variable— at $\alpha = 0.5$. As can be seen, E_a ranged from 109.7 to 254.3 226 kJ/ mol and was largely due to degradation of the cellulose fraction. The average activation energy for cellulose is 189.2 kJ/mol [63].

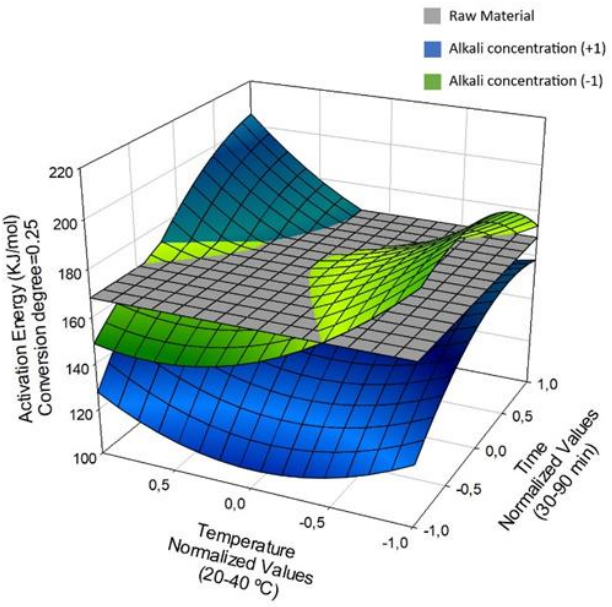


Figure 3. Activation energy contrast in post-CAE solid phases and raw material at α = 0.25, varying conditions.

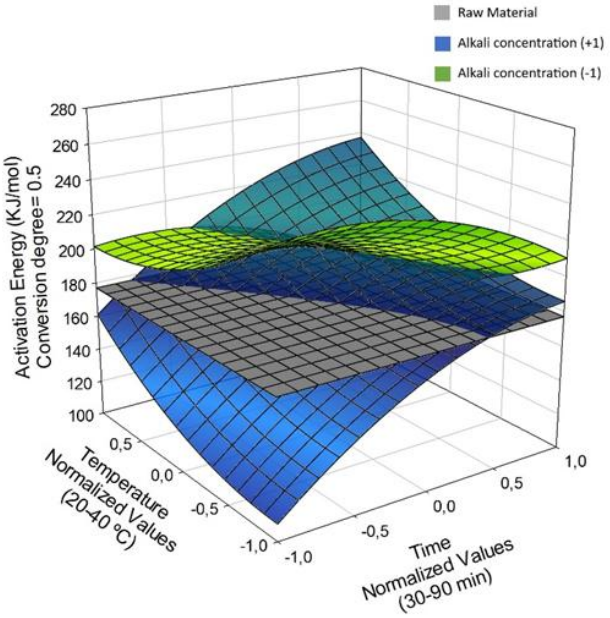


Figure 4. Activation energy constrast in post-CAE solid phases and raw material at α = 0.50, varying conditions.

As can be seen from Figure 5, a combination of the highest alkali concentration, lowest temperature and shortest treatment time led to the lowest E_a values relative to the raw material. On the other hand, E_a remained fairly constant at the lowest alkali level. There was strong correlation between the activation energy and the amount of glucan remaining in the post-CAE solid phase. In fact, as can be seen in Figure 5, constructed at the highest alkali concentration, E_a decreased with increasing proportion of glucan in the solid as a result of the cellulose fraction having a lower activation energy than the polyphenolic fraction.

https://doi.org/10.1038/s41598-024-52052-0

As can be seen in Figure 6, at α = 0.75 the activation energy for the post-CAE solid phases was higher than it was for the raw material under virtually any operating conditions and ranged from 132.9 to 328.5 kJ/mol. Cai et al. [60] reported E_a values of 237.1–266.6 kJ/mol for lignin, whereas Murugan et al. [64] found the isothermal activation energy for the polyphenolic fraction to be 284 kJ/mol.

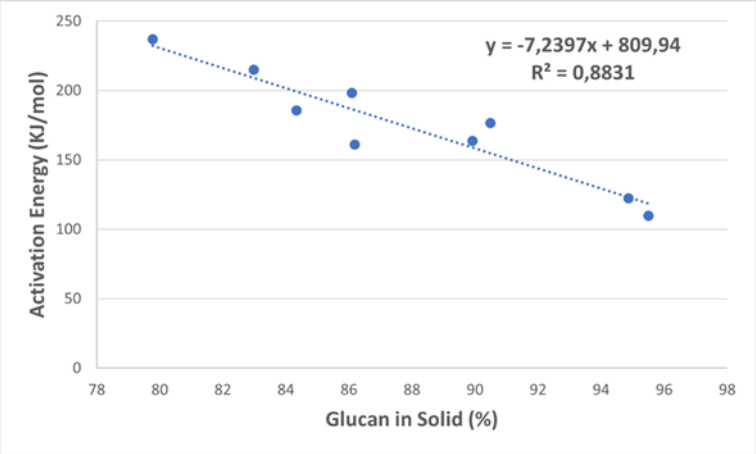


Figure 5. Activation energy change with post-CAE solid phases' glucan content at α = 0.5.

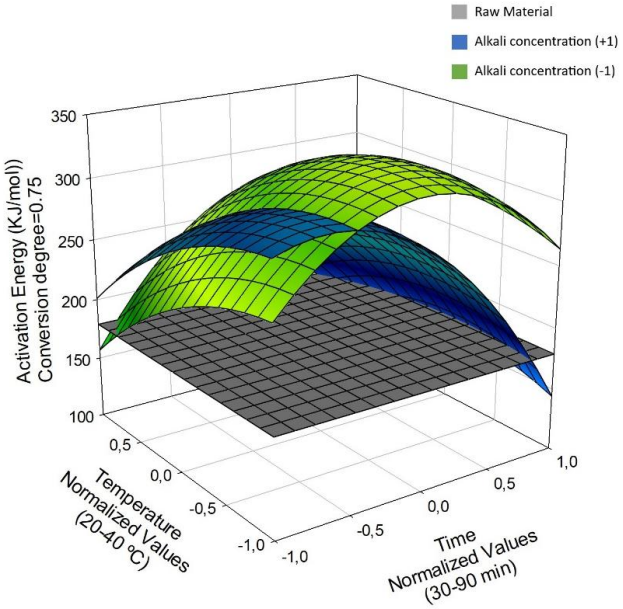


Figure 6. Activation energy contrast in post-CAE solid phases and raw material at α = 0.75, varying conditions.

3.5 Hydrogen production.

The thermogravimetric and kinetic study of the pyrolytic process was followed by assessment of the hydrogen production potential of the post-CAE solid phases on the laboratory-scale reactor described in Section "Modeling and optimization of activation energy".

The TGA curves previously obtained were used to identify the best temperature for hydrogen production. Table 5 shows the selected temperature and the maximum quantity of hydrogen generated for each post-CAE solid phase.

The data in Table 5 underwent multiple regression analysis as a function of the three independent variables (alkali concentration, temperature and treatment time). Similar to E_a, the proportions, in volume, of maximum hydrogen obtained with each post-CAE solid phase were considered. The resulting equation was: $H_2 = 11.85 + 2.32X_A—1.83X_T + 2.94X_A^2—2.24X_T^2—1.65X_AX_T—1.26X_tX_T$ with a quadratic regression coefficient of 0.98 and a coefficient of variation less than 10%. All independent variables had Student's *t*-values greater than 2, so they were deemed statistically significant.

Table 5. Hydrogen production from the post-CAE solid phases.

Operating conditions (X_A, X_t, X_T)			**Temperature** (ºC)	**Hydrogen** (vol. %)
0	0	0	309	13.26
1	1	1	305	6.44
1	1	-1	309	19.07
1	-1	1	313	13.69
1	-1	-1	310	12.76
-1	1	1	315	10.98
-1	1	-1	323	8.31
-1	-1	1	315	7.90
-1	-1	-1	303	6.63
1	0	0	315	8.65
-1	0	0	323	12.94
0	1	0	317	8.84
0	-1	0	315	10.17
0	0	1	318	8.86
0	0	-1	316	11.33
Raw material			372	4.04

Independent variables: X_A alkali concentration, X_T temperature, X_t treatment time.

Figure 7 shows the response surface for hydrogen production. As can be seen, the post-CAE solid phases, but particularly those obtained at the highest alkali concentration, produced greater amounts of hydrogen than did the raw material. On the other hand, as was apparent from Eq. (14), hydrogen production was scarcely affected by the treatment time. Finally, the effect of temperature was found to depend on the alkali concentration; thus, at the highest alkali levels, hydrogen production peaked with medium or high temperatures.

The maximum proportion of hydrogen obtained, in volume, from the post-CAE solid phases ranged from 9.15 to 19.51%, so it was up to 15.57% greater than that provided by the raw material. These results are consistent with previously reported values for species such as *Eucalyptus*

urograndis, where authohydrolysis provided amounts of hydrogen up to 8% greater than the raw material [33]. Similary, the application of acid hydrolysis to *Leucaena leucocephala* resulted in increased hydrogen production [53]. In general, slow pyrolysis, like the process studied in this work, exhibits a range of hydrogen yields between 9 and 44% [65].

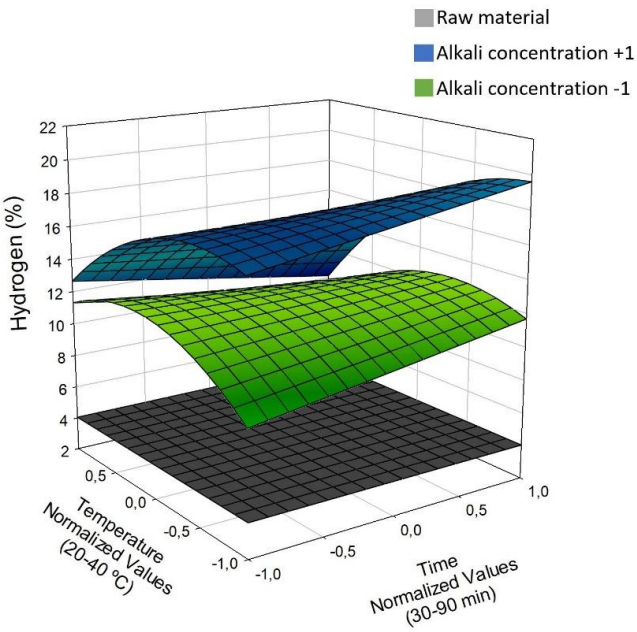


Figure 7. Hydrogen production variation in post-CAE solid phases and raw material at α = 0.50, diverse conditions.

4 Conclusions.

As shown here, ultrasound-assisted cold alkaline extraction provides liquors with increased proportions of hemicelluloses and lignin relative to the absence of ultrasound.

The composition of the raw material and the post-CAE solid phases affect their thermal degradation. In addition, the post-CAE solid phases were more reactive in the thermochemical process than was clone AF2 clone of *Populus*.

The activation energy of the post-CAE solid phases is generally lower than that of the raw material, with alkali concentration proving to be the most influential independent variable in this regard. In turn, E_a decreased with increasing proportion of glucan in the residues.

The ultrasound-assisted CAE process enhances hydrogen production, making this sequential process with CAE and pyrolysis approach a favorable choice for this feedstock valorization.

Author contributions

L.-C.S: Conceptualization, Methodology, Investigation, Formal analysis, Data curation, Visualization, Writing–original draft. **L.J.M**: Conceptualization, Methodology, Investigation, Formal analysis, Data curation, Visualization. **G.J.C**: Conceptualization, Methodology, Funding adquisition,

Supervision, Writing–review & editing. **T.R**: Formal analysis, raw material acquisition, Writing – review & editing. **B.F**: Conceptualization, Methodology, Data curation, Funding acquisition, Supervision, Writing–review & editing, Project administration. All authors reviewed the manuscript and consented to its publication.

Funding

This work was funded by Spain's Ministry of Science and Innovation, and also by the National Research Program Oriented to the Challenges of Society (Project PID2020-112875RB-C21, MCIN/AEI /https://doi.org/10.13039/501100011033), also this publication is part of the PRE2021-097925 support (funded by MCIN/AEI/ https://doi.org/10.13039/501100011033 and by the FSE+), and the University of Huelva/CBUA.

Data availability

All data generated or analyzed during this work are included in this published article.

Ethics approval and consent to participate

The authors declare that this is their original work, and the corresponding manuscript has not been published before and is only submitted to the Journal of Scientific Reports.

Competing interests

The authors declare no competing interests.

Additional information

Correspondence and requests for materials should be addressed to S.L.-C.

Reprints and permissions information is available at www.nature.com/reprints.

Open Access

This article is licensed under a Creative Commons Attribution 4.0 International License, which permits use, sharing, adaptation, distribution and reproduction in any medium or format, as long as you give appropriate credit to the original author(s) and the source, provide a link to the Creative Commons licence, and indicate if changes were made. The images or other third party material in this article are included in the article's Creative Commons licence, unless indicated otherwise in a credit line to the material. If material is not included in the article's Creative Commons licence and your intended use is not permitted by statutory regulation or exceeds the permitted use, you will need to obtain permission directly from the copyright holder. To view a copy of this licence, visit http://creativecommons.org/licenses/by/4.0/.

References

[1] Jiang, Z. et al. Non linear effect of Biomass, fossil fuels and renewable energy usage on the economic Growth: Managing sustainable development through energy sector. Fuel 326, 124943 (2022). https://doi.org/10.1016%2Fj.fuel.2022.124943.

[2] Popp, J., Kovács, S., Oláh, J., Divéki, Z. & Balázs, E. Bioeconomy: Biomass and biomass-based energy supply and demand. N. Biotechnol. 60, 76–84 (2021). https://doi.org/10.1016%2Fj.nbt.2020.10.004.

[3] Schimel, D., Stephens, B. B. & Fisher, J. B. Effect of increasing CO 2 on the terrestrial carbon cycle. Proc. Nat. Acad. Sci. 112, 436–441 (2015). https://doi.org/10.1073/pnas.1407302112.

[4] Welfle, A., Thornley, P. & Röder, M. A review of the role of bioenergy modelling in renewable energy research & policy development. *Biomass Bioenergy.* **136**, 105542 (2020). https://doi.org/10.1016%2Fj.biombioe.2020.105542.

[5] Nie, A. et al. An environmental and economic assessment from bioenergy production and biochar application. J. Saudi Chem. Soc. 25, 101173 (2021). https://doi.org/10.1016%2Fj.jscs.2020.11.006.

[6] Yousaf, I., Nekhili, R. & Umar, M. Extreme connectedness between renewable energy tokens and fossil fuel markets. Energy Econ. 114, 106305 (2022). https://doi.org/10.1016%2Fj.eneco.2022.106305.

[7] Bender, T. A., Dabrowski, J. A. & Gagné, M. R. Homogeneous catalysis for the production of low-volume, high-value chemicals from biomass. Nat. Rev. Chem. 2, 35–46 (2018). https://doi.org/10.1038%2Fs41570-018-0005-y.

[8] Roy, S. et al. Recent nanobiotechnological advancements in lignocellulosic biomass valorization: A review. J. Environ. Manage. 297, 113422 (2021). https://doi.org/10.1016%2Fj.jenvman.2021.113422.

[9] Saravanan, A., Senthil Kumar, P., Jeevanantham, S., Karishma, S. & Vo, D. V. N. Recent advances and sustainable development of biofuels production from lignocellulosic biomass. Bioresour. Technol. 344, 126203 (2022). https://doi.org/10.1016%2Fj.biortech.2021.126203.

[10] Abraham, A. et al. Pretreatment strategies for enhanced biogas production from lignocellulosic biomass. Bioresour. Technol. 301, 122725 (2020). https://doi.org/10.1016%2Fj.biortech.2019.122725.

[11] FitzPatrick, M., Champagne, P., Cunningham, M. F. & Whitney, R. A. A biorefinery processing perspective: Treatment of lignocellulosic materials for the production of value-added products. Bioresour. Technol. 101, 8915–8922 (2010). https://doi.org/10.1016%2Fj.biortech.2010.06.125.

[12] García, J. C. et al. Search for optimum conditions of wheat straw hemicelluloses cold alkaline extraction process. Biochem. Eng. J. 71, 127–133 (2013). https://doi.org/10.1016%2Fj.bej.2012.12.008.

[13] Yuan, Z. et al. Process intensification effect of ball milling on the hydrothermal pretreatment for corn straw enzymolysis. Energy Convers. Manag. 101, 481–488 (2015). https://doi.org/10.1016%2Fj.enconman.2015.05.057.

[14] de Carvalho, D. M., de Queiroz, J. H. & Colodette, J. L. Assessment of alkaline pretreatment for the production of bioethanol from eucalyptus, sugarcane bagasse and sugarcane straw. Ind. Crops Prod. 94, 932–941 (2016). https://doi.org/10.1016%2Fj.indcrop.2016.09.069.

[15] Abejón, R. A bibliometric study of scientific publications regarding hemicellulose valorization during the 2000–2016 period: Identification of alternatives and hot topics. ChemEngineering 2, 7 (2018). https://doi.org/10.3390%2Fchemengineering2010007.

[16] Chen, Z., Zhu, Q., Wang, X., Xiao, B. & Liu, S. Pyrolysis behaviors and kinetic studies on Eucalyptus residues using thermogravimetric analysis. Energy Convers. Manag. 105, 251–259 (2015). https://doi.org/10.1016%2Fj.enconman.2015.07.077.

[17] Bridgwater, A. V. Renewable fuels and chemicals by thermal processing of biomass. Chem. Eng. J. 91, 87–102 (2003). https://doi.org/10.1016%2FS1385-8947%2802%2900142-0.

[18] Zhang, L., Chen, K., He, L. & Peng, L. Reinforcement of the bio-gas conversion from pyrolysis of wheat straw by hot caustic preextraction. Biotechnol. Biofuels. 11, 72 (2018). https://link.springer.com/doi/10.1186/s13068-018-1072-5.

[19] Kan, T., Strezov, V. & Evans, T. J. Lignocellulosic biomass pyrolysis: A review of product properties and effects of pyrolysis parameters. Renew. Sustain. Energy Rev. 57, 1126–1140 (2016). https://doi.org/10.1016%2Fj.rser.2015.12.185.

[20] Yang, H., Yan, R., Chen, H., Lee, D. H. & Zheng, C. Characteristics of hemicellulose, cellulose and lignin pyrolysis. Fuel 86, 1781–1788 (2007). https://doi.org/10.1016%2Fj.fuel.2006.12.013.

[21] Yogalakshmi, K. N. et al. Lignocellulosic biomass-based pyrolysis: A comprehensive review. Chemosphere 286, 131824 (2022). https://doi.org/10.1016%2Fj.chemosphere.2021.131824.

[22] Ni, M., Leung, D. Y. C., Leung, M. K. H. & Sumathy, K. An overview of hydrogen production from biomass. Fuel Process. Technol. 87, 461–472 (2006). https://doi.org/10.1016%2Fj.fuproc.2005.11.003.

[23] Buffi, M., Prussi, M. & Scarlat, N. Energy and environmental assessment of hydrogen from biomass sources: Challenges and perspectives. Biomass Bioenergy 165, 106556 (2022). https://doi.org/10.1016%2Fj.biombioe.2022.106556.

[24] Commission European. Communication from the Commission to the European Parliament, the Council, the European Economic and Social Committee and the Committee of the Regions Youth Opportunities Initiative. 2011.

[25] Nasir Uddin, M., Daud, W. M. A. W. & Abbas, H. F. Potential hydrogen and non-condensable gases production from biomass pyrolysis: Insights into the process variables. Renew. Sustain. Energy Rev. 27, 204–224 (2013). https://doi.org/10.1016%2Fj.rser.2013.06.031.

[26] Demirbaş, A. Gaseous products from biomass by pyrolysis and gasification: Effects of catalyst on hydrogen yield. Energy Convers. Manag. 43, 897–909 (2002). https://doi.org/10.1016%2FS0196-8904%2801%2900080-2.

[27] Widyawati, M., Church, T. L., Florin, N. H. & Harris, A. T. Hydrogen synthesis from biomass pyrolysis with in situ carbon dioxide capture using calcium oxide. Int. J. Hydrogen Energy 36, 4800–4813 (2011). https://doi.org/10.1016%2Fj.ijhydene.2010.11.103.

[28] Sanchez-Silva, L., López-González, D., Villaseñor, J., Sánchez, P. & Valverde, J. L. Thermogravimetric–mass spectrometric analysis of lignocellulosic and marine biomass pyrolysis. Bioresour. Technol. 109, 163–172 (2012). https://doi.org/10.1016%2Fj.biortech.2012.01.001.

[29] Kumar, J. V. & Pratt, B. C. Compositional analysis of some renewable biofuels. Am. Lab. (Fairfield) 28, 15–20 (1996).

[30] Li, S., Xu, S., Liu, S., Yang, C. & Lu, Q. Fast pyrolysis of biomass in free-fall reactor for hydrogen-rich gas. Fuel Process. Technol. 85, 1201–1211 (2004). https://doi.org/10.1016%2Fj.fuproc.2003.11.043.

[31] Wu, C., Wang, Z., Huang, J. & Williams, P. T. Pyrolysis/gasification of cellulose, hemicellulose and lignin for hydrogen production in the presence of various nickel-based catalysts. Fuel 106, 697–706 (2013). https://doi.org/10.1016%2Fj.fuel.2012.10.064.

[32] Jarungthammachote S, Acharya B, Dutta A. Parametric Effect of Agricultural Residues and Woody Biomass on Hydrogen Production through Gasification Process. Proceedings of the international agricultural engineering conference Cutting edge technologies and innovations on sustainable resources for world food sufficiency: Asian Association for Agricultural Engineering. Citeseer; (2007).

[33] Loaiza, J. M. et al. Effect of autohydrolysis on hemicellulose extraction and pyrolytic hydrogen production from Eucalyptus urograndis. Biomass Convers. Biorefin. 12, 4021–4030 (2022). https://link.springer.com/doi/10.1007/s13399-020-00900-0.

[34] González-González, B. D., Oliveira, N., González, I., Cañellas, I. & Sixto, H. Poplar biomass production in short rotation under irrigation: A case study in the Mediterranean. Biomass Bioenergy 107, 198–206 (2017). https://doi.org/10.1016%2Fj.biombioe.2017.10.004.

[35] Sixto, H. et al. Growth potential of different species and genotypes for biomass production in short rotation in Mediterranean environments. For. Ecol. Manage. 354, 291–299 (2015). https://doi.org/10.1016%2Fj.foreco.2015.05.038.

[36] Bloemen, J. et al. Water use of a multigenotype poplar short-rotation coppice from tree to stand scale. GCB Bioenergy 9, 370–384 (2017). https://doi.org/10.1111%2Fgcbb.12345.

[37] Navarro, A., Facciotto, G., Campi, P. & Mastrorilli, M. Physiological adaptations of five poplar genotypes grown under SRC in the semi-arid mediterranean environment. Trees – Struct. Funct. 28, 983–994 (2014). https://link.springer.com/doi/10.1007/s00468-014-1012-3.

[38] di Matteo, G., Nardi, P., Verani, S. & Sperandio, G. Physiological adaptability of Poplar clones selected for bioenergy purposes under non-irrigated and suboptimal site conditions: A case study in Central Italy. Biomass Bioenergy 81, 183–189 (2015). https://doi.org/10.1016%2Fj.biombioe.2015.06.023.

[39] TAPPI T264 cm-07. Preparation of Wood for Chemical Analysis (TAPPI Press, 2007).

[40] TAPPI T212 om-22. One percent sodium hydroxide solubility of wood and pulp (Test Method).

[41] TAPPI T257 cm-85. Sampling and Preparing Wood for Analysis (TAPPI Press, 1999).

[42] TAPPI T204 cm-07. Sampling and Preparing Wood for Analysis (TAPPI Press, 2007).

[43] TAPPI 211 om-02. Ash in Wood, Pulp, Paper and Paperboard: Combustion at 525°C. (TAPPI Press, 2002).

[44] TAPPI T249 cm-09. Carbohydrate Composition of Extractive-Free Wood and Wood Pulp by Gas-Liquid Chromatography (TAPPI Press, 2009).

[45] TAPPI T222 om-11. Acid-Insoluble Lignin in Wood and Pulp (TAPPI Press, 2011).

[46] Montgomery, D. C. Diseño y Análisis de Experimentos (Limusa Wiley, 2003).

[47] Vyazovkin, S. & Sbirrazzuoli, N. Isoconversional kinetic analysis of thermally stimulated processes in polymers. Macromol. Rapid. Commun. 27, 1515–1532 (2006). https://doi.org/10.1002%2Fmarc.200600404.

[48] Starink, M. J. The determination of activation energy from linear heating rate experiments: A comparison of the accuracy of isoconversion methods. Thermochim Acta. 404, 163–176 (2003). https://doi.org/10.1016%2FS0040-6031%2803%2900144-8.

[49] Martín-Lara, M. A., Ronda, A., Blázquez, G., Pérez, A. & Calero, M. Pyrolysis kinetics of the lead-impregnated olive stone by non-isothermal thermogravimetry. Process Safety Environ. Protect. 113, 448–458 (2018). https://doi.org/10.1016%2Fj.psep.2017.11.015.

[50] Friedman, H. L. Kinetics of thermal degradation of char-forming plastics from thermogravimetry. Application to a phenolic plastic. J. Polym. Sci. Part C: Polym. Symposia 6, 183–195 (1964). https://doi.org/10.1002%2Fpolc.5070060121.

[51] Susana Lozano Calvo. Extraction of Polysaccharides in High-Yield Species Using Ultrasound. (2019). https://doi.org/10.1016%2Fj.biortech.2015.10.028.

[52] Methrath Liyakathali, N. A., Muley, P. D., Aita, G. & Boldor, D. Effect of frequency and reaction time in focused ultrasonic pretreatment of energy cane bagasse for bioethanol production. Bioresour. Technol. 200, 262–271 (2016). https://doi.org/10.1016%2Fj.biortech.2015.10.028.

[53] Loaiza, J. M., López, F., García, M. T., García, J. C. & Díaz, M. J. Biomass valorization by using a sequence of acid hydrolysis and pyrolysis processes. Application to Leucaena leucocephala. Fuel 203, 393–402 (2017). https://doi.org/10.1016%2Fj.fuel.2017.04.135.

[54] Pontes, R. et al. Comparative autohydrolysis study of two mixtures of forest and marginal land resources for co-production of biofuels and value-added compounds. Renew. Energy 128, 20–29 (2018). https://doi.org/10.1016%2Fj.renene.2018.05.055.

[55] Dantas, G. A., Legey, L. F. L. & Mazzone, A. Energy from sugarcane bagasse in Brazil: An assessment of the productivity and cost of different technological routes. Renew. Sustain. Energy Rev. 21, 356–364 (2013). https://doi.org/10.1016%2Fj.rser.2012.11.080.

[56] Sebio-Puñal, T., Naya, S., López-Beceiro, J., Tarrío-Saavedra, J. & Artiaga, R. Thermogravimetric analysis of wood, holocellulose, and lignin from five wood species. J. Therm. Anal. Calorim. 109, 1163–1167 (2012). https://link.springer.com/doi/10.1007/s10973-011-2133-1.

[57] Fidalgo, M. L. et al. Comparative study of fractions from alkaline extraction of wheat straw through chemical degradation, analytical pyrolysis, and spectroscopic techniques. J. Agric. Food Chem. 41, 1621–1626 (1993). https://doi.org/10.1021%2Fjf00034a019.

[58] Ramírez, Á., García-Torrent, J. & Tascón, A. Experimental determination of self-heating and self-ignition risks associated with the dusts of agricultural materials commonly stored in silos. J. Hazard Mater. 175, 920–927 (2010). https://doi.org/10.1016%2Fj.jhazmat.2009.10.096.

[59] Carrier, M., Auret, L., Bridgwater, A. & Knoetze, J. H. Using apparent activation energy as a reactivity criterion for biomass pyrolysis. Energy Fuels 30, 7834–7841 (2016). https://doi.org/10.1021%2Facs.energyfuels.6b00794.

[60] Cai, J., Wu, W., Liu, R. & Huber, G. W. A distributed activation energy model for the pyrolysis of lignocellulosic biomass. Green Chem. 15, 1331–1340 (2013). https://doi.org/10.1039%2Fc3gc36958g.

[61] Vyazovkin, S. A time to search: Finding the meaning of variable activation energy. Phys. Chem. Chem. Phys. 18, 18643–18656 (2016). https://doi.org/10.1039%2FC6CP02491B.

[62] Zhou, X., Li, W., Mabon, R. & Broadbelt, L. J. A critical review on hemicellulose pyrolysis. Energy Technol. 5(1), 52–79 (2017). https://doi.org/10.1002%2Fente.201600327.

[63] Chen, D. et al. Insight into biomass pyrolysis mechanism based on cellulose, hemicellulose, and lignin: Evolution of volatiles and kinetics, elucidation of reaction pathways, and characterization of gas, biochar and bio-oil. Combust Flame. 242, 112142 (2022). https://doi.org/10.1016%2Fj.combustflame.2022.112142.

[64] Murugan, P., Mahinpey, N., Johnson, K. E. & Wilson, M. Kinetics of the pyrolysis of lignin using thermogravimetric and differential scanning calorimetry methods. Energy Fuels 22, 2720–2724 (2008). https://doi.org/10.1021%2Fef700730u.

[65] Vuppaladadiyam, A. K. et al. Biomass pyrolysis: A review on recent advancements and green hydrogen production. Bioresour. Technol. 364, 128087 (2022). https://doi.org/10.1016%2Fj.biortech.2022.128087.

Publisher's note

Springer Nature remains neutral with regard to jurisdictional claims in published maps and institutional affiliations.

3.3. Valorización Secuencial del Clon AF2 de *Populus* mediante Extracción Alcalina en Frío y Deslignificación Organosolv.

1 Introducción.

En la actualidad, la búsqueda de materiales celulósicos a partir de recursos lignocelulósicos representa un desafío importante, especialmente ante la necesidad de encontrar alternativas sostenibles a los materiales tradicionales de origen forestal. La creciente presión sobre los recursos naturales, sumada a las exigencias medioambientales y económicas, ha impulsado la búsqueda de nuevas fuentes de biomasa que sean sostenibles, eficientes y de bajo impacto ambiental [1].

En este contexto, los residuos agrícolas han cobrado un notable interés debido a su disponibilidad y bajo costo. Sin embargo, su aprovechamiento presenta limitaciones asociadas a la estacionalidad, la dispersión geográfica, el coste de recolección y transporte [1-3].

Frente a estas limitaciones, los cultivos energéticos de corta rotación y alta productividad (como algunos clones de *Populus*) surgen como una alternativa viable. Estos cultivos ofrecen la posibilidad de un suministro estable y continuo de biomasa, capaz de satisfacer la demanda industrial sin comprometer los recursos forestales tradicionales ni entrar en conflicto con la producción de alimentos [4-6].

Por otro lado, la industria de la pulpa y el papel, que se remonta al primer siglo de nuestra era, continúa siendo un sector en crecimiento. Aunque ha experimentado una transformación significativa con la invasión de las tecnologías digitales y el auge del comercio digital, que ha desplazado su enfoque desde el papel gráfico hacia el embalaje y el envasado, la demanda de productos celulósicos sigue en aumento [7]. Este contexto refuerza la necesidad de explorar nuevas fuentes de celulosa y de desarrollar tecnologías de fraccionamiento más sostenibles y eficientes.

En este sentido, el proceso organosolv se establece cómo una técnica de fraccionamiento prometedora, capaz de satisfacer las necesidades de una estrategia de “lignina-primero”, al tiempo que contribuye al concepto de biorrefinería y al desarrollo de una bioeconomía circular. Además, es económicamente viable, ya que la mayoría de los solventes utilizados pueden recuperarse y reciclarse, debido a sus bajos puntos de ebullición [1,8-12]. Este método fue inventado por Theodor Kleinert en 1968 como una alternativa al proceso Kraft y al sulfito, destacándose por ser más respetuoso con el medio ambiente en comparación con ambos [13]. Aunque fue estudiado ampliamente, el proceso organosolv fue dejado de lado por los avances en la tecnología del proceso Kraft. Sin embargo, recientemente ha vuelto a captar la atención, impulsado por el creciente interés en desarrollar procesos más eficientes para el uso de la biomasa [1,14].

Una de las principales diferencias de este método sobre los procesos más tradicionales es su capacidad de separar la materia prima en una fracción rica en celulosa, una fracción hidrosoluble que contiene productos de degradación de la hemicelulosa y una fracción de lignina disuelta sin azufre [1,15]. Es importante señalar que el grado de fraccionamiento y las propiedades de los componentes extraídos dependerá del solvente empleado, así como de factores como el tiempo, la temperatura y la presión, y de la naturaleza de la materia prima tratada [16]. Entre los diversos solventes que se pueden emplear en el método organosolv, el etanol es el más utilizado debido a su bajo coste, buena solubilidad de la lignina, falta de toxicidad, miscibilidad con agua y fácil recuperación [17-21]. El proceso de organosolv resulta viable para diferentes tipos de biomasa, desde maderas duras y blandas hasta residuos agrícolas y pastos [22,23].

En el fraccionamiento organosolv, la adición de un catalizador juega un papel crucial, ya que aumenta la eficiencia del proceso. Estos catalizadores facilitan la descomposición de la lignina y la hemicelulosa, y ayudan a reducir la cantidad de inhibidores que se producen durante el tratamiento. Se han estudiado diferentes tipos de catalizadores, tanto ácidos como álcalis [1,24].

La opción de catalizar el proceso organosolv mediante ácidos es la más implementada a escala industrial, piloto y laboratorio, ya que estos permiten disminuir la temperatura de operación con concentraciones mínimas [1,24]. Sin embargo, este enfoque presenta algunos desafíos. La temperatura de operación suele ser superior a 150 ºC, donde los ácidos pueden causar la disolución completa de la hemicelulosa y parte de la celulosa, la descomposición de carbohidratos y la formación de inhibidores como el furfural, el ácido levulínico o 5-hidroximetilfurfural. Además, los ácidos pueden contribuir a la corrosión de los equipos y generar altas presiones debido al uso de alcoholes como solventes en el tratamiento [1,25,26].

Por estas razones, el fraccionamiento organosolv catalizado por álcali ha atraído la atención recientemente, en especial en sistemas donde la conservación de carbohidratos es crucial [19,27]. El uso de catalizadores álcalis presentan un avance significativo en la tecnología de conversión de biomasa, ayudando a la descomposición de la estructura de la lignina y aumentando la producción de azúcares valiosos, así como la pureza de las fracciones de celulosa y hemicelulosa [1]. Un ejemplo de estos catalizadores es el hidróxido de sodio, que aumenta la capacidad de deslignificación del etanol [28]. Zhang et al. [29] compararon un proceso etanol-NaOH con el pretratamiento simple de hidróxido de sodio y el proceso organosolv con etanol, concluyendo que la combinación de ambos genera un efecto sinérgico en la deslignificación de la materia prima y, al mismo tiempo, reduce la temperatura de operación.

En este contexto, el presente estudio tiene como objetivo principal realizar un análisis comparativo del proceso organosolv con etanol y el proceso organosolv con etanol catalizado por álcalis, utilizando como materia prima el clon AF2 del *Populus x euramericana.* La hipótesis planteada es que la secuencia del tratamiento de extracción alcalina en frío con ultrasonidos, aprovechando los restos de hidróxido de sodio que permanecen en el sólido post-tratamiento, pueda actuar como catalizador en el siguiente paso del proceso organosolv con etanol. Esto permitiría minimizar las condiciones de operación.

2 Material y metodología.

La biomasa en estudio, el clon AF2 del *Populus x euramericana*, procede de las plantaciones experimentales del departamento de Ciencias Agroforestales de la Universidad de Huelva. Esta biomasa se sometió a un proceso de acondicionamiento, para obtener unas condiciones de tamaño y secado óptimas para ser sometida tanto a la extracción alcalina en frío como al proceso organosolv. Además, se caracterizó acorde con las normas TAPPI para conocer su composición de partida [30-37], se presenta dicha composición en la Tabla 1 de este apartado.

Tabla 1. Composición química y poder calorífico superior (PCS) del clon AF2 *de Populus x euramericana*.

Extractivos al 1% de NaOH	22,3 ± 1,95 %
Extractivos en agua caliente	4,2 ± 0,12 %
Extractivos en etanol-acetona	2,8 ± 0,15 %
α-Celulosa (glucano)	40,3 ± 0,85 %
Lignina Klason	25,1 ± 0,16 %
Xilano	19,3 ± 0,09 %
Arabano	0 %
Grupos acetilo	0,7 ± 0,02 %
Ceniza	1,14 ± 0,04
Poder calorífico superior (PCS)	19,9 ± 30 $KJ*kg^{-1}$ od.b

2.1 Extracción alcalina en frío con ultrasonidos.

El clon AF2 de *Populus x euramericana* fue sometido a un tratamiento de extracción alcalina en frío (EAF) en un baño ultrasónico Power Sonic Serie 500, utilizando una relación constante de líquido/sólido seco de 15. Las condiciones de operación fueron seleccionadas conforme con el estudio desarrollado en el marco de esta tesis doctoral, específicamente según lo establecido en la Publicación 2 de esta memoria.

En dicho estudio se demostró que la aplicación de ultrasonidos incrementaba significativamente la extracción de todas las fracciones lignocelulósicas, especialmente las hemicelulosas y los polifenoles. Por esta razón, se optó por realizar la EAF con aplicación simultánea de ultrasonidos. Además, las condiciones seleccionadas representan un compromiso óptimo entre la cantidad de lignina y hemicelulosas extraídas hacia la fracción líquida.

De este modo, las condiciones operativas empleadas en el presente trabajo fueron: una concentración de 100 g L^{-1} de hidróxido de sodio, un tiempo de operación de 90 minutos, una temperatura de 30 ºC y una potencia ultrasónica de 120W.

Bajo las condiciones establecidas para la extracción alcalina en frío, los sólidos recuperados presentan una composición del 49,5% en glucano, 11,4% de xilano y 25,9% en lignina Klason. Estos valores corresponden al 81,7% del glucano, 39,2% del xilano y 68,7% de lignina Klason respecto a la cantidad original presente en el clon AF2.

Normalmente, la fase sólida obtenida tras el tratamiento se somete a un proceso de lavado y neutralización con agua y ácido acético, con el objetivo de eliminar los restos de hidróxido de sodio que puedan permanecer en los poros del sólido. Sin embargo, en el presente estudio se omite dicha etapa, ya que se pretende aprovechar el carácter alcalino residual del material como catalizador en la siguiente etapa. Esta estrategia permite no solo simplificar el procedimiento, sino también explorar el potencial del residuo alcalino en reacciones subsiguientes, alineándose con un enfoque de aprovechamiento integral y reducción de costos adicionales.

2.2 Proceso organosolv.

El proceso organosolv con etanol se llevó a cabo en un reactor discontinuo de alta presión (Parr 4843), equipado con un cuerpo calefactor y una hélice para asegurar una mezcla uniforme. Los tratamientos se realizaron utilizando la velocidad de calentamiento más alta disponible, precisando de 25 minutos para alcanzar la temperatura de operación de cada experiencia. Una vez alcanzada la temperatura deseada, el sistema cambió a un modo de calentamiento más lento, que permitió mantener dicha temperatura durante el tiempo de operación establecido para cada ensayo. Transcurrido ese periodo, el reactor se enfrió mediante la circulación de agua fría a través de un serpentín interno.

La relación líquido/sólido se fijó en 8. Las variables independientes del proceso organosolv variaron entre dos modalidades: el proceso convencional y un proceso modificado, en el que se aprovechó el carácter alcalino de los sólidos obtenidos en la etapa previa de extracción alcalina en frío. En el primer caso (proceso convencional), la temperatura varió entre 150-180 ºC, el tiempo entre 30-90 minutos y la concentración de etanol entre 35-65% (en volumen respecto al licor). En el segundo caso (con efecto catalítico alcalino), la temperatura osciló entre 135-150 ºC, manteniéndose los mismos rangos de tiempo y concentración de etanol.

Las pulpas obtenidas tras el tratamiento organosolv fueron separadas del licor y lavadas inicialmente con una disolución de etanol en la misma proporción utilizada durante el proceso, con

el fin de evitar la precipitación de la lignina. Posteriormente, se lavaron con abundante agua. Las pulpas resultantes se sometieron a un proceso de desfibrilación durante un minuto.

La preparación de la pulpa para la fabricación de papel se realizó conforme a la norma UNE 57-026. Las hojas se obtuvieron mediante un formador de hojas ENJO F-39, de acuerdo con la norma UNE 57-042-91.

Tanto las pulpas como las hojas obtenidas se caracterizaron mediante: rendimiento de pulpa (TAPPI T-257), número kappa (TAPPI T-236), viscosidad (UNE 57-025), composición química (TAPPI T-249 y TAPPI T-222), índice de tracción (UNE 57-055-79 y UNE 57-028), índice de estallido (UNE 57-055-79 y UNE 57-058), índice de desgarro (UNE 57-055-79 y UNE 57-033) y blancura Iso (UNE 2470-1).

2.3 Modelado y Optimización por Regresión Múltiple-Diseño Experimental.

El proceso organosolv con etanol, catalizado por el carácter alcalino de los sólidos obtenidos en la extracción alcalina en frío, se modeló mediante regresión múltiple, considerando los términos lineales, cuadráticos y de interacción entre las variables independientes. El modelo general utilizado fue el siguiente:

$$Y = a_0 + \sum_{i=1}^{n} b_i X_{ni} + \sum_{i=1}^{n} c_i X_{ni}^2 + \sum_{i=1,j=1}^{n} d_{ij} X_{ni} X_{nj} \quad (i<j) \quad (1)$$

Para limitar el número de experimentos necesarios y minimizar las covarianzas entre variables, se empleó un diseño experimental de composición central, con un total de N experimentos definidos según:

$$N = 2^n + 2n + n_c \qquad (2)$$

donde 2^n representa el número de puntos del diseño factorial, 2n los puntos axiales y n_c los puntos centrales.

Con el fin de eliminar el efecto de los distintos rangos de variación de las variables independientes, estas fueron normalizadas al intervalo [-1,1] utilizanod la siguiente ecuación:

$$X_n = \frac{X - \bar{X}}{(X_{max} - X_{min})/2} \qquad (3)$$

donde X es el valor original de la variable, $\bar{X}$ es su valor medio, y X_{max} y X_{min} son los valores máximo y mínimo del intervalo de estudio, respectivamente.

La inclusión de términos en el modelo se realizó considerando únicamente aquellos estadísticamente significativos, es decir, con un valor de $p<0,1$ según la prueba de *t*-Student, o cuyo intervalo de confianza fuera superior al 95%.

Las variables independientes del proceso fueron: temperatura de operación, tiempo de tratamiento y concentración de etanol. Mientras que las variables de respuesta (dependientes), evaluadas en función de las condiciones de operación, fueron: rendimiento de pulpa, contenidos de glucano, xilano y lignina Klason, índices de tracción, estallido y desgarro, y blancura ISO.

2.4 Precipitación y caracterización de ligninas organosolv.

En ambos procesos organosolv, tanto el convencional como la variante catalizada por el carácter alcalino de los sólidos, se procedió a la precipitación de ligninas a partir del licor obtenido en las condiciones de operación que resultaron en la mayor extracción de este componente.

En el caso del proceso convencional, el licor organosolv fue mezclado con cuatro volúmenes de agua destilada y dejado en reposo durante una hora para favorecer la precipitación de la lignina. Posteriormente, el material precipitado se separó mediante centrifugación y se lavó dos veces con agua destilada en la misma proporción (1:4). Finalmente, las ligninas obtenidas se secaron por liofilización.

Mientras que en el proceso organosolv posterior a la extracción alcalina en frío, el licor, con un pH alcalino, se mezcló con diez volúmenes de agua destilada y se acidificó cuidadosamente mediante la adición controlada de ácido clorhídrico (HCL) 1M hasta alcanzar un pH de 2,5. La lignina precipitada se separó por centrifugación y se sometió a cuatro lavados con agua acidificada al mismo pH (2,5), manteniendo la proporción volumétrica de 1:10. Finalmente, la lignina se secó por liofilización.

La caracterización de ambas ligninas se realizó mediante las siguientes técnicas: **1. Degradación térmica (TGA):** mediante análisis termogravimétrico utilizando un sistema Mettler Toledo TGA/DSC1 STARe, en una atmósfera inerte de nitrógeno. La velocidad de calentamiento empleada fue de 10 ºC min^{-1}, desde temperatura ambiente hasta 800 ºC. Se utilizaron muestras de aproximadamente 10 mg y se realizaron análisis por triplicado**. 2. Hidrólisis ácida cuantitativa:** las muestras se hidrolizaron en dos etapas. En la primera, se empleó ácido sulfúrico (H_2SO_4) al 72% (p/p) durante una hora a 30 ºC en un baño termostático. En la segunda etapa, se utilizó ácido sulfúrico al 4% (p/p) durante una hora a 121 ºC en autoclave. Este procedimiento permitió determinar los contenidos de lignina Klason y los carbohidratos residuales mediante HPLC (según los estándares TAPPI T-249 y TAPPI T-222). **3. Pirólisis analítica (Py-GC/MS):** aproximadamente 100 µg de lignina fueron pirolizados a 550 ºC durante un minuto. Los compuestos volátiles generados fueron analizados mediante cromatografía de gases (GC) acoplada a espectrometría de masas (MS), utilizando helio como gas portador a una velocidad de 1 mL min^{-1}. El análisis se realizó en un pirolizador Pyroprobe 2000 acoplado a un sistema Agilent GC, equipado con un detector de masas y

una columna capilar de sílice fundida DB-17HT (30 m × 0,25 mm × 0,15 µm) (ForTec, Lisboa, Portugal). Los compuestos derivados de las ligninas fueron clasificados según las unidades monoméricas S, G y H, y se calculó su proporción relativa (basada en el área total del pirograma), así como la relación S/G.

3 Resultados y discusión.

Partíamos de la hipótesis inicial de este estudio que era que el carácter alcalino que presentaba los sólidos obtenidos en la extracción alcalina en frío con ultrasonidos, ya optimizada en uno de los capítulos anteriores de esta tesis doctoral, permitiría disminuir la rigurosidad de las condiciones de operación en el proceso organosolv aplicado al clon AF2 del *Populus x euramericana* gracias al poder catalítico del carácter alcalino.

3.1 Proceso Organosolv Convencional.

La Tabla 2 muestra las condiciones de operación que se emplearon en el presente estudio para el caso de los procesos de organosolv convencional (sin etapa alcalina previa) sobre el clon AF2 del *Populus x euramericana*, incluyéndose las variables independientes normalizadas. Mientras que en la Tabla 3 se presenta para las distintas condiciones de operación los resultados obtenidos en cuanto a rendimiento y composición. Ambos respecto a la fracción sólida obtenida en cada proceso.

Tabla 2. Condiciones de operación organosolv convencional con variables normalizadas.

Tiempo (minutos) Xt	**Temperatura** (ºC) X_T	**Concentración etanol** (%) $X_{\%}$
30 [-1]	150 [-1]	35 [-1]
60 [0]	165 [0]	50 [0]
90 [1]	180 [1]	65 [1]

Como se observa en la Tabla 3, a medida que las condiciones de operación se vuelven más rigurosas, el rendimiento disminuye, lo que indica una mayor solubilización de los componentes del clon AF2 en el licor. Simultáneamente, se observa un enriquecimiento en glucano en la pulpa, lo que implica un aumento relativo del contenido de celulosa en la pasta celulósica. En contraste, las hemicelulosas (cuantificadas como xilano), los grupos acetilo y la lignina Klason disminuyen progresivamente en las pulpas a medida que se incrementa la severidad del tratamiento.

El rendimiento obtenido bajo las condiciones de 180 ºC, 90 minutos y una concentración de 65% de etanol es del 64,9%, valor que se encuentra en línea con los reportados por diversos autores. Por ejemplo, Monção et al. [38] obtuvieron un rendimiento del 65,56% al realizar un tratamiento organosolv sobre aserrín de *Picea abies*, operando a 200 ºC durante 30 minutos con una concentración de etanol del 60%. De manera similar, Moral et al. [39] trabajando a 180 ºC durante 60 minutos con una concentración de etanolamina del 60% sobre restos de poda de naranjos, lograron un rendimiento del 62%. En otro estudio, Alaejos et al. [40] emplearon etilenglicol en podas de encina bajo

condiciones cercanas a las de este estudio (180 ºC, 90 minutos y 60% de etilenglicol), alcanzando un rendimiento del 68%.

Por otro lado, en el caso de residuos como la paja de trigo, se observan menores rendimientos, lo que indica una mayor solubilización de los componentes en el licor. Por ejemplo, Jiménez et al. [41], trabajando bajo condiciones similares, obtuvieron un rendimiento del 43,66%.

Tabla 3. Rendimiento y composición de las pulpas del proceso organosolv convencional.

Condiciones de operación X_t X_T $X_{\%}$	**Rendimiento** (%)	**Glucano** (%)	**Xilano** (%)	**Grupos acetilo** (%)	**Lignina Klason** (%)
-1 -1 -1	82,8	39,5	14,7	3,4	39,1
0 0 0	81,5	42,5	12,3	4,2	39
1 1 1	64,9	50,1	10,8	2,2	32,5

En la siguiente tabla se presentan las propiedades de las hojas de papel obtenidas a partir de las tres pulpas derivadas de los tratamientos organosolv convencionales. En el caso de las condiciones mínimas de operación, algunas de las propiedades no pudieron cuantificarse ya que se encontraban fuera de rango.

Las hojas obtenidas con el tratamiento organosolv convencional mostraron propiedades mecánicas débiles, siendo las mejores propiedades alcanzadas bajo las condiciones de operación más intensas, es decir, operando durante 90 minutos a una temperatura de 180 ºC y una proporción de etanol del 65%. Bajo estas condiciones, las propiedades obtenidas fueron comparables a las reportadas por Alaejos et al. [40], quienes realizaron un tratamiento organosolv con etilenglicol sobre madera de encina bajo condiciones similares.

La principal diferencia entre los resultados radica en el valor del número kappa, que en este estudio fue de 77,3, mientras que en el trabajo de Alaejos et al. [40] se reportó un valor de 35. Esta discrepancia se podría atribuir al hecho de que la encina utilizada en dicho estudio contenía una menor cantidad de lignina que el clon AF2 utilizado en el presente estudio.

No obstante, al comparar estos resultados con procesos industriales más extendidos, como es el caso del proceso Kraft, se observan diferencias significativas. Ai et al. [42] realizaron un tratamiento Kraft sobre madera de *Populus* a 170 ºC durante 40 minutos, obteniendo hojas de papel con un número kappa de 27, un brillo de 25,6, un índice de tracción de 42,7 $kN*m*kg^{-1}$ y un índice de desgarro de 4 $N*m^2*kg^{-1}$, lo que indica propiedades mecánicas significativamente superiores a las observadas en el tratamiento organosolv convencional del presente estudio.

Tabla 4. Propiedades físicas hojas de papel del tratamiento organosolv convencional.

Condiciones de operación X_t X_T $X_{\%}$	**Viscosidad** $mL*g^{-1}$	**Kappa**	**Índice de Estallido** $kPa*m^2*g^{-1}$	**Índice de Desgarro** $mN*m^{2*}g^{-1}$	**Índice de Tracción** $N*m*g^{-1}$	**Blancura ISO** %
-1 -1 -1	116,4	69,8	-		-	35,2
0 0 0	268,6	77,6	-	1,29	0,19	27,3
1 1 1	460,2	77,3	0,14	2,05	5,26	19,4

3.2 Proceso Organosolv tras EAF.

La Tabla 5 muestra las condiciones de operación empleadas en el proceso organosolv, realizado tras la extracción alcalina en frío sobre el clon AF2 del *Populus x euramericana*. En este diseño experimental, se buscó aprovechar el efecto alcalino como catalizador en la segunda etapa del tratamiento. Asimismo, se incluyen las variables independientes normalizadas. Por su parte, la Tabla 6 recoge los resultados obtenidos para cada proceso de operación, en relación con el rendimiento y la composición química. Ambos respecto a la fracción sólida obtenida en cada proceso.

Tabla 5. Condiciones de operación organosolv alcalino con variables normalizadas.

Tiempo (minutos) X_t	**Temperatura** (ºC) X_T	**Concentración etanol** (%) $X_{\%}$
30 [-1]	135 [-1]	35 [-1]
60 [0]	142,5 [0]	50 [0]
90 [1]	150[1]	65 [1]

El rendimiento respecto al sólido varió entre un 49,7% y un 60,7%, y estuvo por debajo del rendimiento obtenido en las condiciones de operación más intensas del proceso organosolv convencional (sin etapa alcalina previa), que alcanzó un rendimiento de 64,9%. Esto sugiere que la secuencia de extracción alcalina en frío seguida del proceso organosolv favorece el fraccionamiento del clon AF2, a pesar de operar con temperaturas más bajas a lo largo de todo el diseño experimental.

Una de las mayores solubilizaciones de los componentes del clon AF2 se observó bajo las condiciones más rigurosas, con un rendimiento del 50,5%, lo que podría estar relacionado con una mayor degradación de la celulosa. En estas condiciones, la pulpa resultante presentó un contenido de glucano inferior al de otras condiciones de operación.

El contenido de glucano en la pulpa osciló entre un 47,8% y un 62,5%. Si se considera el contenido inicial de glucano del clon AF2, esto equivale a una permanencia del 65,1% al 88,7% del glucano inicial en las pulpas obtenidas. Por otro lado, el contenido de xilano en la pulpa varió entre un 10,7% y un 16,9%, mientras que la lignina Klason se encontró en un rango de 19% a 36,2%.

Con los datos recogidos en la Tabla 6, se han desarrollado distintos modelos polinómicos para la identificación de las variables de operación con mayor influencia y aproximar así los intervalos óptimos de operación. Dichos modelos, se recogen en la Tabla 7. Para facilitar el análisis de influencia

de las distintas variables de operación se representan las superficies de respuesta correspondientes a los rangos máximos de variación de las variables dependientes de dichos modelos.

Tabla 6. Rendimiento y composición de las pulpas del proceso organosolv alcalino.

Condiciones de operación X_t X_T $X_{\%}$	**Rendimiento** (%)	**Glucano** (%)	**Xilano** (%)	**Lignina Klason** (%)
0 0 0	58,0	56,9	15,0	25,0
0 0 0	57,9	57,8	16,0	24,9
1 1 1	50,5	58,9	14,4	26,5
1 1 -1	49,7	62,5	11,9	20,5
1 -1 1	57,3	57,5	16,0	21,4
1 -1 -1	59,3	53,4	13,5	24,7
-1 1 1	58,3	56,2	16,9	19,1
-1 1 -1	56,2	60,2	13,3	27,2
-1 -1 1	60,3	55,5	15,2	24,8
-1 -1 -1	54,9	47,8	10,7	36,2
1 0 0	54,9	55,3	15,1	22,9
-1 0 0	60,7	53,7	14,4	25,7
0 1 0	53,2	58,2	16,4	22,6
0 -1 0	58,3	53,4	15,4	26,1
0 0 1	60,0	59,6	15,5	19,0
0 0 -1	55,0	59,1	12,2	24,1

Para el rendimiento en este caso se han tenido en cuenta las dos etapas del tratamiento, es decir, la extracción alcalina en frío (condiciones fijas para todo el diseño experimental) y el proceso organosolv.

Tabla 7. Ecuaciones de los modelos polinómicos para el rendimiento y composición de las pulpas del proceso organosolv alcalino.

Variable Dependientes	**Modelos polinómicos**
Rendimiento	$57{,}74-1{,}87X_t-2{,}21X_T+1{,}11X_c-1{,}94X_T^2-1{,}97X_tX_T-1{,}09X_tX_c$
Glucano	$56{,}94+1{,}41X_t+2{,}85X_T-2{,}21X_t^2+2{,}63X_c-2{,}44X_TX_c$
Xilano	$15{,}38+1{,}64X_c-0{,}56X_t^2+0{,}62X_T^2-1{,}46X_c^2-0{,}92X_tX_T-0{,}38X_tX_c$
Lignina Klason	$23{,}62-1{,}7X_t-1{,}72X_T-2{,}18X_c+1{,}95X_tX_T+2{,}78X_tX_c+1{,}57X_TX_c$

Donde X_t es el tiempo de operación, X_T la temperatura del proceso y X_c la proporción de etanol.

En la Figura 1 se representa la superficie de respuesta correspondiente al modelo polinómico ajustado para el rendimiento del proceso secuencial de EAF seguida del proceso organosolv, en función de las variables de operación de esta última etapa. Entre los factores evaluados, la temperatura se identificó como la variable con mayor influencia sobre el rendimiento, tanto por sus términos lineales y cuadráticos cómo de interacción.

Tal como se observa en la figura, los mayores niveles de solubilización de los componentes del clon AF2 en el licor se alcanzan al operar con altas temperaturas y con tiempos prolongados. En estas condiciones, el proceso favorece la ruptura de enlaces estructurales, facilitando la disolución de lignina y hemicelulosas. En contraste, la proporción de etanol mostró una influencia relativamente

menor en las condiciones evaluadas. En la zona de mínimos rendimientos, su efecto es prácticamente nulo, observándose una tendencia hacia menores rendimientos al trabajar con proporciones bajas de etanol.

En cuanto a las condiciones de temperaturas media y baja, los rendimientos obtenidos son similares, aunque se observa una interacción significativa con el tiempo. Específicamente, a temperaturas medias, un mayor tiempo de operación provoca una disminución del rendimiento. Por el contrario, a temperaturas bajas, una reducción del tiempo de operación conlleva una disminución del rendimiento.

En términos generales, la proporción de etanol mostró un comportamiento relativamente constante a lo largo de todo el rango de temperaturas. Mientras que, en condiciones de tiempo de operación bajos, tiene una influencia ligueramente superior, aunque sigue siendo considerablemente menor en comparación con las otras dos variables de operación del proceso organosolv, lo que confirma su baja incidencia sobre el rendimiento global.

La elevada influencia de la temperatura sobre el rendimiento observada en este estudio coincide con lo reportado por diversos autores que han analizado el efecto de las variables de operación del proceso organosolv sobre diferentes materias primas lignocelulósicas. Asimismo, el rango de rendimiento obtenido en el presente trabajo se encuentra dentro de los márgenes informados en la bibliografía, a pesar de que las temperaturas de operación empleadas en este estudio son, en general, inferiores. Esta mejora en el rendimiento a temperaturas más bajas puede atribuirse al efecto catalítico de los restos de NaOH presentes en los sólidos tras el tratamiento previo de EAF. Por ejemplo, Alaejos et al. [40] reportaron rendimientos comprendidos entre 45% y 76,5% al operar entre 180 y 200 ºC. Del mismo modo, Jiménez et al. [41] obtuvieron valores de rendimiento entre 40,73% y 77,55% trabajando con paja de trigo en un rango de temperaturas de 140 a 180 ºC. En otro estudio, Oliet et al. [43] emplearon cardo (*Cynara cardunculusL*) como materia prima, alcanzando rendimientos entre 34,3% y 45,7% al operar en el rango de 180 a 200 ºC. Cabe destacar que tanto la paja de trigo como el cardo son materiales que, en general, presentan mayor susceptibilidad al fraccionamiento que las maderas, lo que refuerza la relevancia de los resultados obtenidos en el presente estudio.

Por otro lado, diversos estudios han evaluado el uso de catalizadores ácidos en el proceso organosolv, demostrando que el aumento en la concentración del catalizador conduce a una mayor solubilización de los componentes lignocelulósicos en el licor, lo que se traduce en una disminución del rendimiento de la pulpa. Por ejemplo, Huijgen et al. [44] estudiaron el efecto catalítico de diferentes ácidos en un sistema etanol-agua, observando que el rendimiento de la pulpa disminuía significativamente al incrementar la concentración de ácido. En el caso de la madera de sauce,

obtuvieron rendimientos del 69,3% sin catalizador y del 57,5% al emplear 2,7% p/p de ácido sulfúrico (H_2SO_4) respecto a la biomasa seca. En la paja de trigo, los rendimientos disminuyeron de 74,4% a 43,8% bajo las mismas condiciones de H_2SO_4. Con ácido clorhídrico (HCl), los rendimientos fueron del 70% al 44% en sauce y del 78,5% al 35% en paja de trigo, también con una concentración del 2,7 p/p.

Estos resultados evidencian que la acción catalítica intensifica el fraccionamiento. De manera análoga, en el presente estudio, la presencia residual de álcali (NaOH) en los sólidos tras el pretratamiento de extracción alcalina en frío actúa como un catalizador, incrementando la eficacia del proceso organosolv. Por lo tanto, el comportamiento observado puede interpretarse como un caso de organosolv catalizado alcalinamente, cuyas consecuencias en el rendimiento y la solubilización se asemejan a las del organosolv ácido descrito en bibliografía.

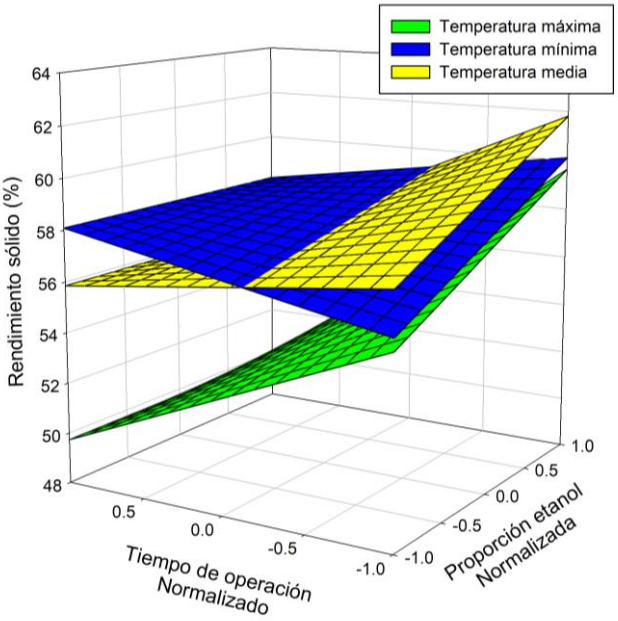


Figura 1. Variación del rendimiento en la pulpa en función de las variables de operación.

En la Figura 2 se representan las superficies de respuestas correspondientes a los modelos polinómicos para el contenido de glucano, xilano y lignina Klason en la pulpa obtenido tras la secuencia de EAF seguida de organosolv, en función de las variables independientes de la última etapa del proceso.

Al analizar la variación del contenido de glucano en la pulpa (Figura 2.A), la variable con mayor influencia sobre dicho contenido es la temperatura, debido a su término lineal y de interacción dentro del modelo matemático ajustado. Se obtiene una pulpa más rica en celulosa (cuantificada cómo glucano) al operar a temperaturas máximas, tiempos de procesamiento medios y proporciones bajas de etanol. Cabe destacar que, en este caso, el tiempo es la variable operativa con menor impacto. Cuando se opera con temperaturas mínimas, el comportamiento del glucano en la pulpa respecto a la

proporción de etanol varía: a altas proporciones de etanol, se mantiene una mayor cantidad de glucano en la pulpa. En general, el contenido de glucano en todas las pulpas, excepto cuando se opera bajo condiciones mínimas (punto -1, -1, -1 para X_t, X_T y X_c, respectivamente), es superior al de las pulpas obtenidas en el proceso organosolv convencional del presente estudio.

En el caso del contenido de xilano y lignina Klason en la pulpa, la variable con mayor impacto en el modelo polinómico es la proporción de etanol, tanto por sus términos lineales y cuadráticos, como por los de interacción.

En la Figura 2.B, se observa una mayor solubilización de hemicelulosas (cuantificadas como xilano) cuando se opera con proporciones bajas de etanol, junto con tiempos y temperaturas mínimas. Sin embargo, la influencia de temperatura y tiempo sobre el contenido de xilano en las pulpas es relativamente similar y mínima.

Por último, en cuanto al contenido de lignina Klason (Figura 2.C), se observa que, en general, los contenidos en la pulpa son menores cuando se opera con altas proporciones de etanol.

La influencia del tiempo sobre el contenido de lignina varía considerablemente en función de la proporción de etanol empleada: a altas proporciones de etanol, el tiempo tiene un impacto mínimo, mientras que, a bajas proporciones, el contenido de lignina disminuye bruscamente a medida que se incrementa el tiempo de operación.

En cuanto a la temperatura, su influencia sobre el contenido de lignina Klason varía en función de la proporción de etanol empleada y el tiempo de operación. A bajas proporciones de etanol, el contenido de lignina disminuye al aumentar la temperatura, independientemente del tiempo de operación. En cambio, a altas proporciones de etanol y tiempos prolongados, el contenido de lignina disminuye cuando se reduce la temperatura; por otro lado, cuando los tiempos de operación son cortos, el contenido de lignina desciende al aumentar la temperatura.

En general, todas las pulpas obtenidas a partir del proceso de dos etapas, con excepción de cuando se opera bajo condiciones mínimas en la segunda etapa (punto -1, -1, -1), presentan un contenido de lignina Klason menor que el de las pulpas obtenidas en el proceso de una sola etapa de organosolv utilizado en este estudio.

Es relevante destacar que el contenido mínimo de lignina Klason se alcanza en el punto -1, 1, 1 (X_t, X_T y X_c, respectivamente), con un valor predicho por el modelo de 18,3%. Este valor es comparable al obtenido en el punto 1, 1, -1, con un contenido de lignina estimado de 20%. Sin embargo, este segundo punto resulta favorable, ya que no solo permite conservar una mayor proporción de glucano en la pulpa, sino que también promueve una significativa solubilización del

xilano en el licor. Además, estas condiciones conducen al menor rendimiento global, lo que indica una mayor separación de los componentes lignocelulósicos del clon AF2 hacia el licor, reflejando una mayor eficacia del proceso en términos de fraccionamiento de la biomasa.

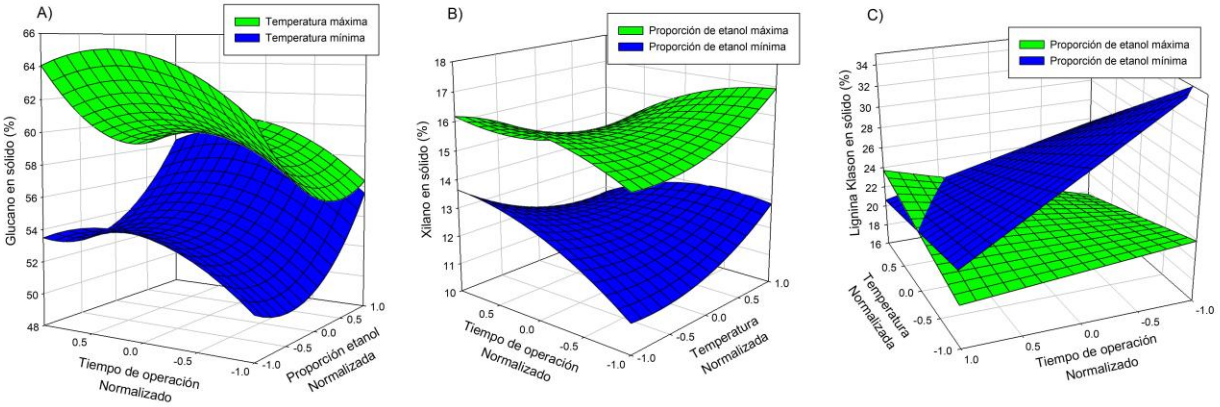


Figura 2. Variación del contenido en glucano (A), xilano (B) y lignina Klason (C) en la pulpa en función de las variables de operación.

En la Tabla 8 se muestran las propiedades de las hojas de papel obtenidas a partir de las diferentes pulpas derivadas del diseño experimental de dos etapas: extracción alcalina en frío con ultrasonidos y organosolv alcalino.

Las viscosidades de las pulpas obtenidas a lo largo del diseño experimental fueron, relativamente bajas, oscilando entre 154,8 mL g^{-1} y 725,7 mL g^{-1}. En cuanto al número kappa, los valores registrados varían entre 18,5 y 82,8, siendo el valor más alto correspondiente a las condiciones de operación más suaves (punto -1, -1, -1 para X_t, X_T y X_c, respectivamente). Exceptuando estas condiciones, el resto de las pulpas presentaron valores de kappa inferiores a los obtenidos en las pulpas procedentes del proceso de una sola etapa de este estudio.

En cuanto a los índices de estallido, desgarro y tracción, los resultados fueron los siguientes: 0,15-2,21 kPa m^2 g^{-1} para estallido, 0,84-5,01 mN m^2 g^{-1} para desgarro y 0,40-19,37 N m g^{-1} para tracción. Finalmente, la blancura de las pulpas varió entre 32,7% y 42,8%.

Por otro lado, en el estudio de Alaejos et al. [40], que evaluaron un proceso organosolv sin catalizador sobre podas de encina con temperaturas entre 180-200ºC, tiempos de 30-90 minutos y una proporción de etanol entre 40-60%, obtuvieron los siguientes rangos para cada propiedad: viscosidad entre 165-789 mL g^{-1}, número kappa de 29,4-72,9, índice de tracción de 2,9-10,1 N m g^{-1}, índice de estallido de 0,08-0,32 kPa m^2 g^{-1} y blancura de 10,3-19,2% ISO.

Comparando estos resultados con los obtenidos en el presente estudio, se observa que, en términos generales, las propiedades de las hojas de papel obtenidas son comparables a los valores reportados por Alaejos et al. [40]. Destaca que, al considerar los mismos puntos de operación normalizados, los

valores de kappa, índices de estallido y tracción y blancura en este estudio son, en su mayoría, superiores.

Tabla 8. Propiedades físicas hojas de papel del tratamiento de dos etapas (EAF + organosolv alcalino).

Condiciones de operación X_t X_T $X_{\%}$	**Viscosidad** $mL*g^{-1}$	**Kappa**	**Índice de Estallido** $kPa*m^2*g^{-1}$	**Índice de Desgarro** $mN*m^{2*}g^{-1}$	**Índice de Tracción** $N*m*g^{-1}$	**Blancura ISO** %
0 0 0	357,3	50,8	0,95	3,62	6,76	37,6
0 0 0	332,3	50,3	0,93	3,08	6,51	37,0
1 1 1	584,4	18,5	0,19	1,70	0,40	42,8
1 1 -1	725,7	27,9	0,15	0,97	7,61	41,4
1 -1 1	369,5	53,7	1,55	5,01	13,05	36,0
1 -1 -1	280,4	60,7	2,21	3,94	19,37	34,9
-1 1 1	471,2	47,9	0,22	1,26	1,67	34,9
-1 1 -1	294,9	56,9	1,21	3,87	10,54	35,1
-1 -1 1	393,7	63,9	0,99	3,75	4,94	34,1
-1 -1 -1	171,7	82,8	1,25	4,07	2,97	32,7
1 0 0	530,1	41,3	1,06	3,35	10,77	38,0
-1 0 0	326,9	60,8	1,33	4,53	9,17	34,4
0 1 0	338,2	33,9	0,64	0,84	1,71	41,3
0 -1 0	154,8	65,9	1,97	3,57	1,28	35,5
0 0 1	553,2	47,2	0,62	2,99	7,48	37,0
0 0 -1	432,3	54,6	0,78	3,71	16,23	35,7

A partir de los datos de las propiedades de las hojas de papel presentados en la Tabla 8, se construyen modelos polinómicos que permiten identificar las variables de operación con mayor impacto en las propiedades y, al mismo tiempo, estimar los rangos óptimos de operación del proceso. Estos se resumen en la Tabla 9, y para facilitar la interpretación de la influencia de cada variable, se han representado las superficies de respuesta correspondientes a los rangos máximos de variación de cada variable dependiente.

Tabla 9. Ecuaciones de los modelos polinómicos para el rendimiento y composición de las pulpas del proceso organosolv alcalino.

Variable Dependientes	**Modelos polinómicos**
Viscosidad	$363,2+83,2X_t+104,4X_T+47X_c+56,1X_t^2-125,9X_T^2+120,4X_c^2+57,4X_tX_T-56,3X_tX_c-4,5X_TX_c$
Kappa	$51,06-11,02X_t-14,17X_T-5,16X_c-3,29X_tX_T+1,42XtXc$
I.Estallido	$1,06-0,57X_T-0,2X_c+0,26X_T^2-0,35X_c^2-0,33X_tX_T$
I.Desgarro	$3,3-0,25X_t-1,17X_T+0,74X_t^2-0,99X_T^2-0,45X_tX_T+0,59X_tX_c-0,33X_TX_c$
I.Tracción	$7,32+2,19X_t-1,97X_T-2,92X_c-6,17X_T^2+4,19X_c^2+3,59X_tX_T$
Blancura	$37,26+2,19X_t+2,23X_T+0,5X_c-1,04X_t^2+1,15X_T^2-0,89X_c^2+1,26X_tX_T$

En la Figura 3 se representa el modelo matemático que describe la viscosidad de las pulpas obtenidas a partir de la secuencia EAF con ultrasonidos seguida del proceso organosolv, en función de las variables de operación de la segunda etapa. De acuerdo con el modelo, la temperatura es la

variable que ejerce el mayor impacto sobre esta propiedad, debido a sus términos lineales, cuadráticos y de interacción.

Los valores más altos de viscosidad se alcanzan al operar a temperaturas medias y altas. En esta región, el tiempo de operación tiene un efecto positivo sobre la viscosidad: a medida que el tiempo aumenta, también lo hace la viscosidad. Por otro lado, la proporción de etanol muestra un comportamiento dual en esta zona. Durante tiempos de operación prolongados, un incremento en la proporción de etanol favorece un aumento de la viscosidad, mientras que, en tiempos más cortos, el aumento de etanol genera una disminución de la viscosidad.

El valor máximo de viscosidad, 725 mL g^{-1}, se obtiene cuando se opera a la temperatura máxima, con un tiempo de operación largo y una proporción mínima de etanol, correspondiente al punto 1, 1, -1 (X_t, X_T y X_c, respectivamente) del diseño experimental.

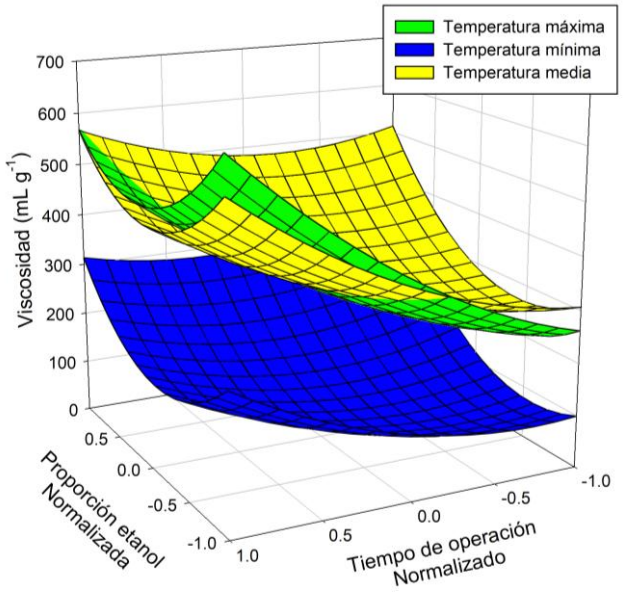


Figura 3. Variación de la viscosidad de las pulpas en función de las variables de operación.

En la Figura 4, se presentan los modelos polinómicos que ajustan el número kappa y la blancura de las pulpas obtenidas en el diseño experimental del proceso de doble etapa, en función de las variables de operación de la etapa organosolv. En ambos modelos, la temperatura es la variable que ejerce mayor influencia sobre estas dos propiedades de las pulpas, debido a sus términos lineales, cuadráticos y de interacción.

En el caso del número kappa (Figura 4.A), los valores más bajos, que generalmente están asociados con un mayor grado de deslignificación, se obtienen al operar a altas temperaturas. Las otras dos variables, tiempo y proporción de etanol, muestran una influencia menos significativa. En particular, el tiempo tiene un efecto negativo sobre el número kappa, ya que a medida que el tiempo de operación

aumenta, el valor de kappa disminuye. En cuanto a la proporción de etanol, su impacto es aún más reducido, evidenciando un efecto casi nulo sobre esta propiedad.

Por otro lado, en la Figura 4.B, que refleja el comportamiento de la blancura de las pulpas en función de las variables de operación del proceso organosolv alcalino, se observa un patrón que sigue lo esperado tras analizar el número kappa. De hecho, cuando el número kappa disminuye, se espera que la blancura aumente. En consecuencia, los mayores porcentajes de blancura se alcanzan al operar a altas temperaturas y con tiempos prolongados. La proporción de etanol, al igual que antes, tiene una influencia casi nula en los valores de blancura.

Al comparar la zona óptima de operación para ambas propiedades, se observa que el número kappa alcanza valores mínimos de 18,5 a 56,9 en el proceso de doble etapa, en comparación con los valores de 69,8 a 77,3 obtenidos en el proceso organosolv convencional de este estudio. Por otro lado, la blancura en estas condiciones óptimas alcanza valores máximos de 34,9 a 42,8%, mientras que en el proceso de una sola etapa los valores de blancura se ubicaron entre 19,4 y 35,2%. Cabe destacar que la temperatura máxima utilizada en el proceso de doble etapa fue de 150 ºC, la cual es la temperatura mínima empleada en el proceso de una sola etapa del proceso organosolv convencional (sin etapa alcalina previa).

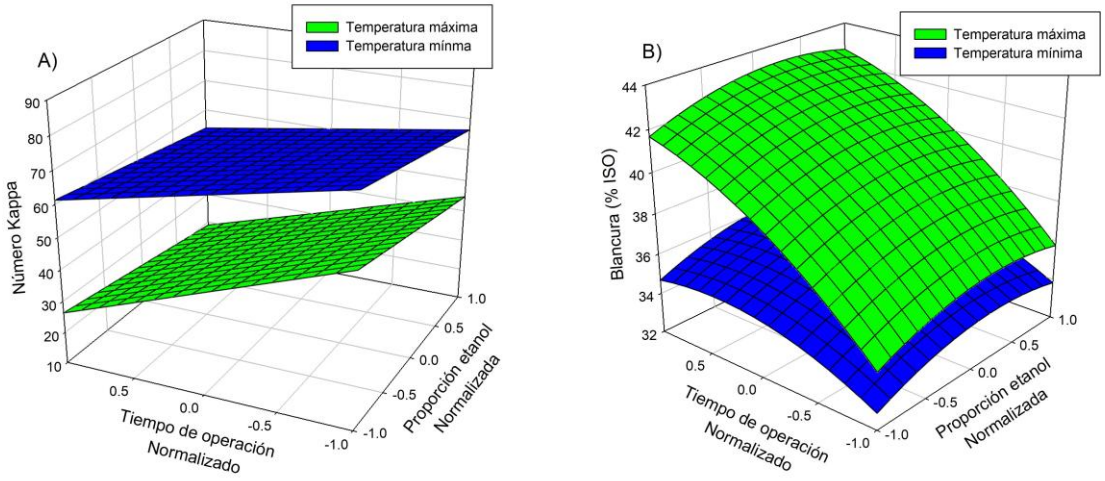


Figura 4. Variación del número Kappa y la blancura de las pulpas en función de las variables de operación.

En la Figura 5, se presentan los modelos matemáticos que describen el comportamiento de los índices de estallido, desgarro y tracción de las pulpas obtenidas a partir del proceso secuencial de EAF con ultrasonidos seguida de organosolv, en función de las variables de operación de esta última etapa. Al igual que en las otras propiedades estudiadas, la temperatura se confirma como la variable con mayor influencia sobre todas las propiedades mecánicas analizadas, obteniéndose los máximos índices cuando se opera a bajas y medias temperaturas.

En el caso del índice de estallido (Figura 5.A), se observa una marcada dependencia con la temperatura, y en menor medida, con el tiempo de operación. El comportamiento de esta segunda variable resulta complejo: a altas temperaturas, una disminución del tiempo tiene un efecto positivo, mejorando la resistencia al estallido de las pulpas; mientras que, a bajas temperaturas, ocurre lo contrario: un mayor tiempo de operación mejora el índice, lo que sugiere que el tiempo puede compensar, en parte, la menor temperatura de procesado en estas condiciones.

En la Figura 5.B, referente al índice de desgarro, los valores máximos se alcanzan a temperaturas medias y con tiempos cortos, logrando el valor máximo al emplear una alta proporción de etanol. No obstante, cabe señalar que, a temperaturas bajas, también se obtienen valores cercanos al óptimo cuando se combinan tiempos prolongados y proporciones elevadas de etanol, lo que permite plantear alternativas operativas más eficientes en términos de consumo energético sin sacrificar significativamente las propiedades mecánicas.

Respecto al índice de tracción (Figura 5.C), los valores máximos se registran al operar a temperaturas medias, siendo el tiempo de operación la segunda variable más influyente, generalmente con un efecto positivo: un mayor tiempo mejora esta propiedad, excepto cuando se trabaja a la temperatura más alta, donde el efecto del tiempo parece neutral o incluso adverso.

En conjunto, estos resultados indican que, aunque las temperaturas elevadas tienden a deteriorar estas tres propiedades mecánicas de las pulpas, probablemente por una mayor degradación de la celulosa, la mayoría de las muestras obtenidas mediante el proceso de doble etapa presentan propiedades superiores a las alcanzadas mediante el proceso organosolv de una sola etapa. Este comportamiento refuerza el potencial del esquema EAF-organosolv como una estrategia eficiente para mejorar la calidad de la pulpa, permitiendo además reducir la temperatura de operación gracias al efecto catalítico derivado del carácter alcalino residual presente tras la extracción alcalina en frío.

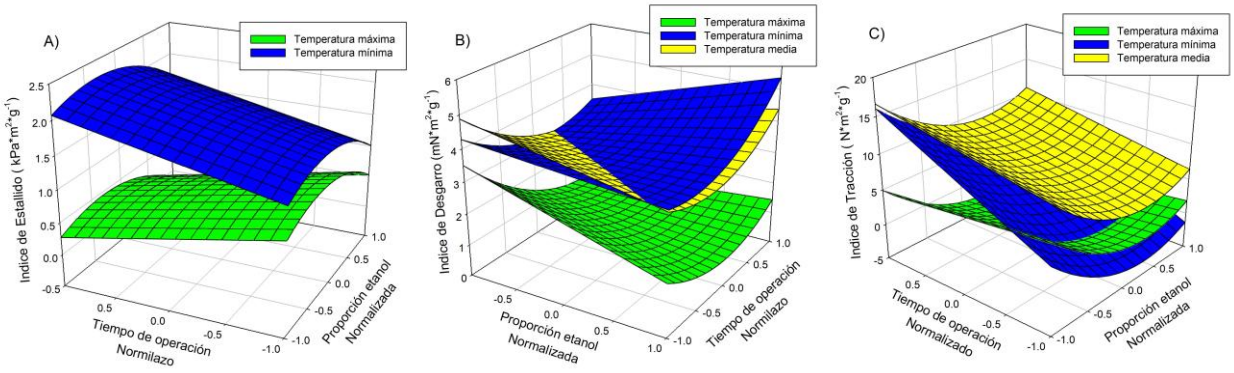


Figura 5. Variación de los índices de estallido (A), desgarro (B) y tracción (C) de las pulpas en función de las variables de operación.

3.3 Caracterización de ligninas.

Para los análisis de pureza, comportamiento térmico y caracterización por espectrometría, se seleccionaron las ligninas obtenidas por precipitación a partir de los licores de dos procesos diferentes: (i) proceso organosolv convencional, sin etapa alcalina previa, operando bajo condiciones severas (90 minutos a 180 ºC con una concentración de etanol del 65%), y (ii) proceso de doble etapa, extracción alcalina en frío con ultrasonidos seguida de un tratamiento organosolv menos severo (90 minutos a 150 ºC con un 35% de etanol).

Ambas condiciones fueron elegidas porque mostraron los menores rendimientos de pulpa, lo cual indica una mayor eficiencia de solubilización de los componentes lignocelulósicos del clon AF2 del *Populus x euramericana* hacia el licor.

Estos análisis se realizaron con el propósito de determinar cómo influye el pretratamiento alcalino sobre la calidad de la lignina organosolv aislada.

3.3.1 Pureza.

En la Tabla 10 se presenta la caracterización de las ligninas precipitadas, considerando su contenido en lignina Klason, carbohidratos residuales, humedad y cenizas.

En el proceso organosolv sin etapa alcalina previa, el contenido de lignina Klason en la pulpa fue del 32,5%, lo que indica que aproximadamente el 84% de la lignina original presente en el clon AF2 permaneció en la fase sólida, extrayéndose solo el 16% al licor. En contraste, en el proceso de doble etapa (condiciones experimentales 1, 1, -1 para X_t, X_T y $X_{\%}$, respectivamente), la pulpa resultante presentó un 20,5% de lignina Klason. Este valor implica que cerca del 76% de la lignina inicial fue solubilizada, distribuyéndose entre un 44,5% en el licor organosolv y un 31,3% en el licor de la EAF con ultrasonidos, lo que evidencia una eficiencia de solubilización notablemente superior.

A pesar de las diferencias en el rendimiento de extracción, las ligninas precipitadas muestran composiciones globalmente similares. No obstante, la lignina obtenida en el proceso de doble etapa presenta un mayor contenido de xilano. Este fenómeno puede atribuirse a las condiciones más suaves del tratamiento organosolv (menor temperatura y proporción de etanol), que limitaron la ruptura de enlaces éter/éster entre las hemicelulosas y la lignina. Por el contrario, el proceso organosolv convencional (sin etapa previa), las condiciones más agresivas y la mayor disponibilidad de protones habrían promovido una mayor ruptura de estos enlaces [45].

Tabla 10. Composición de las ligninas.

Composición	Lignina Organosolv	Lignina EAF + Organosolv
Lignina Klason (%)	81,7 ± 0,09	84,2 ± 0,93
Glucano (%)	0,9 ± 0,05	0,4 ± 0,04
Xilano (%)	1,7 ± 0,18	5,6 ± 0,29
Cenizas (%)	1,8 ± 0,05	1,5 ± 0,03
Humedad (%)	0,5 ± 0,02	2 ± 0,02

3.3.2 Análisis termogravimétrico (TGA):

La estabilidad térmica de ambas ligninas fue evaluada mediante análisis termogravimétrico (TGA) bajo atmósfera inerte, utilizando una velocidad de calentamiento constante de 10 ºC min^{-1}. En la Figura 6 se presentan las curvas TGA de las ligninas precipitadas, las cuales muestran la pérdida de masa en función de la temperatura, así como sus respectivas derivadas de primer orden (DTG), que representa la tasa de pérdida de peso.

La degradación térmica de ambas muestras ocurre en un amplio rango de temperaturas, aproximadamente entre 100 y 700 ºC, comportamiento característico de la lignina debido a su compleja y heterogénea estructura polimérica, como ha sido ampliamente reportado [46-48]. Esta degradación puede dividirse en tres etapas: (i) liberación de humedad hasta aproximadamente los 180ºC, (ii) descomposición de impurezas de hemicelulosas y restos de celulosa entre 180-300 ºC, confirmado por el análisis de pureza, y (iii) degradación principal de la lignina entre 300 y 650 ºC [47,49].

Las tasas máximas de pérdida de masa (DTG_{max}) se observan a 357 ºC para la lignina obtenida mediante el proceso organosolv convencional, con una pérdida de masa del 41,8%, y a 360 ºC para la lignina del proceso de doble etapa, con una pérdida del 39,2%. Estos valores se encuentran dentro del rango típico reportado para ligninas de maderas blandas y duras (350-425 ºC) [15]. Por ejemplo, Kim et al. [50] reportaron DTG_{max} de 352,3 ºC y 367,9 ºC para ligninas organosolv y Kraft, respectivamente, a partir de *Populus*. Por lo general, las ligninas Kraft presentan valores más altos [15].

Los picos de DTG_{max} son indicadores clave de la estabilidad térmica de la muestra analizada [51]; una mayor temperatura de pico indica una mayor estabilidad. En este contexto, puede afirmarse que la lignina obtenida por el proceso de doble etapa presenta una estabilidad térmica ligeramente superior a la del proceso convencional (sin etapa previa alcalina). Esta diferencia podría atribuirse a un mayor contenido de unidades de guayacilo (G), que confiere un mayor peso molecular y lo que se traduce en una mayor estabilidad [52,53].

En ambas ligninas se observa un segundo pico de descomposición en torno a los 300 ºC, el cual podría estar relacionado con la escisión de enlaces β-O-4, como ha sido reportado por Chu et al. [54], quienes identificaron esta ruptura en el intervalo de 250-350 ºC. Sin embargo, la lignina del proceso organosolv convencional presenta una tasa de pérdida de peso superior en esta región, lo que sugiere una mayor presencia de enlaces β-O-4. Este resultado difiere con lo esperado, dado que los procesos organosolv más severos suelen inducir una mayor escisión de dichos enlaces [55,56].

Una posible explicación para este comportamiento radica en la etapa alcalina previa del proceso de doble etapa. Estudios previos han demostrado que los pretratamientos alcalinos tienden a promover la ruptura de enlaces β-O-4. Por ejemplo, Shakeel et al. [57] mostraron que el número creciente de etapas alcalinas en un pretratamiento secuencial aplicado a madera de álamo condujo a una mayor ruptura de estos enlaces.

Finalmente, el residuo carbonizado a 800 ºC fue del 30,31% para la lignina del proceso convencional y del 33,23% para la lignina del proceso de doble etapa.

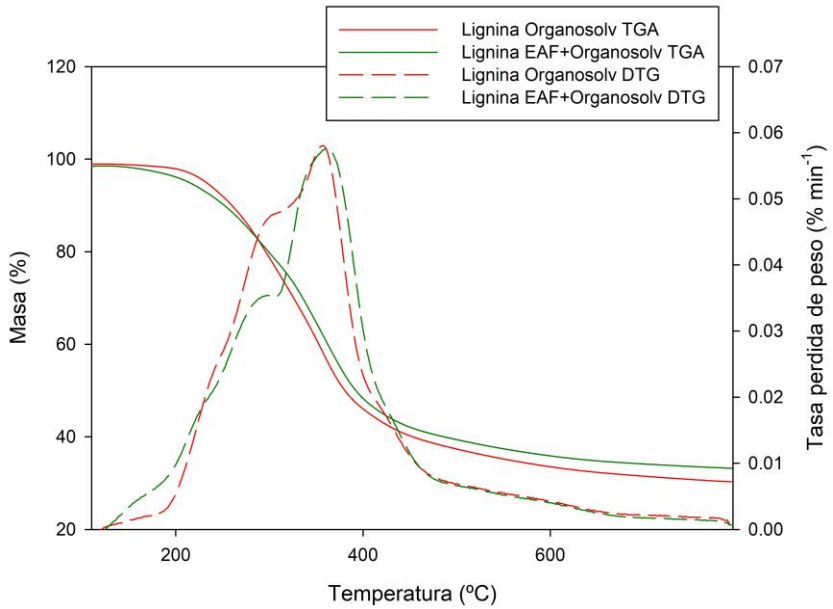


Figura 6. Curvas TGA y DTG de lignina organosolv y lignina EAF + organosolv, velocidad de calentamiento: 10 ºC min^{-1}.

3.3.3 Cromatografía de gases por pirólisis y espectrometría de masas (PY-GC/MS):

La pirólisis combinada con la cromatografía de gases y espectrometría de masas (PY-GC/MS) permite la degradación en línea y el análisis del contenido monomérico de las ligninas, generando una huella digital característica para cada muestra.

La Figura 7 muestra el cromatograma de iones totales (TIC) correspondiente a la pirólisis de la lignina obtenida mediante el proceso organosolv convencional, mientras que la Figura 8 muestra el TIC de la lignina procedente del proceso de doble etapa. En la Tabla 11 se presentan la identificación

y las abundancias molares relativas de los compuestos fenólicos derivados de cada lignina, que se liberan tras la pirólisis. El análisis de los datos mediante bibliotecas de espectros de masas permitió la identificación de 43 compuestos fenólicos individuales, clasificados en función de las microestructuras típicas de las ligninas tipo H, G y S.

Los principales compuestos liberados durante la pirólisis de ambas ligninas correspondieron a fenoles del tipo siringilo, derivados estructurales de unidades de lignina S. Dentro de este grupo, los compuestos más abundantes fueron siringol (pico 10), 4-metilsiringol (pico 14), 4-vinilsiringol (pico 19), propinilsiringol (pico 29), *trans*-4-propenilsiringol (pico 30), siringaldehído (pico 32), homosiringaldehído (pico 34) y *trans*-sinapaldehído (pico 43). En cuanto a los compuestos derivados de la unidad H, el compuesto más representativo fue el fenol (pico 1), mientras que entre los derivados de la unidad G se identificaron predominantemente guayacol (pico 2), 4-metilguayacol (pico 4), 4-vinilguayacol (pico 7), *trans*-eugenol (pico 13) y alcohol *cis*-coniferílico (pico 33).

En cuanto a la distribución relativa de unidades estructurales de lignina, se observó que la lignina obtenida mediante el proceso organosolv convencional (sin etapa alcalina previa) liberó un 19,1% de compuestos procedentes de unidades H, un 54,6% de unidades S y un 26,2% de unidades G. En comparación, la lignina procedente del proceso de doble etapa mostró un 3,3% de unidades H, 55,1% de unidades S y 41,6% de las unidades de lignina G. En consecuencia, las relaciones S/G obtenidas fueron de 2,1, para la lignina organosolv y de 1,3, para la lignina de doble etapa. Estos valores son coherentes con lo reportado por Guan et al. [58], quienes determinaron una relación S/G de 1,37 para el clon 74/76 de *Populus x euramericana* mediante espectroscopía de RMN.

La mayor proporción relativa de unidades G del proceso de doble etapa se asocia con una mayor estabilidad térmica, lo que concuerda con los resultados del análisis termogravimétrico. Las proporciones relativas H/S/G fueron de 1/2,9/1,4 para la lignina organosolv convencional y de 1/16,7/12,6 para la lignina de doble etapa.

Cabe destacar que, además de los compuestos fenólicos derivados de la lignina, se detectaron pequeñas proporciones de compuestos fenólicos no procedentes de las ligninas, siendo más abundantes en la lignina del proceso de doble etapa que la lignina del proceso organosolv convencional. Asimismo, en la lignina organosolv convencional se identificó levoglucosano, lo cual indica la presencia de residuos celulósicos susceptibles a la pirólisis. Estos resultados evidencian la existencia de impurezas en las ligninas obtenidas por ambos procesos, en concordancia con los resultados de pureza reportados previamente, determinados mediante cuantificación de azúcares en el licor de la hidrólisis ácida de las ligninas mediante HPLC.

Finalmente, se identificaron compuestos exclusivos de la lignina de doble etapa que no estuvieron presentes en la lignina obtenida por el proceso organosolv convencional. Entre estos se incluyen 4-metilfenol y 4-vinilfenol (derivados de la unidad H); propenilsiringol (derivados de la unidad S); 4-propilguayacol, cis-eugenol, propiovanillona, butirovanillona y alcohol dihidroconifenílico (derivados de la unidad G). En cambio, los dos únicos compuestos exclusivos de la pirólisis de la lignina organosolv convencional fue la acetoguayacona y el alcohol cis-coniferílico, ambos derivados de la unidad G.

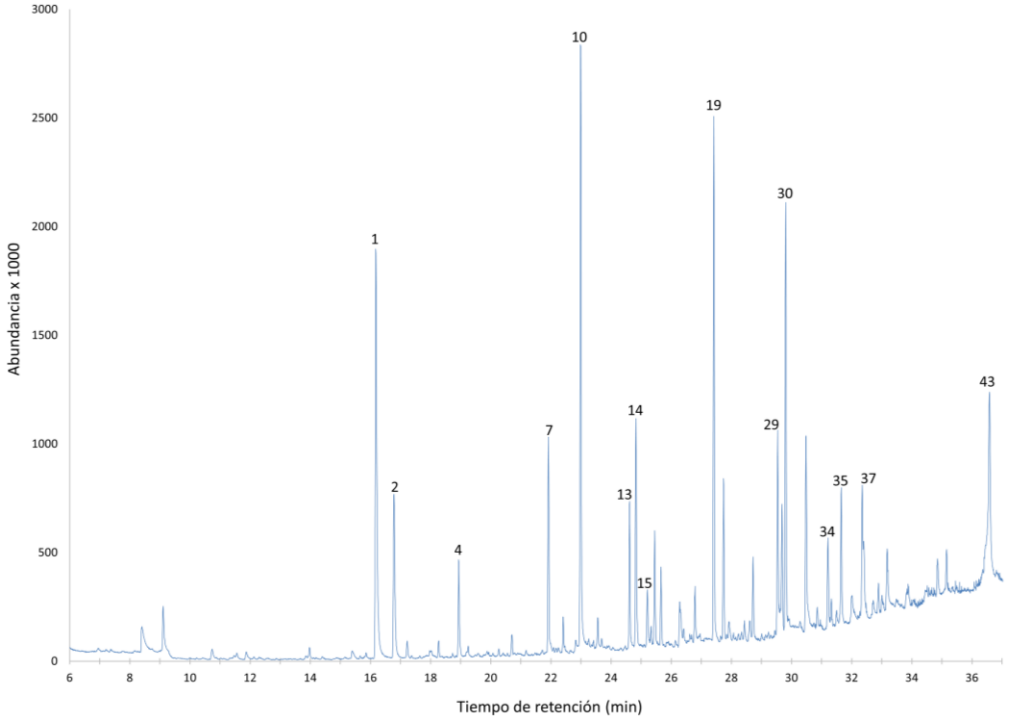


Figura 7. Cromatograma TIC de la lignina obtenida en el proceso organosolv convencional.

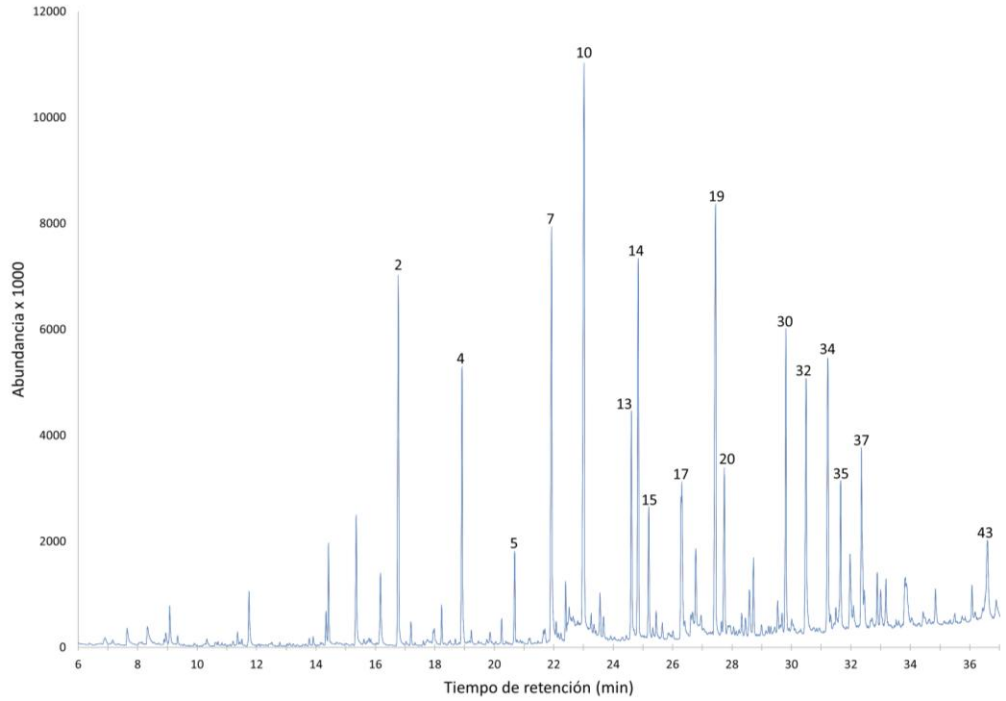


Figura 8. Cromatograma TIC de la lignina obtenida en el de doble etapa.

Tabla 11. Identificación y abundancias molares relativas de los compuestos fenólicos derivados de las ligninas tras Py-GC/MS.

Pico	Tiempo retención	Compuesto	Origen	Lignina Organosolv	Lignina EAF+Organosolv
1	16,174	fenol	H	19,1	2,7
2	16,774	guayacol	G	5,6	8,3
3	17,943	4-metilfenol	H	0,0	0,3
4	18,917	4-metilguayacol	G	2,1	5,6
5	20,685	4-etilguayacol	G	0,4	1,4
6	21,706	4-vinilfenol	H	0,0	0,3
7	21,926	4-vinilguayacol	G	4,2	9,0
8	22,406	eugenol ($g\text{-}ch_2\text{-}ch{=}ch_2$)	G	0,5	0,8
9	22,460	4-propilguayacol	G	0,0	0,2
10	23,024	siringol	S	12,3	13,7
11	23,261	*cis*-isoeugenol	G	0,0	0,4
12	23,558	eugenol ($g\text{-}ch\text{-}ch_2{=}ch_2$)	G	0,6	0,6
13	24,620	*trans*-eugenol	G	2,7	4,1
14	24,846	4-metilsiringol	S	3,8	6,7
15	25,202	vainillina	G	1,3	2,5
16	26,312	4-etilsiringol	S	0,5	1,2
17	26,312	homovainillina	G	0,9	3,1
18	26,674	acetoguayacona	G	1,0	0,0
19	27,446	4-vinilsiringol	S	8,1	7,7
20	27,742	guayacilacetona	G	1,1	1,8
21	27,742	4-alilsiringol	S	1,1	0,8
22	27,742	4-propilsiringol	S	0,3	0,4
23	28,330	propiovainillona	G	0,0	0,4
24	28,585	1'-hidroxieugenol	G	0,2	0,6
25	28,585	guayacil vinil cetona	G	0,3	0,3
26	28,722	butirovanillona	G	0,0	0,3
27	28,722	*cis*-4-pronilsiringol	S	1,2	0,7
28	28,995	propenilsiringol	S	0,0	0,2
29	29,224	propinilsiringol	S	5,0	0,7
30	29,814	*trans*-4-propenilsiringol	S	6,0	4,2
31	30,010	alcohol dihidroconiferílico	G	0,0	0,2
32	30,496	siringaldehído	S	4,1	4,8
33	30,496	alcohol cis-coniferílico	G	4,1	0,0
34	31,226	homosiringaldehído	S	1,5	4,6
35	31,654	acetosingona	S	2,4	2,4
36	31,974	alcohol *trans*-coniferílico	G	1,0	1,6
37	32,360	siringilacetona	S	1,5	2,6
38	32,360	*trans*-coniferaldehído	G	0,3	0,4
39	32,888	propiosiringona	S	0,4	0,7
40	33,001	3-siringol-3-oxopropanal	S	0,2	0,5
41	33,185	siringil vinil cetona	S	0,6	0,1
42	33,185	alcohol t*rans*-sinapaldehído	S	0,6	0,6
43	36,598	*trans*-sinapaldehído	S	5,0	2,6
		H (% molar)		**19,1**	**3,3**
		S (% molar)		**54,6**	**55,1**
		G (% molar)		**26,2**	**41,6**
		S/G		**2,1**	**1,3**

4 Conclusiones.

En el presente trabajo se planteó la hipótesis de que una etapa previa de extracción alcalina en frío con ultrasonidos permitiría mejorar la calidad de la pasta celulósica y reducir la severidad de las condiciones de operación del proceso organosolv, aprovechando el carácter alcalino de la madera del clon AF2 de *Populus x euramericana* tras dicha etapa de EAF. Para validar esta hipótesis, se llevó a cabo un diseño experimental aplicando diferentes condiciones de operación de la etapa organosolv, con el objetivo de evaluar la producción de pulpa y la recuperación de lignina.

Los resultados confirmaron que el tratamiento alcalino previo favorece la solubilización de los componentes lignocelulósicos durante la etapa organosolv, permitiendo operar de forma efectiva a temperaturas más moderadas en comparación con el proceso organosolv convencional.

Las condiciones óptimas determinadas para el proceso organosolv convencional fueron 180 ºC, 90 minutos y una concentración de etanol del 65%. En cambio, para el proceso de doble etapa, la temperatura óptima pudo reducirse hasta 150 ºC, manteniendo el mismo tiempo de operación y utilizando un 35% de etanol, sin comprometer el rendimiento ni la calidad de la pasta celulósica. Bajo estas condiciones de doble etapa, se alcanzaron los mejores valores en términos de viscosidad, número kappa y blancura.

Desde el punto de vista composicional, la pulpa obtenida presentó un contenido de glucano del 62,5% y un contenido de lignina Klason del 20,5%, en comparación con el 50,1% de glucano y 32,5% de lignina Klason de la pulpa producida bajo las condiciones óptimas del proceso organosolv convencional.

Asimismo, la lignina organosolv recuperada del proceso de doble etapa presentó una mayor proporción de unidades guayacílicas, lo que se asoció con una mayor estabilidad térmica, según los análisis de pirólisis.

Por último, si bien las condiciones óptimas para la eficiencia global del proceso se alcanzaron a 150 ºC, el análisis de las propiedades físicas de las hojas de papel sugiere que, para maximizar los índices de estallido, desgarro y tracción, sería recomendable operar a temperaturas intermedias (142,5ºC), buscando un equilibrio entre la eficiencia del proceso, la calidad de la pulpa y las propiedades físicas del papel.

Referencias

[1] T.K. Bedru, B.T. Meshesha, S.A. Mohammed, A.G. Demesa, M. Jayakumar, Efficient Biomass Fractionation via Organosolv for Sustainable Bioenergy Production: A Comprehensive Review, International Journal of Chemical Engineering 2025 (2025) 3120449.

[2] R.A. Quevedo-Amador, B.P. Escalera-Velasco, A.M.R. Arias, H.E. Reynel-Ávila, J.C. Moreno-Piraján, L. Giraldo, A. Bonilla-Petriciolet, Application of waste biomass for the production of biofuels and catalysts: a review, Clean Technol Environ Policy 26 (2024) 943–997. https://doi.org/10.1007/s10098-023-02728-4.

[3] S. Gajula, C.R.K. Reddy, More sustainable biomass production and biorefining to boost the bioeconomy, Biofuels, Bioproducts and Biorefining 15 (2021) 1221–1232. https://doi.org/10.1002/bbb.2227.

[4] R. Moya, C. Tenorio, G. Oporto, Short rotation wood crops in Latin American: A review on status and potential uses as biofuel, Energies (Basel) 12 (2019) 705. https://doi.org/10.3390/en12040705.

[5] I. Porth, Y.A. El-Kassaby, Using Populus as a lignocellulosic feedstock for bioethanol, Biotechnol J 10 (2015) 510–524. https://doi.org/10.1002/biot.201400194.

[6] L. López-Bellido, J. Wery, R.J. López-Bellido, Energy crops: prospects in the context of sustainable agriculture, European Journal of Agronomy 60 (2014) 1–12. https://doi.org/10.1016/j.eja.2014.07.001.

[7] D. Mboowa, A review of the traditional pulping methods and the recent improvements in the pulping processes, Biomass Convers Biorefin 14 (2024) 1–12. https://doi.org/10.1007/s13399-020-01243-6.

[8] A.A. Vaidya, K.D. Murton, D.A. Smith, G. Dedual, A review on organosolv pretreatment of softwood with a focus on enzymatic hydrolysis of cellulose. Biomass Convers Biorefin 12: 5427–5442, (2022). https://doi.org/10.1007/s13399-022-02373-9.

[9] M.N. Borand, F. Karaosmanoğlu, Effects of organosolv pretreatment conditions for lignocellulosic biomass in biorefinery applications: a review, Journal of Renewable and Sustainable Energy 10 (2018). https://doi.org/10.1063/1.5025876.

[10] M.M. Abu-Omar, K. Barta, G.T. Beckham, J.S. Luterbacher, J. Ralph, R. Rinaldi, Y. Román-Leshkov, J.S.M. Samec, B.F. Sels, F. Wang, Guidelines for performing lignin-first biorefining, Energy Environ Sci 14 (2021) 262–292. https://doi.org/10.1039/D0EE02870C.

[11] M. Islam, A.S.K. Sinha, K. Prasad, Organosolv delignification of rice straw cellulose fiber for functional food packaging, Cellulose 31 (2024) 9191–9214. https://doi.org/10.1007/s10570-024-06125-y.

[12] A. Pazzaglia, M. Gelosia, T. Giannoni, G. Fabbrizi, A. Nicolini, B. Castellani, Wood waste valorization: Ethanol based organosolv as a promising recycling process, Waste Management 170 (2023) 75–81. https://doi.org/10.1016/j.wasman.2023.08.003.

[13] T.N. Kleinert, Organosolv pulping and recovery process, (1971).

[14] M. Manfredi, J.L. Gomide, T.T. Barcelos, B. de F.H. Faria, J.L. Colodette, C.M. Silva, Washing, bleaching and characterization of eucalyptus pulp from ethanol pulping, Nord Pulp Paper Res J 29 (2014) 612–619. https://doi.org/10.3183/npprj-2014-29-04-p612-619.

[15] B. Hansen, P. Kusch, M. Schulze, B. Kamm, Qualitative and quantitative analysis of lignin produced from beech wood by different conditions of the Organosolv process, J Polym Environ 24 (2016) 85–97. https://doi.org/10.1007/s10924-015-0746-3.

[16] P.P. Thoresen, L. Matsakas, U. Rova, P. Christakopoulos, Recent advances in organosolv fractionation: Towards biomass fractionation technology of the future, Bioresour Technol 306 (2020) 123189. https://doi.org/10.1016/j.biortech.2020.123189.

[17] Y. Ye, Y. Zhang, J. Fan, J. Chang, Novel method for production of phenolics by combining lignin extraction with lignin depolymerization in aqueous ethanol, Ind Eng Chem Res 51 (2012) 103–110. https://doi.org/10.1021/ie202118d.

[18] X. Zhao, S. Li, R. Wu, D. Liu, Organosolv fractionating pre-treatment of lignocellulosic biomass for efficient enzymatic saccharification: chemistry, kinetics, and substrate structures, Biofuels, Bioproducts and Biorefining 11 (2017) 567–590.

[19] Z. Zhou, F. Lei, P. Li, J. Jiang, Lignocellulosic biomass to biofuels and biochemicals: A comprehensive review with a focus on ethanol organosolv pretreatment technology, Biotechnol Bioeng 115 (2018) 2683–2702. https://doi.org/10.1002/bit.26788.

[20] S. Sun, S. Sun, X. Cao, R. Sun, The role of pretreatment in improving the enzymatic hydrolysis of lignocellulosic materials, Bioresour Technol 199 (2016) 49–58. https://doi.org/10.1016/j.biortech.2015.08.061.

[21] K. Zhang, Z. Pei, D. Wang, Organic solvent pretreatment of lignocellulosic biomass for biofuels and biochemicals: A review, Bioresour Technol 199 (2016) 21–33. https://doi.org/10.1016/j.biortech.2015.08.102.

[22] M. Raita, N. Denchokepraguy, V. Champreda, N. Laosiripojana, Effects of alkaline catalysts on acetone-based organosolv pretreatment of rice straw, 3 Biotech 7 (2017) 1–10. https://doi.org/10.1007/s13205-017-0969-1.

[23] H.A. Ruiz, D.S. Ruzene, D.P. Silva, F.F.M.I. Da Silva, A.A. Vicente, J.A. Teixeira, Development and characterization of an environmentally friendly process sequence (autohydrolysis and organosolv) for wheat straw delignification, Appl Biochem Biotechnol 164 (2011) 629–641. https://doi.org/10.1007/s12010-011-9163-9.

[24] H.D. Zamora Zamora, C. de Freitas, D. Pasquini, F. Masarin, M. Brienzo, Enhanced Fractionation of Guava Seed Cake Using Alkali-Catalyzed Ethanol Organosolv Pretreatment, Bioenergy Res 18 (2025) 1–13. https://doi.org/10.1007/s12155-024-10813-9.

[25] C. Tang, Y. Chen, J. Liu, T. Shen, Z. Cao, J. Shan, C. Zhu, H. Ying, Sustainable biobutanol production using alkali-catalyzed organosolv pretreated cornstalks, Ind Crops Prod 95 (2017) 383–392. https://doi.org/10.1016/j.indcrop.2016.10.048.

[26] C. Tang, J. Shan, Y. Chen, L. Zhong, T. Shen, C. Zhu, H. Ying, Organic amine catalytic organosolv pretreatment of corn stover for enzymatic saccharification and high-quality lignin, Bioresour Technol 232 (2017) 222–228. https://doi.org/10.1016/j.biortech.2017.02.041.

[27] W. Wei, B. Wang, X. Wang, R. Ling, Y. Jin, Comparison of acid and alkali catalyzed ethylene glycol organosolv pretreatment for sugar production from bagasse, Bioresour Technol 320 (2021) 124293. https://doi.org/10.1016/j.biortech.2020.124293.

[28] R. Marton, S. Granzow, Ethanol-alkali pulping, Tappi 65 (1982) 103–106.

[29] C. Zhang, H. Wang, L. Bai, C. Wu, L. Shen, O. Sippula, J. Yang, L. Zhou, C. He, J. Liu, Should industrial bagasse-fired boilers be phased out in China?, J Clean Prod 265 (2020) 121716. https://doi.org/10.1016/j.jclepro.2020.121716.

[30] TAPPI T222 om-11, Acid-insoluble lignin in wood and pulp. TAPPI Press, Atlanta, GA., (2011).

[31] TAPPI T249 cm-09, Carbohydrate composition of extractive-free wood and wood pulp by gas-liquid chromatography. TAPPI Press, Atlanta, GA., (2009).

[32] TAPPI T212 om-22, One percent sodium hydroxide solubility of wood and pulp (Test Method).

[33] TAPPI T257 cm-85, Sampling and preparing wood for analysis. TAPPI Press, Atlanta, GA., (1999).

[34] TAPPI T204 cm-07, Solvent extractives of wood and pulp. TAPPI Press, Atlanta, GA., (2007).

[35] CEN/TS, Solid Biofuels-Method for the Determination of Calorific Value CEN/TS 14918:2005, (2005). https://standards.iteh.ai/catalog/standards/cen/21f53010-bfdf-41aa-8f73-3ad9e2ab444f/cen-ts-14918-2005.

[36] UNE 16001 EX, Solid Biofuels, Method for the determination of calorific value, (2005).

[37] TAPPI 211 om-02, Ash in wood, pulp, paper and paperboard: combustion at 525°C. TAPPI Press, Atlanta, GA., (2002).

[38] M. Monção, A.I. Anukam, K. Hrůzová, U. Rova, P. Christakopoulos, L. Matsakas, A Parametric Study of the Organosolv Fractionation of Norway Spruce Sawdust, Energies (Basel) 17 (2024) 3276. https://doi.org/10.3390/en17133276.

[39] A. Moral, R. Aguado, P. Mutjé, A. Tijero, Papermaking potential of Citrus sinensis trimmings using organosolv pulping, chlorine-free bleaching and refining, J Clean Prod 112 (2016) 980–986. https://doi.org/10.1016/j.jclepro.2015.09.008.

[40] J. Alaejos, F. López, M.E. Eugenio, R. Tapias, Soda–anthraquinone, kraft and organosolv pulping of holm oak trimmings, Bioresour Technol 97 (2006) 2110–2116. https://doi.org/10.1016/j.biortech.2005.09.021.

[41] L. Jiménez, I. Pérez, J.C. Garcıa, A. Rodrıguez, J.L. Ferrer, Influence of ethanol pulping of wheat straw on the resulting paper sheets, Process Biochemistry 37 (2002) 665–672. https://doi.org/10.1016/S0032-9592(01)00255-2.

[42] J. Ai, U. Tschirner, Fiber length and pulping characteristics of switchgrass, alfalfa stems, hybrid poplar and willow biomasses, Bioresour Technol 101 (2010) 215–221. https://doi.org/10.1016/j.biortech.2009.07.090.

[43] M. Oliet, M.A. Gilarranz, J.C. Domínguez, M. V Alonso, F. Rodríguez, Ethanol-based pulping from Cynara cardunculus L, Journal of Chemical Technology & Biotechnology: International Research in Process, Environmental & Clean Technology 80 (2005) 746–753. https://doi.org/10.1002/jctb.1217.

[44] W.J.J. Huijgen, A.T. Smit, J.H. Reith, H. den Uil, Catalytic organosolv fractionation of willow wood and wheat straw as pretreatment for enzymatic cellulose hydrolysis, Journal of Chemical Technology & Biotechnology 86 (2011) 1428–1438. https://doi.org/10.1002/jctb.2654.

[45] Y. Su, C. Huang, C. Lai, Q. Yong, Green solvent pretreatment for enhanced production of sugars and antioxidative lignin from poplar, Bioresour Technol 321 (2021) 124471. https://doi.org/10.1016/J.BIORTECH.2020.124471.

[46] M. Brebu, C. Vasile, Thermal degradation of lignin—a review, Cellulose Chemistry & Technology 44 (2010) 353.

[47] J. Zhao, W. Xiuwen, J. Hu, Q. Liu, D. Shen, R. Xiao, Thermal degradation of softwood lignin and hardwood lignin by TG-FTIR and Py-GC/MS, Polym Degrad Stab 108 (2014) 133–138. https://doi.org/10.1016/j.polymdegradstab.2014.06.006.

[48] C. Wang, J. Pan, J. Li, Z. Yang, Comparative studies of products produced from four different biomass samples via deoxy-liquefaction, Bioresour Technol 99 (2008) 2778–2786. https://doi.org/10.1016/j.biortech.2007.06.023.

[49] V.B.F. Custodis, P. Hemberger, Z. Ma, J.A. van Bokhoven, Mechanism of Fast Pyrolysis of Lignin: Studying Model Compounds, J Phys Chem B 118 (2014) 8524–8531. https://doi.org/10.1021/jp5036579.

[50] J.-Y. Kim, S. Oh, H. Hwang, U.-J. Kim, J.W. Choi, Structural features and thermal degradation properties of various lignin macromolecules obtained from poplar wood (Populus albaglandulosa), Polym Degrad Stab 98 (2013) 1671–1678. https://doi.org/10.1016/j.polymdegradstab.2013.06.008.

[51] L. Abid, V. Landry, T. Stevanovic, Characterization of sugar maple and red oak bark: Efficient lignin extraction via the Organosolv and acidic dioxane process, Journal of Wood Chemistry and Technology 44 (2024) 391–407. https://doi.org/10.1080/02773813.2024.2416656.

[52] W.G. Glasser, R.K. Jain, Lignin derivatives. I. alkanoates, (1993). https://doi.org/10.1515/hfsg.1993.47.3.225.

[53] H. El-Saied, A.-A.M.A. Nada, The thermal behaviour of lignins from wasted black pulping liquors, Polym Degrad Stab 40 (1993) 417–421.

[54] S. Chu, A. V Subrahmanyam, G.W. Huber, The pyrolysis chemistry of a β-O-4 type oligomeric lignin model compound, Green Chemistry 15 (2013) 125–136. https://doi.org/10.1039/C2GC36332A.

[55] B. Wang, X.J. Shen, J.L. Wen, L. Xiao, R.C. Sun, Evaluation of organosolv pretreatment on the structural characteristics of lignin polymers and follow-up enzymatic hydrolysis of the substrates from Eucalyptus wood, Int J Biol Macromol 97 (2017) 447–459. https://doi.org/10.1016/J.IJBIOMAC.2017.01.069.

[56] R. El Hage, N. Brosse, L. Chrusciel, C. Sanchez, P. Sannigrahi, A. Ragauskas, Characterization of milled wood lignin and ethanol organosolv lignin from miscanthus, Polym Degrad Stab 94 (2009) 1632–1638. https://doi.org/10.1016/J.POLYMDEGRADSTAB.2009.07.007.

[57] U. Shakeel, X. Li, B. Wang, F. Geng, Q. Zhang, K. Zhang, X. Xu, J. Xu, Structure and integrity of sequentially extracted lignin during poplar (alkaline) pretreatment, Process Biochemistry 117 (2022) 198–208. https://doi.org/10.1016/J.PROCBIO.2022.03.026.

[58] Y. Guan, T. Shu, H. Gao, L. Zhou, L. Zhang, Comparative studies on lignin structures in normal and tension wood of Populus × euramericana cv. “74/76,” Int J Biol Macromol 172 (2021) 178–185. https://doi.org/10.1016/J.IJBIOMAC.2021.01.005.

3.4. Valorización del Clon AF2 de *Populus* mediante Explosión de vapor, extracción de compuestos bioactivos con disolventes verdes e hidrólisis enzimática.

1 Introducción.

La biomasa lignocelulósica, gracias a su composición química rica en carbohidratos, representa una fuente renovable de interés para la obtención de energía, productos químicos y materiales sostenibles [1,2]. En particular, el género *Populus*, y específicamente el clon AF2 de *Populus x euramericana*, se perfila como una materia prima prometedora para la producción de biocombustibles, gracias a su rápido crecimiento, alta densidad aparente y la posibilidad de cosecha durante todo el año, en comparación con materias primas herbáceas [3].

No obstante, el aprovechamiento de esta biomasa para la producción de azúcares fermentables, precursores clave en la síntesis de biocombustibles y compuestos de plataforma, se ve obstaculizado por la compleja y recalcitrante estructura de la pared celular [4,5]. La lignina, que actúa como barrera física y química, limita la accesibilidad enzimática a los carbohidratos estructurales, reduciendo la eficiencia de la hidrólisis enzimática [6]. Por ello, se requiere la aplicación de un pretratamiento eficaz que modifique la composición y estructura, para así facilitar la posterior liberación de azúcares durante la etapa de hidrólisis enzimática [7,8].

En este contexto, la explosión de vapor (steam explosion) se ha consolidado como uno de los pretratamientos más empleados a nivel industrial [9,10]. Este método fisicoquímico consiste en exponer la biomasa lignocelulósica a vapor a alta presión y temperatura (normalmente entre 160 y 260 ºC), seguido de una despresurización repentina, lo que genera la “explosión” del material, destruyendo parcialmente las paredes celulares [11,12]. Durante este proceso, los grupos acetilados presentes en la biomasa liberan ácidos que catalizan reacciones de autohidrólisis, favoreciendo la solubilización parcial de hemicelulosas y una modificación estructural de la lignina [13,14].

El resultado es una biomasa pretratada con mayor accesibilidad enzimática, debido a la solubilización y degradación de las hemicelulosas, así como a la deslignificación parcial, lo que se traduce en una mayor eficiencia en los procesos posteriores de conversión bioquímica [6,15,16]. En comparación con otros pretratamientos, la explosión de vapor presenta ventajas como una menor inversión de capital, un uso de productos químicos menos peligrosos, un consumo energético relativamente moderado y la posibilidad de utilizar partículas de biomasa de mayor tamaño [11,17]. Estas características, junto a su bajo impacto ambiental y su comprobado desarrollo a escala industrial, lo convierten en una opción atractiva y ampliamente documentada para la valorización de biomasa lignocelulósica [11].

A pesar de las numerosas ventajas del pretratamiento por explosión de vapor, este presenta una desventaja significativa que requiere especial atención, ya que puede afectar negativamente las etapas posteriores. En particular, durante la explosión de vapor se genera diversos productos de degradación de azúcares y lignina, los cuales pueden actuar como inhibidores en la hidrólisis enzimática y en los procesos fermentativos [14,18-20]. Por ello, resulta crucial implementar estrategias eficaces de separación y desintoxicación de estos compuestos inhibidores.

Existen numerosas tecnologías para la eliminación de inhibidores, basadas en enfoques físicos, químicos y biológicos. No obstante, muchas de estas presentan limitaciones importantes, tales como elevados costes, generación de subproductos, procesos complejos y perdida de azúcares fermentables [21]. En este contexto, la extracción con disolventes ha sido una de las estrategias más ampliamente investigadas y aplicadas para la separación de compuestos fenólicos de materiales lignocelulósicos pretratados mediante explosión de vapor o hidrólisis [10,22].

En línea con los principios de la química verde, se impulsa el uso de disolventes más sostenibles, seguros y eficientes, destacando el potencial de los disolventes eutécticos y los disolventes bio-basados como alternativas prometedoras [23-25]. Los disolventes eutécticos consisten en mezclas de dos o más componentes, que da lugar a un punto de fusión más bajo que el de sus componentes individuales [26,27]. Destacan por su bajo costo, alta disponibilidad, estabilidad, biodegradabilidad y adaptabilidad según la aplicación [27,28]. Estas propiedades los hacen adecuados para el pretratamiento de biomasa lignocelulósica y la extracción de compuestos fenólicos [29-31]. Asimismo, los disolventes bio-basados, obtenidos a partir de fuentes renovables, representan una alternativa sostenible frente a los disolventes derivados del petróleo [32].

Por lo tanto, en el presente estudio se evaluó la producción de azúcares fermentables a partir de la madera del clon AF2 de *Populus x euramericana*, mediante un enfoque secuencial que incluye: pretratamiento por explosión de vapor bajo distintas condiciones de operación, eliminación de inhibidores fenólicos utilizando disolventes verdes, e hidrólisis enzimática. Esta estrategia permite una doble valorización de la biomasa: por un lado, la obtención de azúcares, susceptibles de ser empleados en la producción de bioetanol u otros bioproductos; y por otro, la recuperación de compuestos fenólicos con alto valor añadido, debido a su reconocida actividad antioxidante.

2 Material y metodología.

La materia prima del presente estudio fue el clon AF2 del *Populus x Euramericana*, procedente de las plantaciones experimentales del departamento de Ciencias Agroforestales de la Universidad de Huelva. La biomasa fue caracterizada según las normas TAPPI, con el objetivo de determinar la composición química inicial [33-36].

La composición obtenida fue la siguiente: 42,5% de celulosa, 19,8% de hemicelulosa (16,2% de xilano, 1,1% de galactano, 0,12% de arabano y 2,3% de manano), 26,7% de lignina y 0,73% de cenizas.

2.1 Explosión de vapor.

La biomasa fue pretratada en un reactor de 2 L integrado en una planta piloto de explosión de vapor, compuesta por un generador de vapor, un reactor y un ciclón de recuperación, según lo descrito por Ballesteros et al. [37] (CIEMAT, Madrid, España). El reactor fue precalentado hasta alcanzar la temperatura establecida mediante vapor saturado. Por cada ensayo, se procesaron 400 gramos de biomasa seca (contenido de humedad inicial 8,91%).

El pretratamiento por explosión de vapor se llevó a cabo bajo tres condiciones de severidad (baja, media y alta), combinando variaciones de temperatura y presión con un tiempo de residencia constante de 8 minutos. Las condiciones específicas de cada tratamiento se detallan en la Tabla 1.

Tabla 1. Experimentos realizados para evaluar los efectos de la explosión por vapor.

Condiciones	**Temperatura** (ºC)	**Presión** (bares)
Bajas	175	7,8
Medias	200	14,6
Altas	225	24,5

Tras cada pretratamiento, el material explosionado fue enfriado y una fracción de cada muestra fue filtrada al vacío para separar la fracción líquida de la fracción sólida, las cuales se caracterizaron por separado.

La fracción sólida fue lavada con agua destilada para obtener la fracción sólida insoluble en agua (WIS, por sus siglas en inglés). Esta fracción se sometió a hidrólisis ácida en dos etapas con ácido sulfúrico, siguiendo el método descrito en la norma TAPPI T249 [34], y los azúcares resultantes fueron cuantificados mediante cromatografía líquida de alta resolución (HPLC).

Por otro, en la fracción líquida de cada pretratamiento se cuantificaron los azúcares monoméricos por HPLC. Para determinar el contenido de azúcares oligoméricos, se realizó una hidrólisis suave (4% v/v H_2SO_4, 120 ºC, 30 min), transformando los oligómeros en monómeros para ser cuantificados por HPLC.

Finalmente, el material explosionado de cada condición de operación fue almacenado por separado en bolsas herméticas a -18 ºC hasta su posterior uso en las etapas de extracción de compuestos fenólicos e hidrólisis enzimática.

2.2 Extracción de compuestos fenólicos.

Para la extracción de compuestos fenólicos, inhibidores, se emplearon dos disolventes bio-basados: acetato de etilo (EA) y lactato de etilo (EL), seleccionados por su compatibilidad con los principios de la química verde. El objetivo fue evaluar su potencial como agentes de extracción de compuestos inhibidores sobre la biomasa explosionada bajo diferentes condiciones de severidad.

La extracción sólido-líquido se realizó con una proporción de 1:5 (biomasa seca:disolvente). Las muestras se sometieron a agitación orbital a 150 rpm, a una temperatura de 60 ºC durante 1 hora.

Tras el proceso de extracción, las mezclas fueron centrifugadas a 4000 rpm durante 5 minutos para separar la fracción líquida (rica en el disolvente) de la fracción sólida. La fracción líquida fue almacenada en refrigeración para su posterior análisis.

La fracción sólida recuperada se dividió en dos alícuotas:

1. Una parte fue sometida directamente a la etapa de hidrólisis enzimática, con el fin de evaluar el efecto residual del disolvente en el proceso.
2. La segunda parte fue sometida a un proceso de lavado intensivo, que consistió en: tres ciclos consecutivos de lavado con abundante agua, centrifugación a 1400 rpm durante 5 minutos tras cada lavado y un lavado final por filtración a vacío con agua en exceso. Con el fin de eliminar completamente los restos de disolvente.

Este procedimiento permitió evaluar si la presencia de trazas de disolventes tras la extracción influye en el rendimiento de la hidrólisis enzimática.

2.3 Análisis de los compuestos extraídos en disolventes bio-basados.

Las fracciones líquidas obtenidas tras la extracción de la biomasa explosionada con disolventes bio-basados se analizaron con el objetivo de determinar el contenido total de compuestos fenólicos y su actividad antioxidante.

El contenido total de fenoles se cuantificó mediante el método espectrofotométrico de Folin-Ciocalteu, siguiendo la norma ISO 14502-1:2005 [38]. Brevemente, se mezclaron 0,1 mL de reactivo de Folin-Ciocalteu (2N) con 0,1 mL del extracto, manteniéndose en oscuridad durante 3 minutos. Posteriormente, se añadieron 2 mL de una solución de carbonato sódico al 2% (m/v), y la mezcla se dejó reaccionar durante 30 minutos en oscuridad. La absorbancia se midió a 765 nm en un espectrofotómetro UV-Vis (Lambda 365, PerkinElmer). Para la cuantificación, se utilizó una curva de calibrado elaborada con ácido gálico, y los resultados se expresaron como miligramos de equivalentes de ácido gálico por gramo de biomasa explosionada seca (mg GAE/ g biomasa seca).

Todos los análisis se realizaron por triplicado, calculándose los valores medios y sus respectivas desviaciones estándar.

La actividad antioxidante de los extractos se evaluó mediante el método ABTS, según Re et al. [39]. El radical $ABTS^+$ se generó mediante la reacción de una solución madre de ácido 2,2'-azino-bis(3-etilbenztiazolina-6-sulfónico) (ABTS) con persulfato de potasio. La solución madre se diluyó con tampón salino fosfato hasta alcanzar una absorbancia de 0,7 ± 0,02 a 734 nm. Para el análisis, se mezcló 1 mL de la solución madre diluida de ABTS con 10 µL del extracto, midiendo la absorbancia a 734 nm cada 30 segundos durante 6 minutos en el mismo espectrofotómetro UV-Vis. Los resultados se expresaron como miligramos de equivalentes de Trolox por gramo de biomasa explosionada seca (mg Trolox/g biomasa seca). Cada muestra fue analizada por triplicado.

2.4 Hidrólisis enzimática.

La biomasa explosionada (como control) y las fracciones sólidas obtenidas tras la extracción con disolventes bio-basados (tanto las lavadas como las no lavadas) se sometieron a hidrólisis enzimática para evaluar su potencial en la liberación de azúcares fermentables.

La hidrólisis se realizó utilizando una carga enzimática de 5 FPU por gramo de biomasa seca. Las reacciones se llevaron a cabo en tampón de acetato 50 mM (pH 5), a 50 ºC y 100 rpm, durante 72 horas, en un incubador oscilante con control de temperatura. La concentración de sustrato fue del 5% (p/v). Todos los ensayos se realizaron por duplicado.

Se tomaron alícuotas de 400 µL a las 4, 24, 48 y 72 horas de incubación, con el fin de analizar la evolución de la liberación de azúcares. Para detener la actividad enzimática, las muestras se calentaron en un baño térmico a 100 ºC durante 5 minutos. A continuación, se centrifugaron y filtraron mediante membranas de jeringa de nailon de 0,45 µm, y finalmente se inyectaron en el sistema de cromatografía líquida de alta resolución (HPLC) para la determinación de azúcares monoméricos. Todas las mediciones se realizaban por duplicado.

3 Resultados y discusión.

3.1 Pretratamiento. Explosión de vapor.

El clon AF2 de *Populus x euramericana* fue sometido a la explosión de vapor durante 8 minutos, bajo tres niveles de severidad térmica: 175 ºC, 200 ºC y 225 ºC. El incremento de temperatura conllevó también a un aumento de la presión de operación, tal y como se recoge en la Tabla 1.

A medida que se incrementó la severidad del pretratamiento, se observó una disminución progresiva en la recuperación de la fracción sólida insoluble (WIS), acompañada de un aumento en la fracción de sólidos solubles presentes en la fracción líquida (WSS). En concreto, la recuperación

total de sólidos (WIS + WSS) pasó de un 98,7% a 175 ºC a un 81,9% a 225 ºC, lo que refleja una mayor solubilización de los componentes estructurales con el aumento de la temperatura.

Asimismo, se produjo un enriquecimiento relativo a la celulosa y lignina en la fracción sólida (WIS), acompañada de una disminución del contenido de hemicelulosas respecto a la composición inicial de la biomasa. Este fenómeno es consistente con la mayor susceptibilidad de las hemicelulosas a la solubilización y degradación térmica durante el tratamiento, y ha sido ampliamente reportado en literatura [10,40,41].

Como se puede observar en la Tabla 2, es especialmente destacable el incremento del contenido de lignina en el WIS a 225 ºC, mientras que en las condiciones de 175 ºC y 200 ºC su proporción se mantuvo prácticamente constante. Este aumento puede estar asociado tanto a la perdida de hemicelulosas como a fenómenos de condensación de ligninas, típicos de pretratamientos severos [41].

Tabla 2. Recuperación de sólidos y composición de la fracción sólida (WIS).

	Recuperación (%)			Composición (%)		
Severidad	**WIS**	**WSS**	**Total**	**Glucosa**	**Xilosa**	**Lignina**
Baja (175ºC)	96,5	2,1	98,7	43,5	17,2	33,7
Media (200ºC)	74,5	9,0	83,5	56,7	7,2	34,9
Alta (225ºC)	66,4	15,5	81,9	59,1	1,8	46,2

La degradación de hemicelulosas se corroboró mediante el aumento del contenido de xilosa y otros tipos de azúcares hemicelulósicos en la fracción líquida, así como por la presencia creciente de productos de degradación como el furfural, especialmente en las condiciones más severas. Los resultados correspondientes a la fracción líquida se presentan en la Tabla 4. Los resultados son acordes con trabajos previos publicados por otros autores [10,42,43].

Tabla 4. Composición fracción líquida.

Severidad	**Glucosa**	**Xilosa**	**Galactosa**	**Arabinosa**	**Manosa**	**Furfural**	**HMF**	**OH Benzoico**
Baja (175ºC)	1,1	2,8	1,0	1,0	1,5	0,007	0,002	0,070
Media (200ºC)	2,1	26,2	2,1	0,6	3,7	0,308	0,047	0,212
Alta (225ºC)	5,7	11,2	0,9	0,2	3,5	3,640	1,560	1,036

HMF: Hidrometilfurfural. OH benzoico: ácido benzoico.

3.2 Extracción con disolventes bio-basados.

El material explosionado del clon AF2 de *Populus x euramericana*, tratado a diferentes severidades, presentó compuestos inhibidores, los cuales pueden afectar negativamente a la eficacia de la hidrólisis enzimática posterior. Con el objetivo de mitigar este efecto, en el presente estudio se propuso la aplicación de una extracción sólido-líquido utilizando dos disolventes bio-basados: acetato de etilo (EA) y lactato de etilo (EL).

Además, como se ha mencionado en la parte introductoria de este apartado de resultados, se tratan de compuestos fenólicos que se pueden revalorizar como compuestos antioxidantes, lo que abre la posibilidad de una valorización dual de la biomasa. Por ello, las fracciones líquidas obtenidas tras las extracciones fueron analizadas para cuantificar el contenido total de compuestos fenólicos y su actividad antioxidante. Estos análisis permitieron evaluar tanto la eficacia extractiva como la selectividad de cada disolvente hacia este tipo de compuestos.

3.2.1 Contenido total de compuestos fenólicos.

En la Figura 1 se presenta el contenido total de compuestos fenólicos extraídos con acetato de etilo y lactato de etilo a partir de la biomasa explosionada a diferentes severidades. En general, ambos disolventes mostraron una capacidad extractiva similares en las condiciones de baja y media severidad. Sin embargo, a la mayor severidad (225 ºC), el acetato de etilo logró extraer una mayor cantidad de compuestos fenólicos que el lactato de etilo (62,58 y 56,77 mg GAE/g biomasa seca, respectivamente), lo que indica una mejor eficacia bajo condiciones de pretratamiento más intensas.

Asimismo, se observa una tendencia creciente en el contenido de fenoles extraídos a medida que aumenta la severidad del pretratamiento. Este comportamiento se puede asociar a una mayor rotura de la estructura lignocelulósica y a la consecuente degradación de hemicelulosas y lignina, que favorece la liberación de compuestos fenólicos solubles. Esta relación entre severidad del tratamiento y concentración de fenoles extraídos ha sido reportada previamente en la literatura [15,44,45].

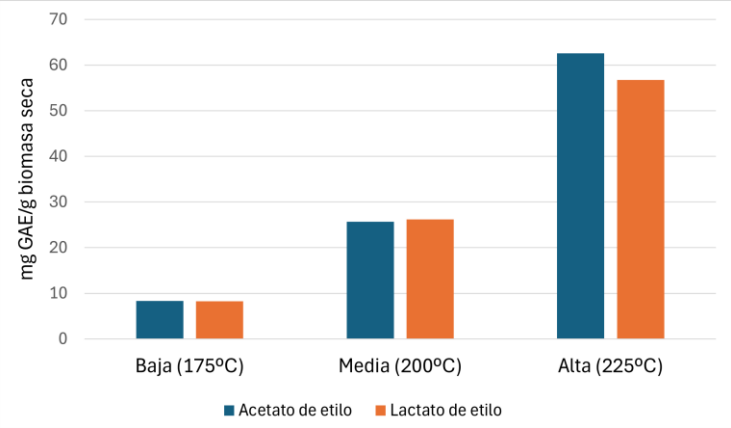


Figura 1. Contenido total de fenoles (CTF) expresado como mg GAE/g biomasa seca de los extractos obtenidos para cada disolvente bio-basado, tras explosionar el clon AF2 a diferentes temperaturas.

3.2.2 Actividad antioxidante.

La Figura 2 muestra la actividad antioxidante de los extractos obtenido mediante extracción sólido-líquido con acetato de etilo (EA) y lactato de etilo (EL), a partir de la biomasa explosionada bajo diferentes condiciones de severidad. En todos los casos, los extractos obtenidos con lactato de etilo presentaron una mayor capacidad antioxidante, expresada como equivalentes de Trolox por gramo de biomasa seca, indicando una mayor eficacia de este disolvente para recuperar compuestos con actividad antioxidante.

Además, se observó una tendencia clara de incremento en la actividad antioxidante con el aumento de la severidad del pretratamiento. En concreto, los valores aumentaron desde 0,007 y 0,011 mg Trolox/g biomasa seca a 175 ºC, hasta 0,032 y 0,038 mg Trolox/g biomasa seca a 225 ºC, para EA y EL, respectivamente. Esta tendencia está relacionada con la mayor liberación y disponibilidad de compuestos fenólicos, que se favorecen por la rotura estructural de la biomasa lignocelulósica a temperaturas más elevadas.

Cabe señalar que, para llevar a cabo una correcta cuantificación de la actividad antioxidante, los extractos fueron diluidos previamente a fin de ajustarse al rango de absorbancia lineal del patrón Trolox. Por ejemplo, en las condiciones menos severas (175 ºC), se empleó una disolución de 1:10, obteniéndose porcentajes de inhibición del 48,31% para EA y 80,17% para EL.

Por lo tanto, estos resultados indican que los compuestos fenólicos extraídos presentan una alta capacidad de actuar como agentes reductores de ABTS.

Estos resultados reflejan no solo la presencia de compuestos fenólicos con una alta capacidad reductora del radical ABTS, sino también el posible efecto sinérgico entre los distintos compuestos presentes en los extractos, particularmente en los obtenidos con el lactato de etilo, lo que podría explicar su mayor actividad antioxidante [46].

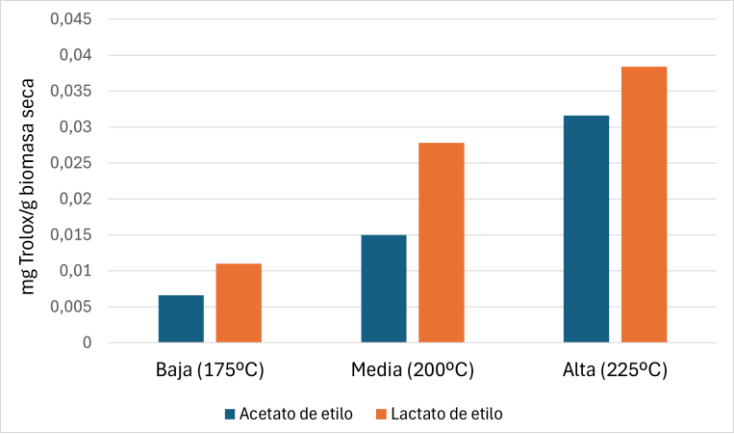


Figura 2. Actividad antioxidante expresado como mg Trolox/g biomasa seca de los extractos obtenidos para cada disolvente bio-basado, tras explosionar el clon AF2 a diferentes temperaturas.

3.3 Hidrólisis enzimática.

Tras realizar una desintoxicación del material explosionado mediante extracción sólido-líquido con disolventes bio-basados, se llevó a cabo la hidrólisis enzimática con el fin de maximizar la producción de azúcares fermentables. Como control, se realizó también la hidrólisis del material explosionado sin someterse a ningún tratamiento de extracción. Además, se compararon los efectos de realizar o no un lavado posterior a la extracción con disolventes, con el objetivo de evaluar si la presencia de trazas de estos compuestos afecta negativamente la actividad enzimática.

La eficacia del proceso se evaluó en función del contenido de glucosa producido durante el transcurso de la hidrólisis. Las Figuras 3, 4 y 5 presentan los resultados obtenidos, organizados en función de la severidad del pretratamiento y de la etapa de lavado posterior a la extracción con disolventes.

En todos los casos, se observó un aumento progresivo de la concentración de glucosa a lo largo del tiempo. En promedio, aproximadamente el 58% del rendimiento total de la hidrólisis (referido al valor de rendimiento a las 72h) se alcanzó en las primeras 24h, lo que indica una elevada actividad enzimática inicial [12,47]. Como tendencia general, la concentración de glucosa aumentó con la severidad del pretratamiento, lo cual está en concordancia con estudios previos [11,12].

En el caso específico del pretratamiento a baja severidad (175 ºC), como se puede observar en la Figura 3, la mayor concentración de glucosa a las 72h se obtuvo a partir del material explosionado que fue extraído con acetato de etilo y posteriormente lavado con agua, alcanzando un valor de 6,89 g L^{-1}. Este valor fue el único tratamiento que superó al obtenido para la muestra de control sin extracción, que alcanzó 5,64 g L^{-1}. En el resto de los casos, las concentraciones de glucosa fueron inferiores al control. Esto sugiere que, a bajas severidades, donde se generan menos productos de degradación, la extracción con acetato de etilo podría favorecer la disponibilidad del sustrato para las enzimas. En cambio, dicha mejora no se observó con el lactato de etilo.

Por otro lado, los casos en los que no se realizó un lavado posterior a la extracción mostraron una menor producción de glucosa en comparación con sus homólogos lavados. Esto indica que la presencia de trazas de disolventes inhibe la actividad enzimática, afectando negativamente el rendimiento del proceso. Esta observación coincide con la literatura, que recomienda eliminar los disolventes antes de la hidrólisis enzimática para evitar inhibiciones [10,48,49].

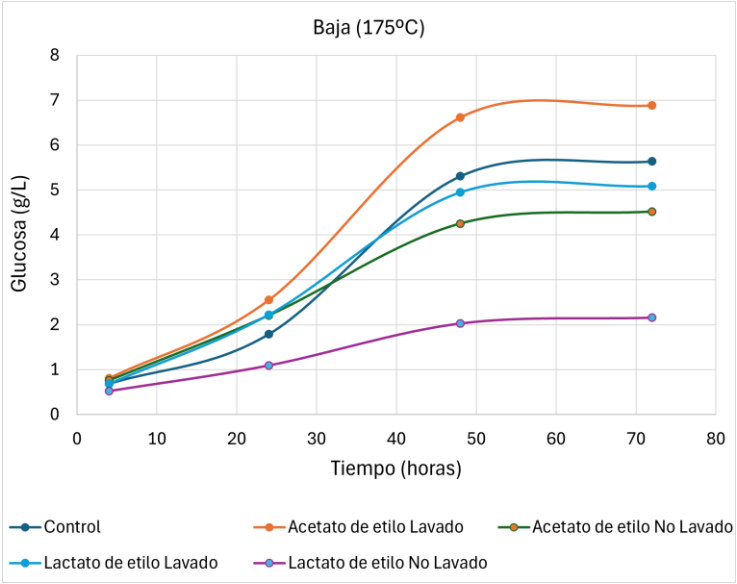


Figura 3. Producción de glucosa (g L^{-1}) a lo largo del tiempo en la hidrólisis enzimática de biomasa explosionada a 175 ºC.

En el caso del material explosionado a 200 ºC, se observa en la Figura 4 que las concentraciones de glucosas son superiores cuando la biomasa se se somete a una extracción con disolvente seguida de un lavado, en comparación con el control (biomasa explosionada sin extracción). La mayor generación de glucosa se obtuvo tras la extracción de compuestos fenólicos con acetato de etilo, alcanzando los 30,06 g L^{-1} a las 72h. En cambio, el control solo alcanzó 15,95 g L^{-1} en el mismo tiempo, lo que supone una mejora de 1,9 veces en la producción de glucosa.

Li et al. [50] también observaron una mejora en la hidrólisis enzimática al incorporar una etapa de extracción con acetato de etilo tras un pretratamiento de explosión de vapor del bagazo de caña azúcar, incrementando la producción de glucosa 1,3 veces y el rendimiento de etanol en un 8,78%.

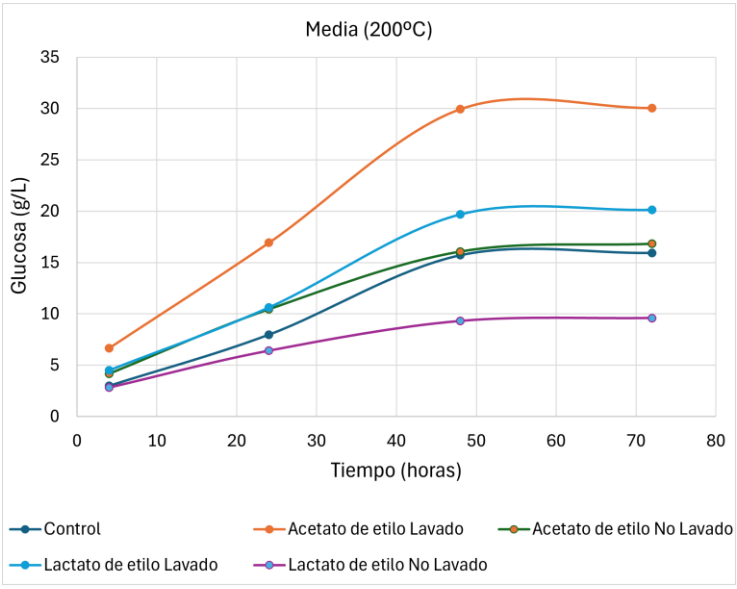


Figura 4. Producción de glucosa (g L^{-1}) a lo largo del tiempo en la hidrólisis enzimática de biomasa explosionada a 200 ºC.

Al igual que en el caso del pretratamiento a baja severidad, la etapa de lavado posterior a la extracción favorece la actividad enzimática. No obstante, en este caso, la extracción con acetato de etilo sin el lavado mostró una concentración de glucosa similar a la del control.

Por último, en el caso del pretratamiento a 225 ºC (Figura 5), todos los tratamientos, excepto la extracción con lactato de etilo sin lavado, mostraron una mayor producción de glucosa en comparación con el control. Tanto el acetato de etilo como el lactato de etilo, cuando se aplicó una etapa de lavado posterior, alcanzaron concentraciones de glucosa entorno a los 36 g L^{-1} a las 72h, siendo ligueramente superior el resultado obtenido con acetato de etilo. En cambio, el control (sin extracción) alcanzó una concentración de 26,07 g L^{-1}, lo que representa una mejora de aproximadamente 1,4 veces.

Estos resultados indican que, bajo las condiciones más severas de pretratamiento, se consigue el mayor rendimiento absoluto de glucosa. Sin embargo, la mayor mejora relativa en comparación con el control se produjo en las condiciones intermedias con la extracción mediante acetato de etilo.

Una vez más, se corrobora la importancia de incorporar una etapa de lavado posterior a la extracción con disolventes. En todos los casos, la ausencia de lavado resultó en menores concentraciones de glucosa, lo que sugiere que las trazas residuales de disolvente afectan negativamente la actividad enzimática.

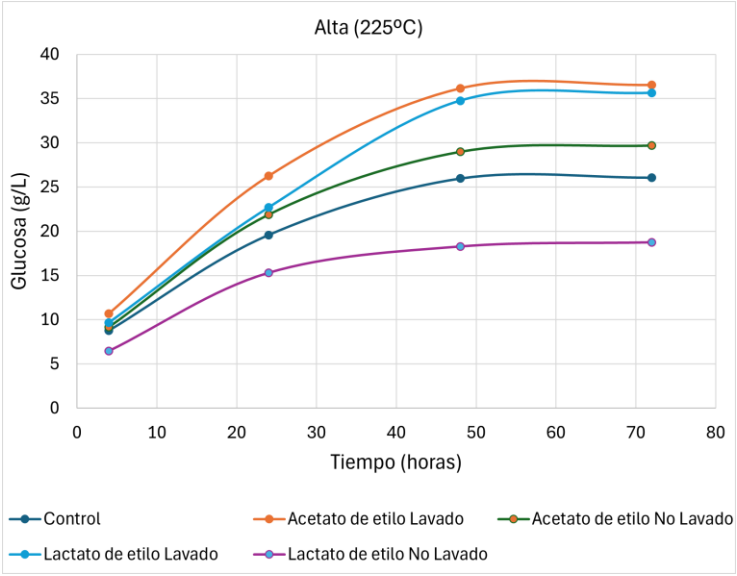


Figura 5. Producción de glucosa (g L^{-1}) a lo largo del tiempo en la hidrólisis enzimática de biomasa explosionada a 200 ºC.

4 Conclusiones.

Los resultados obtenidos demuestran que la incorporación de una etapa de extracción con disolventes verdes tras el pretratamiento por explosión de vapor mejora significativamente la eficacia de la hidrólisis enzimática de la biomasa lignocelulósica. En particular, el acetato de etilo mostró un mayor potencial para mejorar la digestibilidad enzimática, especialmente cuando se aplicó una etapa de lavado con agua posterior, permitiendo alcanzar rendimientos de glucosa superiores al control en todas las condiciones de severidad evaluadas.

Se destaca que el mayor rendimiento absoluto de glucosa se logró con el pretratamiento más severo (225 ºC), alcanzando valores cercanos a 36 g L^{-1} con ambos disolventes. Sin embargo, la mejora relativa más destacada respecto al control se observó a una severidad media (200 ºC), donde la extracción con acetato de etilo casi duplicó la producción de glucosa.

Los resultados también subrayan la importancia de realizar una etapa de lavado posterior a la extracción, ya que la presencia de trazas de disolvente en la biomasa puede inhibir parcialmente la actividad enzimática.

Estos hallazgos no solo contribuyen a mejorar la eficiencia del proceso de hidrólisis enzimática, sino que también apoyan el desarrollo de biorrefinerías sostenibles, al permitir la recuperación simultánea de compuestos fenólicos con actividad antioxidante, favoreciendo así un enfoque integral dentro de la economía circular.

Referencias

[1] F. Carvalheiro, L.C. Duarte, F.M. Gírio, Hemicellulose biorefineries: a review on biomass pretreatments, J Sci Ind Res (India) (2008) 849–864.

[2] P. Alvira, E. Tomás-Pejó, M. Ballesteros, M.J. Negro, Pretreatment technologies for an efficient bioethanol production process based on enzymatic hydrolysis: A review, Bioresour Technol 101 (2010) 4851–4861. https://doi.org/10.1016/j.biortech.2009.11.093.

[3] P. Sannigrahi, A.J. Ragauskas, G.A. Tuskan, Poplar as a feedstock for biofuels: a review of compositional characteristics, Biofuels, Bioproducts and Biorefining 4 (2010) 209–226. https://doi.org/10.1002/bbb.206.

[4] X. Zhao, L. Zhang, D. Liu, Biomass recalcitrance. Part II: Fundamentals of different pre-treatments to increase the enzymatic digestibility of lignocellulose, Biofuels, Bioproducts and Biorefining 6 (2012) 561–579. https://doi.org/10.1002/bbb.1350.

[5] A.K. Kumar, S. Sharma, Recent updates on different methods of pretreatment of lignocellulosic feedstocks: a review, Bioresour Bioprocess 4 (2017) 7. https://doi.org/10.1186/s40643-017-0137-9.

[6] H. Wang, Z. Liu, X. Zheng, X. Pan, L. Hui, J. Li, H. Zhang, Assessment on temperature-pressure severally controlled explosion pretreatment of poplar, Carbohydr Polym 230 (2020) 115622. https://doi.org/10.1016/J.CARBPOL.2019.115622.

[7] N. Sjulander, T. Kikas, Origin, impact and control of lignocellulosic inhibitors in bioethanol production—A review, Energies (Basel) 13 (2020) 4751. https://doi.org/10.3390/en13184751.

[8] H. Xu, J. Peng, Y. Kong, Y. Liu, Z. Su, B. Li, X. Song, S. Liu, W. Tian, Key process parameters for deep eutectic solvents pretreatment of lignocellulosic biomass materials: A review, Bioresour Technol 310 (2020) 123416. https://doi.org/10.1016/J.BIORTECH.2020.123416.

[9] J.D. McMillan, Pretreatment of lignocellulosic biomass, (1994).

[10] R. Cañadas, R. Martín-Sampedro, M. González-Miquel, E.J. González, I. Ballesteros, M.E. Eugenio, D. Ibarra, Green solvents extraction-based detoxification to enhance the enzymatic hydrolysis of steam-exploded lignocellulosic biomass and recover bioactive compounds, J Environ Manage 344 (2023). https://doi.org/10.1016/j.jenvman.2023.118448.

[11] A. Antczak, J. Szadkowski, D. Szadkowska, J. Zawadzki, Assessment of the effectiveness of liquid hot water and steam explosion pretreatments of fast-growing poplar (Populus trichocarpa) wood, Wood Sci Technol (2022) 1–23. https://doi.org/10.1007/s00226-021-01350-1.

[12] E. Ruiz, C. Cara, P. Manzanares, M. Ballesteros, E. Castro, Evaluation of steam explosion pre-treatment for enzymatic hydrolysis of sunflower stalks, Enzyme Microb Technol 42 (2008) 160–166. https://doi.org/10.1016/J.ENZMICTEC.2007.09.002.

[13] J. Li, G. Henriksson, G. Gellerstedt, Carbohydrate reactions during high-temperature steam treatment of aspen wood, Appl Biochem Biotechnol 125 (2005) 175–188. https://doi.org/10.1385/ABAB:125:3:175.

[14] R. Martín-Sampedro, M.E. Eugenio, J.C. García, F. Lopez, J.C. Villar, M.J. Diaz, Steam explosion and enzymatic pre-treatments as an approach to improve the enzymatic hydrolysis of Eucalyptus globulus, Biomass Bioenergy 42 (2012) 97–106. https://doi.org/10.1016/J.BIOMBIOE.2012.03.032.

[15] E. Castro, E. Conde, A. Moure, E. Falqué, C. Cara, E. Ruiz, H. Domínguez, Antioxidant activity of liquors from steam explosion of Olea europea wood, Wood Sci Technol 42 (2008) 579–592. https://doi.org/10.1007/s00226-007-0169-y.

[16] M. Moniruzzaman, Effect of steam explosion on the physicochemical properties and enzymatic saccharification of rice straw, Appl Biochem Biotechnol 59 (1996) 283–297. https://doi.org/10.1007/BF02783570.

[17] B.K. Avellar, W.G. Glasser, Steam-assisted biomass fractionation. I. Process considerations and economic evaluation, Biomass Bioenergy 14 (1998) 205–218. https://doi.org/10.1016/S0961-9534(97)10043-5.

[18] C. Tengborg, M. Galbe, G. Zacchi, Reduced inhibition of enzymatic hydrolysis of steam-pretreated softwood, Enzyme Microb Technol 28 (2001) 835–844. https://doi.org/10.1016/S0141-0229(01)00342-8.

[19] S. Ando, I. Arai, K. Kiyoto, S. Hanai, Identification of aromatic monomers in steam-exploded poplar and their influences on ethanol fermentation by Saccharomyces cerevisiae, Journal of Fermentation Technology 64 (1986) 567–570. https://doi.org/10.1016/0385-6380(86)90084-1.

[20] J.M. Oliva, F. Sáez, I. Ballesteros, A. González, M.J. Negro, P. Manzanares, M. Ballesteros, Effect of lignocellulosic degradation compounds from steam explosion pretreatment on ethanol fermentation by thermotolerant yeast Kluyveromyces marxianus, in: Biotechnology for Fuels and Chemicals: The Twenty-Fourth Symposium, Springer, 2003: pp. 141–153. https://doi.org/10.1007/978-1-4612-0057-4_11.

[21] H. Guo, Y. Zhao, J.S. Chang, D.J. Lee, Inhibitor formation and detoxification during lignocellulose biorefinery: A review, Bioresour Technol 361 (2022) 127666. https://doi.org/10.1016/J.BIORTECH.2022.127666.

[22] J. Li, J. Lin, W. Xiao, Y. Gong, M. Wang, P. Zhou, Z. Liu, Solvent extraction of antioxidants from steam exploded sugarcane bagasse and enzymatic convertibility of the solid fraction, Bioresour Technol 130 (2013) 8–15. https://doi.org/10.1016/J.BIORTECH.2012.11.143.

[23] W. Wang, D.J. Lee, Lignocellulosic biomass pretreatment by deep eutectic solvents on lignin extraction and saccharification enhancement: A review, Bioresour Technol 339 (2021) 125587. https://doi.org/10.1016/J.BIORTECH.2021.125587.

[24] V. Sharma, M.L. Tsai, C.W. Chen, P.P. Sun, A.K. Patel, R.R. Singhania, P. Nargotra, C. Di Dong, Deep eutectic solvents as promising pretreatment agents for sustainable lignocellulosic biorefineries: A review, Bioresour Technol 360 (2022) 127631. https://doi.org/10.1016/J.BIORTECH.2022.127631.

[25] T. Welton, Solvents and sustainable chemistry, Proceedings of the Royal Society A: Mathematical, Physical and Engineering Sciences 471 (2015) 20150502. https://doi.org/10.1098/rspa.2015.0502.

[26] T. Jiao, X. Qin, H. Zhang, W. Zhang, Y. Zhang, P. Liang, Separation of phenol and pyridine from coal tar via liquid–liquid extraction using deep eutectic solvents, Chemical Engineering Research and Design 145 (2019) 112–121. https://doi.org/10.1016/j.cherd.2019.03.006.

[27] A.P. Abbott, G. Capper, D.L. Davies, R.K. Rasheed, V. Tambyrajah, Novel solvent properties of choline chloride/urea mixtures, Chemical Communications (2003) 70–71. https://doi.org/10.1039/B210714G.

[28] A.P. Abbott, D. Boothby, G. Capper, D.L. Davies, R.K. Rasheed, Deep eutectic solvents formed between choline chloride and carboxylic acids: versatile alternatives to ionic liquids, J Am Chem Soc 126 (2004) 9142–9147. https://doi.org/10.1021/ja048266j.

[29] B. Sáenz de Miera, R. Cañadas, R. Santiago, I. Díaz, M. González-Miquel, E.J. González, A pathway to improve detoxification processes by selective extraction of phenols and sugars from aqueous media using sustainable solvents, Sep Purif Technol 299 (2022) 121675. https://doi.org/10.1016/J.SEPPUR.2022.121675.

[30] B. Gullón, A. Muñiz-Mouro, T.A. Lú-Chau, M.T. Moreira, J.M. Lema, G. Eibes, Green approaches for the extraction of antioxidants from eucalyptus leaves, Ind Crops Prod 138 (2019) 111473. https://doi.org/10.1016/J.INDCROP.2019.111473.

[31] N.S. Ab Rasid, A. Shamjuddin, A.Z. Abdul Rahman, N.A.S. Amin, Recent advances in green pre-treatment methods of lignocellulosic biomass for enhanced biofuel production, J Clean Prod 321 (2021) 129038. https://doi.org/10.1016/J.JCLEPRO.2021.129038.

[32] C. Breil, A. Meullemiestre, M. Vian, F. Chemat, Bio-based solvents for green extraction of lipids from oleaginous yeast biomass for sustainable aviation biofuel, Molecules 21 (2016) 196. https://doi.org/10.3390/molecules21020196.

[33] TAPPI T222 om-11, Acid-insoluble lignin in wood and pulp. TAPPI Press, Atlanta, GA., (2011).

[34] TAPPI T249 cm-09, Carbohydrate composition of extractive-free wood and wood pulp by gas-liquid chromatography. TAPPI Press, Atlanta, GA., (2009).

[35] TAPPI T257 cm-85, Sampling and preparing wood for analysis. TAPPI Press, Atlanta, GA., (1999).

[36] TAPPI 211 om-02, Ash in wood, pulp, paper and paperboard: combustion at 525°C. TAPPI Press, Atlanta, GA., (2002).

[37] M. Ballesteros, J.M. Oliva, M.J. Negro, P. Manzanares, I. Ballesteros, Ethanol from lignocellulosic materials by a simultaneous saccharification and fermentation process (SFS) with Kluyveromyces marxianus CECT 10875, Process Biochemistry 39 (2004) 1843–1848. https://doi.org/10.1016/J.PROCBIO.2003.09.011.

[38] I.S.O. ISO, 14502-1. Determination of substances characteristic of green and black tea-Part 1: Content of total polyphenols in tea-colorimetric method using Folin-Ciocalteu reagent, (2005).

[39] R. Re, N. Pellegrini, A. Proteggente, A. Pannala, M. Yang, C. Rice-Evans, Antioxidant activity applying an improved ABTS radical cation decolorization assay, Free Radic Biol Med 26 (1999) 1231–1237. https://doi.org/10.1016/S0891-5849(98)00315-3.

[40] S.J. Horn, V.G.H. Eijsink, Enzymatic hydrolysis of steam-exploded hardwood using short processing times, Biosci Biotechnol Biochem 74 (2010) 1157–1163. https://doi.org/10.1271/bbb.90762.

[41] A. Antczak, J. Szadkowski, M. Marchwicka, F. Akus-Szylberg, O. Bytner, J. Zawadzki, The study of chemical composition and enzymatic hydrolysis efficiency of poplar wood (Populus deltoides x maximowiczii) after steam explosion pretreatment, Ann WULS-SGGW for Wood Technol 104 (2018) 139–146.

[42] C. Cara, E. Ruiz, I. Ballesteros, M.J. Negro, E. Castro, Enhanced enzymatic hydrolysis of olive tree wood by steam explosion and alkaline peroxide delignification, Process Biochemistry 41 (2006) 423–429. https://doi.org/10.1016/J.PROCBIO.2005.07.007.

[43] L.J. Jönsson, C. Martín, Pretreatment of lignocellulose: Formation of inhibitory by-products and strategies for minimizing their effects, Bioresour Technol 199 (2016) 103–112. https://doi.org/10.1016/J.BIORTECH.2015.10.009.

[44] Ö. Seçmeler, Ö. Güçlü Üstündağ, J. Fernández-Bolaños, G. Rodríguez-Gutiérrez, Effect of subcritical water and steam explosion pretreatments on the recovery of sterols, phenols and oil from olive pomace, Food Chem 265 (2018) 298–307. https://doi.org/10.1016/J.FOODCHEM.2018.05.088.

[45] E. Conde, C. Cara, A. Moure, E. Ruiz, E. Castro, H. Domínguez, Antioxidant activity of the phenolic compounds released by hydrothermal treatments of olive tree pruning, Food Chem 114 (2009) 806–812. https://doi.org/10.1016/J.FOODCHEM.2008.10.017.

[46] E. Conde, A. Moure, H. Domínguez, J.C. Parajó, Production of antioxidants by non-isothermal autohydrolysis of lignocellulosic wastes, LWT - Food Science and Technology 44 (2011) 436–442. https://doi.org/10.1016/J.LWT.2010.08.006.

[47] T. Jeoh, F.A. Agblevor, Characterization and fermentation of steam exploded cotton gin waste, Biomass Bioenergy 21 (2001) 109–120. https://doi.org/10.1016/S0961-9534(01)00028-9.

[48] Y. Sun, J. Cheng, Hydrolysis of lignocellulosic materials for ethanol production: a review, Bioresour Technol 83 (2002) 1–11. https://doi.org/10.1016/S0960-8524(01)00212-7.

[49] A. Kumar, K. Dhar, S.S. Kanwar, P.K. Arora, Lipase catalysis in organic solvents: advantages and applications, Biol Proced Online 18 (2016) 1–11. https://doi.org/10.1186/s12575-016-0033-2.

[50] J. Li, K. Wu, W. Xiao, J. Zhang, J. Lin, Y. Gong, Z. Liu, Effect of antioxidant extraction on the enzymatic hydrolysis and bioethanol production of the extracted steam-exploded sugarcane bagasse, Biochem Eng J 82 (2014) 91–96. https://doi.org/10.1016/J.BEJ.2013.11.005.

3.5. Análisis de la influencia del origen de la biomasa y los métodos de fraccionamiento en la pirólisis de las principales fracciones lignocelulósicas.

Los resultados obtenidos en este trabajo se detallan en la publicación: **Assessing the influence of biomass origin and fractionation methods on pyrolysis of primary biomass fractions.** N. Almagro-Herrera, S. Lozano-Calvo, A. Palma, J.C. García and M.J. Díaz. Fuel 367 (2024) 131501. (**Publicación 4**).

A continuación, se presenta una contextualización y un resumen de los principales hallazgos de este estudio.

En un contexto de creciente demanda de soluciones energéticas sostenibles, el proceso termoquímico de pirólisis se ha revelado como una tecnología prometedora para el aprovechamiento eficiente de la biomasa lignocelulósica, contribuyendo a la reducción de la dependencia de los combustibles fósiles. Este proceso permite la obtención de una amplia variedad de productos de alto valor añadido, lo que resalta su relevancia en las investigaciones actuales.

El comportamiento de la biomasa lignocelulósica durante la pirólisis está determinada por el tipo y la composición de la materia prima, lo que tiene un impacto significativo en la tasa de conversión y la eficiencia del proceso. Cada una de las fracciones que componen la biomasa presentan propiedades físicas y termoquímicas diversas, lo que influye en el desarrollo del proceso de pirólisis.

Entre las variables operativas clave de la pirólisis destacan la temperatura y la energía de activación, las cuales dependen de la composición específica de la biomasa. Por ello, comprender la influencia de la composición sobre la cinética del proceso es crucial, resultando esencial examinar y entender los mecanismos subyacentes que determinan este proceso.

El objetivo principal de este estudio es evaluar comparativamente la pirólisis de las principales fracciones de la biomasa lignocelulósica (celulosa, hemicelulosa y lignina), considerando distintos orígenes (arbórea, arbustiva y herbácea) y métodos de fraccionamiento (EAF, Kraft y Sosa-antraquinona). Se analizó la cinética del proceso, la evolución de la energía de activación y la composición de los gases generados.

Las materias primas seleccionadas fueron: *Populus x euramericana* (clon AF2) como representante de biomasa frondosa, *Chamaecytisus proliferus* (Tagasaste) como biomasa arbustiva y la paja de trigo como residuo agrícola. El interés de los dos primeros se debe a que son especies de alto rendimiento, por lo que presentan potencial para el suministro de biomasa.

Para la obtención de las fracciones principales de cada biomasa, primero se realizó una extracción alcalina en frío para la separación de las hemicelulosas. Posteriormente, se aplicaron dos métodos de deslignificación para la obtención de celulosa en el sólido y lignina en el licor negro: Kraft y sosa-antraquinona.

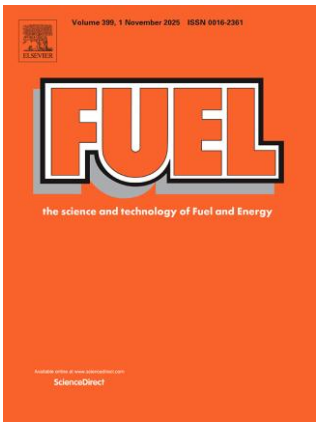
Las fracciones obtenidas fueron analizadas mediante termogravimetría (TGA) para cuantificar su grado de conversión y determinar la energía de activación en función del grado de conversión, mediante los modelos cinéticos diferenciales de Friedman y el método integral de Flynn-Wall-Ozawa (FWO). Finalmente, las muestras de gas generadas durante la pirólisis fueron recogidas a través de tubos de adsorción y analizadas por cromatografía de gases acoplada a espectrometría de masas (GC-MS).

Los resultados revelaron que la energía de activación está influenciada por múltiples factores, entre ellos el método de fraccionamiento y el origen de la biomasa. En particular, la hemicelulosa presentó valores de E_a en el rango de 200-300 kJ mol^{-1}, mientras que la celulosa presentó valores alrededor de 180-220 kJ mol^{-1}. Por el contrario, la lignina exhibió una mayor variabilidad en la E_a, siendo especialmente sensibles al método de fraccionamiento aplicado. En cuanto a los modelos cinéticos evaluados, el método integral de FWO se identificó como el más eficiente.

PUBLICACIÓN 4.

Assessing the influence of biomass origin and fractionation methods on pyrolysis of primary biomass fractions.

N. Almagro-Herrera, S. Lozano-Calvo, A. Palma, J.C. García and M.J. Díaz.



Fuel
Elsevier
Volumen: 367, 131501 (2024)
DOI: 10.1016/j.fuel.2024.131501

Categoría	Clasificación revista/Número total de revistas	Cuartil (Porcentaje)
Ingeniería Química	23/170	Q1 (86,8%)
Energía y combustibles	46/171	Q2 (73,4%)
Factor de impacto	6,7	

Assessing the Influence of Biomass Origin and Fractionation Methods on Pyrolysis of Primary Biomass Fractions.

Almagro-Herrera, N.[a]; Lozano-Calvo, S.[a*]; Palma, A.[a]; García, J.C.[a]; Díaz, M.J.[a]

*Corresponding author: susana.lozano@diq.uhu.es

[a]Research Centre for Technology of Products and Chemical Processes (PRO²TECS), Department of Chemical Engineering, University of Huelva, Av. 3 de marzo s/n, 21071 Huelva, Spain.

Abstract.

Pyrolysis has emerged as a highly promising technology for the efficient utilization of organic materials, particularly lignocellulosic materials. This study investigates the behavior and influence of three primary biomass fractions (cellulose, hemicellulose, and lignin) derived from different sources (trees, shrubs, and agricultural residues) on the kinetic of the pyrolysis process. With this objective, different fragmentation methods were employed to isolate the main components of the lignocellulosic biomass, followed by thermogravimetric analysis to examine the pyrolysis process. The activation energy was determined using both, the Friedman differential kinetic models of and the Flynn-Wall-Ozawa integrated method, with the latter being found to be more efficient. The activation energy (E_a) was found to be influenced by several factors, including the fractionation process and the origin of the raw material. For hemicellulose, the E_a was in the range of 200-300 kJ mol^{-1}, while cellulose showed E_a values of about 180-220 kJ mol^{-1}. In contrast, lignin displayed a wider range of E_a variation, with its values being more sensitive to the fractionation method used. Gas samples were collected through adsorption tubes during pyrolysis for analysis of gas stream compositions from different lignocellulosic fractions using gas chromatography/mass spectrometry. Furfural, among other compounds, was predominantly detected in the pyrolysis of hemicellulose fractions, ranging from 6.6% to 19.3%.

Keyword: Activation energy, Fractionation methods, Lignocellulosic biomass, Pyrolysis gases, TD/GC-MS.

1 Introduction.

Biomass can be used as an alternative to fossil fuels to reduce greenhouse gas emissions and promote sustainable development [1]. One of the most promising uses is to produce fuels such as bio-oil, renewable diesel, methane, and hydrogen through processes such as pyrolysis and hydrotreatment [2]. Biomass can also be used to produce a range of valuable chemicals, materials and products through biorefineries, similar to oil refineries and petrochemical plants [3]. These processes have both positive and negative ecological impacts, and therefore need to be optimized from both a technical and economic point of view [4,5].

https://doi.org/10.1016/j.fuel.2024.131501

In this context, in order to successfully achieve biomass valorisation, there are several needs that must be addressed, among which stand out (i) the optimisation of pre-treatments due to the fact that biomass is a complex and recalcitrant material that must undergo pre-treatment to decompose its structure and make it more accessible to conversion processes [6]; (ii) the selection of the optimal valorisation technology depending on the characteristics of the biomass [7,8]; and (iii) the proper integration of the technology used with existing industries such as agriculture, forestry and biorefineries. This approach can also contribute to the creation of a circular economy in which waste materials are transformed into valuable products [9].

There are numerous technologies for biomass valorisation, such as direct combustion, biochemicals such as fermentation or anaerobic digestion, and thermochemical including pyrolysis, gasification, or hydrothermal liquefaction. Among them, pyrolysis is an efficient thermochemical process that can convert biomass into pyrolytic gas, bio-oil and solid biochar, meeting the requirements mentioned above [10,11]. In general, the pyrolysis process involves heating biomass in the absence of oxygen to temperatures between 300 and 800 °C. In addition, the pyrolysis process can be easily integrated with other biomass valorisation processes, such as anaerobic digestion, to increase the overall biomass conversion efficiency [12].

The kinetics of the pyrolysis process, regulated by reaction rate, temperature, and residence time, must be carefully controlled to optimize the yield and quality of the pyrolysis products. Biomass composition, primarily comprising cellulose, hemicelluloses, and lignin, has a significant influence on pyrolysis rate and efficiency [13]. These polymers have different physical behavior and thermochemical properties depending on feedstock, biomass, and other required properties [14]. Furthermore, significant variations in biomass behavior during pyrolysis arise from differences in the structure and chemistry of polymers, resulting in different decomposition ratios, temperatures, and forms [15]. The operating variables of the pyrolysis process must be carefully controlled to optimize its efficiency. For example, higher temperatures tend to increase the yield of gaseous products, whereas lower temperatures favor the production of liquid bio-oil [16]. Similarly, longer residence times result in higher char yield, while shorter residence times enhance the yield of gaseous and liquid products [17]. In pyrolysis, the key operating variables are the temperature and the activation energy, which vary depending on the biomass components. Some studies suggest that the activation energy depends on the degree of polymerisation of the components [13].

Consequently, understanding the influence of biomass composition and pyrolysis process kinetics are critical factors. In this sense, the relative influence of each of the fractions on the kinetics of the process, and therefore on the products generated, has not been studied in depth. Some articles with

https://doi.org/10.1016/j.fuel.2024.131501

pure compounds have been found [16,18–20], but no comparison of the comparative influence between different types of cellulose, hemicelluloses and lignin has been made.

In order to understand the impact of each major fraction lignocellulosic biomass, it is essential to fragment the biomass. Various treatments can be used sequentially for this purpose. One such treatment is cold alkaline extraction, which offers operational and environmental advantages as it operates below 40 ºC [21]. Other methods that can be utilized include the kraft and soda-anthraquinone processes to obtain the cellulosic and lignocellulosic fraction. The kraft process, a traditional and widely used method, solubilizes more than half of the hemicelluloses and almost all of the lignin from the fibers, while the cellulose undergoes partial degradation without dissolution, leading to an increase in its crystallinity degree [22–24]. Alternatively, soda-anthraquinone, serves as an alkaline, non-sulphur alternative to the kraft process. However, the cellulose pulp produced by the soda-anthraquinone process has lower strength compared to kraft [25].

The aim of this study is, therefore, to explore the comparative valorization of the pyrolysis (kinetic, and gasses) of the main biomass fractions (cellulose, hemicellulose, lignin) with different characteristics and origins (tree, shrub, agricultural residue) and under different types of fractionations (kraft and soda-anthraquinone), focusing on its potential applications.

2 Materials and Methods.

2.1 Materials.

Three types of biomasses with different characteristics and compositions have been evaluated. *Populus x-Euramericana* clone AF2 (Poplar) as a tree, Tagasaste as a shrub (because both are high-yielding species) and Wheat Straw as agroforestry waste have been selected. The Agroforestry Department of University of Huelva has supplied these raw materials. For all the raw materials studied, the initial conditioning consists of a mechanical treatment based on the reduction of the sliver size that runs on a disposer conventional (Mill Retsch) with a sieve of mesh size 20 mm and, later, sieved to obtain the length and width average of chips between 1-3 cm and 0.5 cm, respectively. Finally, the chips are stored at room temperature to maintain a constant moisture level and then packed in airtight containers. The main chemical characteristics of the materials used in Table 1 are shown, and the main parameters of industrial interest and elemental analysis of the biomasses under study in Table 2 are shown.

https://doi.org/10.1016/j.fuel.2024.131501

Table 1. Chemical characterization of studied raw materials.

Characterization/Raw Material	Poplar	Tagasaste	Wheat Straw
Removable in ethanol (% p/p)	12.13 ± 1.32	11.36 ± 1.10	20.35 ± 4.23
Glucan (% p/p)	40.31 ± 5.15	41.42 ± 4.02	34.12 ± 6.86
Xylan (% p/p)	19.35 ± 1.04	18.56 ± 1.25	14.33 ± 4.14
Araban (% p/p)	0.23 ± 0.15	0.65 ± 0.21	2.35 ± 0.15
Acetyl Groups (% p/p)	2.88 ± 0.39	3.31 ± 0.17	2.12 ± 0.17
Lignin Klason (% p/p)	19.53 ± 1.65	20.1 ± 1.72	21.62 ± 2.38
Ash (% p/p)	1.4 ± 1.41	0.8 ± 0.90	4.02 ± 0.31

Table 2. Proximate, ultimate and calorific values for studied biomasses.

	Proximate[a]		Ultimate[b]			Calorimetry[c]
	Volatile (%)	**Fixed Carbon** (%)	**H** (%)	**C** (%)	**N** (%)	**HHV** (MJ/kg)
Poplar	85.61 ± 2.3	12.30 ± 0.4	6.21 ± 0.2	48.68 ± 0.7	1.05 ± 0.1	14.35 ± 1.2
Tagasaste	78.84 ± 1.9	18.65 ± 0.8	6.58 ± 0.2	47.31 ± 0.9	4.23 ± 0.1	16.27 ± 1.5
Wheat Straw	73.55 ± 1.2	15.21 ± 0.5	5.41 ± 0.2	43.16 ± 0.6	0.30 ± 0.1	16.82 ± 1.3

[a]Proximate analysis was done according to ASTM D5142-09.

[b]Ultimate analysis was conducted using a modified ASTM D5373-10 method.

[c]Heating value (HHV) were determined with a calorimeter using ASTM D5865-10.

2.2 Biomass Treatments.

Three replicates for each of the tested treatments have been performed.

2.2.1 Alkali Pretreatment: Hemicellulose extraction.

Alkaline pretreatments are used in biorefinery for delignification to improve the accessibility and digestibility of polysaccharides as a step before enzymatic hydrolysis or microbial digestion [26]. Among the alkaline treatments, cold alkaline extraction (CAE) is widely used. This operation breaks down the biomass into hemicelluloses and soluble lignins in alkali and waste through the separation of heteropolysaccharides polymer of the fiber source. In this way, it facilitates the use of these components in higher value products with minimal chemical and physical changes. In this case, the hemicelluloses are extracted from the biomass in the liquor with a polymeric structure without significant degradation [27,28]. The used conditions were: 40 ºC operating temperature; 90 min operating time and 100 $g.L^{-1}$ alkali concentration for Wheat Straw [27] and 120 $g.L^{-1}$ for Tagasaste and Poplar [29]. The difference lies in the type of lignocellulosic biomass. Wheat is herbaceous and has a greater capacity for hemicelluloses extraction, while the nature of the others requires a higher alkali concentration to extract the hemicelluloses. The resulting solid from the cold alkaline extraction is repeatedly washed with water to remove any traces of NaOH according to TAPPI standard T264 cm-07 [30].

https://doi.org/10.1016/j.fuel.2024.131501

2.2.2 Delignification Kraft treatment.

The solid obtained is the cellulose-rich pre-treatment and contains most of the lignin from the biomass. The kraft process is currently the dominant delignification method for paper pulp production due to its advantages over other methods for the same purpose [31]. The operating conditions for a batch pulp mill were as follows: a liquid to solid ratio of 3.5; a sulphide content of 25%, a cooking temperature of 165 ºC and a cooking time of 50 minutes [32].

2.2.3 Delignification soda-anthraquinone treatment.

Among the alternative methods, the most widely used is an alkaline (NaOH), sulphur-free process using anthraquinone (AQ) as a catalyst. The cellulose obtained is more difficult to bleach and has poorer resistance properties than that obtained by the kraft process [33]. For this delignification process, 13% active alkali; a temperature of 143 ºC and a time of 90 minutes for all the biomasses studied [32] has been used.

2.2.4 Chemical analysis.

The standards: TAPPI T264 [30] to determine the moisture content of the raw material; TAPPI T204 [33] standard to measure extractable compounds such as hydrocarbons, non-volatile low molecular weight carbohydrates, phytosterols, salts, waxes, polyphenols, resins, fats and other compounds; TAPPI T222 [34] for the quantitative determination of monomeric compounds and lignin and TAPPI T249 [35] to the determination of monomeric sugars, i.e. xylose, glucose and arabinose, acetic acid and possibly 5-hydroxymethylfurfural and furfural by HPLC, have been successfully used.

2.3 Thermogravimetric analysis.

The thermogravimetric experiments applied to each of the different biomasses and fractions studied were carried out on the Mettler Toledo TGA/DSC1 STARe system. The samples of the different starting materials were previously ground and homogenized. In the pyrolysis experiments, nitrogen was used as an inert gas to avoid secondary reactions. The pyrolysis processes were carried out in two steps: (i) heating the sample from 25 to 105 °C with a heating rate of 15°C min-1 and an inert nitrogen atmosphere with a flow rate of 15 mL min^{-1}; (ii) heating from 105 to 800 °C with different heating rates (5, 10, 15, 20 and 25 °C min^{-1}) with a nitrogen flow rate of 30 mL min-1. The initial sample mass was approximately 10 mg in all cases and the experiments were carried out in triplicate and the mean values recorded.

2.4 Kinetic models.

Iso-conversional kinetic methods are those in which the variation of the activation energy is estimated as a function of the conversion degree. These models are of great importance in systems where there is a variation of the activation energy as a function of the conversion degree. This type

https://doi.org/10.1016/j.fuel.2024.131501

of method is particularly useful for biomass, which degrades at different temperatures due to the diverse and heterogeneous nature of its components [36]. Within this type, there are two groups: differential methods and integral methods [37]. These models are used to determine the kinetic parameters of the reaction by using the Arrhenius equation (Eq. 1), and that all the reactions are of order 1, because there is an excess of the sample, in these models are assumed.

$$k(T) = A\, e^{\left(\frac{-E_a}{RT}\right)} \qquad (1)$$

Where: A: preexponential factor (s-1); E_a: activation energy (kJ mol^{-1})); and R: universal gas constant (8,8145 kJ mol^{-1} K).

In general, in the differential kinetic models data from dα/dt as a function of T (Eq.2) are fitted.

$$\frac{d\,\alpha}{dt} = A\, e^{\left(\frac{-E_a}{RT}\right)} f(\alpha) \qquad (2)$$

Where: dα/dt: ratio of reaction, represented as the variation of the conversion (α), calculated through the loss of mass, with respect to time (t); and f(α): dependent on temperature (T) function of the conversion.

However, when working in conditions that are not isothermal, the temperature will vary with time and will produce a specific heating rate (β) and the Eq. 3 will be obtained.

$$\frac{d\,\alpha}{dT} = \frac{A}{\beta}\, e^{\left(\frac{-E_a}{RT}\right)} f(\alpha) \qquad (3)$$

Integral methods, by separating the variables and integrating with respect to the limits α and 0; T and T_0, which is then simplified to 0 since the reaction ratio is significant from the initial temperature, Eq. 4 can be obtained.

$$g(\alpha) = \int_0^{\alpha} \frac{d\,\alpha}{dT} = \frac{A}{\beta} \int_{T_0}^{T} e^{\left(\frac{-E_a}{RT}\right)} d\,T \approx \frac{A}{\beta} \int_0^{T} e^{\left(\frac{-E_a}{RT}\right)} dT \qquad (4)$$

g(α): conversion dependent function.

The integrated models used data α, or an integral of α as a function of t, or T. In this sense, the Flynn-Wall-Ozawa (FWO) method [38,39], which faithfully represents systems where there is more than one simultaneous reaction [40]. The equation for this method is shown in Eq. 5.

$$ln(\beta) = ln\left(\frac{A\,E_a}{R\,g(\alpha)}\right) = 5{,}523 - 1{,}052\,\left(\frac{E_a}{RT}\right) \qquad (5)$$

Using the Eq. 5 for each of the conversion degrees, we get the Eq. 6.

$$ln(\beta) = ln\left(\frac{A\,E_a}{R}\right) - ln\, g(\alpha) - 0{,}4567\,\left(\frac{E_a}{RT}\right) \qquad (6)$$

For each conversion value (α), by plotting lnβ versus 1/T, a line with a slope of -0.4567 E_a/R can be obtained and the activation energy calculated. The pre-exponential factor (A) can be found by intersecting the line with the axes.

https://doi.org/10.1016/j.fuel.2024.131501

On the other hand, the values of the DTG curve (Differential Thermogravimetric Analysis) are used for the differential methods. The method developed by Friedman [41] is the most widely used differential method. This method is based on the application of logarithms to equation 3, which results in Eq. 7.

$$ln\left(\beta\frac{d\alpha}{dT}\right) = ln\left(\frac{d\,\alpha}{dt}\right) = ln[A\,f(\alpha)]\,\frac{-E_a}{RT} \qquad (7)$$

For each conversion degree (a) and heating rate (b), the plot of ln(dα/dt) versus 1/T gives a straight line whose slope is $-E_a/R$. From this slope, the value of the activation energy for each of the conversions is determined [40].

2.5 Pyrolysis products analysis by TD/GC-MS.

To obtain the pyrolysis products (pyrolytic gases) from different fractions (cellulose, hemicellulose, and lignin) of the three biomass species studied, a laboratory-scale reactor was used. The reactor comprises a temperature-controlled furnace housing a quartz tube measuring 10 mm in diameter and 140 cm in length. A horizontal actuator is employed to introduce the sample, typically around 1 g. The residence time was systematically set a 7 min and nitrogen (250 $cm^3\ min^{-1}$) was used as transport gas.

Volatile compounds samples from the pyrolysis process at the peak temperature ranges of the different biomasses and fractions obtained (hemicellulose, kraft cellulose, soda-AQ cellulose, kraft lignin, and soda-AQ lignin) sere collected at the exit of the Laboratory-scale pyrolysis reactor in fritted glass TD tubes (Supelco, Bellefonte, PA; O.D.: 6.35 mm; length: 88.9 mm) for 15 s. These tubes contained 100 mg of Tenax® TA (80-100 mesh purchased from Supelco, Bellefonte, PA) packed in synthesized glass wool layers. After collecting samples in TD tubes, the analysis was performed using TD/GC-MS. Therma desorption (TD) was employed to release the volatile compounds captured by the sorbent material in the tubes, facilitating their identification and quantification on the GC/MS. TD was carried out using a thermal desorption system unit (TD-20, Shimadzu, Japan) equipped with an HP-5 MS column (column length: 60 m, inner diameter: 0.25 mm, film thickness: 0.25 μm, J&W Scientific, Agilent Technologies, Santa Clara, California, USA), involving two steps: tube desorption and trap desorption. The mass spectrometer operated in scan mode (41-450 m/*z*), and volatile organic compounds were identified by comparing their mass spectra with those in the NIST11 library database, using 1-bromo-3-chlorobenzene as an internal standard (Figure 1).

https://doi.org/10.1016/j.fuel.2024.131501

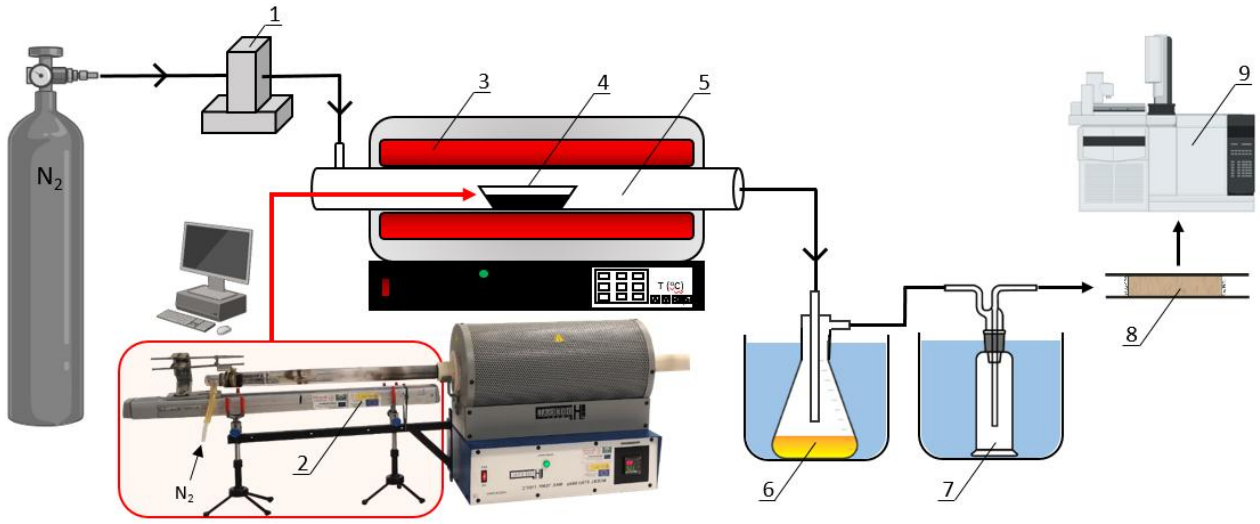


Figure 1. Schematic of pyrolysis experimental system: (1) Flowmeter, (2) Automatic Sample System, (3) furnace, (4) sample, (5) quartz reaction tube, (6) condenser, (7) cold trap, (8) gas collection (Tenax®), (9) TD-GC/MS.

3 Results and discussion.

3.1 Cold alkaline extraction (CAE).

Cold alkaline extractions were utilized to extract hemicelluloses in a liquid medium. The extraction process resulted in solid rich in cellulose and lignin after the removal of hemicelluloses. In Table 3, the main components of the solid residue following hemicellulose extraction from the selected raw materials are shown. The hemicellulose yields are referred to as the quantity of dry hemicellulose obtained relative to the quantity of raw material introduced in the cold alkaline extraction process.

Table 3. Material balance for the Cold Alkaline Extraction.

	Hemicelluloses Yield (% w/w)[a]	**Glucan** (% w/w)[b]	**Xylan** (% w/w)[b]	**Araban** (% w/w)[b]	**Acetyl Groups** (% w/w)[b]	**Klason Lignin** (% w/w)[b]
Poplar	4.59 ± 1.35	45.5 ± 8.25	16.67 ± 1.45	1.24 ± 0.10	2.2 ± 0.01	22.41 ± 4.48
Tagasaste	7.23 ± 2.13	48.18 ± 8.13	14.50 ± 2.60	0.8 ± 0.11	2.65 ± 0.01	21.24 ± 3.76
Wheat Straw	15.52 ± 2.88	49.35 ± 6.18	12.29 ± 0.88	2.61 ± 0.20	2.98 ± 0.01	20.52 ± 1.23

[a]Percentages based on quantity raw material.
[b]Percentages based on obtained solid.

The yield of hemicellulose obtained from Poplar after cold alkaline extraction is less than 5% as shown in Table 3. This is mainly attributed to the structural characteristics of Poplar which make the alkaline liquor difficult to penetrate and act on, resulting in a low yield of hemicellulose. Hemicellulose yield is directly related to cold alkaline extraction process yield. It has been observed that woody materials exhibit lower extraction yields compared to herbaceous materials, as demonstrated by various studies. For instance, Carvalho et al. [21] achieved extraction yields of 4.52% and 37.7% from eucalyptus and straw, respectively. The composition of obtained solid in the cold alkaline extraction process from Tagasaste was found to be intermediate between those of Poplar and Wheat Straw, containing significant amounts of glucan and xylan. This extraction treatment is

selective for the hemicelluloses but does not prevent the extraction of part of the lignin content of the raw material. This means that the extracted hemicellulose fractions are not pure, and their behavior must be further analysed by thermogravimetric analysis.

3.2 Kraft process delignification.

Delignification by the kraft process was carried out on the materials studied. The characteristics of the solids obtained are given in Table 4. The yield indicates the amount of pulp produced in relation to the solid obtained from the cold alkaline extraction process; a lower yield means less solid obtained, i.e. a higher extraction in the liquid phase. On the other hand, the kappa index is directly related to the lignin content of the pulp, i.e. the higher the kappa index, the more lignin is found in the pulp and vice versa.

Table 4 shows the characteristics of products obtained through kraft delignification of Poplar, Tagasaste, and Sheat Straw. The yield of the solids obtained from Poplar was the highest at 60.1%, followed by Tagasaste at 57.84%, and Wheat Straw at 53.30%. The Kappa number was highest for Poplar at 16.27, followed by Tagasaste at 14.81 and Wheat Straw at 12.93, indicating that Wheat Straw pulp has the lowest lignin content. The glucan content was highest for Wheat Straw at 78.02%, followed by Tagasaste at 72.03% and Poplar at 70.95%. The xylan content was highest for Poplar at 10.03%, followed by Tagasaste and Wheat Straw at 8.65% and 6.24%, respectively. However, the araban content was highest for Wheat Straw at 1.47%, followed by Tagasaste at 0.26% and 0.2% for Poplar.

The higher extraction observed in agricultural residues, as occurred with Wheat Straw, after kraft treatment results in a lower yield, a phenomenon previously noted by several authors. These results are consistent with those reported in the literature. For instance, in a study involving a simple kraft process, the solid yield for *Eucalyptus Citriodora* was 47% with a kappa number of 20.9 [42]. In another study, which focused on optimizing of kraft conditions for wheat straw, the solid yield ranged from 40.02% to 44.11%, while the kappa number varied from 18.7 to 47.6 [43].

Table 4. Characteristics of solids obtained in kraft delignification.

	Yield Pulp (% w/w)[a]	**Kappa Index**	**Glucan** (% w/w)[b]	**Xylan** (% w/w)[b]	**Araban** (% w/w)[b]	**Klason Lignin** (% w/w)[b]
Poplar	60.1 ± 6.84	16.27 ± 3.47	70.95 ± 2.21	10.03 ± 1.05	0.20 ± 0.01	8.34 ± 1.01
Tagasaste	57.84 ± 9.78	14.81 ± 2.02	72.03 ± 2.63	8.65 ± 0.88	0.26 ± 0.05	7.27 ± 0.74
Wheat Straw	53.30 ± 6.82	12.93 ± 1.75	78.02 ± 2.84	6.24 ± 0.62	1.47 ± 0.10	6.56 ± 0.62

[a]Percentages based on solids obtained in CAE.

[b]Percentages based on the kraft pulps obtained.

https://doi.org/10.1016/j.fuel.2024.131501

3.3 Soda-Anthraquinone process delignification.

Delignification by the soda-Anthraquinone process was carried out on the materials studied. Table 5 shows the characteristics of the obtained solids in the soda-anthraquinone delignification of Poplar, Tagasaste and Wheat Straw.

The results show that Poplar had the highest yield of 70.89%, followed by Tagasaste with 65.57% and Wheat Straw with 60.94%. Poplar also had the highest kappa number of 42.03, followed by Tagasaste with 33.01 and Wheat Straw with 17.98, in particular the Poplar pulp had 17.73% of lignin content. The highest glucan content was found in Wheat Straw with 68.02%, followed by Tagasaste with 64.65% and Poplar with 58.47%. The highest xylan content was found in Poplar with 14.17%, followed by Tagasaste with 11.33% and Wheat Straw with 9.03%. The highest araban content was found in Wheat Straw with 2.35%, followed by Tagasaste with 1.21% and Poplar with 0.33%.

Comparing the data presented in Tables 4 and 5, it is clear evident that the pulp yield obtained by soda-anthraquinone delignification exceeds that obtained through kraft delignification. Also, the kappa index obtained with soda-anthraquinone delignification is significantly higher than that obtained with kraft delignification, indicating a greater degree of delignification in kraft process. This difference between the two processes has been observed in various studies, including the work of Alaejos et al. [44], where the holm yield for kraft and soda-antraquinone processes was reported to be 50.5% and 55.0%, respectively, while the corresponding kappa numbers were 20 and 23.7, respectively.

Consequently, the three pulps obtained from different raw material using soda-anthraquinone have slightly less glucan, and more xylan, araban and Klason lignin compared to kraft.

Table 5. Characteristics of solids obtained in soda-anthraquinone delignification.

	Yield Pulp (% w/w)[a]	**Kappa Index**	**Glucan** (% w/w)[b]	**Xylan** (% w/w)[b]	**Araban** (% w/w)[b]	**Klason Lignin** (% w/w)[b]
Poplar	70.89 ± 7.45	42.03 ± 9.58	58.47 ± 5.39	14.17 ± 4.21	0.33 ± 0.07	17.73 ± 4.32
Tagasaste	65.57 ± 9.41	33.01 ± 2.84	64.65 ± 5.96	11.33 ± 2.58	1.21 ± 0.26	15.17 ± 2.15
Wheat Straw	60.94 ± 5.50	17.98 ± 2.05	68.02 ± 7.63	9.03 ± 0.94	2.35 ± 0.46	12.45 ± 1.21

[a]Percentages based on solid obtained in CAE.

[b]Percentages based on solid obtained in soda-anthraquinone process.

3.4 Thermogravimetric analysis (TGA).

3.4.1 Raw materials pyrolytic degradation.

The TGA and DTG curves shown in Figure 2 were obtained from Poplar, Tagasaste and Wheat Straw raw materials at a heating rate of 20 ºC min^{-1}. The TGA curves show an initial drop, corresponding to the initial peak of the DTG curves, which indicates the loss of moisture from the

sample at a temperature of approximately 112 ºC for the three raw materials. During this initial phase of dehydration, the sample loses approximately 3.20% for Poplar, 4.95% for Tagasaste and 6.01% for Wheat Straw. This is followed by the active pyrolysis stage (112–500ºC), during which the sample loses most of its weight due to the thermal degradation of the biomass, which is mainly composed of cellulose, hemicellulose, and lignin. The first peak observed in the pyrolysis active region represents the degradation of hemicelluloses andlignin. Hemicelluloses start to degrade at around 200 ºC and continue to degrade up to around 500 ºC due to their relatively low thermal stability [19,34].

After this stage, at around 300 ºC, cellulose degradation begins. This follows a similar process to that of hemicellulose, with degradation continuing up to about 600ºC [46]. Lignin, on the other hand, has a more complex structure, which makes it more thermally stable. It undergoes bulk degradation in the temperature range of 150–600 ºC [47] and has a lower degradation peak. Therefore, the DTG curve of lignin overlaps with that of hemicelluloses and cellulose. Although cellulose is more thermally stable than hemicellulose, it undergoes degradation in a temperature range of about 390–600 ºC due to its crystalline structure. During the active pyrolysis stage, the sample loses 72.17% of its weight. The final stage of pyrolysis begins at around 500 ºC, the passive pyrolysis stage, during which the weight loss of the sample is minimal, and the degradation of lignin is completed.

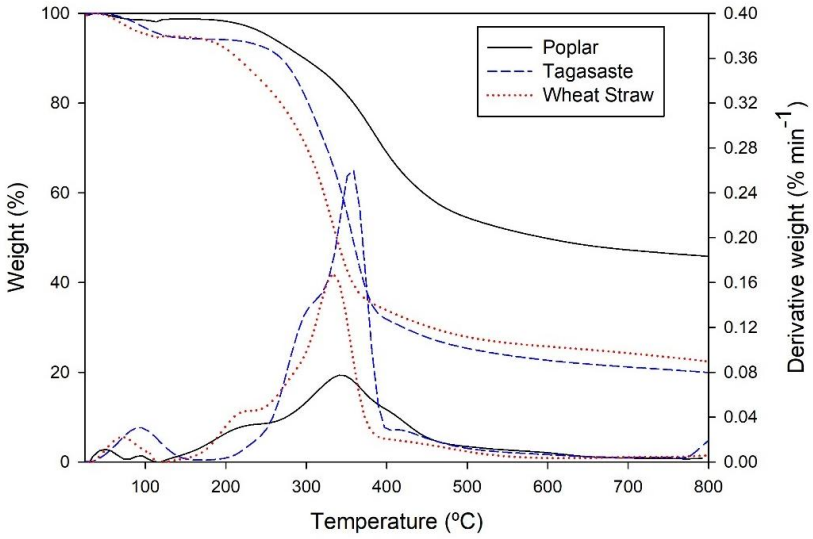


Figure 2. Pyrolytic evolution (TGA and DTG) curves obtained from Poplar, Tagasaste and Wheat Straw as raw materials under nitrogen atmosphere at 20 ºC min^{-1}.

3.4.2 Hemicelluloses pyrolytic degradation.

Figure 3 shows the evolution during pyrolysis (DTG) of hemicelluloses obtained by cold alkaline extraction of the selected raw materials. As can be seen in Figure 3, both degradation rate of and chemical changes can vary depending on the specific characteristics of the hemicellulose sample being analyzed.

https://doi.org/10.1016/j.fuel.2024.131501

The DTG curves show the three typical phases of hemicellulose degradation. The first phase causes dehydration of the hemicelluloses and results in an average weight loss of 10% for the three materials. This is mainly due to the moisture remaining in the hemicelluloses after extraction and to the removal of some volatile organic compounds from the hemicellulose. The second phase involves active degradation of the hemicelluloses by pyrolysis (breaking of glycosidic bonds) in the range of 250-350 ºC, with a total weight loss of 63.94%, 42.23% and 60.27% for Poplar, Tagasaste and Wheat Straw respectively at 400 ºC. The maximum degradation occurs at around 300 ºC, mainly due to the depolymerisation of sugars such as xylan, a major component of hemicelluloses [48]. This phase can be further divided into primary and secondary reactions. In the primary reaction, thermal depolymerization of hemicelluloses triggers the production of volatile components such as acetic acid, furfural, and 5-HMF. In the secondary reaction, these volatile compounds further transform into liquid and solid products, such as phenols and aromatics [49]. Finally, the third stage is the passive pyrolysis stage, which occurs at temperatures above 450ºC and involves the transformation of the remaining hemicellulose fragments into a more stable carbonaceous char, through reactions with aromatic compounds and the cracking of carbon-hydrogen and carbon-oxygen bonds [45].

It should be noted that the peaks found in this study for hemicellulose fractions coming from the selected raw materials are smaller than those found in commercial hemicelluloses. This discrepancy could be attributed to the degradation of these linkages during the cold alkaline extraction process, which mainly affects the weaker linkages while preserving the main structure of the hemicelluloses. In addition, commercially available hemicelluloses undergo purification which is not part of the cold alkaline extraction process.

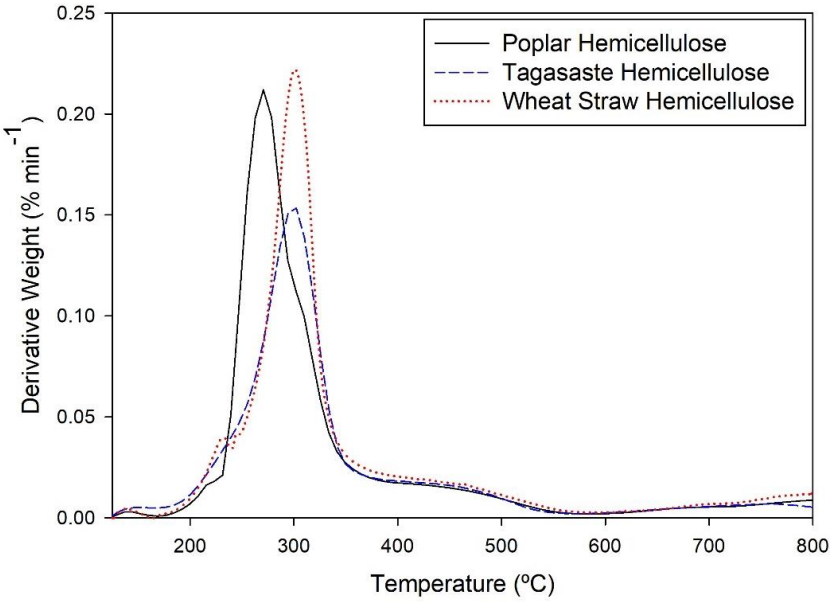


Figure 3. Pyrolytic evolution (DTG) curves obtained from Poplar, Tagasaste and Wheat Straw extracted hemicelluloses under nitrogen atmosphere at 20 ºC min^{-1}.

https://doi.org/10.1016/j.fuel.2024.131501

3.4.3 Celluloses pyrolytic degradation.

The major component of the obtained pulps is cellulose. Figure 4 shows the DTG curves of kraft and soda-anthraquinone pulp for the selected raw materials. Similar to what was found for hemicelluloses, the rate of degradation can also vary depending on the specific characteristics of the cellulose sample being degraded. However, both temperature and degradation intervals appear to be similar between different starting materials and delignification methods. As can be seen, cellulose decomposition occurs in two stages; the first phase takes place at temperatures up to 300 °C and results in the highest weight loss of 80.3% for all pulps tested. This phase involves the dehydrogenation and decarbonisation of cellulose, leading to the production of levoglucosan, volatile compounds such as levoglucosan (a major product), furans, acetic acid and other oligosaccharides through transglycosylation [50]. Similar to hemicelluloses, the degradation phase of cellulose pyrolysis can be further divided into primary and secondary reactions. The primary reaction involves depolymerisation of the cellulose, releasing volatile organic compounds at the start of the process. The secondary reaction involves the production of liquid and solid products through various chemical reactions in the later stages of the process [16]. The second phase occurs above 500 °C and involves the conversion of volatiles and chars through reactions with aromatics and cracking of the carbon-hydrogen and carbon-oxygen bonds [50]. Both the Kraft and soda-anthraquinone processes exhibit similar cellulose fractions obtained degradation behavior, and both show a single peak representing cellulose degradation, but some differences were observed. For the species studied, the soda-anthraquinone pulps suffers from a higher degradation rate and a higher weight loss compared to those for the kraft process. These differences in the different cellulose fractions contents (Tables 4 and 5) obtained from the different delignification processes may be due to the fact that the soda-anthraquinone process delignifies less due to the lower cellulose content in the final pulp.

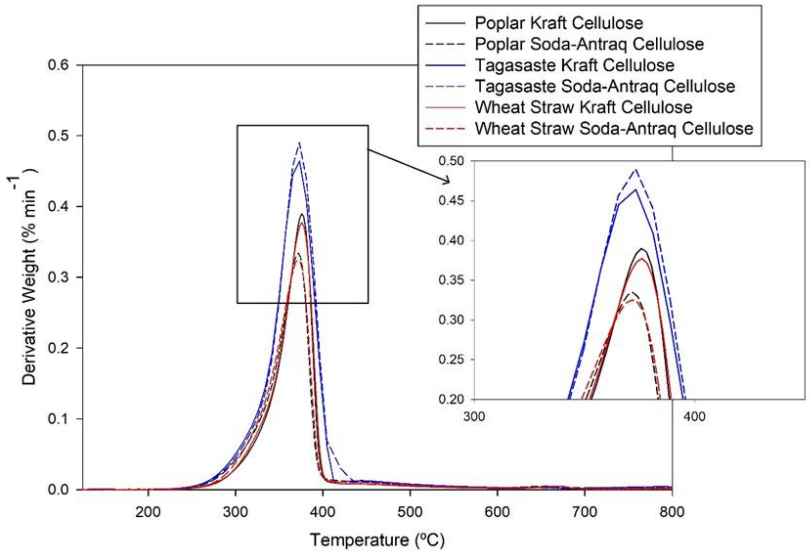


Figure 4. Pyrolytic evolution (DTG) curves obtained from Poplar, Tagasaste and Wheat Straw kraft and soda-Anthraquinone celluloses under nitrogen atmosphere at 20 ºC min^{-1}.

https://doi.org/10.1016/j.fuel.2024.131501

3.4.4 Lignin pyrolytic degradation.

Figure 5 shows the DTG curves of lignin fractions obtained from the acid hydrolysis of the kraft process and soda-anthraquinone treatment of the selected raw materials. Acid hydrolysis quantitatively extracts Klason lignin, which is further analyzed. A similar evolution to those found for hemicellulose and cellulose has been found for lignin. Also the degradation intervals of lignin pyrolysis can vary depending on factors such as the source of lignin and the delignification method. Lignin is a very complex and heterogeneous polymer, and its behavior during pyrolysis can be influenced by the presence of other components or by the different specific structures of lignin (depending on the feedstock). In this sense, the temperature ranges for lignin pyrolysis can vary depending on the specific conditions of the delignification process. However, the general temperature range for lignin pyrolysis is between 250 °C and 800 °C [36]. Lignin degradation occurs in a wide temperature range due to its complex structure containing various functional groups connected by strong linear and weak bonds, different degradation maxima are observed in the DTG curves.

During lignin pyrolysis, the lignin undergoes three main decomposition phases. The first phase (200-300 ºC), shown in Figure 5, to the degradation of hemicelluloses and celluloses, present as impurities in the lignin due to the delignification process, can be attributed. The second phase (300-500 ºC) is the one with the highest rate and weight loss (40.46% weight loss as an average of the different materials and treatments), which is attributed to the degradation of β-O-4 alkyl-aryl-ether bonds, resulting in the formation of small molecular weight compounds such as phenolic compounds, such as guayacol, syringol, and catechol, as well as aromatic hydrocarbons and gasses like carbon dioxide, carbon monoxide, and methane [51]. The third phase (500-800 ºC), with a low rate of weight loss (10.15% weight loss on average for the different materials and treatments), may be due to the degradation of the remaining lignin structures, which undergo thermal cracking to form biochar and a carbon-rich solid residue [52].

Note that, the lignin fractions curves of both processes exhibit noise, which is due to the complexity of reactions and gas flow during the measurement. Comparing the lignin of Wheat Straw from the kraft process to the soda-anthraquinone process reveals differences, including a more reactive sample with a bulk degradation to lower temperatures, and a stronger first stage due to the presence of sulphur in kraft process causing increased rupture of carbon-carbon bonds in lignin. The sample from the soda-anthraquinone process experiences the highest weight loss (39.42%) in the second stage of pyrolysis.

https://doi.org/10.1016/j.fuel.2024.131501

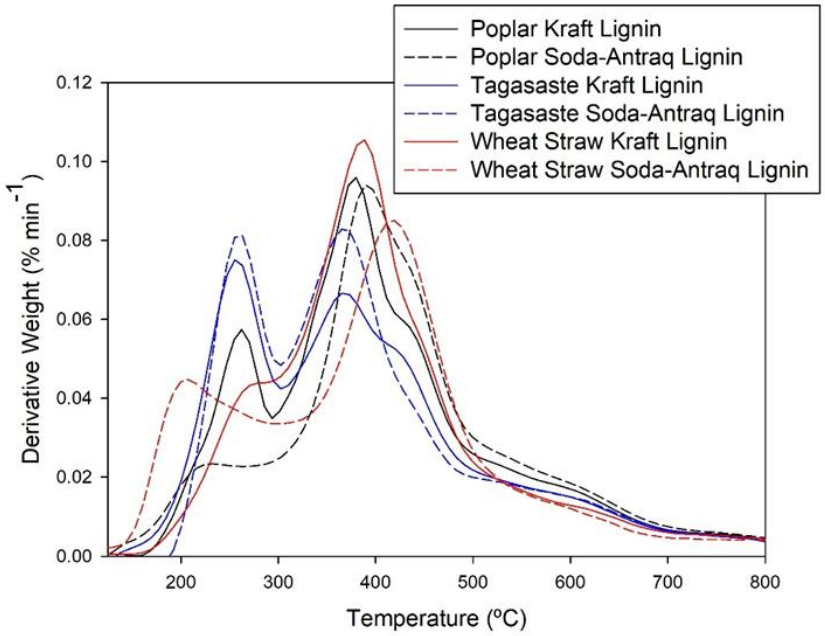


Figure 5. Pyrolytic evolution (DTG) curves obtained from Poplar, Tagasaste and Wheat Straw Kraft and Soda-Anthraquinone lignins under nitrogen atmosphere at 20 ºC min-1.

3.5 Kinetic analysis.

Two kinetic models, the Friedman differential, and the Flynn-Wall-Ozawa (FWO) integral, are compared for all samples tested. Figures 6-8 show the lines obtained in the plot of ln(dα/dt) vs 1/T for the Friedman method and lnβ vs 1/T for the Flynn-Wall-Ozawa method for all the samples studied. In these figures, the values obtained with the highest (0.90) and lowest (0.10) conversions grade have been excluded because they do not represent the behavior of the sample in the initial and final pyrolysis reactions.

3.5.1 Hemicelluloses kinetic analysis.

As can be seen in Figure 6, the use of both methods has resulted in remarkably high regression coefficients (R^2>0.98) when analyzing hemicellulose fractions from different sources. Furthermore, it can be concluded that the FWO method gives more favorable results than the Friedman method, as evidenced by the fact that the lines are more parallel when analyzing hemicellulose fractions.

Observing the change in slope in the figures, apart from what is observed in Figure 3, it is clear that different reactions have taken place during the pyrolytic degradation of hemicelluloses. This is because a change in slope implies a change in activation energy, which in turn implies different reactions involved in the degradation, depending on the conversion degree of the sample. Therefore, by observing this fact in the figures, it is possible to identify the different reactions that have taken place during the pyrolytic degradation of hemicelluloses.

https://doi.org/10.1016/j.fuel.2024.131501

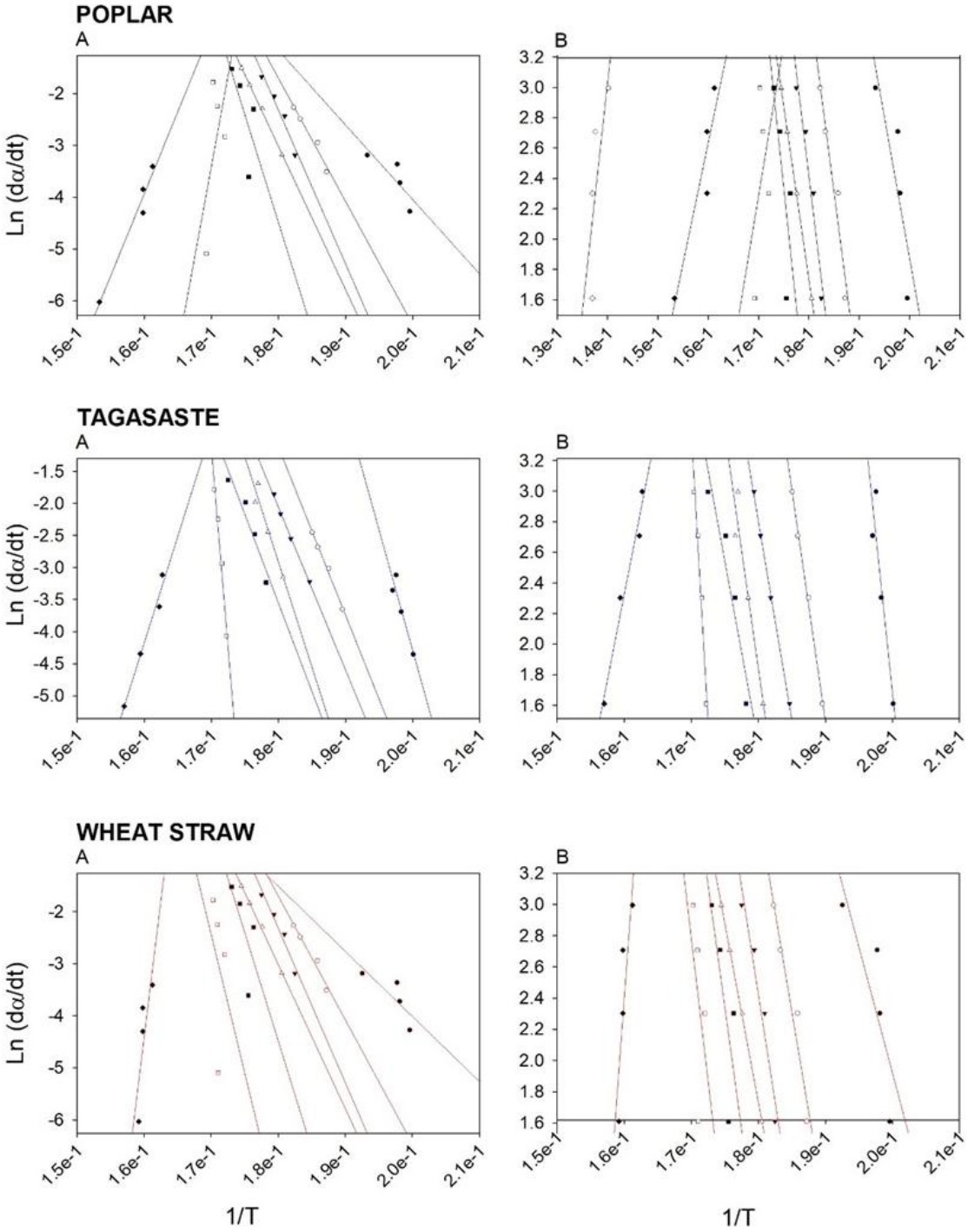


Figure 6. Evolution of the Friedman (A) and FWO (B) lines for hemicelluloses as a function of the conversion degree (symbols) and the regression lines obtained.

Figure 7 shows the evolution of the activation energy (obtained from the slope of the calculated regression lines) during the pyrolysis of hemicelluloses obtained by cold alkaline extraction for the three species studied. According to H. Wang et al. [53], the degradation process of hemicellulose is characterized by a low initial activation energy during the degradation process, which gradually increases as the reaction progresses.

https://doi.org/10.1016/j.fuel.2024.131501

In the samples studied, the calculated activation energy for hemicellulose pyrolysis is in the range of 200-300 kJ mol^{-1}. This value is higher than those reported by some authors, which can be attributed to the characteristics of hemicellulose, the method used for its extraction and the type of modelling performed. For instance, in a review of Zhou et al. [19] the one-reaction/stage models estimated the activation energy of hemicellulose pyrolysis to be in the range of 100-220 kJ mol^{-1}, while the multiple-reaction/stage models estimated the E_a in the range between 26-271 kJ mol^{-1}. There are several possible reasons why the activation energy of hemicellulose extracted by cold alkaline extraction is higher than those reported in the literature. Among them, the alkaline extraction method used in the study could result in different chemical structures, properties, and composition of the extracted hemicellulose. For example, the extracted hemicellulose could be contaminated with other compounds, which could affect the pyrolysis behavior and the activation energy. Figure 2 also suggests that the alkaline extraction method used in the study could result in different chemical structures and properties of the extracted hemicellulose depending on the feedstock.

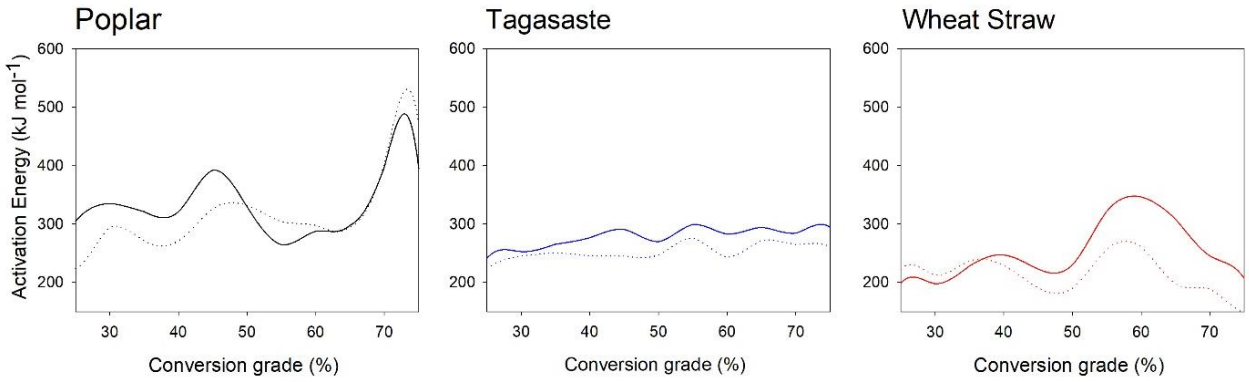


Figure 7. Activation Energy evolution for extracted hemicelluloses. Continuous lines for Friedman method and discontinuous lines for FWO method.

3.5.2 Celluloses kinetic analysis.

Similar to what was observed for hemicelluloses, the use of both methods has resulted in remarkably high regression coefficients (R^2>0.99) when analyzing celluloses obtained from different sources and processes. The high R^2 values obtained with both methods indicate that they are reliable in predicting the pyrolysis behavior of cellulose and can be used to estimate the activation energy of cellulose pyrolysis. In addition, based on the high calculated regression coefficients, it is found that the pyrolysis of cellulose follows first order reaction kinetics, as stated by H. Fan et al. [54].Furthermore, similar to what was found for hemicelluloses, it can be inferred that the FWO method gives more favorable results (higher R^2) than the Friedman method also for celluloses [48,55]. This suggests that the FWO method is more accurate in predicting the pyrolysis behavior of cellulose than the Friedman method.

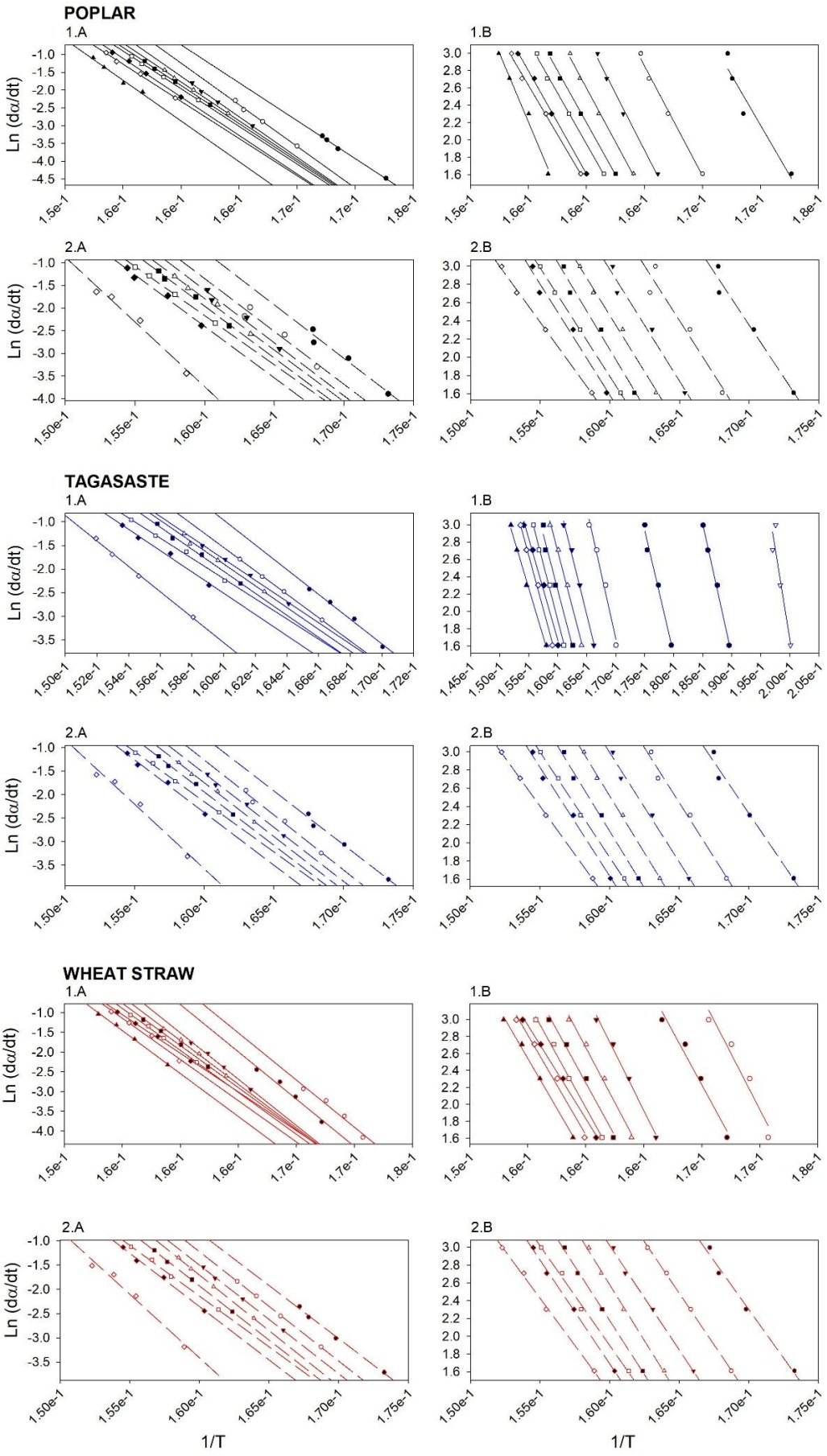


Figure 8. Evolution of the Friedman (A) and FWO (B) lines for Kraft (1) and Soda-Antraquinone (2) celluloses as a function of the conversion degree (symbols) and the regression lines obtained.

https://doi.org/10.1016/j.fuel.2024.131501

In Figure 8, a similar slope for almost all measured reaction degrees can be observed. This may be attributed to the high purity of cellulose extracted using both studied delignification methods. In this case, the Friedman method shows a closer resemblance in slope compared to the Flynn method.

Figure 9 illustrates the evolution of activation energy during the pyrolysis of the obtained celluloses. This figure shows that the activation energy increases as the reaction degree increases, which is in agreement with the literature.

For the cases studied, the values calculated by the FWO method are always higher than those found by the Friedman method. Moreover, the calculated values by the FWO method (180-220 kJ mol^{-1}) are within the range calculated by other authors.

In this sense, the activation energy of cellulose pyrolysis has been reported to be in the range of 114-288 kJ mol^{-1} [50,56,57]. The average pyrolysis activation energy of cellulose has been reported to be 189.2 kJ mol^{-1}[16]. Therefore, it is important to consider the experimental conditions and the method used when comparing the activation energy values reported in different studies.

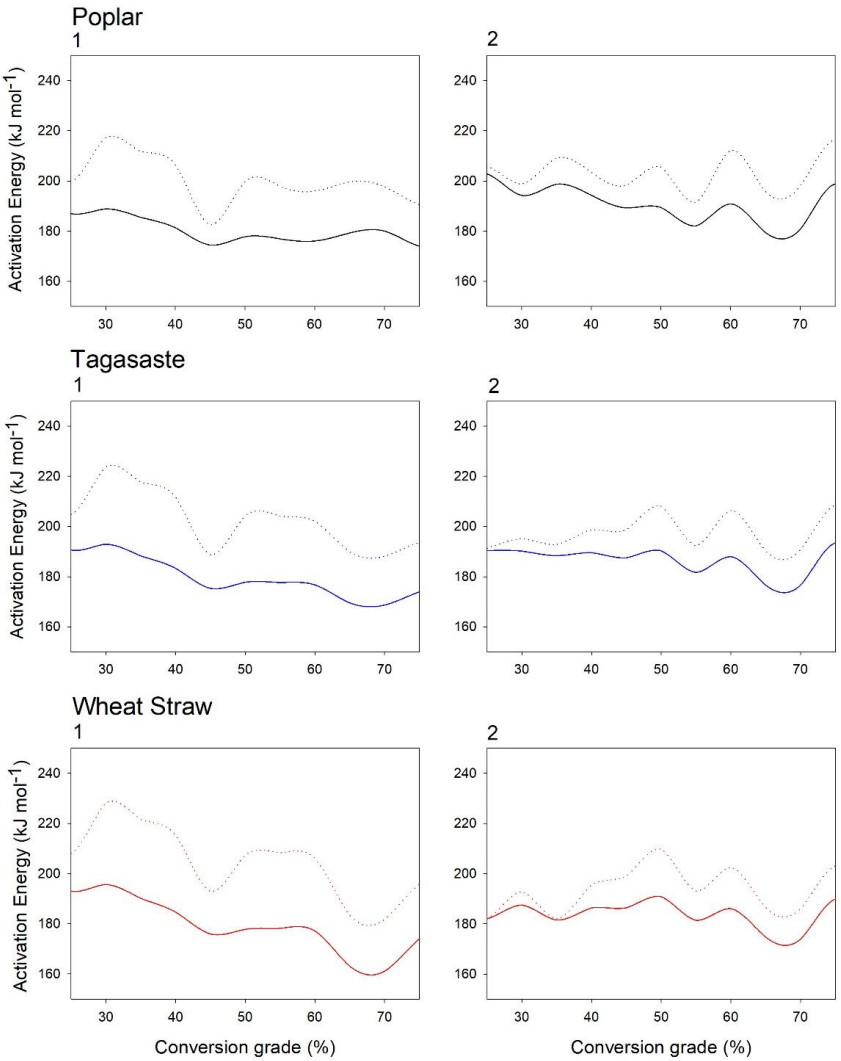


Figure 9. Activation Energy evolution for kraft (1) and Soda-Antraquinone (2) celluloses by Friedman (continuous lines) and FWO (discontinuous lines) methods.

https://doi.org/10.1016/j.fuel.2024.131501

3.5.3 Lignins kinetic analysis.

Figure 10 presents an insightful analysis of the kinetic evolution of lignin, utilizing both the Friedman and FWO methods.

According to the studies conducted by L. Luo et al. and Matusiak et al. [57, 58], the activation energies obtained through both methods do not demonstrate a clear linear trend with lignin content as the degree of reaction progresses. This observation can be attributed to the intricate nature of lignin decomposition, which involves multiple reactions with varying activation energies due to the diverse range of bonds and the multi-phasic character of its conversion Radojević et al. [59]. This complexity is reflected in Figure 10 through the different slopes depicted.

Figure 11 illustrates the evolution of activation energy during the pyrolysis of the obtained lignins.

Figure 11 shows that the activation energy required to break chemical bonds in lignin is higher than that for cellulose. It should be noted that similar values of activation energy were found between the two kinetic models for the different lignins under investigation. According to L. Li, et al. and L. Luo et al. [60,57], the results show that the activation energy of lignin increases as the conversion degree progresses, indicating a higher energy requirement to break lignin bonds. This observation holds true for all three species and the two delignification methods investigated in the study. The increase in activation energy can be attributed to several factors. First, as lignin is depolymerised, the larger lignin molecules exhibit increased resistance to pyrolytic degradation. Secondly, the pyrolysis of lignin involves a complex interplay of reactions including fragmentation, condensation, and recombination. As the pyrolysis reaction progresses, the composition of the reaction mixture changes, leading to the dominance of different reaction pathways [61].

It should be noted that the evolution of the activation energy during the pyrolysis of the different lignins studied is different, since this evolution can be influenced by several factors, including the origin and composition of the lignin and the delignification method used. Different chemical compositions and structures of lignin, resulting in variations in pyrolysis kinetics and activation energy profiles, according to the literature cited.

In this case, the figure 11 shows that the delignification method has a strong influence on the activation energy, more so than the hemicelluloses and celluloses present in the lignin samples. The literature indicates that lignin has relatively high activation energy values [58], which range from 126 to 200 kJ mol^{-1}, depending on the study and the method used to estimate it [54,62,63].

https://doi.org/10.1016/j.fuel.2024.131501

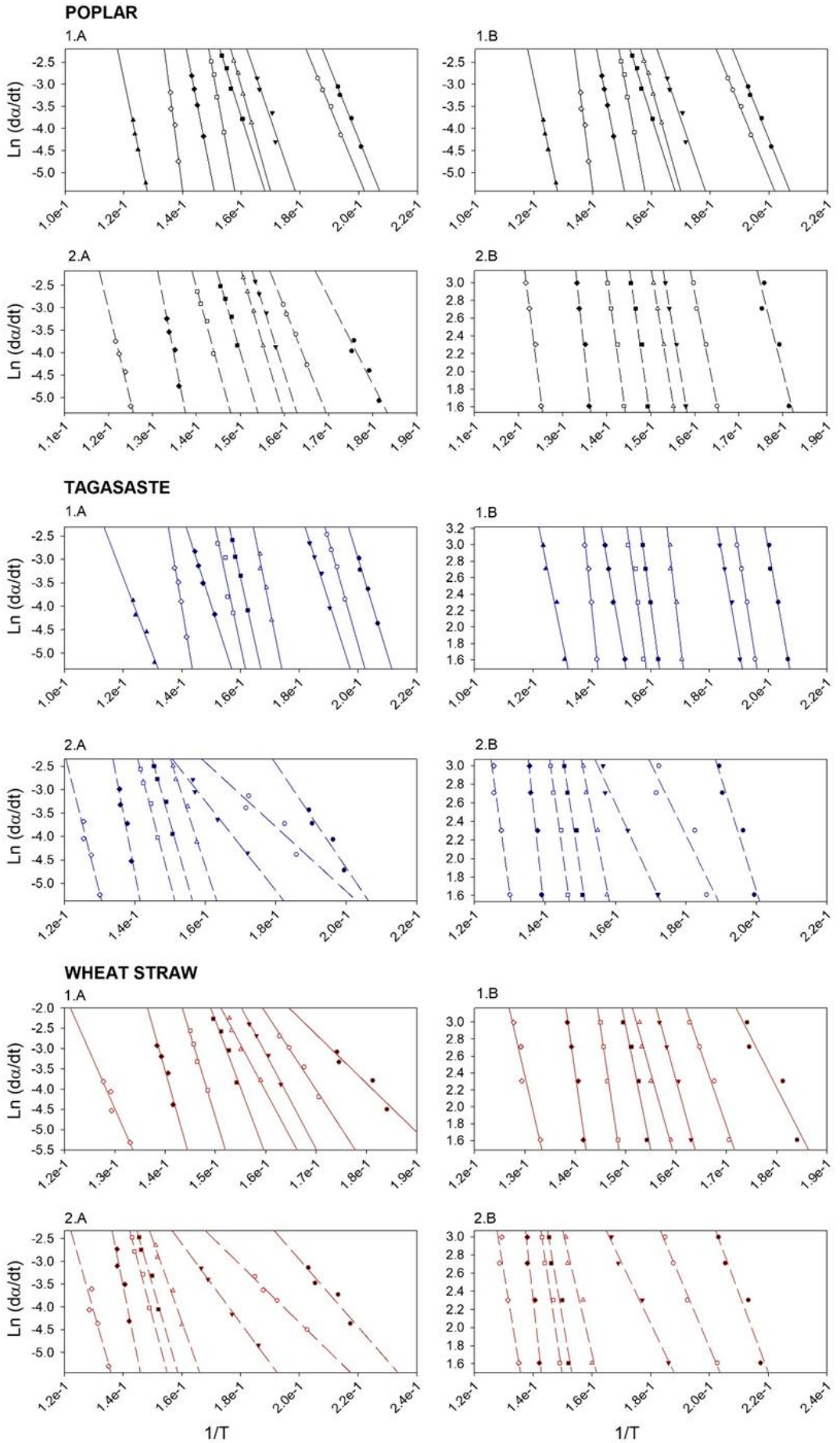


Figure 10. Evolution of the Friedman (A) and FWO (B) lines for kraft (1) and Soda-Antraquinone (2) lignins as a function of the conversion degree (symbols) and the regression lines obtained.

https://doi.org/10.1016/j.fuel.2024.131501

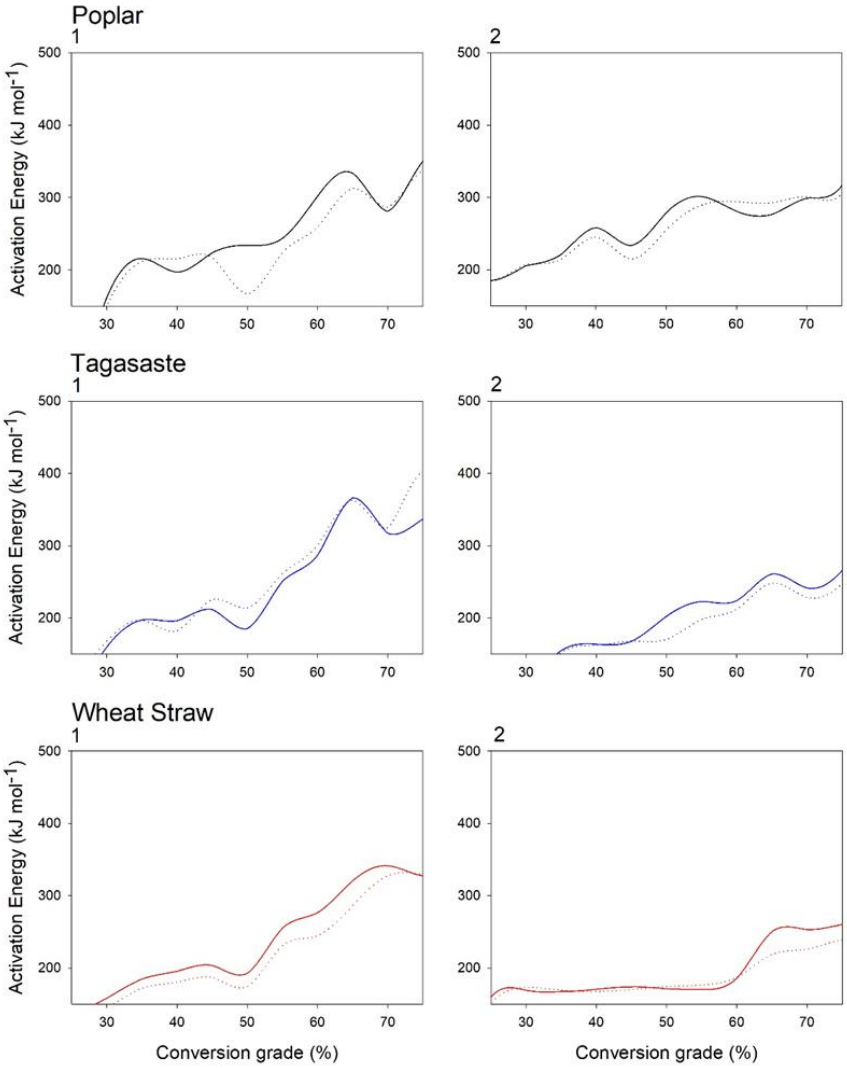


Figure 11. Activation Energy evolution for kraft (1) and Soda-Antraquinone (2) lignins by Friedman (continuous lines) and FWO (discontinuous lines) methods.

3.6 Obtained gasses by pyrolysis from different fractions.

It's essential to emphasize that temperature ranges and the composition of evolved gasses during the pyrolysis of the different lignocellulosic biomass fractions may exhibit variations influenced by factors such as the source plant, experimental conditions, and heating rate [64,65].

Figure 12 shows the families of compounds detected during the pyrolysis of the different fraction. These gas streams have the potential for uses as fuel. Currently, there is a growing interest in selectively separating these compounds for specific applications [66]. For instance, among the compounds detected was acetic acid, which can be utilized as a platform chemical for the productions of different chemicals and materials [60]. Furthermore, apart from these non-condensable gases, a substantial amount of lighter gases, such as carbon dioxide, hydrogen, carbon monoxide, and methane, have been reported by other authors [65,67, 68].

https://doi.org/10.1016/j.fuel.2024.131501

One family of compounds commonly associated whit the hemicellulose and cellulose degradation are furans, with hemicellulose being more prone to their formation, as observed in Figure 12. Poplar wood and Wheat Straw primarily yielded fundamentally esters (28.9% and 31.1%, respectively), furans (20.2% and 22.6%, respectively), and aromatic hydrocarbons (16% and 21.7%, respectively). In contrast, Tagasaste predominantly produced aldehydes (32.4%), carboxylic acid (13%), and furans (11.9%). The variation observed can be attributed to the inherent properties of the raw materials. This is due to the fact that the composition and the degree of acetylation of the hemicelluloses are dependent on the raw material used. For instance, the divergence stems from the differing sugar monomers present in the raw materials, which decompose at different temperatures and produce different gas products. Hardwoods contain predominantly xylose, whereas softwoods contain a combination of xylose, mannose, and galactose [69,70]. If we refer back to the DTG-curve of hemicellulose fractions (Figure 3), we can observe a difference in the degradation of Tagasaste's hemicellulose fractions compared to that found for Poplar and Wheat Straw.

Focusing on the cellulose fractions, it is observed in the gas stream produced during pyrolysis that the most prominent compounds are aldehydes, and phenols, while in the Poplar case by the second one, the carboxylic acids. Therefore, as mentioned above, the production of specific compounds and their amounts depend on the initial raw material. With regard to the cellulose fraction, the crystallinity and degree of polymerization vary among different feedstocks. For example, softwoods generally have a higher crystallinity than hardwoods and agricultural residues [71-73]. Sun et al. [74] reported that cellulose pyrolysis produces aldehydes, acids, alcohols, ketones, carbohydrates, and other. In Poplar, a significant amount of the aldehyde prop-2-enal (29.5%) was identified, while the primary aldehyde in the cellulose fractions of Tagasaste and Wheat Straw was 3-Methylbutanal (14.2% and 18.1%, respectively).

Regarding the lignin fractions, the differences between Tagasaste, Poplar and Wheat Straw are similar to those observed in the hemicellulose fractions. In this case, the most abundant family of compounds obtained from Poplar and Wheat Straw was aromatic hydrocarbons, predominantly toluene (40.8% and 31.6%, respectively). However, in Tagasaste's lignin fraction, the predominant group of compounds were phenols (28.2%). For this fraction, there is also a correlation between the feedstock and the pyrolytic gases, as the lignin composition is also influenced by the feedstock's composition. Specifically, softwoods have a higher lignin content with a predominantly guaiacyl units, whereas hardwoods contain a higher proportion of syringyl units [75].

One compound deserving special mention is furfural, which has been recognized as one of the top biomass-derived platform compounds by the US Department of Energy [76]. Furfural has the potential to yield high-value products, including liquid hydrocarbon fuels, fuel additives, and furfural

derivatives with various applications [77,78]. In summary, the furfural serves as a valuable source of derivatives that have the potential to become biofuel components [79]. In this work, we observed that pyrolysis produced a significant quantity of furans, especially furfural, primarily originating from hemicellulose fractions. Wheat Straw exhibited the highest furfural production, accounting for 19.3%, followed by Poplar with 16.9%, and Tagasaste with the lowest at 6.6%.

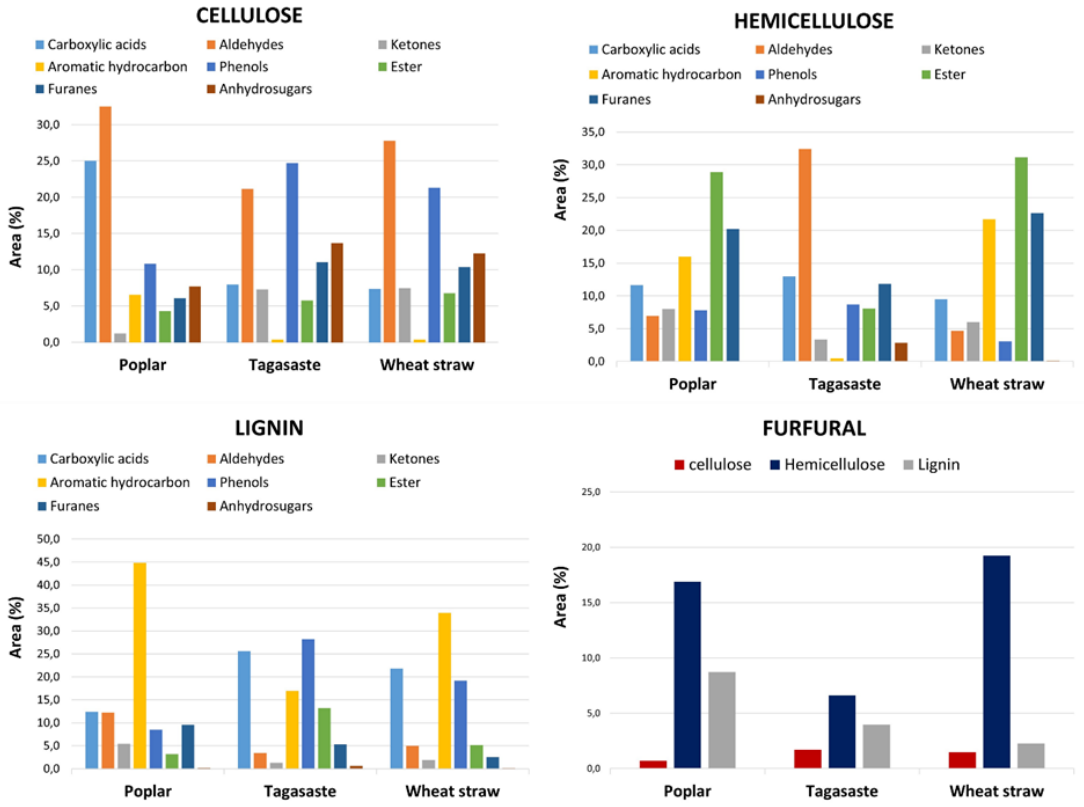


Figure 12. Pyrolysis-gas products (% area) of the different fractions (cellulose, hemicellulose, and lignin) of Poplar, Tagasaste and Wheat Straw, and furfural production from the different fractions.

4 Conclusions.

The thermogravimetric analysis revealed similar degradation patterns across the studied raw materials (Poplar, Tagasaste, and Wheat Straw), with distinct characteristics for each lignocellulosic fraction. Cellulose exhibited a single peak around 370 ºC, hemicellulose degraded earlier (250 – 300 ºC) with a smoother profile, and lignin showed a broader range (15 – 600 ºC) that is less prevalent in raw materials due to overlapping degradation with other components. The activation energy (E_a) required for degradation varied depending on the fraction and conversion degree, with hemicellulose (200 – 300 kJ mol^{-1}) requiring slightly higher E_a than cellulose (180 – 220 kJ mol^{-1}). Lignin fractions displayed the highest E_a; variations exist among different lignins, influenced by factors such as the origin of the raw material and the delignification method employed to obtain the lignin fraction. The pyrolysis process generated a diverse gas stream, with a wide range of components, originating from different lignocellulosic fractions. Highlighting the presence of furfural, more pronounced in the pyrolysis of hemicellulose fractions, especially in hemicellulose obtained from Wheat Straw. This

observation underscores a potential avenue for the targeted production of high-value-added chemicals from specific biomass sources.

CRediT authorship contribution statement

N. Almagro-Herrera: Visualization, Methodology, Investigation, Formal analysis, Data curation, Conceptualization. **S. Lozano-Calvo:** Writing – original draft, Visualization, Methodology, Investigation, Formal analysis, Data curation, Conceptualization. **A. Palma:** Writing – review & editing, Visualization, Methodology, Investigation, Formal analysis, Data curation, Conceptualization. **J.C. García:** Conceptualization, Methodology, Funding acquisition, Supervision, Project administration. **M.J. Díaz:** Conceptualization, Methodology, Formal analysis, Data curation, Funding acquisition, Supervision, Writing – review & editing, Project administration.

Funding

This study was supported by the Ministry of Science and Innovation (Spain), as well as by the National Research Program Oriented to the Challenges of Society (Project PID2020-112875RB-C21 funded by MCIN/AEI /https://doi.org/10.13039/501100011033), also this publication is part of the PRE2021-097925 support (funded by MCIN/AEI/ https://doi.org/10.13039/501100011033 and by the FSE+). Funding for open access charge: Universidad de Huelva/CBUA.

Data availability

All data generated or analyzed during this work are included in this published article.

Declaration of competing interest

The authors declare that they have no known competing financial interests or personal relationships that could have appeared to influence the work reported in this paper.

Ethics approval and consent to participate

The authors declare that this is their original work, and the corresponding manuscript has not been published before and is only submitted to Fuel.

Consent for publication

All authors reviewed the manuscript and consented to its publication.

Availability of data and materials

All data generated or analyzed during this work are included in this published article.

References

[1] Alper K, Tekin K, Karagöz S, Ragauskas AJ. Sustainable energy and fuels from biomass: a review focusing on hydrothermal biomass processing. Sustain Energy Fuels 2020; 4:4390–414. https://doi.org/10.1039/D0SE00784F.

[2] Roy P, Jahromi H, Rahman T, Baltrusaitis J, Hassan EB, Torbert A, et al. Hydrotreatment of pyrolysis bio-oil with non-edible carinata oil and poultry fat for producing transportation fuels. Fuel Processing Technology 2023; 245:107753. https://doi.org/10.1016/J.FUPROC.2023.107753.

[3] Sharma V, Tsai ML, Nargotra P, Chen CW, Sun PP, Singhania RR, et al. Journey of lignin from a roadblock to bridge for lignocellulose biorefineries: A comprehensive review. Science of The Total Environment 2023; 861:160560. https://doi.org/10.1016/J.SCITOTENV.2022.160560.

[4] Ayub Y, Zhou J, Shi T, Ren J. Process safety assessment of thermal technologies for biomass valorization by numerical descriptive approach. Process Safety and Environmental Protection 2023; 171:803–11. https://doi.org/10.1016/J.PSEP.2023.01.075.

[5] Troiano DT, Hofmann T, Brethauer S, Studer MHP. Toward optimal use of biomass as carbon source for chemical bioproduction. Curr Opin Biotechnol 2023; 81:102942. https://doi.org/10.1016/J.COPBIO.2023.102942.

[6] Akram HA, Imran M, Javaid A, Latif S, Rizvi NB, Jesionowski T, et al. Pretreatment and catalytic conversion of lignocellulosic and algal biomass into biofuels by metal organic frameworks. Molecular Catalysis 2023; 539:112893. https://doi.org/10.1016/J.MCAT.2022.112893.

[7] Zhan Q, Lin Q, Wu Y, Liu Y, Wang X, Ren J. A fractionation strategy of cellulose, hemicellulose, and lignin from wheat straw via the biphasic pretreatment for biomass valorization. Bioresour Technol 2023; 376:128887. https://doi.org/10.1016/J.BIORTECH.2023.128887.

[8] Fan Q, Fu P, Song C, Fan Y. Valorization of waste biomass through hydrothermal liquefaction: A review with focus on linking hydrothermal factors to products characteristics. Ind Crops Prod 2023; 191:116017. https://doi.org/10.1016/J.INDCROP.2022.116017.

[9] Mujtaba M, Fraceto L, Fazeli M, Mukherjee S, Savassa SM, Araujo de Medeiros G, et al. Lignocellulosic biomass from agricultural waste to the circular economy: a review with focus on biofuels, biocomposites and bioplastics. J Clean Prod 2023; 402:136815. https://doi.org/10.1016/J.JCLEPRO.2023.136815.

[10] Amenaghawon AN, Anyalewechi CL, Okieimen CO, Kusuma HS. Biomass pyrolysis technologies for value-added products: a state-of-the-art review. Environ Dev Sustain 2021; 23:14324–78. https://doi.org/10.1007/s10668-021-01276-5.

[11] Vuppaladadiyam AK, Vuppaladadiyam SSV, Sahoo A, Murugavelh S, Anthony E, Bhashkar T, et al. Bio-oil and biochar from the pyrolytic conversion of biomass: A current and future perspective on the trade-off between economic, environmental, and technical indicators. Science of The Total Environment 2023; 857:159155. https://doi.org/10.1016/J.SCITOTENV.2022.159155.

[12] Okolie JA, Epelle EI, Tabat ME, Orivri U, Amenaghawon AN, Okoye PU, et al. Waste biomass valorization for the production of biofuels and value-added products: A comprehensive review of thermochemical, biological and integrated processes. Process Safety and Environmental Protection 2022; 159:323–44. https://doi.org/10.1016/J.PSEP.2021.12.049.

[13] Eugenio ME, Ruiz-Montoya M, Martín-Sampedro R, Ibarra D, Díaz MJ. Influence of Cellulose Characteristics on Pyrolysis Suitability. Processes 2021;9. https://doi.org/10.3390/pr9091584.

[14] Madanayake BN, Gan S, Eastwick C, Ng HK. Biomass as an energy source in coal co-firing and its feasibility enhancement via pre-treatment techniques. Fuel Processing Technology 2017; 159:287–305. https://doi.org/10.1016/J.FUPROC.2017.01.029.

[15] Wu W, Mei Y, Zhang L, Liu R, Cai J. Effective Activation Energies of Lignocellulosic Biomass Pyrolysis. Energy & Fuels 2014; 28:3916–23. https://doi.org/10.1021/ef5005896.

[16] Chen D, Cen K, Zhuang X, Gan Z, Zhou J, Zhang Y, et al. Insight into biomass pyrolysis mechanism based on cellulose, hemicellulose, and lignin: Evolution of volatiles and kinetics, elucidation of reaction pathways, and characterization of gas, biochar and bio-oil. Combust Flame 2022; 242:112142. https://doi.org/10.1016/J.COMBUSTFLAME.2022.112142.

[17] Al-Rumaihi A, Shahbaz M, Mckay G, Mackey H, Al-Ansari T. A review of pyrolysis technologies and feedstock: A blending approach for plastic and biomass towards optimum biochar yield. Renewable and Sustainable Energy Reviews 2022; 167:112715. https://doi.org/10.1016/J.RSER.2022.112715.

[18] Stefanidis SD, Kalogiannis KG, Iliopoulou EF, Michailof CM, Pilavachi PA, Lappas AA. A study of lignocellulosic biomass pyrolysis via the pyrolysis of cellulose, hemicellulose and lignin. J Anal Appl Pyrolysis 2014; 105:143–50. https://doi.org/10.1016/J.JAAP.2013.10.013.

[19] Zhou X, Li W, Mabon R, Broadbelt LJ. A Critical Review on Hemicellulose Pyrolysis. Energy Technology 2017; 5:52–79. https://doi.org/https://doi.org/10.1002/ente.201600327.

[20] Carrier M, Windt M, Ziegler B, Appelt J, Saake B, Meier D, et al. Quantitative Insights into the Fast Pyrolysis of Extracted Cellulose, Hemicelluloses, and Lignin. ChemSusChem 2017; 10:3212–24. https://doi.org/https://doi.org/10.1002/cssc.201700984.

[21] de Carvalho DM, Sevastyanova O, Queiroz JH de, Colodette JL. Cold alkaline extraction as a pretreatment for bioethanol production from eucalyptus, sugarcane bagasse and sugarcane straw. Energy Convers Manag 2016; 124:315–24. https://doi.org/10.1016/j.enconman.2016.07.029.

[22] Hult E-L, Larsson PT, Iversen T. A comparative CP/MAS 13C-NMR study of cellulose structure in spruce wood and kraft pulp. Cellulose 2000; 7:35–55.

[23] Newman RH, Hemmingson JA, Suckling ID. Carbon-13 nuclear magnetic resonance studies of kraft pulping 1993.

[24] Gustafson RR, Sleicher CA, McKean WT, Finlayson BA. Theoretical model of the kraft pulping process. Industrial & Engineering Chemistry Process Design and Development 1983; 22:87–96.

[25] Martínez JM, Reguant J, Salvadó J, Farriol X. Soda-anthraquinone pulping of a softwood mixture: Applying a pseudo-kinetic severity parameter. Bioresour Technol 1997; 60:161–7.

[26] Rabemanolontsoa H, Saka S. Various pretreatments of lignocellulosics. Bioresour Technol 2016; 199:83–91. https://doi.org/10.1016/J.BIORTECH.2015.08.029.

[27] García JC, Díaz MJ, Garcia MT, Feria MJ, Gómez DM, López F. Search for optimum conditions of wheat straw hemicelluloses cold alkaline extraction process. Biochem Eng J 2013; 71:127–33. https://doi.org/10.1016/j.bej.2012.12.008.

[28] Park YC, Kim JS. Comparison of various alkaline pretreatment methods of lignocellulosic biomass. Energy 2012; 47:31–5. https://doi.org/10.1016/j.energy.2012.08.010.

[29] Lozano Calvo S. Extracción de Polisacáridos en Especies de Alta Productividad Aplicando Ultrasonidos. Huelva: 2019.

[30] TAPPI T264 cm-07. Preparation of wood for chemical analysis.TAPPI Press, Atlanta, GA. 2007.

[31] Pola L, Collado S, Oulego P, Díaz M. Kraft black liquor as a renewable source of value-added chemicals. Chemical Engineering Journal 2022; 448:137728. https://doi.org/10.1016/J.CEJ.2022.137728.

[32] López F, Trinidad García M, Mena V, Loaiza JM, Zamudio MAM, García JC. Can acceptable pulp be obtained from Eucalyptus globulus wood chips after hemicellulose extraction? vol. 10. 2015.

[33] TAPPI T204 cm-07. Solvent extractives of wood and pulp. TAPPI Press, Atlanta, GA. 2007.

[34] TAPPI T222 om-11. Acid-insoluble lignin in wood and pulp. TAPPI Press, Atlanta, GA. 2011.

[35] TAPPI T249 cm-09. Carbohydrate composition of extractive-free wood and wood pulp by gas-liquid chromatography. TAPPI Press, Atlanta, GA. 2009.

[36] Van de Velden M, Baeyens J, Brems A, Janssens B, Dewil R. Fundamentals, kinetics and endothermicity of the biomass pyrolysis reaction. Renew Energy 2010; 35:232–42. https://doi.org/10.1016/J.RENENE.2009.04.019.

[37] Siddiqi H, Bal M, Kumari U, Meikap BC. In-depth physiochemical characterization and detailed thermo-kinetic study of biomass wastes to analyze its energy potential. Renew Energy 2020; 148:756–71. https://doi.org/10.1016/J.RENENE.2019.10.162.

[38] Ozawa T. A New Method of Analyzing Thermogravimetric Data. Bull Chem Soc Jpn 1965; 38:1881–6. https://doi.org/10.1246/bcsj.38.1881.

[39] Flynn JH, Wall LA. A quick, direct method for the determination of activation energy from thermogravimetric data. J Polym Sci B 1966; 4:323–8. https://doi.org/https://doi.org/10.1002/pol.1966.110040504.

[40] Venkatesh M, Ravi P, Tewari SP. Isoconversional Kinetic Analysis of Decomposition of Nitroimidazoles: Friedman method vs Flynn–Wall–Ozawa Method. J Phys Chem A 2013; 117:10162–9. https://doi.org/10.1021/jp407526r.

[41] Friedman HL. Kinetics of thermal degradation of char-forming plastics from thermogravimetry. Application to a phenolic plastic. Journal of polymer science part C: polymer symposia, vol. 6, Wiley Online Library; 1964, p. 183–95.

[42] Khristova P, Kordsachia O, Patt R, Dafaalla S. Alkaline pulping of some eucalypts from Sudan. Bioresour Technol 2006; 97:535–44. https://doi.org/10.1016/J.BIORTECH.2005.04.006.

[43] Deniz I, Kirci H, Ates S. Optimisation of wheat straw Triticum drum kraft pulping. Ind Crops Prod 2004; 19:237–43. https://doi.org/10.1016/J.INDCROP.2003.10.011.

[44] Alaejos J, López F, Eugenio ME, Tapias R. Soda–anthraquinone, kraft and organosolv pulping of holm oak trimmings. Bioresour Technol 2006; 97:2110–6. https://doi.org/10.1016/J.BIORTECH.2005.09.021.

[45] Ma H, Zhang Y, Wang L, Zhu Z, Chen Y, Wang H, et al. Kinetic Analysis of the Pyrolysis of Apricot Stone and its Main Components via Distributed Activation Energy Mode. vol. 15. 2019.

[46] SriBala G, Vargas DC, Kostetskyy P, de Vijver R, Broadbelt LJ, Marin GB, et al. New Perspectives into Cellulose Fast Pyrolysis Kinetics Using a Py-GC × GC-FID/MS System. ACS Engineering Au 2022; 2:320–32. https://doi.org/10.1021/acsengineeringau.2c00006.

[47] Domínguez JC, Santos TM, Rigual V, Oliet M, Alonso M V., Rodriguez F. Thermal stability, degradation kinetics, and molecular weight of organosolv lignins from Pinus radiata. Ind Crops Prod 2018; 111:889–98. https://doi.org/10.1016/J.INDCROP.2017.10.059.

[48] Yeo JY, Chin BLF, Tan JK, Loh YS. Comparative studies on the pyrolysis of cellulose, hemicellulose, and lignin based on combined kinetics. Journal of the Energy Institute 2019; 92:27–37. https://doi.org/10.1016/J.JOEI.2017.12.003.

[49] Collard FX, Blin J. A review on pyrolysis of biomass constituents: Mechanisms and composition of the products obtained from the conversion of cellulose, hemicelluloses and lignin. Renewable and Sustainable Energy Reviews 2014; 38:594–608. https://doi.org/10.1016/J.RSER.2014.06.013.

[50] Zhang X, Yang W, Dong C. Levoglucosan formation mechanisms during cellulose pyrolysis. J Anal Appl Pyrolysis 2013; 104:19–27. https://doi.org/10.1016/J.JAAP.2013.09.015.

[51] Custodis VBF, Hemberger P, Ma Z, van Bokhoven JA. Mechanism of Fast Pyrolysis of Lignin: Studying Model Compounds. J Phys Chem B 2014; 118:8524–31. https://doi.org/10.1021/jp5036579.

[52] Mandlekar N, Cayla A, Rault F, Giraud S, Salaün F, Malucelli G, et al. Thermal Stability and Fire Retardant Properties of Polyamide 11 Microcomposites Containing Different Lignins. Ind Eng Chem Res 2017; 56:13704–14. https://doi.org/10.1021/acs.iecr.7b03085.

[53] Wang H, Yao Q, Wang C, Fan B, Xiong Y, Chen Y, et al. New Insight on Promoted thermostability of poplar wood modified by MnFe2O4 nanoparticles through the pyrolysis behaviors and kinetic study. Sci Rep 2017; 7:1418. https://doi.org/10.1038/s41598-017-01597-4.

[54] Fan H, Gu J, Wang Y, Yuan H, Chen Y. Insight into the pyrolysis kinetics of cellulose, xylan and lignin with the addition of potassium and calcium based on distributed activation energy model. Energy 2022; 243:122816. https://doi.org/10.1016/J.ENERGY.2021.122816.

[55] Zhu L, Zhong Z. Effects of cellulose, hemicellulose and lignin on biomass pyrolysis kinetics. Korean Journal of Chemical Engineering 2020; 37:1660–8. https://doi.org/10.1007/s11814-020-0553-y.

[56] Anca-Couce A, Tsekos C, Retschitzegger S, Zimbardi F, Funke A, Banks S, et al. Biomass pyrolysis TGA assessment with an international round robin. Fuel 2020; 276:118002. https://doi.org/10.1016/J.FUEL.2020.118002.

[57] Luo L, Guo X, Zhang Z, Chai M, Rahman MdM, Zhang X, et al. Insight into Pyrolysis Kinetics of Lignocellulosic Biomass: Isoconversional Kinetic Analysis by the Modified Friedman Method. Energy & Fuels 2020; 34:4874–81.

[58] Matusiak M, Ślęzak R, Ledakowicz S. Thermogravimetric Kinetics of Selected Energy Crops Pyrolysis. Energies (Basel) 2020;13. https://doi.org/10.3390/en13153977https://doi.org/10.1021/acs.energyfuels.0c00275.

[59] Radojević M, Janković B, Jovanović V, Stojiljković D, Manić N. Comparative pyrolysis kinetics of various biomasses based on model-free and DAEM approaches improved with numerical optimization procedure. PLoS One 2018;13. https://doi.org/10.1371/journal.pone.0206657.

[60] Li L, Rowbotham JS, Christopher Greenwell H, Dyer PW. An Introduction to Pyrolysis and Catalytic Pyrolysis: Versatile Techniques for Biomass Conversion. New and Future Developments in Catalysis: Catalytic Biomass Conversion 2013:173–208. https://doi.org/10.1016/B978-0-444-53878-9.00009-6.

[61] Wang S, Dai G, Yang H, Luo Z. Lignocellulosic biomass pyrolysis mechanism: A state-of-the-art review. Prog Energy Combust Sci 2017; 62:33–86. https://doi.org/10.1016/J.PECS.2017.05.004.

[62] Liu M, Yang J, Liu Z, He W, Liu Q, Li Y, et al. Cleavage of Covalent Bonds in the Pyrolysis of Lignin, Cellulose, and Hemicellulose. Energy & Fuels 2015; 29:5773–80. https://doi.org/10.1021/acs.energyfuels.5b00983.

[63] Kristanto J, Azis MM, Purwono S. Multi-distribution activation energy model on slow pyrolysis of cellulose and lignin in TGA/DSC. Heliyon 2021;7:e07669. https://doi.org/10.1016/J.HELIYON.2021.E07669.

[64] Carrier M, Fournet R, Sirjean B, Amsbury S, Alfonso YB, Pontalier P-Y, et al. Fast Pyrolysis of Hemicelluloses into Short-Chain Acids: An Investigation on Concerted Mechanisms. Energy & Fuels 2020; 34:14232–48. https://doi.org/10.1021/acs.energyfuels.0c02901.

[65] Huang Y, Wang H, Zhang X, Zhang Q, Wang C, Ma L. CO2 pyrolysis kinetics and characteristics of lignin-rich hydrolysis residue produced from a tandem process of steam-stripping and acid hydrolysis. Fuel 2022; 316:123361. https://doi.org/10.1016/J.FUEL.2022.123361.

[66] Clemente-Castro S, Palma A, Ruiz-Montoya M, Giráldez I, Díaz MJ. Optimizing pyrolysis parameters and product analysis of a fluidized bed pilot plant for Leucaena leucocephala biomass. Environ Sci Eur 2023; 35:88. https://doi.org/10.1186/s12302-023-00800-w.

[67] Pielsticker S, Gövert B, Umeki K, Kneer R. Flash Pyrolysis Kinetics of Extracted Lignocellulosic Biomass Components. Front Energy Res 2021;9. https://doi.org/10.3389/fenrg.2021.737011.

[68] Li H, Wang L, Ji Y, Xue S, Wang Z. Study on the mechanism of gas component release for biomass pyrolysis. E3S Web of Conferences, vol. 118, EDP Sciences; 2019, p. 03058.

[69] Popa VI, Spiridon J. Hemicelluloses: structure and properties. Polysaccharides: Structural Diversity and Functional Versatility Marcel Dekker, New York 1998:297–311.

[70] Xiao L-P, Song G-Y, Sun R-C. Effect of hydrothermal processing on hemicellulose structure. Hydrothermal Processing in Biorefineries: Production of Bioethanol and High Added-Value Compounds of Second and Third Generation Biomass 2017:45–94.

[71] Adachi H, Sugiyama J, Kondo Y, Okano T. THE DIFFERENCE OF CELLULOSE CRYSTAL BETWEEN SOFTWOODS AND HARDWOODS. Sen'i Gakkaishi 1991; 47:580–4. https://doi.org/10.2115/fiber.47.11_580.

[72] Newman RH. Crystalline Forms of Cellulose in Softwoods and Hardwoods. Journal of Wood Chemistry and Technology 1994; 14:451–66. https://doi.org/10.1080/02773819408003107.

[73] Lichtenegger H, Reiterer A, Stanzl-Tschegg SE, Fratzl P. Variation of Cellulose Microfibril Angles in Softwoods and Hardwoods—A Possible Strategy of Mechanical Optimization. J Struct Biol 1999; 128:257–69. https://doi.org/10.1006/JSBI.1999.4194.

[74] Sun T, Zhang L, Yang Y, Li Y, Ren S, Dong L, et al. Fast Pyrolysis of Cellulose and the Effect of a Catalyst on Product Distribution. Int J Environ Res Public Health 2022;19. https://doi.org/10.3390/ijerph192416837.

[75] Lourenço A, Pereira H. Compositional variability of lignin in biomass. Lignin-Trends and Applications 2018:65–98.

[76] Luo Y, Li Z, Li X, Liu X, Fan J, Clark JH, et al. The production of furfural directly from hemicellulose in lignocellulosic biomass: A review. Catal Today 2019; 319:14–24. https://doi.org/10.1016/j.cattod.2018.06.042.

[77] Machado G, Leon S, Santos F, Lourega R, Dullius J, Mollmann ME, et al. Literature Review on Furfural Production from Lignocellulosic Biomass. Natural Resources 2016; 07:115–29. https://doi.org/10.4236/nr.2016.73012.

[78] Li X, Jia P, Wang T. Furfural: A Promising Platform Compound for Sustainable Production of C4 and C5 Chemicals. ACS Catal 2016; 6:7621–40. https://doi.org/10.1021/acscatal.6b01838.

[79] Lange JP, Van Der Heide E, Van Buijtenen J, Price R. Furfural-A promising platform for lignocellulosic biofuels. ChemSusChem 2012; 5:150–66. https://doi.org/10.1002/cssc.201100648.

CAPÍTULO 4

Conclusiones



4.1. Conclusiones.

La presente Tesis Doctoral tuvo como objetivo evaluar, modelizar y optimizar el fraccionamiento del clon AF2 de *Populus x euramericana* bajo un enfoque integral de biorrefinería lignocelulósica. A lo largo de este trabajo se ha demostrado la versatilidad y el potencial de esta biomasa como materia prima para esquemas de biorrefinería, mediante su valorización secuencial a través de diferentes plataformas.

Se desarrollaron estrategias de fraccionamiento físico-químico y termoquímico aplicadas tanto al clon AF2 como a otras biomasas de comparación, integrando tratamientos suaves (extracción alcalina en frío), tratamientos intensivos (explosión de vapor y organosolv) y procesos de conversión (pirólisis e hidrólisis enzimática).

En primer lugar, se validó la eficacia de la extracción alcalina en frío (EAF) como herramienta selectiva para disolver la fracción hemicelulósica, manteniendo una elevada integridad estructural en la celulosa y la lignina. El clon AF2 mostró una respuesta favorable al tratamiento, especialmente cuando se aplicó simultáneamente la tecnología de ultrasonidos, lo que incrementó tanto el rendimiento en hemicelulosas solubilizadas en el licor como el poder calorífico de la fracción sólida. En comparación, este tratamiento fue menos eficaz en *Robinia Pseudoacaia*, mientras que en el caso de la hierba elefante también se logró una solubilización selectiva de las hemicelulosas sin necesidad de incorporar ultrasonidos, lo que se relaciona con su carácter herbáceo. Esta etapa permite la recuperación de compuestos fenólicos y azúcares, sentando las bases para rutas de valorización química.

Posteriormente, se demostró que la fracción sólida del clon AF2 tras la extracción alcalina en frío presenta una mayor reactividad térmica y una reducción de la energía de activación, especialmente cuando se aplicaron ultrasonidos durante la etapa alcalina. Esta mejora se correlacionó positivamente con el enriquecimiento en glucano y la disminución relativa de lignina, lo que implicó una mayor eficiencia en la generación de productos volátiles y gases ricos en hidrógeno mediante pirólisis, destacando así su potencial como plataforma energética.

La integración de la extracción alcalina en frío con el tratamiento organosolv representó una estrategia sinérgica, que permitió operar a menores temperaturas y concentraciones de disolvente en comparación con el proceso organosolv convencional (sin etapa alcalina previa), sin comprometer la calidad de la pasta celulósica ni la recuperación de lignina. Se obtuvo una pasta con mayor pureza y mejores propiedades físicas, así como una lignina con características térmicas mejoradas, lo que amplía su campo de aplicación en materiales o química verde.

Por su parte, el uso del pretratamiento de explosión de vapor, seguido de una extracción con disolventes verdes y una posterior hidrólisis enzimática, evidenció una mejora sustancial en la conversión de celulosa a glucosa, especialmente cuando se utilizó acetato de etilo y se operó bajo condiciones moderadas de pretratamiento. Este enfoque permitió, además, recuperar compuestos fenólicos con potencial antioxidante, reforzando la sostenibilidad del proceso y el esquema de doble valorización.

Finalmente, el estudio comparativo entre distintos tipos de biomasa (clon AF2, tagasaste y paja de trigo) y métodos de fraccionamiento permitió evaluar cómo el origen y el pretratamiento influyen en el comportamiento de las fracciones lignocelulósicas durante la pirólisis. Se observaron diferencias marcadas en los perfiles de degradación y en la energía de activación, siendo la lignina la fracción más sensible al método de fraccionamiento. Además, los hallazgos de este estudio abren la posibilidad de orientar la pirólisis hacia la obtención de productos específicos, como el furfural a partir de hemicelulosas seleccionadas.

En conjunto, los resultados permiten concluir que el clon AF2 de *Populus x euramericana* constituye una materia prima estratégica para biorrefinerías lignocelulósicas. Se evidencia que la estrategia de extracción alcalina en frío no solo mejora la eficiencia de cada etapa de valorización, sino que también promueve un aprovechamiento integral y sostenible de esta biomasa de rápido crecimiento. La tesis establece un marco técnico y científico para el diseño modular de procesos, demostrando que la integración de etapas suaves e intensivas puede optimizar el rendimiento global, mejorar la eficiencia energética, facilitar la obtención de productos de valor añadido y reducir la severidad de las condiciones de operación.

Esta investigación no solo aporta conocimientos relevantes sobre el comportamiento y valorización del clon AF2 de *Populus x euramericana*, sino que también contribuye a la implementación de esquemas de biorrefinería más sostenibles y adaptativos, en consonancia con los principios de la economía circular y la transición energética.

4.2. Conclusions.

The aim of this Doctoral Thesis was to evaluate, model, and optimise the fractionation of clone AF2 of *Populus x euramericana* within an integrated lignocellulosic biorefinery framework. Throughout this study, the versatility and potential of this biomass as a feedstock for biorefinery applications have been demostrated, through its sequential valorisation via different platforms.

Physicochemical and thermochemical fractionation strategies were developed and applied to clone AF2 and other comparative biomasses. These strategies integrated mild treatments (cold alkaline extraction), intensive treatments (steam explosion and organosolv), and conversion processes (pyrolysis and enzymatic hydrolysis).

Firstly, the efficiency of cold alkaline extraction (CAE) was validated as a selective method for dissolving the hemicelulosic fraction while preserving the structural integrity of cellulose and lignin. Clone AF2 exhibited a favourable response to the treatment, especially when ultrasound technology was simultaneously applied, which increased both the yield of solubilised hemicelluloses in the liquor and the calorific value of the solid fraction. In comparison, the treatments was less efficient on *Robinia Pseudoacaia*, whereas in elephant grass, a selective solubilisation of hemicelluloses was achieved without the need for ultrasound, likely due to its herbaceous nature. This stage enabled the recovery of phenolic compounds and sugars, laying the groundwork for subsequent chemical valorisation routes.

Subsequently, the solid fraction obtained from cold alkaline extraction of clone AF2 exhibited high thermal reactivity and a reduction in activation energy, particularly when ultrasound was applied during the alkaline stage. This improvement correlated positively with glucan enrichment and a relative decrease in lignin content, leading to greater efficiency in the generation of volatile products and hydrogen-rich gases via pyrolysis, thus highlihting its potential as an energy platform.

The integration of cold alkaline extraction with organosolv treatment represented a synergistic strategy, allowing operation at lower temperatures and solvent concentrations than the traditional organosolv process (without the prior alkaline stage), without compromising cellulose pulp quality or lignin recovery. The resulting pulp exhibited higher purity and improved physical propeties, while the lignin displayed enhanced termal characteristics, broadening its potential applications in materials and green chemistry.

The use of steam explosion pretreatment, followed by green solvent extraction and subsequent enzymatic hydrolysis, resulted in a substantial improvement in cellulose to glucose conversion, particularly when ethyl acetate was used and moderate pretreatment conditions were applied. This

approach also enabled the recovery of phenolic compunds with antioxidant potential, reinforcing both the sustainability of the process and the dual valorisation strategy.

Finally, the comparative study of different biomass types (clone AF2, tagasaste, and wheat straw) and different fractionation methods enabled the evaluation of how both biomass origin and pretreatment influence the behaviour of lignocellulosic fractions during pyrolysis. Marked differences in degradation profiles and activation energies were observed, with lignin being the fraction most sensitive to the fractionation method. Furthermore, the findings of this study open the possibility of targeting pyrolysis toward the production of specific compounds, such as furfural from selected hemicelluloses.

Overall, the results support the conclusion that clone AF2 of *Populus x euramericana* is a strategic feedstock for lignocellulosic biorefinery. It is evident that cold alkaline extraction not only enhances the efficiency of each valorisation stage, but also promotes an integrated and sustainable use of this fast-growing biomass. This doctoral thesis establishes a theoretical and scientific framework for modular process design, demonstrating that the integration of mild and intensive treatments can optimise overall yield, improve energy efficiency, facilitate the production of value-added products, and reduce the severity of operational conditions.

This research not only to contributes valuable knowledge regarding the behaviour and valorisation of clone AF2 of *Populus x euramericana*, but also supports the implementation of more sustainable and adaptive biorefinery schemes, aligned with the principles of the circular economy and the energy transition.

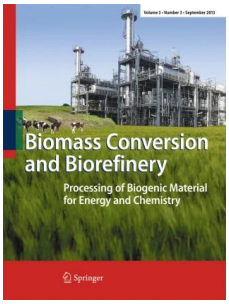
ANEXOS



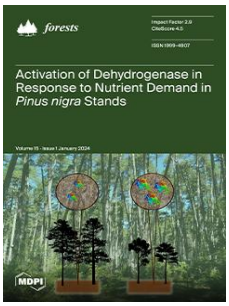
1. Publicaciones.

- **Artículos derivados de la Tesis Doctoral.**

☐ J.C. García, A. Alfaro, J.M. Loaiza, S. Lozano-Calvo, F. López, Cold alkaline extraction of Elephant Grass for optimal subsequent extraction of hemicelluloses and energy production.
Biomass Convers Biorefin 14 (2024) 8307-8320.
https://doi.org/10.1007/s13399-022-03054-3.



☐ S. Lozano-Calvo, J.M. Loaiza, J.C. García, M.T. García, F. López, Ultrasound-Assisted Cold Akaline Extraction: Increasing Hemicellulose Extraction and Energy Production from Populus Wood.
Forests 15 (2024) 109.
https://doi.org/10.3390/f15010109.



☐ S. Lozano-Calvo, J.M. Loaiza, J.C. García, R. Tapias, F. López, Kinetic and hydrogen production analysis in the sequential valorization of *Populus* clone by cold alkaline extraction and pyrolysis.
Sci Rep 14 (2024) 1509.
https://doi.org/10.1038/s41598-024-52052-0.



☐ N. Almagro-Herrera, S. Lozano-Calvo, A. Palma, J.C. García, M.J. Díaz, Assessing the influence of biomass origin and fractionation methods on pyrolysis biomass fractions.
Fuel 367 (2024) 131501.
https://doi.org/10.1016/j.fuel.2024.131501.



- **Otros Artículos publicados a lo largo de la Tesis Doctoral.**

☐ J.M. Loaiza, M.A. Zamudio, L. Susana, A. Alfaro, M.T. García, J.C. García, F. López, Characterization and Usage of Tule (Typha domingensis Pers) to Obtain Cellulose Pulp in a Biorefinery Framework.
Bioresources 16 (2021) 3328-3347.
https://doi.org/10.15376/biores.16.2.3328-3347.



☐ M. Ruiz-Montoya, A. Palma, S. Lozano-Calvo, E. Morales, M.J. Díaz, Kinetic synergistic effect in co-pyrolysis of *Eucalyptus Globulus* with high and low density polyethylene.
Energy Reports 8 (2022) 10688-10704.
https://doi.org/10.1016/j.egyr.2022.08.200.



Biomass Conversion and Biorefinery
https://doi.org/10.1007/s13399-022-03054-3

ORIGINAL ARTICLE

Cold alkaline extraction of Elephant grass for optimal subsequent extraction of hemicelluloses and energy production

J. C. García[1] · A. Alfaro[2] · J. M. Loaiza[1] · S. Lozano-Calvo[1] · F. López[1]

Received: 22 March 2022 / Revised: 5 July 2022 / Accepted: 7 July 2022
© The Author(s) 2022

Abstract

There is growing scientific and industrial interest in obtaining useful substances by fractionating lignocellulosic biomass from non-food plant crops for use by the bioenergy industry. The primary goals are to ensure process sustainability and to comply with the principles of circular economy. In this work, we optimized energy production from Elephant grass by previously using cold alkaline extraction to remove its hemicellulose fraction. Elephant grass contains a high proportion of lignin (20%) and hemicelluloses (27.4%), and therefore is an excellent alternative to wood materials for energy production by direct burning. Energy production was optimized to identify the best operating conditions among those tested, namely: alkali concentrations of 80–120 g NaOH L^{-1}, temperatures of 20–40 °C, and treatment times of 30–90 min. Using the optimum conditions thus established (viz., 100 g NaOH L^{-1}, 30 °C, and 30 min) raised the high heating value (HHV) to 19.151 MJ kg^{-1} (i.e., by 4% relative to the starting material). Also, it allowed the content in elemental C to be preserved, that in H increased by 4.86% and, more environmentally significant, most sulphur (46.9%) to be removed from the solid phase upon treatment. Cold alkaline extraction of the raw material additionally enabled relatively selective separation of the hemicellulose fraction from the cellulose and lignin fractions. Thus, 30.1% of all hemicellulose was dissolved in the treatment liquor and made valorizable while 93.0% of cellulose and 82.1% of lignin present in the raw material remained in the solid phase.

Keywords Biorefinery · Cold alkaline extraction · Elephant grass · Hemicelluloses · Bioenergy

1 Introduction

Biorefining is becoming increasingly essential to ensure sustainable development, especially when using raw materials based on non-food plants such as perennial grasses, which escape the food versus fuel dilemma [1–3]. In fact, using biomass as a renewable energy source can be useful to fulfil the goals of the current European energy policy, which is increasingly favouring the establishment of sustainable energy crops not compromising food production [4, 5]. A fraction of 17.9% of all energy used in the word in 2018 was obtained from renewable sources—and 67% of it from biomass—2.2% from nuclear power and 79.9% from fossil fuels [6]. The European Union has set the goal that, by 2030, 37% of all energy should be produced from renewable sources [7, 8]. In the process, fossil fuels should be gradually replaced with renewable energy sources to reduce greenhouse gas emissions, diversify energy supply, and alleviate the currently strong dependence on oil markets while creating new jobs, fostering industrial entrepreneurship, and boosting economic growth [9, 10].

Energy from biomass can be used in the traditional manner (i.e., by burning, which uses 57.7% of lignocellulosic biomass) or as "modern bioenergy," which uses the remainder portion of biomass (specifically, 20.8% for industrial heating, 10% for home heating, 8.3% for transportation, and 3.3% for electricity production) [6].

A number of plant species are currently being used for energy production worldwide. Especially prominent among the non-wood species are perennial grasses such as giant reed (*Arundo donax*, L.), miscanthus (*Miscanthus x giganteus*), energy cane (*Saccharum spontaneum hybrids*), switchgrass (*Panicum virgatum L.*), bulbous canary grass

✉ A. Alfaro
ascension.alfaro@uhu.es

[1] Research Center in Technology of Products and Chemical Processes, PRO2TECS- Chemical Engineering Department, University of Huelva, Av. 3 de marzo s/n, 21071 Huelva, Spain

[2] Department of Forest Engineering, University of Huelva, Huelva, Spain

Published online: 27 July 2022

(*Phalaris aquatica L.*), elephant grass (*Pennisetum purpureum* Schum.) [11–13], and bagasse from eating sugarcane [14, 15]. These plants are especially suitable for energy production by virtue of their low cropping costs, and also of their ability to grow in a variety of environments or even on marginal land [16]. Also, they produce large amounts of biomass [17], use water and nutrients highly efficiently [18, 19], contain more cellulose and lignin than deciduous species, and have a relatively low moisture content at the end of their growth cycle [2, 20, 21]. Even more important, they have the potential for use on marginal land and hence for improving the social and economic status of some rural areas [22].

Pennisetum purpureum Schum is a perennial grass of the family Poaceae from tropical Africa. Popularly known by the names "Elephant grass," "giant zacate," "fake sugarcane," "Napier grass," "merkeron," "Uganda grass" and "king grass," this plant has traditionally been used as fodder in tropical and subtropical countries. Each plant of Elephant grass has a number of branching stems radiating from the same stand. Its stems can be up to 8 m tall and 2.5 cm thick, and resemble those of sugarcane in appearance [1, 23]. Elephant grass grows well in temperate, subtropical, and tropical regions with a dry season. Also, it can grow in many types of land, but especially on thick, light-textured, well-drained soils [24], as well as on acid soils previously amended with biochar [25]. This species is highly resistant to disease and tolerant of drought [26]. Its ability to grow on contaminated soils has allowed its cropping in engineered wetlands to exploit its phytoremediating effects and use the resulting biomass for ethanol and butanol production [27]. Among others, elephant grass has additionally been used to reclaim water bodies contaminated with high concentrations of arsenic [21].

Like miscanthus and switchgrass, Elephant grass is a C4-type plant whose high photosynthetic efficiency leads to also high lignocellulose production [17, 28–30]. In fact, Elephant grass produces in the region of 45 t dry matter ha^{-1} $year^{-1}$ [1, 23, 31, 32] depending on the particular genotype, soil fertility, and crop management practices. Thus, [33] and [34] reported yields of 12–150 and 45–67 t ha^{-1} $year^{-1}$, respectively, so high biomass production yields, and the fact that Elephant grass can be harvested up to four times each year, make it especially attractive for energy production [1, 33].

Industrially, Elephant grass has been used to obtain chemicals such as cellulose and xylanase [35], monosaccharides and ethanol [36], xylitol and ethanol [37], hemicelluloses [38, 39], lignin nanoparticles [40], cellulose pulp [32, 41], and corrosion inhibitor extracts [42]. Also, it has been used to obtain fuels such as ethanol [33, 34, 43–45] or methane [24, 46–48], pyrolysis products [34, 49–52], thermal and electrical energy [17, 24, 53–58], and densified solid biofuels [19]. These uses testify to the high potential of Elephant grass for energy production and have fostered research into genetic breeding methods for improving its properties as a raw material and optimizing its use [24, 53, 59–61].

In this scenario, our group envisaged the development of a process for obtaining energy from Elephant grass and using its lignocellulose fraction as a source of chemicals. This is the way biorefining schemes are typically used to fractionate lignocellulosic materials stepwise for optimal use of the ensuing fractions. In this work, we used cold alkaline extraction (CAE) prior to fractionation of Elephant grass on the grounds of its operational and environmental advantages over other alkaline and hydrolysis treatments [26, 62]. The most salient advantage of CAE over alternative biomass fractionation methods is its ability to separate hemicelluloses in a selective manner for their subsequent alcoholic precipitation with minimal degradation to furfural [63–67]. In addition, CAE requires no high temperatures or pressures, and hence uses energy sparingly. In fact, most CAE-based processes are conducted at mild temperatures (20–40 °C) [68]. However, the efficiency of the CAE treatment is strongly dependent on the particular raw material and greater with grassy lignocellulosic materials than with woody plants (i.e., it allows lignocellulose to be more efficiently extracted from grasses) [63, 69–71].

With the aims of ensuring sustainability in the process and complying with the principles of circular economy, in this work, we optimized the efficiency of Elephant grass as an energy crop by subjecting the raw material to cold alkaline extraction in order to remove its hemicellulose fraction in the treatment liquor and use the resulting solid phase for energy production with increased economic and environmental efficiency in the overall process.

2 Materials and methods

Figure 1 shows the sequential scheme of the experimental work carried out with the Elephant grass.

2.1 Chemical and energy characterization

The material studied was elephant grass grown at an experimental station of the Pulp and Paper Laboratory of the Federal University of Viçosa (Minas Gerais, Brazil) that was ground by hand to obtain fragments of variable length and 1–4 cm in width. The material was characterized in chemical and energy terms by using the same methods as with the CAE liquor and solid phase.

For chemical analysis, samples were ground to variably sized particles in Wiley mill. The particles were sieved according to TAPPI T257-cm85 and those ranging from 40 to 60 mm in size retained. Moisture was determined by

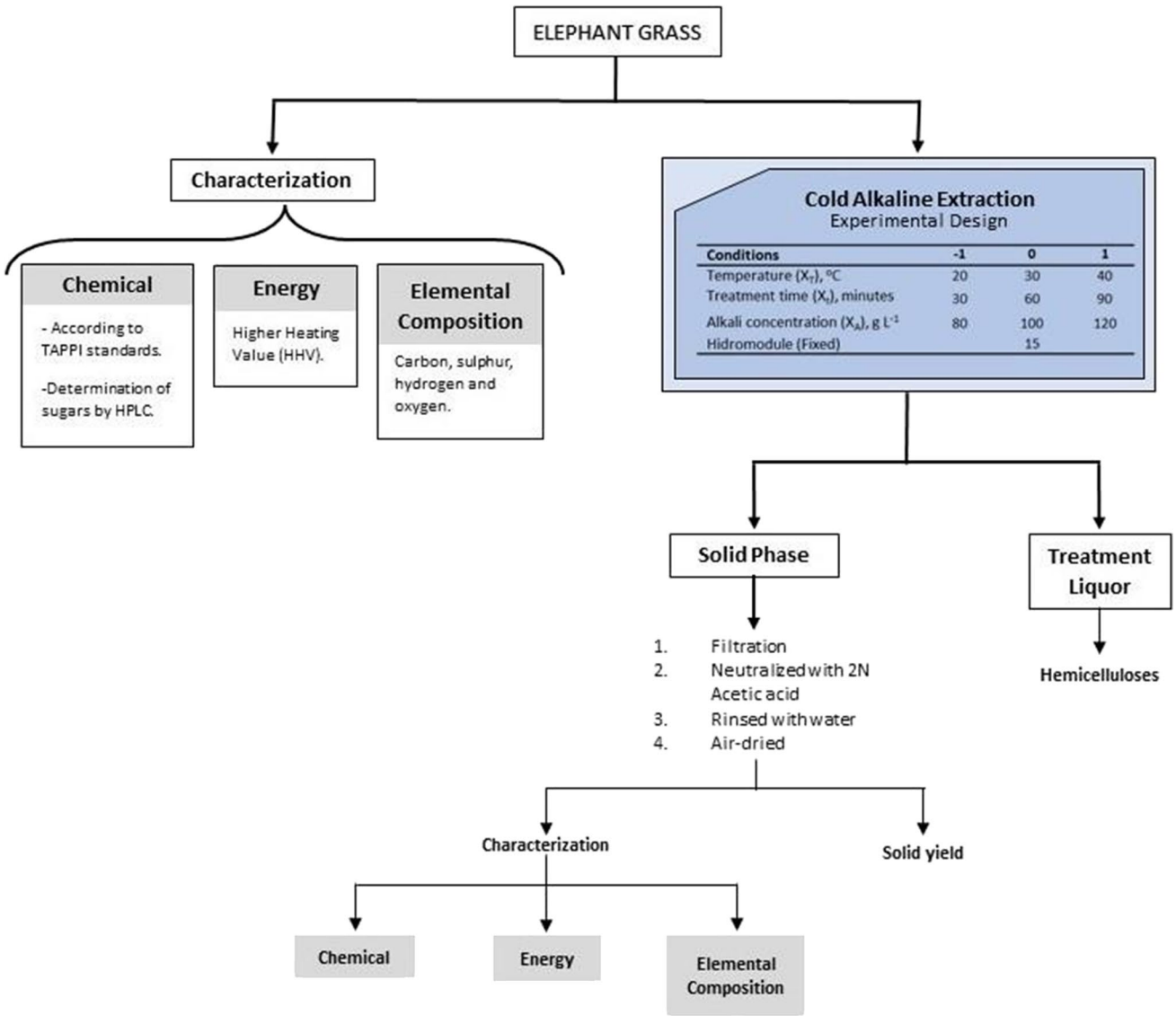


Fig. 1 Scheme of the work carried out

drying to a constant weight at 105 °C (TAPPI T-264-cm-07). The samples, raw material, and CAE solid phase were all hydrolysed with 5 mL of 72% H_2SO_4 acid at 30 °C for 1 h and the -hydrolysed by adding water to reduce the acid concentration down to 4% while heating at 121 °C for 60 min according to TAPPI T 249 cm-09. The resulting solid residue was recovered by filtration and labelled Klason lignin (TAPPI T 222 om-06). Soluble lignin was determined according to TAPPI T UM 25, and the hydrolysate used to determine, glucan, and hemicelluloses (xylan, araban, galactan, and mannan) in the material on an Agilent 1100 HPLC instrument equipped with a BioRaden ion-exchange column and a refractive index detector. The working temperature was 50 °C, and the mobile phase consisted of 0.005 M H_2SO_4 and was circulated at 0–0.6 mL/min. All measurements were made in triplicate and the resulting coefficient of variation was less than 4%.

The raw materials and the solid phases were analysed for carbon, sulphur, hydrogen, and oxygen on an Eltra Helios CHS analyser. Also, they were used to determine their higher heating value (HHV) at a constant volume in accordance with CEN/TS 14,918 (2005) and UNE 16,001 EX (2005) on a Parr 6300 automatic isoperibol bomb calorimeter.

2.2 Cold alkaline extraction and determination of hemicelluloses

Alkaline extraction was done by immersing the raw material in a bath containing an NaOH solution, using a constant solid/liquid ratio on a dry basis of 15 in all tests. The

independent variables of the process were the soda concentration, temperature, and treatment time.

The solid fraction was recovered by filtration, neutralized with 2 N acetic acid, rinsed with water, and air-dried for weighing in order to estimate yield. The proportions of glucan and hemicelluloses from the raw material present in the extraction liquor were determined as described in the previous Sect. (2.1). The solid fraction was also subjected to the determinations described in it.

2.3 Multiple regression models and experimental design of cold alkaline extraction

The CAE process was modelled in order to maximize extraction of hemicellulose derivatives while ensuring that the resulting solid would have a high heating value for energy production. A $2n$ factorial design with a central point was used to reduce the number of tests needed and also to avoid significant covariances between the dependent variables. The number of tests needed, N, was calculated as $2^n + 2n + n_C$, where 2^n is the number of points constituting the design, $2n$ that of axial points and n_C that of central points.

The independent variables were normalized by using the following Eq. (1):

$$X_n = \frac{X - \mathrm{X}}{(X_{\max} - X_{\min})/2} \tag{1}$$

where X is the absolute value of the variable concerned, and $\bar{X}$, $X_{\max}$, and $X_{\min}$ are its mean, maximum, and minimum value, respectively.

As can be seen in Table 1, each independent variable was examined at three different values. The results were used to establish second-order polynomials for each dependent variable, the polynomials including linear and quadratic terms of the independent variables, and their mutual interactions, and being fitted by multiple regression:

$$Y = a_0 + \sum_{i=1}^{n} b_i X_{ni} + \sum_{i=1}^{n} c_i X_{ni}^2 + \sum_{i=1 i=1}^{n} d_{ij} X_{ni} X_{nj} (i < j) \tag{2}$$

where X denotes independent variables, Y dependent variables, and coefficients a_o, b_i, c_i, and d_{ij} are constants for each model obtained from the experimental results. The dependent variables were yield, glucan, xylan, araban, galactan, mannan, Klason lignin, and soluble lignin, and the independent variables were soda concentration, temperature, and time.

The independent variables present in the polynomials are those which exhibited statistically significant coefficients. In fact, no term with $p < 0.05$ as per Student's t-test or spanning a confidence interval narrower than 95% was included.

The results were processed with the software Statistica v. 10.0 (StatSoft, Inc., Tulsa, OK, USA) and additionally used to calculate R^2 and Snedecor's F-value, those with $R^2 > 0.85$ or $F > 5$ being deemed acceptable.

Table 1 Conditions of CAE experimental design

Conditions	−1	0	1
Temperature (X_T), °C	20	30	40
Treatment time (X_t), minutes	30	60	90
Alkali concentration (X_A), g L^{-1}	80	100	120
Hidromodule (fixed)	15		

3 Results and discussion

As noted earlier, the primary aims of this work were to optimize the use of Elephant grass by subjecting the raw material to cold alkaline extraction (CAE) in order to remove its hemicellulose fraction in the treatment liquor and facilitate energy production from the resulting solid phase under the assumption that CAE would increase the heat capacity and decrease the sulphur content of the solidphase while enabling selective extraction of hemicellulose derivatives for their valorization. For this purpose, the starting material was characterized in chemical and energy terms, and the CAE process was modelled for optimal energy production. Finally, the efficiency with which hemicellulose derivatives were extracted, and its dependence on the operating conditions, were assessed.

3.1 Chemical and energy characterization

Based on recent studies [24], Elephant grass can store dry matter more efficiently than other plant species. This results in favourable quality-related biomass properties including high heating value (HHV), and cellulose, hemicellulose, lignin, and ash contents. These properties make elephant grass an effective alternative to lignocellulosic raw materials for energy production by burning. Table 2 shows the chemical composition of Elephant grass as determined by our group and other authors. As can be seen, coefficients of variation were relatively high (viz. 136% for cellulose, 105% hemicellulose, 69% for lignin, and 25% for ash), which can be ascribed to differences in plant growth environment. In any case, our results fall within the chemical composition ranges previously reported by other authors. Also, the differences in composition can have arisen from differences among the 85 genotypes studied [33], which spanned cellulose and lignin contents over the range 38.5–48.9% and 6.4–12.4%, respectively.

The chemical composition of Elephant grass is compared with those of other grass species and a reference material (*Eucalyptus globulus*) used for bioenergy production and

Table 2 Chemical characterization of Elephant grass

Component (%)	This work	Oluwasina [38]	Gomes [32]	Pandey [21]	Cardona [72]	De Conto [49]
Glucan	41.7	55.33	38.2	36.34	22.6	30.37
Xylan	23.1	–	9.6	–	–	–
Arabinan	2.9	–	0.2	–	–	–
Galactan	0.95	–	0.8	–	–	–
Manan	0.45	–	0.6	–	–	–
Hemicelluloses	27.4	16.6	–	34.12	20.9	31.31
Klason lignin	19.3	2.79	–	–	–	–
Soluble lignin	1.56	24.0	2.2	–	–	–
Lignin	20.9		18	30.40	19.4	26.02
Holocelluloses	69.1	69.60	–	–	–	–
Ash	–	8.87	–	–	11.1	–

other industrial purposes in Table 3. The cellulose content of the plant material used here (41.7%) was higher than that of other grasses such as switchgrass (31.0%) and sugarcane bagasse (39.0%), but somewhat lower than that of *Miscanthus giganteus* (48.6%) and eucalyptus wood (48.1%). The material had a high content in hemicellulose (27.4%), which is especially useful for biorefining by selective extraction of the hemicellulose fraction. This content exceeds the combined xylan and araban content reported by Oluwasina [38] for the same species (17.6%) and is comparable to the upper ends of the ranges for other materials such as rice straw (23–28%), wheat straw (26–32%), sugarcane bagasse (27–32%), and bamboo (15–26%) [80]. Xylan was the major component of the hemicellulose fraction and present in considerably higher proportions (23.1%) than in other materials (e.g., 8.4% in eucalyptus wood or 17.3% in sugarcane bagasse) [81]. The proportion of lignin in Elephant grass (20.9%) was higher than those in other residual grass materials such as wheat straw, tricolor sorghum, or corn stover (18.6%) [73], but slightly lower than those of grass species such as *M. Giganteus* and sugarcane bagasse, and wood species such as eucalyptus (26.9%), poplar (25.2%), and leucaena (24%) [75, 77, 82, 83]. Finally, the lignin contents of elephant straw were similar to those of other raw materials such as rice straw (15–25%) [84, 85] and fell in the overall ranges for grass species (10–30%) [73].

In terms of energy potential, the high heating value (HHV) of Elephant grass, calculated as described under Materials and Methods, was 18.44 MJ kg^{-1}, which is very similar to that reported by Reza et al., [50] (18.55 MJ kg^{-1}) but higher than that obtained by Tsai [86] (16.3 MJ kg^{-1}). These differences are quite normal because HHV changes with plant age (e.g., from 16.96 MJ kg^{-1} at 4 months to 22.04 MJ kg^{-1} at 6) [87]. HHV for Elephant grass was similar to the values for a number of wood species (in the region of 20 MJ kg^{-1}) according to [88], and also similar to or slightly greater than those of short-lifecycle plant species used for energy production such as *Leucaena leucocephala* (19.3–20.6 MJ kg^{-1}) [83], switchgrass (18.8 MJ kg^{-1}), or wheat straw (18.55 MJ kg^{-1}) [74].

An elemental composition analysis conducted as described under Materials and Methods provided the C, O,

Table 3 Chemical composition of selected lignocellulosic crops of industrial and bioenergetic interest

Component (%)	Switchgrass [73, 74]	*Miscanthus* x *giganteus* [75, 76]	Sugarcane bagasse [32]	Eucalyptus [73, 77, 78]	Wheat straw [73, 79]	Bicolor sorghum [73]
Glucan	30.97, 38	48.64, 39.5	39.01	48.07, 49.4, 46.8	32.64, 41.8	34.01
Xylan	20.42, 22.8	nd, 19.0	22.05	10.42, 12, 16.6	19.22, 25.4	14.14
Arabinan	2.75, 3.7	nd, 1.8	2.06	0.3, 0.3, 0.5	2.35, 2.5	1.65
Galactan	0.92, 1.3		0.46	0.74, 1.2	0.75, 0.7	0.52
Mannan	0.29		0.35	1.23, 0.9	0.31	0.2
Hemicelluloses	24.55	18.67				
Lignin	17.56, 22.1	27.2	23.09	26.91, 27.2, 22.9	16.85	16.09
Holocellulose		67.31		nd, nd, 66.9		
Ash	5.76, 3.7	5.49	3.66	1.22	10.22	5.04
Extractives	16.99		3.76	4.15	12.95	22.03

H, and S contents that are compared with those reported by Reza et al. [50] and those for various other raw materials in Table 4. The chemical composition of a raw material can be expected to influence that of the gases it releases and the amount of heat it produces upon burning. The fact that the C and H contents of Elephant grass were somewhat higher than those of other materials suggested that it might be more efficient for energy production. On the other hand, the S content of Elephant grass was similar to those of other lignocellulosic raw materials and substantially lower than those of fossil fuels.

Table 4 Elemental composition of Elephant grass and other lignocellulosic materials

Species	C (%)	H (%)	S (%)	O (%)
Elephant grass[(1)]	48.999	6.790	0.12125	44.09
Elephant grass[(2)]	43.23	5.8	0.11	50.86
Clon AF2 Populus[(1)]	52.101	6.023	0.016	41.86
Leucaena[(1)]	50.623	6.117	0.024	43.236
Robinia[(1)]	51.38	6.301	0.023	42.296
Eucalyptus globulus[(1)]	51.924	6.326	0.01	41.74
Olmo[(1)]	52.916	6.406	0.017	40.661
Pino[(1)]	57.746	6.942	0.12	35.192
Ethiopian rapeseed[(3)]	46.3	6.1	0.49	47.11
Populus[(3)]	48.19	5.9	0.05	45.86

[(1)]This work, [(2)] [50], [(3)] [89]

3.2 Modelling and optimization of the higher heating value and elemental composition of the post-CAE liquor and solid phase

Table 5 shows the HHV and elemental composition (C, H, S, and O) of the solid fraction from the CAE treatment as determined under variable operating conditions selected in accordance with the experimental design used. The polynomial equations of the design are shown in Table 6, which includes one for CAE solid yield. As can be seen, the differences between observed and calculated values never exceeded 10% and correlation coefficients were all higher than 0.95. Table 5 also includes CAE yield.

As can be seen from Eq. 1 in Table 6, HHV for the post-CAE solid phase from Elephant grass was strongly dependent on the quadratic terms of the process variables. Clearly, the values and signs of the coefficients for the treatment time suggest that times in the lower end of the operating range should result in increased HHV levels. Also clearly, using alkali concentrations and temperatures at the ends of the operating ranges would detract from HHV as the very likely result of poor extraction of hemicelluloses into the CAE liquor at low temperatures and excessive extraction of polyphenols (lignin) at high temperatures. As confirmed by Fig. 2A, it was therefore advisable to use medium alkali concentrations and temperatures. Thus, Eq. 1 in Table 6 predicts HHV = 19.151 MJ kg^{-1}, which was nearly 4% higher than the value for the starting material.

Table 5 HHV and elemental composition of the post-CAE solid phase obtained under different operating conditions

T (°C), t (min), NaOH concentration (g L^{-1})	C (%)	H (%)	S (%)	O (%)	HHV (MJ/kg)	Yield (%)
0, 0, 0	47.581	7.089	0.0865	52.333	18.745	74.6
0, 0, 0	47.656	7.061	0.0827	52.261	18,863	75.3
1, 1, 1	47.185	6.747	0.0019	52.813	18.200	66.9
1, 1, –1	46.170	6.724	0.0018	53.828	17.777	71.8
1, –1, 1	47.027	6.862	0.0040	52.969	18.449	79.4
1, –1, –1	46.866	6.931	0.0035	53.131	18.045	82.8
–1, 1, 1	47.052	6.755	0.0084	52.940	18.122	75.3
–1, 1, –1	46.956	6.703	0.0118	53.032	18.278	72.1
–1, –1, 1	46.956	6.810	0.0384	53.006	18.429	84.7
–1, –1, –1	47.585	6.850	0.0384	52.377	18.374	86.8
1, 0, 0	46.172	6.975	0.0232	53.805	18.435	70.5
–1, 0, 0	46.263	6.869	0.0520	53.685	18.402	76.1
0, 1, 0	48.388	7.056	0.0613	51.551	18.866	70.6
0, –1, 0	48.871	7.067	0.0891	51.040	19.244	82.5
0, 0, 1	46.891	6.982	0.0831	53.026	18,590	77.4
0, 0, –1	47.077	6.975	0.0844	52.839	18.470	80.6
Raw material	48.999	6.790	0.12125	57.912	18.440	

Y_{HHV} high heating value (HHV). Y_C, Y_H, and Y_S content in carbon, hydrogen, and sulphur (%). Y_{yield} CAE yield (%). X_A, X_T, X_t normalized alkali concentration, temperature, and treatment time, respectively

Table 6 Polynomial models for HHV, C, H, S, and yield

Eq	Polynomial	r^2	F
1	$Y_{HHV} = 18.850 + 0.0938 \cdot X_A - 0.121 \cdot X_t - 0.070 \cdot X_T - 0.346 \cdot X_A^2 + 0.179 \cdot X_t^2 - 0.458 \cdot X_T^2 + 0.116 \cdot X_A \cdot X_T$	0.940	34.5
2	$Y_C = 47.513 - 0.279 \cdot X_t - 0.302 \cdot X_T - 0.476 \cdot X_A^2 + 1.170 \cdot X_t^2 - 1.242 \cdot X_T^2$	0.945	52.6
3	$Y_S = 0.0887 - 0.0097 \cdot X_t - 0.0112 \cdot X_T - 0.0070 \cdot X_A^2 - 0.0156 \cdot X_t^2 - 0.0532 \cdot X_T^2 + 0.0070 \cdot X_T \cdot X_t$	0.982	140.4
4	$Y_H = 7.073 - 0.047\ X_t + 0.035 \cdot X_T - 0.104 \cdot X_A^2 - 0.160 \cdot X_T^2 + 0.0316 \cdot X_A \cdot X_t$	0.956	66.9
5	$Y_{yield} = 75.56 - 2.35\ X_T - 5.96\ X_t - 1.04\ X_A - 1.94\ X_T^2 + 3.78\ X_A^2 - 1.19\ X_t X_A$	0.987	57.61

Y_{HHV} high heating value (HHV). Y_C, Y_H, and Y_S content in carbon, hydrogen, and sulphur (%). Y_{yield} CAE yield (%). X_A, X_T, X_t normalized alkali concentration, temperature, and treatment time, respectively

Equations 2 and 4 in Table 6 show the modelled results for the C and H contents of the post-CAE solid phase. The conditions needed to maximize HHV and both contents were identical. Again, the quadratic terms were especially influential and interaction terms virtually uninfluential. As with HHV, maximizing the C and H contents of the post-CAE solid phase would require using medium alkali concentrations and temperatures in combination with short treatment times. Under these conditions, Eqs. 2 and 4 in Table 6 predict a content in C of 48.961% and one in H of 7.120%. While the C content was similar to that of the raw material, the H content was 4.86% higher. The response surface for the C content, not shown, was similar to that of Fig. 2A.

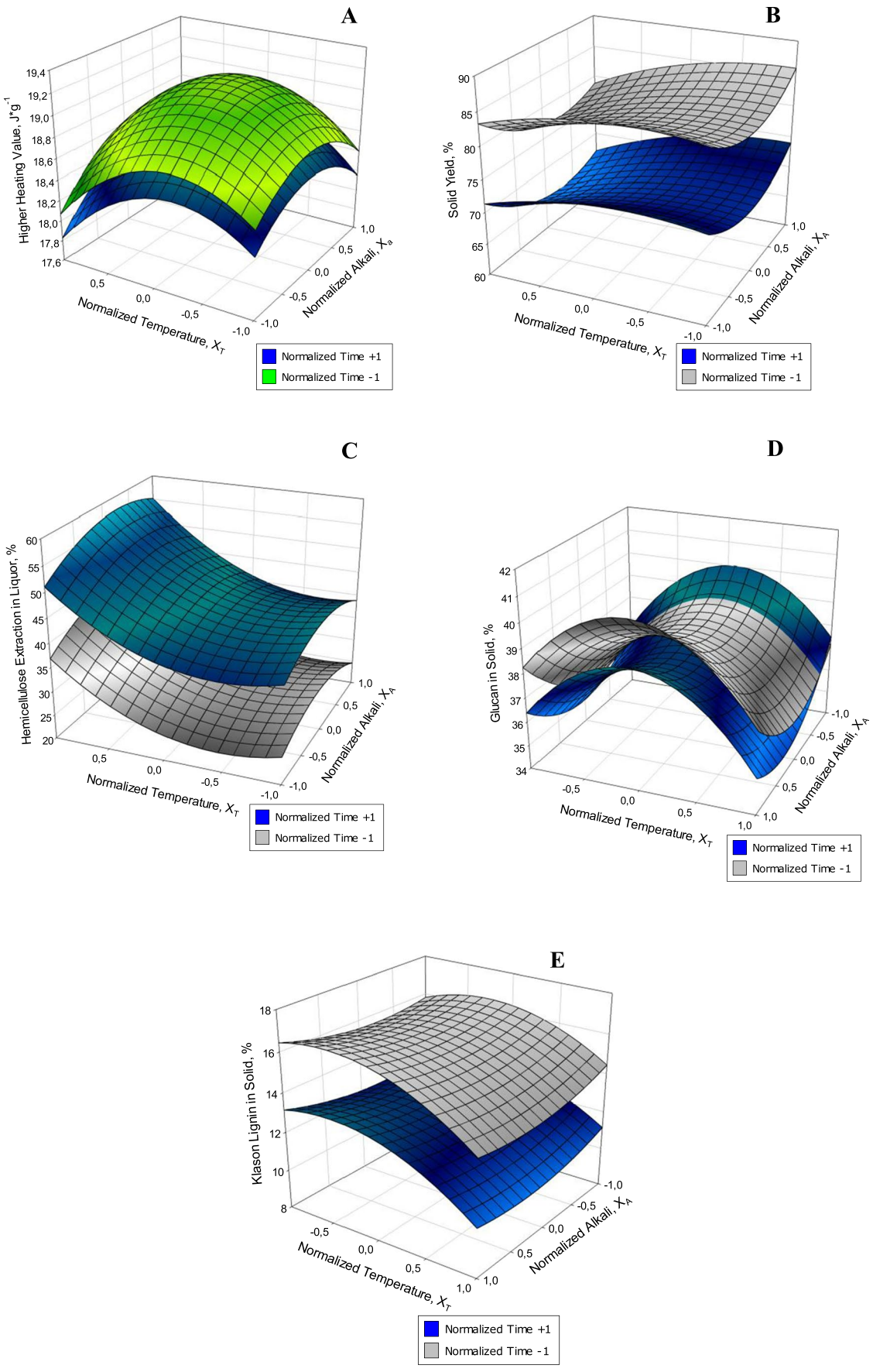
Based on the predictions of Eq. 3 in Table 6, the operating conditions maximizing energy production, and the C and H contents, should lead to increased S contents in the post-CAE solid phase. Although this might be an unwanted outcome of the treatment, the S content of the starting biomass was so low that it was unlikely to raise environmental concerns. Also, the CAE treatment considerably reduced the S content by 26.6–98.5% depending on the particular conditions (46.9% with the optimum settings). In this way, CAE facilitated use of the material for energy production with little emission of sulphur dioxide. This is an added advantage to the above-mentioned increased energy yield and valorization of the hemicellulose fraction relative to burning of the raw material. Also, the increased energy yield need not be accompanied by an excessive decrease in solid yield. In fact, hemicellulose extraction should be selective providing most cellulose and lignin remain in the post-CAE solid phase.

As can be seen from Table 5, the CAE treatment resulted in little biomass loss. Thus, solid yields ranged from 66.9 to 86.8% and exceeded those obtained by García et al. [63] treating wheat straw (viz., 61.1% by using an NaOH concentration of 100 g L^{-1}, a temperature of 40 °C, and a treatment time of 90 min). The yield from Elephant grass under similar temperature and time conditions amounted to 71.8 and 66.9% with an NaOH concentration of 80 and 120 g L^{-1}, respectively. There were no substantial changes in yield with temperature or the alkali concentration, however. By contrast, time considerably influenced the results. Thus, the highest yields were obtained at short times (30 min, normalized value –1) and, with little difference, low temperatures (20 °C, –1) and high alkali concentrations (120 g NaOH L^{-1}, + 1). As can be seen from Fig. 2B, using short treatment times and medium temperatures (normalized value 0) provided the highest solid yields. Based on Eq. 5 in Table 6, using medium temperatures and alkali concentrations in combination with short times (–1) would lead to a yield of 81.5% in the post-CAE solid phase. This is quite acceptable if one considers that the highest possible yield was 85.6% (Eq. 5, Table 6).

3.3 Modelling and optimization of monosaccharide contents in the post-CAE liquor and solid phase

Table 7 shows the contents in Klason and soluble lignin, individual monomers from the polysaccharide fraction, their combination, and monomers from the hemicellulose fraction (xylan, arabinan, galactan, and mannan) of the post-CAE solid fraction as a function of the operating conditions used. The results were used to calculate the proportion of each fraction that was extracted into the CAE liquor. Table 8 shows the proportions such fractions but relative to the percent content of each polymer in the starting material.

Not all chemical characterization results shown in Tables 7 and 8 were modelled. In fact, some components were present in too small amounts in both the raw material and the post-CAE solid phase for any useful conclusions to be drawn. Rather, we used multiple regression on the major dependent variables suggested by the experimental design in addition to total hemicellulose in order to consider two minor saccharides (mannan and galactan). On the other hand, the liquid fraction was modelled for extracted lignin, extracted glucan, and total extracted hemicellulose (viz., the combination of all monomers listed in Table 8 except glucan). The models used, and their statistical figures of merit, are shown in Table 9. As can be seen, the differences between experimental and calculated values never exceeded 10% and correlation coefficients (R^2) were all higher than 0.95.


A
Higher Heating Value, J*g-1
19,4
19,2
19,0
18,8
18,6
18,4
18,2
18,0
17,8
17,6
0,5
0,0
-0,5
-1,0
Normalized Temperature, XT
1,0
0,5
0,0
-0,5
-1,0
Normalized Alkali, XA
Normalized Time +1
Normalized Time -1
B
Solid Yield, %
90
85
80
75
70
65
60
0,5
0,0
-0,5
-1,0
Normalized Temperature, XT
1,0
0,5
0,0
-0,5
-1,0
Normalized Alkali, XA
Normalized Time +1
Normalized Time -1
C
Hemicellulose Extraction in Liquor, %
60
55
50
45
40
35
30
25
20
0,5
0,0
-0,5
-1,0
Normalized Temperature, XT
1,0
0,5
0,0
-0,5
-1,0
Normalized Alkali, XA
Normalized Time +1
Normalized Time -1
D
Glucan in Solid, %
42
41
40
39
38
37
36
35
34
-0,5
0,0
0,5
1,0
Normalized Temperature, XT
-1,0
-0,5
0,0
0,5
1,0
Normalized Alkali, XA
Normalized Time +1
Normalized Time -1
E
Klason Lignin in Solid, %
18
16
14
12
10
8
-0,5
0,0
0,5
1,0
Normalized Temperature, XT
-1,0
-0,5
0,0
0,5
1,0
Normalized Alkali, XA
Normalized Time +1
Normalized Time -1

◂**Fig. 2** **A** HHV response surface. **B** CAE yield response surface. **C** Hemicellulose extraction in the CAE liquor. **D** Percent cellulose content, as glucan, in the post-CAE solid phase. **E** Percent Klason lignin in the post-CAE solid phase

The values of the dependent variables of Table 9 were used to construct response surfaces in order to facilitate comparisons and identification of the optimum CAE conditions. The *z*-axis represents each of the most influential variables at two different response levels (+1 and –1).

CAE allowed hemicelluloses to be relatively selectively extracted in the form of highly pure polymers [90]. In fact, only 6.6–20.1% of all glucan present in the raw material—which accounted for an average 11.3% in it—was removed (i.e., 2.8–84% of all starting material). By contrast, 25.4–56.0% of the whole hemicellulose fraction (viz., 7.0–15.3% of raw material) was extracted. CAE additionally resulted in substantial delignification. Thus, 16.3–46.4% of the initial amount of Klason lignin (3.2–9.0% of all raw material) was extracted into the CAE liquor.

The post-CAE liquor contained various monomers, xylo-oligomers, minerals, proteins, degradation products (furfural and 5-hydroxymethylfurfural), gluco-oligomers, arabanoligomers, extractables, dissolved lignin, and non-volatile solids [83]. Overall, hemicelluloses were the most efficiently extracted lignocellulosic fraction (especially xylan). Galactan and mannan monomers supplied only small amounts of monosaccharides to the post-CAE liquor owing to their low proportion in the raw material (less than 1% and 0.5%, respectively). Also, araban was less markedly extracted into the CAE liquor than was xylan. As expected, extraction peaked under the most drastic operating conditions.

Figure 2C illustrates the dependence of hemicellulose extraction into the CAE liquor on the operating conditions. As can be seen, the highest proportion of hemicellulose in the liquor (57.1%) was obtained by using a medium alkali concentration (100 g NaOH L^{-1}, normalized value = 0), a high temperature (40 °C, + 1), and a long treatment time (90 min, + 1). In any case, the first variable was scarcely influential. Other authors previously reported similar hemicellulose extraction values. Thus, Sun et al. [91] dissolved 89.3% of all hemicelluloses in poplar wood by using a similar alkali concentration (8.5% vs 10% here) but a much longer treatment time (16 h). Cheng et al. [65] obtained high xylan extraction yields (> 90%) from corn stover by using an NaOH concentration of 10%, a temperature of 75 °C and a time of 2 h. Under optimum conditions (viz., an alkaline mass fraction of 9.5%, 78 °C, and 252 min), Shao [92] obtained a hemicellulose extraction yield of 52.8% from poplar wood

In this work, we chose to restrict hemicellulose extraction in order to avoid cellulose depolymerization and extensive delignification—which would have diminished the high heating value (HHV) of the post-CAE solid phase. In fact, biomass for thermal energy production by burning should contain high proportions of lignin and cellulose, and possess a high C/N ratio, and high heating value but low moisture, ash, and nitrogen contents [57]. Thus, although the glucan fraction supplied monosaccharides to the CAE liquor, cellulose should ideally remain in the solid phase as a polymer in order to preserve its heating value—and so should lignin, which possesses a high thermal potential. Specifically, cellulose, hemicellulose, and lignin have an HHV of 17.36, 17.54, and 25.8 MJ kg^{-1}, respectively (i.e., cellulose and hemicellulose have a similar HHV which, however, is 48% lower than that of lignin) [93]. Using the operating conditions needed to maximize HHV in the post-CAE solid phase resulted in a hemicellulose extraction yield of 30.1%, which was lower than that obtained under the most drastic conditions (55.1%) but allowed relatively selective extraction of hemicelluloses over glucan and lignin.

As can be seen from Fig. 2D, minimizing the proportion of cellulose dissolved in the post-CAE liquor would require using high alkali concentrations, medium temperatures, and short treatment times.

It is necessary to take into account the synergy of the operating variables on the extraction of glucan. In our case, time and temperature are much more influential than the alkali concentration (see Eq. 2 in Table 9 or Fig. 2D). As the NaOH concentration is scarcely influential, so it allowed medium values to be used instead of high levels (i.e., the most suitable conditions for maximizing energy production). The percentages of glucan in solid can also rise if the extraction process is more selective towards the other fractions. As predicted by Eq. 2 in Table 9, such conditions would lead to a proportion of 38.7% of cellulose (glucan) in the post-CAE solid phase (i.e., 93% of all cellulose present in the starting material would remain in that phase). Also, as predicted by Eq. 7 in Table 9, only 7.15% of the initial amount of glucan would be dissolved in the CAE liquor (compared to 30.1% of all hemicellulose). These numbers testify to the ability of CAE to selectively extract hemicelluloses over cellulose.

Restricting delignification in order to allow as much lignin as possible to remain in the solid phase (Fig. 2E) would require using low temperatures and short treatment times with any alkali concentration. As can be seen, however, normalized temperatures over the range –1 to 0 scarcely influenced the lignin content of the post-CAE solid phase. As predicted by Eq. 6 in Table 9, the conditions needed to maximize HHV would result in 18.0% of all lignin being extracted into the CAE liquor.

Based on the foregoing, increasing the heating value of the post-CAE solid phase while ensuring adequate, selective extraction of hemicelluloses would require using the following, optimum conditions: a medium alkali concentration

Table7 Composition of the solid resulting from the CAE in percentage with respect to the raw material

T(°C), *t*(min), Conc. NaOH (g/L)	Lignin, %		Carbohydrates, %						Total hemicellulose
	Klason	Soluble	Glucan	Xylan	Arabinan	Galactan	Mannan	Total CHO	
0 0 0	13.6	0.8	36,3	13,3	2,2	0,7	0,2	52,8	16,4
0 0 0	13,4	0.8	36.7	13.5	2.2	0.7	0.2	53.2	16.6
1 1 1	10.4	0.6	36.0	9.3	1.8	0.6	0.3	48.1	12.1
1 1 – 1	11.3	0.6	36.8	10.7	1.9	0.7	0.3	50.4	13.5
1 – 1 1	14.0	0.9	37.0	12.8	2.5	0.9	0.4	53.7	16.6
1 – 1 – 1	14.3	1.0	37.2	13.3	2.6	0.9	0.4	54.4	17.2
– 1 1 1	13.5	0.8	36.3	13.4	2.4	0.8	0.3	53.1	16.8
– 1 1 – 1	12.4	1.0	36.9	13.0	2.5	0.8	0.3	53.5	16.6
– 1 – 1 1	16.1	1.4	38.9	16.4	2.8	0.9	0.3	59.3	20.4
– 1 – 1 – 1	15.9	1.5	35.8	16.0	2.7	0.9	0.4	55.8	20.0
1 0 0	11.2	0.9	33.3	9.7	2.0	0.7	0.3	46.0	12.7
– 1 0 0	13.3	1.2	33.9	13.6	2.3	0.8	0.3	50.9	17.0
0 1 0	12.2	0.5	37.9	12.3	2.1	0.7	0.1	53.1	15.2
0 – 1 0	16.2	0.8	38.8	15.7	2.5	0.9	0.2	58.0	19.2
0 0 1	13.8	0.8	37.7	13.7	2.5	0.7	0.3	54.8	17.1
0 0 – 1	14.2	0.8	38.5	14.6	2.3	0.8	0.3	56.5	18.0

Table 8 Percentages of extraction in liquid phase relative to the percent content of each polymer in the starting material

T(°C), *t*(min), Conc. NaOH (g/L)	Extraction in percentage in liquid phase with respect to the initial polymer (%)							% Total hemicellulos extracted in liquid
	Klason lignin	Soluble lignin	Glucan	Xylan	Arabinan	Galactan	Mannan	
0 0 0	29.5	49.5	12.8	42.3	25.4	24.4	53.9	40.0
0 0 0	30.8	50.4	11.9	41.8	24.8	24.9	51.1	39.5
1 1 1	46.4	64.1	13.5	59.6	36.6	33.1	40.6	55.9
1 1 – 1	41.2	62.2	11.6	53.8	34.4	28.9	36.2	50.6
1 – 1 1	27.7	44.9	11.1	44.7	12.4	3.9	11.8	39.3
1 – 1 – 1	26.0	33.9	10.8	42.3	10.0	4.1	17.2	37.1
– 1 1 1	30.3	50.7	12.9	42.0	18.2	20.7	33.1	38.6
– 1 1 – 1	35.5	35.6	11.5	43.9	13.0	12.8	36.0	39.4
– 1 – 1 1	16.8	10.4	6.6	29.2	3.1	1.9	24.7	25.4
– 1 – 1 – 1	17.7	0.8	14.1	30.7	5.7	4.0	22.8	27.0
1 0 0	42.1	40.2	20.1	58.0	30.7	25.8	36.4	53.7
– 1 0 0	31.2	21.5	18.7	41.1	20.0	19.9	32.4	38.0
0 1 0	36.7	71.2	9.1	46.7	29.2	22.0	76.5	44.4
0 – 1 0	16.3	49.1	7.0	32.0	14.7	4.6	63.4	29.8
0 0 1	28.4	50.0	9.6	40.9	14.6	26.8	31.2	37.4
0 0 – 1	26.3	51.5	7.7	36.8	19.4	19.4	28.4	34.3

(100 g NaOH L^{-1}, normalized value = 0), a medium temperature (30 °C, 0), and a short treatment time (30 min, –1). These conditions are milder than those used by García et al., (2013) [63] to obtain a hemicellulose-rich valorizable liquor and a solid fraction suitable for producing cellulose pulp (viz., 100 g NaOH L^{-1}, 40 °C, and 90 min, which allowed them to extract all hemicellulose present in the raw material and 10.3% of lignin). As predicted by Eq. 8 in Table 9, these conditions would allow 55.1% of all hemicellulose and 46.8% of all lignin present in elephant grass to be extracted. Therefore, as suggested by the results of García et al. [63], (2017), the alkaline treatment was more efficient with elephant grass than it was with wheat straw. Also, based on the results of De Carvalho et al. [94], it was comparably efficient for extraction from sugarcane straw. Thus, using 110 g NaOH L^{-1}, 33 °C, and 60 min in combination allowed them

Table 9 Models for the dependent variables after the CAE process

No. Eq	Solid residue equations	r^2	*F*-Snedecor
1	$YligK = 13.48 - 1.00\ X_T - 1.65\ X_t - 1.25\ X_T^2 + 0.70\ X_t^2 + 0.54\ X_A^2 - 0.32\ X_T X_A$	0.984	92.69
2	$Yglu = 36.52 - 0.38\ X_t - 2.96\ X_T^2 + 1.78\ X_t^2 + 1.52\ X_A^2 - 0.44\ X_T X_A - 0.55\ X_t X_A$	0.942	24.41
3	$Yxil = 13.36 - 1.65\ X_T - 1.55\ X_t - 0.21\ X_A - 1.69\ X_T^2 + 0.69\ X_t^2 + 0.77\ X_A^2 - 0.33\ X_T X_A$	0.984	72.44
4	$Yara = 2.19 - 0.20\ X_T - 0.26\ X_t + 0.23\ X_A^2 - 0.07\ X_T \cdot X_t$	0.945	47.33
5	$Yhmt = 16.49 - 1.87\ X_T - 1.93\ X_t - 0.23\ X_A - 1.65\ X_T^2 + 0.74\ X_t^2 + 1.08\ X_A^2 - 0.34\ X_T \cdot X_A$	0.992	138.91
No. Eq	**Extraction liquor equations**	r^2	***F*-Snedecor**
6	$Yligex = 30.16 + 5.18\ X_T + 8.55\ X_t + 6.50\ X_T^2 - 3.64\ X_t^2 - 2.81\ X_A^2 + 1.63\ X_T X_A$	0.984	92.69
7	$Ygluex = 12.33 + 0.90\ X_t + 7.11\ X_T^2 - 4.28\ X_t^2 - 3.66\ X_A^2 + 1.05\ X_T X_A + 1.32\ X_t X_A$	0.942	24.41
8	$Yhmtex = 39.80 + 6.83\ X_T + 7.04\ X_t + 0.83\ X_A + 6.01\ X_T^2 - 2.69\ X_t^2 - 3.95\ X_A^2 + 1.22\ X_T \cdot X_A$	0.992	138.91

YligK, klason lignin content in the solid; *Yglu*, glucan content in the solid; *Yxil*, xylan content in the solid; *Yara*, araban content in the solid; *Yhmt*, hemicelluloses conten in the solid; *Yligex*, lignin extracted; *Ygluex*, glucan extracted; *Yhmtex*, hemicelluloses extracted; *XA, XT, Xt*, normalized value of the alkali concentration, temperature, and time, respectively

to extract 52.5% of all hemicellulose in their raw material compared to 25.7–55.1% from elephant grass here.

4 Conclusions

Elephant grass has been deemed an excellent alternative to woody materials for energy production by direct burning, basically by virtue of its substantial contents in lignin (20.86%) and hemicelluloses (27.4%).

Using the optimal operating conditions for pre-burning cold alkaline extraction (CAE) of Elephant grass (viz., an alkali concentration of 100 g NaOH L^{-1}, a temperature of 30 °C, and a treatment time of 30 min) allowed its high heating value to be raised by 4% (to 19.151 MJ kg^{-1}) while preserving the proportion of elemental C and increasing that of H with respect to the raw material, and deriving the environmental advantage of reducing the sulphur content by 46.9% from the starting material to the post-CAE solid phase.

Cold alkaline extraction of the raw material additionally enabled relatively selective separation of the hemicellulose fraction from the cellulose and lignin fractions. Thus, 30.1% of all hemicellulose was dissolved in the treatment liquor and made valorizable while 93.0% of cellulose and 82.1% of lignin present in the raw material remained in the solid phase.

Acknowledgements The authors would like to thank the Laboratorio de Celulosa e Paper of the Federal University of Viçosa, Minas Gerais, Brazil, where part of the work of this paper was developed.

Author contribution All authors contributed to the study conception and design and have collaborated in the different phases of the work. The aspects on which the authors have worked most intensively are highlighted as follows: Juan Carlos García: contribution in the methodology, statistical analysis, and making graphics. Ascensión Alfaro: writing in the first draft, review, and editing; data analysis; and results and graphs. Javier Mauricio Loaiza: contribution in experimental work and methology and writing in the first draft. Susana Lozano-Calvo: contribution in experimental work and methodology and writing in the first draft. Francisco López: conceptualización, funding acquision, project manager, and general supervision.

Funding Open Access funding provided thanks to the CRUE-CSIC agreement with Springer Nature. Funding for open acces charge: Universidad de Huelva/CBUA. This study was funded by the Spanish Ministry of Economy and Competitiveness through the National Programme for Research Aimed at the Challenges of Society (CTQ2017-85251-C2-1and 2-R and PID2020-112875RB-C21), additional cofunding, in an 80:20 proportion, by FEDER (Project Green Asphalt, ref. 802C1800001) and the Andalusian Regional Government (Economy, Knowledge, Enterprises and University Council/IDEA Agency) and by micro-projects of research "Cátedra de la provincia" of the University of Huelva.

Declarations

Conflict of interest The authors declare no competing interests.

Open Access This article is licensed under a Creative Commons Attribution 4.0 International License, which permits use, sharing, adaptation, distribution and reproduction in any medium or format, as long as you give appropriate credit to the original author(s) and the source, provide a link to the Creative Commons licence, and indicate if changes were made. The images or other third party material in this article are included in the article's Creative Commons licence, unless indicated otherwise in a credit line to the material. If material is not included in the article's Creative Commons licence and your intended use is not permitted by statutory regulation or exceeds the permitted use, you will need to obtain permission directly from the copyright holder. To view a copy of this licence, visit http://creativecommons.org/licenses/by/4.0/.

References

1. Singh BP, Singh HP, Obeng E (2013) Elephantgrass. In: Singh BP (ed) Biofuel crops: production, physiology and genetics. CABI, Wallingford, pp 271–291
2. Chen HG, Zhang Y-HHP (2015) New biorefineries and sustainable agriculture: increased food, biofuels, and ecosystem security. Renew Sustain Energy Rev 47:117–132

3. Yadav P, Priyanka P, Kumar D et al (2019) Bioenergy crops: recent advances and future outlook. pp 315–335
4. Hulthom T, Robertsen L, Lönnberg B et al (1998) The IDE process. A new concept suitable for softwood, hardwood and non-wood, p 577–588
5. European Parliament (2006) Report on a strategy for biomass and biofuels (2006/2082 (INI)). https://www.europarl.europa.eu/doceo/document/A-6-2006-0347_EN.html. Accessed 8 Nov 2021
6. REN21 (2020) Renewables 2020. https://www.ren21.net/gsr-2020/. Accessed 9 Nov 2021
7. European Parliament (2021) Fact sheets on the European Union. Renewable energy. https://www.europarl.europa.eu/factsheets/en/section/192/industrial-energy-and-research-policies. Accessed 8 Nov 2021
8. Eurostat (2021) Database. In: Share Renew. energy gross Final energy Consum. https://ec.europa.eu/eurostat/databrowser/view/t2020_31/default/bar?lang=en,. Accessed 9 Nov 2021
9. European Commission (2020) In focus: Renewable energy in Europe. https://ec.europa.eu/info/news/focus-renewable-energy-europe-2020-mar-18_en. Accessed 9 Nov 2021
10. Haribabu K, Sivasubramanian V, Deepanraj B, Ong HC (2021) Thematic issue: bioenergy and biorefinery approaches for environmental sustainability. Biomass Convers Biorefin. https://doi.org/10.1007/s13399-021-01989-7
11. Korndörfer (2011) Biomass and energy yields of bioenergy germplasm grown on sandy soils in Florida. University of Florida
12. Nazli RI, Tansi V, Öztürk HH, Kusvuran A (2018) Miscanthus, switchgrass, giant reed, and bulbous canary grass as potential bioenergy crops in a semi-arid Mediterranean environment. Ind Crops Prod 125:9–23. https://doi.org/10.1016/j.indcrop.2018.08.090
13. Cosentino SL, Scordia D, Testa G et al (2018) The importance of perennial grasses as a feedstock for bioenergy and bioproducts. In: Perennial Grasses for Bioenergy and Bioproducts. pp 1–33
14. Nie S, Zhang C, Zhang Q et al (2018) Enzymatic and cold alkaline pretreatments of sugarcane bagasse pulp to produce cellulose nanofibrils using a mechanical method. Ind Crops Prod 124:435–441. https://doi.org/10.1016/j.indcrop.2018.08.033
15. Lu Y, Tao P, Zhang N, Nie S (2020) Preparation and thermal stability evaluation of cellulose nanofibrils from bagasse pulp with differing hemicelluloses contents. Carbohydr Polym 245:116463. https://doi.org/10.1016/j.carbpol.2020.116463
16. Sosa LL, Jozami E, Oakley LJ et al (2019) Using C4 perennial rangeland grasses for bioenergy. Biomass Bioenergy 128:105299. https://doi.org/10.1016/j.biombioe.2019.105299
17. McKendry P (2002) Energy production from biomass (part 1): Overview of biomass. Bioresour Technol 83:37–46. https://doi.org/10.1016/S0960-8524(01)00118-3
18. Lewandowski I, Scurlock JMO, Lindvall E, Christou M (2003) The development and current status of perennial rhizomatous grasses as energy crops in the US and Europe. Biomass Bioenergy 25:335–361. https://doi.org/10.1016/S0961-9534(03)00030-8
19. Samson R, Mani S, Boddey R et al (2005) The potential of C4 perennial grasses for developing a global BIOHEAT Industry. CRC Crit Rev Plant Sci 24:461–495
20. Dien BS, Jung HJG, Vogel KP et al (2006) Chemical composition and response to dilute-acid pretreatment and enzymatic saccharification of alfalfa, reed canarygrass, and switchgrass. Biomass Bioenergy 30:880–891. https://doi.org/10.1016/j.biombioe.2006.02.004
21. Pandey VC, Patel D, Jasrotia S, Singh DP (2020) Potential of Napier grass (Pennisetum purpureum Schumach.) for phytoremediation and biofuel production. In: Phytoremediation Potential of Perennial Grasses. Elsevier, pp 283–302
22. Scordia D, Cosentino S (2019) Perennial energy grasses: resilient crops in a changing European agriculture. Agriculture 9:169. https://doi.org/10.3390/agriculture9080169
23. Martín Torrealba B, Diaz Dominguez A, Chinea Correa E, Delgado Hdez B (1989) Posibilidad de cultivo y aprovechamiento del"pasto elefante" ("pennisetum purpureum" schum) en Tenerife (Islas Canarias). Pastos 79–86
24. Marafon AC, Machado JC, Cavalcante de Amorim EL et al (2021) Elephant grass as a feedstoc for bioenergy production. BSS Mag
25. Nguyen BT, Le LB, Pham LP et al (2021) The effects of biochar on the biomass yield of elephant grass (Pennisetum Purpureum Schumach) and properties of acidic soils. Ind Crops Prod 161:113224. https://doi.org/10.1016/j.indcrop.2020.113224
26. Negawo AT, Teshome A, Kumar A et al (2017) Opportunities for napier grass (Pennisetum purpureum) improvement using molecular genetics. Agronomy 7:28
27. Osman NA, Roslan AM, Ibrahim MF, Hassan MA (2020) Potential use of pennisetum purpureum for phytoremediation and bioenergy production: a mini review. Asia-Pac J Mol Biol Biotechnol 28:14–26. https://doi.org/10.35118/apjmbb.2020.028.1.02
28. Byrt CS, Grof CPL, Furbank RT (2011) C4 Plants as biofuel feedstocks: optimising biomass production and feedstock quality from a lignocellulosic perspective. J Integr Plant Biol 53:120–135
29. Varnero CS, Urrutia MV, Ibaceta SV (2018) Bioenergy from perennial grasses. In: Advances in Biofuels and Bioenergy. InTech, p
30. van der Weijde T, Alvim Kamei CL, Torres AF et al (2013) The potential of C4 grasses for cellulosic biofuel production. Front Plant Sci 4:107
31. Cerdas R, Vallejos E (2010) Productividad del pasto Camerún (Pennisetum purpureum) con varias dosis de nitrógeno y frecuencias de corte en la zona seca de Costa Rica. InterSedes Rev las Sedes Reg XI:180–195
32. Gomes FJB, Colodette JL, Burnet A et al (2013) Potential of elephant grass for pulp production. BioResources 8:4359–4379. https://doi.org/10.15376/biores.8.3.4359-4379
33. Basso V, Machado JC, da Silva Lédo FJ et al (2014) Different elephant grass (Pennisetum purpureum) accessions as substrates for enzyme production for the hydrolysis of lignocellulosic materials. Biomass Bioenergy 71:155–161. https://doi.org/10.1016/j.biombioe.2014.10.011
34. Rengsirikul K, Ishii Y, Kangvansaichol K et al (2013) Biomass yield, chemical composition and potential ethanol yields of 8 cultivars of napiergrass (*Pennisetum purpureum* Schumach.) harvested 3-monthly in Central Thailand. J Sustain Bioenergy Syst 03:107–112. https://doi.org/10.4236/jsbs.2013.32015
35. Menegol D, Scholl AL, Dillon AJP, Camassola M (2016) Influence of different chemical pretreatments of elephant grass (Pennisetum purpureum, Schum.) used as a substrate for cellulase and xylanase production in submerged cultivation. Bioprocess Biosyst Eng 39:1455–1464. https://doi.org/10.1007/s00449-016-1623-8
36. Dien BS, Anderson WF, Cheng MH et al (2020) Field productivities of napier grass for production of sugars and ethanol. ACS Sustain Chem Eng 8:2052–2060. https://doi.org/10.1021/acssuschemeng.9b06637
37. Antunes FAF, Machado PEM, Rocha TM et al (2021) Column reactors in fluidized bed configuration as intensification system for xylitol and ethanol production from napier grass (Pennisetum Purpureum). Chem Eng Process Process Intensif 164. https://doi.org/10.1016/j.cep.2021.108399
38. Oluwasina OO, Lajide L (2016) Evaluation of compositional properties of some plant wastes for industrial applications. FUTA J Res Sci 12:180–187
39. Haldar D, Purkait MK (2020) Thermochemical pretreatment enhanced bioconversion of elephant grass (Pennisetum purpureum): insight on the production of sugars and lignin. Biomass Convers Biorefin. https://doi.org/10.1007/s13399-020-00689-y

40. Trevisan H, Rezende CA (2020) Pure, stable and highly antioxidant lignin nanoparticles from elephant grass. Ind Crops Prod 145. https://doi.org/10.1016/j.indcrop.2020.112105
41. Nandal P, Arora A, Virmani S (2021) An appraisal on valorization of lignin: a byproduct from biorefineries and paper industries. Biomass Bioenergy 155:106295. https://doi.org/10.1016/j.biombioe.2021.106295
42. Alaneme KK, Olusegun SJ, Alo AW (2016) Co rrosion inhibitory properties of elephant grass (Pennisetum purpureum) extract: effect on mild steel corrosion in 1 M HCl solution. Alex Eng J 55:1069–1076. https://doi.org/10.1016/j.aej.2016.03.012
43. Campos BB, Diniz RHS, da Silveira FA et al (2019) ELEPHANT GRASS (Pennisetum purpureum Schumach) IS A PROMISING FEEDSTOCK FOR ETHANOL PRODUCTION BY THE THERMOTOLERANT YEAST Kluyveromyces marxianus CCT 7735. Brazilian J Chem Eng 36:43–49. https://doi.org/10.1590/0104-6632.20190361s20170263
44. Rueda JA, de Guerrero-Rodríguez JD, Ramírez-Ordoñes S et al (2020) Morphological composition and fiber partitioning along regrowth in elephant grass CT115 intended for ethanol production. Sci Rep 10. https://doi.org/10.1038/s41598-020-72169-2
45. Yasuda M, Ishii Y, Ohta K (2014) Napier grass (Pennisetum purpureum Schumach) as raw material for bioethanol production: pretreatment, saccharification, and fermentation. Biotechnol Bioprocess Eng 19:943–950
46. Rocha-Meneses L, Otor OF, Bonturi N et al (2020) Bioenergy yields from sequential bioethanol and biomethane production: an optimized process flow. Sustain 12:1–19. https://doi.org/10.3390/su12010272
47. Pardang P, Sonwai A, Pholchan P et al (2020) Potential of lignin-rich grass, pennisetum purpureum × pennisetum typhoideum, as a feedstock for biogas production. J Environ Eng 146:04020074. https://doi.org/10.1061/(ASCE)EE.1943-7870.0001741
48. Phuttaro C, Reungsang A, Boonsawang P, Chaiprapat S (2019) Integrative effects of sonication and particle size on biomethanation of tropical grass Pennisetum purpureum using superior diverse inocula cultures. Energies 12:4226. https://doi.org/10.3390/en12224226
49. De Conto D, Silvestre WP, Baldasso C, Godinho M (2016) Performance of rotary kiln reactor for the elephant grass pyrolysis. Bioresour Technol 218:153–160. https://doi.org/10.1016/j.biortech.2016.06.082
50. Reza MS, Islam SN, Afroze S et al (2020) Evaluation of the bioenergy potential of invasive Pennisetum purpureum through pyrolysis and thermogravimetric analysis. Energy Ecol Environ 5:118–133. https://doi.org/10.1007/s40974-019-00139-0
51. Cai C, Wang L, Wang G et al (2020) Effects of dry explosion pretreatment on physicochemical and fuel properties of hybrid pennisetum (Pennisetum americanum × P. purpureum). Bioresour Technol 297:122–508. https://doi.org/10.1016/j.biortech.2019.122508
52. Strezov V, Evans TJ, Hayman C (2008) Thermal conversion of elephant grass (Pennisetum Purpureum Schum) to bio-gas, bio-oil and charcoal. Bioresour Technol 99:8394–8399. https://doi.org/10.1016/j.biortech.2008.02.039
53. de Morais RF, de Souza BJ, Leite JM et al (2009) Elephant grass genotypes for bioenergy production by direct biomass combustion. Pesqui Agropecuária Bras 44:133–140. https://doi.org/10.1590/s0100-204x2009000200004
54. Brandon AG, Scheller HV (2020) Engineering of bioenergy crops: dominant genetic approaches to improve polysaccharide properties and composition in biomass. Front Plant Sci 11
55. Danquah JA, Roberts CO, Appiah M (2018) Elephant grass (Pennisetum purpureum): a potential source of biomass for power generation in Ghana. Curr J Appl Sci Technol 30:1–12. https://doi.org/10.9734/cjast/2018/45224
56. do Amaral Santos de Carvalho Rocha JR, Machado JC, Carneiro PCS et al (2017) Bioenergetic potential and genetic diversity of elephantgrass via morpho-agronomic and biomass quality traits. Ind Crops Prod 95:485–492. https://doi.org/10.1016/j.indcrop.2016.10.060
57. do Amaral Santos de Carvalho Rocha JR, Machado JC, Carneiro PCS et al (2017) Elephant grass ecotypes for bioenergy production via direct combustion of biomass. Ind Crops Prod 95:27–32. https://doi.org/10.1016/j.indcrop.2016.10.014
58. Marafon AC, Amaral AFC, Machado JC et al (2021) Chemical composition and calorific value of elephant grass varieties and other feedstocks intended for direct combustion. Grassl Sci 67:241–249. https://doi.org/10.1111/grs.12311
59. Brito da Silva V, Daher RF, de Souza YP et al (2020) Assessment of energy production in full-sibling families of elephant grass by mixed models. Renew Energy 146:744–749. https://doi.org/10.1016/j.renene.2019.06.152
60. Flores RA, Urquiaga S, Alves BJR et al (2012) Yield and quality of elephant grass biomass produced in the cerrados region for bioenergy. Eng Agric 32:831–839. https://doi.org/10.1590/S0100-69162012000500003
61. Ferreira FM, do Amaral JR, Lopes L et al (2021) Optimal harvest number and genotypic evaluation of total dry biomass, stability, and adaptability of elephant grass clones for bioenergy purposes. Biomass Bioenergy 149
62. Kumar AK, Sharma S (2017) Recent updates on different methods of pretreatment of lignocellulosic feedstocks: a review. Bioresour Bioprocess 4:7. https://doi.org/10.1186/s40643-017-0137-9
63. García JC, Díaz MJ, Garcia MT et al (2013) Search for optimum conditions of wheat straw hemicelluloses cold alkaline extraction process. Biochem Eng J 71:127–133. https://doi.org/10.1016/j.bej.2012.12.008
64. García MT, Alfaro A, Garcia JC et al (2017) Obtainment of hemicellulose derivatives and cellulose pulp from wheat straw following cold alkaline extraction. Cellul Chem Technol 51:465–475
65. Cheng H, Zhan H, Fu S, Lucia LA (2011) Alkali extraction of hemicellulose from depithed corn stover and effects on soda-AQ pulping. Bioresources 6:196–206. https://doi.org/10.15376/biores.6.1.196-206
66. Arnoul-Jarriault B, Lachenal D, Chirat C, Heux L (2015) Upgrading softwood bleached kraft pulp to dissolving pulp by cold caustic treatment and acid-hot caustic treatment. Ind Crops Prod 65:565–571. https://doi.org/10.1016/j.indcrop.2014.09.051
67. Steinbach D, Kruse A, Sauer J (2017) Pretreatment technologies of lignocellulosic biomass in water in view of furfural and 5-hydroxymethylfurfural production- a review. Biomass Convers Biorefinery 7:247–274. https://doi.org/10.1007/s13399-017-0243-0
68. Peng F, Peng P, Xu F, Sun RC (2012) Fractional purification and bioconversion of hemicelluloses. Biotechnol Adv 30:879–903
69. Longue Júnior D, Colodette JL, Gomes VJ (2010) Remoção de hemiceluloses da madeira por tratamento de lixiviação alcalina com NaOH. Cerne 16:423–429. https://doi.org/10.1590/S0104-77602010000400001
70. Hutterer C, Schild G, Potthast A (2016) A precise study on effects that trigger alkaline hemicellulose extraction efficiency. Bioresour Technol 214:460–467. https://doi.org/10.1016/j.biortech.2016.04.114
71. Park YC, Kim JS (2012) Comparison of various alkaline pretreatment methods of lignocellulosic biomass. Energy 47:31–35. https://doi.org/10.1016/j.energy.2012.08.010
72. Cardona EM, Rios JA, Peña JD, Rios LA (2013) Pretratamiento Alcalino de Pasto Elefante (Pennisetum sp) y King Grass (Pennisetum hybridum) Cultivados en Colombia para la Producción de Bioetanol. Inf Tecnol 24:69–80. https://doi.org/10.4067/S0718-07642013000500009

73. Prinsen P (2010) Composición química de diversos materiales lignocelulósicos de interés industrial y análisis estructural de sus ligninas
74. Hu Z, Sykes R, Davis MF et al (2010) Chemical profiles of switchgrass. Bioresour Technol 101:3253–3257. https://doi.org/10.1016/j.biortech.2009.12.033
75. Tsalagkas D, Börcsök Z, Pásztory Z et al (2021) Assessment of the papermaking potential of processed Miscanthus × giganteus stalks using alkaline pre-treatment and hydrodynamic cavitation for delignification. Ultrason Sonochem 72:105462. https://doi.org/10.1016/j.ultsonch.2021.105462
76. Devrije T (2002) Pretreatment of Miscanthus for hydrogen production by Thermotoga elfii. Int J Hydrog Energy 27:1381–1390. https://doi.org/10.1016/S0360-3199(02)00124-6
77. Matei JC, Soares M, Bonato ACH et al (2020) Enzymatic delignification of sugar cane bagasse and rice husks and its effect in saccharification. Renew Energy 157:987–997. https://doi.org/10.1016/j.renene.2020.05.028
78. Garrote G (2003) Hydrothermal and pulp processing of Eucalyptus. Bioresour Technol 88:61–68. https://doi.org/10.1016/S0960-8524(02)00256-0
79. Persson T, Ren JL, Joelsson E, Jönsson A-S (2009) Fractionation of wheat and barley straw to access high-molecular-mass hemicelluloses prior to ethanol production. Bioresour Technol 100:3906–3913. https://doi.org/10.1016/j.biortech.2009.02.063
80. Finell M (2003) The use of reed canary-grass (Phalaris arundinacea) as a short fibre raw material for the pulp and paper industry. Swedish University of Agricultural Sciences. Umea, Sweden
81. de Carvalho DM, de Queiroz JH, Colodette JL (2016) Assessment of alkaline pretreatment for the production of bioethanol from eucalyptus, sugarcane bagasse and sugarcane straw. Ind Crops Prod 94:932–941. https://doi.org/10.1016/j.indcrop.2016.09.069
82. Ai J, Tschirner U (2010) Fiber length and pulping characteristics of switchgrass, alfalfa stems, hybrid poplar and willow biomasses. Bioresour Technol 101:215–221. https://doi.org/10.1016/j.biortech.2009.07.090
83. Feria MJ, López F, García JC et al (2011) Valorization of Leucaena leucocephala for energy and chemicals from autohydrolysis. Biomass Bioenergy 35:2224–2233. https://doi.org/10.1016/j.biombioe.2011.02.038
84. Jeetah P, Golaup N, Buddynauth K (2015) Production of cardboard from waste rice husk. J Environ Chem Eng 3:52–59. https://doi.org/10.1016/j.jece.2014.11.013
85. Gao Y, Guo X, Liu Y et al (2018) A full utilization of rice husk to evaluate phytochemical bioactivities and prepare cellulose nanocrystals. Sci Rep 8. https://doi.org/10.1038/s41598-018-27635-3
86. Tsai WT, Tsai YL (2016) Thermochemical characterization of napier grass as an energy source and its environmental and economic benefit analysis. Energy Sources B Econ Plan Policy 11:130–136. https://doi.org/10.1080/15567249.2011.590847
87. Rodriguez B, Romero J (2017) EVALUACIÓN DEL POTENCIAL ENERGÉTICO DEL ZACATE " KING GRASS " (Pennisetum purpureum). Universidad del Salvador, EN EL SALVADOR
88. Raveendran K, Ganesh A (1996) Heating value of biomass and biomass pyrolysis products. Fuel 75:1715–1720. https://doi.org/10.1016/S0016-2361(96)00158-5
89. Martínez S (2009) Evaluación de la biomasa como recurso energético renovable en Cataluña
90. Glasser WG, Kaar WE, Jain RK, Sealey JE (2000) Isolation options for non-cellulosic heteropolysaccharides (HetPS). Cellulose 7:299–317. https://doi.org/10.1023/A:1009277009836
91. Sun RC, Fang JM, Tomkinson J et al (2001) Fractional isolation, physico-chemical characterization and homogeneous esterification of hemicelluloses from fast-growing poplar wood. Carbohydr Polym 44:29–39. https://doi.org/10.1016/S0144-8617(00)00196-X
92. Shao H, Hu Y, Sun H et al (2019) Response surface optimization of alkali extraction and characterization of poplar hemicellulose. Bioresources 14:3844–3859. https://doi.org/10.15376/biores.14.2.3844-3859
93. Maksimuk Y, Antonava Z, Krouk V et al (2021) Prediction of higher heating value (HHV) based on the structural composition for biomass. Fuel 299:120860. https://doi.org/10.1016/j.fuel.2021.120860
94. de Carvalho DM, Sevastyanova O, de Queiroz JH, Colodette JL (2016) Cold alkaline extraction as a pretreatment for bioethanol production from eucalyptus, sugarcane bagasse and sugarcane straw. Energy Convers Manag 124:315–324. https://doi.org/10.1016/j.enconman.2016.07.029

Publisher's Note Springer Nature remains neutral with regard to jurisdictional claims in published maps and institutional affiliations.

According to the journal policy, we confirm that neither the manuscript nor any parts of its content are currently under consideration or published in another journal and its publication is approved by all the authors.

forests

MDPI

Article

Ultrasound-Assisted Cold Alkaline Extraction: Increasing Hemicellulose Extraction and Energy Production from Populus Wood

S. Lozano-Calvo *, J. M. Loaiza, J. C. García, M. T. García and F. López

Research Centre for Technology of Products and Chemical Processes (PRO2TECS), Department of Chemical Engineering, University of Huelva, Av. 3 de marzo s/n, 21071 Huelva, Spain; javiermauricio.loiza@diq.uhu.es (J.M.L.); juan.garcia@diq.uhu.es (J.C.G.); mtrinidad.garcia@diq.uhu.es (M.T.G.); baldovin@diq.uhu.es (F.L.)

* Correspondence: susana.lozano@diq.uhu.es

Abstract: Alkaline pretreatments are considered highly effective for the separation of the different components of lignocellulosic biomass. However, cold alkaline extraction (CAE) exhibits minimal modification/degradation of hemicellulosic fraction and successfully accomplishes efficient delignification. In this research, the fast-growing clone AF2 of *Populus x euramericana* wood was utilized as the raw material and subjected to ultrasound-assisted CAE. The objective of incorporating ultrasound into cold alkaline extraction is to increase the yield of a hemicellulosic-rich liquid phase that can be used to produce high-value products such as furfural or xylitol. Simultaneously, it aims to obtain a solid phase with a higher calorific value compared to the raw material. The results, obtained from a central composite factorial design, demonstrated that the CAE process for 90 min at a sodium hydroxide concentration of 100 g L^{-1}, a temperature of 30 °C, and with ultrasound assistance maximized hemicellulose extraction in the liquid phase (60.8% was extracted) and improved the heating value of solid phase.

Keywords: biomass; delignification; hemicelluloses; pre-treatment; ultrasound

check for updates

Citation: Lozano-Calvo, S.; Loaiza, J.M.; García, J.C.; García, M.T.; López, F. Ultrasound-Assisted Cold Alkaline Extraction: Increasing Hemicellulose Extraction and Energy Production from Populus Wood. *Forests* **2024**, *15*, 109. https://doi.org/10.3390/f15010109

Academic Editor: Sabrina Palanti

Received: 11 December 2023
Revised: 24 December 2023
Accepted: 30 December 2023
Published: 5 January 2024

Copyright: © 2024 by the authors. Licensee MDPI, Basel, Switzerland. This article is an open access article distributed under the terms and conditions of the Creative Commons Attribution (CC BY) license (https://creativecommons.org/licenses/by/4.0/).

1. Introduction

International commitments of the European Union to mitigate climate change have promoted a search for clean, renewable energy sources including biomass [1]. More than 60% of the amount of energy produced from biomass in the world is obtained from renewable sources, which account for up to 19.3% of the whole energy output [2]. The use of lignocellulosic biomass has expanded steadily in recent times and is expected to continue to grow in the coming years by virtue of the value-added products that can be obtained from chips, pellets, biogas, and other biorefinery materials [3,4]. However, conventional agro-forestry systems cannot by themselves meet the growing demand, so fast-growing woody species are being increasingly planted for this purpose [5]. In this scenario, converting biomass through biorefinery processes has a high potential judging by their sustainability, and also by the fact that they use waste materials to provide alternative energies and high value-added products according to the principles of sustainable development [6,7]. In addition, commitments to a circular economy, the need to reduce the dependence on raw materials from non-renewable fossil resources, and the consequences of climate change all necessitate the adoption of novel technologies within conventional production sectors. This transition aims to supplant the prevailing industrialization model with efficient use of natural resources as far as possible [8,9].

A number of plant species of the genera *Populus*, *Salix*, *Eucalyptus*, *Miscanthus*, *Cynara*, *Paulownia*, *Robinia*, *Casuarina*, and *Leucaena*, among others, are being used as short-rotation energy crops on a global scale [6,10,11]. Some are multi-purpose species that provide a

variety of goods such as forage or paper pulp, and services such as soil restoration or carbon sequestration. These industrial lignocellulosic crops are expected to cover 5–10% of the global forest area by 2050 [12]. In Europe alone, farmland has undergone degradation to such an extent that 45% of its soils have low organic matter contents (<2%); also, 15% have problems due to over-fertilization with inorganic nitrogen, and more than 147 million hectares are seriously eroded [13]. Fortunately, at least 70% of all degraded land is under a climate allowing plants such as *Robinia pseudoacacia, Ulmus pumila, Eucalyptus* sp., and/or *Populus* sp. to grow. It can thus be useful to assess biomass production, industrial use, and the environmental impact of their intensive production on already poor, degraded soils with a view to their potential exploitation [14]. The limited research carried out in this area has indicated that the results are influenced by specific plant species, cultivation conditions, and environmental factors [15,16].

Recent studies have shown the genus *Populus* can easily adapt to varying environmental conditions; also, it possesses a high hybridization capacity and ease of vegetative propagation. These advantages, together with its fast growth, have boosted the development of a very broad clonal offer that allows clones to be selected for optimal growth at specific sites and for specific purposes [11].

The principal components of lignocellulosic biomass are cellulose, hemicellulose, and lignin. All of these components have the potential to yield high-value products. However, achieving this goal necessitates the utilization of a biorefinery scheme for the selective separation and recovery of these fractions [17]. Often, it is particularly useful to carry out the fractionation in two steps. The first step involves hydrolysis under relatively mild conditions to extract the hemicelluloses (which have low resistance). Additionally, this helps prevent excessive degradation of cellulose fibers. The second step involves oxidative delignification or organosolv treatment to remove the lignin fraction [18]. Among the various pretreatment methods available, alkaline pretreatment offers significant advantages, including the use of environmentally friendly and non-corrosive chemicals, as well as milder operating conditions [19]. Cold Alkaline Extraction (CAE) is one such pretreatment that offers the added benefit of yielding hemicelluloses for use as food additives or in the production of furfural and polymers [12]. The CAE, conducted at 20-40 ºC, does not necessitate high pressures, resulting in reduced energy consumption [20]. Nevertheless, the primary advantage of CAE compared to other biomass fractionation techniques lies in its capacity to selectively extract hemicelluloses with minimal degradation and enable straightforward separation through alcoholic precipitation [21].

However, CAE has its disadvantages, and the most significant one is likely its efficiency, which strongly depends on the specific raw material. This pretreatment has been extensively studied for various applications, and it has been observed that the extraction of hemicelluloses is more efficient in herbaceous lignocellulosic materials than in wood [21–24].

The pretreatment's effectiveness can be enhanced through supplementary procedures, including prehydrolysis, impregnation, or novel techniques such as ultrasound-assisted extraction, sub-critical and supercritical fluid extraction, microwave-assisted extraction, or solvent-accelerated extraction [25,26]. The application of ultrasound can be employed as either a pretreatment step or during the treatment process, providing a clean and eco-friendly extraction method with several benefits [25,27]. Extraction is improved by the transmission of ultrasound, which induces acoustic cavitation. This, in turn, triggers the spontaneous creation of microbubbles. When these microbubbles collapse, they produce localized shock waves and hot spots, releasing high temperatures and pressure. This disintegrates the crystalline structure of solid particles [28]. Ultrasound-assisted fractionation improves the efficiency of conventional processes, and results in a high product yield and selectivity [29]. A. García et al., 2011 [29] investigated various lignocellulosic biomass fractionation processes with ultrasound assistance. The results showed that this technology produced a liquid richer in hemicelluloses and lignin compared to when it was not used.

On the other hand, direct combustion is a method for generating chemical energy. This process leads to the emission of CO_2, particulate matter, sulfur dioxide, and other compounds. However, the quantities released are relatively lower than those produced by the combustion of fossil fuels [30,31].

There are numerous scientific investigations on the extraction of hemicellulosic derivatives using various alkaline processes, both with and without ultrasound assistance [32,33]. In this work, we combined a cold alkaline treatment with ultrasound technology. This approach lacks references in the literature, representing a significant aspect of academic originality and scientific novelty. Furthermore, the efficiency of CAE is highly dependent on the raw material used, adding another point of scientific and academic novelty when testing these processes on a raw material such as the AF2 clone of *Populus x euramericana*. To the best of the authors' knowledge, there are no bibliographic references exploring its utilization for the simultaneous valorization of the hemicellulosic liquid and energy application of the solid residue, despite numerous studies on the value-added product of hemicellulosic, as demonstrated by A. Tareen et al., 2020 [34]. The AF2 clone of *Populus x euramericana* is a high-yield energy crop, and optimizing the conditions for the industrial biorefinery process holds great potential, especially for potential scaling to a semi-industrial or industrial level of exploitation.

For these purposes, the AF2 clone of *Populus x euramericana* was evaluated as a raw material for hemicellulose extraction using CAE, both with and without ultrasound assistance. The process included modeling and optimization through multiple regression, a widely employed approach for optimizing biomass and waste stream valorization [35,36]. The aim was to obtain a high-value liquid fraction and energy from the resulting solid residue, within the context of comprehensive utilization (biorefining).

2. Materials and Methods

2.1. Characterization and Storage of Raw Materials

The raw material utilized was wood from the AF2 clone of *Populus x euramericana*, from the province of Huelva, located in southwestern Spain. The material was subject to cold grinding in a Resch mill for 4 min and then sieved to obtain chips approximately 1–3 cm long and 0.5 cm wide. These chips were allowed to equilibrate with ambient moisture and temperature before being stored in tightly closed containers during the period between obtaining the wood chips and their use in the CAE process.

For characterization, the chips were further ground to a size of less than 0.5 mm using an Ika Werke mill. Tests were conducted following international standards, including TAPPI T264 cm-07 for moisture [37], TAPPI 211 om-02 for ash [38], and TAPPI T204 cm-07 in combination with Soxhlet extraction (95% ethanol, 5 h) for extractives [39].

Following gravimetric testing, the material was subjected to quantitative acid hydrolysis with 72% H_2SO_4, and the hydrolysate was analyzed for monomeric sugars (glucose, xylose, and arabinose) according to TAPPI T249 cm-09 [40]. This analysis was conducted using high-performance liquid chromatography (HPLC) with an AMinex HPX-87H ion-exchange column (Bio-Rad Laboratories, Alcobendas, Madrid, Spain) at 30 °C as the stationary phase and 0.005 M H2SO4 at a flow rate of 0.6 mL min^{-1} as the mobile phase [41]. Klason lignin was determined following the guidelines of TAPPI T222 om-11 [42].

2.2. Cold Alkaline Extraction (CAE) with and without Ultrasound

Hemicelluloses were subjected to CAE in a Power Sonic Series 500 ultrasonic bath, using a constant liquid/solid ratio of 15 Kg of water per kg of raw material on a dry basis (odb). The independent operational variables of the process were temperature (20, 30, or 40 °C), time (30, 60, or 90 min), and sodium hydroxide concentration (80, 100, or 120 g L^{-1}).

The resulting CAE liquor was filtered, and the solid residue was washed with water. Then, the solid fraction was air-dried to determine moisture content and weighed to calculate the process yield. The solid fraction underwent chemical characterization using the same test as the raw material. Additionally, it was analyzed for calorific value following

CEN/TS 14918:2005 E [43] and UNE 16001 EX [44]. This analysis used a Parr 6300 automatic Isoperibol calorimeter (Parr Instrument Company, Moline, IL, USA), a CGA 540 connector, 99.5% pure oxygen, and a maximum pressure of 2500 psig. Furthermore, the solid was subjected to elemental analysis (C, N, O, and H) using a C/H/S-Analyser autosampler Eltra Helos.

The statistical dispersion of the results from chemical and energetic characterization will not be analyzed using the typical parameters of univariate statistics (standard deviation). As this is a multivariate modeling approach aimed at replicating experimental results, it is important to take into account the dispersion between the experimental values and those calculated using the models detailed in Section 2.3, expressed in terms of the coefficient of variation. The analysis and discussion of this coefficient will be conducted in the results section.

2.3. Modeling and Optimization by Multiple Regression-Experimental Design

The CAE process was modeled by multiple regression with provision for linear, quadratic, and interaction terms among the independent variables:

$$Y = a_0 + \sum_{i=1}^{n} b_i X_{ni} + \sum_{i=1}^{n} c_i X_{ni}^2 + \sum_{i=1,j=1}^{n} d_{ij} X_{ni} x_{nj} \quad (i < j) \tag{1}$$

The number of tests needed was decreased and covariance between variables was reduced by using a central composition design with N tests such that $N = 2^n + 2 \cdot n + n_c$, 2^n being the number of points constituting the design, $2 \cdot n$ that of axial points and n_c that of central points. The effect of the different ranges spanned by the variables was suppressed by normalizing their values to 0, 1, and –1 with the following equation:

$$X_n = \frac{X - \overline{X}}{(X_{max} - X_{min})/2} \tag{2}$$

where X, $\overline{X}$, X_{max}, and X_{min} represent the value of a particular independent variable, and its mean, maximum, and minimum values, respectively. The dependent variables under examination included yield, glucan, xylan, Klason lignin, and lower heating value (LHV).

The statistical models developed in this study to represent the various dependent variables should exhibit globally significant model values, such as the R-squared (R^2) and Snedecor F statistics, that are sufficiently high for the models to have statistical relevance. The "appropriate" threshold for these statistics will vary depending on the type of results and models used, whether working with variables of a more "social" nature or more deterministic ones, as in laboratory experiments. However, in the context of our study, values of R^2 greater than 0.85 and Snedecor F values above 5 are considered very appropriate. In the results section, the statistical significance of each model will be addressed according to these criteria. Furthermore, the statistical importance of each coefficient associated with the independent variables will be evaluated. In this context, a conventional criterion is used, which considers an independent variable to be statistically significant in the model when its significance level "p" is less than 0.05 or the value of the Student-*t* test is greater than 2. The variables included in the models presented in the results section adhere to this conventional criterion.

Furthermore, in order to simplify interpretation, polynomial equations were employed to generate response surfaces. These surfaces were created by plotting two of the three independent process variables on two horizontal axes while displaying the maximum and minimum levels of the third independent variable. This enables a comprehensive representation of the entire range of variation for each dependent variable in relation to all independent process variables (in our case, alkali concentration, treatment time, and temperature).

3. Results and Discussion

The initial hypothesis was that the cold alkaline extraction (CAE) of clone AF2 of *Populus x euramericana* would be more efficient than that of other woody species such as eucalyptus (the reference species here). Furthermore, it was hypothesized that the use of ultrasound during the process would result in increased extraction of hemicelluloses in the liquor. If the process were highly selective for hemicelluloses, there would be the additional benefit of an increased calorific value in the solid residue from CAE. This hypothesis was tested by analyzing the raw material and modeling the results obtained with and without ultrasound for comparison.

3.1. Chemical Characterization of the Raw Material

As previously mentioned, *Populus x euramericana* is a tree species with a wide range of clones [45,46]. In this work, we selected clone AF2 due to its fast growth and adaptability. Under the conditions described above, this clone yielded over 25 tons of dry biomass per hectare per year when harvested at 3-year intervals. The biomass used in this study primarily consisted of stems and branches with a thickness of 2.5–10.0 cm, accounting for 67.5% of the total biomass. The bark content of the biomass, which should ideally be minimized to maintain quality, ranged from 31% in the thickest stems to 12% in those 5.0–10.0 cm thick. The primary criterion for selecting this poplar clone was its sustainability as a crop. Indeed, after 9 years, the target plantation had significantly improved soil quality by increasing the organic matter content by 0.23 percentage points (from 0.80% -typical values in poor soils- to 1.03%) and the nitrogen content by 0.03 percentage points (from 0.12% to 0.15%).

Table 1 displays the results of chip characterization and compares them with the results from Constantí et al., 1998 [47] for the *Populus* genus and those from studies on other lignocellulosic raw materials conducted elsewhere. These results represent various raw materials obtained prior to the extraction process and were acquired by different authors following international standards (TAPPI standards). The table also shows the higher heating value (HHV) for the clone and the other materials. Additional determinations for AF2 included the contents of extractives soluble in 1% NaOH (22.3%, -1.95-), hot water (4.22%, -0.12-), and ethanol–acetone mixtures (2.8%, -0.15-). The similarity between the content of xylan and that in NaOH-soluble extractives suggests that the hemicellulose fraction of the studied clone is primarily composed of that polysaccharide. The elemental composition of the biomass was 6.11% hydrogen (H), 0.00019% sulfur (S), 48.67% carbon (C), and 44.13% oxygen (O).

As shown in Table 1, the lignin and xylan contents of the clone exceeded those of most of the species compared, especially the reference material (*E. globulus*) and the *Populus* species examined by Constantí et al., 1998, and Ebringerová et al., 2010 [47,48]. These differences are quite normal as the materials had different natures despite their common origin. In line with the results of Constantí et al., 1998, and Ebringerová et al., 2010 [47,48], clone AF2 contained no arabinan. Additionally, its α-cellulose and glucan contents were slightly lower, yet still similar to those of *E. globulus* and those reported by Constantí et al., 1998, and Ebringerová et al., 2010 [47,48] for a different *Populus* species. In contrast, the higher heating value (HHV) significantly exceeded that of most of the other materials, including *E. globulus*.

3.2. Cold Alkaline Extraction of Hemicelluloses with and without Ultrasound Assistance

Table 2 presents the yields, glucan, xylan, and lignin results obtained at each point in the experimental design for the CAE process with and without ultrasound. The values in the table are expressed as a percentage of each polymer in the initial raw material. They could be converted into percentages relative to the raw material by multiplying the value by the corresponding amount in the initial raw material and dividing by 100. However, if this value is divided by the yield and then multiplied by 100, it would represent the percentage of the polymer relative to the solid phase.

Table 1. Chemical Composition and Higher Calorific Value (HCV) of Clone AF2 of *Populus euroamericana*, and Comparison with Other Materials.

Composition	(1)	(2)	(3)	(4)	(5)	(6)	(7)	(8)
α Cellulose (glucan) (%)	40.3 ± 0.85	41.1 ± 2.1	38.9 ± 3.4	38.0 ± 2.4	44.0 ± 3.3	42.8 ± 2.0	33.8 ± 1.6	55.4 ± 2.6
Klason Lignin (%)	25.1 ± 0.16	24.1 ± 1.8	19.8 ± 1.9	19.0 ± 2.5	27.8 ± 1.1	21.2 ± 0.9	19.9 ± 0.5	16 ± 0.3
Xylan (%)	19.3 ± 0.09	17.0 ± 0.5	19.9 ± 1.3	15.7 ± 0.1	15.7 ± 0.2	17.1 ± 0.3	23.9 ± 0.1	34.6 ± 0.4
Araban (%)	0	-----	0.6 ± 0.3	1.5 ± 0.3	1.1 ± 0.1	0.7 ± 0.1	0.37 ± 0.2	5.6 ± 0.3
Acetyl groups (%)	0.7 ± 0.02	-----	4.4 ± 0.6	3.3 ± 0.5	4.4 ± 0.2	3.5 ± 0.1	4.32 ± 0.1	-----
HHV, KJul/kg od.b.	19,982 ± 30	-----	19,592 ± 28	18,981 ± 95	20,300 ± 53	19,326 ± 84	17,259 ± 25	-----

Raw material percentages (100 kg dry matter); 1—Genus *Populus* (Poplar clone AF2). Present study; 2—Genus *Populus* [47]; 3—Tagasaste (*Chamaecytisus proliferus*) [49,50]; 4—Leucaena (*Leucaena diversifolia*) [51,52]; 5—Paulownia trihybrid (fortunei x tormentose x elongata) [53,54]; 6—*Eucalyptus globulus* [55,56]; 7—Sunflower stalks [52]; 8—Wheat straw [57].

Table 2. Normalized values of the process variables and composition of the solid fractions obtained in the two processes of cold alkaline extraction with and without ultrasound assistance of the *Populus x euroamericana* (Clone AF2). Additionally, the glucan, xylan, and lignin contents are expressed as percentages relative to the raw material.

Variables			With Ultrasound				Without Ultrasound			
X_A	X_t	X_T	Yield (%)	Glucan (%)	Xylan (%)	Klason Lignin (%)	Yield (%)	Glucan (%)	Xylan (%)	Klason Lignin (%)
0	0	0	68.8	86.4	40.4	67.0	73.2	89.8	45.4	88.5
0	0	0	68.8	86.4	40.4	67.0	73.2	89.8	45.4	88.5
1	1	1	63.3	80.4	45.0	58.4	68.5	93.2	56.8	80.1
1	1	−1	67.9	84.3	43.5	62.4	77.8	95.7	49.3	83.4
1	−1	1	69.0	84.8	49.5	73.9	73.3	96.5	54.7	97.5
1	−1	−1	75.0	95.8	50.2	67.4	80.8	98.2	47.4	90.6
−1	1	1	64.7	96.2	47.2	51.5	69.3	98.1	43.3	71.6
−1	1	−1	70.9	96.2	51.6	66.7	77.6	98.2	51.3	90.9
−1	−1	1	69.5	85.7	49.9	69.2	71.6	89.8	53.0	89.5
−1	−1	−1	74.6	87.6	55.7	77.7	78.5	92.1	60.2	98.9
1	0	0	67.3	91.0	44.4	60.9	72.7	98.7	47.4	79.7
−1	0	0	69.4	95.6	50.3	61.3	73.1	97.4	47.6	79.6
0	1	0	66.5	81.7	39.2	68.7	73.7	88.1	46.4	93.3
0	−1	0	71.0	84.6	44.2	74.4	75.4	85.1	52.0	98.1
0	0	1	68.6	82.1	40.9	68.4	71.1	86.3	49.5	90.6
0	0	−1	73.5	84.1	42.6	72.9	78.7	87.8	50.1	96.0

X_A alkali concentration, X_t time, X_T temperature.

The results were modeled using Equations (3)–(10) from Table 3, as described in Sections 2.2 and 2.3. By analyzing the residuals between the experimental (observed) values and those predicted by the polynomial multiple regression models, it was observed that the prediction errors were all less than 10% and, in some cases, even less than 5%. This percentage is understood as the percentage change within the range of each dependent variable, rather than as the percentage change in the maximum or minimum value. Therefore, the obtained values demonstrate the robustness of the models.

Also, the quadratic regression coefficients, R^2, all exceeded 0.95, which was considered acceptable given the simultaneous calculations involving several independent variables. The Snedecor's *F*-values significantly exceeded 5, which is the minimum value required to assume a good fit. All independent variables included in the models had individual Student's *t*-values greater than 2 or *p*-values less than 0.05, including their statistical significance at the 95% confidence level. For easier interpretation, the polynomial equations were employed to create the response surfaces in Figures 1 and 2 (refer to Section 2.3).

Table 3. Equations of the polynomial models for the dependent variables of the cold alkaline extraction (CAE) with and without ultrasound assistance of the *Populus x euroamericana* wood (Clone AF2).

Equation with Ultrasounds	Equation Number	Adjusted R^2/Snedecor's *F-Value*
$YI = 68.5 - 0.67X_A - 2.57X_t - 2.66X_T - 1.83X_t^2 + 2.58X_T^2$	(3)	0.95/56
$GL = 87.0 - 2.50X_A - 1.87X_T + 5.98X_A^2 - 4.03X_T^2 - 4.39X_AX_t - 1.6X_AX_T + 1.19X_tX_T$	(4)	0.98/59
$X = 40.2 - 2.28X_A - 2.24X_t - 1.12X_T + 7.23X_A^2 + 1.62X_T^2 - 0.56X_AX_t + 1.37X_AX_T + 0.44X_tX_T$	(5)	0.98/138
$KL = 66.6 - 5.96X_t - 2.57X_T - 5.33X_A^2 + 4.58X_T^2 + 1.04X_AX_t + 3.28X_AX_T - 2.34X_tX_T$	(6)	0.98/114
Equation without Ultrasounds	**Equation Number**	**Adjusted R^2/Snedecor's *F-Value***
$YI = 73.0 + 0.3\ X_A - 1.38X_t - 3.97X_T + 1.68X_T^2 - 0.57X_AX_t - 0.42X_tX_T$	(7)	0.98/202
$GL = 89.7 + 0.67X_A + 1.16X_t - 0.80X_T + 8.37X_A^2 - 2.86X_T^2 - 2.53X_AX_t$	(8)	0.99/189
$X = 45.2 - 2.02X_t + 2.39X_A^2 + 4.39X_T^2 + 2.84X_AX_t + 3.76X_AX_T$	(9)	0.99/211
$KL = 88.04 - 6.08X_t - 3.05X_T - 8.14X_A^2 + 2.61X_t^2 + 5.24X_T^2 + 4.05X_AX_T - 2.75X_tX_T$	(10)	0.99/251

Dependent variables: YI yield (%), GL glucan (%), X xylan (%), KL Klason lignin (%). Independent variables: X_A: alkali concentration, X_t and X_T: treatment time and temperature. The differences between the experimental values and those estimated using the equations never exceeded 10% of the former.

The values predicted by the quadratic Equations (3)–(15) can be easily calculated using these equations and, as mentioned, replicate the experimental results with coefficients of variation below 10% of the range of variation of each dependent variable.

Before delving into the data in Tables 2 and 3, it is important to note that our initial hypothesis was confirmed (i.e., clone AF2 of *Populus x euramericana* proved a suitable raw material for the intended purpose). The CAE yields obtained in the absence of ultrasound were significantly higher than those obtained by Carvalho et al., 2016, and Fernández et al., 2020 [20,58] with eucalyptus (ranging 3.2% to 5.0%), but lower than those observed for grassy materials such as wheat (ranging from 25.5% 38.8%; [16,21]). A lower yield implies a higher extraction yield in the liquid phase. These results are consistent with our earlier discussion on the introduction that CAE efficiency depends on the specific raw material. For instance, eucalyptus wood, which is resistant to CAE fractionation [20], can be efficiently extracted at temperatures, such as those used by Alfaro et al., 2010, and Carvalho et al., 2016 [20,49], which reached temperatures of up to 175 °C, resulting in yields of 5.0% to 32.9%. This confirmation aligns with the proportions of different polymers extracted in our study.

Based on Equations (3) and (7) in Table 3, it is evident that temperature had the most significant impact on yield as an individual operational variable, both in the presence and absence of ultrasound. Figures 1A and 2A depict a similar response to the other two independent variables, although over considerably different ranges, ranging from 63.3% to 75.0% with sonication and from 68.5% to 80.8% without it. These findings underscore the pronounced influence of ultrasound on CAE yield. Indeed, experimental yields were notably lower with ultrasound, which was reflected in their mean values and the predictions made by the multiple regression models presented in Equations (3) and (7), particularly at the central points of the experimental design (68.5% with ultrasound and 73.0% without it). It is important to note that a lower yield was preferable as CAE efficiently removed structural components (cellulose, hemicellulose, and lignin) from the raw material. In fact, ultrasound-assisted CAE removed 25.0% to 36.7% of these initial structural components present in the material.

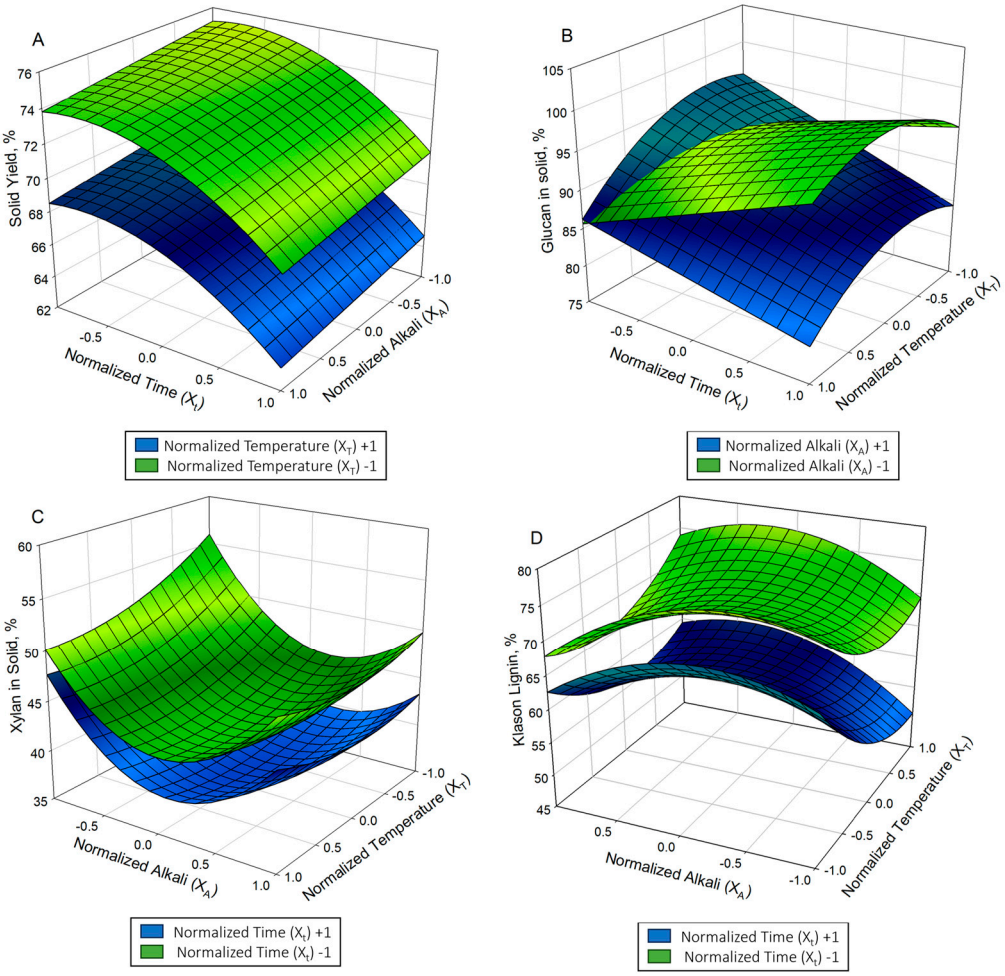


Figure 1. Surface responses for yield (**A**), as well as the glucan (**B**), xylan (**C**), and lignin contents (**D**) (percentage relative to the polymer content in raw material) in the solid residue obtained from the process of Cold Alkaline Extraction using ultrasound on the Popular Wood (clone AF2).

As observed in the glucan surface responses shown in Figures 1 and 2, the glucan content of the CAE solid residue decreased with increasing alkali concentration, treatment time, and solid yield. However, according to Equations (4) and (8), the alkali concentration was the most influential variable on the glucan content. Furthermore, the difference between the predicted values for glucan content at the central point of the experimental design (87.0% with ultrasound and 89.7% without it) was much smaller than that of the corresponding mean yields. Therefore, the yield ranges, both with (81.7%–95.6%) and without ultrasound (85.1%–98.7%), were more similar. Therefore, as previously found by García et al., 2013, and Carvalho et al., 2016 [20,21], ultrasound had a notably selective effect on the hemicellulose and lignin fractions. This was particularly true for xylan, the primary component of the hemicellulose fraction, characterized by its low polymerization and non-crystallinity structure that makes it more susceptible to decomposition into monosaccharides. These findings support the initial hypothesis that ultrasound enhances hemicellulose extraction in the CAE liquor while preserving or even increasing the calorific potential of the solid residue.

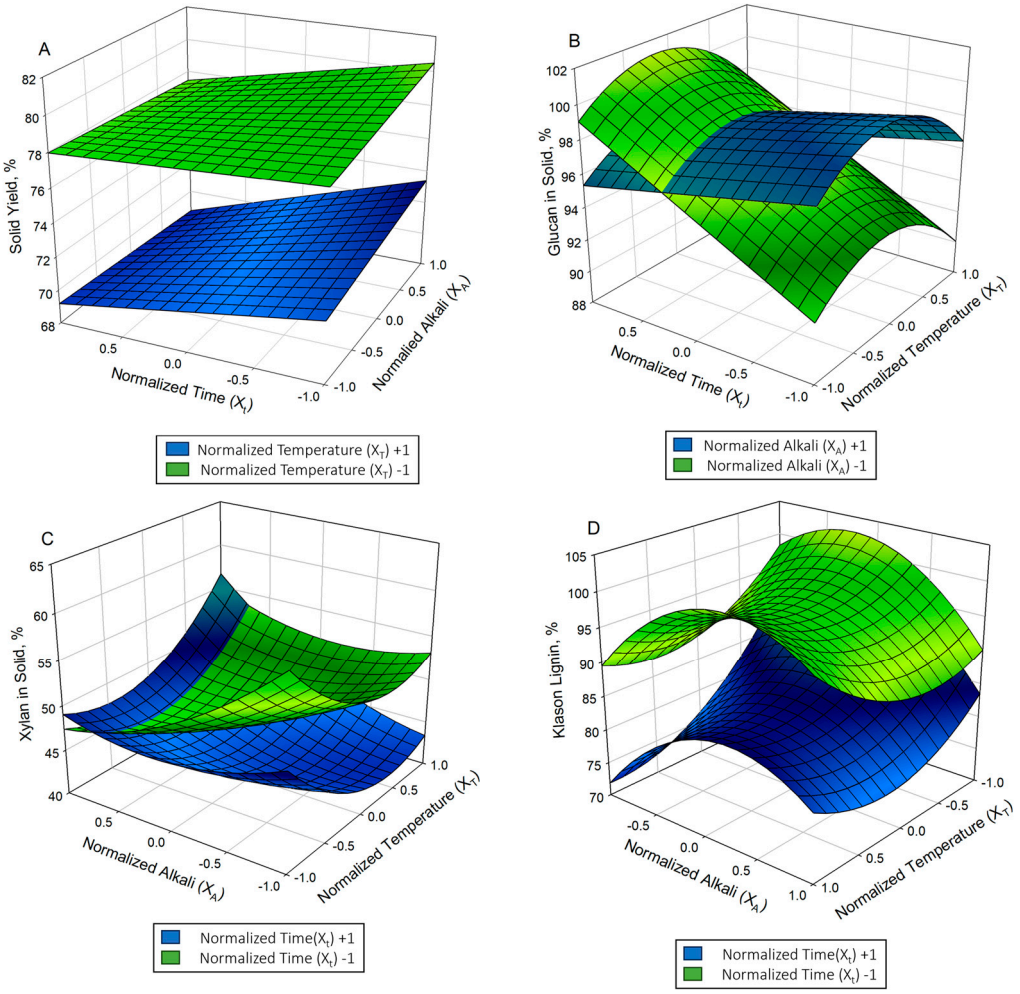


Figure 2. Surface responses for yield (**A**), as well as the glucan (**B**), xylan (**C**), and lignin contents (**D**) (percentage relative to the polymer content in raw material) in the solid residue obtained from the process of Cold Alkaline Extraction without ultrasound on the Popular Wood (clone AF2).

In fact, when comparing the experimental ranges for hemicelluloses (xylan) extraction in the presence and absence of ultrasound (44.3%–60.8% vs. 39.8%–56.7%) with the predicted values at the central points based on Equations (5) and (9) (59.8% and 54.8%, respectively), it becomes evident that CAE had a much more selective effect on the hemicellulose fraction (xylan) than on the cellulose fraction (glucan). This difference was even more pronounced in the presence of ultrasound. This suggests that, notably, the CAE process exhibits a high selectivity for hemicelluloses while preserving the integrity of glucan. Alkaline treatments typically alter the structure of lignocellulosic materials by reducing the crystallinity and degree of polymerization of cellulose, thereby increasing the inner surface area, and facilitating release into the extraction medium [59].

Equations (6) and (10) do not provide a clear indication of the independent variable with the strongest influence on hemicellulose extraction into the CAE liquor. Figures 1C and 2C represent extreme values of treatment time, as it was clearly the independent variable that most strongly influenced CAE yield in a linear manner, without ultrasound. In the presence of ultrasound, the highest xylan contents of the solid residue (i.e., the lowest extraction of xylan into the CAE liquor) were achieved with extended treatment times, moderate alkali concentrations, and temperatures. The alkali concentration had little influence. Xylan extraction without ultrasound yielded similar results, although with lower hemicellulose extraction levels. These results were considerably higher than those reported by Carvalho et al., 2016 and Fernández et al., 2018 [20,60] for eucalyptus

(46%) but comparable to those of García et al., 2013, and Madejón et al., 2016 [16,21] for wheat straw.

In theory, preserving glucan integrity while maximizing hemicellulose extraction into the CAE liquor would be easiest by using a long treatment time, a medium temperature, and a medium-to-high alkali concentration. Below are described the results of the elemental analysis of the CAE solid residue in the presence of ultrasound to confirm the practicality of these operating conditions.

Obviously, preserving most of the glucan in the raw material in the CAE solid residue is of interest when considering the thermal stability of this component. In fact, the cellulose fraction has the highest energy content among the constituents of lignocellulosic biomass [60].

The amount of lignin remaining in the solid was also interest. Cold alkaline extraction partially delignifies the raw material, potentially facilitating subsequent delignification of the solid residue, making it useful for applications such as cellulose pulping, or increasing energy production through thermochemical treatment. Lignin acts as a seal protecting the lignocellulosic fraction, which needs to be broken down to fully exploit the raw material. Due to its abundance of benzene rings, lignin has the highest activation energy and thermal stability [61]. The use of ultrasound significantly facilitated its extraction. Delignification at the central point of the experimental design was estimated to be 33.4% in the presence of ultrasound and 12.0% in its absence (Table 3). Lignin was extracted by 22.3%–48.5% with ultrasound and 1.9%–28.4% without it (Table 2). However, lignin was consistently extracted to a lesser extent than hemicelluloses, indicating that CAE was less selective toward the lignin fraction. Therefore, longer treatment times at the upper end of the range (Equations (4) and (8)), along with medium temperatures (Figure 1D) and alkali concentrations (Figure 2D), may be suitable for effective delignification and hemicellulose extraction while preserving glucan integrity. Since lignin is the most structurally complex component and resistant to extraction from lignocellulosic materials, the treatment time will be especially influential on the efficiency of the chemical treatment and the cavitational effects of ultrasound, leading to cleavage of lignin–cellulose bonds [62].

In summary, these comparisons regarding the yield, glucan, hemicelluloses, and lignin content in the CAE processes with and without ultrasound assistance confirm the initial hypothesis and demonstrate a significant synergistic effect when ultrasound and CAE are applied simultaneously, enhancing both the selectivity and efficiency of hemicellulose extraction and the potential for increased energy yield from the post-treatment solid phase.

Another interesting point is the dependence of the elemental composition of the CAE solid residue on the operating conditions in the presence of ultrasound. This information can be useful for identifying the optimal operating conditions for extracting hemicelluloses from the target clone. The results are presented in Table 4, along with the lower heating value (LHV) (it is considered that the water vapor generated during combustion does not condense into liquid water, unlike in the case of higher heating value, where vapor condensation is taken into account) and moisture content. Table 5 displays the equations of the polynomial models derived from these results. Figure 3 illustrates the response surfaces for the contents in C, H, S and O, while Figure 4 shows the response surface for LHV.

Table 4. Values of the process variables and elemental composition (hydrogen, H; Sulphur, S; Carbon, C; and Oxygen, O) of the solid fractions obtained in the Cold alkaline extraction (CAE) with and without the use of ultrasound on *Populus x euroamericana* wood (Clone AF2).

Normalized Values			**Cold Alkaline Extraction (CAE) with Ultrasound**					
X_A	X_t	X_T	**H (%)**	**S (%)**	**C (%)**	**O (%)**	**Moisture (%)**	**LHV at Constant Volume (J/g o.d.b.)**
0	0	0	6.105	0.00018	45.60	47.19	9.9	18,843
1	1	1	5.867	0.00000	41.01	52.03	8.2	19,233
1	1	−1	5.872	0.00000	42.36	50.68	7.8	19,033

Table 4. *Cont.*

Normalized Values			Cold Alkaline Extraction (CAE) with Ultrasound					
X_A	X_t	X_T	H (%)	S (%)	C (%)	O (%)	Moisture (%)	LHV at Constant Volume (J/g o.d.b.)
1	−1	1	5.918	0.00024	44.70	48.23	10.0	18,115
1	−1	−1	5.922	0.00011	45.18	47.81	8.1	18,570
−1	1	1	5.841	0.00000	42.00	51.07	11.2	18,504
−1	1	−1	5.858	0.00016	43.88	49.17	8.2	18,530
−1	−1	1	5.861	0.00020	43.85	49.20	10.0	18,516
−1	−1	−1	5.908	0.00032	44.15	48.86	8.9	18,675
1	0	0	6.023	0.00014	44.00	49.01	11.2	18,965
−1	0	0	5.981	0.00030	44.25	48.71	8.8	18,872
0	1	0	5.972	0.00004	44.69	48.25	8.2	18,734
0	−1	0	5.962	0.000140	45.547	47.4	8.1	18,477
0	0	1	5.870	0.000165	44.359	48.78	9.8	18,482
0	0	−1	5.890	0.000205	45.076	47.78	9.7	18,686

Table 5. Equations of the polynomial models for the dependent variables of the cold alkaline extraction (CAE) with ultrasound assistance of the clone AF2 of *Populus euroamericana*.

Equation with Ultrasounds	Equation Number	Adjusted R^2/Snedecor's *F-Value*
$H = 6.100 + 0.015X_A - 0.016X_t - 0.093{X_A}^2 + 0.092{X_t}^2 - 0.220{X_T}^2$	(11)	0.96/70
$S = 0.000180 - 0.000049X_A - 0.000086X_t - 0.000019X_T + 0.000036{X_A}^2 - 0.000089{X_t}^2 + 0.000050X_AX_T - 0.000023X_tX_T$	(12)	0.95/40
$C = 45.62 - 1.02X_t - 0.470X_T - 1.514{X_A}^2 - 0.711{X_T}^2 - 0.549X_AX_t - 0.363X_tX_T$	(13)	0.97/77
$O = 47.22 + 1.04X_t + 0.50X_T + 1.60{X_A}^2 + 0.81{X_T}^2 + 0.56X_AX_t$	(14)	0.97/79
$LHV = 18{,}881 + 82X_A + 186X_t - 64X_T - 251{X_T}^2 + 217X_AX_t + 90X_tX_T$	(15)	0.95/27

Dependent variables: Hydrogen (%), Sulphur (%), Carbon (%), Oxygen (%), and LHV Low heating value. Independent variables: X_A: alkali concentration, X_t and X_T: treatment time and temperature of the cold alkaline extraction (CAE) with ultrasound of the target clone. The differences between the experimental values and those estimated using the equations never exceeded 10% of the former.

As shown in Figure 3A, the lowest hydrogen contents in the solid residues from ultrasound-assisted CAE were obtained at extreme temperatures and were scarcely dependent on the other independent variables. The sulfur content exhibited a similar behavior to the extraction yield and glucan content; thus, it decreased with increasing values of the three independent variables. In contrast, the carbon and oxygen contents increased with rising temperature, alkali concentration, and treatment time. This is consistent with the fact that the latter was a derivative quantity, and the former was the major element. The amount of carbon present in the CAE solid residue peaked at treatment times in the lower end of the range, where the temperature and alkali concentration had little influence, even though the highest carbon contents in the residue were obtained in the central ranges of the two variables. Since the carbon and hydrogen contents have contradictory effects on LHV, it is uncertain whether it is better to use treatment times in the lower or upper end of the range. Nevertheless, medium temperatures and alkali concentrations are the best choices to maximize LHV.

The H and C contents influence the calorific value of the material. LHV should increase with a decrease in H content and an increase in C content—although the former element is present in much smaller amounts than C. As demonstrated by Equation (11) in Table 5, the quadratic term of temperature had the most significant impact on the H content of the CAE solid residue obtained with ultrasound. Additionally, the lowest H contents were observed at low temperatures, regardless of the alkali concentration and treatment time employed. Nonetheless, the highest lower heating values, and consequently the greatest energy output, were achieved with longer treatment times, along with medium temperatures and alkali concentrations.

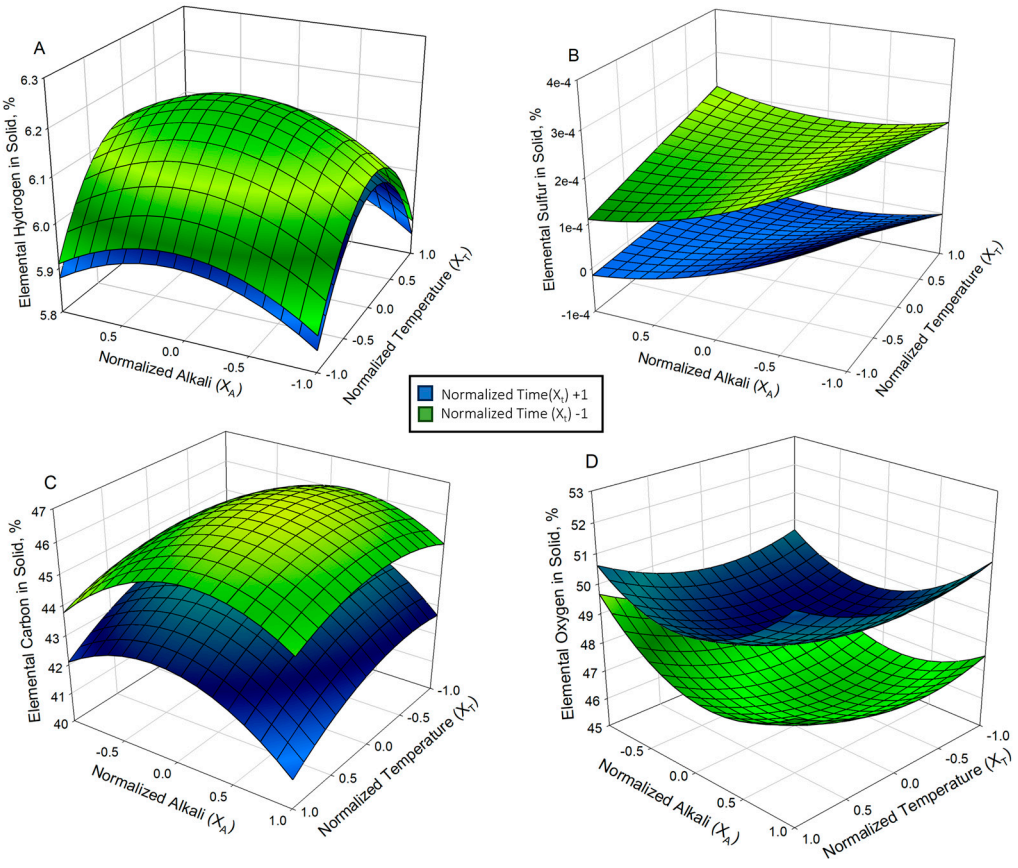


Figure 3. Response surfaces for elemental hydrogen (**A**), sulfur (**B**), carbon (**C**), and oxygen (**D**), all presented as percentages in the solid residue obtained from the Cold Alkaline Extraction process using ultrasound on the Popular Wood (clone AF2).

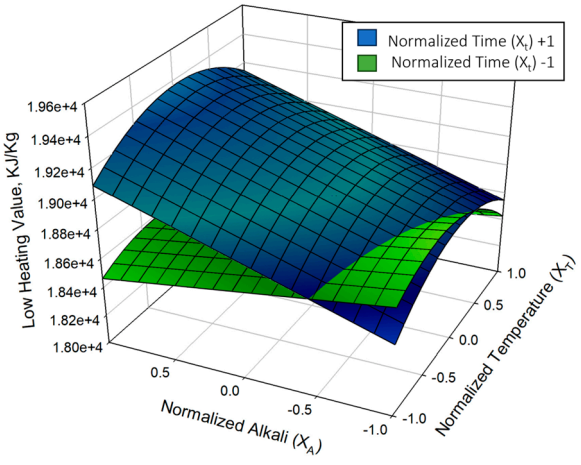


Figure 4. Response surface for lower heating values in the solid residue from the Cold Alkaline Extraction process using ultrasound on the Popular Wood (clone AF2).

Overall, utilizing extended durations, medium-to-high alkali concentrations, and moderate temperatures in conjunction with ultrasound yielded CAE solid residues with the highest glucan contents and lowest lignin contents. It also maximized hemicellulose extraction into the CAE liquor and the energy content (LHV) of the solid residue.

One other noteworthy point is the influence of ultrasound on LHV and the hemicellulose content of the CAE solid residue. As depicted in Figure 5, illustrating their variations at a constant treatment time (90 min, +1), it becomes evident that LHV was significantly

influenced by the presence of ultrasound. Therefore, LHV = 20,880 − 44.85 × hemicellulose content of solid (Equation (16)) (R^2 = 0.79). When ultrasound was employed, longer treatment times increased LHV and reduced the proportion of hemicelluloses in the CAE solid residue, subsequently increasing their concentration in the liquor. The effect was more pronounced at medium temperatures and, to a somewhat lesser extent, at medium alkali concentrations.

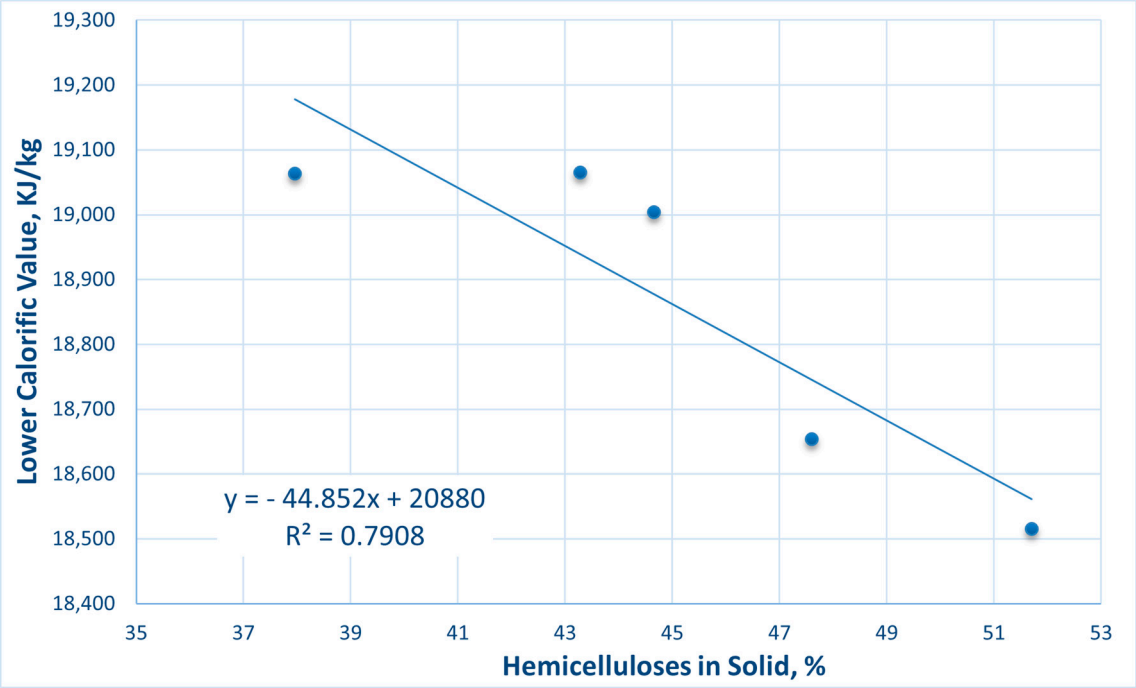


Figure 5. Predicted LHV (Equation (15)) against predicted xylan content (Equation (5)) of the solid residue obtained from the process of Cold Alkaline Extraction using ultrasound of the Popular Wood (clone AF2) at a constant treatment time of 90 min (experimental point, normalized time value = +1).

4. Conclusions

Clone AF2 of *Populus x euramericana* was found to have lignin and xylan contents slightly higher than those of *Eucalyptus globulus* and other species containing large amounts of biomass. Also, in common with other *Populus* species, the hemicellulose fraction of the clone contained no arabinan derivatives. However, its lower heating value (LHV) was considerably higher than that of *E. globulus* and other energy crops, and, unlike that of *Eucalyptus*, which was used as a reference here, it is suitable for the cold alkaline extraction (CAE) of hemicelluloses.

Using ultrasound increased the selectivity of CAE toward the hemicellulose and lignin fractions in the raw material. Thus, it increased hemicellulose extraction into the liquor while preserving or increasing the calorific value of the solid residue due to the cellulose fraction remaining in it.

The optimal conditions vary depending on the performance and property indices. However, overall, utilizing extended treatment times, medium-to-high alkali concentrations, and moderate temperatures with ultrasound-assisted CAE maximized the glucan content and minimized the lignin content of the resulting solid residue. It also maximized the extraction of hemicelluloses into the liquor and the energy content (LHV) of the solid residue.

Author Contributions: S.L.-C.: Conceptualization, Methodology, Investigation, Formal analysis, Data curation, Visualization, review. J.M.L.: Conceptualization, Methodology, Investigation, Formal analysis, Data curation, Visualization. J.C.G.: Conceptualization, Methodology, Funding acquisition, Supervision, Writing—review and editing. M.T.G.: Conceptualization, Methodology, Investigation, Formal analysis, Data curation, Visualization. F.L.: Conceptualization, Methodology, Data curation, Funding acquisition, Supervision, Writing—original draft, Project administration. All authors have read and agreed to the published version of the manuscript.

Funding: This work was funded by Spain's Ministry of Science and Innovation, and also by the National Research Program Oriented to the Challenges of Society (Project PID2020-112875RB-C21, MCIN/AEI /10.13039/501100011033), also this publication is part of the PRE2021-097925 support (funded by MCIN/AEI/10.13039/501100011033 and by the FSE+), and the University of Huelva/CBUA.

Data Availability Statement: All data generated or analyzed during this work are included in this published article.

Conflicts of Interest: The authors declare that they have no competing interests.

References

1. European Parliament. Directive (EU) 2018/2001 of the European Parliament and of the Council on the promotion of the use of energy from renewable sources. *Off. J. Eur. Union* **2018**, *2018*, 82–209.
2. REN21. *Renewables 2020 Global Status Report*; Renewable and Sustainable Energy Reviews; REN21 Secretariat: Paris, France, 2020; ISBN 978-3-948393-00-7. Available online: https://www.ren21.net/gsr-2020/ (accessed on 11 December 2023).
3. Domínguez, E.; Nóvoa, T.; del Río, P.G.; Garrote, G.; Romaní, A. Sequential two-stage autohydrolysis biorefinery for the production of bioethanol from fast-growing Paulownia biomass. *Energy Convers. Manag.* **2020**, *226*, 113517. [CrossRef]
4. Ginni, G.; Kavitha, S.; Kannah, Y.; Bhatia, S.K.; Kumar, A.; Rajkumar, M.; Kumar, G.; Pugazhendhi, A.; Chi, N.T.L. Valorization of agricultural residues: Different biorefinery routes. *J. Environ. Chem. Eng.* **2021**, *9*, 105435. [CrossRef]
5. World Energy Outlook 2017 [Internet]. OECD, 2017. Available online: https://www.oecd-ilibrary.org/energy/world-energy-outlook-2017_weo-2017-en (accessed on 11 May 2021).
6. Seserman, D.-M.; Pohle, I.; Veste, M.; Freese, D. Simulating climate change impacts on hybrid-poplar and black locust short rotation coppices. *Forests* **2018**, *9*, 419. [CrossRef]
7. Montero, G.; Serrada, R. *La Situación de los Bosques y el Sector Forestal en España*; ISFE: Pontevedra, Spain, 2013.
8. del Mar Contreras, M.; Romero, I.; Moya, M.; Castro, E. Olive-derived biomass as a renewable source of value-added products. *Process Biochem.* **2020**, *97*, 43–56. [CrossRef]
9. Ning, P.; Yang, G.; Hu, L.; Sun, J.; Shi, L.; Zhou, Y.; Wang, Z.; Yang, J. Recent advances in the valorization of plant biomass. *Biotechnol. Biofuels* **2021**, *14*, 102. [CrossRef]
10. Cristóbal, J.; Matos, C.T.; Aurambout, J.P.; Manfredi, S.; Kavalov, B. Environmental sustainability assessment of bioeconomy value chains. *Biomass Bioenergy* **2016**, *89*, 159–171. [CrossRef]
11. Ruiz, H.A.; Conrad, M.; Sun, S.N.; Sanchez, A.; Rocha, G.J.M.; Romaní, A.; Castro, E.; Torres, A.; Rodríguez-Jasso, R.M.; Andrade, L.P.; et al. Engineering aspects of hydrothermal pretreatment: From batch to continuous operation, scale-up and pilot reactor under biorefinery concept. *Bioresour. Technol.* **2020**, *299*, 122685. [CrossRef]
12. Sixto, H.; Cañellas, I.; van Arendonk, J.; Ciria, P.; Camps, F.; Sánchez, M.; Sánchez-González, M. Growth potential of different species and genotypes for biomass production in short rotation in Mediterranean environments. *For. Ecol. Manag.* **2015**, *354*, 291–299. [CrossRef]
13. FAO. *The Future of Food and Agriculture—Trends and Challenges*; FAO: Rome, Italy, 2017; ISBN 978-92-5-109551-5. Available online: https://www.fao.org/3/i6583e/i6583e.pdf (accessed on 11 December 2023).
14. Lauri, P.; Havlík, P.; Kindermann, G.; Forsell, N.; Böttcher, H.; Obersteiner, M. Woody biomass energy potential in 2050. *Energy Policy* **2014**, *66*, 19–31. [CrossRef]
15. Vanguelova, E.; Pitman, R. Impacts of short rotation forestry on soil sustainability. Short rotation forestry: Review of growth and environmental impacts. *For. Res. Monogr.* **2011**, *2*, 37–77.
16. Madejón, P.; Alaejos, J.; García-Álbala, J.; Fernández, M.; Madejón, E. Three-year study of fast-growing trees in degraded soils amended with composts: Effects on soil fertility and productivity. *J. Environ. Manag.* **2016**, *169*, 18–26. [CrossRef] [PubMed]
17. Madadi, M.; Song, G.; Karimi, K.; Zhu, D.; Elsayed, M.; Sun, F.; Abomohra, A. One-step lignocellulose fractionation using acid/pentanol pretreatment for enhanced fermentable sugar and reactive lignin production with efficient pentanol retrievability. *Bioresour. Technol.* **2022**, *359*, 127503. [CrossRef] [PubMed]
18. Penín, L.; Peleteiro, S.; Rivas, S.; Santos, V.; Parajó, J.C. Production of 5-hydroxymethylfurfural from pine wood via biorefinery technologies based on fractionation and reaction in ionic liquids. *Bioresources* **2019**, *14*, 4733–4747. [CrossRef]
19. Kim, J.S.; Lee, Y.Y.; Kim, T.H. A review on alkaline pretreatment technology for bioconversion of lignocellulosic biomass. *Bioresour. Technol.* **2016**, *199*, 42–48. [CrossRef]

20. de Carvalho, D.M.; Sevastyanova, O.; de Queiroz, J.H.; Colodette, J.L. Cold alkaline extraction as a pretreatment for bioethanol production from eucalyptus, sugarcane bagasse and sugarcane straw. *Energy Convers. Manag.* **2016**, *124*, 315–324. [CrossRef]
21. García, J.C.; Díaz, M.J.; Garcia, M.T.; Feria, M.J.; Gómez, D.M.; López, F. Search for optimum conditions of wheat straw hemicelluloses cold alkaline extraction process. *Biochem. Eng. J.* **2013**, *71*, 127–133. [CrossRef]
22. Hutterer, C.; Schild, G.; Potthast, A. A precise study on effects that trigger alkaline hemicellulose extraction efficiency. *Bioresour. Technol.* **2016**, *214*, 460–467. [CrossRef]
23. Park, Y.C.; Kim, J.S. Comparison of various alkaline pretreatment methods of lignocellulosic biomass. *Energy* **2012**, *47*, 31–35. [CrossRef]
24. Longue Júnior, D.; Colodette, J.L.; Gomes, V.J. Extraction of wood hemicelluloses through NaOH leaching | Remoção de hemiceluloses da madeira por tratamento de lixiviação alcalina com NaOH. *Cerne* **2010**, *16*, 423–429. [CrossRef]
25. Tiwari, B.K. Ultrasound: A clean, green extraction technology. *TrAC-Trends Anal. Chem.* **2015**, *71*, 100–109. [CrossRef]
26. Yuan, Z.; Long, J.; Wang, T.; Shu, R.; Zhang, Q.; Ma, L. Process intensification effect of ball milling on the hydrothermal pretreatment for corn straw enzymolysis. *Energy Convers. Manag.* **2015**, *101*, 481–488. [CrossRef]
27. Saikia, M.; Das, T.; Hower, J.C.; Silva, L.F.O.; Fan, X.; Saikia, B.K. Oxidative chemical beneficiation of low-quality coals under low-energy ultrasonic and microwave irradiation: An environmental-friendly approach. *J. Environ. Chem. Eng.* **2021**, *9*, 104830. [CrossRef]
28. Ashokkumar, M. The characterization of acoustic cavitation bubbles—An overview. *Ultrason. Sonochem.* **2011**, *18*, 864–872. [CrossRef] [PubMed]
29. García, A.; Alriols, M.G.; Llano-Ponte, R.; Labidi, J. Ultrasound-assisted fractionation of the lignocellulosic material. *Bioresour. Technol.* **2011**, *102*, 6326–6330. [CrossRef] [PubMed]
30. Raihan, A.; Ibrahim, S.; Muhtasim, D.A. Dynamic impacts of economic growth, energy use, tourism, and agricultural productivity on carbon dioxide emissions in Egypt. *World Dev. Sustain.* **2023**, *2*, 100059. [CrossRef]
31. Li, F.; Li, Y.; Novoselov, K.S.; Liang, F.; Meng, J.; Ho, S.-H.; Zhao, T.; Zhou, H.; Ahmad, A.; Zhu, Y.; et al. Bioresource Upgrade for Sustainable Energy, Environment, and Biomedicine. *Nano-Micro Lett.* **2023**, *15*, 35. [CrossRef]
32. Puițel, A.C.; Suditu, G.D.; Drăgoi, E.N.; Danu, M.; Ailiesei, G.-L.; Balan, C.D.; Chicet, D.-L.; Nechita, M.T. Optimization of Alkaline Extraction of Xylan-Based Hemicelluloses from Wheat Straws: Effects of Microwave, Ultrasound, and Freeze–Thaw Cycles. *Polymers* **2023**, *15*, 1038. [CrossRef]
33. Gufe, C.; Thantsha, M.S.; Malgas, S. Recovery of xylan from Acacia mearnsii using ultrasound-assisted alkaline extraction. *Biofuels Bioprod. Biorefining* **2023**, *17*, 976–987. [CrossRef]
34. Tareen, A.K.; Punsuvon, V.; Parakulsuksatid, P. Conversion of steam exploded hydrolyzate of oil palm trunk to furfural by using sulfuric acid, solid acid, and base catalysts in one pot. *Energy Sources Part A Recovery Util. Environ. Eff.* **2020**, 1–12. [CrossRef]
35. Gil, M.V.; Jablonka, K.M.; García, S.; Pevida, C.; Smit, B. Biomass to energy: A machine learning model for optimum gasification pathways. *Digit. Discov.* **2023**, *2*. [CrossRef]
36. Tofani, G.; Cornet, I.; Tavernier, S. Multiple linear regression to predict the brightness of waste fibres mixtures before bleaching. *Chem. Pap.* **2022**, *76*, 4351–4365. [CrossRef]
37. *TAPPI T264 cm-07*; Preparation of Wood for Chemical Analysis. TAPPI Press: Atlanta, GA, USA, 2007.
38. *TAPPI 211 om-02*; Ash in Wood, Pulp, Paper and Paperboard: Combustion at 525 °C. TAPPI Press: Atlanta, GA, USA, 2002.
39. *TAPPI T204 cm-07*; Solvent Extractives of Wood and Pulp. TAPPI Press: Atlanta, GA, USA, 2007.
40. *TAPPI T249 cm-09*; Carbohydrate Composition of Extractive-Free Wood and Wood Pulp by Gas-Liquid Chromatography. TAPPI Press: Atlanta, GA, USA, 2009.
41. Romaní, A.; Garrote, G.; Ballesteros, I.; Ballesteros, M. Second generation bioethanol from steam exploded Eucalyptus globulus wood. *Fuel* **2013**, *111*, 66–74. [CrossRef]
42. *TAPPI T222 om-11*; Acid-Insoluble Lignin in Wood and Pulp. TAPPI Press: Atlanta, GA, USA, 2011.
43. CEN/TS Solid Biofuels-Method for the Determination of Calorific Value CEN/TS 14918:2005. 2005. Available online: https://standards.iteh.ai/catalog/standards/cen/21f53010-bfdf-41aa-8f73-3ad9e2ab444f/cen-ts-14918-2005 (accessed on 11 December 2023).
44. *UNE 16001 EX*; Solid Biofuels, Method for the Determination of Calorific Value. Spanish Association for Standardization: Madrid, Spain, 2005. Available online: https://infostore.saiglobal.com/preview/is/en/2005/i.s.cents14918-2005.pdf?sku=675235 (accessed on 11 December 2023).
45. Civitarese, V.; Faugno, S.; Picchio, R.; Assirelli, A.; Sperandio, G.; Saulino, L.; Crimaldi, M.; Sannino, M. Production of selected short-rotation wood crop species and quality of obtained biomass. *Eur. J. For. Res.* **2018**, *137*, 541–552. [CrossRef]
46. Magagnotti, N.; Spinelli, R.; Kärhä, K.; Mederski, P.S. Multi-tree cut-to-length harvesting of short-rotation poplar plantations. *Eur. J. For. Res.* **2020**, *140*, 345–354. [CrossRef]
47. Constantí, M.; Reguant, C.; Poblet, M.; Zamora, F.; Mas, A.; Guillamón, J.M. Molecular analysis of yeast population dynamics: Effect of sulphur dioxide and inoculum on must fermentation. *Int. J. Food Microbiol.* **1998**, *41*, 169–175. [CrossRef] [PubMed]
48. Ebringerová, A.; Hromádková, Z. An overview on the application of ultrasound in extraction, separation and purification of plant polysaccharides. *Cent. Eur. J. Chem.* **2010**, *8*, 243–257. [CrossRef]
49. Alfaro, A.; López, F.; Pérez, A.; García, J.C.; Rodríguez, A. Integral valorization of tagasaste (*Chamaecytisus proliferus*) under hydrothermal and pulp processing. *Bioresour. Technol.* **2010**, *101*, 7635–7640. [CrossRef]

50. López, F.; Alfaro, A.; García, M.; Díaz, M.J.; Calero, A.M.; Ariza, J. Pulp and paper from tagasaste (*Chamaecytisus proliferus* L.F. ssp. palmensis). *Chem. Eng. Res. Des.* **2004**, *82*, 1029–1036. [CrossRef]
51. Feria, M.J.; García, J.C.; Pérez, A.; Gomide, J.L.; Colodette, J.L.; López, F. Process optimization in kraft pulping, bleaching, and beating of Leucaena diversifolia. *Bioresources* **2012**, *7*, 283–297. [CrossRef]
52. Caparrós, S.; Ariza, J.; López, F.; Nacimiento, J.A.; Garrote, G.; Jiménez, L. Hydrothermal treatment and ethanol pulping of sunflower stalks. *Bioresour. Technol.* **2008**, *99*, 1368–1372. [CrossRef] [PubMed]
53. García, J.C.; Zamudio, M.A.M.; Pérez, A.; De Alva, H.E.; López, F. Paulownia as a raw material for the production of pulp by soda-anthraquinone cooking with or without previous autohydrolysis. *J. Chem. Technol. Biotechnol.* **2011**, *86*, 608–615. [CrossRef]
54. López, F.; Pérez, A.; Zamudio, M.A.M.; De Alva, H.E.; García, J.C. Paulownia as raw material for solid biofuel and cellulose pulp. *Biomass Bioenergy* **2012**, *45*, 77–86. [CrossRef]
55. Loaiza, J.M.; López, F.; García, M.T.; Fernández, O.; Díaz, M.J.; García, J.C. Selecting the pre-hydrolysis conditions for eucalyptus wood in a fractional exploitation biorefining scheme. *J. Wood Chem. Technol.* **2016**, *36*, 211–223. [CrossRef]
56. López, F.; García, M.; Feria, M.; García, J.; de Diego, C.; Zamudio, M.; Díaz, M. Optimization of furfural production by acid hydrolysis of eucalyptus globulus in two stages. *Chem. Eng. J.* **2014**, *240*, 195–201. [CrossRef]
57. Pan, X.; Sano, Y. Fractionation of wheat straw by atmospheric acetic acid process. *Bioresour. Technol.* **2005**, *96*, 1256–1263. [CrossRef]
58. Fernández, M.; Alaejos, J.; Andivia, E.; Madejón, P.; Díaz, M.J.; Tapias, R. Short rotation coppice of leguminous tree Leucaena spp. improves soil fertility while producing high biomass yields in Mediterranean environment. *Ind. Crops Prod.* **2020**, *157*, 112911. [CrossRef]
59. Hu, M.; Chen, Z.; Wang, S.; Guo, D.; Ma, C.; Zhou, Y.; Chen, J.; Laghari, M.; Fazal, S.; Xiao, B.; et al. Thermogravimetric kinetics of lignocellulosic biomass slow pyrolysis using distributed activation energy model, Fraser-Suzuki deconvolution, and iso-conversional method. *Energy Convers. Manag.* **2016**, *118*, 1–11. [CrossRef]
60. Fernández, M.; Alaejos, J.; Andivia, E.; Vázquez-Piqué, J.; Ruiz, F.; López, F.; Tapias, R. Eucalyptus x urograndis biomass production for energy purposes exposed to a Mediterranean climate under different irrigation and fertilisation regimes. *Biomass Bioenergy* **2018**, *111*, 22–30. [CrossRef]
61. Chen, Z.; Zhu, Q.; Wang, X.; Xiao, B.; Liu, S. Pyrolysis behaviors and kinetic studies on Eucalyptus residues using thermogravimetric analysis. *Energy Convers. Manag.* **2015**, *105*, 251–259. [CrossRef]
62. Methrath Liyakathali, N.A.; Muley, P.D.; Aita, G.; Boldor, D. Effect of frequency and reaction time in focused ultrasonic pretreatment of energy cane bagasse for bioethanol production. *Bioresour. Technol.* **2016**, *200*, 262–271. [CrossRef] [PubMed]

Disclaimer/Publisher's Note: The statements, opinions and data contained in all publications are solely those of the individual author(s) and contributor(s) and not of MDPI and/or the editor(s). MDPI and/or the editor(s) disclaim responsibility for any injury to people or property resulting from any ideas, methods, instructions or products referred to in the content.

scientific reports

Check for updates

OPEN

Kinetic and hydrogen production analysis in the sequential valorization of a *Populus* clone by cold alkaline extraction and pyrolysis

S. Lozano-Calvo[1]✉, J. M. Loaiza[1], J. C. García[1], R. Tapias[2] & F. López[1]

This work employed a two-step biorefining process, consisting of a hemicellulose-rich liquor production through ultrasound-assisted cold alkaline extraction (CAE), followed by thermochemical treatment of the resultant solid phase. The post-CAE solid phase's pyrolytic potential was assessed by application of thermogravimetric analysis (TGA) and Friedman's isoconversional method, and also from hydrogen production. The solid phases remaining after the CAE treatment were more reactive than the untreated raw material. Notably, the alkali concentration employed in the first step was the individual variable most pronounced influence on their activation energy (E_a). Thus, at a degree of conversion α = 0.50, E_a ranged from 109.7 to 254.3 kJ/mol for the solid phases, compared to 177 kJ/mol for the raw material; this value decreased with rising glucan content. At maximal degradation, the post-CAE solid phases produced up to 15.57% v/v more hydrogen than did the untreated raw material.

Economic growth and expansive economies have led to an increasingly poorer environmental quality in many countries, especially as regards ecological systems, biodiversity and human health. Economic development is closely related to energy consumption[1] and, at present, 81% of all primary energy is obtained from fossil fuels, 5% from nuclear fission and only 14% from renewable sources[2]. As a result, atmospheric CO_2 levels continue to rise steadily. In fact, they have risen by 42% since 1950 and worsened the global problem posed by climate change[3]. In response to this pressing challenge, international institutions have adopted initiatives such as the Paris Agreement, by which countries such as United Kingdom, Spain, France and New Zealand have committed to be carbon–neutral by 2050, and others such as Sweden and Norway expect to meet this goal by 2045 and 2030, respectively[4]. Because societies can hardly be sustainable unless they use low-carbon fuels[5], growing concern with dramatic climate events and the exhaustion of fossil fuels has emerged over the last few decades that has boosted a search for renewable sources of energy on a global scale[6].

Biomass is a clean, sustainable choice for a smooth transition from oil-based to biorenewable energy[7,8]. Lignocellulosic biomass is especially effective as a renewable resource because it is widely available in vast amounts, and also because its chemical components are highly suitable and its production does not compete with that of food[8,9]. As a result, second-generation biofuels are being increasingly obtained from lignocellulosic biomass for the production of renewable energy[10].

Biorefining lignocellulosic materials allows biomass to be fractioned into its three main precursors (cellulose, hemicellulose and lignin) and the precursors to be processed in order to obtain products with a high added value[11]. One of the treatments used for this purpose is cold alkaline extraction, which is especially advantageous in operational and environmental terms. Also, however, it is subject to one major disadvantage: the optimum operating conditions depend on the particular type of biomass to be treated. Thus, CAE is usually much more efficient with grass than it is with wood[12] and the latter usually requires additional measures for efficient processing[13]. Also, CAE removes both hemicelluloses and polyphenols[14]. The potential applications of the hemicellulosic franction are extensive and have been explored by numerous researchers. For instance, sugar extracted from hemicellulose can subjected to biological conversion for biofuel production, such as ethanol; utilized in

[1]Research Centre for Technology of Products and Chemical Processes (PRO2TECS), Department of Chemical Engineering, University of Huelva, Av. 3 de Marzo S/N, 21071 Huelva, Spain. [2]Department of Forest Engineering, University of Huelva, Huelva, Spain. ✉email: susana.lozano@diq.uhu.es

chemical processes for the production of substances like xylitol or lactic acid; or chemical conversion produces furfural, 5-hydroxyfurfural, and levulinic acid, crucial precursors for synthesizing various organic derivatives[15]. In addition, the CAE decreases the lignin content of the material and leading to a reduced activation energy upon thermochemical treatment as a result of the polyphenol fraction consisting largely of benzene rings —which possess increased E_a values and thermal stability[16].

Thermochemical treatments of lignocellulosic biomass provide a promising technology for producing fuels with a high added value[17]. Highlighting pyrolysis as the most popular and versatile process[18] for the efficient production of bio-coal, bio-oil and pyrolytic gas (a mixture of carbon monoxide and dioxide, hydrogen, light hydrocarbons and small amounts of other compounds)[19]. Pyrolysing lignocellulosic biomass affects its three main components (cellulose, hemicellulose and lignin)[20] and involves a number of chemical reactions the span three steps, namely: (1) evaporation of moisture; (2) primary degradation of biomass (200–400 °C); and (3) side reactions[21]. A number of studies have examined the pyrolysis of various types of lignocellulosic biomass and their individual fractions with a view to better understanding their rate and extent of thermal degradation, the products formed and their proportions[22].

Pyrolysing biomass is also one way of obtaining hydrogen (H_2) from renewable resources[23]. Hydrogen is one of the major energy vectors for decarbonization strategies in Europe[24] and pyrolysis produces not only gaseous hydrogen, but also additional hydrogen formed in water–gas exchange reactions with carbon monoxide[25]. Hydrogen production is influenced by several variable, and it has been observed that as the pyrolysis temperature rises, the output of gaseous products increases while the formation of biochar and bio-oil decreases[26]. Thus, a temperature of 750 °C produces about 50% of hydrogen, whereas one of 500 °C gives only about 35%[25]. This is a result of the gas forming in very small amounts in primary reactions relative to tar cracking, reforming and coal decomposition at increased temperatures[27,28].

Hydrogen production also increases with increasing proportion of cellulose and hemicelluloses, but not lignin[29,30]. In fact, hydrogen forms largely from the cellulose fraction[31]. Ligneous biomass has been found to provide more hydrogen than agricultural residues[32]. Thus, Loaiza et al.[33] found extracting hemicelluloses from *Eucalytpus urograndis* by pyrolysis to provide solids whose pyrolysis led to a decreased activation energy and increased hydrogen production (6–8%) relative to the untreated, raw material.

The lignocellulosic biomass used in this work was obtained from clone AF2 of the genus *Populus* (viz., *Populus nigra x Populus deltoides*). *Populus* is a fast-growing plant that affords short, highly productive rotation[34]. Also, it is especially well adapted to Mediterranean areas with cold winters[35] and adequate soil moisture[36], so its productivity can be affected by climate change[34]. This has promoted the use of hybrid clones capable of growing under suboptimal conditions[37]. Some studies have shown clone AF2 of *Populus* to outperform others under conditions of limited water availability and long droughts[38].

The main aim of this work was to optimize exploitation of clone AF2 by using a two-step biorefining scheme involving ultrasound-assisted CAE and the subsequent pyrolysis of the resulting solid phase. The degree of conversion was assessed by thermogravimetric analysis (TGA) and non-isothermal kinetic parameters were determined by using Friedman's differential isoconversional method. Also, the kinetics of the pyrolytic process was modelled in terms of E_a in order to maximize hydrogen production, which was quantified as a function of the operating conditions of the ultrasound-assisted CAE treatment.

Materials and methods

Characterization of the raw material

The lignocellulosic biomass used was from clone AF2 of *Populus* and collected from plantations on La Rabida Campus (University of Huelva, Spain). The collected material was cold ground to obtain chips approximately 1–3 cm long and 0.5 cm wide.

The raw material was previously characterized by some members of our group in terms of moisture[39], solubility in 1% soda[40], solubility in hot water[41], ethanol–acetone extractives[42] and ash[43]. In addition, the material was subjected to acid hydrolysis in two steps involving treatment with 72% sulphuric acid at 30 °C for 1 h to cleave polysaccharides into oligomers and 4% sulphuric acid at 121 °C for 1 h to convert the oligomers into monomers. Monomeric sugars and Klason lignin were determined by HPLC according to[44] and[45], respectively. The results of the previous determinations are summarized in Table 1.

1% NaOH extractives	22.3 ± 1.95
Hot water extractives	4.22 ± 0.12
Ethanol–acetone extractives	2.8 ± 0.15
α-Cellulose (glucan)	40.3 ± 0.85
Klason lignin	25.1 ± 0.16
Xylan	19.3 ± 0.09
Arabinan	0
Acetyl groups	0.7 ± 0.02
Ash	1.14 ± 0.04

Table 1. Percent composition of the raw material.

Ultrasound-assisted cold alkaline extraction

A CAE treatment was used to maximize extraction of hemicelluloses into the liquor and ensure that they would remain stable for potential subsequent processing. The treatment was conducted in a Power Sonic Series 500 bath, using a water modulus (i.e., a liquid/solid ratio) of 15 kg water/ kg raw material on a dry basis, an ultrasound power of 120 W, an alkali concentration of 80–120 g/L, a temperature of 20–40 °C (temperature was kept constant by cooling the bath) and a treatment time of 30–90 min. The process was followed by filtration to separate the liquor from the remaining solid phase.

The CAE liquor was neutralized with 37% v/v hydrochloric acid, and the hemicellulose fraction precipitated with ethanol. The solid phase was neutralized with acetic acid, rinsed in water, centrifuged and dried at room temperature to determine moisture as described in Section "Characterization of the raw material" and calculate CAE yield by weighing. The solid was additionally hydrolysed in two steps as described in Section "Characterization of the raw material" in order to determine its composition.

The previous conditions were used in combination with a central composite factor design and response surface analysis[46] to optimize the CAE treatment by examining the influence of the independent variables of the process (viz., alkali concentration, temperature and treatment time) on the composition of the post-CAE solid phase (viz., glucan, xylan and Klason lignin), the activation energy of the solid and its pyrolytic hydrogen production capacity.

The factor design used allowed second-order polynomials to be established whose coefficients were a measure of the statistical significance of the influence of each independent variable on the dependent variables. For easier comparison, the independent variables were normalized by using the following equation:

$$X_n = 2 * \frac{X - \overline{X}}{(X_{max} - X_{min})/2} \tag{1}$$

where X, $\overline{X}$, X_{max} and X_{min} are the absolute, mean, maximum and minimum value, respectively, of the variable concerned. The design was applied at three different alkali concentrations (80, 100 and 120 g/L), temperatures (20, 30 and 40 °C) and treatment times (30, 60 and 90 min). It encompassed three groups of experimental points, namely: 2^n points for the factor design proper, $2n$ axial points and n_c central points. Therefore, the total number of experiments required, given by $2^n + 2n + n_c$, was 16.

Experimental data were modelled by fitting the results for the dependent variables to the following polynomial equation:

$$Y = a_0 + \sum_{i=1}^{n} b_i X_{ni} + \sum_{i=1}^{n} c_i X_{ni}^2 + \sum_{i=1,j=1}^{n} d_{ij} X_{ni} X_{nj} (i < j) \tag{2}$$

where X denotes independent variables and Y dependent variables, and the coefficients a_0, b_i, c_i and d_{ij} were estimated individually for each independent variable.

The independent terms selected were those having a statistically significant coefficient ($p < 0.05$). The conditions imposed on the overall statistics were $R^2 > 0.9$ and $F_{Snedecor} > 5$. All statistical processing was done with the software Statistica v. 10.0 from Statsoft, Inc. (Tulsa, OK, USA).

Thermogravimetric analyses

The raw material and the different post-CAE solid phases were subjected to non-isothermal thermogravimetric analysis (TGA) on a TGA/DSC1 STARe System from Mettler Toledo. In each test, an amount of ca. 13 g of sample was heated from 25 to 800 °C at four different rates (5, 10, 15 and 20 °C/min), using nitrogen at a flow-rate of 10 mL/min as inert gas. The experiments were performed in triplicate recorded the average values.

Friedman's analytical method

Friedman's method was used here to examine the kinetics of the pyrolysis reactions and determine their activation energy. The overall kinetics of the biomass pyrolysis process can be represented as follows:

$$\frac{d\alpha}{dt} = k(T) \cdot f(\alpha) \tag{3}$$

where α is the conversion fraction $[(W_0 - W_t)/(W_0 - W_\infty)]$, W denoting the mass of sample, and W_0, W_t and W_∞ its initial value, that at time t and that at the end of the process, respectively; $f(\alpha)$ the differential conversion function; T (K) temperature; and $k(T)$ the rate constant in the Arrhenius equation $[k(T) = A \cdot \exp(-E_a/RT)$, with A the pre-exponential factor, E_a the apparent activation energy and R the universal gas constant (8.314 J/mol·K)]. The reaction rate can be expressed as follows:

$$\frac{d\alpha}{dT} = \left(\frac{A}{\delta}\right) \cdot \exp\left(-\frac{Ea}{R \cdot T}\right) \cdot f(\alpha) \tag{4}$$

where δ is the linear heating rate ($\delta = dT/dt$), which is constant.

For convenience, Eq. (4) can be expressed in integral form:

$$\int_0^\alpha \frac{d\alpha}{f(\alpha)} = G(\alpha) = \left(\frac{A}{\beta}\right) \cdot \int_{T_0}^{T} \exp\left(-\frac{E_a}{R \cdot T}\right) dT = \left(\frac{A}{\beta}\right) \cdot p(x) \tag{5}$$

where $G(\alpha)$ and $p(x)$ are the integrals of the conversion function and temperature, respectively. The latter function cannot be solved exactly, so it has to be estimated or integrated numerically[47].

Some empirical methods allow the kinetic parameters to be calculated from the data for the thermal analysis. Such methods are of either the isoconversional or the fitting type. In this work, we used an isoconversional method to calculate the kinetic parameters for no specific form of the reaction model to enable the accurate determination of the activation energy[48,49]. The most widely used isoconversional method is Friedman's differential method[50]. In natural logarithmic form, Eq. (4) becomes:

$$\ln\left(\beta \cdot \frac{d\alpha}{dT}\right) = \ln\left[A \cdot f(\alpha)\right] - \frac{E_a}{R \cdot T} \tag{6}$$

Friedman's method assumes the extent of biomass decomposition to depend solely on the mass loss rate. Therefore, a plot of ln (dα/dt) against 1/T allows he activation energy to be calculated from the slope ($-E_a$/R) and conversion from the intercept [ln [A·f(α)].

Modeling and optimization of activation energy

The modeling and optimization of the E_a results, as a function of the independent operating variables of the CAE process with ultrasounds, has been conducted following the methodology outlined in section "Thermogravimetric analysis (TGA) of the pyrolytic process".

The experimental design points for the central composite design are consistent with those utilized for modeling and optimizing the composition of the solid phase.

The same procedures, including response surface analysis, normalization of independent variables, analysis of coefficients, statistical assessment of model validity and/or uncertainty, and the selection of statistically significant coefficients, have been applied. It is noteworthy that the results of the dependent variable (E_a) were obtained in accordance with the description provided in sections "Thermogravimetric analyses" and "Friedman's analytical method".

Quantifying hydrogen production in a pyrolytic reactor

The amount of hydrogen resulting from pyrolysis of the lignocellulosic biomass and the CAE solid phases was evaluated using a laboratory-scale reactor. The reactor consisted of a 140 cm length and 10 mm wide quartz tube, within which approximately 2 g of the sample was uniformly introduced and placed in a furnace at a constant temperature for 4 min, using nitrogen at a flow-rate of 150 mL/min as carrier gas. The operating variables of this laboratory-scale reactor are the furnace temperature, the residence time of the sample in the furnace, and the flow-rate of carrier gas. While it is at a laboratory scale, we believe the results would be scalable. The reactor design is an original design from the research group, and efforts have been made to operate it in a manner resembling that of a semi-pilot reactor.

Hydrogen production was measured by collecting samples in Tedlar bags at the reactor outlet. Samples were collected at the highest degradation temperature in each test for 1 min. Four different samples were taken in each experiment to determine the maximum H_2, which was produced between minutes 2 and 3. These samples were analyzed using a precalibrated MultiRAE IR PGM-54 gas analyser from RAE Systems (San José, CA, USA). All measurements were made in triplicate and averaged to calculate the volume of pyrolytic gas of the analyzed sample and disregarding the carrier gas.

Ethics approval and consent to participate

The authors declare that this is their original work, and the corresponding manuscript has not been published before and is only submitted to the Journal of Scientific Reports.

Results

Ultrasound-assisted cold alkaline extraction of hemicellulose

Previous studies by our group[51] revealed that using ultrasound in the CAE of clone AF2 of *Populus* resulted in increased extraction of all lignocellulosic fractions but especially those of hemicelluloses and polyphenols. Specifically, extraction of hemicelluloses, measured as xylan, from the raw material into the CAE liquor ranged from 39.8 to 56.7% in the absence of ultrasound and from 44.3 to 60.8% in its presence. Also, the hemicellulose content of the post-CAE solid phase decreased from 60.2–43.3% to 55.7–39.2% of the content in the starting material. On the other hand, the lignin content of the solid increased from 51.5 to 77.7% with sonication to 71.6–98.9% without it. Finally, cellulose was scarcely extracted into the CAE liquor and remained in the solid phase by 80.4–96.2% with ultrasound and by 85.1–98.7% without it.

These results allowed polynomial models relating the dependent variables (glucan, xylan and Klason lignin in the post-CAE solid phase) to the independent variables (alkali concentration, temperature and treatment time) to be developed. Table 2 shows the equations for the models, which were used to predict the effect of each independent variable of the ultrasound-assisted CAE process on the cellulose, hemicellulose and polyphenol contents of the resulting solid phase. Such contents (specifically, those of glucan, xylan and Klason lignin) are referred to their initial levels in the starting, raw material.

As can be seen from Eq. (8) in Table 2, the alkali concentration was the most influential variable on the glucan content of the post-CAE solid phase. Cellulose extraction into the liquor was maximal at the greatest alkali concentration, temperature and time values studied. As noted earlier, however, glucan was scarcely extracted into the liquor (20.22% at most).

Equation	Adjusted R^2	Adjusted Snedecor's F
$GL = 87.0 - 2.50X_A - 1.87X_T + 5.98X_A^2 - 4.03X_T^2 - 4.39X_AX_t - 1.60X_AX_T + 1.19X_tX_T$ (8)	0.98	59
$X = 40.2 - 2.28X_A - 2.24X_t - 1.12X_T + 7.23X_A^2 + 1.62X_T^2 - 0.56X_AX_t + 1.37X_AX_T + 0.44X_tX_T$ (9)	0.89	138
$KL = 66.6 - 5.96X_t - 2.57X_T - 5.33X_A^2 + 4.58X_T^2 + 1.04X_AX_t + 3.28X_AX_T - 2.34X_tX_T$ (10)	0.98	114

Table 2. Equations of the polynomial models for the dependent variables in the ultrasound-assisted CAE treatment. Dependent variables: GL glucan (%), X xylan (%), KL Klason lignin (%). Independent variables: X_A alkali concentration, X_T temperature, X_t treatment time. The differences between the experimental values and those estimated with the equations never exceeded 10% of the former.

Based on Eq. (9) in Table 2, medium alkali concentrations and temperatures in combination with long treatment times should result in maximal hemicellulose extraction into the CAE liquor. Finally, Eq. (10) suggests that long CAE treatment times should result in increased delignification (i.e., in increased proportions of lignin in the CAE liquor). This prediction is consistent with the results of Methrath Liyakathali et al.[52], who found the treatment time and sonication to influence the cleavage of lignin–cellulose bonds to an extent increasing with the former variable. Accordingly, lignin extraction into the CAE liquor was especially high in the upper range of treatment times (90 min).

The post-CAE solid phase was rich in cellulose, but poor in lignin by effect of the polyphenol fraction being largely extracted into the liquor. In theory, this must decrease the pyrolysis activation energy since the polyphenol fraction is that with the highest E_a value[16]. Also, it should result in increased hydrogen production relative to the starting material[53]. These two expectations warranted the present work, where we examined the pyrolytic process as described below.

Thermogravimetric analysis (TGA) of the pyrolytic process

The CAE treatment provided a highly valorizable liquor by effect of the extraction process being especially selective for hemicelluloses. Also, the treatment provided a solid phase enriched with a cellulose fraction potentially useful for purposes such as producing energy, hydrogen, biofuels, pulp, paper or polyphenol derivatives. In this work, we examined the potential of the process for obtaining energy and a high added value product: hydrogen. Removing most of the hemicellulose fraction and part of the polyphenol fraction decreased the activation energy of the pyrolysis process[16,33], thereby presumably facilitating it. It should be noted that, as shown for treatments other than CAE, the operating conditions —or rather, their combination—influence the activation energy and kinetics of the thermal treatment[54].

Because using all 16 points of the experimental design would have been impractical, we selected those corresponding to the lowest and highest extraction of hemicelluloses (viz., 80 g/L, 90 min, 20 °C and 100 g/L, 60 min, 30 °C, respectively) and the lowest and highest extraction of Klason lignin (viz., 80 g/L, 30 min, 20 °C and 80 g/L, 90 min, 40 °C, respectively) in addition to the raw material.

Figure 1 is a weight loss versus temperature plot. As can be seen, the initial temperature of the second step of process, known as "active pyrolysis", was higher for the raw material (224 °C) than it was with the lowest and highest extraction of hemicelluloses (172 and 180 °C, respectively) and lignin (177 and 172 °C, respectively). The decreased temperatures for the post-CAE solid phases relative to the raw material can be ascribed to selective extraction of hemicelluloses and polyphenols into the CAE liquor. Also, residual lignin in the resulting solid contained fewer bonds and was thus less thermally stable. The affinity of alkaline treatments for soluble lignin and the cleavage of C–C bonds in polyphenols remaining in the solid fraction was previously observed by other authors[54]. The cleavage of bonds in the lignin fraction decreases its strength and degree of polymerization, thus facilitating hydrolysis of polysaccharides[55].

Heating the post-CAE solid phase with the highest content in hemicelluloses at 5 °C/min led to an extended loss of fixed carbon that was not considered in calculating the activation energy. Nor was the result for the residue heated at 15 °C/min leading to the lowest extraction of lignin.

Derivative thermogravimetry (DTG)

Figure 2 shows the rate of weight loss (%/min) as a function of temperature (i.e., the DTG curves) for the raw material and the four post-CAE solid phases examined in the previous section. As can be seen, there were three distinct regions typical of biomass pyrolysis corresponding to water evaporation, active pyrolysis ad side reactions[21]. The main pyrolysis step spanned the range 200–400 °C and two sub-steps involving degradation of the cellulose and hemicellulose fractions. Whereas the raw material exhibited two well-defined peaks, the post-CAE solid phases showed a poorly defined peak for hemicellulose degradation. This was a result of structural and compositional differences between the samples directly influencing hemicellulose and cellulose degradation[56].

Thermal degradation in the active pyrolysis step started at 230 °C in the raw material and at around 190 °C in the post-CAE solid phases, possibly as a result of increased extraction of hemicelluloses and lignin from the latter. Thus, the CAE treatment caused a portion of the polyphenolic fraction to be extracted into the liquor and

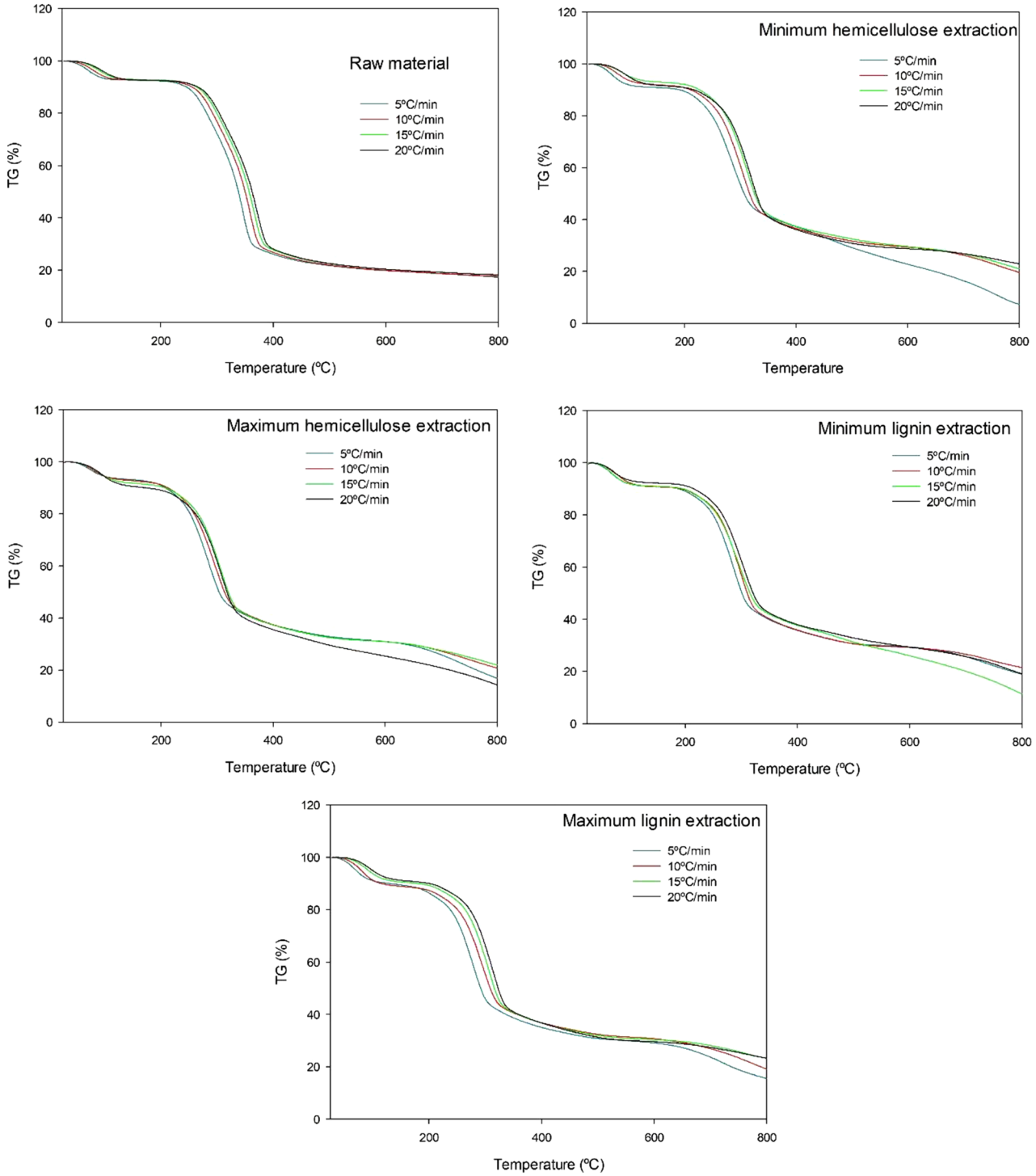


Figure 1. TGA at different heating rates of the raw material and the four post-CAE solid phases.

the rest, which remained in the solid, to break more easily as a consequence of its having a decreased number of C–C bonds —and being less thermally stable as a result[57].

As can also be seen from Fig. 2, the maximum loss temperature (T_{max}) was 372 °C for the raw material and lower (302–320 °C) for the post-CAE solid phases. T_{max} is known to be inversely related to reactivity[58]. Again, the post-CAE solid phases were less thermally stable than the raw material. Also, T_{max} coincided with the main peak in the DTG curves, which was primarily associated with cellulose degradation[55].

The maximum reaction rate at a heating rate of 20 °C/min was 22.59%/min for the raw material (40.3 wt% glucan), about 19.50%/min for the post-CAE solid phases resulting from the lowest extraction of hemicelluloses and highest extraction of lignin (38.3 and 39.0 wt% glucan, respectively), and in the region of 16.3%/min for those with the highest extraction of hemicelluloses and lowest extraction of lignin (35.0 and 35.7 wt% glucan,

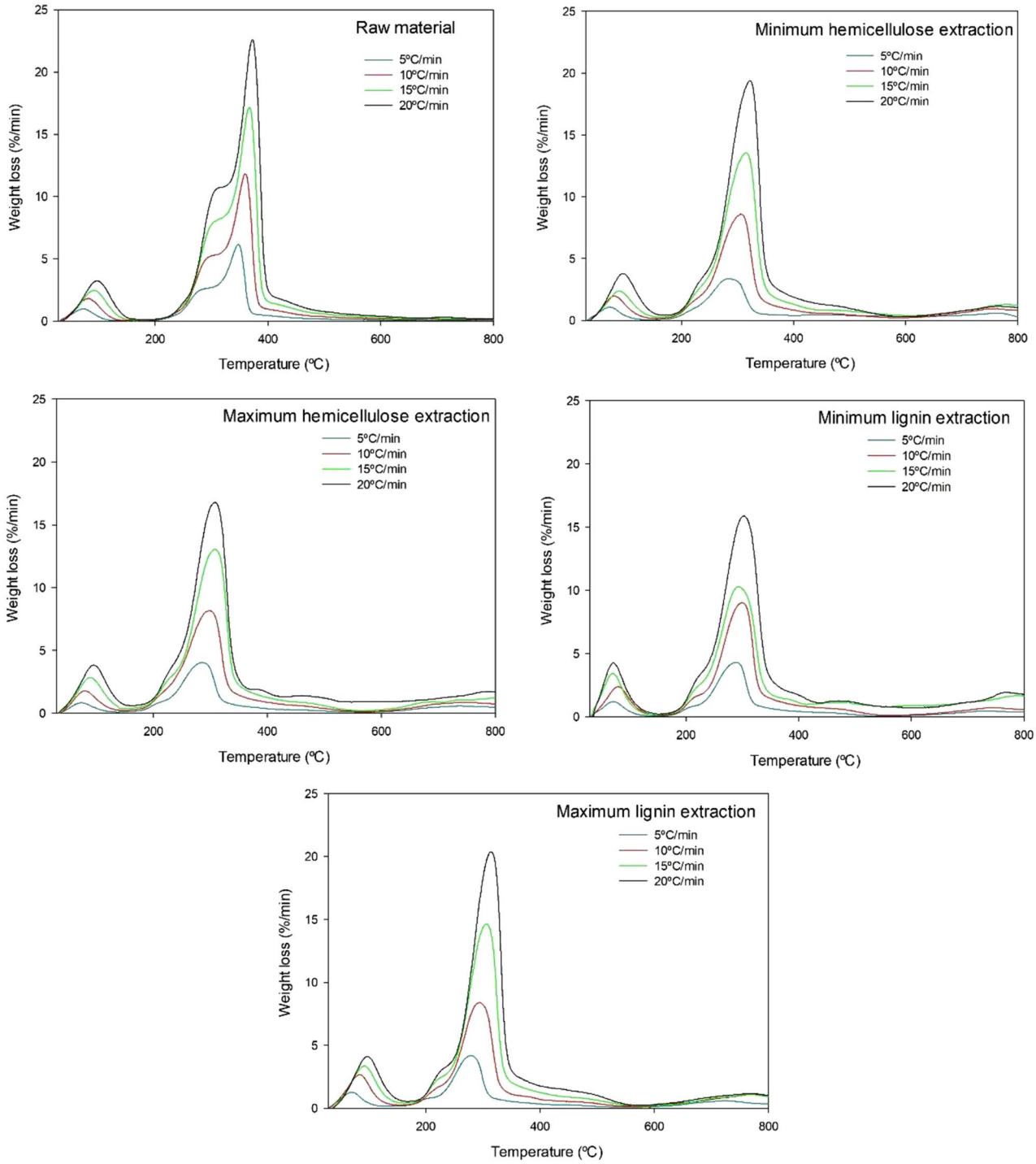


Figure 2. DTG of the raw material and the four post-CAE solid phases.

respectively). Therefore, it can be observed that the maximum reaction rate increases alongside the glucan content. It can be asserted that the primary degradation, which occurs in this peak of the DTG curves, largely corresponds to the degradation of the cellulose fraction.

Kinetic analysis of the pyrolytic process

The pyrolysis kinetics of the raw material and the post-CAE solid phases allowed the influence of the independent variables of the treatment on the thermochemistry of the process to be established. The activation energy E_a at a given degree of conversion α was calculated by applying Friedman's isoconversional method to the results obtained at the heating rates 5, 10, 15 and 20 °C/min. Table 3 shows the E_a values thus obtained as the average of at least three determinations each. The relative standard deviation was less than 5% in all instances.

Operating conditions (X_A, X_t, X_T)			E_a (kJ/mol)		
			α = 0.25	α = 0.50	α = 0.75
0	0	0	145.7	179.5	285.9
1	1	1	215.4	227.1	139.1
1	1	−1	152.9	195.3	135.1
1	−1	1	127.6	158.8	195.4
1	−1	−1	131.9	164.4	265.4
−1	1	1	177.6	153.6	253.3
−1	1	−1	165.8	211.9	262.7
−1	−1	1	154.8	190.5	167.3
−1	−1	−1	186.8	262.2	255.4
1	0	0	141.1	170.9	282.9
−1	0	0	174.5	209.6	312.8
0	1	0	133.8	166.1	198.3
0	−1	0	108.2	145.1	222.9
0	0	1	156.5	183.2	212.3
0	0	−1	152.9	185.8	290.3

Table 3. Activation energy as calculated with Friedman's isoconversional method at different degrees of conversion for the post-CAE solid phases. Independent variables: X_A alkali concentration, X_T temperature, X_t treatment time.

E_a for the raw material was 168, 177 and 179 kJ/mol at a degree of conversion of 0.25, 0.50 and 0.75, respectively. As can be seen, the activation energy changed with α, both in the raw material and in the post-CAE solid phases. This was a result of the pyrolysis of such highly complex materials as lignocellulosic biomass being an intricate process involving a number of steps. Some authors have reported an average E_a value for the whole conversion range whereas others believe that the effective activation energy of lignocellulosic biomass depends on those of decomposition of each fraction[59–61].

The data in Table 3 were subjected to multiple regression analysis on E_a as a function of the three independent variables (alkali concentration, temperature, and treatment time) at the different degrees of conversion considered. The equations for the models thus established are shown in Table 4. The coefficients of variation between the predicted and experimental results were all less than 10% and the quadratic regression coefficients, R^2, greater than 0.95. Student's-t values for the individual variables were all greater than 2, so the results were statistically significant at $p < 0.05$.

Figures 3, 4, 5 show the response surfaces for the models, which were used to identify the ranges of the independent variables leading to the lowest activation energy for the post-CAE solid phases relative to the raw material. Surfaces were plotted at two different levels of alkali concentration, which was the individual independent variable most strongly influencing E_a. For easier viewing and understanding, the activation energy for the initial, untreated biomass was plotted on a fixed plane so it would not change along the axes representing the CAE operating conditions.

Figure 3, which corresponds to Eq. (11), shows the variation of E_a for the post-CAE solid phases as a function of temperature and time at the highest and lowest alkali concentration studied. As can be seen, E_a was independent of both variables throughout their operation ranges. Also, at α = 0.25 it was lower for the post-CAE solid phases than it was for the raw material. Thus, E_a spanned the range 108.4–205.1 kJ/mol, which is similar to those for hemicelluloses reported by other authors. Some overall kinetic methods for hemicellulose pyrolysis have provided E_a values from 100 to 220 kJ/mol[62].

Equation	α
$E_a = 137.91 - 9.18X_A + 13.73X_t + 21.81X_A^2 - 14.95X_t^2 + 18.74X_T^2 + 13.50X_AX_t + 12.04X_AX_T + 11.57X_tX_T$ (11)	0.25
$E_a = 173.91 - 16.18X_A + 8.3X_t + 18.68X_A^2 - 16.01X_t^2 + 12.92X_T^2 + 29.62X_AX_t + 25.57X_AX_T$ (12)	0.50
$E_a = 276.27 - 18.69X_A - 16.48X_t - 28.84X_T + 23.98X_A^2 - 63.23X_t^2 - 22.54X_T^2 - 40.84X_AX_t + 23.22X_tX_T$ (13)	0.75

Table 4. Equations of the polynomial models for the activation energy. Independent variables: X_A alkali concentration, X_T temperature, X_t treatment time.

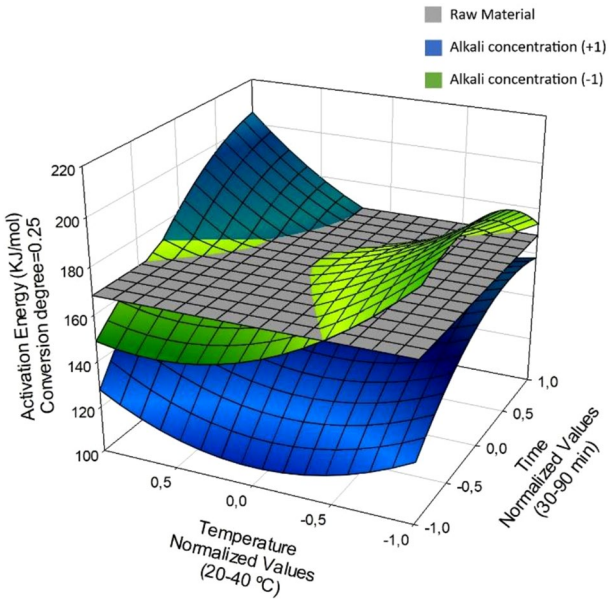


Figure 3. Activation energy contrast in post-CAE solid phases and raw material at α = 0.25, varying conditions.

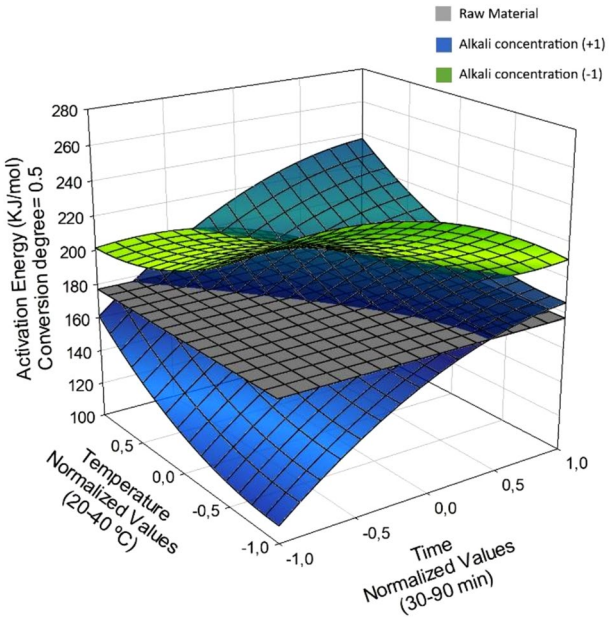


Figure 4. Activation energy constrast in post-CAE solid phases and raw material at α = 0.50, varying conditions.

It should be noted that E_a was lowest for the post-CAE solid phases resulting from treatments at high alkali concentrations and short times, the temperature having little effect on the results.

Figure 4 shows the variation of E_a with the treatment temperature and time at the highest and lowest alkali concentration —the most influential variable— at α = 0.5. As can be seen, E_a ranged from 109.7 to 254.3 226 kJ/mol and was largely due to degradation of the cellulose fraction. The average activation energy for cellulose is 189.2 kJ/mol[63].

As can be seen from Fig. 5, a combination of the highest alkali concentration, lowest temperature and shortest treatment time led to the lowest E_a values relative to the raw material. On the other hand, E_a remained fairly constant at the lowest alkali level. There was strong correlation between the activation energy and the amount of glucan remaining in the post-CAE solid phase. In fact, as can be seen in Fig. 5, constructed at the highest alkali concentration, E_a decreased with increasing proportion of glucan in the solid as a result of the cellulose fraction having a lower activation energy than the polyphenolic fraction.

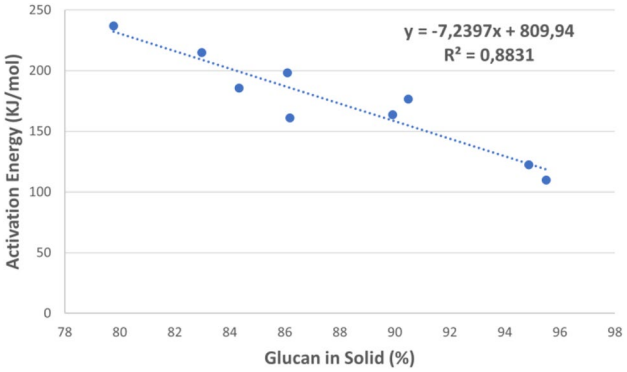


Figure 5. Activation energy change with post-CAE solid phases' glucan content at α = 0.5.

As can be seen in Fig. 6, at α = 0.75 the activation energy for the post-CAE solid phases was higher than it was for the raw material under virtually any operating conditions and ranged from 132.9 to 328.5 kJ/mol. Cai et al.[60] reported E_a values of 237.1–266.6 kJ/mol for lignin, whereas Murugan et al.[64] found the isothermal activation energy for the polyphenolic fraction to be 284 kJ/mol.

Hydrogen production

The thermogravimetric and kinetic study of the pyrolytic process was followed by assessment of the hydrogen production potential of the post-CAE solid phases on the laboratory-scale reactor described in Section "Modeling and optimization of activation energy".

The TGA curves previously obtained were used to identify the best temperature for hydrogen production. Table 5 shows the selected temperature and the maximum quantity of hydrogen generated for each post-CAE solid phase.

The data in Table 5 underwent multiple regression analysis as a function of the three independent variables (alkali concentration, temperature and treatment time). Similar to E_a, the proportions, in volume, of maximum hydrogen obtained with each post-CAE solid phase were considered. The resulting equation was: $H_2 = 11.85 + 2.32X_A - 1.83X_T + 2.94X_A^2 - 2.24X_T^2 - 1.65X_AX_T - 1.26X_tX_T$ with a quadratic regression coefficient of 0.98 and a coefficient of variation less than 10%. All independent variables had Student's *t*-values greater than 2, so they were deemed statistically significant.

Figure 7 shows the response surface for hydrogen production. As can be seen, the post-CAE solid phases, but particularly those obtained at the highest alkali concentration, produced greater amounts of hydrogen than did the raw material. On the other hand, as was apparent from Eq. (14), hydrogen production was scarcely affected

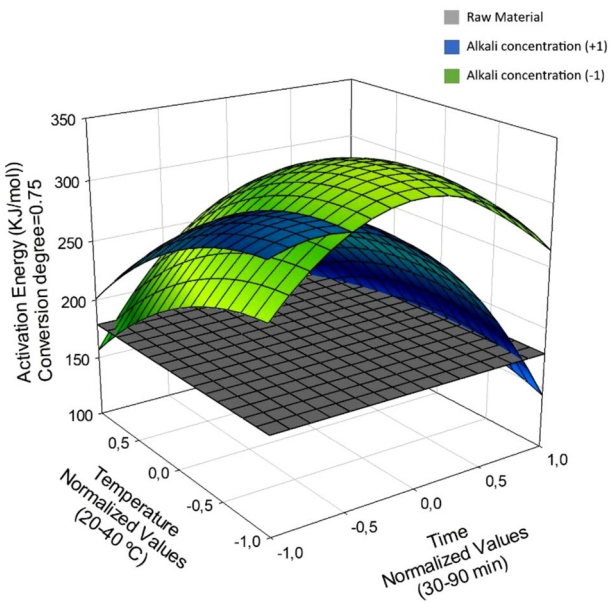


Figure 6. Activation energy contrast in post-CAE solid phases and raw material at α = 0.75, varying conditions.

Operating conditions (X_A, X_t, X_T)			Temperature (°C)	Hydrogen (vol. %)
0	0	0	309	13.26
1	1	1	305	6.44
1	1	−1	309	19.07
1	−1	1	313	13.69
1	−1	−1	310	12.76
−1	1	1	315	10.98
−1	1	−1	323	8.31
−1	−1	1	315	7.90
−1	−1	−1	303	6.63
1	0	0	315	8.65
−1	0	0	323	12.94
0	1	0	317	8.84
0	−1	0	315	10.17
0	0	1	318	8.86
0	0	−1	316	11.33
Raw material			372	4.04

Table 5. Hydrogen production from the post-CAE solid phases. Independent variables: X_A alkali concentration, X_T temperature, X_t treatment time.

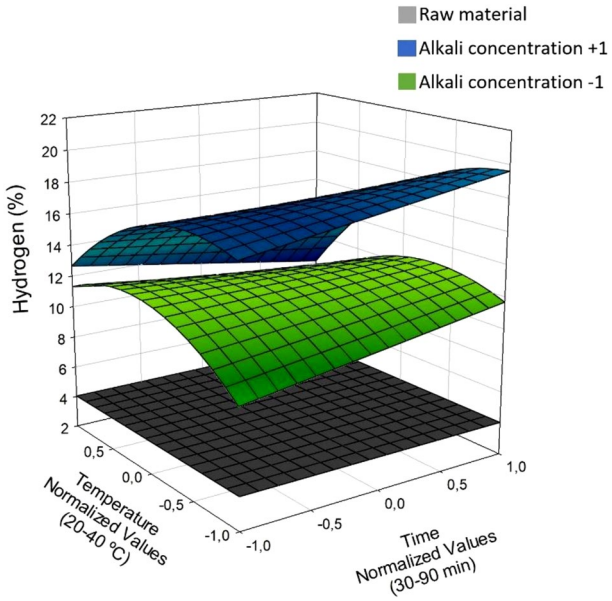


Figure 7. Hydrogen production variation in post-CAE solid phases and raw material at α = 0.50, diverse conditions.

by the treatment time. Finally, the effect of temperature was found to depend on the alkali concentration; thus, at the highest alkali levels, hydrogen production peaked with medium or high temperatures.

The maximum proportion of hydrogen obtained, in volume, from the post-CAE solid phases ranged from 9.15 to 19.51%, so it was up to 15.57% greater than that provided by the raw material. These results are consistent with previously reported values for species such as *Eucalyptus urograndis*, where authohydrolysis provided amounts of hydrogen up to 8% greater than the raw material[33]. Similary, the application of acid hydrolysis to *Leucaena leucocephala* resulted in increased hydrogen production[53]. In general, slow pyrolysis, like the process studied in this work, exhibits a range of hydrogen yields between 9 and 44%[65].

Conclusions

As shown here, ultrasound-assisted cold alkaline extraction provides liquors with increased proportions of hemicelluloses and lignin relative to the absence of ultrasound.

The composition of the raw material and the post-CAE solid phases affect their thermal degradation. In addition, the post-CAE solid phases were more reactive in the thermochemical process than was clone AF2 clone of *Populus*.

The activation energy of the post-CAE solid phases is generally lower than that of the raw material, with alkali concentration proving to be the most influential independent variable in this regard. In turn, E_a decreased with increasing proportion of glucan in the residues.

The ultrasound-assisted CAE process enhances hydrogen production, making this sequential process with CAE and pyrolysis approach a favorable choice for this feedstock valorization.

Data availability

All data generated or analyzed during this work are included in this published article.

Received: 20 October 2023; Accepted: 12 January 2024
Published online: 17 January 2024

References

1. Jiang, Z. *et al.* Non linear effect of Biomass, fossil fuels and renewable energy usage on the economic Growth: Managing sustainable development through energy sector. *Fuel* **326**, 124943 (2022).
2. Popp, J., Kovács, S., Oláh, J., Divéki, Z. & Balázs, E. Bioeconomy: Biomass and biomass-based energy supply and demand. *N. Biotechnol.* **60**, 76–84 (2021).
3. Schimel, D., Stephens, B. B. & Fisher, J. B. Effect of increasing CO_2 on the terrestrial carbon cycle. *Proc. Nat. Acad. Sci.* **112**, 436–441. https://doi.org/10.1073/pnas.1407302112 (2015).
4. Welfle, A., Thornley, P. & Röder, M. A review of the role of bioenergy modelling in renewable energy research & policy development. *Biomass Bioenergy.* **136**, 105542 (2020).
5. Nie, A. *et al.* An environmental and economic assessment from bioenergy production and biochar application. *J. Saudi Chem. Soc.* **25**, 101173 (2021).
6. Yousaf, I., Nekhili, R. & Umar, M. Extreme connectedness between renewable energy tokens and fossil fuel markets. *Energy Econ.* **114**, 106305 (2022).
7. Bender, T. A., Dabrowski, J. A. & Gagné, M. R. Homogeneous catalysis for the production of low-volume, high-value chemicals from biomass. *Nat. Rev. Chem.* **2**, 35–46 (2018).
8. Roy, S. *et al.* Recent nanobiotechnological advancements in lignocellulosic biomass valorization: A review. *J. Environ. Manage.* **297**, 113422 (2021).
9. Saravanan, A., Senthil Kumar, P., Jeevanantham, S., Karishma, S. & Vo, D. V. N. Recent advances and sustainable development of biofuels production from lignocellulosic biomass. *Bioresour. Technol.* **344**, 126203 (2022).
10. Abraham, A. *et al.* Pretreatment strategies for enhanced biogas production from lignocellulosic biomass. *Bioresour. Technol.* **301**, 122725 (2020).
11. FitzPatrick, M., Champagne, P., Cunningham, M. F. & Whitney, R. A. A biorefinery processing perspective: Treatment of lignocellulosic materials for the production of value-added products. *Bioresour. Technol.* **101**, 8915–8922 (2010).
12. García, J. C. *et al.* Search for optimum conditions of wheat straw hemicelluloses cold alkaline extraction process. *Biochem. Eng. J.* **71**, 127–133 (2013).
13. Yuan, Z. *et al.* Process intensification effect of ball milling on the hydrothermal pretreatment for corn straw enzymolysis. *Energy Convers. Manag.* **101**, 481–488 (2015).
14. de Carvalho, D. M., de Queiroz, J. H. & Colodette, J. L. Assessment of alkaline pretreatment for the production of bioethanol from eucalyptus, sugarcane bagasse and sugarcane straw. *Ind. Crops Prod.* **94**, 932–941. https://doi.org/10.1016/j.indcrop.2016.09.069 (2016).
15. Abejón, R. A bibliometric study of scientific publications regarding hemicellulose valorization during the 2000–2016 period: Identification of alternatives and hot topics. *ChemEngineering* **2**, 7 (2018).
16. Chen, Z., Zhu, Q., Wang, X., Xiao, B. & Liu, S. Pyrolysis behaviors and kinetic studies on Eucalyptus residues using thermogravimetric analysis. *Energy Convers. Manag.* **105**, 251–259. https://doi.org/10.1016/j.enconman.2015.07.077 (2015).
17. Bridgwater, A. V. Renewable fuels and chemicals by thermal processing of biomass. *Chem. Eng. J.* **91**, 87–102 (2003).
18. Zhang, L., Chen, K., He, L. & Peng, L. Reinforcement of the bio-gas conversion from pyrolysis of wheat straw by hot caustic pre-extraction. *Biotechnol. Biofuels.* **11**, 72. https://doi.org/10.1186/s13068-018-1072-5 (2018).
19. Kan, T., Strezov, V. & Evans, T. J. Lignocellulosic biomass pyrolysis: A review of product properties and effects of pyrolysis parameters. *Renew. Sustain. Energy Rev.* **57**, 1126–1140 (2016).
20. Yang, H., Yan, R., Chen, H., Lee, D. H. & Zheng, C. Characteristics of hemicellulose, cellulose and lignin pyrolysis. *Fuel* **86**, 1781–1788 (2007).
21. Yogalakshmi, K. N. *et al.* Lignocellulosic biomass-based pyrolysis: A comprehensive review. *Chemosphere* **286**, 131824. https://doi.org/10.1016/j.chemosphere.2021.131824 (2022).
22. Ni, M., Leung, D. Y. C., Leung, M. K. H. & Sumathy, K. An overview of hydrogen production from biomass. *Fuel Process. Technol.* **87**, 461–472 (2006).
23. Buffi, M., Prussi, M. & Scarlat, N. Energy and environmental assessment of hydrogen from biomass sources: Challenges and perspectives. *Biomass Bioenergy* **165**, 106556 (2022).
24. Commission European. Communication from the Commission to the European Parliament, the Council, the European Economic and Social Committee and the Committee of the Regions Youth Opportunities Initiative. 2011;
25. Nasir Uddin, M., Daud, W. M. A. W. & Abbas, H. F. Potential hydrogen and non-condensable gases production from biomass pyrolysis: Insights into the process variables. *Renew. Sustain. Energy Rev.* **27**, 204–224 (2013).
26. Demirbaş, A. Gaseous products from biomass by pyrolysis and gasification: Effects of catalyst on hydrogen yield. *Energy Convers. Manag.* **43**, 897–909 (2002).
27. Widyawati, M., Church, T. L., Florin, N. H. & Harris, A. T. Hydrogen synthesis from biomass pyrolysis with in situ carbon dioxide capture using calcium oxide. *Int. J. Hydrogen Energy* **36**, 4800–4813 (2011).
28. Sanchez-Silva, L., López-González, D., Villaseñor, J., Sánchez, P. & Valverde, J. L. Thermogravimetric–mass spectrometric analysis of lignocellulosic and marine biomass pyrolysis. *Bioresour. Technol.* **109**, 163–172 (2012).
29. Kumar, J. V. & Pratt, B. C. Compositional analysis of some renewable biofuels. *Am. Lab. (Fairfield)* **28**, 15–20 (1996).
30. Li, S., Xu, S., Liu, S., Yang, C. & Lu, Q. Fast pyrolysis of biomass in free-fall reactor for hydrogen-rich gas. *Fuel Process. Technol.* **85**, 1201–1211 (2004).
31. Wu, C., Wang, Z., Huang, J. & Williams, P. T. Pyrolysis/gasification of cellulose, hemicellulose and lignin for hydrogen production in the presence of various nickel-based catalysts. *Fuel* **106**, 697–706 (2013).

32. Jarungthammachote S, Acharya B, Dutta A. Parametric Effect of Agricultural Residues and Woody Biomass on Hydrogen Production through Gasification Process. Proceedings of the international agricultural engineering conference Cutting edge technologies and innovations on sustainable resources for world food sufficiency: Asian Association for Agricultural Engineering. Citeseer; 2007.
33. Loaiza, J. M. *et al.* Effect of autohydrolysis on hemicellulose extraction and pyrolytic hydrogen production from Eucalyptus urograndis. *Biomass Convers. Biorefin.* **12**, 4021–4030. https://doi.org/10.1007/s13399-020-00900-0 (2022).
34. González-González, B. D., Oliveira, N., González, I., Cañellas, I. & Sixto, H. Poplar biomass production in short rotation under irrigation: A case study in the Mediterranean. *Biomass Bioenergy* **107**, 198–206 (2017).
35. Sixto, H. *et al.* Growth potential of different species and genotypes for biomass production in short rotation in Mediterranean environments. *For. Ecol. Manage.* **354**, 291–299 (2015).
36. Bloemen, J. *et al.* Water use of a multigenotype poplar short-rotation coppice from tree to stand scale. *GCB Bioenergy* **9**, 370–384. https://doi.org/10.1111/gcbb.12345 (2017).
37. Navarro, A., Facciotto, G., Campi, P. & Mastrorilli, M. Physiological adaptations of five poplar genotypes grown under SRC in the semi-arid mediterranean environment. *Trees – Struct. Funct.* **28**, 983–994. https://doi.org/10.1007/s00468-014-1012-3 (2014).
38. di Matteo, G., Nardi, P., Verani, S. & Sperandio, G. Physiological adaptability of Poplar clones selected for bioenergy purposes under non-irrigated and suboptimal site conditions: A case study in Central Italy. *Biomass Bioenergy* **81**, 183–189 (2015).
39. TAPPI T264 cm-07. *Preparation of Wood for Chemical Analysis* (TAPPI Press, 2007).
40. TAPPI T212 om-22. One percent sodium hydroxide solubility of wood and pulp (Test Method).
41. TAPPI T257 cm-85. *Sampling and Preparing Wood for Analysis* (TAPPI Press, 1999).
42. TAPPI T204 cm-07. *Sampling and Preparing Wood for Analysis* (TAPPI Press, 2007).
43. TAPPI 211 om-02. *Ash in Wood, Pulp, Paper and Paperboard: Combustion at 525°C.* (TAPPI Press, 2002).
44. TAPPI T249 cm-09. *Carbohydrate Composition of Extractive-Free Wood and Wood Pulp by Gas-Liquid Chromatography* (TAPPI Press, 2009).
45. TAPPI T222 om-11. *Acid-Insoluble Lignin in Wood and Pulp* (TAPPI Press, 2011).
46. Montgomery, D. C. *Diseño y Análisis de Experimentos* (Limusa Wiley, 2003).
47. Vyazovkin, S. & Sbirrazzuoli, N. Isoconversional kinetic analysis of thermally stimulated processes in polymers. *Macromol. Rapid. Commun.* **27**, 1515–1532. https://doi.org/10.1002/marc.200600404 (2006).
48. Starink, M. J. The determination of activation energy from linear heating rate experiments: A comparison of the accuracy of isoconversion methods. *Thermochim Acta.* **404**, 163–176 (2003).
49. Martín-Lara, M. A., Ronda, A., Blázquez, G., Pérez, A. & Calero, M. Pyrolysis kinetics of the lead-impregnated olive stone by non-isothermal thermogravimetry. *Process Safety Environ. Protect.* **113**, 448–458 (2018).
50. Friedman, H. L. Kinetics of thermal degradation of char-forming plastics from thermogravimetry. Application to a phenolic plastic. *J. Polym. Sci. Part C: Polym. Symposia* **6**, 183–195 (1964).
51. Susana Lozano Calvo. Extraction of Polysaccharides in High-Yield Species Using Ultrasound. 2019.
52. Methrath Liyakathali, N. A., Muley, P. D., Aita, G. & Boldor, D. Effect of frequency and reaction time in focused ultrasonic pretreatment of energy cane bagasse for bioethanol production. *Bioresour. Technol.* **200**, 262–271 (2016).
53. Loaiza, J. M., López, F., García, M. T., García, J. C. & Díaz, M. J. Biomass valorization by using a sequence of acid hydrolysis and pyrolysis processes. Application to Leucaena leucocephala. *Fuel* **203**, 393–402 (2017).
54. Pontes, R. *et al.* Comparative autohydrolysis study of two mixtures of forest and marginal land resources for co-production of biofuels and value-added compounds. *Renew. Energy* **128**, 20–29 (2018).
55. Dantas, G. A., Legey, L. F. L. & Mazzone, A. Energy from sugarcane bagasse in Brazil: An assessment of the productivity and cost of different technological routes. *Renew. Sustain. Energy Rev.* **21**, 356–364 (2013).
56. Sebio-Puñal, T., Naya, S., López-Beceiro, J., Tarrío-Saavedra, J. & Artiaga, R. Thermogravimetric analysis of wood, holocellulose, and lignin from five wood species. *J. Therm. Anal. Calorim.* **109**, 1163–1167. https://doi.org/10.1007/s10973-011-2133-1 (2012).
57. Fidalgo, M. L. *et al.* Comparative study of fractions from alkaline extraction of wheat straw through chemical degradation, analytical pyrolysis, and spectroscopic techniques. *J. Agric. Food Chem.* **41**, 1621–1626. https://doi.org/10.1021/jf00034a019 (1993).
58. Ramírez, Á., García-Torrent, J. & Tascón, A. Experimental determination of self-heating and self-ignition risks associated with the dusts of agricultural materials commonly stored in silos. *J. Hazard Mater.* **175**, 920–927 (2010).
59. Carrier, M., Auret, L., Bridgwater, A. & Knoetze, J. H. Using apparent activation energy as a reactivity criterion for biomass pyrolysis. *Energy Fuels* **30**, 7834–7841 (2016).
60. Cai, J., Wu, W., Liu, R. & Huber, G. W. A distributed activation energy model for the pyrolysis of lignocellulosic biomass. *Green Chem.* **15**, 1331–1340 (2013).
61. Vyazovkin, S. A time to search: Finding the meaning of variable activation energy. *Phys. Chem. Chem. Phys.* **18**, 18643–18656 (2016).
62. Zhou, X., Li, W., Mabon, R. & Broadbelt, L. J. A critical review on hemicellulose pyrolysis. *Energy Technol.* **5**(1), 52–79. https://doi.org/10.1002/ente.201600327 (2017).
63. Chen, D. *et al.* Insight into biomass pyrolysis mechanism based on cellulose, hemicellulose, and lignin: Evolution of volatiles and kinetics, elucidation of reaction pathways, and characterization of gas, biochar and bio-oil. *Combust Flame.* **242**, 112142 (2022).
64. Murugan, P., Mahinpey, N., Johnson, K. E. & Wilson, M. Kinetics of the pyrolysis of lignin using thermogravimetric and differential scanning calorimetry methods. *Energy Fuels* **22**, 2720–2724 (2008).
65. Vuppaladadiyam, A. K. *et al.* Biomass pyrolysis: A review on recent advancements and green hydrogen production. *Bioresour. Technol.* **364**, 128087 (2022).

Author contributions

L.-C.: Conceptualization, Methodology, Investigation, Formal analysis, Data curation, Visualization, Writing – original draft. L.J.M: Conceptualization, Methodology, Investigation, Formal analysis, Data curation, Visualization. G.J.C: Conceptualization, Methodology, Funding adquisition, Supervision, Writing – review & editing. T.R: Formal analysis, raw material acquisition, Writing – review & editing. B.F: Conceptualization, Methodology, Data curation, Funding acquisition, Supervision, Writing – review & editing, Project administration. All authors reviewed the manuscript and consented to its publication.

Funding

This work was funded by Spain's Ministry of Science and Innovation, and also by the National Research Program Oriented to the Challenges of Society (Project PID2020-112875RB-C21, MCIN/AEI /https://doi.org/10.13039/501100011033), also this publication is part of the PRE2021-097925 support (funded by MCIN/AEI/https://doi.org/10.13039/501100011033 and by the FSE +), and the University of Huelva/CBUA.

Competing interests
The authors declare no competing interests.

Additional information
Correspondence and requests for materials should be addressed to S.L.-C.

Reprints and permissions information is available at www.nature.com/reprints.

Publisher's note Springer Nature remains neutral with regard to jurisdictional claims in published maps and institutional affiliations.

Open Access This article is licensed under a Creative Commons Attribution 4.0 International License, which permits use, sharing, adaptation, distribution and reproduction in any medium or format, as long as you give appropriate credit to the original author(s) and the source, provide a link to the Creative Commons licence, and indicate if changes were made. The images or other third party material in this article are included in the article's Creative Commons licence, unless indicated otherwise in a credit line to the material. If material is not included in the article's Creative Commons licence and your intended use is not permitted by statutory regulation or exceeds the permitted use, you will need to obtain permission directly from the copyright holder. To view a copy of this licence, visit http://creativecommons.org/licenses/by/4.0/.

© The Author(s) 2024

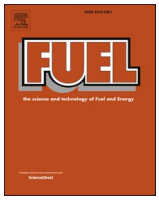
Fuel 367 (2024) 131501



Contents lists available at ScienceDirect

Fuel

journal homepage: www.elsevier.com/locate/fuel



Full Length Article

Assessing the influence of biomass origin and fractionation methods on pyrolysis of primary biomass fractions

N. Almagro-Herrera, S. Lozano-Calvo *, A. Palma, J.C. García, M.J. Díaz

Research Centre for Technology of Products and Chemical Processes (PRO^{2}TECS), Department of Chemical Engineering, University of Huelva, Av. 3 de marzo s/n, 21071 Huelva, Spain

ARTICLE INFO

Keywords:
Activation energy
Fractionation methods
Lignocellulosic biomass
Pyrolysis gases
TD/GC–MS

ABSTRACT

Pyrolysis has emerged as a highly promising technology for the efficient utilization of organic materials, particularly lignocellulosic materials. This study investigates the behavior and influence of three primary biomass fractions (cellulose, hemicellulose, and lignin) derived from different sources (trees, shrubs, and agricultural residues) on the kinetic of the pyrolysis process. With this objective, different fragmentation methods were employed to isolate the main components of the lignocellulosic biomass, followed by thermogravimetric analysis to examine the pyrolysis process. The activation energy was determined using both, the Friedman differential kinetic models of and the Flynn-Wall-Ozawa integrated method, with the latter being found to be more efficient. The activation energy (Ea) was found to be influenced by several factors, including the fractionation process and the origin of the raw material. For hemicellulose, the Ea was in the range of 200–300 kJ mol^{-1}, while cellulose showed Ea values of about 180–220 kJ mol^{-1}. In contrast, lignin displayed a wider range of Ea variation, with its values being more sensitive to the fractionation method used. Gas samples were collected through adsorption tubes during pyrolysis for analysis of gas stream compositions from different lignocellulosic fractions using gas chromatography/mass spectrometry. Furfural, among other compounds, was predominantly detected in the pyrolysis of hemicellulose fractions, ranging from 6.6 % to 19.3 %.

1. Introduction

Biomass can be used as an alternative to fossil fuels to reduce greenhouse gas emissions and promote sustainable development [1]. One of the most promising uses is to produce fuels such as bio-oil, renewable diesel, methane, and hydrogen through processes such as pyrolysis and hydrotreatment [2].Biomass can also be used to produce a range of valuable chemicals, materials and products through biorefineries, similar to oil refineries and petrochemical plants [3]. These processes have both positive and negative ecological impacts, and therefore need to be optimized from both a technical and economic point of view [4,5].

In this context, in order to successfully achieve biomass valorisation, there are several needs that must be addressed, among which stand out (i) the optimisation of pre-treatments due to the fact that biomass is a complex and recalcitrant material that must undergo pre-treatment to decompose its structure and make it more accessible to conversion processes [6]; (ii)the selection of the optimal valorisation technology depending on the characteristics of the biomass [7,8]; and (iii) the proper integration of the technology used with existing industries such as agriculture, forestry and biorefineries. This approach can also contribute to the creation of a circular economy in which waste materials are transformed into valuable products [9].

There are numerous technologies for biomass valorisation, such as direct combustion, biochemicals such as fermentation or anaerobic digestion, and thermochemical including pyrolysis, gasification, or hydrothermal liquefaction. Among them, pyrolysis is an efficient thermochemical process that can convert biomass into pyrolytic gas, bio-oil and solid biochar, meeting the requirements mentioned above [10,11]. In general, the pyrolysis process involves heating biomass in the absence of oxygen to temperatures between 300 and 800 °C. In addition, the pyrolysis process can be easily integrated with other biomass valorisation processes, such as anaerobic digestion, to increase the overall biomass conversion efficiency [12].

The kinetics of the pyrolysis process, regulated by reaction rate, temperature, and residence time, must be carefully controlled to optimize the yield and quality of the pyrolysis products. Biomass composition, primarily comprising cellulose, hemicelluloses, and lignin, has a

* Corresponding author.
E-mail address: susana.lozano@diq.uhu.es (S. Lozano-Calvo).

https://doi.org/10.1016/j.fuel.2024.131501
Received 12 December 2023; Received in revised form 13 March 2024; Accepted 15 March 2024
Available online 16 March 2024
0016-2361/© 2024 Published by Elsevier Ltd.

significant influence on pyrolysis rate and efficiency [13]. These polymers have different physical behavior and thermochemical properties depending on feedstock, biomass, and other required properties [14]. Furthermore, significant variations in biomass behavior during pyrolysis arise from differences in the structure and chemistry of polymers, resulting in different decomposition ratios, temperatures, and forms [15].The operating variables of the pyrolysis process must be carefully controlled to optimize its efficiency. For example, higher temperatures tend to increase the yield of gaseous products, whereas lower temperatures favor the production of liquid bio-oil [16]. Similarly, longer residence times result in higher char yield, while shorter residence times enhance the yield of gaseous and liquid products [17]. In pyrolysis, the key operating variables are the temperature and the activation energy, which vary depending on the biomass components. Some studies suggest that the activation energy depends on the degree of polymerisation of the components [13].

Consequently, understanding the influence of biomass composition and pyrolysis process kinetics are critical factors. In this sense, the relative influence of each of the fractions on the kinetics of the process, and therefore on the products generated, has not been studied in depth. Some articles with pure compounds have been found [16,18–20], but no comparison of the comparative influence between different types of cellulose, hemicelluloses and lignin has been made.

In order to understand the impact of each major fraction lignocellulosic biomass, it is essential to fragment the biomass. Various treatments can be used sequentially for this purpose. One such treatmentis cold alkaline extraction, which offers operational and environmental advantages as it operates below 40 °C [21]. Other methods that can be utilized include the kraft and soda-anthraquinone processes to obtain the cellulosic and lignocellulosic fraction. The kraft process, a traditional and widely used method, solubilizes more than half of the hemicelluloses and almost all of the lignin from the fibers, while the cellulose undergoes partial degradation without dissolution, leading to an increase in its crystallinity degree [22–24]. Alternatively, soda-anthraquinone, serves as an alkaline, non-sulphur alternative to the kraft process. However, the cellulose pulp produced by the soda-anthraquinone process has lower strength compared to kraft [25].

The aim of this study is, therefore, to explore the comparative valorization of the pyrolysis (kinetic, and gasses) of the main biomass fractions (cellulose, hemicellulose, lignin) with different characteristics and origins (tree, shrub, agricultural residue) and under different types of fractionations (kraft and soda-anthraquinone), focusing on its potential applications.

2. Materials and methods

2.1. Materials

Three types of biomasses with different characteristics and compositions have been evaluated. *Populus x-Euroamericana* clone AF2 (Poplar) as a tree, Tagasaste as a shrub (because both are high-yielding species) and Wheat Straw as agroforestry waste have been selected. The Agroforestry Department of University of Huelva has supplied these raw materials. For all the raw materials studied, the initial conditioning consists of a mechanical treatment based on the reduction of the sliver size that runs on a disposer conventional (Mill Retsch) with a sieve of mesh size 20 mm and, later, sieved to obtain the length and width average of chips between 1 and 3 cm and 0.5 cm, respectively. Finally, the chips are stored at room temperature to maintain a constant moisture level and then packed in airtight containers. The main chemical characteristics of the materials used in Table 1 are shown, and the main parameters of industrial interest and elemental analysis of the biomasses under study in Table 2 are shown.

Table 1
Chemical characterization of studied raw materials.

Characterization/Raw Material	Poplar	Tagasaste	Wheat Straw
Removable in ethanol (% p/p)	12.13 ± 1.32	11.36 ± 1.10	20.35 ± 4.23
Glucan (% p/p)	40.31 ± 5.15	41.42 ± 4.02	34.12 ± 6.86
Xylan (% p/p)	19.35 ± 1.04	18.56 ± 1.25	14.33 ± 4.14
Araban (% p/p)	0.23 ± 0.15	0.65 ± 0.21	2.35 ± 0.15
Acetyl Groups (% p/p)	2.88 ± 0.39	3.31 ± 0.17	2.12 ± 0.17
Lignin Klason (% p/p)	19.53 ± 1.65	20.1 ± 1.72	21.62 ± 2.38
Ash (% p/p)	1.4 ± 1.41	0.8 ± 0.90	4.02 ± 0.31

Table 2
Proximate, ultimate and calorific values for studied biomasses.

	Proximate[a]		Ultimate[b]			Calorimetry[c]
	Volatile (%)	Fixed Carbon (%)	H (%)	C (%)	N (%)	HHV (MJ/kg)
Poplar	85.61 ± 2.3	12.30 ± 0.4	6.21 ± 0.2	48.68 ± 0.7	1.05 ± 0.1	14.35 ± 1.2
Tagasaste	78.84 ± 1.9	18.65 ± 0.8	6.58 ± 0.2	47.31 ± 0.9	4.23 ± 0.1	16.27 ± 1.5
Wheat Straw	73.55 ± 1.2	15.21 ± 0.5	5.41 ± 0.2	43.16 ± 0.6	0.30 ± 0.1	16.82 ± 1.3

[a] Proximate analysis was done according to ASTM D5142-09.
[b] Ultimate analysis was conducted using a modified ASTM D5373-10 method.
[c] Heating value (HHV) were determined with a calorimeter using ASTM D5865-10.

2.2. Biomass treatments

Three replicates for each of the tested treatments have been performed.

2.2.1. Alkali Pretreatment: Hemicellulose extraction

Alkaline pretreatments are used in biorefinery for delignification to improve the accessibility and digestibility of polysaccharides as a step before enzymatic hydrolysis or microbial digestion [26]. Among the alkaline treatments, cold alkaline extraction (CAE) is widely used. This operation breaks down the biomass into hemicelluloses and soluble lignins in alkali and waste through the separation of heteropolysaccharides polymer of the fiber source. In this way, it facilitates the use of these components in higher value products with minimal chemical and physical changes. In this case, the hemicelluloses are extracted from the biomass in the liquor with a polymeric structure without significant degradation [27,28]. The used conditions were: 40 °C operating temperature; 90 min operating time and 100 $g.L^{-1}$ alkali concentration for Wheat Straw [27] and 120 $g.L^{-1}$ for Tagasaste and Poplar [29]. The difference lies in the type of lignocellulosic biomass. Wheat is herbaceous and has a greater capacity for hemicelluloses extraction, while the nature of the others requires a higher alkali concentration to extract the hemicelluloses. The resulting solid from the cold alkaline extraction is repeatedly washed with water to remove any traces of NaOH according to TAPPI standard T264 cm-07 [30].

2.2.2. Delignification kraft treatment

The solid obtained is the cellulose-rich pre-treatment and contains most of the lignin from the biomass. The kraft process is currently the dominant delignification method for paper pulp production due to its advantages over other methods for the same purpose [31]. The operating conditions for a batch pulp mill were as follows: a liquid to solid ratio of 3.5; a sulphide content of 25 %, a cooking temperature of 165 °C and a cooking time of 50 min [32].

2.2.3. Delignification soda-anthraquinone treatment

Among the alternative methods, the most widely used is an alkaline

(NaOH), sulphur-free process using anthraquinone (AQ) as a catalyst. The cellulose obtained is more difficult to bleach and has poorer resistance properties than that obtained by the kraft process [33]. For this delignification process, 13 % active alkali; a temperature of 143 °C and a time of 90 min for all the biomasses studied [32] has been used.

2.2.4. Chemical analysis

The standards: TAPPI T264 cm-07 [30] to determine the moisture content of the raw material; TAPPI T204 cm-07 [33] standard to measure extractable compounds such as hydrocarbons, non-volatile low molecular weight carbohydrates, phytosterols, salts, waxes, polyphenols, resins, fats and other compounds; TAPPI T222 [34] for the quantitative determination of monomeric compounds and lignin and TAPPI T249 [35] to the determination of monomeric sugars, i.e. xylose, glucose and arabinose, acetic acid and possibly 5-hydroxymethylfurfural and furfural by HPLC, have been successfully used.

2.3. Thermogravimetric analysis

The thermogravimetric experiments applied to each of the different biomasses and fractions studied were carried out on the Mettler Toledo TGA/DSC1 STARe system. The samples of the different starting materials were previously ground and homogenized. In the pyrolysis experiments, nitrogen was used as an inert gas to avoid secondary reactions. The pyrolysis processes were carried out in two steps: (i) heating the sample from 25 to 105 °C with a heating rate of 15 °C min^{-1} and an inert nitrogen atmosphere with a flow rate of 15 mL min^{-1}; (ii) heating from 105 to 800 °C with different heating rates (5, 10, 15, 20 and 25 °C min^{-1}) with a nitrogen flow rate of 30 mL min^{-1}. The initial sample mass was approximately 10 mg in all cases and the experiments were carried out in triplicate and the mean values recorded.

2.4. Kinetic models

Iso-conversional kinetic methods are those in which the variation of the activation energy is estimated as a function of the conversion degree. These models are of great importance in systems where there is a variation of the activation energy as a function of the conversion degree. This type of method is particularly useful for biomass, which degrades at different temperatures due to the diverse and heterogeneous nature of its components [36]. Within this type, there are two groups: differential methods and integral methods [37]. These models are used to determine the kinetic parameters of the reaction by using the Arrhenius equation (Eq. (1), and that all the reactions are of order 1, because there is an excess of the sample, in these models are assumed.

$$k(T) = Ae^{\left(\frac{-E_a}{RT}\right)} \tag{1}$$

Where: A: preexponential factor (s^{-1}); E_a: activation energy (kJ mol^{-1})); and R: universal gas constant (8,8145 kJ mol^{-1}K).

In general, in the differential kinetic models data from dα/dt as a function of T (Eq.2) are fitted.

$$\frac{d\alpha}{dt} = Ae^{\left(\frac{-E_a}{RT}\right)} f(\alpha) \tag{2}$$

Where: dα/dt: ratio of reaction, represented as the variation of the conversion (α), calculated through the loss of mass, with respect to time (t); and f(α): dependent on temperature (T) function of the conversion.

However, when working in conditions that are not isothermal, the temperature will vary with time and will produce a specific heating rate (β) and the Eq. (3) will be obtained.

$$\frac{d\alpha}{dT} = \frac{A}{\beta}e^{\left(\frac{-E_a}{RT}\right)} f(\alpha) \tag{3}$$

Integral methods, by separating the variables and integrating with respect to the limits α and 0; T and T0, which is then simplified to 0 since the reaction ratio is significant from the initial temperature, Eq. (4) can be obtained.

$$g(\alpha) = \int_0^\alpha \frac{d\alpha}{dT} = \frac{A}{\beta}\int_{T_0}^{T} e^{\left(\frac{-E_a}{RT}\right)} dT \approx \frac{A}{\beta}\int_0^T e^{\left(\frac{-E_a}{RT}\right)} dT \tag{4}$$

g(α): conversion dependent function.

The integrated models used data α, or an integral of α as a function of t, or T. In this sense, the Flynn-Wall-Ozawa (FWO) method [38,39], which faithfully represents systems where there is more than one simultaneous reaction [40]. The equation for this method is shown in Eq. (5).

$$ln(\beta) = ln\left(\frac{AE_a}{Rg(\alpha)}\right) = 5,523 - 1,052\left(\frac{E_a}{RT}\right) \tag{5}$$

Using the Eq. (5) for each of the conversion degrees, we get the Eq. (6).

$$ln(\beta) = ln\left(\frac{AE_a}{R}\right) - lng(\alpha) - 0,4567\left(\frac{E_a}{RT}\right) \tag{6}$$

For each conversion value (α), by plotting lnβ versus 1/T, a line with a slope of −0.4567 E_a/R can be obtained and the activation energy calculated. The pre-exponential factor (A) can be found by intersecting the line with the axes.

On the other hand, the values of the DTG curve (Differential Thermogravimetric Analysis) are used for the differential methods. The method developed by Friedman [41] is the most widely used differential method. This method is based on the application of logarithms to equation (3), which results in Eq. (7).

$$ln\left(\beta\frac{d\alpha}{dT}\right) = ln\left(\frac{d\alpha}{dt}\right) = ln[Af(\alpha)]\frac{-E_a}{RT} \tag{7}$$

For each conversion degree (a) and heating rate (b), the plot of ln(dα/dt) versus 1/T gives a straight line whose slope is -E_a/R. From this slope, the value of the activation energy for each of the conversions is determined [40].

2.5. Pyrolysis products analysis by TD/GC–MS

To obtain the pyrolysis products (pyrolytic gases) from different fractions (cellulose, hemicellulose, and lignin) of the three biomass species studied, a laboratory-scale reactor was used. The reactor comprises a temperature-controlled furnace housing a quartz tube measuring 10 mm in diameter and 140 cm in length. A horizontal actuator is employed to introduce the sample, typically around 1 g. The residence time was systematically set a 7 min and nitrogen (250 cm^3 min^{-1}) was used as transport gas.

Volatile compounds samples from the pyrolysis process at the peak temperature ranges of the different biomasses and fractions obtained (hemicellulose, kraft cellulose, soda-AQ cellulose, kraft lignin, and soda-AQ lignin) sere collected at the exit of the Laboratory-scale pyrolysis reactor in fritted glass TD tubes (Supelco, Bellefonte, PA; O.D.: 6.35 mm; length: 88.9 mm) for 15 s. These tubes contained 100 mg of Tenax® TA (80–100 mesh purchased from Supelco, Bellefonte, PA) packed in synthesized glass wool layers. After collecting samples in TD tubes, the analysis was performed using TD/GC–MS. Therma desorption (TD) was employed to release the volatile compounds captured by the sorbent material in the tubes, facilitating their identification and quantification on the GC/MS. TD was carried out using a thermal desorption system

unit (TD-20, Shimadzu, Japan) equipped with an HP-5 MS column (column length: 60 m, inner diameter: 0.25 mm, film thickness: 0.25 μm, J&W Scientific, Agilent Technologies, Santa Clara, California, USA), involving two steps: tube desorption and trap desorption. The mass spectrometer operated in scan mode (41–450 m/z), and volatile organic compounds were identified by comparing their mass spectra with those in the NIST11 library database, using 1-bromo-3-chlorobenzene as an internal standard (Fig. 1).

3. Results and discussion

3.1. Cold alkaline extraction (CAE)

Cold alkaline extractions were utilized to extract hemicelluloses in a liquid medium. The extraction process resulted in solid rich in cellulose and lignin after the removal of hemicelluloses. In Table 3, the main components of the solid residue following hemicellulose extraction from the selected raw materials are shown. The hemicellulose yields are referred to as the quantity of dry hemicellulose obtained relative to the quantity of raw material introduced in the cold alkaline extraction process.

The yield of hemicellulose obtained from Poplar after cold alkaline extraction is less than 5 % as shown in Table 3. This is mainly attributed to the structural characteristics of Poplar which make the alkaline liquor difficult to penetrate and act on, resulting in a low yield of hemicellulose. Hemicellulose yield is directly related to cold alkaline extraction process yield. It has been observed that woody materials exhibit lower extraction yields compared to herbaceous materials, as demonstrated by various studies. For instance, Carvalho et al. 2016 [21] achieved extraction yields of 4.52 % and 37.7 % from eucalyptus and straw, respectively. The composition of obtained solid in the cold alkaline extraction process from Tagasaste was found to be intermediate between those of Poplar and Wheat Straw, containing significant amounts of glucan and xylan. This extraction treatment is selective for the hemicelluloses but does not prevent the extraction of part of the lignin content of the raw material. This means that the extracted hemicellulose fractions are not pure, and their behavior must be further analysed by thermogravimetric analysis.

3.2. Kraft process delignification

Delignification by the kraft process was carried out on the materials studied. The characteristics of the solids obtained are given in Table 4. The yield indicates the amount of pulp produced in relation to the solid obtained from the cold alkaline extraction process; a lower yield means less solid obtained, i.e. a higher extraction in the liquid phase. On the other hand, the kappa index is directly related to the lignin content of the pulp, i.e. the higher the kappa index, the more lignin is found in the pulp and vice versa.

Table 4 shows the characteristics of products obtained through kraft delignification of Poplar, Tagasaste, and Sheat Straw. The yield of the solids obtained from Poplar was the highest at 60.1 %, followed by Tagasaste at 57.84 %, and Wheat Straw at 53.30 %. The Kappa number was highest for Poplar at 16.27, followed by Tagasaste at 14.81 and Wheat Straw at 12.93, indicating that Wheat Straw pulp has the lowest lignin content. The glucan content was highest for Wheat Straw at 78.02 %, followed by Tagasaste at 72.03 % and Poplar at 70.95 %. The xylan content was highest for Poplar at 10.03 %, followed by Tagasaste and Wheat Straw at 8.65 % and 6.24 %, respectively. However, the araban content was highest for Wheat Straw at 1.47 %, followed by Tagasaste at 0.26 % and 0.2 % for Poplar.

The higher extraction observed in agricultural residues, as occurred with Wheat Straw, after kraft treatment results in a lower yield, a phenomenon previously noted by several authors. These results are consistent with those reported in the literature. For instance, in a study involving a simple kraft process, the solid yield for Eucalyptus Citriodora was 47 % with a kappa number of 20.9 [42]. In another study, which focused on optimizing of kraft conditions for wheat straw, the solid yield ranged from 40.02 % to 44.11 %, while the kappa number varied from 18.7 to 47.6 [43].

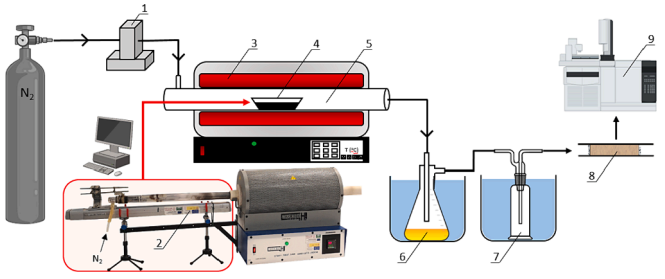


Fig. 1. Schematic of pyrolysis experimental system: (1) Flowmeter, (2) Automatic Sample System, (3) furnace, (4) sample, (5) quartz reaction tube, (6) condenser, (7) cold trap, (8) gas collection (Tenax®), (9) TD-GC/MS.

3.3. Soda-Anthraquinone process delignification

Delignification by the soda-Anthraquinone process was carried out on the materials studied. Table 5 shows the characteristics of the obtained solids in the soda-anthraquinone delignification of Poplar, Tagasaste and Wheat Straw.

The results show that Poplar had the highest yield of 70.89 %, followed by Tagasaste with 65.57 % and Wheat Straw with 60.94 %. Poplar also had the highest kappa number of 42.03, followed by Tagasaste with 33.01 and Wheat Straw with 17.98, in particular the Poplar pulp had 17.73 % of lignin content. The highest glucan content was found in Wheat Straw with 68.02 %, followed by Tagasaste with 64.65 % and Poplar with 58.47 %. The highest xylan content was found in Poplar with 14.17 %, followed by Tagasaste with 11.33 % and Wheat Straw with 9.03 %. The highest araban content was found in Wheat Straw with 2.35 %, followed by Tagasaste with 1.21 % and Poplar with 0.33 %.

Comparing the data presented in Tables 4 and 5, it is clear evident that the pulp yield obtained by soda-anthraquinone delignification exceeds that obtained through kraft delignification. Also, the kappa index obtained with soda-anthraquinone delignification is significantly higher than that obtained with kraft delignification, indicating a greater degree of delignification in kraft process. This difference between the two processes has been observed in various studies, including the work of Alaejos et al. (2006) [44], where the holm yield for kraft and soda-antraquinone processes was reported to be 50.5 % and 55.0 %, respectively, while the corresponding kappa numbers were 20 and 23.7, respectively.

Consequently, the three pulps obtained from different raw material using soda-anthraquinone have slightly less glucan, and more xylan, araban and Klason lignin compared to kraft.

3.4. Thermogravimetric analysis (TGA-DSC)

3.4.1. Raw materials pyrolytic degradation

The TGA and DTG curves shown in Fig. 2 were obtained from Poplar, Tagasaste and Wheat Straw raw materials at a heating rate of 20 °C min^{-1}. The TGA curves show an initial drop, corresponding to the initial peak of the DTG curves, which indicates the loss of moisture from the sample at a temperature of approximately 112 °C for the three raw materials. During this initial phase of dehydration, the sample loses approximately 3.20 % for Poplar, 4.95 % for Tagasaste and 6.01 % for Wheat Straw. This is followed by the active pyrolysis stage (112–500 °C), during which the sample loses most of its weight due to the thermal degradation of the biomass, which is mainly composed of cellulose, hemicellulose, and lignin. The first peak observed in the pyrolysis active region represents the degradation of hemicelluloses and

Table 3
Material balance for the Cold Alkaline Extraction.

	Hemicelluloses Yield (% w/w)[a]	Glucan (% w/w)[b]	Xylan (% w/w)[b]	Araban (% w/w)[b]	Acetyl Groups (% w/w)[b]	Klason Lignin (% w/w)[b]
Poplar	4.59 ± 1.35	45.5 ± 8.25	16.67 ± 1.45	1.24 ± 0.10	2.2 ± 0.01	22.41 ± 4.48
Tagasaste	7.23 ± 2.13	48.18 ± 8.13	14.50 ± 2.60	0.8 ± 0.11	2.65 ± 0.01	21.24 ± 3.76
Wheat Straw	15.52 ± 2.88	49.35 ± 6.18	12.29 ± 0.88	2.61 ± 0.20	2.98 ± 0.01	20.52 ± 1.23

[a] Percentages based on quantity raw material.
[b] Percentages based on obtained solid.

Table 4
Characteristics of solids obtained in kraft delignification.

	Yield Pulp (% w/w)[a]	Kappa Index	Glucan (% w/w)[b]	Xylan (% w/w)[b]	Araban (% w/w)[b]	Klason Lignin (% w/w)[b]
Poplar	60.1 ± 6.84	16.27 ± 3.47	70.95 ± 2.21	10.03 ± 1.05	0.20 ± 0.01	8.34 ± 1.01
Tagasaste	57.84 ± 9.78	14.81 ± 2.02	72.03 ± 2.63	8.65 ± 0.88	0.26 ± 0.05	7.27 ± 0.74
Wheat Straw	53.30 ± 6.82	12.93 ± 1.75	78.02 ± 2.84	6.24 ± 0.62	1.47 ± 0.10	6.56 ± 0.62

[a] Percentages based on solids obtained in CAE.
[b] Percentages based on the kraft pulps obtained.

Table 5
Characteristics of solids obtained in soda-anthraquinone delignification.

	Yield Pulp (% w/w)[a]	Kappa Index	Glucan (% w/w)[b]	Xylan (% w/w)[b]	Araban (% w/w)[b]	Klason Lignin (% w/w)[b]
Poplar	70.89 ± 7.45	42.03 ± 9.58	58.47 ± 5.39	14.17 ± 4.21	0.33 ± 0.07	17.73 ± 4.32
Tagasaste	65.57 ± 9.41	33.01 ± 2.84	64.65 ± 5.96	11.33 ± 2.58	1.21 ± 0.26	15.17 ± 2.15
Wheat Straw	60.94 ± 5.50	17.98 ± 2.05	68.02 ± 7.63	9.03 ± 0.94	2.35 ± 0.46	12.45 ± 1.21

[a] Percentages based on solid obtained in CAE.
[b] Percentages based on solid obtained in soda-anthraquinone process.

lignin. Hemicelluloses start to degrade at around 200 °C and continue to degrade up to around 500 °C due to their relatively low thermal stability [19,34].

After this stage, at around 300 °C, cellulose degradation begins. This follows a similar process to that of hemicellulose, with degradation continuing up to about 600 °C [46]. Lignin, on the other hand, has a more complex structure, which makes it more thermally stable. It undergoes bulk degradation in the temperature range of 150–600 °C [47] and has a lower degradation peak. Therefore, the DTG curve of lignin overlaps with that of hemicelluloses and cellulose. Although cellulose is more thermally stable than hemicellulose, it undergoes degradation in a temperature range of about 390–600 °C due to its crystalline structure. During the active pyrolysis stage, the sample loses 72.17 % of its weight. The final stage of pyrolysis begins at around 500 °C, the passive pyrolysis stage, during which the weight loss of the sample is minimal, and the degradation of lignin is completed.

3.4.2. *Hemicelluloses pyrolytic degradation*

Fig. 3 shows the evolution during pyrolysis (DTG) of hemicelluloses obtained by cold alkaline extraction of the selected raw materials. As can be seen in Fig. 3, both degradation rate of and chemical changes can vary depending on the specific characteristics of the hemicellulose sample being analyzed.

The DTG curves show the three typical phases of hemicellulose degradation. The first phase causes dehydration of the hemicelluloses and results in an average weight loss of 10 % for the three materials. This is mainly due to the moisture remaining in the hemicelluloses after extraction and to the removal of some volatile organic compounds from the hemicellulose. The second phase involves active degradation of the hemicelluloses by pyrolysis (breaking of glycosidic bonds) in the range

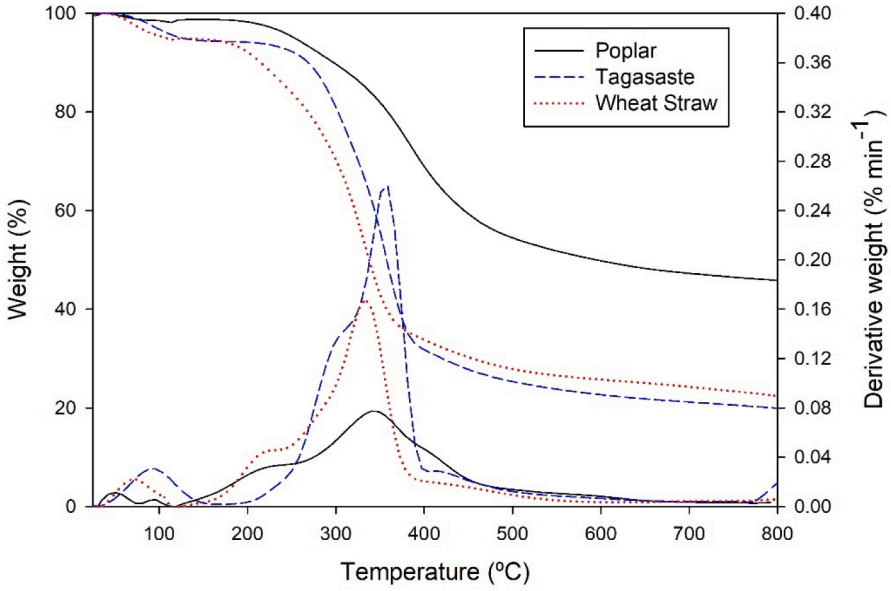


Fig. 2. Pyrolytic evolution (TGA and DTG) curves obtained from Poplar, Tagasaste and Wheat Straw as raw materials under nitrogen atmosphere at 20 °C min^{-1}.

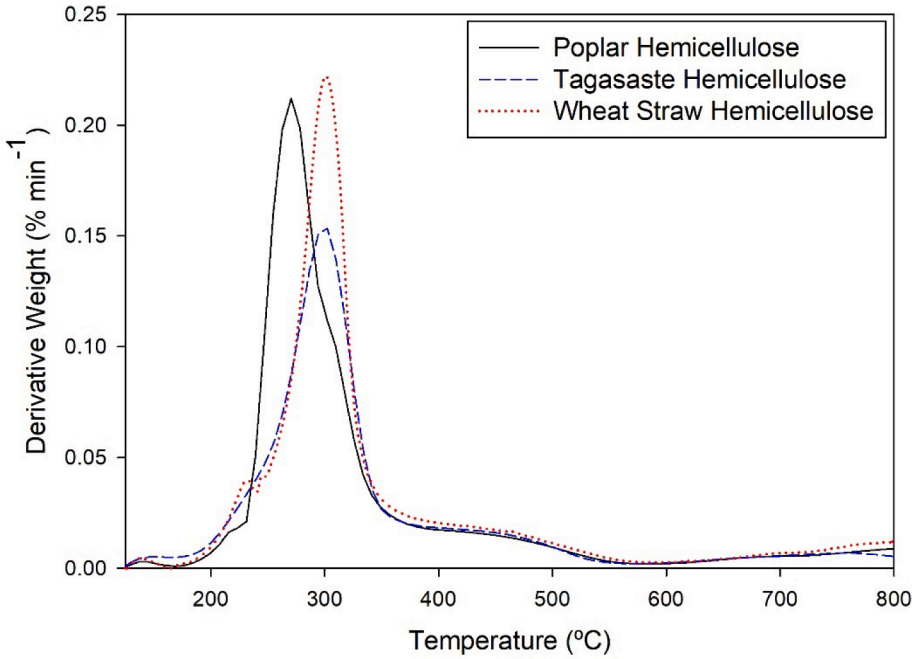


Fig. 3. Pyrolytic evolution (DTG) curves obtained from Poplar, Tagasaste and Wheat Straw extracted hemicelluloses under nitrogen atmosphere at 20 °C min^{-1}.

of 250–350 °C, with a total weight loss of 63.94 %, 42.23 % and 60.27 % for Poplar, Tagasaste and Wheat Straw respectively at 400 °C. The maximum degradation occurs at around 300 °C, mainly due to the depolymerisation of sugars such as xylan, a major component of hemicelluloses [48]. This phase can be further divided into primary and secondary reactions. In the primary reaction, thermal depolymerization of hemicelluloses triggers the production of volatile components such as acetic acid, furfural, and 5-HMF. In the secondary reaction, these volatile compounds further transform into liquid and solid products, such as phenols and aromatics [49]. Finally, the third stage is the passive pyrolysis stage, which occurs at temperatures above 450 °C and involves the transformation of the remaining hemicellulose fragments into a more stable carbonaceous char, through reactions with aromatic compounds and the cracking of carbon-hydrogen and carbon–oxygen bonds [45].

It should be noted that the peaks found in this study for hemicellulose fractions coming from the selected raw materials are smaller than those found in commercial hemicelluloses. This discrepancy could be attributed to the degradation of these linkages during the cold alkaline extraction process, which mainly affects the weaker linkages while preserving the main structure of the hemicelluloses. In addition, commercially available hemicelluloses undergo purification which is not part of the cold alkaline extraction process.

3.4.3. *Celluloses pyrolytic degradation*

The major component of the obtained pulps is cellulose. Fig. 4 shows

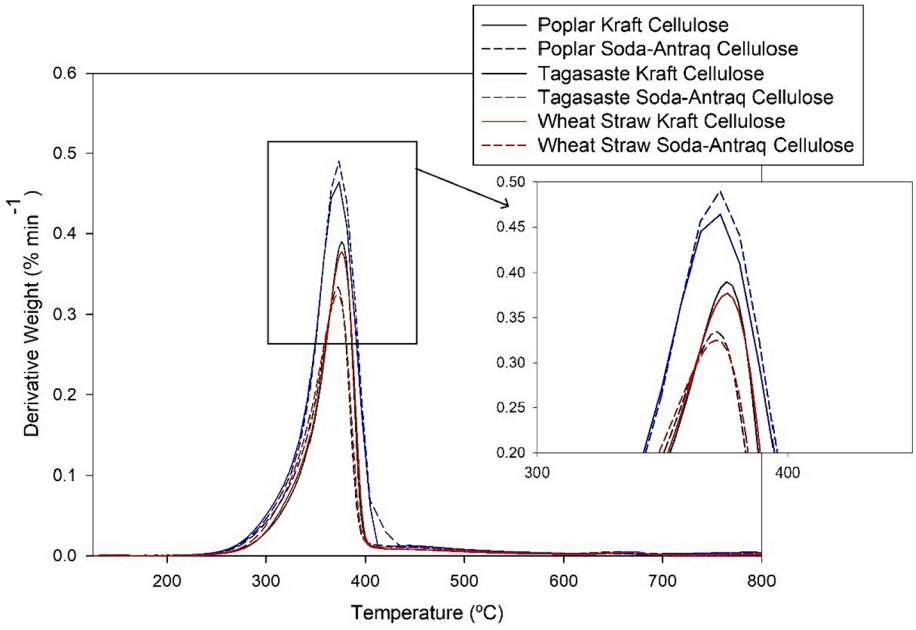


Fig. 4. Pyrolytic evolution (DTG) curves obtained from Poplar, Tagasaste and Wheat Straw kraft and soda-Anthraquinone celluloses under nitrogen atmosphere at 20 °C min^{-1}.

the DTG curves of kraft and soda-anthraquinone pulp for the selected raw materials. Similar to what was found for hemicelluloses, the rate of degradation can also vary depending on the specific characteristics of the cellulose sample being degraded. However, both temperature and degradation intervals appear to be similar between different starting materials and delignification methods. As can be seen, cellulose decomposition occurs in two stages; the first phase takes place at temperatures up to 300 °C and results in the highest weight loss of 80.3 % for all pulps tested. This phase involves the dehydrogenation and decarbonisation of cellulose, leading to the production of levoglucosan, volatile compounds such as levoglucosan (a major product), furans, acetic acid and other oligosaccharides through transglicosilación [50]. Similar to hemicelluloses, the degradation phase of cellulose pyrolysis can be further divided into primary and secondary reactions. The primary reaction involves depolymerisation of the cellulose, releasing volatile organic compounds at the start of the process. The secondary reaction involves the production of liquid and solid products through various chemical reactions in the later stages of the process [16]. The second phase occurs above 500 °C and involves the conversion of volatiles and chars through reactions with aromatics and cracking of the carbon-hydrogen and carbon–oxygen bonds [50]. Both the Kraft and soda-anthraquinone processes exhibit similar cellulose fractions obtained degradation behavior, and both show a single peak representing cellulose degradation, but some differences were observed. For the species studied, the soda-anthraquinone pulps suffers from a higher degradation rate and a higher weight loss compared to those for the kraft process. These differences in the different cellulose fractions contents (Tables 4 and 5) obtained from the different delignification processes may be due to the fact that the soda-anthraquinone process delignifies less due to the lower cellulose content in the final pulp.

3.4.4. *Lignin pyrolytic degradation*

Fig. 5 shows the DTG curves of lignin fractions obtained from the acid hydrolysis of the kraft process and soda-anthraquinone treatment of the selected raw materials. Acid hydrolysis quantitatively extracts Klason lignin, which is further analyzed. A similar evolution to those found for hemicellulose and cellulose has been found for lignin. Also the degradation intervals of lignin pyrolysis can vary depending on factors such as the source of lignin and the delignification method. Lignin is a very complex and heterogeneous polymer, and its behavior during pyrolysis can be influenced by the presence of other components or by the different specific structures of lignin (depending on the feedstock). In this sense, the temperature ranges for lignin pyrolysis can vary depending on the specific conditions of the delignification process. However, the general temperature range for lignin pyrolysis is between 250 °C and 800 °C [36]. Lignin degradation occurs in a wide temperature range due to its complex structure containing various functional groups connected by strong linear and weak bonds, different degradation maxima are observed in the DTG curves.

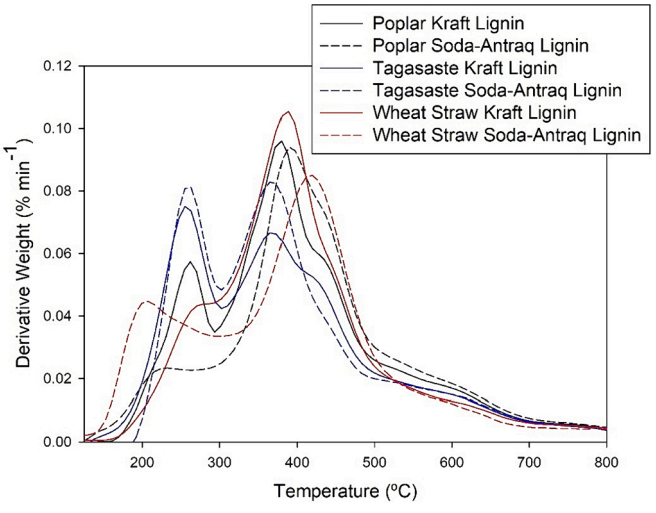


Fig. 5. Pyrolytic evolution (DTG) curves obtained from Poplar, Tagasaste and Wheat Straw Kraft and Soda-Anthraquinone lignins under nitrogen atmosphere at 20 °C min^{-1}.

During lignin pyrolysis, the lignin undergoes three main decomposition phases. The first phase (200–300 °C), shown in Fig. 5, to the degradation of hemicelluloses and celluloses, present as impurities in the lignin due to the delignification process, can be attributed. The second phase (300–500 °C) is the one with the highest rate and weight loss (40.46 % weight loss as an average of the different materials and treatments), which is attributed to the degradation of β-O-4 alkyl-aryl-ether bonds, resulting in the formation of small molecular weight compounds such as phenolic compounds, such as guaiacol, syringol, and catechol, as well as aromatic hydrocarbons and gasses like carbon dioxide, carbon monoxide, and methane [51]. The third phase (500–800 °C), with a low rate of weight loss (10.15 % weight loss on average for the different materials and treatments), may be due to the degradation of the remaining lignin structures, which undergo thermal cracking to form biochar and a carbon-rich solid residue [52].

Note that, the lignin fractions curves of both processes exhibit noise, which is due to the complexity of reactions and gas flow during the measurement. Comparing the lignin of Wheat Straw from the kraft process to the soda-anthraquinone process reveals differences, including a more reactive sample with a bulk degradation to lower temperatures, and a stronger first stage due to the presence of sulphur in kraft process causing increased rupture of carbon–carbon bonds in lignin. The sample from the soda-anthraquinone process experiences the highest weight loss (39.42 %) in the second stage of pyrolysis.

3.5. *Kinetic analysis.*

Two kinetic models, the Friedman differential, and the Flynn-Wall-Ozawa (FWO) integral, are compared for all samples tested. Figs. 6-8 show the lines obtained in the plot of $\ln(d\alpha/dt)$ vs $1/T$ for the Friedman method and $\ln\beta$ vs $1/T$ for the Flynn-Wall-Ozawa method for all the samples studied. In these figures, the values obtained with the highest (0.90) and lowest (0.10) conversions grade have been excluded because they do not represent the behavior of the sample in the initial and final pyrolysis reactions.

3.5.1. *Hemicelluloses kinetic analysis.*

As can be seen in Fig. 6, the use of both methods has resulted in remarkably high regression coefficients ($R^2 > 0.98$) when analyzing hemicellulose fractions from different sources. Furthermore, it can be concluded that the FWO method gives more favorable results than the Friedman method, as evidenced by the fact that the lines are more parallel when analyzing hemicellulose fractions.

Observing the change in slope in the figures, apart from what is observed in Fig. 3, it is clear that different reactions have taken place during the pyrolytic degradation of hemicelluloses. This is because a change in slope implies a change in activation energy, which in turn implies different reactions involved in the degradation, depending on the conversion degree of the sample. Therefore, by observing this fact in the figures, it is possible to identify the different reactions that have taken place during the pyrolytic degradation of hemicelluloses.

Fig. 7 shows the evolution of the activation energy (obtained from the slope of the calculated regression lines) during the pyrolysis of hemicelluloses obtained by cold alkaline extraction for the three species studied. According to H. Wang et al., (2017) [53], the degradation process of hemicellulose is characterized by a low initial activation energy during the degradation process, which gradually increases as the reaction progresses.

In the samples studied, the calculated activation energy for hemicellulose pyrolysis is in the range of 200–300 kJ mol^{-1}. This value is

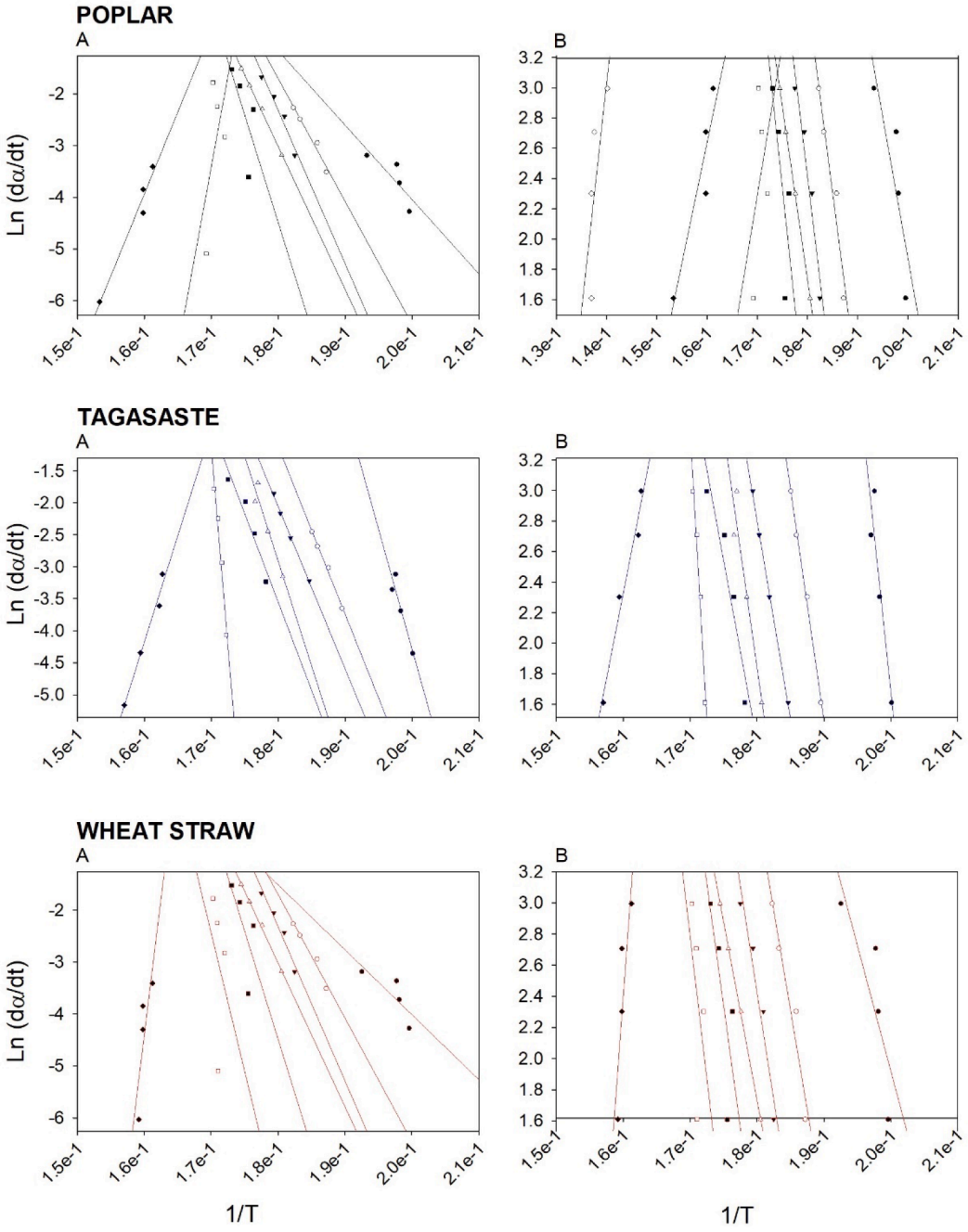


Fig. 6. Evolution of the Friedman (A) and FWO (B) lines for hemicelluloses as a function of the conversion degree (symbols) and the regression lines obtained.

higher than those reported by some authors, which can be attributed to the characteristics of hemicellulose, the method used for its extraction and the type of modelling performed. For instance, in a review of Zhou et al., 2017 [19] the one-reaction/stage models estimated the activation energy of hemicellulose pyrolysis to be in the range of 100–220 kJ mol^{-1}, while the multiple-reaction/stage models estimated the E_a in the range between 26 and 271 kJ mol^{-1}. There are several possible reasons why the activation energy of hemicellulose extracted by cold alkaline extraction is higher than those reported in the literature. Among them, the alkaline extraction method used in the study could result in different chemical structures, properties, and composition of the extracted hemicellulose. For example, the extracted hemicellulose could be contaminated with other compounds, which could affect the pyrolysis behavior and the activation energy. Fig. 2 also suggests that the alkaline extraction method used in the study could result in different chemical structures and properties of the extracted hemicellulose depending on the feedstock.

3.5.2. *Celluloses kinetic analysis.*

Similar to what was observed for hemicelluloses, the use of both methods has resulted in remarkably high regression coefficients ($R^2 >$ 0.99) when analyzing celluloses obtained from different sources and processes. The high R^2 values obtained with both methods indicate that they are reliable in predicting the pyrolysis behavior of cellulose and can be used to estimate the activation energy of cellulose pyrolysis. In addition, based on the high calculated regression coefficients, it is found that the pyrolysis of cellulose follows first order reaction kinetics, as stated by H. Fan et al., 2022 [54].Furthermore, similar to what was found for hemicelluloses, it can be inferred that the FWO method gives more favorable results (higher R^2) than the Friedman method also for

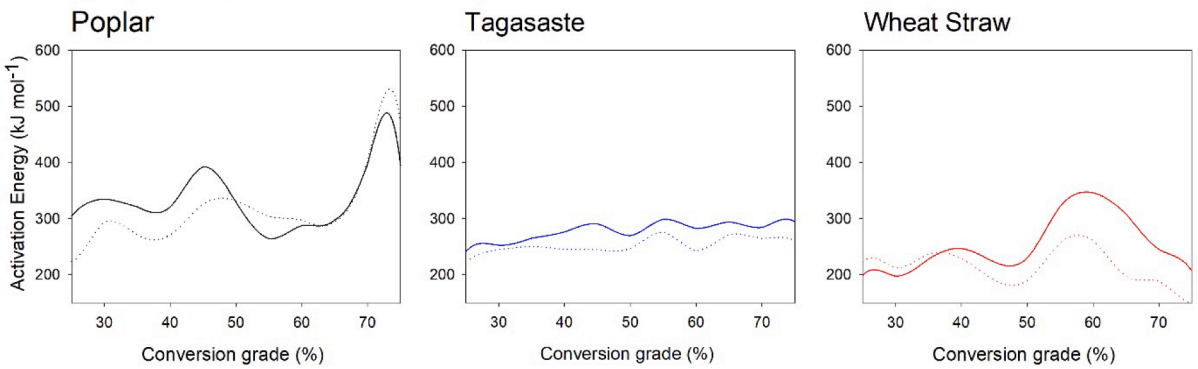


Fig. 7. Activation Energy evolution for extracted hemicelluloses. Continuous lines for Friedman method and discontinuous lines for FWO method.

celluloses [48,55]. This suggests that the FWO method is more accurate in predicting the pyrolysis behavior of cellulose than the Friedman method.

In Fig. 8, a similar slope for almost all measured reaction degrees can be observed. This may be attributed to the high purity of cellulose extracted using both studied delignification methods. In this case, the Friedman method shows a closer resemblance in slope compared to the Flynn method.

Fig. 9 illustrates the evolution of activation energy during the pyrolysis of the obtained celluloses. This figure shows that the activation energy increases as the reaction degree increases, which is in agreement with the literature.

For the cases studied, the values calculated by the FWO method are always higher than those found by the Friedman method. Moreover, the calculated values by the FWO method (180–220 kJ mol^{-1}) are within the range calculated by other authors.

In this sense, the activation energy of cellulose pyrolysis has been reported to be in the range of 114–288 kJ mol^{-1} [50,56,57]. The average pyrolysis activation energy of cellulose has been reported to be 189.2 kJ mol^{-1}[16]. Therefore, it is important to consider the experimental conditions and the method used when comparing the activation energy values reported in different studies.

3.5.3. *Lignins kinetic analysis.*

Fig. 10 presents an insightful analysis of the kinetic evolution of lignin, utilizing both the Friedman and FWO methods.

According to the studies conducted by L. Luo et al., 2020 and Matusiak et al., 2020 [57,58], the activation energies obtained through both methods do not demonstrate a clear linear trend with lignin content as the degree of reaction progresses. This observation can be attributed to the intricate nature of lignin decomposition, which involves multiple reactions with varying activation energies due to the diverse range of bonds and the multi-phasic character of its conversion Radojević et al., 2018 [59]. This complexity is reflected in Fig. 10 through the different slopes depicted.

Fig. 11 illustrates the evolution of activation energy during the pyrolysis of the obtained lignins.

Fig. 11 shows that the activation energy required to break chemical bonds in lignin is higher than that for cellulose. It should be noted that similar values of activation energy were found between the two kinetic models for the different lignins under investigation. According to L. Li, et al., 2013 and L. Luo et al., 2020 [60,57], the results show that the activation energy of lignin increases as the conversion degree progresses, indicating a higher energy requirement to break lignin bonds. This observation holds true for all three species and the two delignification methods investigated in the study. The increase in activation energy can be attributed to several factors. First, as lignin is depolymerised, the larger lignin molecules exhibit increased resistance to pyrolytic degradation. Secondly, the pyrolysis of lignin involves a complex interplay of reactions including fragmentation, condensation, and recombination. As the pyrolysis reaction progresses, the composition of the reaction mixture changes, leading to the dominance of different reaction pathways [61].

It should be noted that the evolution of the activation energy during the pyrolysis of the different lignins studied is different, since this evolution can be influenced by several factors, including the origin and composition of the lignin and the delignification method used. Different chemical compositions and structures of lignin, resulting in variations in pyrolysis kinetics and activation energy profiles, according to the literature cited.

In this case, the Fig. 11 shows that the delignification method has a strong influence on the activation energy, more so than the hemicelluloses and celluloses present in the lignin samples. The literature indicates that lignin has relatively high activation energy values [58], which range from 126 to 200 kJ mol^{-1}, depending on the study and the method used to estimate it [54,62,63].

3.6. *Obtained gasses by pyrolysis from different fractions*

It's essential to emphasize that temperature ranges and the composition of evolved gasses during the pyrolysis of the different lignocellulosic biomass fractions may exhibit variations influenced by factors such as the source plant, experimental conditions, and heating rate [64,65].

Fig. 12 shows the families of compounds detected during the pyrolysis of the different fraction. These gas streams have the potential for uses as fuel. Currently, there is a growing interest in selectively separating these compounds for specific applications [66]. For instance, among the compounds detected was acetic acid, which can be utilized as a platform chemical for the productions of different chemicals and materials [60]. Furthermore, apart from these non-condensable gases, a substantial amount of lighter gases, such as carbon dioxide, hydrogen, carbon monoxide, and methane, have been reported by other authors [65,67,68].

One family of compounds commonly associated whit the hemicellulose and cellulose degradation are furans, with hemicellulose being more prone to their formation, as observed in Fig. 12. Poplar wood and Wheat Straw primarily yielded fundamentally esters (28.9 % and 31.1 %, respectively), furans (20.2 % and 22.6 %, respectively), and aromatic hydrocarbons (16 % and 21.7 %, respectively). In contrast, Tagasaste predominantly produced aldehydes (32.4 %), carboxylic acid (13 %), and furans (11.9 %). The variation observed can be attributed to the inherent properties of the raw materials. This is due to the fact that the composition and the degree of acetylation of the hemicelluloses are dependent on the raw material used. For instance, the divergence stems from the differing sugar monomers present in the raw materials, which decompose at different temperatures and produce different gas products. Hardwoods contain predominantly xylose, whereas softwoods

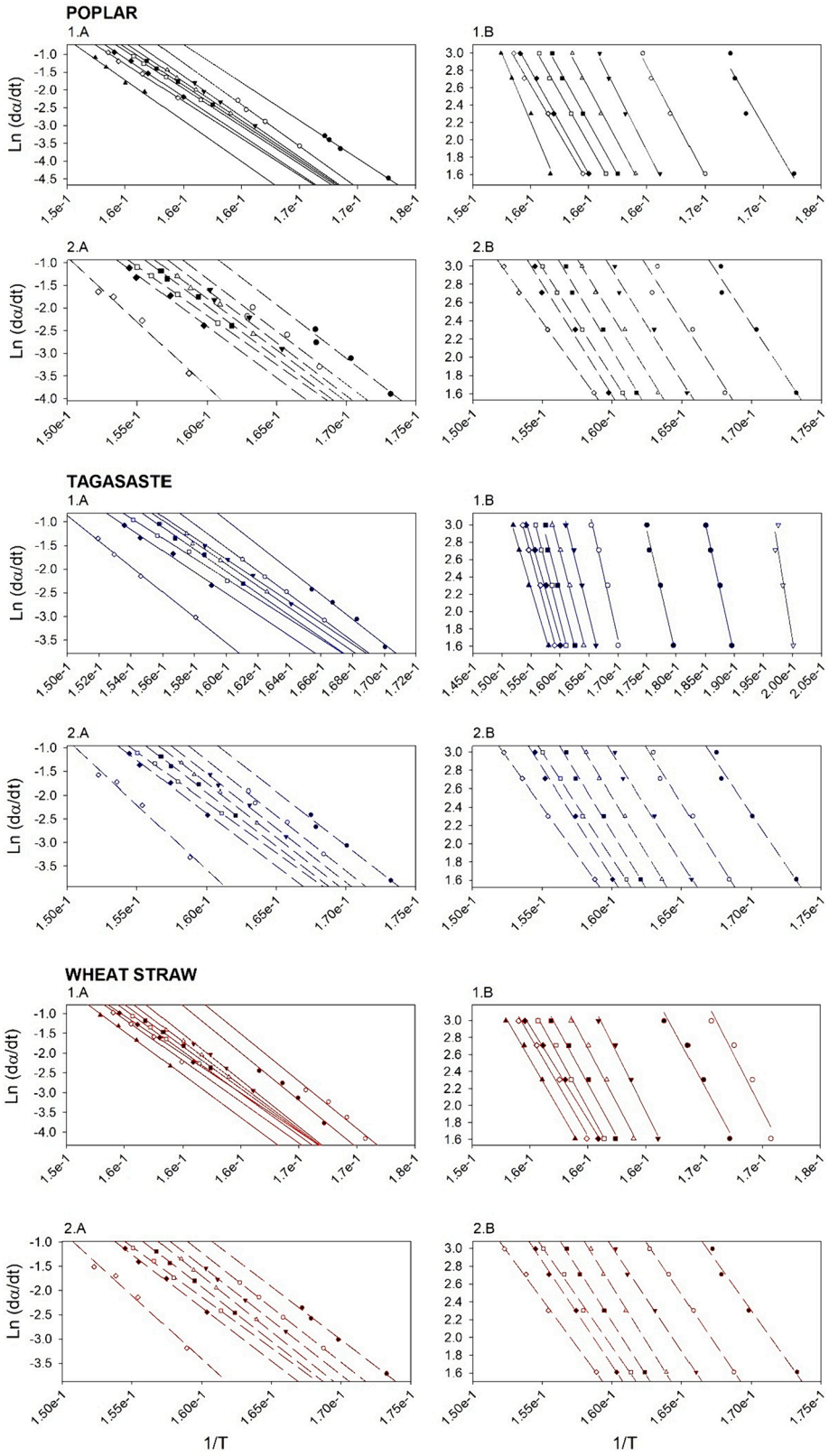


Fig. 8. Evolution of the Friedman (A) and FWO (B) lines for Kraft (1) and Soda-Antraquinone (2) celluloses as a function of the conversion degree (symbols) and the regression lines obtained.

contain a combination of xylose, mannose, and galactose [69,70]. If we refer back to the DTG-curve of hemicellulose fractions (Fig. 3), we can observe a difference in the degradation of Tagasaste's hemicellulose fractions compared to that found for Poplar and Wheat Straw.

Focusing on the cellulose fractions, it is observed in the gas stream produced during pyrolysis that the most prominent compounds are aldehydes, and phenols, while in the Poplar case by the second one, the carboxylic acids. Therefore, as mentioned above, the production of

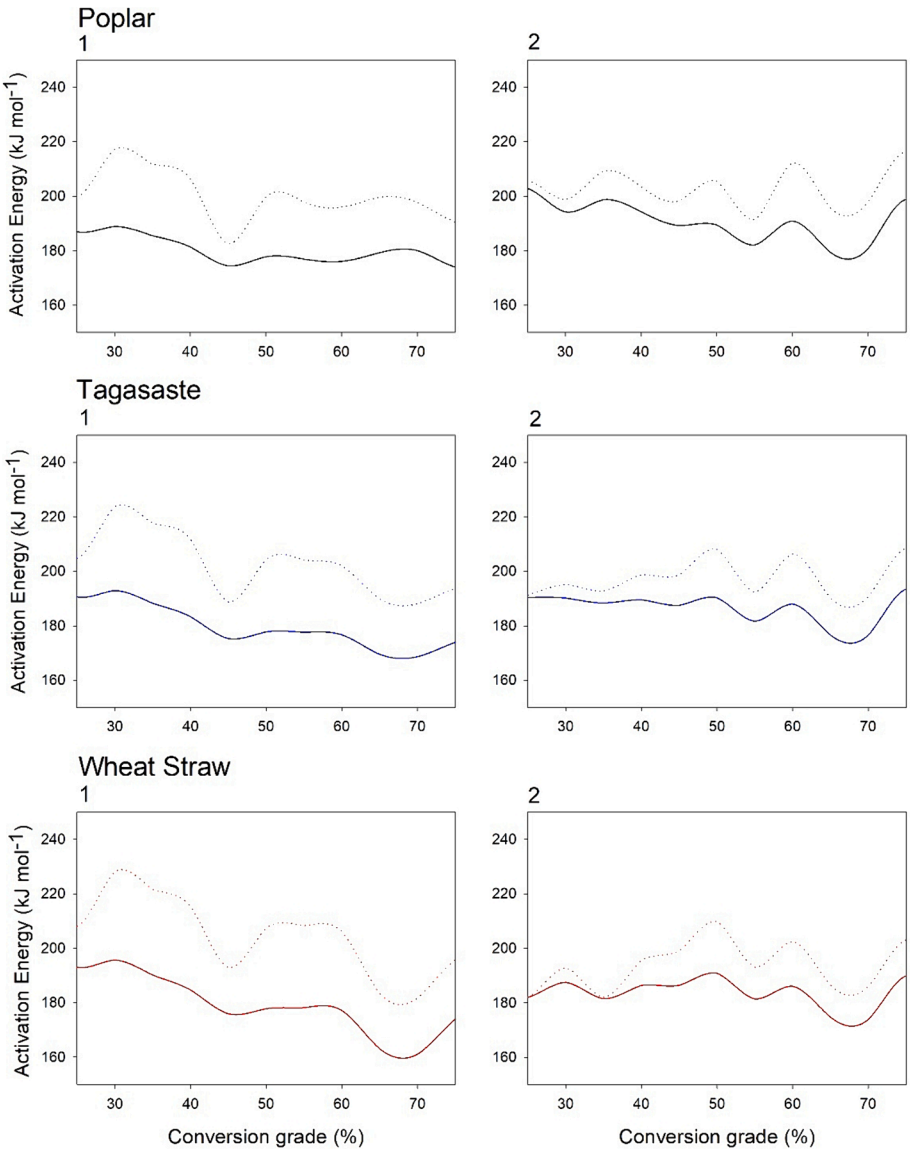


Fig. 9. Activation Energy evolution for kraft (1) and Soda-Antraquinone (2) celluloses by Friedman (continuous lines) and FWO (discontinuous lines) methods.

specific compounds and their amounts depend on the initial raw material. With regard to the cellulose fraction, the crystallinity and degree of polymerization vary among different feedstocks. For example, softwoods generally have a higher crystallinity than hardwoods and agricultural residues [71–73]. Sun et al., 2022 [74] reported that cellulose pyrolysis produces aldehydes, acids, alcohols, ketones, carbohydrates, and other. In Poplar, a significant amount of the aldehyde prop-2-enal (29.5 %) was identified, while the primary aldehyde in the cellulose fractions of Tagasaste and Wheat Straw was 3-Methylbutanal (14.2 % and 18.1 %, respectively).

Regarding the lignin fractions, the differences between Tagasaste, Poplar and Wheat Straw are similar to those observed in the hemicellulose fractions. In this case, the most abundant family of compounds obtained from Poplar and Wheat Straw was aromatic hydrocarbons, predominantly toluene (40.8 % and 31.6 %, respectively). However, in Tagasaste's lignin fraction, the predominant group of compounds were phenols (28.2 %). For this fraction, there is also a correlation between the feedstock and the pyrolytic gases, as the lignin composition is also influenced by the feedstock's composition. Specifically, softwoods have a higher lignin content with a predominantly guaiacyl units, whereas hardwoods contain a higher proportion of syringyl units [75].

One compound deserving special mention is furfural, which has been recognized as one of the top biomass-derived platform compounds by the US Department of Energy [76]. Furfural has the potential to yield high-value products, including liquid hydrocarbon fuels, fuel additives, and furfural derivatives with various applications [77,78]. In summary, the furfural serves as a valuable source of derivatives that have the potential to become biofuel components [79]. In this work, we observed that pyrolysis produced a significant quantity of furans, especially furfural, primarily originating from hemicellulose fractions. Wheat Straw exhibited the highest furfural production, accounting for 19.3 %, followed by Poplar with 16.9 %, and Tagasaste with the lowest at 6.6 %.

4. Conclusions

The thermogravimetric analysis revealed similar degradation patterns across the studied raw materials (Poplar, Tagasaste, and Wheat Straw), with distinct characteristics for each lignocellulosic fraction. Cellulose exhibited a single peak around 370 °C, hemicellulose degraded earlier (250 – 300 °C) with a smoother profile, and lignin showed a broader range (15 – 600 °C) that is less prevalent in raw materials due to overlapping degradation with other components. The activation energy (E_a) required for degradation varied depending on the fraction and conversion degree, with hemicellulose (200–300 kJ mol^{-1}) requiring

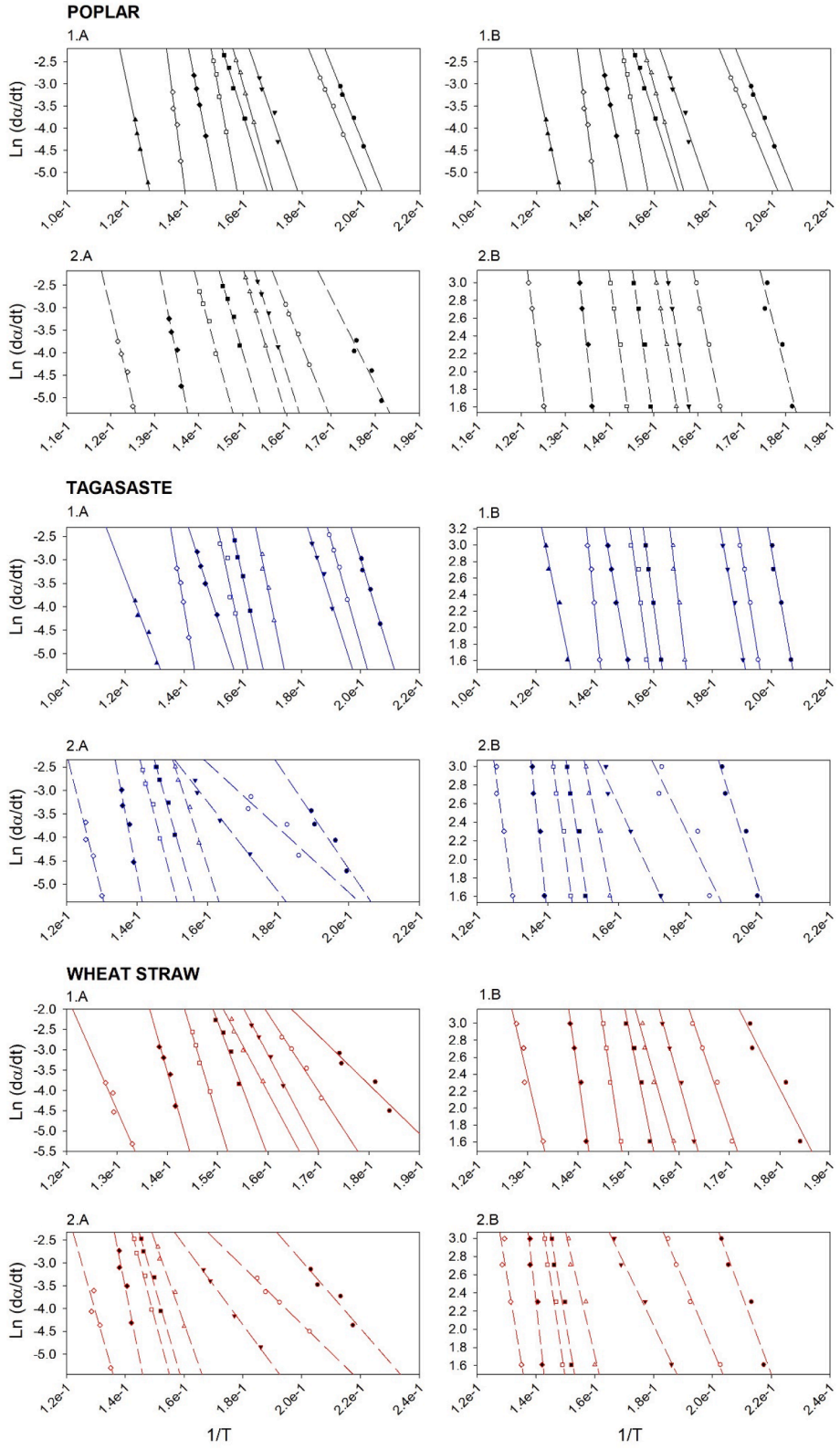


Fig. 10. Evolution of the Friedman (A) and FWO (B) lines for kraft (1) and Soda-Antraquinone (2) lignins as a function of the conversion degree (symbols) and the regression lines obtained.

slightly higher E_a than cellulose (180–220 kJ mol^{-1}). Lignin fractions displayed the highest E_a; variations exist among different lignins, influenced by factors such as the origin of the raw material and the delignification method employed to obtain the lignin fraction. The pyrolysis process generated a diverse gas stream, with a wide range of components, originating from different lignocellulosic fractions. Highlighting the presence of furfural, more pronounced in the pyrolysis of hemicellulose fractions, especially in hemicellulose obtained from Wheat Straw. This observation underscores a potential avenue for the targeted production of high-value-added chemicals from specific

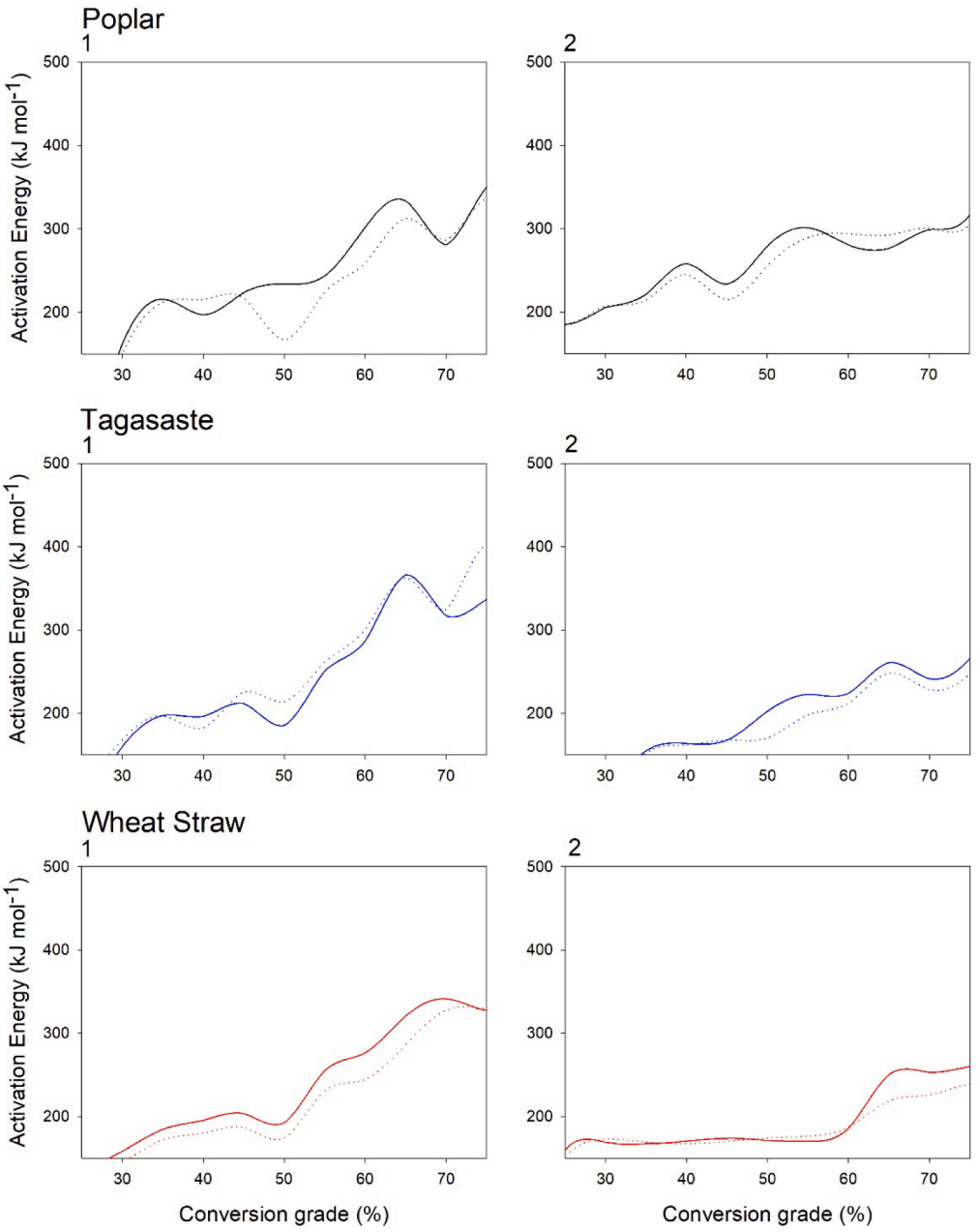


Fig. 11. Activation Energy evolution for kraft (1) and Soda-Antraquinone (2) lignins by Friedman (continuous lines) and FWO (discontinuous lines) methods.

biomass sources.

Ethics approval and consent to participate

The authors declare that this is their original work, and the corresponding manuscript has not been published before and is only submitted to Fuel.

Consent for publication

All authors reviewed the manuscript and consented to its publication.

Availability of data and materials

All data generated or analyzed during this work are included in this published article.

Funding

This study was supported by the Ministry of Science and Innovation (Spain), as well as by the National Research Program Oriented to the Challenges of Society (Project PID2020-112875RB-C21 funded by MCIN/AEI /https://doi.org/10.13039/501100011033), also this publication is part of the PRE2021-097925 support (funded by MCIN/AEI/ https://doi.org/10.13039/501100011033 and by the FSE+). Funding for open access charge: Universidad de Huelva/CBUA.

CRediT authorship contribution statement

N. Almagro-Herrera: Visualization, Methodology, Investigation, Formal analysis, Data curation, Conceptualization. **S. Lozano-Calvo:** Writing – original draft, Visualization, Methodology, Investigation, Formal analysis, Data curation, Conceptualization. **A. Palma:** Writing – review & editing, Visualization, Methodology, Investigation, Formal analysis, Data curation, Conceptualization. **J.C. García:** Conceptualization, Methodology, Funding acquisition, Supervision, Project administration. **M.J. Díaz:** Conceptualization, Methodology, Formal analysis, Data curation, Funding acquisition, Supervision, Writing – review & editing, Project administration.

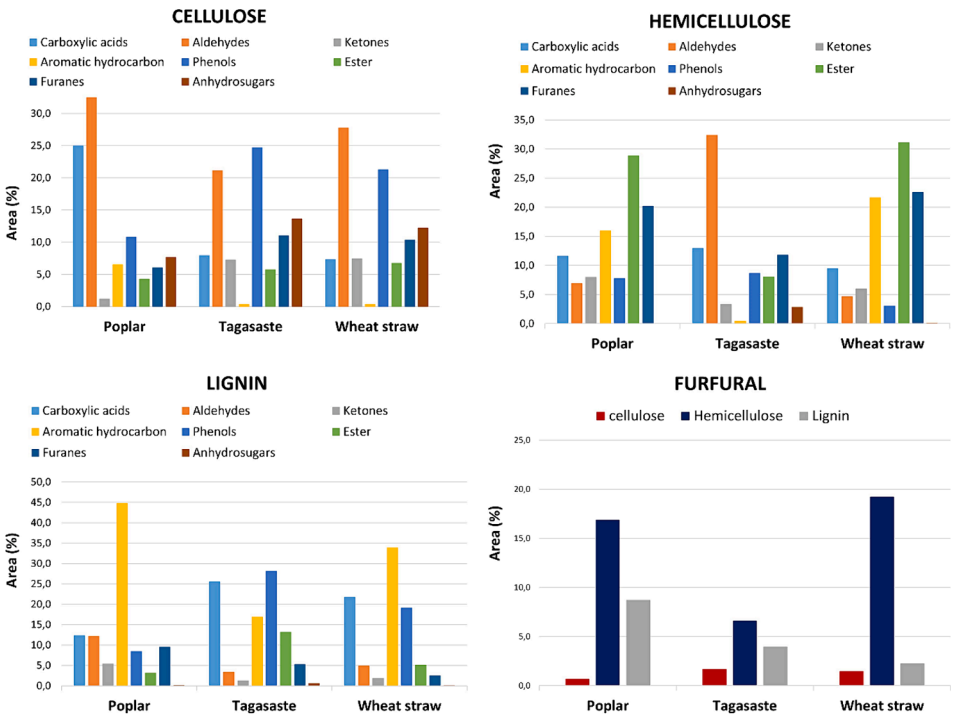


Fig. 12. Pyrolysis-gas products (% area) of the different fractions (cellulose, hemicellulose, and lignin) of Poplar, Tagasaste and Wheat Straw, and furfural production from the different fractions.

Declaration of competing interest

The authors declare that they have no known competing financial interests or personal relationships that could have appeared to influence the work reported in this paper.

Data availability

All data generated or analyzed during this work are included in this published article.

References

[1] Alper K, Tekin K, Karagöz S, Ragauskas AJ. Sustainable energy and fuels from biomass: a review focusing on hydrothermal biomass processing. Sustain Energy Fuels 2020;4:4390–414. https://doi.org/10.1039/D0SE00784F.

[2] Roy P, Jahromi H, Rahman T, Baltrusaitis J, Hassan EB, Torbert A, et al. Hydrotreatment of pyrolysis bio-oil with non-edible carinata oil and poultry fat for producing transportation fuels. Fuel Process Technol 2023;245:107753. https://doi.org/10.1016/J.FUPROC.2023.107753.

[3] Sharma V, Tsai ML, Nargotra P, Chen CW, Sun PP, Singhania RR, et al. Journey of lignin from a roadblock to bridge for lignocellulose biorefineries: a comprehensive review. Sci Total Environ 2023;861:160560. https://doi.org/10.1016/J.SCITOTENV.2022.160560.

[4] Ayub Y, Zhou J, Shi T, Ren J. Process safety assessment of thermal technologies for biomass valorization by numerical descriptive approach. Process Saf Environ Prot 2023;171:803–11. https://doi.org/10.1016/J.PSEP.2023.01.075.

[5] Troiano DT, Hofmann T, Brethauer S, Studer MHP. Toward optimal use of biomass as carbon source for chemical bioproduction. Curr Opin Biotechnol 2023;81:102942. https://doi.org/10.1016/J.COPBIO.2023.102942.

[6] Akram HA, Imran M, Javaid A, Latif S, Rizvi NB, Jesionowski T, et al. Pretreatment and catalytic conversion of lignocellulosic and algal biomass into biofuels by metal organic frameworks. Mol Catal 2023;539:112893. https://doi.org/10.1016/J.MCAT.2022.112893.

[7] Zhan Q, Lin Q, Wu Y, Liu Y, Wang X, Ren J. A fractionation strategy of cellulose, hemicellulose, and lignin from wheat straw via the biphasic pretreatment for biomass valorization. Bioresour Technol 2023;376:128887. https://doi.org/10.1016/J.BIORTECH.2023.128887.

[8] Fan Q, Fu P, Song C, Fan Y. Valorization of waste biomass through hydrothermal liquefaction: a review with focus on linking hydrothermal factors to products characteristics. Ind Crops Prod 2023;191:116017. https://doi.org/10.1016/J.INDCROP.2022.116017.

[9] Mujtaba M, Fraceto L, Fazeli M, Mukherjee S, Savassa SM, Araujo de Medeiros G, et al. Lignocellulosic biomass from agricultural waste to the circular economy: a review with focus on biofuels, biocomposites and bioplastics. J Clean Prod 2023;402:136815. https://doi.org/10.1016/J.JCLEPRO.2023.136815.

[10] Amenaghawon AN, Anyalewechi CL, Okieimen CO, Kusuma HS. Biomass pyrolysis technologies for value-added products: a state-of-the-art review. Environ Dev Sustain 2021;23:14324–78. https://doi.org/10.1007/s10668-021-01276-5.

[11] Vuppaladadiyam AK, Vuppaladadiyam SSV, Sahoo A, Murugavelh S, Anthony E, Bhashkar T, et al. Bio-oil and biochar from the pyrolytic conversion of biomass: a current and future perspective on the trade-off between economic, environmental, and technical indicators. Sci Total Environ 2023;857:159155. https://doi.org/10.1016/J.SCITOTENV.2022.159155.

[12] Okolie JA, Epelle EI, Tabat ME, Orivri U, Amenaghawon AN, Okoye PU, et al. Waste biomass valorization for the production of biofuels and value-added products: a comprehensive review of thermochemical, biological and integrated processes. Process Saf Environ Prot 2022;159:323–44. https://doi.org/10.1016/J.PSEP.2021.12.049.

[13] Eugenio ME, Ruiz-Montoya M, Martín-Sampedro R, Ibarra D, Díaz MJ. Influence of cellulose Characteristics on pyrolysis suitability. Processes 2021;9. https://doi.org/10.3390/pr9091584.

[14] Madanayake BN, Gan S, Eastwick C, Ng HK. Biomass as an energy source in coal co-firing and its feasibility enhancement via pre-treatment techniques. Fuel Process Technol 2017;159:287–305. https://doi.org/10.1016/J.FUPROC.2017.01.029.

[15] Wu W, Mei Y, Zhang L, Liu R, Cai J. Effective activation energies of lignocellulosic biomass pyrolysis. Energy Fuel 2014;28:3916–23. https://doi.org/10.1021/ef5005896.

[16] Chen D, Cen K, Zhuang X, Gan Z, Zhou J, Zhang Y, et al. Insight into biomass pyrolysis mechanism based on cellulose, hemicellulose, and lignin: evolution of volatiles and kinetics, elucidation of reaction pathways, and characterization of gas, biochar and bio-oil. Combust Flame 2022;242:112142. https://doi.org/10.1016/J.COMBUSTFLAME.2022.112142.

[17] Al-Rumaihi A, Shahbaz M, Mckay G, Mackey H, Al-Ansari T. A review of pyrolysis technologies and feedstock: a blending approach for plastic and biomass towards optimum biochar yield. Renew Sustain Energy Rev 2022;167:112715. https://doi.org/10.1016/J.RSER.2022.112715.

[18] Stefanidis SD, Kalogiannis KG, Iliopoulou EF, Michailof CM, Pilavachi PA, Lappas AA. A study of lignocellulosic biomass pyrolysis via the pyrolysis of cellulose, hemicellulose and lignin. J Anal Appl Pyrolysis 2014;105:143–50. https://doi.org/10.1016/J.JAAP.2013.10.013.

[19] Zhou X, Li W, Mabon R, Broadbelt LJ. A critical review on hemicellulose pyrolysis. Energ Technol 2017;5:52–79. https://doi.org/10.1002/ente.201600327.

[20] Carrier M, Windt M, Ziegler B, Appelt J, Saake B, Meier D, et al. Quantitative insights into the fast pyrolysis of Extracted cellulose, hemicelluloses, and lignin. ChemSusChem 2017;10:3212–24. https://doi.org/10.1002/cssc.201700984.

[21] de Carvalho DM, Sevastyanova O, de Queiroz JH, Colodette JL. Cold alkaline extraction as a pretreatment for bioethanol production from eucalyptus, sugarcane bagasse and sugarcane straw. Energy Convers Manag 2016;124:315–24. https://doi.org/10.1016/j.enconman.2016.07.029.

[22] Hult E-L, Larsson PT, Iversen T. A comparative CP/MAS 13C-NMR study of cellulose structure in spruce wood and kraft pulp. Cellul 2000;7:35–55.

[23] Newman RH, Hemmingson JA, Suckling ID. Carbon-13 nuclear magnetic resonance studies of kraft pulping; 1993.
[24] Gustafson RR, Sleicher CA, McKean WT, Finlayson BA. Theoretical model of the kraft pulping process. Ind Eng Chem Process Des Dev 1983;22:87–96.
[25] Martínez JM, Reguant J, Salvadó J, Farriol X. Soda-anthraquinone pulping of a softwood mixture: applying a pseudo-kinetic severity parameter. Bioresour Technol 1997;60:161–7.
[26] Rabemanolontsoa H, Saka S. Various pretreatments of lignocellulosics. Bioresour Technol 2016;199:83–91. https://doi.org/10.1016/J.BIORTECH.2015.08.029.
[27] García JC, Díaz MJ, Garcia MT, Feria MJ, Gómez DM, López F. Search for optimum conditions of wheat straw hemicelluloses cold alkaline extraction process. Biochem Eng J 2013;71:127–33. https://doi.org/10.1016/j.bej.2012.12.008.
[28] Park YC, Kim JS. Comparison of various alkaline pretreatment methods of lignocellulosic biomass. Energy 2012;47:31–5. https://doi.org/10.1016/j.energy.2012.08.010.
[29] Lozano Calvo S. Extracción de Polisacáridos en Especies de Alta Productividad Aplicando Ultrasonidos. Huelva: 2019.
[30] TAPPI T264 cm-07. Preparation of wood for chemical analysis.TAPPI Press, Atlanta, GA. 2007.
[31] Pola L, Collado S, Oulego P, Díaz M. Kraft black liquor as a renewable source of value-added chemicals. Chem Eng J 2022;448:137728. https://doi.org/10.1016/J.CEJ.2022.137728.
[32] López F, Trinidad García M, Mena V, Loaiza JM, Zamudio MAM, García JC. Can acceptable pulp be obtained from Eucalyptus globulus wood chips after hemicellulose extraction? vol. 10. 2015.
[33] TAPPI T204 cm-07. Solvent extractives of wood and pulp. TAPPI Press, Atlanta, GA. 2007.
[34] TAPPI T222 om-11. Acid-insoluble lignin in wood and pulp. TAPPI Press, Atlanta, GA. 2011.
[35] TAPPI T249 cm-09. Carbohydrate composition of extractive-free wood and wood pulp by gas-liquid chromatography. TAPPI Press, Atlanta, GA. 2009.
[36] Van de Velden M, Baeyens J, Brems A, Janssens B, Dewil R. Fundamentals, kinetics and endothermicity of the biomass pyrolysis reaction. Renew Energy 2010;35:232–42. https://doi.org/10.1016/J.RENENE.2009.04.019.
[37] Siddiqi H, Bal M, Kumari U, Meikap BC. In-depth physiochemical characterization and detailed thermo-kinetic study of biomass wastes to analyze its energy potential. Renew Energy 2020;148:756–71. https://doi.org/10.1016/J.RENENE.2019.10.162.
[38] Ozawa T. A new method of analyzing thermogravimetric data. Bull Chem Soc Jpn 1965;38:1881–6. https://doi.org/10.1246/bcsj.38.1881.
[39] Flynn JH, Wall LA. A quick, direct method for the determination of activation energy from thermogravimetric data. J Polym Sci B 1966;4:323–8. https://doi.org/10.1002/pol.1966.110040504.
[40] Venkatesh M, Ravi P, Tewari SP. Isoconversional kinetic analysis of decomposition of nitroimidazoles: friedman method vs Flynn–Wall–Ozawa method. J Phys Chem A 2013;117:10162–9. https://doi.org/10.1021/jp407526r.
[41] Friedman HL. Kinetics of thermal degradation of char-forming plastics from thermogravimetry. application to a phenolic plastic. J Polym Sci Part C: Polym Symposia Wiley Online Library 1964;6:183–95.
[42] Khristova P, Kordsachia O, Patt R, Dafaalla S. Alkaline pulping of some eucalypts from Sudan. Bioresour Technol 2006;97:535–44. https://doi.org/10.1016/J.BIORTECH.2005.04.006.
[43] Deniz I, Kirci H, Ates S. Optimisation of wheat straw Triticum drum kraft pulping. Ind Crops Prod 2004;19:237–43. https://doi.org/10.1016/J.INDCROP.2003.10.011.
[44] Alaejos J, López F, Eugenio ME, Tapias R. Soda–anthraquinone, kraft and organosolv pulping of holm oak trimmings. Bioresour Technol 2006;97:2110–6. https://doi.org/10.1016/J.BIORTECH.2005.09.021.
[45] Ma H, Zhang Y, Wang L, Zhu Z, Chen Y, Wang H, et al. Kinetic Analysis of the Pyrolysis of Apricot Stone and its Main Components via Distributed Activation Energy Mode. vol. 15. 2019.
[46] SriBala G, Vargas DC, Kostetskyy P, de Vijver R, Broadbelt LJ, Marin GB, et al. New perspectives into cellulose fast pyrolysis kinetics using a py-GC × GC-FID/MS system. ACS Engineering Au 2022;2:320–32. https://doi.org/10.1021/acsengineeringau.2c00006.
[47] Domínguez JC, Santos TM, Rigual V, Oliet M, Alonso MV, Rodriguez F. Thermal stability, degradation kinetics, and molecular weight of organosolv lignins from Pinus radiata. Ind Crops Prod 2018;111:889–98. https://doi.org/10.1016/J.INDCROP.2017.10.059.
[48] Yeo JY, Chin BLF, Tan JK, Loh YS. Comparative studies on the pyrolysis of cellulose, hemicellulose, and lignin based on combined kinetics. J Energy Inst 2019;92:27–37. https://doi.org/10.1016/J.JOEI.2017.12.003.
[49] Collard FX, Blin J. A review on pyrolysis of biomass constituents: mechanisms and composition of the products obtained from the conversion of cellulose, hemicelluloses and lignin. Renew Sustain Energy Rev 2014;38:594–608. https://doi.org/10.1016/J.RSER.2014.06.013.
[50] Zhang X, Yang W, Dong C. Levoglucosan formation mechanisms during cellulose pyrolysis. J Anal Appl Pyrolysis 2013;104:19–27. https://doi.org/10.1016/J.JAAP.2013.09.015.
[51] Custodis VBF, Hemberger P, Ma Z, van Bokhoven JA. Mechanism of fast pyrolysis of lignin: studying model compounds. J Phys Chem B 2014;118:8524–31. https://doi.org/10.1021/jp5036579.
[52] Mandlekar N, Cayla A, Rault F, Giraud S, Salaün F, Malucelli G, et al. Thermal stability and fire Retardant properties of polyamide 11 microcomposites containing different lignins. Ind Eng Chem Res 2017;56:13704–14. https://doi.org/10.1021/acs.iecr.7b03085.
[53] Wang H, Yao Q, Wang C, Fan B, Xiong Y, Chen Y, et al. New insight on promoted thermostability of poplar wood modified by MnFe2O4 nanoparticles through the pyrolysis behaviors and kinetic study. Sci Rep 2017;7:1418. https://doi.org/10.1038/s41598-017-01597-4.
[54] Fan H, Gu J, Wang Y, Yuan H, Chen Y. Insight into the pyrolysis kinetics of cellulose, xylan and lignin with the addition of potassium and calcium based on distributed activation energy model. Energy 2022;243:122816. https://doi.org/10.1016/J.ENERGY.2021.122816.
[55] Zhu L, Zhong Z. Effects of cellulose, hemicellulose and lignin on biomass pyrolysis kinetics. Korean J Chem Eng 2020;37:1660–8. https://doi.org/10.1007/s11814-020-0553-y.
[56] Anca-Couce A, Tsekos C, Retschitzegger S, Zimbardi F, Funke A, Banks S, et al. Biomass pyrolysis TGA assessment with an international round robin. Fuel 2020;276:118002. https://doi.org/10.1016/J.FUEL.2020.118002.
[57] Luo L, Guo X, Zhang Z, Chai M, Rahman MM, Zhang X, et al. Insight into pyrolysis kinetics of lignocellulosic biomass: isoconversional kinetic analysis by the modified Friedman method. Energy Fuel 2020;34:4874–81.
[58] Matusiak M, Ślęzak R, Ledakowicz S. Thermogravimetric kinetics of selected energy crops pyrolysis. Energies (Basel) 2020;13. https://doi.org/10.3390/en13153977https://doi.org/10.1021/acs.energyfuels.0c00275.
[59] Radojević M, Janković B, Jovanović V, Stojiljković D, Manić N. Comparative pyrolysis kinetics of various biomasses based on model-free and DAEM approaches improved with numerical optimization procedure. PLoS One 2018;13. https://doi.org/10.1371/journal.pone.0206657.
[60] Li L, Rowbotham JS, Christopher Greenwell H, Dyer PW. An introduction to pyrolysis and catalytic pyrolysis: versatile techniques for biomass conversion. New Future Devel Catal: Catal Biomass Convers 2013:173–208. https://doi.org/10.1016/B978-0-444-53878-9.00009-6.
[61] Wang S, Dai G, Yang H, Luo Z. Lignocellulosic biomass pyrolysis mechanism: a state-of-the-art review. Prog Energy Combust Sci 2017;62:33–86. https://doi.org/10.1016/J.PECS.2017.05.004.
[62] Liu M, Yang J, Liu Z, He W, Liu Q, Li Y, et al. Cleavage of covalent bonds in the pyrolysis of lignin, cellulose, and hemicellulose. Energy Fuel 2015;29:5773–80. https://doi.org/10.1021/acs.energyfuels.5b00983.
[63] Kristanto J, Azis MM, Purwono S. Multi-distribution activation energy model on slow pyrolysis of cellulose and lignin in TGA/DSC. Heliyon 2021;7:e07669.
[64] Carrier M, Fournet R, Sirjean B, Amsbury S, Alfonso YB, Pontalier P-Y, et al. Fast pyrolysis of hemicelluloses into short-chain acids: an investigation on concerted mechanisms. Energy Fuel 2020;34:14232–48. https://doi.org/10.1021/acs.energyfuels.0c02901.
[65] Huang Y, Wang H, Zhang X, Zhang Q, Wang C, Ma L. CO2 pyrolysis kinetics and characteristics of lignin-rich hydrolysis residue produced from a tandem process of steam-stripping and acid hydrolysis. Fuel 2022;316:123361. https://doi.org/10.1016/J.FUEL.2022.123361.
[66] Clemente-Castro S, Palma A, Ruiz-Montoya M, Giráldez I, Díaz MJ. Optimizing pyrolysis parameters and product analysis of a fluidized bed pilot plant for Leucaena leucocephala biomass. Environ Sci Eur 2023;35:88. https://doi.org/10.1186/s12302-023-00800-w.
[67] Pielsticker S, Gövert B, Umeki K, Kneer R. Flash pyrolysis kinetics of Extracted lignocellulosic biomass components. Front Energy Res 2021:9. https://doi.org/10.3389/fenrg.2021.737011.
[68] Li H, Wang L, Ji Y, Xue S, Wang Z. Study on the mechanism of gas component release for biomass pyrolysis. E3S Web of Conferences, vol. 118, EDP Sciences; 2019, p. 03058.
[69] Popa VI, Spiridon J. Hemicelluloses: structure and properties. Polysaccharides: Structural Diversity and Functional Versatility Marcel Dekker, New York 1998:297–311.
[70] Xiao L-P, Song G-Y, Sun R-C. Effect of hydrothermal processing on hemicellulose structure. Hydrothermal processing in biorefineries: production of bioethanol and high added-value compounds of second and third generation biomass 2017:45–94.
[71] Adachi H, Sugiyama J, Kondo Y, Okano T. The difference of cellulose crystal between softwoods and hardwoods. Sen'i Gakkaishi 1991;47:580–4. https://doi.org/10.2115/fiber.47.11_580.
[72] Newman RH. Crystalline forms of cellulose in softwoods and Hardwoods. J Wood Chem Technol 1994;14:451–66. https://doi.org/10.1080/02773819408003107.
[73] Lichtenegger H, Reiterer A, Stanzl-Tschegg SE, Fratzl P. Variation of cellulose microfibril angles in softwoods and Hardwoods—a possible strategy of mechanical optimization. J Struct Biol 1999;128:257–69. https://doi.org/10.1006/JSBI.1999.4194.
[74] Sun T, Zhang L, Yang Y, Li Y, Ren S, Dong L, et al. Fast pyrolysis of cellulose and the effect of a catalyst on product distribution. Int J Environ Res Public Health 2022:19. https://doi.org/10.3390/ijerph192416837.
[75] Lourenço A, Pereira H. Compositional variability of lignin in biomass. Lignin-Trends Appl 2018:65–98.
[76] Luo Y, Li Z, Li X, Liu X, Fan J, Clark JH, et al. The production of furfural directly from hemicellulose in lignocellulosic biomass: a review. Catal Today 2019;319:14–24. https://doi.org/10.1016/j.cattod.2018.06.042.
[77] Machado G, Leon S, Santos F, Lourega R, Dullius J, Mollmann ME, et al. Literature review on furfural production from lignocellulosic biomass. Nat Resour 2016;07:115–29. https://doi.org/10.4236/nr.2016.73012.
[78] Li X, Jia P, Wang T. Furfural: a promising platform compound for sustainable production of C4 and C5 chemicals. ACS Catal 2016;6:7621–40. https://doi.org/10.1021/acscatal.6b01838.
[79] Lange JP, Van Der Heide E, Van Buijtenen J, Price R. Furfural-a promising platform for lignocellulosic biofuels. ChemSusChem 2012;5:150–66. https://doi.org/10.1002/cssc.201100648.

2. Comunicaciones en congresos.

- **Autores:** J.M. Loaiza, S. Lozano-Calvo, J.C. García, M.T. García, M.J. Díaz, F. López.
  Título: Energy valuation and otaining hydrogen from post-hydrolysis phases (cold alkaline extraction with ultrasound) of the genus Populus (Poplar clone AF2).
  Tipo de participación: Exposición oral de Póster.
  Congreso: XXV TECNICELPA-International Forest, Pulp and Paper Conference | XI CIADICYP.
  Lugar de celebración: Online.
  Fecha: 9-12 Marzo 2021.

- **Autores:** S. Lozano-Calvo, M.T. García, J.C. García, F. López, J.M. Loaiza.
  Título: Valorization by acid hydrolysis from three industrial crops (Tagasaste, Leucaena and Paulownia trihybrid).
  Tipo de participación: Exposición oral de Póster.
  Congreso: 2nd International Webinar on "Recycling and Waste Management".
  Lugar de celebración: Online.
  Fecha: 29-30 Marzo 2021.

- **Autores:** S. Lozano-Calvo, J.M. Loaiza, A. Palma, J.C. García, M.T. García, M.J. Díaz, F. López.
  Título: Optimizing isothermal autohydrolysis of wheat Straw for furfural production.
  Tipo de participación: Exposición oral de Póster.
  Congreso: 2nd International Conference on Recycling and Waste Management.
  Lugar de celebración: Online.
  Fecha: 5-6 Julio 2021.

- **Autores:** S. Lozano-Calvo, J.M. Loaiza, M.T. García, A. Palma, F. López, J.C. García.
  Título: Comparison of different double stage biorefinery schemes on *Eucalyptus globulus*.
  Tipo de participación: Presentación oral.
  Congreso: 4th Online International Conference on "Recycling and Waste Management".
  Lugar de celebración: Online.
  Fecha: 28-29 Marzo 2022.

- **Autores:** S. Lozano-Calvo, A. Alfaro, J.M. Loaiza, M.T. García, F. López, J.C. García.
  Título: Application of cold alkaline extraction process of the elephant grass to optimize the energy use and valorization of the hemicellulosic fraction.
  Tipo de participación: Presentación oral.
  Congreso: Iberoamerican Congress on Pulp and Paper Research (CIADICYP).
  Lugar de celebración: Girona (España).
  Fecha: 28 Junio - 1 Julio 2022.

- **Autores:** J.M. Loaiza, M.T. García, S. Lozano-Calvo, M.J. Díaz, J.C. García, F. López.
  Título: Obtaining furfural by isothermal autohydrolysis from agricultural by-product.
  Tipo de participación: Presentación Póster.
  Congreso: Iberoamerican Congress on Pulp and Paper Research (CIADICYP).
  Lugar de celebración: Girona (España).
  Fecha: 28 Junio - 1 Julio 2022.

- **Autores:** S. Lozano-Calvo, Mª. Trejo-Cáceres, M. Delgado-Aguilar, Q. Tarrés, J.C. García, P. Partal, F. López.
  Título: Prospective characterization of lignocellulosic biomasses to obtain biorefinery fractions of interest in asphalts.
  Tipo de participación: Presentación Póster.
  Congreso: Iberoamerican Congress on Pulp and Paper Research (CIADICYP).
  Lugar de celebración: Girona (España).
  Fecha: 28 Junio - 1 Julio 2022.

- **Autores:** J.F. Rubio-Valle, M. Trejo-Cáceres, M.A. Martín-Alfonso, S. Lozano-Calvo, J.E. Martín-Alfonso.
  Título: Influence o fan alkali treatment on the acetylation process of Kraft pulp.
  Tipo de participación: Presentación Póster.
  Congreso: Congreso Internacional del Centro de Biotecnología FEMSA.
  Lugar de celebración: Monterrey, Nuevo León (México).
  Fecha: 24-26 Agosto 2022.

- **Autores:** S. Lozano-Calvo, N. Almagro, A. Palma, J.C. García, M.T. García, M.J. Díaz.
  Título: Optimization of the fracctionation of an agroforestry waste in the different lignocellulosic components and its energetic valorization.
  Tipo de participación: Presentación Póster.
  Congreso: 3rd International Workshop on Biorefinery of Lignocellulosic Materials
  Lugar de celebración: Córdoba (España).
  Fecha: 12-15 Septiembre 2023.

- **Autores:** M.T. García, R. Rengel, J.M. Loaiza, S. Lozano-Calvo, F. López, J.C. García.
  Título: Furfural production by acid hydrolysis of Poplar clone AF2, *Ulmus minor* and *Leucaena L.* in two stages.
  Tipo de participación: Presentación Póster.
  Congreso: 3rd International Workshop on Biorefinery of Lignocellulosic Materials
  Lugar de celebración: Córdoba (España).
  Fecha: 12-15 Septiembre 2023.

- **Autores:** S. Lozano-Calvo, J.M. Loaiza, M.T. García, F. López, A. Valenzuela, J.C. García.
  Título: Optimization of cold alkaline extraction of hemicelluloses with ultrasound from *Robinia Pseudoacacia*.
  Tipo de participación: Presentación Póster.
  Congreso: XXVI International Conference – Forest Biobased Materials – TECNICELPA.
  Lugar de celebración: Coimbra (Portugal).
  Fecha: 11-13 Octubre 2023.

- **Autores:** S. Lozano-Calvo, N. Almagro, A. Palma, J.M. Loaiza, M.T. García, M.J. Díaz, F. López, J.C. García.
  Título: Evaluation of the influence on pyrolysis of main biomass fractions, fractionation methods and biomass origin.
  Tipo de participación: Presentación Póster.
  Congreso: 5th Iberoamerican congress on Biorefineries (5th-CIAB).
  Lugar de celebración: Jaén (España).
  Fecha: 2-4 Octubre 2024.

- **Autores:** S. Lozano-Calvo, R. Rengel, A. Palma, M.T. García, J.M. Loaiza, J.C. García, R. León, M.J. Díaz.
  Título: Synergistic effects in the pyrolysis of algae and main biomass fractions mixtures.
  Tipo de participación: Presentación Póster.
  Congreso: 5th Iberoamerican congress on Biorefineries (5th-CIAB).
  Lugar de celebración: Jaén (España).
  Fecha: 2-4 Octubre 2024.

- **Autores:** J.M. Loaiza, E. Gutiérrez, S. Lozano-Calvo, M.T. García, A. Valenzuela, R. Rengel, F. López, J.C. García.
  Título: Effect of Cold Alkaline Extraction in Obtaining Hemicelluloses and Cellulose Nanofibers (CNF) From High-yield Forest Species.
  Tipo de participación: Presentación Póster.
  Congreso: 5th Iberoamerican congress on Biorefineries (5th-CIAB).
  Lugar de celebración: Jaén (España).
  Fecha: 2-4 Octubre 2024.

- **Autores:** R. Rengel, A.M. Molina, S. Lozano-Calvo, M.T. García, J.M. Loaiza, A. Palma, R. León, J.C. García.
  Título: Biorefinery scheme for the synergistic use of lignocellulosic and microalgae biomass for the production of bioethanol and other high-added value compounds.
  Tipo de participación: Presentación Póster.
  Congreso: 5th Iberoamerican congress on Biorefineries (5th-CIAB).
  Lugar de celebración: Jaén (España).
  Fecha: 2-4 Octubre 2024.